ERRATA

1. VOLUME I: Page 222 (Fig. 209) is missing
(Email JC Turner to get this page).

2. VOLUME IV. At the end of Appendix 2009 (see heading CWH KNOTS) there are three pages numbered 197, i and ii.
Disgard these three pages, as they do not belong in the book.

THE BRAIDER

VOLUME III

ALBERTUS GEORG SCHAAKE

THE BRAIDER

VOLUME III : Issue Numbers 31–45

ALBERTUS GEORG SCHAAKE

— August 2002 to February 2006 —

PREFACE

This is the third of four volumes on the Theory and Practice of Braiding. It brings together the third fifteen issues of a Journal called simply *THE BRAIDER*.

Albertus Georg Schaake was born in Holland in 1933. He studied Engineering at Delft Technical University, before emigrating to New Zealand in 1962. His career has been spent first as a Public Works Engineer, and then as a Tutor in Engineering subjects at the Waikato Polytechnic in Hamilton.

For the last thirty years he has devoted countless hours to the study and practice of braiding : to the creation of decorative braids in particular. Towards the end of the 1980s, he began a project to publish his discoveries, occasionally collaborating with other authors, to produce a stream of books, pamphlets, articles and research papers on a variety of topics in braiding theory. These publications range from books on Regular Knots, Fiador Knots and Herringbone Knots through to extensive pamphlets on the braiding of Wheel-knots. For a lengthy account of the progress and philosophy of this work up to 1995, the reader is referred to chapter twelve of *History and Science of Knots* edited by J C Turner and P van de Griend, and published by World Scientific (1995).

In 1995, such was the large output of Schaake's ideas on the subject, that he decided to produce a quarterly Journal which would summarize and extend the description of his work. He called the Journal *The Braider*; and in the next eleven years, virtually single-handedly, he produced 60 issues. Such was his industry and application, that when he stopped his researches, due to illness in 2006, he had already prepared quarterly issues which would take the series up to November 2009.

In total, some 1600 pages of ideas, philosophies, theories, and instruction on design and production of decorative braids, have flowed from his computer and have been included in the issues of *The Braider*. In all the issues there are numerous diagrams which illustrate the theories and techniques. All of these were produced by Schaake by means of a computer-aided design package.

Now, in 2007, it is my privilege to bring together all sixty of the issues, unchanged and unedited, into a collection of four spirally-bound Volumes. They will be available for future generations of braiders to study and further the great body of work that Schaake has initiated.

Georg Schaake may truly be said to be the father of Modern Braiding Theory; very little of consequence existed before he began his researches.

The four-volume collection may be taken as a text for all braiders, from beginners to the most advanced. It is essential reading for all serious decorative braiders.

John C. Turner,
Honorary Fellow,
University of Waikato,
Hamilton,
New Zealand (August, 2007).
email: jcturner@clear.net.nz

THE BRAIDER — Issue Numbers 31–45

CONTENTS

No. 31 Solutions to the Questions in Issue No. 30
Nested Cylindrical Braids
Pitfalls in knot design
The Braider's Notebook 707–728

No. 32 A Button Saga
Designing Interbraided Knots
APPENDIX 2002 : Leading Braiders up the Garden Path,
Errata — *The Braider* 729–754

No. 33 Nested Cylindrical Braids
Designing Interbraided Knots
Historical Events and their fictitious renderings 755-782

No. 34 The separate half-cycle tables for each essential string in the example on pp. 756–767
Solution to the Question in Issue No. 33
Nested Cylindrical Braids
Toggle Knots at the end of a 4-string Round Braid 783–806

No. 35 Solutions to the Questions in Issue No. 34
A Hanger (Lanyard) with colourful knots
Nested Cylindrical Braids
An Integrated Pineapple Knot for an 8-string 2u-2o Round Braid 807–830

No. 36 A pair of South American Hobbles
Nested Cylindrical Braids
APPENDIX 2003 : Errata — *The Braider* 831–854

No. 37 Solutions to the Questions in Issue No. 36
Rectangular Right Prismatic Braids 855–880

No. 38 Solution to the Question in Issue No. 37
The Braider's Notebook
A Six Thong Round Braid Start 881–902

No. 39 The Flores Knots 903–924

No. 40 Solutions to the Questions in Issue No. 39
The Flores Knots 927–954

No. 41 Solutions to the Questions in Issue No. 40
Transition from two Round Braids
to one Round Braid, and vice versa
The Braider's Notebook 955–980

No. 42 Braided Slit Braids
The Components of Semi-Perfect Herringbone
Pineapple Knots 981–1004

No. 43 The Braider's Notebook
Braid Design 1005–1030

No. 44 Solution to the Question in Issue No. 43
Braid Design
Checkered Pineapple Knots
Round Braids and their string sizes 1031–1054

No. 45 The Glen Vandy Knots
Braid Design
Grant Knots
The Single Bugler's Braid 1055–1076

A complete **INDEX** may be found at the end of Volume *IV*

THE BRAIDER

No.31 **AUGUST 2002.**

CONTENTS

pg.

Solutions to the Questions in Issue No.30 707

Nested Cylindrical Braids 710

Pitfalls in knot design 719

The Braider's Notebook 725

A quarterly publication
for
the braiding artisan

Resale of this publication or copies thereof
is strictly prohibited

Copyright ©2002 by:

A.G. Schaake; 21 Sundown Cresc.; Hamilton; New Zealand.
D. Van Tassel; Box 335; Craig, Co 81626-0335; U.S.A.
F.J.M. Masurel; Ganzenzijde 4; 2317XG .Leiden; Nederland.

All rights reserved. No part of this publication may be reproduced, stored in a retrieval system, or transmitted, in any form or by any means, electronic, mechanical, photo-copying, recording, or otherwise, without prior written permission.

This publication is available to braiding artisans only.

Copies may be obtained from:

A.G. Schaake,
21 Sundown Cresc.,
Hamilton,
New Zealand.

SEE NOTE BELOW.

No. 31

NOTE : the first Fig. number in this Issue is 554, but should have been 584 instead. Hence the Fig. numbers 554 - 583 not only appear in *The Braider*, Issue No. 30, but the numbers 554 - 574 appear again in *The Braider*, Issue No. 31 and the numbers 575 - 583 appear again in *The Braider*, Issue No. 32. This was noted too late for rectification.

No. 32

See NOTE under No. 31 above.

Solutions to the Questions in Issue No. 30

Question on pg. 695.

Method I–1:

Since we have the cycle consisting of the successive half-cycles $1 \to 1$ and $A \leftarrow 1$, we have the cycle which consists of the successive half-cycles $A \to 2$ and $(A-1) \leftarrow 2$. We can obtain the value for y from the half-cycle $A \to 2$:

$$y = |2(A-A) + x + 2(A-2)|_{2A} = |x-4|_{2A}.$$

Since $\Delta = A-1$, it follows that $y = A-1$ or $y = 2A-1$. The enlargement will create only one additional nest of bights on the left-hand bight-edge and one additional nest of bights on the right-hand bight-edge, hence:

$$|(A-A) + x + 2(A-2) + (A-(A-1))|_B = 0, \text{ hence } |2A+x-3|_{AB^*} = 0.$$

(i.) For $y = A-1$:

$$x-4 = 2n'A + A - 1, \text{ hence } x = (2n'+1)A + 3 = (2n-3)A + 3,$$

where n is a natural number (recall from *The Braider*, Issue No. 25, pg. 564 that $x \geq 2-A$).

$$|2A+x-3|_{AB^*} = |(2n-1)A|_{AB^*} = 0, \text{ hence } B^* = \frac{2n-1}{m},$$

where m and n are natural numbers, and m divides into $2n-1$.

$$P = 2A + x - 2 = (2n-1)A + 1 = mAB^* + 1.$$

Since $B_e^* = B^* + 1$ it follows that $P_e = mAB_e^* + 1 = mAB^* + mA + 1 = P + mA$, and since $P_e = P + (x_e - x)$ it follows that $x_e = x + mA$.
Furthermore, $y_e = |y + (x_e - x)|_{2A} = |y + mA|_{2A} = |(m+1)A - 1|_{2A}$.

(ii.) For $y = 2A-1$:

$$x-4 = 2n'A + 2A - 1, \text{ hence } x = (2n'+2)A + 3 = (2n-2)A + 3,$$

where n is a natural number (recall from *The Braider*, Issue No. 25, pg. 564 that $x \geq 2-A$).

$$|2A+x-3|_{AB^*} = |2nA|_{AB^*} = 0, \text{ hence } B^* = \frac{2n}{m},$$

where m and n are natural numbers, and m divides into $2n$.

$$P = 2A + x - 2 = 2nA + 1 = mAB^* + 1.$$

Since $B_e^* = B^* + 1$ it follows that $P_e = mAB_e^* + 1 = mAB^* + mA + 1 = P + mA$, and since $P_e = P + (x_e - x)$ it follows that $x_e = x + mA$.
Furthermore, $y_e = |y + (x_e - x)|_{2A} = |y + mA|_{2A} = |mA - 1|_{2A}$.

Method I–2:

We have the cycle consisting of the successive half-cycles $1 \to A$ and $2 \leftarrow A$. From the half-cycle $1 \to A$ we can obtain the value for y:

$$y = |2(A-1) + x + 2(A-A)|_{2A} = |x-2|_{2A}.$$

Since $\Delta = 1$, it follows that $y = A+1$ or $y = 1$. The enlargement will create only one additional nest of bights on the left-hand bight-edge and one additional nest of bights on the right-hand bight-edge, hence:

$$|(A-1) + x + 2(A-A) + (A-2)|_B = 0, \text{ hence } |2A+x-3|_{AB^*} = 0.$$

(i.) For $y = A+1$:

$$x-2 = 2n'A + A + 1, \text{ hence } x = (2n'+1)A + 3 = (2n-3)A + 3,$$

where n is a natural number (recall from *The Braider*, Issue No. 25, pg. 564 that $x \geq 2-A$).

$$|2A+x-3|_{AB^*} = |(2n-1)A|_{AB^*} = 0\,,\ \text{hence}\ B^* = \frac{2n-1}{m}\,,$$

where m and n are natural numbers, and m divides into $2n-1$.

$$P = 2A+x-2 = (2n-1)A+1 = mAB^*+1\,.$$

Since $B^*_e = B^*+1$ it follows that $P_e = mAB^*_e+1 = mAB^*+mA+1 = P+mA$, and since $P_e = P+(x_e-x)$ it follows that $x_e = x+mA$.
Furthermore, $y_e = |y+(x_e-x)|_{2A} = |y+mA|_{2A} = |(m+1)A+1|_{2A}$.

(ii.) For $y=1$:

$$x-2 = 2n'A+1\,,\ \text{hence}\ x = 2n'A+3 = (2n-2)A+3\,,$$

where n is a natural number (recall from *The Braider*, Issue No. 25, pg. 564 that $x \geq 2-A$).

$$|2A+x-3|_{AB^*} = |2nA|_{AB^*} = 0\,,\ \text{hence}\ B^* = \frac{2n}{m}\,,$$

where m and n are natural numbers, and m divides into $2n$.

$$P = 2A+x-2 = 2nA+1 = mAB^*+1\,.$$

Since $B^*_e = B^*+1$ it follows that $P_e = mAB^*_e+1 = mAB^*+mA+1 = P+mA$, and since $P_e = P+(x_e-x)$ it follows that $x_e = x+mA$.
Furthermore, $y_e = |y+(x_e-x)|_{2A} = |y+mA|_{2A} = |mA+1|_{2A}$.

Method II–1 :

Since we have the cycle consisting of the successive half-cycles $A \rightarrow A$ and $1 \leftarrow A$, we have the cycle which consists of the successive half-cycles $1 \rightarrow (A-1)$ and $2 \leftarrow (A-1)$. We can obtain the value for y from the half-cycle $1 \rightarrow (A-1)$:

$$y = |2(A-1)+x+2(A-(A-1))|_{2A} = |x|_{2A}\,.$$

Since $\Delta = 1$, it follows that $y = A+1$ or $y = 1$. The enlargement will create only one additional nest of bights on the left-hand bight-edge and one additional nest of bights on the right-hand bight-edge, hence:

$$|(A-1)+x+2(A-(A-1))+(A-2)|_B = 0\,,\ \text{hence}\ |2A+x-1|_{AB^*} = 0\,.$$

(i.) For $y = A+1$:

$$x = 2n'A+A+1\,,\ \text{hence}\ x = (2n'+1)A+1 = (2n-1)A+1\,,$$

where n is a natural number (recall from *The Braider*, Issue No. 25, pg. 564 that $x \geq 2-A$).

$$|2A+x-1|_{AB^*} = |(2n+1)A|_{AB^*} = 0\,,\ \text{hence}\ B^* = \frac{2n+1}{m}\,,$$

where m and n are natural numbers, and m divides into $2n+1$.

$$P = 2A+x-2 = (2n+1)A-1 = mAB^*-1\,.$$

Since $B^*_e = B^*+1$ it follows that $P_e = mAB^*_e-1 = mAB^*+mA-1 = P+mA$, and since $P_e = P+(x_e-x)$ it follows that $x_e = x+mA$.
Furthermore, $y_e = |y+(x_e-x)|_{2A} = |y+mA|_{2A} = |(m+1)A+1|_{2A}$.

(ii.) For $y=1$:

$$x = 2n'A+1\,,\ \text{hence}\ x = (2n-2)A+1\,,$$

where n is a natural number (recall from *The Braider*, Issue No. 25, pg. 564 that $x \geq 2-A$).

$$|2A+x-1|_{AB^*} = |2nA|_{AB^*} = 0\,,\ \text{hence}\ B^* = \frac{2n}{m}\,,$$

where m and n are natural numbers, and m divides into $2n$.

$$P = 2A+x-2 = 2nA-1 = mAB^*-1\,.$$

Since $B_e^* = B^* + 1$ it follows that $P_e = mAB_e^* - 1 = mAB^* + mA - 1 = P + mA$, and since $P_e = P + (x_e - x)$ it follows that $x_e = x + mA$.
Furthermore, $y_e = |y + (x_e - x)|_{2A} = |y + mA|_{2A} = |mA + 1|_{2A}$.

Method II–2:

We have the cycle consisting of the successive half-cycles $A \to 1$ and $(A-1) \leftarrow 1$. From the half-cycle $A \to 1$ we can obtain the value for y :

$$y = |2(A - A) + x + 2(A - 1)|_{2A} = |x - 2|_{2A}\,.$$

Since $\Delta = A - 1$, it follows that $y = A - 1$ or $y = 2A - 1$. The enlargement will create only one additional nest of bights on the left-hand bight-edge and one additional nest of bights on the right-hand bight-edge, hence:

$$|(A - A) + x + 2(A - 1) + (A - (A - 1))|_B = 0\,,\ \text{hence}\ |2A + x - 1|_{AB^*} = 0\,.$$

(i.) For $y = A - 1$:

$$x = 2n'A + A + 1\,,\ \text{hence}\ x = (2n' + 1)A + 1 = (2n - 1)A + 1\,,$$

where n is a natural number (recall from *The Braider*, Issue No. 25, pg. 564 that $x \geq 2 - A$).

$$|2A + x - 1|_{AB^*} = |(2n + 1)A|_{AB^*} = 0\,,\ \text{hence}\ B^* = \frac{2n + 1}{m}\,,$$

where m and n are natural numbers, and m divides into $2n + 1$.

$$P = 2A + x - 2 = (2n + 1)A - 1 = mAB^* - 1\,.$$

Since $B_e^* = B^* + 1$ it follows that $P_e = mAB_e^* - 1 = mAB^* + mA - 1 = P + mA$, and since $P_e = P + (x_e - x)$ it follows that $x_e = x + mA$.
Furthermore, $y_e = |y + (x_e - x)|_{2A} = |y + mA|_{2A} = |(m + 1)A - 1|_{2A}$.

(ii.) For $y = 2A - 1$:

$$x = (2n' + 2)A + 1\,,\ \text{hence}\ x = (2n - 2)A + 1\,,$$

where n is a natural number (recall from *The Braider*, Issue No. 25, pg. 564 that $x \geq 2 - A$).

$$|2A + x - 1|_{AB^*} = |2nA|_{AB^*} = 0\,,\ \text{hence}\ B^* = \frac{2n}{m}\,,$$

where m and n are natural numbers, and m divides into $2n$.

$$P = 2A + x - 2 = 2nA - 1 = mAB^* - 1\,.$$

Since $B_e^* = B^* + 1$ it follows that $P_e = mAB_e^* - 1 = mAB^* + mA - 1 = P + mA$, and since $P_e = P + (x_e - x)$ it follows that $x_e = x + mA$.
Furthermore, $y_e = |y + (x_e - x)|_{2A} = |y + mA|_{2A} = |mA - 1|_{2A}$.

Question on pg. 705.

The sequence of i-values is the complementary cyclic bight-number scheme and is directly related to the cyclic bight-number scheme, the sequence in which the string-run visits the bight-points on a bight-boundary.[†]

For $\Delta^* = 1$ and the Standing-End half-cycle from lower-left to upper-right, the successive odd-numbered half-cycles are being laid down adjacent to each other **below** the Standing-End half-cycle. For $\Delta^* = 1$, hence $|p|_b = b - 1$, we obtain $p = nb + b - 1 = (n + 1)b - 1$ where n is a whole number, or $p = n'b - 1$ where n' is a natural number.

[†] See *The Braider*, Issue No. 5, pg. 93.

An alternative proof may be obtained from the algorithm diagram: since $\Delta^* = 1$, it follows that $|(p-1)\Delta^*|_b = b-2$ (recall that $(p-1)\Delta^* + \Delta^* = b-1$)[†]. Hence $|p-1|_b = b-2$, and thus $p = (n+1)b-1$ where n is a whole number.

For $\Delta^* = b-1$ and the Standing-End half-cycle from lower-left to upper-right, the successive odd-numbered half-cycles are being laid down adjacent to each other **above** the Standing-End half-cycle. For $\Delta^* = b-1$, hence $|p|_b = 1$, we obtain $p = nb+1$ where n is a whole number (note, however, that for $n = 0$, hence for $p = 1$, no knot of practical use will be obtained).

An alternative proof may be obtained from the algorithm diagram: since $\Delta^* = b-1$, it follows that $|(p-1)\Delta^*|_b = 0$ (recall that $(p-1)\Delta^* + \Delta^* = b-1$)[†]. Hence $|(p-1)(b-1)|_b = 0$, and thus $p = nb+1$ where n is a whole number.

Nested Cylindrical Braids

Instead of two algorithm tables (one for the odd half-cycles and one for the even half-cycles) for a Semi-Perfect Regular Nested Cylindrical Braid as discussed in *The Braider*, Issue No. 29, pp. 671–682, some braiders might prefer to have two algorithm tables (one for the odd half-cycles and one for the even half-cycles) for each of its sub-components. This certainly makes reading of the half-cycle braiding algorithms easier. For example, in Example 5 on pp. 677–679 we can replace the two algorithm tables in Fig. 549 by the algorithm tables in Fig. 554, where the two upper algorithm tables are associated with the first sub-component (hence with the half-cycles 1 to 20), and the two lower algorithm tables are associated with the second sub-component (hence with the half-cycles 21 to 40).

The Pineapple Knot depicted in *The Braider*, Issue No. 14, Fig. 287, pg. 324 is a Compound Regular Nested Cylindrical Braid shown once again in Fig. 558. It is an interbraid of two components, each being a Perfect Regular Nested Knot.

The foundation knot (the first knot) comprises the half-cycles 1 to 16, and the second knot comprises the half-cycles 17 to 32. For the first knot $A = 2$, $x = 9$, $B^* = 4$, hence $P_{c_1} = 2A + x - 2 = 11$, and for the second knot $A = 2$, $x = 7$, $B^* = 4$, hence $P_{c_2} = 2A + x - 2 = 9$.

The first-return string-run of each component and the half-cycle pattern obtained from them is shown in Fig. 555. From the half-cycle pattern we can again assemble the two algorithm tables in Fig. 556 from which we can read the half-cycle braiding algorithms for each of the two components. These half-cycle braiding algorithms were given on pg. 324.

Instead of obtaining the half-cycle braiding algorithms from the two algorithm tables in Fig. 556, it may be preferred to obtain the half-cycle braiding algorithms of each component from its associated algorithm tables shown in Fig. 557. The upper two tables in Fig. 557 are associated with the foundation knot (the first component with the half-cycles 1 to 16), and the lower two tables in Fig. 557 are associated with the second knot (the component with the half-cycles 17 to 32).

[†] See *The Braider*, Issue No. 7, pg. 133: it follows from $a^* + b^* = b - 1$.

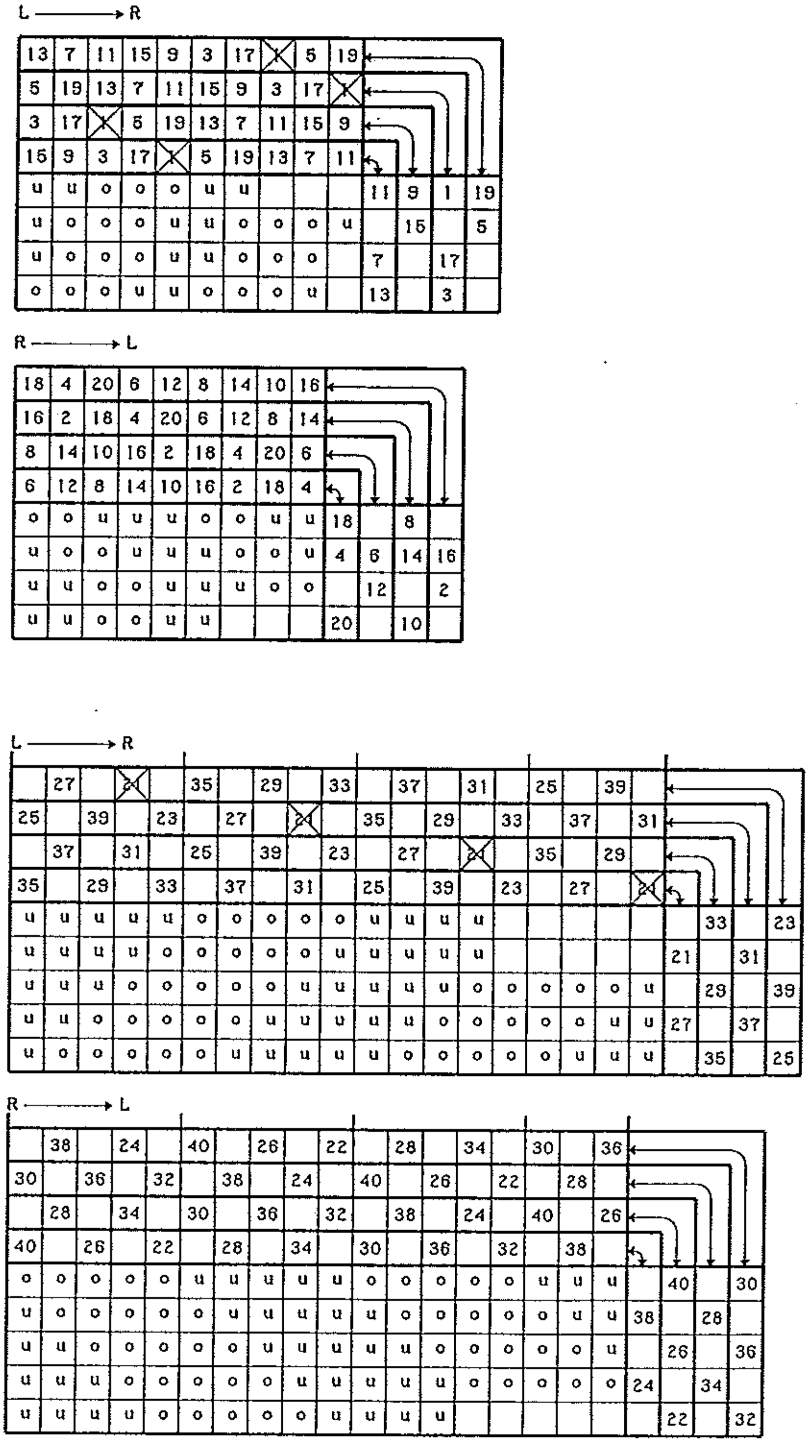

L → R

13	7	11	15	9	3	17	~~1~~	5	19				
5	19	13	7	11	15	9	3	17	~~1~~				
3	17	~~1~~	5	19	13	7	11	15	9				
15	9	3	17	~~1~~	5	19	13	7	11				
u	u	o	o	o	u	u				11	9	1	19
u	o	o	o	u	u	o	o	o	u		15		5
u	o	o	o	u	u	o	o	o		7		17	
o	o	o	u	u	o	o	o	u		13		3	

R → L

18	4	20	6	12	8	14	10	16				
16	2	18	4	20	6	12	8	14				
8	14	10	16	2	18	4	20	6				
6	12	8	14	10	16	2	18	4				
o	o	u	u	u	o	o	u	u	18		8	
u	o	o	u	u	u	o	o	u	4	6	14	16
u	u	o	o	u	u	u	o	o		12		2
u	u	o	o	u	u				20		10	

L → R

	27		~~21~~		35		29		33		37		31		25		39					
25		39		23		27		~~21~~		35		29		33		37		31				
	37		31		25		39		23		27		~~21~~		35		29					
35		29		33		37		31		25		39		23		27		~~21~~				
u	u	u	u	u	o	o	o	o	o	u	u	u	u							33		23
u	u	u	u	o	o	o	o	o	u	u	u	u	u						21		31	
u	u	u	o	o	o	o	o	u	u	u	u	u	o	o	o	o	o	u		29		39
u	u	o	o	o	o	o	u	u	u	u	u	o	o	o	o	o	u	u	27		37	
u	o	o	o	o	o	u	u	u	u	u	o	o	o	o	o	u	u	u		35		25

R → L

	38		24		40		26		22		28		34		30		36				
30		36		32		38		24		40		26		22		28					
	28		34		30		36		32		38		24		40		26				
40		26		22		28		34		30		36		32		38					
o	o	o	o	o	u	u	u	u	u	o	o	o	o	o	u	u	u		40		30
u	o	o	o	o	o	u	u	u	u	u	o	o	o	o	o	u	u	38		28	
u	u	o	o	o	o	o	u	u	u	u	u	o	o	o	o	o	u		26		36
u	u	u	o	o	o	o	o	u	u	u	u	u	o	o	o	o	o	24		34	
u	u	u	u	o	o	o	o	o	u	u	u	u							22		32

Fig. 554 — The algorithm tables of the sub-components in Example 5, pp. 677–679.

Since the bight-boundaries associated with one component are not associated with any other component, the algorithm tables of a component are easier to compile than the algorithm tables of a sub-component. Therefore compiling and working with algorithm tables of components as compared to compiling and working with algorithm tables of the overall braid offers greater advantages than the compiling and working with algorithm tables of sub-components as compared to compiling and working with algorithm tables of the overall component.

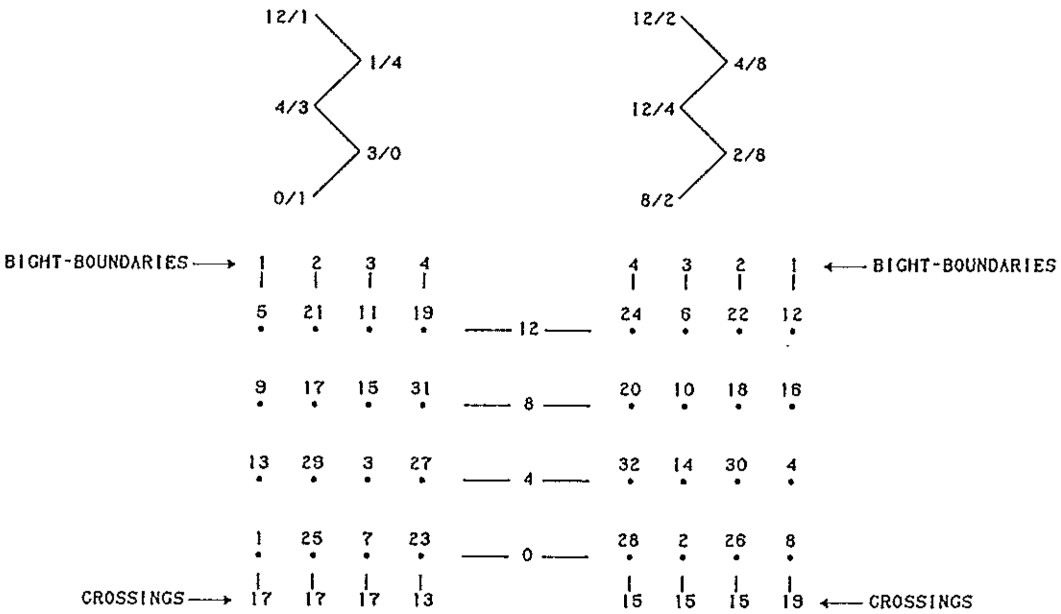

Fig. 555 — First-return string-runs and half-cycle pattern of the knot on pg. 324 and in Fig. 558.

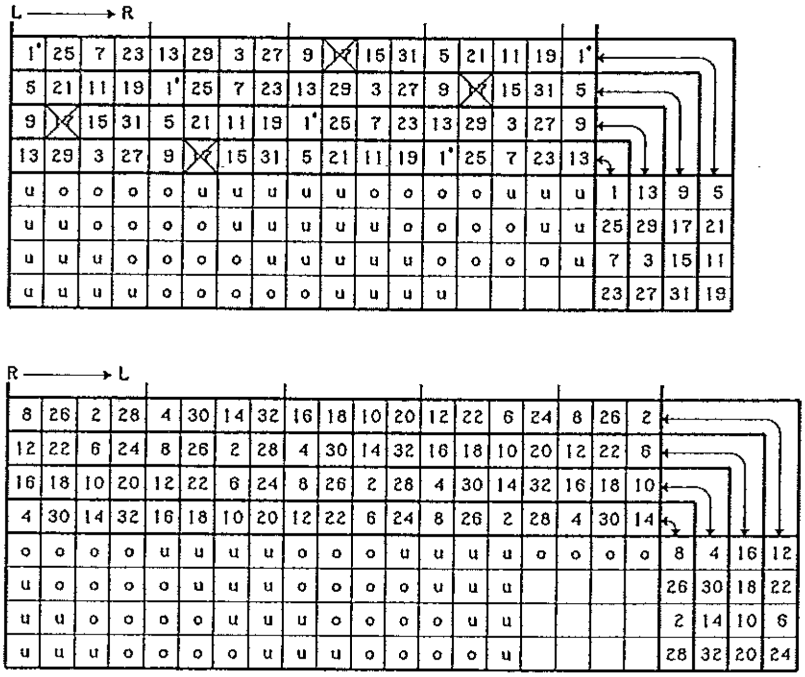

L → R

1•	25	7	23	13	29	3	27	9	~~17~~	15	31	5	21	11	19	1•				
5	21	11	19	1•	25	7	23	13	29	3	27	9	~~17~~	15	31	5				
9	~~17~~	15	31	5	21	11	19	1•	25	7	23	13	29	3	27	9				
13	29	3	27	9	~~17~~	15	31	5	21	11	19	1•	25	7	23	13				
u	o	o	o	o	u	u	u	u	u	o	o	o	o	u	u	u	1	13	9	5
u	u	o	o	o	o	u	u	u	u	u	o	o	o	o	u	u	25	29	17	21
u	u	u	o	o	o	o	u	u	u	u	u	o	o	o	o	u	7	3	15	11
u	u	u	u	o	o	o	o	o	u	u	u	u					23	27	31	19

R → L

8	26	2	28	4	30	14	32	16	18	10	20	12	22	6	24	8	26	2				
12	22	6	24	8	26	2	28	4	30	14	32	16	18	10	20	12	22	6				
16	18	10	20	12	22	6	24	8	26	2	28	4	30	14	32	16	18	10				
4	30	14	32	16	18	10	20	12	22	6	24	8	26	2	28	4	30	14				
o	o	o	o	u	u	u	u	o	o	o	u	u	u	u	o	o	o	o	8	4	16	12
u	o	o	o	o	u	u	u	o	o	o	o	u	u	u					26	30	18	22
u	u	o	o	o	o	u	u	u	o	o	o	o	u	u					2	14	10	6
u	u	u	o	o	o	o	u	u	u	o	o	o	o	u					28	32	20	24

Fig. 556 — Algorithm tables of the knot on pg. 324 and in Fig. 558.

Note that the left bight-boundaries 1 & 3 and the right bight-boundaries 1 & 3 are associated with the string-run of the foundation knot (the first component), and that the left bight-boundaries 2 & 4 and the right bight-boundaries 2 & 4 are associated with the second component.

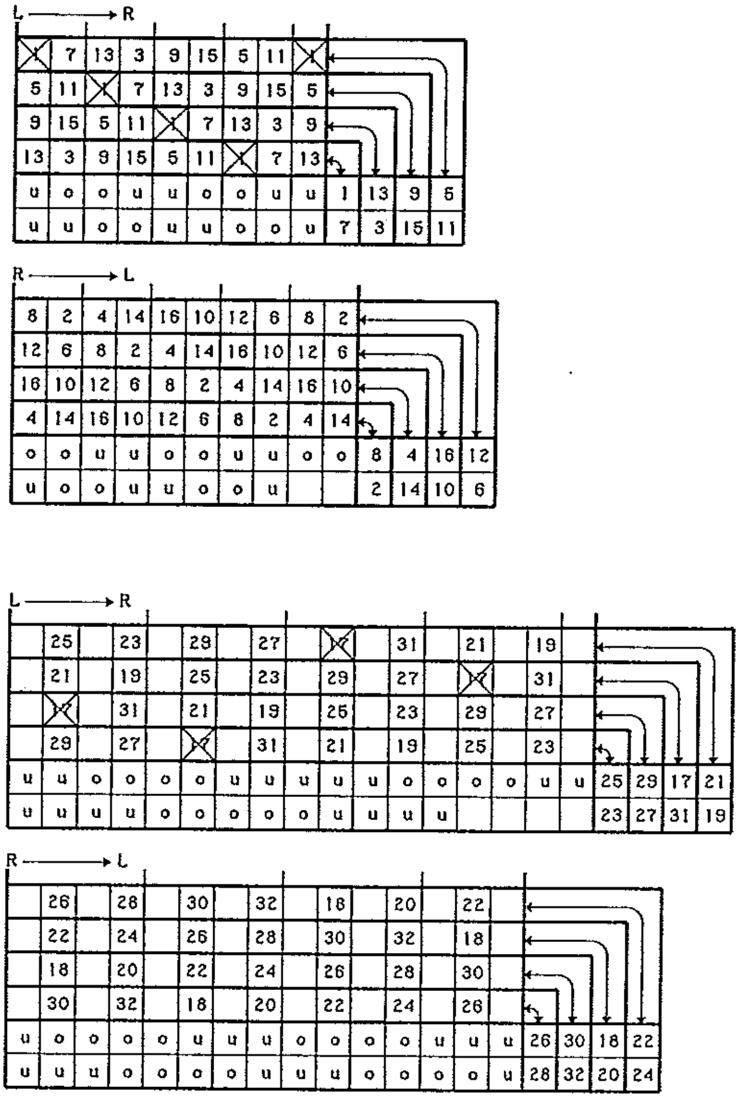

L → R

~~1~~	7	13	3	9	15	5	11	~~1~~				
5	11	~~1~~	7	13	3	9	15	5				
9	15	5	11	~~1~~	7	13	3	9				
13	3	9	15	5	11	~~1~~	7	13				
u	o	o	u	u	o	o	u	u	1	13	9	5
u	u	o	o	u	u	o	o	u	7	3	15	11

R → L

8	2	4	14	16	10	12	6	8	2				
12	6	8	2	4	14	16	10	12	6				
16	10	12	6	8	2	4	14	16	10				
4	14	16	10	12	6	8	2	4	14				
o	o	u	u	o	o	u	u	o	o	8	4	16	12
u	o	o	u	u	o	o	u			2	14	10	6

L → R

	25		23		29		27		~~17~~		31		21		19					
	21		19		25		23		29		27		~~17~~		31					
	~~17~~		31		21		19		25		23		29		27					
	29		27		~~17~~		31		21		19		25		23					
u	u	o	o	o	o	u	u	u	u	u	o	o	o	o	u	u	25	29	17	21
u	u	u	u	o	o	o	o	o	u	u	u	u					23	27	31	19

R → L

	26		28		30		32		18		20		22					
	22		24		26		28		30		32		18					
	18		20		22		24		26		28		30					
	30		32		18		20		22		24		26					
u	o	o	o	o	u	u	u	o	o	o	o	u	u	u	26	30	18	22
u	u	u	o	o	o	o	u	u	u	o	o	o	o	u	28	32	20	24

Fig. 557 — Algorithm tables for the components of the knot on pg. 324 and in Fig. 558.

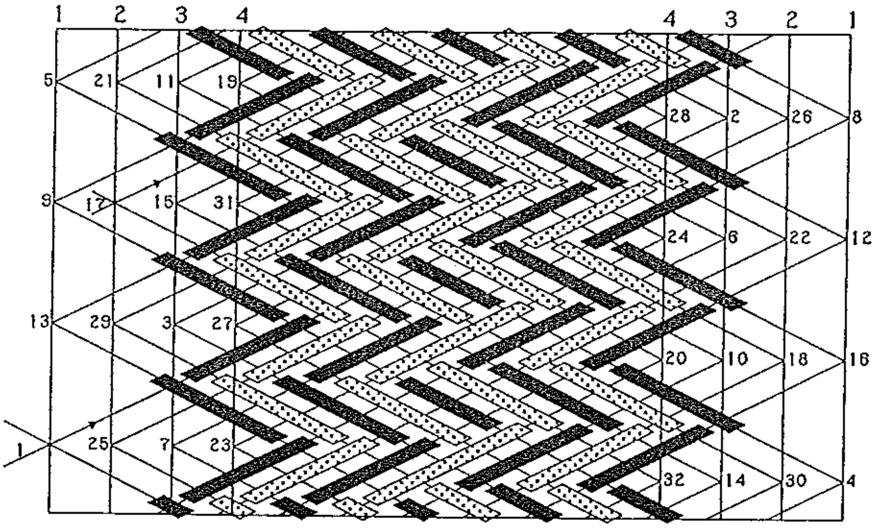

Fig. 558 — The Compound Regular Nested Cylindrical Braid on pg. 324.

Let's revisit the Regular Nested Cylindrical Braids in Issues No. 16, pg. 367, No. 13, pg. 298, and No. 12, pg. 272 of *The Braider*, and see what their associated algorithm tables are.

The Braider, Issue No. 16, pg. 367:

The uppermost Glen Vandy Knot on pg. 367 is an interbraid of the knots X and Y in Fig. 559. Both these knots are column-coded Regular Knots with $p/b = 4/5$, and with Euclid's algorithm, the path-formula, and the path in the RKT are as shown in Fig. 559. From the path in the RKT follows that $\Delta^* = 1$, and hence the algorithm diagram of knot X as the foundation knot is as shown in Fig. 559. Instead of its algorithm diagram we may prefer to use its depicted algorithm tables. Knot Y is the second knot, which is to be interbraided with knot X, and hence its algorithm diagram is as shown in Fig. 559. Again we may prefer to use its depicted algorithm tables. From the algorithm diagrams, or from the algorithm tables, we read and compile the uppermost half-cycle braiding algorithms shown in Fig. 313 on pg. 367.

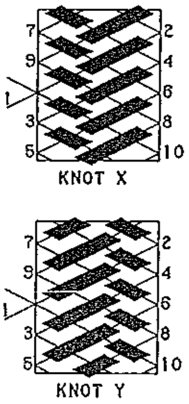

0	5	4
1	4	5
4	1	4

[0;1,3,1]

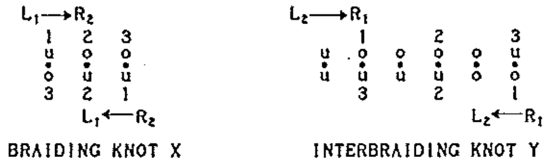

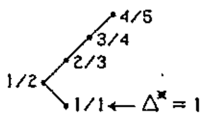

$L_1 \rightarrow R_2$

1	2	3	ODD HALF-CYCLES
u	o	o	

$R_2 \rightarrow L_1$

1	2	3	EVEN HALF-CYCLES
u	u	o	

BRAIDING KNOT X

$L_2 \rightarrow R_1$

	1		2		3	ODD HALF-CYCLES
u	o	o	o	o	u	

$R_1 \rightarrow L_2$

1		2		3		EVEN HALF-CYCLES
o	o	u	u	u	u	

INTERBRAIDING KNOT Y

Fig. 559 — The two interbraided Regular Knots X and Y.

The general string-run specification for this Glen Vandy Knot is $(2/6/2)\{12/21\}B$, where $B = 8n + 2$ or $B = 8n + 6$ with n a whole number.

For $B = 8n + 2$ the interbraided Regular Knots each have $p/b = 4/(4n + 1)$, while for $B = 8n + 6$ the interbraided Regular Knots each have $p/b = 4/(4n + 3)$.

0	4n+1	4
n	4	4n+1
4	1	4

[0;n,3,1]

0	4n+3	4
n	4	4n+3
1	3	4
3	1	3

[0;n,1,2,1]

$L_1 \rightarrow R_2$

n	2n	3n	ODD HALF-CYCLES
u	o	o	

$R_2 \rightarrow L_1$

n	2n	3n	EVEN HALF-CYCLES
u	u	o	

BRAIDING KNOT X WITH b=4n+1

$L_2 \rightarrow R_1$

	n		2n		3n	ODD HALF-CYCLES
u	o	o	o	o	u	

$R_1 \rightarrow L_2$

n		2n		3n		EVEN HALF-CYCLES
o	o	u	u	u	u	

INTERBRAIDING KNOT Y WITH b=4n+1

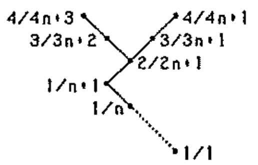

$L_1 \rightarrow R_2$

3n+2	2n+1	n	ODD HALF-CYCLES
u	o	o	

$R_2 \rightarrow L_1$

3n+2	2n+1	n	EVEN HALF-CYCLES
u	u	o	

BRAIDING KNOT X WITH b=4n+3

$L_1 \rightarrow R_2$

	3n+2		2n+1		n	ODD HALF-CYCLES
u	o	o	o	o	u	

$R_2 \rightarrow L_1$

3n+2		2n+1		n		EVEN HALF-CYCLES
o	o	u	u	u	u	

INTERBRAIDING KNOT Y WITH b=4n+3

Fig. 560 — The interbraided Regular Knots for $B = 8n + 2$ and for $B = 8n + 6$.

In Fig. 560 are shown Euclid's algorithm, path-formula, and path in the RKT for $p/b = 4/(4n+1)$ and for $p/b = 4/(4n+3)$. From the paths in the RKT it follows that $\Delta^* = n$ for $p/b = 4/(4n+1)$, and $\Delta^* = 3n+2$ for $p/b = 4/(4n+3)$.

The algorithm tables associated with each interbraided pair of Regular Knots can now readily be drawn up as shown in Fig. 560.

The Braider, Issue No. 13, pg. 298 :

This Regular Nested Cylindrical Braid is an interbraid of three identical over–under coded Regular Knots, each with $p/b = 8/5$. Euclid's algorithm, path-formula, and the path in the RKT for $p/b = 8/5$ are shown in Fig. 561.

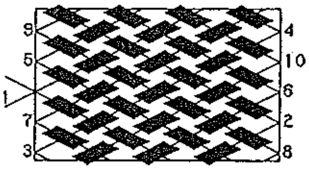

$$\begin{array}{c|c|c|}
1 & 5 & 8 \\
1 & 3 & 5 \\
1 & 2 & 3 \\
2 & 1 & 2
\end{array}$$

$$[1;1,1,1,1]$$

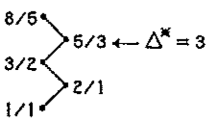

$L_1 \longrightarrow R_3$

3	1	4	2	0	3	1	ODD HALF-CYCLES
u	o	u	o	u	o	u	

$R_3 \longrightarrow L_1$

3	1	4	2	0	3	1	EVEN HALF-CYCLES
o	u	o	u	o	u	o	

$L_2 \longrightarrow R_2$

	3		1		4		2		0		3		1	ODD HALF-CYCLES
u	u	o	o	u	u	o	o	u	u	u	o	o	u	

$R_2 \longrightarrow L_2$

3		1		4		2		0		3		1		EVEN HALF-CYCLES
o	o	u	u	o	o	u	u	o	o	u	o	o	u	

$L_3 \longrightarrow R_1$

		3			1			4			2			0			3			1	ODD HALF-CYCLES
u	u	u	o	o	o	u	u	u	u	o	o	o	u	u	u	u	o	o	o	u	

$R_1 \longrightarrow L_3$

3			1			4			2			0			3			1			EVEN HALF-CYCLES
o	o	o	u	u	u	o	o	o	u	u	o	o	o	u	u	o	o	o	u	u	

Fig. 561 — The three interbraided over–under coded Regular Knots $p/b = 5/8$.

From the path in the RKT it follows that $\Delta^* = 3$, and thus we can now draw up the algorithm tables.

In Fig. 561 the algorithm tables for the foundation knot (the first knot) are at the upper-right, the algorithm tables for the second knot are at the lower-left, and the algorithm tables for the third knot are at the lower-right. We can read and compile from the algorithm tables the half-cycle braiding algorithms shown on pg. 298.

$(22/20/22)\{132/312\}B$, where $B = 24n+3$ or $B = 24n+9$ or $B = 24n+15$ or $B = 24n+21$ with n a whole number, is the general string-run specification for this Regular Nested Knot. The respective p/b-values of the three identical interbraided over–under coded Regular Knots are therefore $8/(8n+1)$ or $8/(8n+3)$ or $8/(8n+5)$ or $8/(8n+7)$. Euclid's algorithms for these p/b-values, path-fomulae, and paths in the RKT are shown in Fig. 562. From the paths in the RKT it follows that $\Delta^* = n$ for $p/b = 8/(8n+1)$, $\Delta^* = 3n+1$ for $p/b = 8/(8n+3)$, $\Delta^* = 5n+3$ for $p/b = 8/(8n+5)$, and $\Delta^* = 7n+6$ for $p/b = 8/(8n+7)$. This enables us to draw up the algorithm tables.

The upper two algorithm tables are associated with the foundation knot (the first knot), the central two algorithm tables with the second knot, and the lower two algorithm tables with the third knot.

The Braider, Issue No. 12, pg. 272 :

This Regular Nested Cylindrical Braid is an interbraid of two identical over–under coded Regular Knots X with $p/b = 8/5$ and one over–under coded Regular Knot Y with $p/b = 6/5$. Euclid's algorithms, path-formulae, and the paths in the RKT for $p/b = 8/5$ and $p/b = 6/5$ are shown in Fig. 563. From the paths in the RKT it follows that $\Delta^* = 3$ for $p/b = 8/5$, and $\Delta^* = 4$ for $p/b = 6/5$. This enables us to draw up the algorithm tables.

0	8n+1	8
n	8	8n+1
8	1	8

[0;n,7,1]

0	8n+3	8
n	8	8n+3
2	3	8
1	2	3
2	1	2

[0;n,2,1,1,1]

0	8n+5	8
n	8	8n+5
1	5	8
1	3	5
1	2	3
2	1	2

[0;n,1,1,1,1,1]

0	8n+7	8
n	8	8n+7
1	7	8
7	1	7

[0;n,1,6,1]

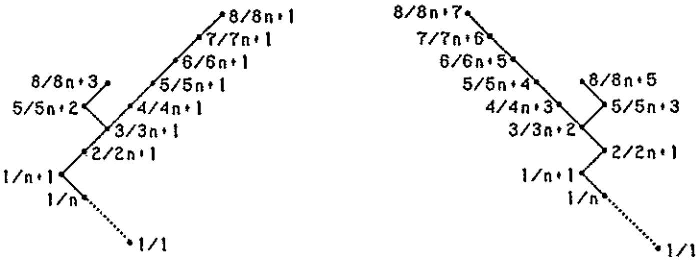

$L_1 \rightarrow R_3$

n	2n	3n	4n	5n	6n	7n	b=8n+1	ODD HALF-CYCLES
3n+1	6n+2	n	4n+1	7n+2	2n	5n+1	b=8n+3	
5n+3	2n+1	7n+4	4n+2	n	6n+3	3n+1	b=8n+5	
7n+6	6n+5	5n+4	4n+3	3n+2	2n+1	n	b=8n+7	
u	o	u	o	u	o	u		

$R_3 \rightarrow L_1$

n	2n	3n	4n	5n	6n	7n	b=8n+1	EVEN HALF-CYCLES
3n+1	6n+2	n	4n+1	7n+2	2n	5n+1	b=8n+3	
5n+3	2n+1	7n+4	4n+2	n	6n+3	3n+1	b=8n+5	
7n+6	6n+5	5n+4	4n+3	3n+2	2n+1	n	b=8n+7	
o	u	o	u	o	u	o		

$L_2 \rightarrow R_2$

	n		2n		3n		4n		5n		6n		7n	b=8n+1	ODD HALF-CYCLES
	3n+1		6n+2		n		4n+1		7n+2		2n		5n+1	b=8n+3	
	5n+3		2n+1		7n+4		4n+2		n		6n+3		n+1	b=8n+5	
	7n+6		6n+5		5n+4		4n+3		3n+2		2n+1		n	b=8n+7	
u	u	o	o	u	u	o	o	u	u	u	o	o	u		

$R_2 \rightarrow L_2$

n		2n		3n		4n		5n		6n		7n		b=8n+1	EVEN HALF-CYCLES
3n+1		6n+2		n		4n+1		7n+2		2n		5n+1		b=8n+3	
5n+3		2n+1		7n+4		4n+2		n		6n+3		n+1		b=8n+5	
7n+6		6n+5		5n+4		4n+3		3n+2		2n+1		n		b=8n+7	
o	o	u	u	o	o	u	u	o	o	u	o	o	u		

$L_3 \rightarrow R_1$

		n			2n			3n			4n			5n			6n			7n	b=8n+1	ODD HALF-CYCLES
		3n+1			6n+2			n			4n+1			7n+2			2n			5n+1	b=8n+3	
		5n+3			2n+1			7n+4			4n+2			n			6n+3			n+1	b=8n+5	
		7n+6			6n+5			5n+4			4n+3			3n+2			2n+1			n	b=8n+7	
u	u	u	o	o	o	u	u	u	u	o	o	o	u	u	u	u	o	o	o	u		

$R_1 \rightarrow L_3$

n			2n			3n			4n			5n			6n			7n			b=8n+1	EVEN HALF-CYCLES
3n+1			6n+2			n			4n+1			7n+2			2n			5n+1			b=8n+3	
5n+3			2n+1			7n+4			4n+2			n			6n+3			n+1			b=8n+5	
7n+6			6n+5			5n+4			4n+3			3n+2			2n+1			n			b=8n+7	
o	o	o	u	u	u	o	o	o	u	u	o	o	o	u	u	o	o	o	u	u		

Fig. 562 — The interbraided over–under coded Regular Knots for $B = 24n + 3$, $B = 24n + 9$, $B = 24n + 15$, and $B = 24n + 21$.

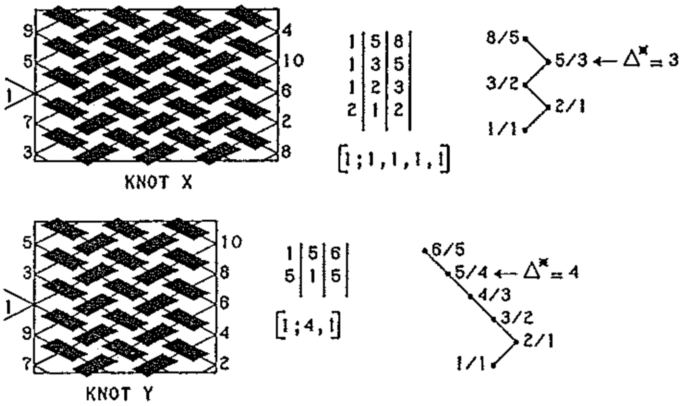

$L_1 \rightarrow R_2$

3	1	4	2	0	3	1	ODD HALF-CYCLES
u	o	u	o	u	o	u	

$R_2 \rightarrow L_1$

3	1	4	2	0	3	1	EVEN HALF-CYCLES
o	u	o	u	o	u	o	

$L_2 \rightarrow R_1$

	3		1		4		2		0		3		1	ODD HALF-CYCLES
u	u	o	o	u	u	u	o	o	u	u	o	o	u	

$R_1 \rightarrow L_2$

3		1		4		2		0		3		1		EVEN HALF-CYCLES
o	o	u	u	o	o	u	o	o	u	u	o	o	u	

$L_3 \rightarrow R_3$

		4			3			2			1			0			ODD HALF-CYCLES
u	u	u	o	o	o	u	o	u	o	u	o	o	o	u	u	u	

$R_3 \rightarrow L_3$

		4			3			2			1			0			EVEN HALF-CYCLES
u	u	o	o	o	u	u	o	o	o	u	u	o	o	o	u	u	

Fig. 563 — The three interbraided over–under coded Regular Knots $p/b = 8/5$, $p/b = 8/5$, and $p/b = 6/5$.

In Fig. 563 the upper-right two algorithm tables are associated with the over–under coded foundation knot $p/b = 8/5$, the lower-left two algorithm tables are associated with the second $p/b = 8/5$ over–under coded Regular Knot, and the lower-right two algorithm tables are associated with the third over–under coded $p/b = 6/5$ Regular Knot. From the algorithm tables we can read and compile the half-cycle braiding algorithms shown on pg. 272.

$(22/18/22)\{132/231\}B$, where $B = 18m + 3$ or $B = 18m + 15$ with m a whole number, is the general string-run specification for this Regular Nested Knot. The respective p/b-values of the three interbraided over–under coded Regular Knots are therefore $8/(6m+1)$, $8/(6m+1)$, and $6/(6m+1)$ or $8/(6m+5)$, $8/(6m+5)$, and $6/(6m+5)$. For these p/b-values Euclid's algorithms, path-fomulae, and paths in the RKT are shown in Fig. 564.

$n = \frac{6m+1-|6m+1|_8}{8}$ for $b = 6m+1$, then from the paths in the RKT it follows that:
$\Delta^* = n$ for $p/b = 8/(6m+1) = 8/(8n+1)$,
$\Delta^* = 3n+1$ for $p/b = 8/(6m+1) = 8/(8n+3)$,
$\Delta^* = 5n+3$ for $p/b = 8/(6m+1) = 8/(8n+5)$,
$\Delta^* = 7n+6$ for $p/b = 8/(6m+1) = 8/(8n+7)$,
$n = \frac{6m+5-|6m+5|_8}{8}$ for $b = 6m+5$, then from the paths in the RKT it follows that:
$\Delta^* = n$ for $p/b = 8/(6m+5) = 8/(8n+1)$,
$\Delta^* = 3n+1$ for $p/b = 8/(6m+5) = 8/(8n+3)$,
$\Delta^* = 5n+3$ for $p/b = 8/(6m+5) = 8/(8n+5)$,
$\Delta^* = 7n+6$ for $p/b = 8/(6m+5) = 8/(8n+7)$,

Furthermore it follows from the paths in the RKT that:
$\Delta^* = m$ for $p/b = 6/(6m+1)$,
$\Delta^* = 5m+4$ for $p/b = 6/(6m+5)$.

This enables us to draw up the algorithm tables.

The upper two algorithm tables are associated with the foundation knot (the first knot), the central two algorithm tables with the second knot, and the lower two algorithm tables with the third knot.

0	8n+1	8
n	8	8n+1
8	1	8

[0;n,7,1]

0	8n+3	8
n	8	8n+3
2	3	8
1	2	3
2	1	2

[0;n,2,1,1,1]

0	8n+5	8
n	8	8n+5
1	5	8
1	3	5
1	2	3
2	1	2

[0;n,1,1,1,1,1]

0	8n+7	8
n	8	8n+7
1	7	8
7	1	7

[0;n,1,6,1]

0	6m+1	6
m	6	6m+1
6	1	6

[0;m,5,1]

0	6m+5	6
m	6	6m+5
1	5	6
5	1	5

[0;m,1,4,1]

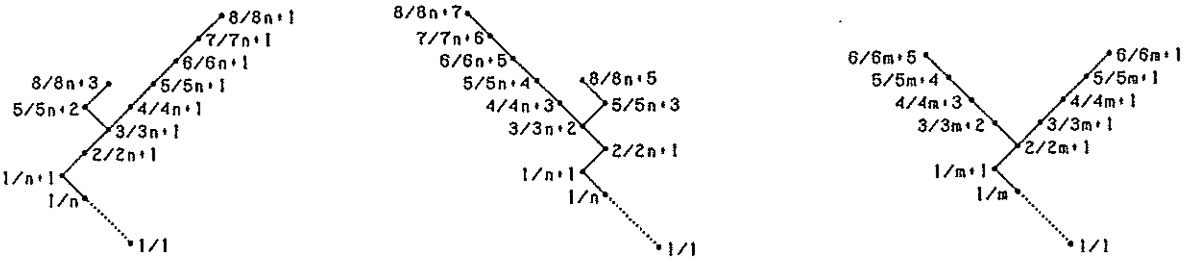

L$_1$ → R$_2$

n	2n	3n	4n	5n	6n	7n	b=8n+1	ODD HALF-CYCLES
3n+1	6n+2	n	4n+1	7n+2	2n	5n+1	b=8n+3	
5n+3	2n+1	7n+4	4n+2	n	6n+3	3n+1	b=8n+5	
7n+6	6n+5	5n+4	4n+3	3n+2	2n+1	n	b=8n+7	
u	o	u	o	u	.o	u		

R$_2$ → L$_1$

n	2n	3n	4n	5n	6n	7n	b=8n+1	EVEN HALF-CYCLES
3n+1	6n+2	n	4n+1	7n+2	2n	5n+1	b=8n+3	
5n+3	2n+1	7n+4	4n+2	n	6n+3	3n+1	b=8n+5	
7n+6	6n+5	5n+4	4n+3	3n+2	2n+1	n	b=8n+7	
o	u	o	u	o	u	o		

FOR $b' = 6m+1 \rightarrow n = \frac{6m+1-|6m+1|_8}{8} \rightarrow b = 8n+|6m+1|_8$

FOR $b' = 6m+5 \rightarrow n = \frac{6m+5-|6m+5|_8}{8} \rightarrow b = 8n+|6m+5|_8$

L$_2$ → R$_1$

	n		2n		3n		4n		5n		6n		7n	b=8n+1	ODD HALF-CYCLES
	3n+1		6n+2		n		4n+1		7n+2		2n		5n+1	b=8n+3	
	5n+3		2n+1		7n+4		4n+2		n		6n+3		n+1	b=8n+5	
	7n+6		6n+5		5n+4		4n+3		3n+2		2n+1		n	b=8n+7	
u	u	o	o	u	u	u	o	o	u	u	o	o	u		

R$_1$ → L$_2$

n		2n		3n		4n		5n		6n		7n		b=8n+1	EVEN HALF-CYCLES
3n+1		6n+2		n		4n+1		7n+2		2n		5n+1		b=8n+3	
5n+3		2n+1		7n+4		4n+2		n		6n+3		n+1		b=8n+5	
7n+6		6n+5		5n+4		4n+3		3n+2		2n+1		n		b=8n+7	
o	o	u	u	o	o	u	o	o	u	u	o	o	u		

L$_3$ → R$_3$

		m			2m			3m			4m			5m			b'=6m+1	ODD HALF-CYCLES
		5m+4			4m+3			3m+2			2m+1			m			b'=6m+5	
u	u	u	o	o	o	u	o	u	o	u	o	o	o	u	u	u		

R$_3$ → L$_3$

		m			2m			3m			4m			5m			b'=6m+1	EVEN HALF-CYCLES
		5m+4			4m+3			3m+2			2m+1			m			b'=6m+5	
u	u	o	o	o	u	u	o	o	o	u	u	o	o	o	u	u		

Fig. 564 — The interbraided over–under coded Regular Knots for $B = 18m + 3$ and $B = 18m + 15$.

Pitfalls in knot design

The Pampas Button, much in vogue in the gaucho regions of the Argentine Pampas according to Bruce Grant and described in his *Encyclopedia of Rawhide and Leather Braiding* on pp. 438–439, suffers not only from a similar central lopsided design as the small Pampas knot we discussed in *The Braider*, Issue No. 30, pp. 704–706, but has furthermore two dissimilar end-sections which, due to the small difference in their lengths, cannot be regarded as being satisfactory for an orientation purpose. The grid-diagram of this Pampas Button is shown in Fig. 565.

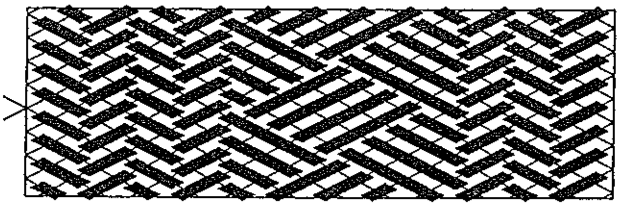

Fig. 565 — The Pampas Button in the *Encyclopedia of Rawhide and Leather Braiding.*

This Pampas Button with $p/b = 25/8$ is most likely the result of using "the running method of making woven knots", or what may be called pattern-braiding, in the design of knots (note that we have also here, as with the small Pampas knot, a typical case[†] of $p = nb + 1$ with $n = 3$).

The lopsided coding of the central section of the Pampas Button, shown by the leftmost diagram in Fig. 566, can readily be made symmetrical in two ways as shown by the central and rightmost diagrams in Fig. 566.

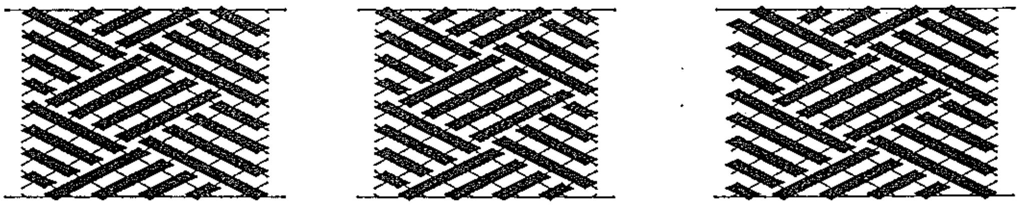

Fig. 566 — The coding of the central section of the Pampas Button and alternative modified coding arrangements.

Since the coding arrangements of the central section has a periodicity of 4 bights, we require b to be a multiple of 4. For the modified coding of the central section there are either 9 crossings (central coding arrangement in Fig. 566) or 11 crossings (rightmost coding arrangement in Fig. 566) on a half-cycle section, and hence if we make the overall knot symmetrical then the total number of crossings on a half-cycle will be odd and thus p will be even.[‡] Since $b = 4n$, where n is a natural number, hence even, and since p is even with each one of the modified central coding arrangements, it follows that a single string knot is not possible (g.c.d. $(p, b) > 1$). Thus in order to obtain a single string knot we must modify the coding of the central section further.

[†] Refer to *The Braider*, Issue No. 30, pg. 705.

[‡] The total number of crossings on a half-cycle is equal to number of crossings on a half-cycle section in the central-section coding arrangement plus twice the number of crossings on a half-cycle section in an end-section coding arrangement. The number of parts p is equal to the total number of crossings on a half-cycle plus 1.

Instead of using the central coding arrangement with a periodicity of 4 bights, we can use a similar coding arrangement with a periodicity of 3 bights. An example of such a similar arrangement is depicted in Fig. 567. We have furthermore assured that the coding of the overall knot will be symmetrical by using suitably coded end-sections.

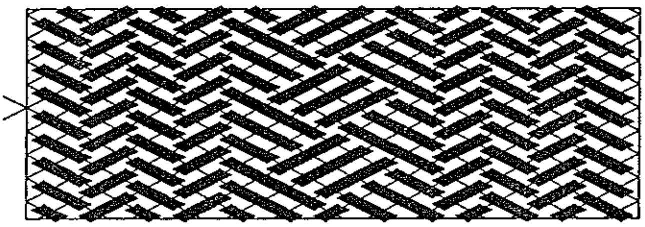

Fig. 567 — A single string Pampas type knot with a periodicity of 3 bights.

The algorithm tables of this knot are presented in Fig. 568. In these tables the *i*-values are above the horizontal thick line and the half-cycle numbers are to the right of the vertical thick line in line with their associated half-cycle coding sequences.

L → R BRAIDING UPWARDS

1	2	3	4	5	6	7	8	0	1	2	3	4	5	6	7	8	0	1	2	3	4	5	6	7			
u	u	o	o	u	u	o	o	u	u	u	o	o	o	u	u	u	o	o	u	u	o	o	u	u	1	7	13
u	u	o	o	u	u	o	o	u	u	u	u	o	o	o	u	u	o	o	u	u	o	o	u	u	3	9	15
u	u	o	o	u	u	o	o	u	u	o	o	o	u	u	u	u	o	o	u	u	o	o	u	u	5	11	17

R → L BRAIDING UPWARDS

1	2	3	4	5	6	7	8	0	1	2	3	4	5	6	7	8	0	1	2	3	4	5	6	7			
o	o	u	u	o	o	u	u	o	o	u	u	u	o	o	o	o	u	u	o	o	u	u	o	o	2	8	14
o	o	u	u	o	o	u	u	o	o	o	u	u	u	o	o	o	u	u	o	o	u	u	o	o	4	10	16
o	o	u	u	o	o	u	u	o	o	o	o	u	u	u	o	o	u	u	o	o	u	u	o	o	6	12	18

L → R BRAIDING DOWNWARDS

1	2	3	4	5	6	7	8	0	1	2	3	4	5	6	7	8	0	1	2	3	4	5	6	7			
o	o	u	u	o	o	u	u	o	o	u	u	u	o	o	o	o	u	u	o	o	u	u	o	o	1	7	13
o	o	u	u	o	o	u	u	o	o	o	u	u	u	o	o	o	u	u	o	o	u	u	o	o	3	9	15
o	o	u	u	o	o	u	u	o	o	o	o	u	u	u	o	o	u	u	o	o	u	u	o	o	5	11	17

R → L BRAIDING DOWNWARDS

1	2	3	4	5	6	7	8	0	1	2	3	4	5	6	7	8	0	1	2	3	4	5	6	7			
u	u	o	o	u	u	o	o	u	u	u	u	o	o	o	u	u	o	o	u	u	o	o	u	u	2	8	14
u	u	o	o	u	u	o	o	u	u	o	o	o	u	u	u	u	o	o	u	u	o	o	u	u	4	10	16
u	u	o	o	u	u	o	o	u	u	u	o	o	o	u	u	u	o	o	u	u	o	o	u	u	6	12	18

2	9	26
1	8	9
8	1	8

[2;1,7,1]

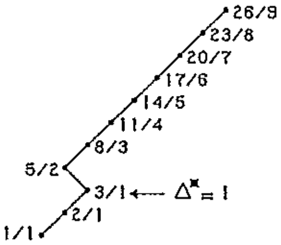

Fig. 568 — The algorithm tables of the Pampas type knot in Fig. 567.

From these algorithm tables we read the following half-cycle braiding algorithms:

1. Free run.
2. $o - u$.
3. $u - o$.
4. $3o - 2u$.
5. $3u - 2o$.
6. $5o - 2u - o$.
7. $5u - 2o - u$.
8. $2o - u - 2o - 4u - 2o$.
9. $2u - o - 4u - 2o - 2u$.
10. $2o - 2u - 3o - 4u - 2o - u$.
11. $2u - 2o - 2u - 5o - 2u - o$.
12. $2o - 2u - 5o - 4u - 2o - 2u$.
13. $2u - 2o - 4u - 5o - 2u - 2o$.
14. $2o - 2u - 4o - 3u - 2o - 2u - 2o - 2u - o$.
15. $2u - 2o - 6u - 5o - 2u - 2o - u$.
16. $2o - 2u - 2o - u - 3o - 3u - 2o - 2u - 2o - 2u - 2o$.
17. $2u - 2o - 2u - o - 2u - 3o - 3u - 2o - 2u - 2o - 2u$.
18. $2o - 2u - 2o - 2u - 4o - 3u - 2o - 2u - 2o - 2u - 2o$.

We would normally braid the knot by starting at the centre of the string-length, hence braid half the string-length upwards and the other half downwards. Thus starting at the centre of the string-length, we would braid the half-cycles 1–9 upwards, then continue with braiding the Standing End and hence the remaining half-cycles downwards:

10. $2u - 2o - 2u - 5o - 2u - o$.
11. $2o - 2u - 4o - 3u - 2o - u$.
12. $2u - 2o - 4u - 5o - 2u - 2o$.
13. $2o - 2u - 3o - 3u - o - 2u - 2o - 2u$.
14. $2u - 2o - 6u - 5o - 2u - 2o - u$.
15. $2o - 2u - 5o - 3u - o - 2u - 2o - 2u - o$.
16. $2u - 2o - 2u - o - 2u - 3o - 3u - 2o - 2u - 2o - 2u$.
17. $2o - 2u - 2o - u - 4o - 3u - o - 2u - 2o - 2u - 2o$.
18. $2u - 2o - 2u - 2o - 3u - 3o - 3u - 2o - 2u - 2o - 2u$.

In designing long knots we often 'couple' some shorter knots with symmetric coding-patterns together in series. For example, we could 'couple' in series with one of the previously discussed modified 4-bight periodic Pampas Buttons the *Three section Fan Knot or Botón Oriental* described by Bruce Grant in his *Encyclopedia of Rawhide and Leather Braiding*, pp. 430–431 and depicted below in Fig. 569.

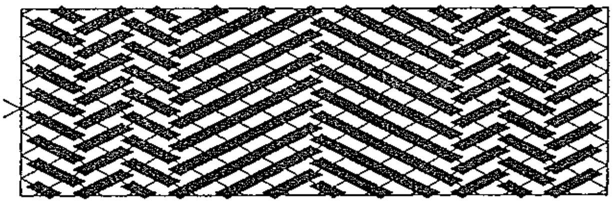

Fig. 569 — The Three section Fan Knot or Botón Oriental.

The resulting knot has then two end-sections and three sections between these end-sections. The central modified section of the Pampas Button and the central fan section of the Three section Fan Knot supply orientation to the knot and in order to accentuate this we should ensure that the central section of the overall knot (the section between the modified central section of the Pampas Button and the central section of the Three section Fan Knot) has some symmetric coding-pattern relative to its centre while the two end sections should have a balanced coding-pattern with respect to the overall knot. An easy way to achieve the latter is to make the two end sections symmetric with respect to each other, hence we could choose two-pass Headhunter's-coded end sections as those found in the Three section Fan Knot and Pampas Button, or two-pass Gaucho-coded end sections as the one found in the Pampas Button. Whichever choice we make, the combined number of intersection-columns in the two end sections, the modified central Pampas Button section and the central fan section is odd (since the number of intersection-columns is even in each end section and in the central fan section, but odd only in the modified central Pampas Button section). Thus for a single string knot the number of intersection-columns in the section between the modified central section of the Pampas Button and the central section of the Three section Fan Knot must be odd (the number of parts in the overall knot must be odd since the number of bights has to be a multiple of 4 due to the 4-bight periodicity of the modified central Pampas Button section). Hence for the central section of the overall knot we cannot use the two-pass Gaucho-coded section resulting from the two 'coupled' two-pass Headhunter's-coded end sections of the Pampas Button and the Three section Fan Knot. We must, for example, use instead a two-pass Headhunter's-coded section in which the central two intersection-columns are replaced by three intersection-columns as shown in the grid-diagrams of Figs. 570 & 571.

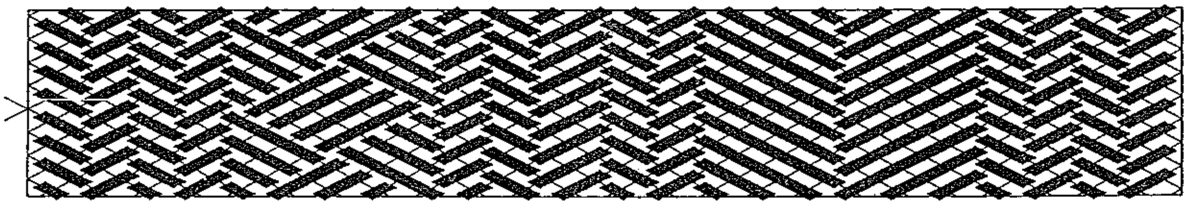

Fig. 570 — The long knot with the central depicted modification in Fig. 566.

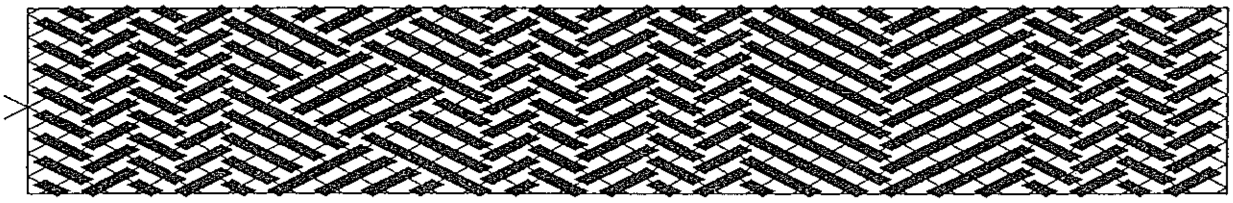

Fig. 571 — The long knot with the rightmost depicted modification in Fig. 566.

The algorithm tables of the knot in Fig. 570 are shown in Fig. 572. From these tables we read the following half-cycle braiding algorithms:

1. Free run.
2. $6o$.
3. $o - u - o - u - 2o$.
4. $6o - u - 5o$.
5. $2o - 2u - 2o - 2u - 4o$.
6. $u - 2o - u - 2o - u - 2o - 2u - 4o - u - 2o$.
7. $u - 2o - 3u - 3o - 3u - 3o - u - 2o$.
8. $2u - 2o - 2u - 2o - 2u - 3o - 2u - 5o - 2u - 2o$.
9. $2u - 6o - u - 3o - 4u - 4o - 2u - 2o$.
10. $o - 2u - 2o - 3u - 3o - 2u - 4o - 2u - o - 4u - 2o - 2u - 2o$.

11. $o - 2u - 6o - 3u - 4o - 4u - 6o - 2u - 2o$.
12. $2o - 2u - 2o - 4u - 4o - 2u - 2o - u - 2o - 2u - o - 4u - 4o - 2u - 2o$.
13. $2o - 2u - 6o - 2u - o - 2u - 5o - 4u - 8o - 2u - 2o$.
14. $u - 2o - 2u - 2o - 5u - 5o - 2u - 2o - 2u - 2o - 2u - o - 4u - 3o - u - 2o - 2u - 2o$.
15. $u - 2o - 2u - 6o - 3u - 2o - 2u - 3o - u - 2o - 5u - 6o - u - 2o - 2u - 2o$.
16. $2u - 2o - 2u - 2o - 6u - 6o - 2u - 2o - 3u - 2o - 2u - o - 4u - 4o - 2u - 2o - 2u - 2o$.

Starting at the centre of the string, braid upwards the half-cycles 1–8. Then continue with braiding the Standing End downwards:

9. $2o - 6u - o - 3u - 4o - 4u - 2o - 2u$.
10. $u - 2o - 2u - 3o - 3u - 2o - 4u - 2o - u - 4o - 2u - 2o - 2u$.
11. $u - 2o - 6u - 3o - 4u - 4o - 6u - 2o - 2u$.
12. $2u - 2o - 2u - 4o - 4u - 2o - 2u - o - 2u - 2o - u - 4o - 4u - 2o - 2u$.
13. $2u - 2o - 6u - 2o - u - 2o - 5u - 4o - 8u - 2o - 2u$.
14. $o - 2u - 2o - 2u - 5o - 5u - 2o - 2u - 2o - 2u - 2o - u - 4o - 3u - o - 2u - 2o - 2u$.
15. $o - 2u - 2o - 6u - 3o - 2u - 2o - 3u - o - 2u - 5o - 6u - o - 2u - 2o - 2u$.
16. $2o - 2u - 2o - 2u - 6o - 6u - 2o - 2u - 3o - 2u - 2o - u - 4o - 4u - 2o - 2u - 2o - 2u$.

L → R BRAIDING UPWARDS

7	6	5	4	3	2	1	0	7	6	5	4	3	2	1	0	7	6	5	4	3	2	1	0	7	6	5	4	3	2	1	0	7	6	5	4	3	2	1	0	7	6	5	4	3	2	1	0		
u	u	o	o	u	u	o	o	u	u	u	u	o	o	o	o	u	o	o	u	u	o	o	o	u	u	o	o	u	u	u	u	u	u	o	o	o	o	o	o	u	u	o	o	u	u	o	o	1	9
u	u	o	o	u	u	o	o	u	u	u	o	o	o	o	u	u	o	o	u	u	o	o	o	u	u	o	o	u	u	u	u	u	u	o	o	o	o	o	o	u	u	o	o	u	u	o	o	3	11
u	u	o	o	u	u	o	o	u	u	o	o	o	o	u	u	u	o	o	u	u	o	o	o	u	u	o	o	u	u	u	u	u	u	o	o	o	o	o	o	u	u	o	o	u	u	o	o	5	13
u	u	o	o	u	u	o	o	u	o	o	o	o	u	u	u	u	o	o	u	u	o	o	o	u	u	o	o	u	u	u	u	u	u	o	o	o	o	o	o	u	u	o	o	u	u	o	o	7	15

R → L BRAIDING UPWARDS

7	6	5	4	3	2	1	0	7	6	5	4	3	2	1	0	7	6	5	4	3	2	1	0	7	6	5	4	3	2	1	0	7	6	5	4	3	2	1	0	7	6	5	4	3	2	1	0		
u	u	o	o	u	u	o	o	u	u	u	u	u	u	o	o	o	o	o	o	u	u	o	o	u	u	u	o	o	u	u	o	o	o	o	u	u	u	u	o	u	u	o	o	u	u	o	o	2	10
u	u	o	o	u	u	o	o	u	u	u	u	u	u	o	o	o	o	o	o	u	u	o	o	u	u	u	o	o	u	u	o	o	o	u	u	u	u	o	o	u	u	o	o	u	u	o	o	4	12
u	u	o	o	u	u	o	o	u	u	u	u	u	u	o	o	o	o	o	o	u	u	o	o	u	u	u	o	o	u	u	o	o	u	u	u	u	o	o	o	u	u	o	o	u	u	o	o	6	14
u	u	o	o	u	u	o	o	u	u	u	u	u	u	o	o	o	o	o	o	u	u	o	o	u	u	u	o	o	u	u	o	u	u	u	u	o	o	o	o	u	u	o	o	u	u	o	o	8	16

L → R BRAIDING DOWNWARDS

7	6	5	4	3	2	1	0	7	6	5	4	3	2	1	0	7	6	5	4	3	2	1	0	7	6	5	4	3	2	1	0	7	6	5	4	3	2	1	0	7	6	5	4	3	2	1	0		
o	o	u	u	o	o	u	u	o	o	o	o	u	u	u	u	o	u	u	o	o	u	u	u	o	o	u	u	o	o	o	o	o	o	u	u	u	u	u	u	o	o	u	u	o	o	u	u	1	9
o	o	u	u	o	o	u	u	o	o	o	u	u	u	u	o	o	u	u	o	o	u	u	u	o	o	u	u	o	o	o	o	o	o	u	u	u	u	u	u	o	o	u	u	o	o	u	u	3	11
o	o	u	u	o	o	u	u	o	o	u	u	u	u	o	o	o	u	u	o	o	u	u	u	o	o	u	u	o	o	o	o	o	o	u	u	u	u	u	u	o	o	u	u	o	o	u	u	5	13
o	o	u	u	o	o	u	u	o	u	u	u	u	o	o	o	o	u	u	o	o	u	u	u	o	o	u	u	o	o	o	o	o	o	u	u	u	u	u	u	o	o	u	u	o	o	u	u	7	15

R → L BRAIDING DOWNWARDS

7	6	5	4	3	2	1	0	7	6	5	4	3	2	1	0	7	6	5	4	3	2	1	0	7	6	5	4	3	2	1	0	7	6	5	4	3	2	1	0	7	6	5	4	3	2	1	0		
o	o	u	u	o	o	u	u	o	o	o	o	o	o	u	u	u	u	u	u	o	o	u	u	o	o	o	u	u	o	o	u	u	u	u	o	o	o	o	u	o	o	u	u	o	o	u	u	2	10
o	o	u	u	o	o	u	u	o	o	o	o	o	o	u	u	u	u	u	u	o	o	u	u	o	o	o	u	u	o	o	u	u	u	o	o	o	o	u	u	o	o	u	u	o	o	u	u	4	12
o	o	u	u	o	o	u	u	o	o	o	o	o	o	u	u	u	u	u	u	o	o	u	u	o	o	o	u	u	o	o	u	u	o	o	o	o	u	u	u	o	o	u	u	o	o	u	u	6	14
o	o	u	u	o	o	u	u	o	o	o	o	o	o	u	u	u	u	u	u	o	o	u	u	o	o	o	u	u	o	o	u	o	o	o	o	u	u	u	u	o	o	u	u	o	o	u	u	8	16

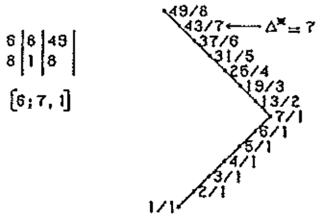

Fig. 572 — The algorithm tables of the knot in Fig. 570.

The algorithm tables of the knot in Fig. 571 are shown in Fig. 573.

L → R

BRAIDING UPWARDS

5	2	7	4	1	6	3	0	5	2	7	4	1	6	3	0	5	2	7	4	1	6	3	0	5	2	7	4	1	6	3	0	5	2	7	4	1	6	3	0	5	2	7	4	1	6	3	0	5	2		
u	u	o	o	u	u	o	o	u	u	u	u	u	o	o	o	o	u	u	o	o	u	u	o	o	o	u	u	o	o	u	u	u	u	u	u	o	o	o	o	o	o	u	u	o	o	u	u	o	o	1	9
u	u	o	o	u	u	o	o	u	u	o	o	o	o	u	u	u	u	u	o	o	u	u	o	o	o	u	u	o	o	u	u	u	u	u	u	o	o	o	o	o	o	u	u	o	o	u	u	o	o	3	11
u	u	o	o	u	u	o	o	u	u	u	o	o	o	o	u	u	u	u	o	o	u	u	o	o	o	u	u	o	o	u	u	u	u	u	u	o	o	o	o	o	o	u	u	o	o	u	u	o	o	5	13
u	u	o	o	u	u	o	o	u	u	u	u	o	o	o	o	u	u	u	o	o	u	u	o	o	o	u	u	o	o	u	u	u	u	u	u	o	o	o	o	o	o	u	u	o	o	u	u	o	o	7	15

R → L

BRAIDING UPWARDS

5	2	7	4	1	6	3	0	5	2	7	4	1	6	3	0	5	2	7	4	1	6	3	0	5	2	7	4	1	6	3	0	5	2	7	4	1	6	3	0	5	2	7	4	1	6	3	0	5	2		
u	u	o	o	u	u	o	o	u	u	u	u	u	u	o	o	o	o	o	o	u	u	o	o	u	u	u	o	o	u	u	o	o	o	o	u	u	u	u	o	o	o	u	u	o	o	u	u	o	o	2	10
u	u	o	o	u	u	o	o	u	u	u	u	u	u	o	o	o	o	o	o	u	u	o	o	u	u	u	o	o	u	u	o	o	o	o	o	u	u	u	u	o	o	u	u	o	o	u	u	o	o	4	12
u	u	o	o	u	u	o	o	u	u	u	u	u	u	o	o	o	o	o	o	u	u	o	o	u	u	u	o	o	u	u	o	o	u	u	u	u	o	o	o	o	o	u	u	o	o	u	u	o	o	6	14
u	u	o	o	u	u	o	o	u	u	u	u	u	u	o	o	o	o	o	o	u	u	o	o	u	u	u	o	o	u	u	o	o	o	u	u	u	u	o	o	o	o	u	u	o	o	u	u	o	o	8	16

L → R

BRAIDING DOWNWARDS

5	2	7	4	1	6	3	0	5	2	7	4	1	6	3	0	5	2	7	4	1	6	3	0	5	2	7	4	1	6	3	0	5	2	7	4	1	6	3	0	5	2	7	4	1	6	3	0	5	2		
o	o	u	u	o	o	u	u	o	o	o	o	u	u	u	u	o	o	o	u	u	o	o	u	u	u	o	o	u	u	o	o	o	o	o	o	u	u	u	u	u	u	o	o	u	u	o	o	u	u	1	9
o	o	u	u	o	o	u	u	o	o	o	o	o	u	u	u	u	o	o	u	u	o	o	u	u	u	o	o	u	u	o	o	o	o	o	o	u	u	u	u	u	u	o	o	u	u	o	o	u	u	3	11
o	o	u	u	o	o	u	u	o	o	u	u	u	u	o	o	o	o	o	u	u	o	o	u	u	u	o	o	u	u	o	o	o	o	o	o	u	u	u	u	u	u	o	o	u	u	o	o	u	u	5	13
o	o	u	u	o	o	u	u	o	o	o	u	u	u	u	o	o	o	o	u	u	o	o	u	u	u	o	o	u	u	o	o	o	o	o	o	u	u	u	u	u	u	o	o	u	u	o	o	u	u	7	15

R → L

BRAIDING DOWNWARDS

5	2	7	4	1	6	3	0	5	2	7	4	1	6	3	0	5	2	7	4	1	6	3	0	5	2	7	4	1	6	3	0	5	2	7	4	1	6	3	0	5	2	7	4	1	6	3	0	5	2		
o	o	u	u	o	o	u	u	o	o	o	o	o	o	u	u	u	u	u	u	o	o	u	u	o	o	o	u	u	o	o	u	u	u	o	o	o	o	u	u	u	u	o	o	u	u	o	o	u	u	2	10
o	o	u	u	o	o	u	u	o	o	o	o	o	o	u	u	u	u	u	u	o	o	u	u	o	o	o	u	u	o	o	u	u	u	u	o	o	o	o	u	u	u	o	o	u	u	o	o	u	u	4	12
o	o	u	u	o	o	u	u	o	o	o	o	o	o	u	u	u	u	u	u	o	o	u	u	o	o	o	u	u	o	o	u	u	u	u	u	o	o	o	o	u	u	o	o	u	u	o	o	u	u	6	14
o	o	u	u	o	o	u	u	o	o	o	o	o	o	u	u	u	u	u	u	o	o	u	u	o	o	o	u	u	o	o	u	u	o	o	o	o	u	u	u	u	u	o	o	u	u	o	o	u	u	8	16

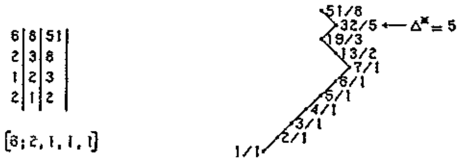

Fig. 573 — The algorithm tables of the knot in Fig. 571.

From these tables we read the following half-cycle braiding algorithms:

1. Free run.
2. $5o - u$.
3. $o - u - o - u - o - u$.
4. $u - o - u - o - u - 3o - 2u - o - u$.
5. $u - 2o - u - 3o - u - 3o - u$.
6. $2u - o - 2u - 2o - u - o - u - 2o - 2u - 3o - u - o$.
7. $2u - o - u - 2o - u - 4o - 2u - 4o - u - o$.
8. $2u - 2o - 2u - 3o - u - 2o - u - o - u - 2o - u - 4o - 2u - o$.
9. $2u - 2o - 2u - 2o - u - o - u - 3o - 3u - 5o - 2u - o$.
10. $u - o - u - 2o - 3u - 4o - u - 2o - u - 2o - u - 2o - 3u - 2o - u - o - 2u - o$.
11. $u - o - u - 2o - u - 2o - 3u - 2o - u - 2o - u - o - 4u - 4o - u - o - 2u - o$.
12. $2u - o - u - 2o - 4u - 5o - u - 2o - 2u - 2o - u - 4o - 3u - 2o - u - o - 2u - 2o$.
13. $2u - o - u - 2o - 2u - 3o - 3u - 2o - u - 3o - u - o - 5u - 5o - u - o - 2u - 2o$.
14. $2u - o - 2u - 2o - 5u - 5o - 2u - 2o - 2u - 2o - 2u - 2o - 3u - 5o - u - 2o - 2u - 2o$.
15. $2u - o - 2u - 2o - 3u - 4o - 2u - 2o - 2u - 3o - u - 2o - 5u - 6o - u - 2o - 2u - 2o$.
16. $2u - 2o - 2u - 2o - 6u - 6o - 2u - 2o - 3u - 2o - 2u - 3o - 4u - 4o - 2u - 2o - 2u - 2o$.

Starting at the centre of the string, braid upwards the half-cycles 1–8. Then continue with braiding the Standing End downwards:

9. $2o - 2u - o - 3u - o - u - o - 3u - 3o - 5u - 2o - u$.
10. $o - u - o - 2u - 3o - 4u - o - 2u - o - 2u - o - 2u - 2o - 3u - o - u - 2o - u$.
11. $o - u - o - 2u - 3o - 2u - o - 2u - o - 2u - o - u - 4o - 4u - o - u - 2o - u$.
12. $2o - u - o - 2u - 4o - 5u - o - 2u - 2o - 2u - o - 3u - 3o - 3u - o - u - 2o - 2u$.
13. $2o - u - o - 2u - 2o - 2u - 4o - 2u - o - 3u - o - u - 5o - 5u - o - u - 2o - 2u$.
14. $2o - u - 2o - 2u - 5o - 5u - 2o - 2u - 2o - 2u - 2o - 4u - 4o - 2u - o - 2u - 2o - 2u$.
15. $2o - u - 2o - 2u - 2o - 4u - 3o - 2u - 2o - 3u - o - 2u - 5o - 6u - o - 2u - 2o - 2u$.
16. $2o - 2u - 2o - 2u - 6o - 6u - 2o - 2u - 3o - 2u - 2o - 2u - 4o - 5u - 2o - 2u - 2o - 2u$.

An 8-bight knot will in general be of little value, hence a greater multiple of 4 for the number of bights is normally required in order to cover the intended object properly. A greater multiple of 4 gives the modified central Pampas Button section also a much better appearance. For the knot in Fig. 570 with $p = 49$ we can take for b the values $4, 8, 12, 16, 20, 24, 32, 36, 40, 44, 48, 52, 60, \cdots$, and for the knot in Fig. 571 with $p = 51$ we can take for b the values $4, 8, 16, 20, 28, 32, 40, 44, 52, 56, 64, \cdots$. Note that in the algorithm tables the o/u bodies of the tables do not change and that only the i-values change due to the Δ^*-values and the half-cycle numbers are extended. This makes the algorithm tables of much greater value than a list of half-cycle braiding algorithms, consequently the more experienced braider may prefer to braid directly from the algorithm tables rather then from half-cycle braiding algorithms.

THE BRAIDER'S NOTEBOOK

At times one comes across a general statement which is, besides not being quite true, an obvious extrapolation of a relatioship found for a few cases. Invariably one looks in vain for an explanation and/or proof, and often such a general statement is incomplete. A typical case of such a general statement can be found in an article by Barney Belford entitled *"The 7 Part, 5 Bight Turk's-head"* published in *The Australian Whipmaker, No. 42*. In that article we come across the following lines: *"As there are 2 more parts than bights over half the knot is tied before having to take the working end under at all. The 5 part 3 bight turkshead is quick to tie for this reason and so is the 9 part 7 bight one"*, it then continues with the erroneous statement: *"but none of these can be made into larger turksheads in the way standard knots can"*. Although what *"standard knots"* are has not been defined, it can only be assumed that these also are *"turksheads"* or more correctly called "over–under coded Regular Knots". In the quoted knots and in the extrapolated statement (concerning over–under coded Regular Knots with an **odd** number of bights) it are exactly the first half (and hence **not** over half) of the total number of half-cycles which are being laid down without having to take the Working End under at all. Barney Belford's general statement (concerning over–under coded Regular Knots with an **odd** number of bights) does not mention the case where there are two less parts than bights, in which case over half the knot is tied before having to take the Working End under at all. Let's therefore have a look at both cases: the case where the number of parts is 2 less than the number of bights and the case where the number of parts is 2 more than the number of bights; in both cases the number of bights is **odd** as required for a single string string-run.

Details concerning the over–under coded Regular Knot $p/b = (x-2)/x$, where x is an odd positive integer, are shown at the left in Fig. 574, and details concerning the over–under coded Regular Knot $p/b = (x+2)/x$, where x is an odd positive integer, are shown at the right in Fig. 574.

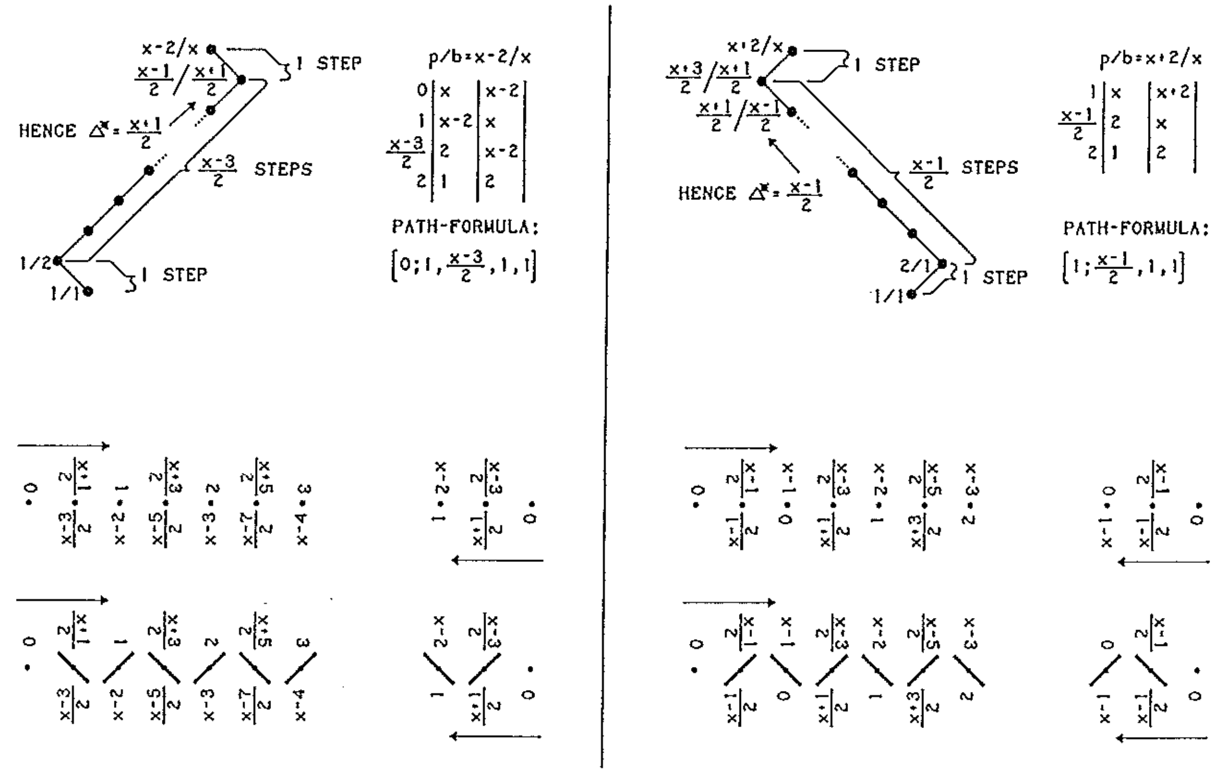

Fig. 574 — The over–under coded Regular Knots $p/b = (x-2)/x$ and $p/b = (x+2)/x$.

With the aid of Euclid's algorithm we determine the path-formula which enables us to plot the path in the RKT. From the path in the RKT we establish the Δ*-value with which we calculate the i-values in the algorithm diagram. Next we place on the inner $(p-1)$ dots of the algorithm diagram (the intersection-columns of the knot) the codings for the consecutive half-cycles, using for each half-cycle **over** codings where free dots are available and fulfil the requirement of an over–under coded Regular Knot.

The case $p = x - 2$:

$$\Delta^* = \frac{x+1}{2}.$$

$$2\Delta^* = \left|\frac{2(x+1)}{2}\right|_b = \left|\frac{2(x+1)}{2}\right|_x = |x+1|_x = 1.$$

$$3\Delta^* = \left|\frac{3(x+1)}{2}\right|_b = \left|\frac{3(x+1)}{2}\right|_x = \left|\frac{3x+3}{2}\right|_x = \frac{x+3}{2}.$$

$$4\Delta^* = \left|\frac{4(x+1)}{2}\right|_b = \left|\frac{4(x+1)}{2}\right|_x = |2x+2|_x = 2\,.$$

$$5\Delta^* = \left|\frac{5(x+1)}{2}\right|_b = \left|\frac{5(x+1)}{2}\right|_x = \left|\frac{5x+5}{2}\right|_x = \frac{x+5}{2}\,.$$

$$\vdots$$

Thus the last free dot in the algorithm diagram for a half-cycle from lower-right to upper-left, able to receive an over coding, is the dot above $i = |(p-1)\Delta^*|_b = \left|(x-3)\left(\frac{x+1}{2}\right)\right|_x = \left|(x+1)\left(\frac{x-3}{2}\right)\right|_x = \frac{x-3}{2}$, and the last free dot for a half-cycle from lower-left to upper-right, able to receive an over coding, is the dot below $i = |(p-1)\Delta^*|_b = \left|(x-3)\left(\frac{x+1}{2}\right)\right|_x = \frac{x-3}{2}$. The i-value $\frac{x-1}{2}$, the next greater i-value above $\frac{x-3}{2}$, does not appear in the algorithm diagram since it would be associated with the dot for intersection-column $(p+1)$ which of couse does not exist in a Regular Knot having p parts. Hence the last half-cycle with all over crossings is half-cycle $h_o = 2\left\{\frac{x-1}{2}\right\} + 3 = x+2$. Since the knot has $2x$ half-cycles, the first half plus two of the total number of half-cycles can thus be laid down without having to take the Working End under any already laid down half-cycle.

The case $p = x+2$:

$$\Delta^* = \frac{x-1}{2}\,.$$

$$2\Delta^* = \left|\frac{2(x-1)}{2}\right|_b = \left|\frac{2(x-1)}{2}\right|_x = |x-1|_x = x-1\,.$$

$$3\Delta^* = \left|\frac{3(x-1)}{2}\right|_b = \left|\frac{3(x-1)}{2}\right|_x = \left|\frac{3x-3}{2}\right|_x = \frac{x-3}{2}\,.$$

$$4\Delta^* = \left|\frac{4(x-1)}{2}\right|_b = \left|\frac{4(x-1)}{2}\right|_x = |2x-2|_x = x-2\,.$$

$$5\Delta^* = \left|\frac{5(x-1)}{2}\right|_b = \left|\frac{5(x-1)}{2}\right|_x = \left|\frac{5x-5}{2}\right|_x = \frac{x-5}{2}\,.$$

$$\vdots$$

Thus the last free dot in the algorithm diagram for a half-cycle from lower-right to upper-left, able to receive an over coding, is the dot above $i = |3\Delta^*|_b = \left|3\left(\frac{x-1}{2}\right)\right|_x = \frac{x-3}{2}$, and the last free dot for a half-cycle from lower-left to upper-right, able to receive an over crossing, is the dot below $i = |3\Delta^*|_b = \left|3\left(\frac{x-1}{2}\right)\right|_x = \frac{x-3}{2}$. Note that the outermost intersection columns have the same i-value for both the lower-right to upper-left and the lower-left to upper-right half-cycles ($i = |(p-1)\Delta^*|_b = \left|(x+1)\left(\frac{x-1}{2}\right)\right|_x = \frac{x-1}{2} = \Delta^*$), hence cannot be given over codings and at the same time fulfil the coding requirements of an over–under coded Regular Knot. Thus the last half-cycle with all over crossings is half-cycle $h_o = 2\left\{\frac{x-3}{2}\right\} + 3 = x$. Since the knot has $2x$ half-cycles, the first half of the total number of half-cycles can thus be laid down without having to take the Working End under any already laid down half-cycle.

Note that in the algorithm diagram the i-value associated with the dot representing the last intersection-column for the half-cycles from lower-right to upper-left and for the half-cycles from lower-left to upper-right can more readily be calculated from the relationship $a^* + b^* = b - 1 = x - 1$ (see *The Braider*, Issue No. 7, pg. 133).

Besides the above way at looking at the two cases of single string over–under coded Regular Knots where respectively the number of parts is 2 less than the number of bights and the number of parts is 2 more than the number of bights, we can also look at them in the following way:

The case $p = x - 2$:

From the path in the RKT, which we could plot with the aid of the path-formula obtained with Euclid's algorithm, we see that the over–under coded $p/b = (x-2)/x$ Regular Knot is obtained from the $p/b = 1/1$ Regular Knot by an n-order Method I enlargement (where $n = 1 + \frac{x-3}{2} = \frac{x-1}{2}$) followed by a first-order Method I enlargement. The first enlargement stage (the n-order Method I enlargement) brings us from $p/b = 1/1$ to $p/b = \left(\frac{x-1}{2}\right) / \left(\frac{x+1}{2}\right)$. This are $(x+1)$ half-cycles in which the Working End is not taken under any previous laid down half-cycle (assuming that we want the least number of 'unders' possible; refer to *The Braider*, Issue No. 7). The first track-splitting half-cycle is then also without 'unders', hence overall we have the first $(x+2)$ half-cycles without 'unders'. Since the total number of half-cycles in the $p/b = (x-2)/x$ over–under coded Regular Knot is equal to $2x$, we see that the first half plus two of these are without 'unders'.

The case $p = x + 2$:

From the path in the RKT, which we could plot with the aid of the path-formula obtained with Euclid's algorithm, we see that the over–under coded $p/b = (x+2)/x$ Regular Knot is obtained from the $p/b = 1/1$ Regular Knot by an n-order Method II enlargement (where $n = 1 + \frac{x-1}{2} = \frac{x+1}{2}$) followed by a first-order Method II enlargement. The first enlargement stage (the n-order Method II enlargement) brings us from $p/b = 1/1$ to $p/b = \left(\frac{x+3}{2}\right) / \left(\frac{x+1}{2}\right)$. This are $(x+1)$ half-cycles, however, the last of these half-cycles has as the last crossing an 'under', hence we have the first x half-cycles without 'unders' (assuming that we want the least number of 'unders' possible; refer to *The Braider*, Issue No. 7). Since the total number of half-cycles in the $p/b = (x+2)/x$ over–under coded Regular Knot is equal to $2x$, we see that the first half of these are without 'unders'.

It will be obvious that too many initial half-cycles without any 'unders' besides 'overs' makes the braiding of the knot without the aid of a mandrel with pins cumbersome. For example, the $p/b = 7/72$ over–under coded Regular Knot may be regarded as being impossible to braid without the aid of a mandrel with pins since the first 83 half-cycles are without any 'unders', assuming that we want the least number of 'unders' possible. Only small knots with a relative large number of initial half-cycles which do not have both 'overs' and 'unders' don't give any trouble in braiding them, but even slightly bigger ones become difficult to braid without a mandrel with pins due to the initial lack of formfastness.

THE BRAIDER

No.32 NOVEMBER 2002.

CONTENTS

pg.
A Button Knot Saga 729
Designing Interbraided Knots 733

A quarterly publication for the braiding artisan

Resale of this publication or copies thereof is strictly prohibited

Copyright ©2002 by:

A.G. Schaake; 21 Sundown Cresc.; Hamilton; New Zealand.
D. Van Tassel; Box 335; Craig, Co 81626-0335; U.S.A.
F.J.M. Masurel; Ganzenzijde 4; 2317 XG Leiden; Nederland.

All rights reserved. No part of this publication may be reproduced, stored in a retrieval system, or transmitted, in any form or by any means, electronic, mechanical, photo-copying, recording, or otherwise, without prior written permission.

This publication is available to braiding artisans only.

Copies may be obtained from:

A.G. Schaake,
21 Sundown Cresc.,
Hamilton,
New Zealand.

SEE NOTE BELOW.

No. 31

NOTE: the first Fig. number in this Issue is 554, but should have been 584 instead. Hence the Fig. numbers 554 - 583 not only appear in *The Braider*, Issue No. 30, but the numbers 554 - 574 appear again in *The Braider*, Issue No. 31 and the numbers 575 - 583 appear again in *The Braider*, Issue No. 32. This was noted too late for rectification.

No. 32

See NOTE under No. 31 above.

A Button Knot Saga

There are several Lanyard Knots which after a suitable deformation can serve as 'Button Knots', but should nevertheless not be regarded as true Button Knots. Since those so-called 'Button Knots' are only deformed Lanyard Knots, they have as such a distinct weakness as a Button Knot. Sometimes we encounter in the braiding literature an article about some of those so-called 'Button Knots' in which relationships between their construction methods are discussed and illustrated in a pictorial way. Often such discussions not only leave much to be desired, but since a pictorial drawing cannot show the whole braid, a pictorial drawing is never able to show relationships in a simple and clear manner. In the Australian Plaiters and Whipmakers Association's Journal *The Australian Whipmaker, issue No.51*, we find such a discussion about the 'Crown Button Knot', the 'Chinese Button Knot' and the 'Diamond Button Knot'. Of these three 'Button Knots' only the 'Crown Button Knot' may be regarded as a true Button Knot. The 'Chinese Button Knot' and the 'Diamond Button Knot' are suitably deformed Lanyard Knots, each based on a different 2-string $p/b = 3/4$ over–under coded Regular open-ender. The 'Crown Button Knot' comes in two forms which are each others complement (see the two leftmost grid-diagrams I and IV in Fig. 575). The 'Chinese Button Knot' and the 'Diamond Button Knot' also come each in two complementary forms as do the Lanyard Knots from which they are derived (for the complementary Lanyard Knots from which the complementary forms of the 'Chinese Button Knots' are derived see the central two grid-diagrams II and V in Fig. 575, and for the complementary Lanyard Knots from which the complementary forms of the 'Diamond Button Knots' are derived see the rightmost two grid-diagrams III and VI in Fig. 575). The 'Chinese Button knots' and the 'Diamond Button Knots' are obtained from their associated Lanyard Knots by working the loop away. The essential difference in the construction of the 'Crown Button Knot', the 'Chinese Button Knot' and the 'Diamond Button Knot' is indicated by the dotted string-sections and for the Diamond Knot by the additional rearrangement of the loop position (the loop can simply be slid into the indicated position). In the 'Crown Button Knot' the dotted string-sections are cut off.

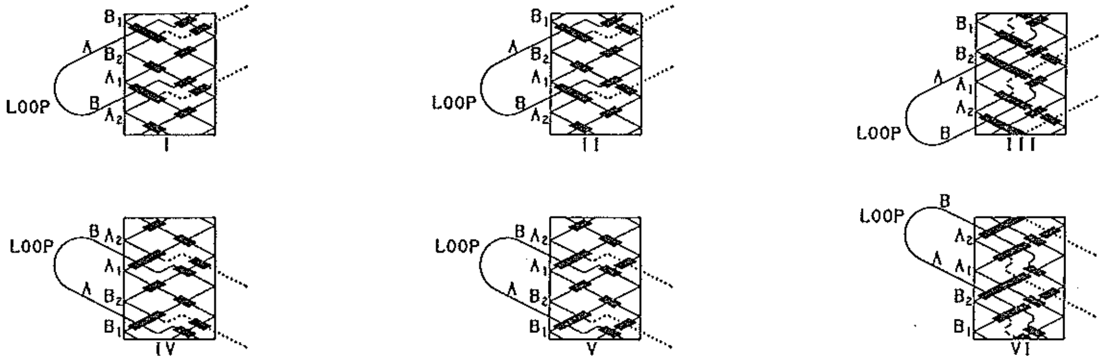

Fig. 575 — The 'Crown Button Knot' and the Lanyard Knots from which the 'Chinese Button Knot' and the 'Diamond Button Knot' are obtained.

The weakness in the 'Chinese Button Knot' and the 'Diamond Button Knot' as a Button Knot lies in the worked away loop which tends to sink somewhat down into the knot.

The 2-string Lanyard Knots from which the 'Chinese Button Knot' and the 'Diamond Button Knot' are obtained have a crown on the right bight-boundary of their depicted grid-diagrams in Fig. 575. This crown can be rolled over to the left whereby Lanyard Knot II goes over into the reversed Lanyard Knot II_{R}, Lanyard Knot V goes over into the reversed Lanyard Knot V_{R}, Lanyard Knot III goes over into the reversed Lanyard Knot $\mathrm{III}_{\mathrm{R}}$, and Lanyard Knot VI goes over into the reversed Lanyard Knot VI_{R} (see Fig. 576).

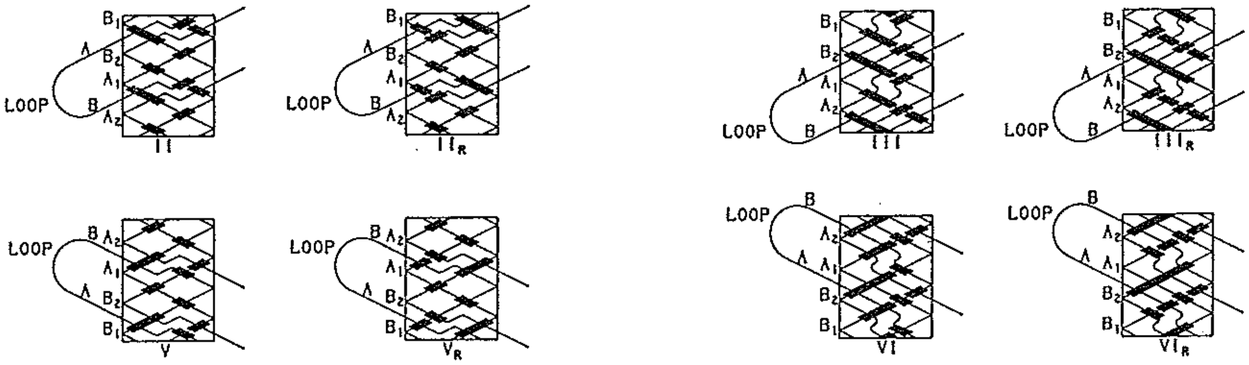
LOOP
A
B
B_1
B_2
A_1
A_2
II
II_{R}
III
$\mathrm{III}_{\mathrm{R}}$
V
V_{R}
VI
VI_{R}

Fig. 576 — The 2-string Lanyard Knots II, V ; III, VI and their reversed forms.

Similar to the formation of 'Button Knots' from the 2-string over–under coded Regular Lanyard Knots $p/b = 3/4$, 'Button Knots' can of course also be formed from the 2-string over–under coded Regular Lanyard Knots $p/b = 3/2$ and $p/b = 4/6$. The weakness, pointed out above, in those 'Button Knots' becomes, however, more apparent with increased p/b values.

Of some special interest are the 2-string over–under coded Regular Lanyard Knots $p/b = 3/2$ and the 'Button Knots' obtained from them by working away the loop. The complementary lanyard forms II, V, and the complementary lanyard forms III, VI, as well as their reversed forms, are depicted in Fig. 577.

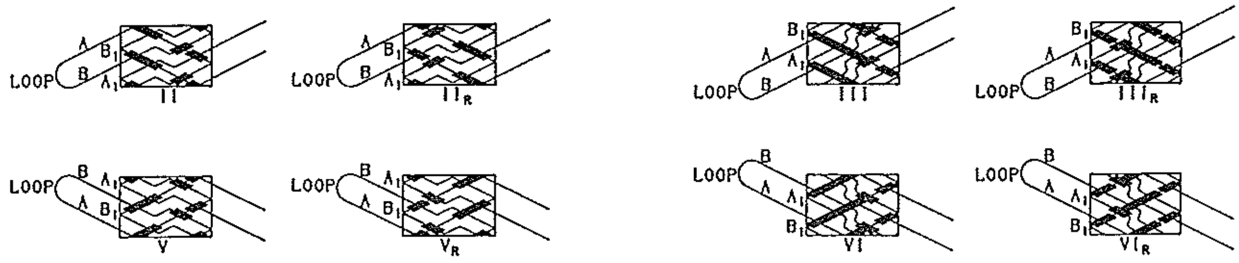
LOOP
A
B
B_1
A_1
II
II_{R}
III
$\mathrm{III}_{\mathrm{R}}$
V
V_{R}
VI
VI_{R}

Fig. 577 — The Lanyard Knots $p/b = 3/2$.

Note how the complementary lanyard forms II and IV relate to the 2-string complementary Footrope Knots and complementary Ashley's Bends (see *The Braider*, Issue No. 5, pg. 95–106; Issue No. 20, pp. 452–456; Appendix 1997; Appendix 1999).

When the bights A_1 and B_1 of the 'Button Knots' obtained from the Lanyard Knots II and V in Fig. 577 are pulled up to form loops we create the respective left-hand and right-hand loop knots in Fig. 578. Hence we can form the Lanyard Knots II and V from these respective loop knots as shown in Fig. 579. An obvious modification of the loop knots in Fig. 578 leads to the useful loop knots in Fig. 580.

Similarly, the bights A_1 and B_1 of the 'Button Knots' obtained from the Lanyard Knots III and VI in Fig. 577 can be pulled up to form loops in order to create the respective left-hand and right-hand loop knots in Fig. 581. Hence we can form the

Lanyard Knots III and VI from these respective loop knots as shown in Fig. 582. An obvious modification of the loop knots in Fig. 582 leads to the useful loop knots in Fig. 583.

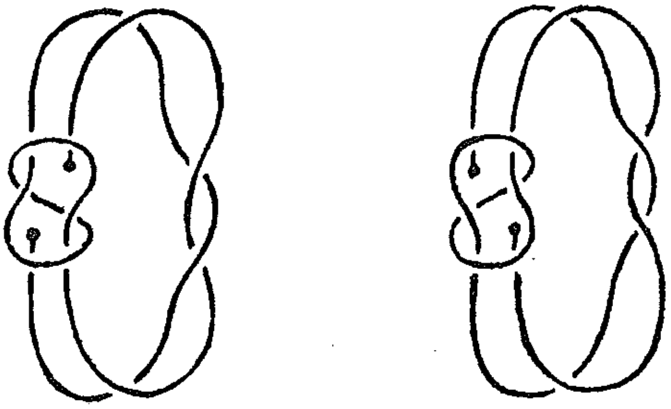

Fig. 578 — The loop knots created from the 'Button Knots' obtained from the Lanyard Knots II and V in Fig. 577.

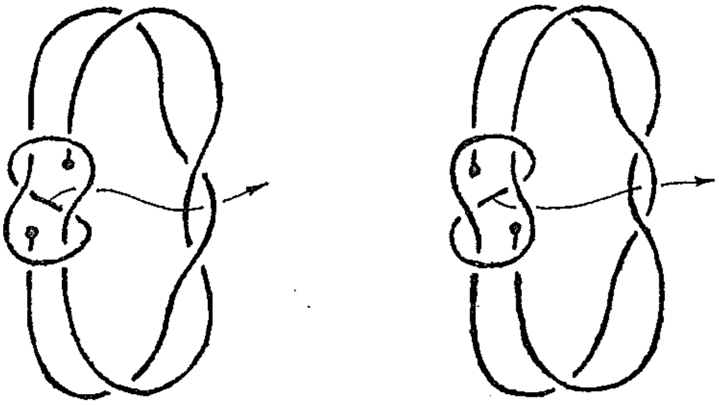

Fig. 579 — The construction of the Lanyard Knots II and V in Fig. 577 from the loop knots in Fig. 578.

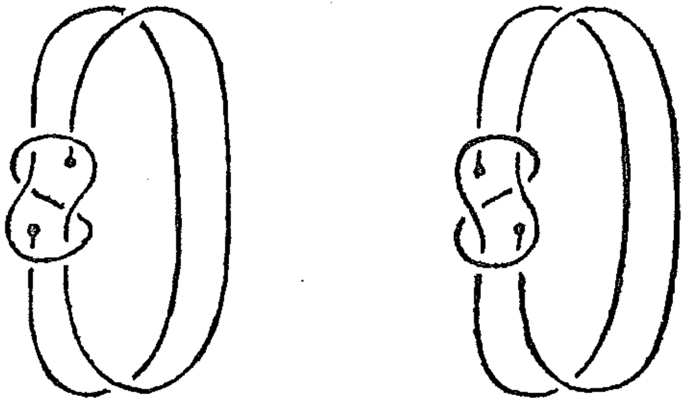

Fig. 580 — The modification of the loop knots in Fig. 578.

The reversed forms of the Lanyard Knots II, V and II, VI in Fig. 577 may be obtained by rolling the crown on their right bight-boundary over to the left. The Lanyard Knots

II$_{\mathrm{R}}$, V$_{\mathrm{R}}$, III$_{\mathrm{R}}$ and VI$_{\mathrm{R}}$, in Figs. 576 and 577 do not lend themselves to the creation of 'Button Knots' in a way similar to the one used for the Lanyard Knots II, V, III and VI.

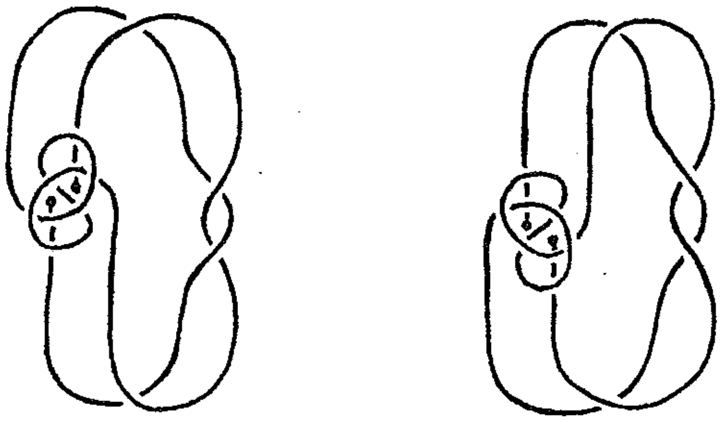

Fig. 581 — The loop knots created from the 'Button Knots' obtained from the Lanyard Knots III and VI in Fig. 577.

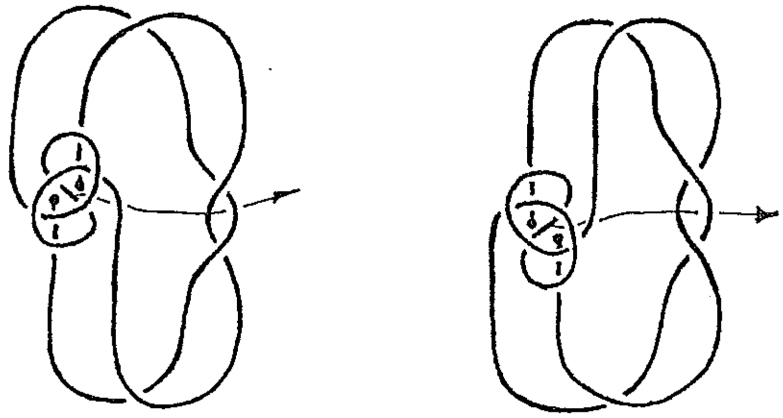

Fig. 582 — The construction of the Lanyard Knots III and VI in Fig. 577 from the loop knots in Fig. 581.

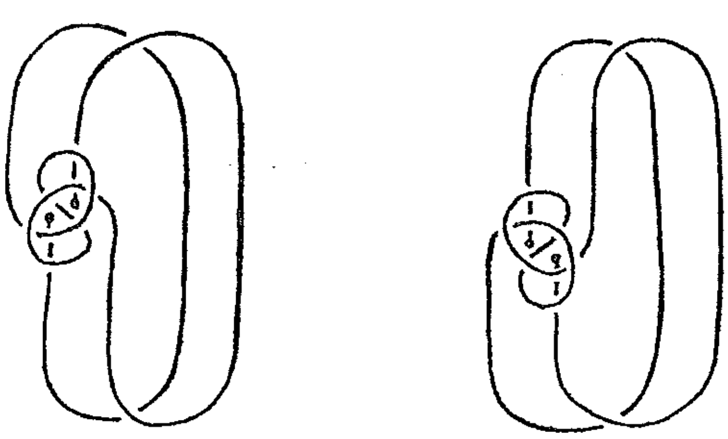

Fig. 583 — The modification of the loop knots in Fig. 581.

Designing Interbraided Knots

The interbraiding of knots not only gives us a means of creating colour-patterns, but also gives us the means of creating braiding-patterns (as opposed to colour-patterns) which we otherwise would not be able to create. For Interbraided Cylindrical Braids we do like the interbraid to have a great deal of flexibility with regards its possible number of bights since this determines its applicability rating with respect to diameter sizes it can properly cover. When the interbraid consists of more than two interbraided knots it is advantageous if at least each sequential interbraiding stage of these knots gives us a useful interbraid as well since this increases the overall usefulness of the sequential interbraids. The algorithm diagrams for the determination of the half-cycle braiding algorithms will be kept simple when we use for interbraiding Column-coded Regular Knots with identical p/b values. We shall discuss here four such interbraids which give us a pleasing colour-pattern and are easy to braid.

Say that we like our interbraid to consist of three interbraided Regular Column-coded Knots each with the same p/b value, but not necessarily the same coding. For the earlier mentioned flexibility we not only like the value of p to be a prime number, but we also like the coding-periodicity to be equal to the number of interbraided knots, hence in our case to be equal to 3, This can readily be accomplished since the three interbraided Regular Knots are column-coded. The interbraid will thus possess a number of three differently coded half-cycles from lower-left to upper-right and an identical number of three differently coded half-cycles from lower-right to upper-left.

Let the interbraided knot be a Regular Cylindrical Braid with the coding as in the diagram of Fig. 584.

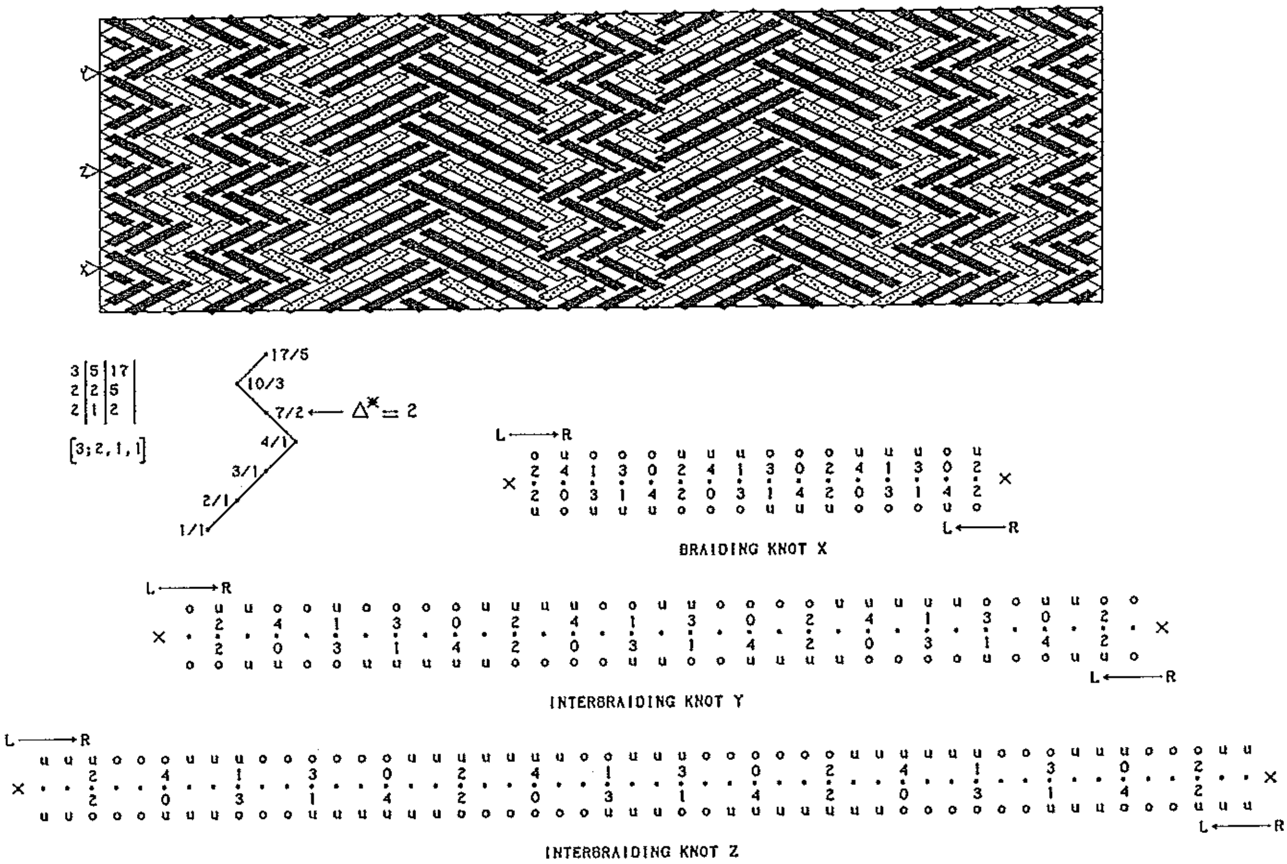

Fig. 584 — An interbraided Regular Cylindrical Knot.

The three interbraided components X, Y and Z of the knot in Fig. 584, and the interbraid of the components X and Y are depicted in Fig. 585.

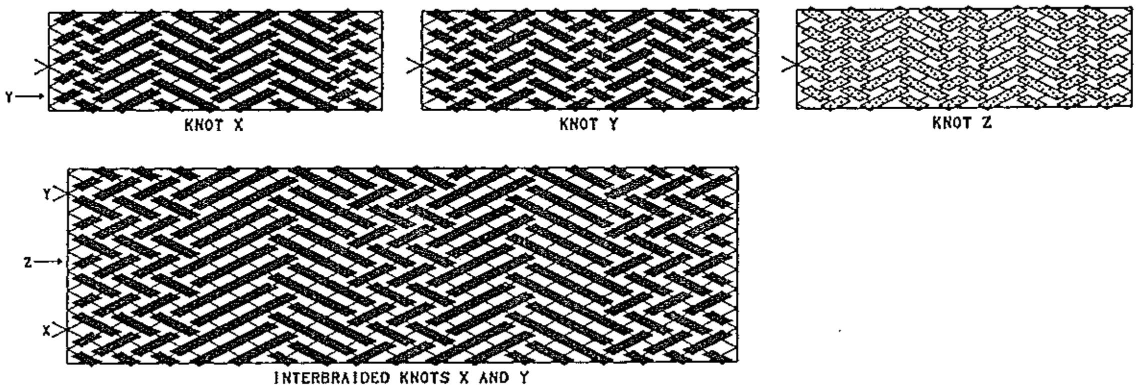

Fig. 585 — Components X, Y, Z and interbraid of X and Y of the knot in Fig. 584.

First we braid knot X which we then interbraid with knot Y. Next we interbraid the interbraid of knots X and Y with knot Z. For the Standing Ends of the knots X, Y and Z to be regularly distributed over the left bight-boundary as indicated in Fig. 584, we place the Standing End of knot Y in the knot X and the Standing End of knot Z in the interbraided knots X and Y as indicated by the respective arrows in Fig. 585.

Braiding knot X:

1. : Free run.
2. $i = 0$: $3o$.
3. $i = 0$: $3o$.
4. $i \leq 1$: $2o - u - o - u - o$.
5. $i \leq 1$: $2o - u - o - u - o$.
6. $i \leq 2$: $3o - 2u - 2o - u - o - u$.
7. $i \leq 2$: $3o - 2u - 2o - u - o - u$.
8. $i \leq 3$: $4o - 2u - 3o - 2u - o - u$.
9. $i \leq 3$: $4o - 2u - 3o - 2u - o - u$.
10. $i \leq 4$: $o - u - 3o - 3u - 3o - 3u - o - u$.

Interbraiding knot Y:

1. : $o - u - 3o - 2u - o - u - 2o - 3u - o - u - o$.
2. $i = 0$: $o - u - 4o - 2u - o - u - 3o - 3u - o - 2u - o$.
3. $i = 0$: $o - u - 4o - 2u - o - u - 3o - 3u - o - 2u - o$.
4. $i \leq 1$: $o - u - o - u - 3o - 2u - 2o - u - 3o - 4u - o - 2u - o$.
5. $i \leq 1$: $o - u - o - u - 3o - 2u - 2o - u - 3o - 4u - o - 2u - o$.
6. $i \leq 2$: $o - 2u - o - u - 3o - 3u - 2o - u - 4o - 4u - o - 2u - 2o$.
7. $i \leq 2$: $o - 2u - o - u - 3o - 3u - 2o - u - 4o - 4u - o - 2u - 2o$.
8. $i \leq 3$: $o - 2u - o - u - 4o - 3u - 2o - 2u - 4o - 4u - 2o - 2u - 2o$.
9. $i \leq 3$: $o - 2u - o - u - 4o - 3u - 2o - 2u - 4o - 4u - 2o - 2u - 2o$.
10. $i \leq 4$: $o - 2u - 2o - u - 4o - 4u - 2o - 2u - 4o - 5u - 2o - 2u - 2o$.

Interbraiding knot Z:

1. : $2u - 2o - 2u - 4o - 5u - o - 2u - 4o - 4u - 2o - 2u - 2o - 2u$.
2. $i = 0$: $2u - 2o - 2u - 5o - 5u - o - 2u - 5o - 4u - 2o - 3u - 2o - 2u$.
3. $i = 0$: $2u - 2o - 2u - 5o - 5u - o - 2u - 5o - 4u - 2o - 3u - 2o - 2u$.
4. $i \leq 1$: $2u - 2o - 3u - 5o - 5u - 2o - 2u - 5o - 5u - 2o - 3u - 2o - 2u$.
5. $i \leq 1$: $2u - 2o - 3u - 5o - 5u - 2o - 2u - 5o - 5u - 2o - 3u - 2o - 2u$.

6. $i \leq 2:$ $3u - 2o - 3u - 5o - 6u - 2o - 2u - 6o - 5u - 2o - 3u - 3o - 2u\,.$
7. $i \leq 2:$ $3u - 2o - 3u - 5o - 6u - 2o - 2u - 6o - 5u - 2o - 3u - 3o - 2u\,.$
8. $i \leq 3:$ $3u - 2o - 3u - 6o - 6u - 2o - 3u - 6o - 5u - 3o - 3u - 3o - 2u\,.$
9. $i \leq 3:$ $3u - 2o - 3u - 6o - 6u - 2o - 3u - 6o - 5u - 3o - 3u - 3o - 2u\,.$
10. $i \leq 4:$ $3u - 3o - 3u - 6o - 7u - 2o - 3u - 6o - 6u - 3o - 3u - 3o - 2u\,.$

Since each of the knots X , Y and Z have a symmetric coding-pattern, not only do the knots X and Y give us a useful interbraid, but the interbraids of the knots X and Z and the knots Y and Z also give us useful interbraids. In Fig. 586 we find again the interbraid of knots X and Y depicted in Fig. 585, but note that for using this interbraid as the final braid, the Standing Ends of knots X and Y are regularly distributed over the left bight-boundary and consequently the Standing End of knot Y is placed in knot X as indicated by the arrow in Fig. 586. Since the coding-pattern of knot Z is identical to the coding-pattern of knot Y, we can in the interbraid of knots X and Y replace knot Y by knot Z (see Fig. 586).

The half-cycle braiding algorithms for knot X and the interbraiding of knot Y (and of course the replacement of Y by Z) are the half-cycle braiding algorithms for these knots on pg. 734.

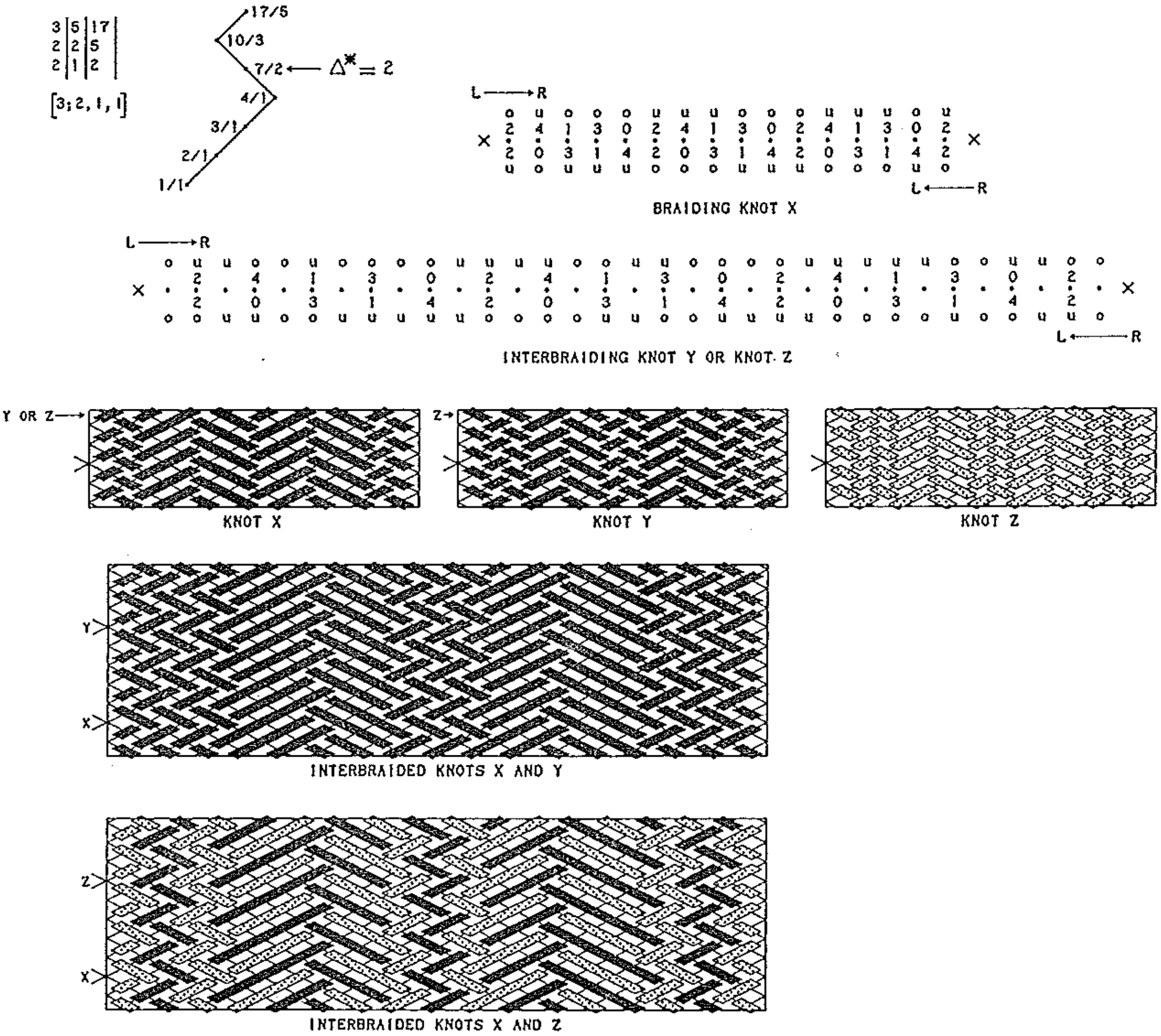
3 | 5 | 17
2 | 2 | 5
2 | 1 | 2
[3; 2, 1, 1]
17/5
10/3
7/2 ← Δ* = 2
4/1
3/1
2/1
1/1
L → R
o u o o o u u u o o o u u u o u
X 2 4 1 3 0 2 4 1 3 0 2 4 1 3 0 2 X
2 0 3 1 4 2 0 3 1 4 2 0 3 1 4 2
u o u u u o o o u u u o o o u o
L ← R
BRAIDING KNOT X
L → R
o u u o o u o o o o u u u u o o u u o o o o u u u u u o o u u o o
X 2 4 1 3 0 2 4 1 3 0 2 4 1 3 0 2 X
2 0 3 1 4 2 0 3 1 4 2 0 3 1 4 2
o o u u o o u u u u u o o o o u u o o u u u u o o o o u o o u u o
L ← R
INTERBRAIDING KNOT Y OR KNOT Z
Y OR Z →
KNOT X
Z →
KNOT Y
KNOT Z
Y
X
INTERBRAIDED KNOTS X AND Y
Z
X
INTERBRAIDED KNOTS X AND Z

Fig. 586 — Interbraided knots X and Y, and the replacement of knot Y by knot Z.

The interbraid of knots X and Z is depicted in Fig. 587, and for the same reason as above, knot Z can be replaced by knot Y. The half-cycle braiding algorithms for knot X are the ones for this knot on pg. 734, and the half-cycle braiding algorithms for the interbraiding of knot Z (and of course the replacement of Z by Y) can be read from the algorithm diagram in Fig. 587 as follows:

Interbraiding knot Z:

1. : $u - o - u - 2o - 4u - 2o - 2u - o - u - o - u$.
2. $i = 0$: $u - o - u - 3o - 4u - 3o - 2u - o - 2u - o - u$.
3. $i = 0$: $u - o - u - 3o - 4u - 3o - 2u - o - 2u - o - u$.
4. $i \leq 1$: $u - o - 2u - 3o - 3u - o - u - 3o - 3u - o - 2u - o - u$.
5. $i \leq 1$: $u - o - 2u - 3o - 3u - o - u - 3o - 3u - o - 2u - o - u$.
6. $i \leq 2$: $2u - o - 2u - 3o - 4u - o - u - 4o - 3u - o - 2u - 2o - u$.
7. $i \leq 2$: $2u - o - 2u - 3o - 4u - o - u - 4o - 3u - o - 2u - 2o - u$.
8. $i \leq 3$: $2u - o - 2u - 4o - 4u - o - 2u - 4o - 3u - 2o - 2u - 2o - u$.
9. $i \leq 3$: $2u - o - 2u - 4o - 4u - o - 2u - 4o - 3u - 2o - 2u - 2o - u$.
10. $i \leq 4$: $2u - 2o - 2u - 4o - 5u - o - 2u - 4o - 4u - 2o - 2u - 2o - u$.

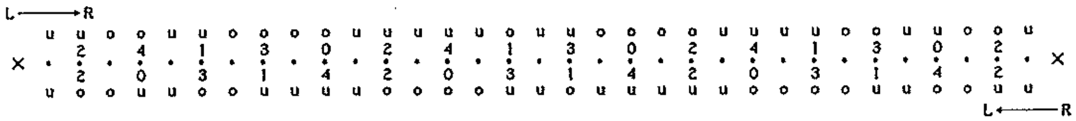
L → R
u u o o u u o o o o u u u u u o u u o o o o u u u u o o u u o o u
2 4 1 3 0 2 4 1 3 0 2 4 1 3 0 2
X X
2 0 3 1 4 2 0 3 1 4 2 0 3 1 4 2
u o o u u o o u u u u o o o o u u o u u u u u o o o o u u o o u u
L ← R

INTERBRAIDING KNOT Z OR Y

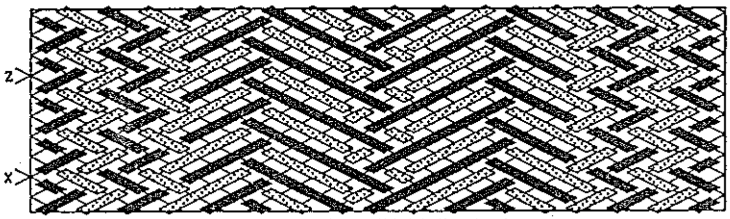

INTERBRAIDED KNOTS X AND Z

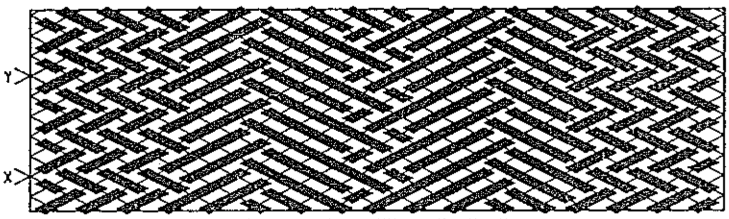

INTERBRAIDED KNOTS X AND Y

Fig. 587 — Interbraided knots X and Z, and the replacement of knot Z by knot Y.

The interbraid of knots Y and Z is depicted in Fig. 588, and again for the same reason as mentioned earlier, knot Z can be replaced by knot Y. First we braid knot Y which we then interbraid with knot Z. Note that for using this interbraid as the final braid, the Standing Ends of knots Y and Z are regularly distributed over the left bight-boundary and consequently the Standing End of knot Z is placed in the knot Y as indicated by the arrow in Fig. 586. Since the coding-pattern of knot Z is identical to the coding-pattern of knot Y, we can in the interbraid of knots Y and Z replace knot Z by knot Y (see Fig. 588). The half-cycle braiding algorithms for knot Y and the half-cycle braiding algorithms for the interbraiding of knot Z (and of course the replacement of Z by Y) can be read from the algorithm diagrams in Fig. 588 as follows:

Braiding knot Y:

1. : Free run.

2. $i=0$: $2o-u$.
3. $i=0$: $2o-u$.
4. $i\leq 1$: $u-3o-2u$.
5. $i\leq 1$: $u-3o-2u$.
6. $i\leq 2$: $2u-o-u-3o-2u-o$.
7. $i\leq 2$: $2u-o-u-3o-2u-o$.
8. $i\leq 3$: $2u-2o-u-o-u-2o-u-o-u-o$.
9. $i\leq 3$: $2u-2o-u-o-u-2o-u-o-u-o$.
10. $i\leq 4$: $u-o-u-2o-2u-o-u-2o-2u-o-u-o$.

Interbraiding knot Z:

1. : $u-o-u-2o-2u-o-u-2o-2u-o-u-o-u$.
2. $i=0$: $u-o-u-3o-2u-o-u-3o-2u-o-2u-o-u$.
3. $i=0$: $u-o-u-3o-2u-o-u-3o-2u-o-2u-o-u$.
4. $i\leq 1$: $u-o-2u-3o-2u-2o-u-3o-3u-o-2u-o-u$.
5. $i\leq 1$: $u-o-2u-3o-2u-2o-u-3o-3u-o-2u-o-u$.
6. $i\leq 2$: $2u-o-2u-3o-3u-2o-u-4o-3u-o-2u-2o-u$.
7. $i\leq 2$: $2u-o-2u-3o-3u-2o-u-4o-3u-o-2u-2o-u$.
8. $i\leq 3$: $2u-o-2u-4o-3u-2o-2u-4o-3u-2o-2u-2o-u$.
9. $i\leq 3$: $2u-o-2u-4o-3u-2o-2u-4o-3u-2o-2u-2o-u$.
10. $i\leq 4$: $2u-2o-2u-4o-4u-2o-2u-4o-4u-2o-2u-2o-u$.

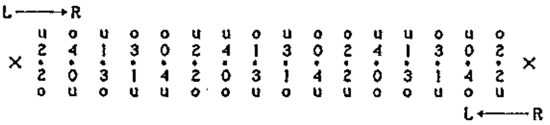

BRAIDING KNOT Y

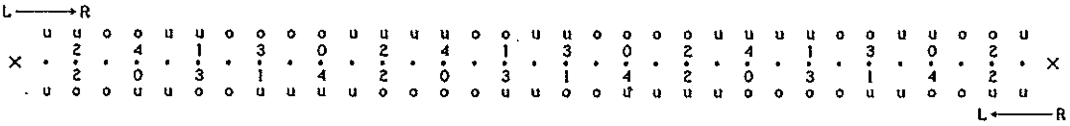
L → R
u u o o u u o o o o u u u u o o u u o o o o u u u u o o u u o o u
2 4 1 3 0 2 4 1 3 0 2 4 1 3 0 2
X X
2 0 3 1 4 2 0 3 1 4 2 0 3 1 4 2
u o o u u o o u u u u o o o o u u o o u u u u o o o o u u o o u u
L ← R

INTERBRAIDING KNOT Z OR Y

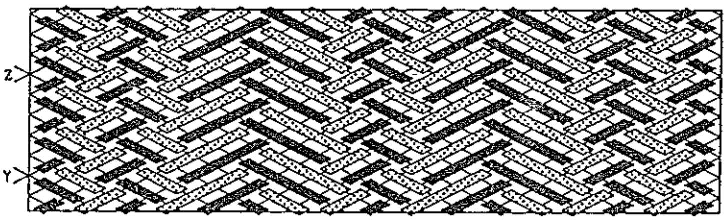

INTERBRAIDED KNOTS Y AND Z

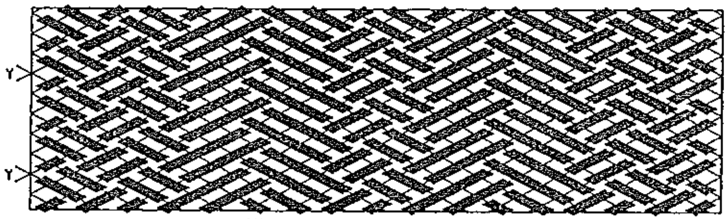

INTERBRAIDED KNOTS Y AND Y

Fig. 588 — Interbraided knots Y and Z, and the replacement of knot Z by knot Y.

In many applications we require the Interbraided Cylindrical Knot to have constricting ends. The grid-diagram offers us the ideal braid representation which facilitates the modification from a Regular Cylindrical Braid to a Regular Nested Cylindrical Braid (a Nested Cylindrical Braid in general) or vice versa. The Interbraided Regular Cylindrical Knot of Fig. 584 has been modified to the Interbraided Regular Nested Cylindrical Knot of Fig. 589.

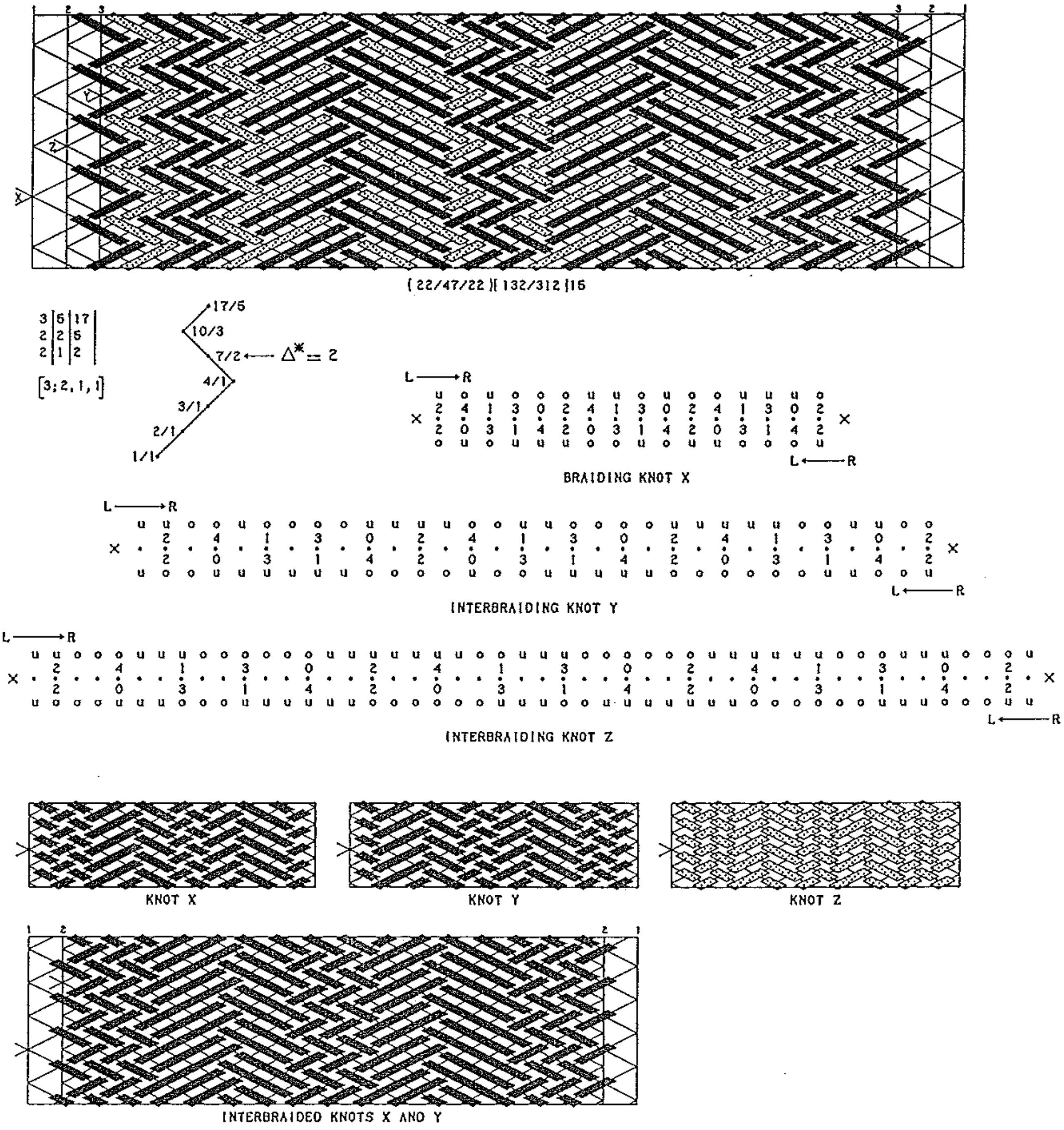
1 2 3
3 2 1
Y
Z
X
(22/47/22)(132/312)16
3 | 5 | 17
2 | 2 | 5
2 | 1 | 2
[3; 2, 1, 1]
17/5
10/3
7/2 ← Δ* = 2
4/1
3/1
2/1
1/1
L → R
u o u o o o u u o u o o u u u o
X 2 4 1 3 0 2 4 1 3 0 2 4 1 3 0 2 X
2 0 3 1 4 2 0 3 1 4 2 0 3 1 4 2
o u o u u u o o u o u u o o o u
L ← R
BRAIDING KNOT X
L → R
u u o o u o o o o u u u u o o u u o o o o u u u u u o o u u o o
X · 2 · 4 · 1 · 3 · 0 · 2 · 4 · 1 · 3 · 0 · 2 · 4 · 1 · 3 · 0 · 2 X
2 0 3 1 4 2 0 3 1 4 2 0 3 1 4 2
u o o u u u u u u o o o o u o o u u u u u o o o o o o u u o o u
L ← R
INTERBRAIDING KNOT Y
L → R
u u o o o u u u o o o o o o u u u u u u u o o u u u o o o o o o u u u u u u o o o u u u o o o u
X · 2 · · 4 · · 1 · · 3 · · 0 · · 2 · · 4 · · 1 · · 3 · · 0 · · 2 · · 4 · · 1 · · 3 · · 0 · · 2 · X
2 0 3 1 4 2 0 3 1 4 2 0 3 1 4 2
u o o o u u u o o o u u u u u u o o o o o o u u u o o u u u u u u u o o o o o o u u u o o o u u
L ← R
INTERBRAIDING KNOT Z
KNOT X
KNOT Y
KNOT Z
1 2
2 1
INTERBRAIDED KNOTS X AND Y

Fig. 589 — The Regular Nested interbraid of knots X , Y and Z.

First we braid knot X; its left bight-boundary is 1 and its right bight-boundary is 3 in the final interbraid of the knots X , Y and Z. Then we interbraid knot Y; its left bight-boundary is 3 and its right bight-boundary is 1 in the final interbraid of the knots X , Y and Z. Finally we interbraid knot Z; its left bight-boundary is 2 and its right bight-boundary is 2 in the final interbraid of the knots X , Y and Z. Note that the coding of knot Z in Fig. 589 is identical to the coding of knot Z in Fig. 584, but that the codings of knots X and Y in Fig. 589 differ from their respective codings in Fig. 584. The half-cycle braiding algorithms for the respective braiding stages may be obtained from the algorithm diagrams in Fig. 589.

Braiding knot X :

1. : Free run.
2. $i = 0$: $u - o - u$.
3. $i = 0$: $o - 2u$.
4. $i \leq 1$: $o - 2u - o - 2u$.
5. $i \leq 1$: $u - o - 4u$.
6. $i \leq 2$: $u - o - 3u - o - 3u - o$.
7. $i \leq 2$: $2u - 2o - 2u - o - 2u - o$.
8. $i \leq 3$: $u - 2o - 3u - 2o - 2u - o - u - o$.
9. $i \leq 3$: $2u - 3o - u - o - u - o - 3u - o$.
10. $i \leq 4$: $u - 3o - 2u - o - u - 2o - 3u - o - u - o$.

Interbraiding knot Y :

1. : $u - o - u - 2o - 2u - o - u - 2o - 2u - o - u - o$.
2. $i = 0$: $o - u - 4o - 3u - o - u - 2o - 4u - o - u$.
3. $i = 0$: $u - o - u - 2o - 3u - o - u - 3o - 2u - o - 2u - o$.
4. $i \leq 1$: $o - 2u - 4o - 4u - o - u - 2o - 5u - o - u$.
5. $i \leq 1$: $u - o - u - 3o - 3u - o - 2u - 3o - 3u - o - 2u - o$.
6. $i \leq 2$: $u - o - 2u - 5o - 4u - o - u - 3o - 5u - 2o - u$.
7. $i \leq 2$: $2u - o - u - 3o - 4u - o - 2u - 3o - 4u - o - 2u - 2o$.
8. $i \leq 3$: $u - o - 2u - 6o - 4u - 2o - u - 3o - 6u - 2o - u$.
9. $i \leq 3$: $2u - o - u - 4o - 4u - o - 2u - 4o - 4u - 2o - 2u - 2o$.
10. $i \leq 4$: $u - 2o - 2u - 6o - 5u - 2o - u - 4o - 6u - 2o - u$.

Interbraiding knot Z :

1. : $u - 2o - 2u - 4o - 5u - o - 2u - 4o - 4u - 2o - 2u - 2o - u$.
2. $i = 0$: $u - 2o - 2u - 5o - 5u - o - 2u - 5o - 4u - 2o - 3u - 2o - u$.
3. $i = 0$: $u - 2o - 2u - 5o - 5u - o - 2u - 5o - 4u - 2o - 3u - 2o - u$.
4. $i \leq 1$: $u - 2o - 3u - 5o - 5u - 2o - 2u - 5o - 5u - 2o - 3u - 2o - u$.
5. $i \leq 1$: $u - 2o - 3u - 5o - 5u - 2o - 2u - 5o - 5u - 2o - 3u - 2o - u$.
6. $i \leq 2$: $2u - 2o - 3u - 5o - 6u - 2o - 2u - 6o - 5u - 2o - 3u - 3o - u$.
7. $i \leq 2$: $2u - 2o - 3u - 5o - 6u - 2o - 2u - 6o - 5u - 2o - 3u - 3o - u$.
8. $i \leq 3$: $2u - 2o - 3u - 6o - 6u - 2o - 3u - 6o - 5u - 3o - 3u - 3o - u$.
9. $i \leq 3$: $2u - 2o - 3u - 6o - 6u - 2o - 3u - 6o - 5u - 3o - 3u - 3o - u$.
10. $i \leq 4$: $2u - 3o - 3u - 6o - 7u - 2o - 3u - 6o - 6u - 3o - 3u - 3o - u$.

The Regular Nested interbraid of knots X and Y gives us also a useful symmetrical knot.

The Regular Nested interbraid of knots X and Z, depicted by the uppermost grid-diagram in Fig. 590, does not give us a useful knot, which is of course not surprising since knot X has no symmetrical coding-pattern whereas knot Z does have a symmetrical coding-pattern. We can, however, readily make two changes: one which does neither affect the coding of knot X nor the coding of knot Z, but only the coding of the interbraid, and one which extends knot X by two parts to the right in order to enable us to make its coding-pattern symmetrical (see in Fig. 590 knot X^*). The Δ^*-value of knot X^* is 1, and since the string-run of knot Z does not change, its Δ^*-value does not change either, hence remains equal to 2. The grid-diagram of the Regular Nested interbraid of knots X^* and Z is depicted in Fig. 590. First we braid knot X^* and next we interbraid it with knot Z. The associated half-cycle braiding algorithms are read from the respective algorithm diagrams in Fig. 590.

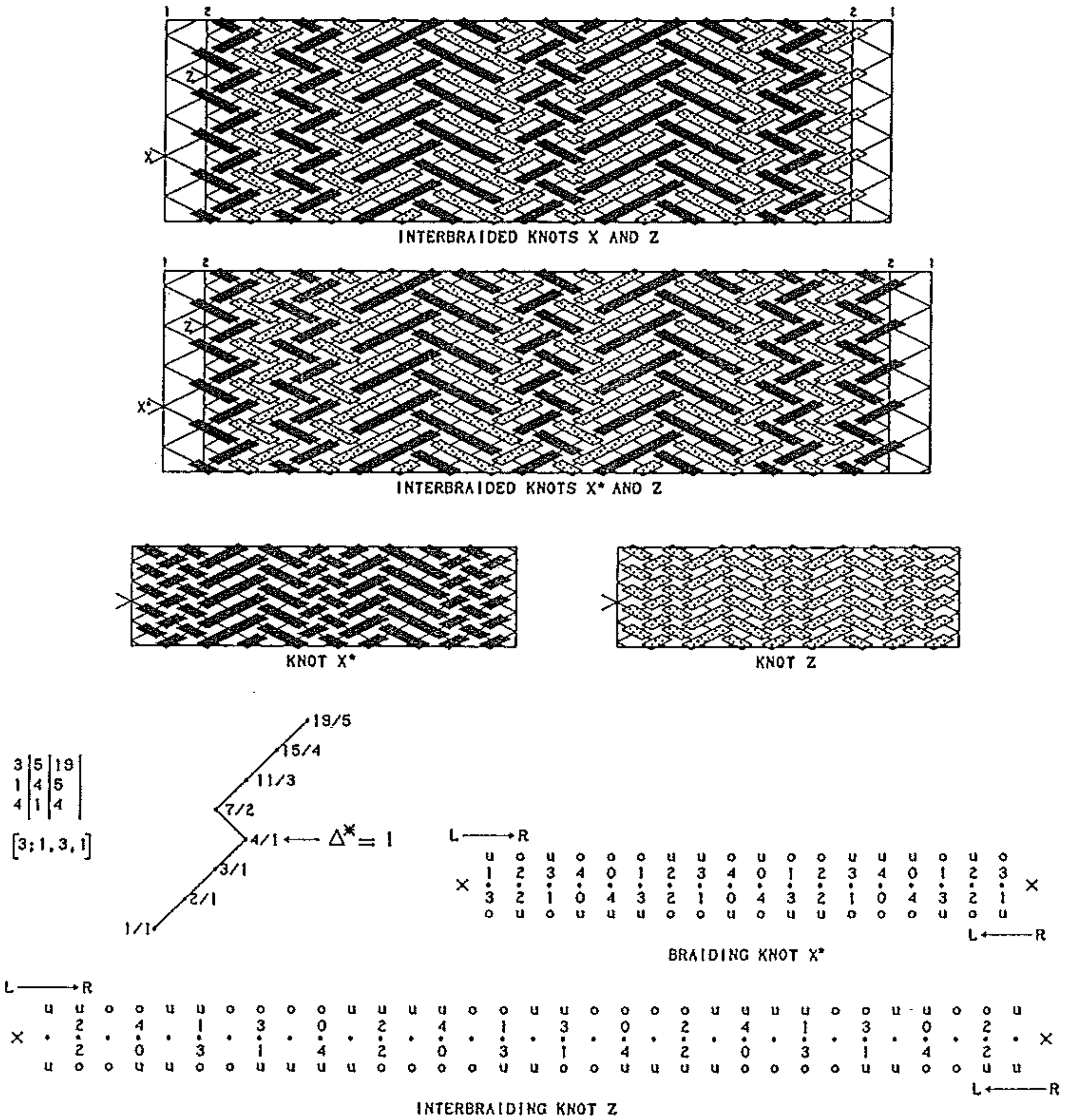

Fig. 590 — The Regular Nested interbraids of knots X^* and Z.

Braiding knot X^*:

1. : Free run.
2. $i = 0$: $o - 2u$.
3. $i = 0$: $o - 2u$.
4. $i \leq 1$: $u - 2o - u - o - u - o$.
5. $i \leq 1$: $u - 2o - u - o - u - o$.
6. $i \leq 2$: $u - 3o - 2u - 2o - u - o - u$.
7. $i \leq 2$: $u - 3o - 2u - 2o - u - o - u$.
8. $i \leq 3$: $u - o - u - 2o - 3u - 2o - 2u - o - u - o$.
9. $i \leq 3$: $u - o - u - 2o - 3u - 2o - 2u - o - u - o$.
10. $i \leq 4$: $u - o - u - 3o - 2u - o - u - 2o - 3u - o - u - o$.

Interbraiding knot Z:

1. : $u - o - u - 2o - 2u - o - u - 2o - 2u - o - u - o - u$.
2. $i = 0$: $u - o - u - 3o - 2u - o - u - 3o - 2u - o - 2u - o - u$.
3. $i = 0$: $u - o - u - 3o - 2u - o - u - 3o - 2u - o - 2u - o - u$.
4. $i \leq 1$: $u - o - 2u - 3o - 2u - 2o - u - 3o - 3u - o - 2u - o - u$.

5. $i \leq 1$: $u - o - 2u - 3o - 2u - 2o - u - 3o - 3u - o - 2u - o - u$.
6. $i \leq 2$: $2u - o - 2u - 3o - 3u - 2o - u - 4o - 3u - o - 2u - 2o - u$.
7. $i \leq 2$: $2u - o - 2u - 3o - 3u - 2o - u - 4o - 3u - o - 2u - 2o - u$.
8. $i \leq 3$: $2u - o - 2u - 4o - 3u - 2o - 2u - 4o - 3u - 2o - 2u - 2o - u$.
9. $i \leq 3$: $2u - o - 2u - 4o - 3u - 2o - 2u - 4o - 3u - 2o - 2u - 2o - u$.
10. $i \leq 4$: $2u - 2o - 2u - 4o - 4u - 2o - 2u - 4o - 4u - 2o - 2u - 2o - u$.

The Regular Nested interbraid of the knots Y and Z is the mirror image of the Regular Nested interbraid of the knots X and Z depicted by the uppermost grid-diagram in Fig. 590, and is for the same reason not a useful interbraid. When we make similar changes to the interbraid of knots Y and Z as we did above to the interbraid of the knots X and Z, then we extend knot Y by two parts to the left. The resulting interbraid will be identical to the interbraid of the knots X^* and Z.

The two component interbraids in Figs. 586, 587, 588, 590 are of course not the only suitable arrangements here, in fact several other useful interbraids can readily be derived from them. For example, the interbraids in Fig. 591 are derived from the interbraids in Fig. 587.

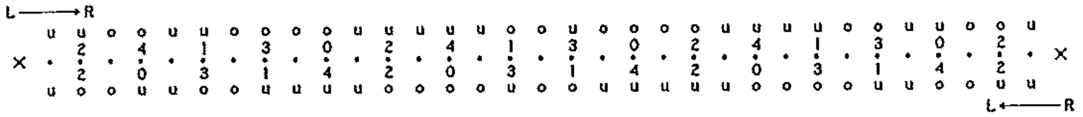
L → R
u u o o u u o o o o u u u u u o o u o o o o u u u u o o u u o o u
2 4 1 3 0 2 4 1 3 0 2 4 1 3 0 2
X
2 0 3 1 4 2 0 3 1 4 2 0 3 1 4 2
u o o u u o o u u u u o o o o u o o u u u u u o o o o u u o o u u
L ← R

INTERBRAIDING KNOT Z OR Y

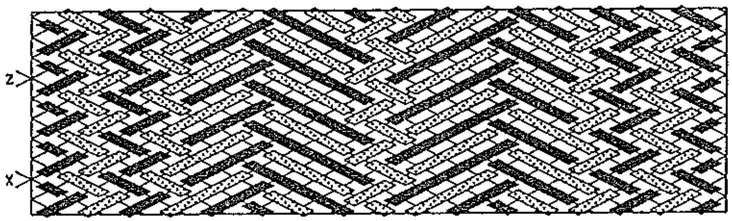

INTERBRAIDED KNOTS X AND Z

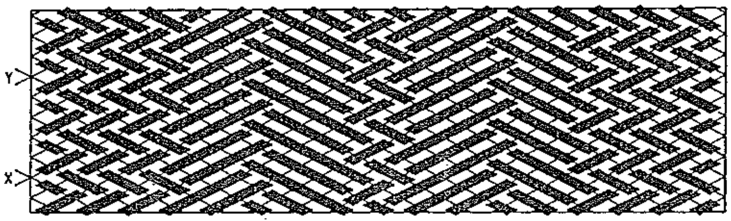

INTERBRAIDED KNOTS X AND Y

Fig. 591 — Interbraided knots X and Z or Y.

Observe that the interbraids in Fig. 591 do not affect the coding of the knots X, Y and Z in Fig. 586, but only affect the coding of the interbraids and hence only the coding of the algorithm diagram for interbraiding knot Z or Y when knot X is the first knot to be braided. Thus the half-cycle braiding algorithms for knot X are those on pg. 734. The half-cycle braiding algorithms for interbraiding knot Z or knot Y are read from the algorithm diagram in Fig. 591 as follows:

Interbraiding knot Z or Y:

1. : $u - o - u - 2o - 3u - 3o - 2u - o - u - o - u$.
2. $i = 0$: $u - o - u - 3o - 3u - 4o - 2u - o - 2u - o - u$.
3. $i = 0$: $u - o - u - 3o - 3u - 4o - 2u - o - 2u - o - u$.
4. $i \leq 1$: $u - o - 2u - 3o - 3u - 5o - 3u - o - 2u - o - u$.

5. $i \leq 1:$ $u - o - 2u - 3o - 3u - 5o - 3u - o - 2u - o - u$.
6. $i \leq 2:$ $2u - o - 2u - 3o - 4u - 6o - 3u - o - 2u - 2o - u$.
7. $i \leq 2:$ $2u - o - 2u - 3o - 4u - 6o - 3u - o - 2u - 2o - u$.
8. $i \leq 3:$ $2u - o - 2u - 4o - 4u - 2o - u - 4o - 3u - 2o - 2u - 2o - u$.
9. $i \leq 3:$ $2u - o - 2u - 4o - 4u - 2o - u - 4o - 3u - 2o - 2u - 2o - u$.
10. $i \leq 4:$ $2u - 2o - 2u - 4o - 5u - 2o - u - 4o - 4u - 2o - 2u - 2o - u$.

Although all the above useful interbraids have symmetrical coding-patterns, none of these coding-patterns can be regarded as being balanced since in the cicumferential direction they point in one specific way. This shortcoming can be overcome by turning one of the two directional coding arrangements into the opposite direction as has been done in Fig. 592.

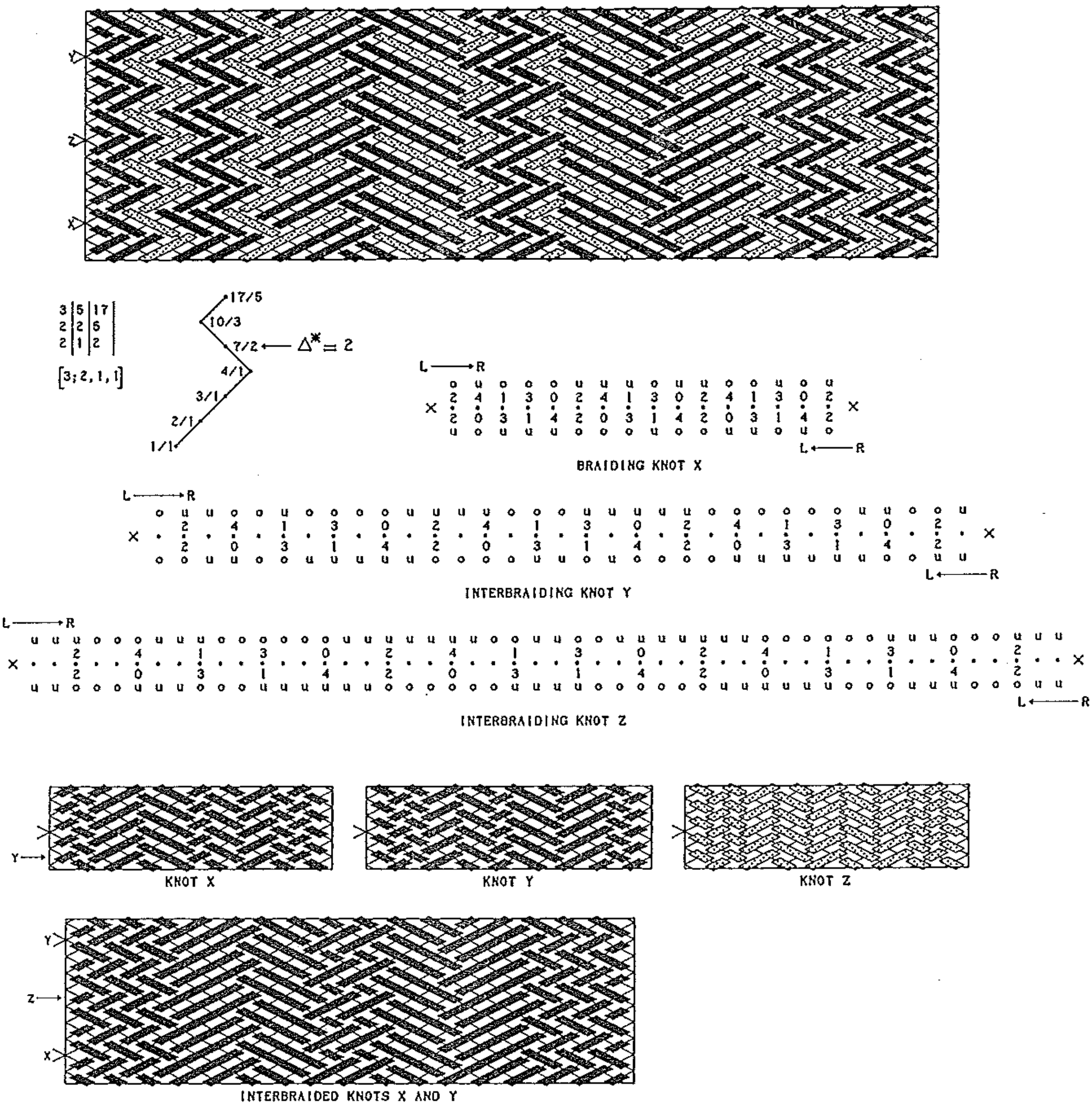

Fig. 592 — An interbraided Regular Cylindrical Braid of knots X, Y and Z.

The sequential half-cycle braiding algorithms for the knots X, Y and Z may be read from the sequential algorithm diagrams in Fig. 592 as follows:

Braiding knot X:

1. : Free run.
2. $i = 0$: $u - 2o$.
3. $i = 0$: $o - u - o$.
4. $i \leq 1$: $o - 2u - o - u - o$.
5. $i \leq 1$: $2o - 2u - 2o$.
6. $i \leq 2$: $2o - u - o - u - 2o - u - o - u$.
7. $i \leq 2$: $3o - 4u - 2o - u$.
8. $i \leq 3$: $2o - 2u - o - u - 3o - 2u - o - u$.
9. $i \leq 3$: $4o - 2u - o - 2u - o - u - o - u$.
10. $i \leq 4$: $o - u - o - 2u - 2o - u - 3o - 3u - o - u$.

Interbraiding knot Y:

1. : $o - u - 3o - 2u - 2o - 2u - 3o - u - o - u$.
2. $i = 0$: $u - o - 4u - 2o - 2u - 3o - 3u - o - 2u - o$.
3. $i = 0$: $o - u - 4o - 2u - 2o - 3u - 3o - 2u - o - u$.
4. $i \leq 1$: $u - o - 5u - 2o - u - o - u - 3o - 4u - o - 2u - o$.
5. $i \leq 1$: $o - u - o - u - 3o - 2u - 3o - 3u - 4o - 2u - o - u$.
6. $i \leq 2$: $2u - o - 5u - 3o - u - o - u - 4o - 4u - o - 2u - 2o$.
7. $i \leq 2$: $o - 2u - o - u - 3o - 3u - 3o - 4u - 4o - 2u - 2o - u$.
8. $i \leq 3$: $2u - o - 6u - 3o - u - o - 2u - 4o - 4u - 2o - 2u - 2o$.
9. $i \leq 3$: $o - 2u - o - u - 4o - 3u - 3o - 5u - 5o - 2u - 2o - u$.
10. $i \leq 4$: $2u - 2o - 6u - 4o - u - o - 2u - 4o - 5u - 2o - 2u - 2o$.

Interbraiding knot Z:

1. : $2u - 2o - 2u - 4o - 5u - o - 2u - o - 5u - 4o - 2u - 2o - 2u$.
2. $i = 0$: $2u - 2o - 2u - 2o - 5u - 4o - 2u - 5o - 4u - 2o - 3u - 2o - 2u$.
3. $i = 0$: $2u - 2o - 2u - 5o - 5u - o - 2u - o - 6u - 4o - 2u - 3o - 2u$.
4. $i \leq 1$: $2u - 2o - 2u - 3o - 5u - 4o - 3u - 5o - 5u - 2o - 3u - 2o - 2u$.
5. $i \leq 1$: $2u - 2o - 3u - 5o - 5u - 2o - 2u - o - 6u - 5o - 2u - 3o - 2u$.
6. $i \leq 2$: $2u - 3o - 2u - 3o - 5u - 5o - 3u - 6o - 5u - 2o - 3u - 3o - 2u$.
7. $i \leq 2$: $3u - 2o - 3u - 5o - 6u - 2o - 2u - o - 7u - 5o - 2u - 3o - 3u$.
8. $i \leq 3$: $2u - 3o - 2u - 3o - 6u - 5o - 4u - 6o - 5u - 3o - 3u - 3o - 2u$.
9. $i \leq 3$: $3u - 2o - 3u - 6o - 6u - 2o - 2u - 2o - 7u - 5o - 3u - 3o - 3u$.
10. $i \leq 4$: $2u - 3o - 3u - 3o - 6u - 6o - 4u - 6o - 6u - 3o - 3u - 3o - 2u$.

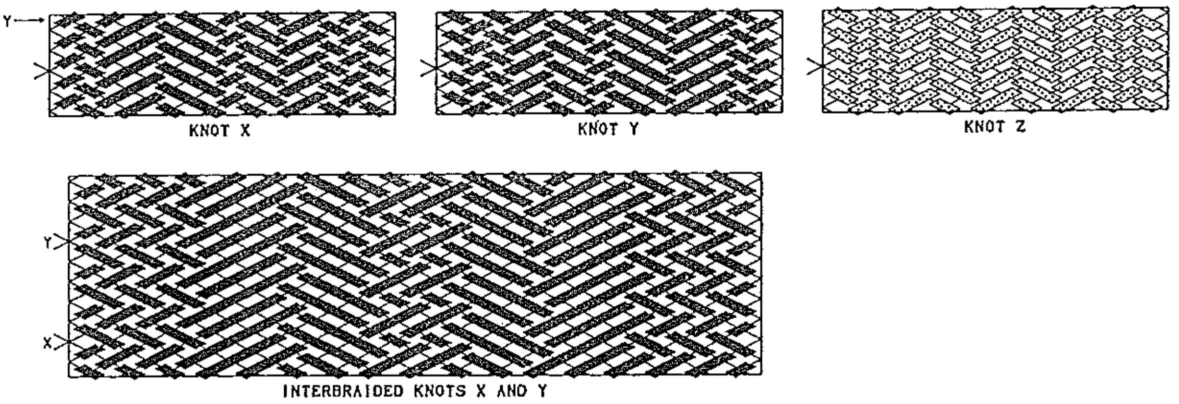

Fig. 593 — Interbraided knots X and Y.

In Fig. 593 we find again the interbraid of knots X and Y depicted in Fig. 592, but note that for using this interbraid as the final braid, the Standing Ends of knots X and Y are regularly distributed over the left bight-boundary and consequently the Standing End of knot Y is placed in knot X as indicated by the arrow in Fig. 593. The half-cycle braiding algorithms for knot X and the interbraiding of knot Y are the half-cycle braiding algorithms for these knots on pg. 743.

The Regular Cylindrical interbraid of knots X and Z, depicted by the uppermost grid-diagram in Fig. 594, does not give us a useful knot, which is of course not surprising since knot X has no symmetrical coding-pattern whereas knot Z does have a symmetrical coding-pattern. We can, however, readily make a coding change which does neither affect the coding of knot X nor the coding of knot Z, but only the coding of the interbraid (see the lower grid-diagram in Fig. 594).

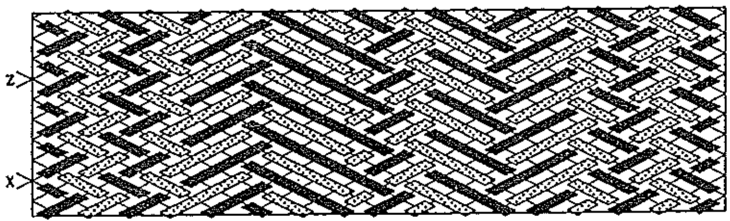

INTERBRAIDED KNOTS X AND Z

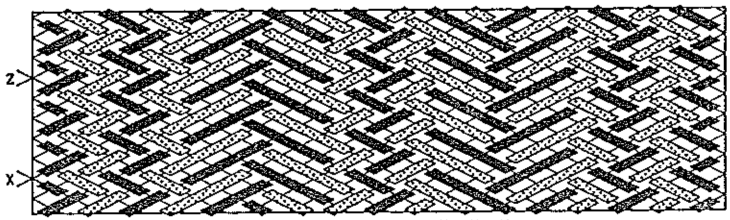

INTERBRAIDED KNOTS X AND Z

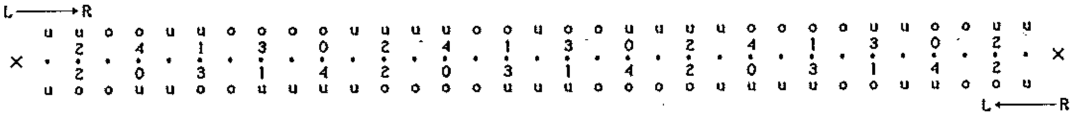
L → R
u u o o u u o o o o u u u u o o u o o u u u u o o o o u u o o u u
2 4 1 3 0 2 4 1 3 0 2 4 1 3 0 2
X
X
2 0 3 1 4 2 0 3 1 4 2 0 3 1 4 2
u o o u u o o u u u u o o o o u u u o o o o u u u u o o u u o o u
L ← R

INTERBRAIDING KNOT Z

Fig. 594 — The interbraid of knots X and Z, and its modification.

For the modified interbraid of the knots X and Z, first knot X is braided in accordance with its half-cycle braiding algorithms on pg. 743. Next knot Z is interbraided; the associated half-cycle braiding algorithms are read from the algorithm diagram in Fig. 594 as follows:

Interbraiding knot Z:

1. : $u - o - u - 2o - 2u - o - u - o - 2u - 2o - u - o - u$.
2. $i = 0$: $u - o - u - o - 3u - 2o - u - 3o - 2u - o - 2u - o - u$.
3. $i = 0$: $u - o - u - 3o - 2u - o - u - o - 3u - 2o - u - 2o - u$.
4. $i \leq 1$: $u - o - u - 2o - 3u - 2o - 2u - 3o - 3u - o - 2u - o - u$.
5. $i \leq 1$: $u - o - 2u - 3o - 2u - 2o - u - o - 3u - 3o - u - 2o - u$.
6. $i \leq 2$: $u - 2o - u - 2o - 3u - 3o - 2u - 4o - 3u - o - 2u - 2o - u$.
7. $i \leq 2$: $2u - o - 2u - 3o - 3u - 2o - u - o - 4u - 3o - u - 2o - 2u$.
8. $i \leq 3$: $u - 2o - u - 2o - 4u - 3o - 3u - 4o - 3u - 2o - 2u - 2o - u$.
9. $i \leq 3$: $2u - o - 2u - 4o - 3u - 2o - u - 2o - 4u - 3o - 2u - 2o - 2u$.
10. $i \leq 4$: $u - 2o - 2u - 2o - 4u - 4o - 3u - 4o - 4u - 2o - 2u - 2o - u$.

This particular interbraid visually appears to have a symmetrical and balanced pattern, but this is a false impression created by the domineering effect of the colour-pattern. The coding-pattern is not symmetrical, and even the colour-pattern is not of a true symmetrical nature either. In certain applications we can use this interbraid in series, but not necessarily adjacent, with its mirror-imaged interbraid depicted by the lowermost grid-diagram in Fig. 595.

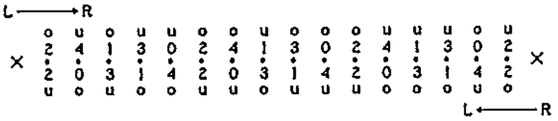
L → R
o u o u u o o u o o o u u u o u
X 2 4 1 3 0 2 4 1 3 0 2 4 1 3 0 2 X
2 0 3 1 4 2 0 3 1 4 2 0 3 1 4 2
u o u o o u u o u u u o o o u o
L ← R

BRAIDING KNOT X_m

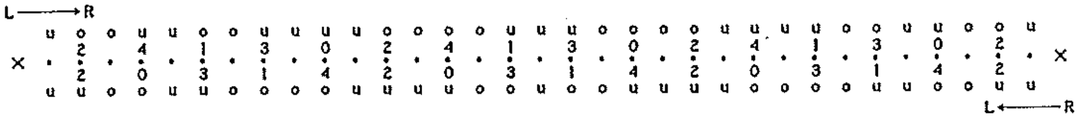
L → R
u o o u u o o u u u u o o o o u u u o o o o u u u u o o u u o o u
2 4 1 3 0 2 4 1 3 0 2 4 1 3 0 2
X X
2 0 3 1 4 2 0 3 1 4 2 0 3 1 4 2
u u o o u u o o o o u u u u o o u o o u u u u o o o o u u o o u u
L ← R

INTERBRAIDING KNOT Z_m

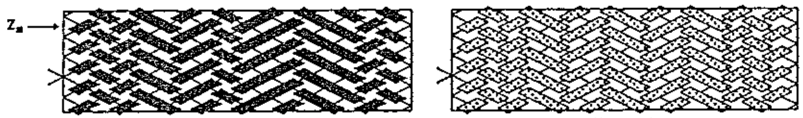

KNOT X_m KNOT Z_m

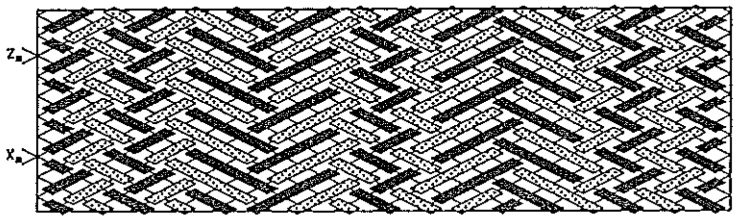

INTERBRAIDED KNOTS X_m AND Z_m

Fig. 595 — The interbraid of knots X_m and Z_m.

The half-cycle braiding algorithms for the knot X_m and for interbraiding knot Z_m may be read from the respective algorithm diagrams in Fig. 595 as follows:

Braiding knot X_m :

1. : Free run.
2. $i = 0$: $o - u - o$.
3. $i = 0$: $u - 2o$.
4. $i \leq 1$: $2o - 2u - 2o$.
5. $i \leq 1$: $o - 2u - o - u - o$.
6. $i \leq 2$: $3o - 4u - 2o - u$.
7. $i \leq 2$: $2o - u - o - u - 2o - u - o - u$.
8. $i \leq 3$: $4o - 2u - o - 2u - o - u - o - u$.
9. $i \leq 3$: $2o - 2u - o - u - 3o - 2u - o - u$.
10. $i \leq 4$: $o - u - 3o - 3u - o - 2u - 2o - u - o - u$.

Interbraiding knot Z_m :

1. : $u - o - u - o - 2u - 2o - u - 2o - 2u - o - u - o - u$.
2. $i = 0$: $u - o - u - 3o - 2u - o - u - o - 3u - 2o - u - 2o - u$.
3. $i = 0$: $u - o - u - o - 3u - 2o - u - 3o - 2u - o - 2u - o - u$.
4. $i \leq 1$: $u - o - 2u - 3o - 2u - 2o - u - o - 3u - 3o - u - 2o - u$.
5. $i \leq 1$: $u - o - u - 2o - 3u - 2o - 2u - 3o - 3u - o - 2u - o - u$.
6. $i \leq 2$: $2u - o - 2u - 3o - 3u - 2o - u - o - 4u - 3o - u - 2o - 2u$.
7. $i \leq 2$: $u - 2o - u - 2o - 3u - 3o - 2u - 4o - 3u - o - 2u - 2o - u$.

8. $i \le 3$: $2u - o - 2u - 4o - 3u - 2o - u - 2o - 4u - 3o - 2u - 2o - 2u$.
9. $i \le 3$: $u - 2o - u - 2o - 4u - 3o - 3u - 4o - 3u - 2o - 2u - 2o - u$.
10. $i \le 4$: $2u - 2o - 2u - 4o - 4u - 2o - u - 2o - 4u - 4o - 2u - 2o - 2u$.

We can also form a symmetrical and balanced knot by combining parts of the mirror imaged knots in Figs. 594 & 595 as depicted in Fig. 596. The half-cycle braiding algorithms for the interbraided knots X and Z in Fig. 596 are as follows:

Braiding knot X:

1. : Free run.
2. $i = 0$: $o - u - 3o - u$.
3. $i = 0$: $o - u - 3o - u$.
4. $i \le 1$: $3o - 2u - o - u - 4o - u$.
5. $i \le 1$: $3o - 2u - o - u - 4o - u$.
6. $i \le 2$: $3o - u - o - u - o - u - o - 2u - 4o - u - o - u$.
7. $i \le 2$: $3o - u - o - u - o - u - o - 2u - 4o - u - o - u$.
8. $i \le 3$: $u - 3o - 2u - o - u - 2o - u - 2o - 2u - o - u - 3o - 2u - o - u$.
9. $i \le 3$: $u - 3o - 2u - o - u - 2o - u - 2o - 2u - o - u - 3o - 2u - o - u$.
10. $i \le 4$: $o - u - 3o - 3u - o - 2u - 2o - u - o - u - o - 2u - 2o - u - 3o - 3u - o - u$.

Interbraiding knot Z:

1. : $u - o - u - 2o - 2u - o - u - o - 2u - 2o - u - o - u - o - 2u - 2o - u - 2o - 2u - o - u - o - u$.
2. $i = 0$: $u - o - u - 3o - 2u - o - u - o - 3u - 2o - u - 2o - u - o - 2u - 3o - u - 3o - 2u - o - u - 2o - u$.
3. $i = 0$: $u - o - u - 3o - 2u - o - u - o - 3u - 2o - u - 2o - u - o - 2u - 3o - u - 3o - 2u - o - u - 2o - u$.
4. $i \le 1$: $u - o - u - 4o - 2u - o - u - 2o - 3u - 2o - 2u - 2o - u - o - 3u - 3o - u - 4o - 2u - o - 2u - 2o - u$.
5. $i \le 1$: $u - o - u - 4o - 2u - o - u - 2o - 3u - 2o - 2u - 2o - u - o - 3u - 3o - u - 4o - 2u - o - 2u - 2o - u$.
6. $i \le 2$: $u - o - 2u - 4o - 2u - 2o - u - 2o - 3u - 3o - 2u - 2o - u - o - 4u - 3o - 2u - 4o - 2u - 2o - 2u - 2o - u$.
7. $i \le 2$: $u - o - 2u - 4o - 2u - 2o - u - 2o - 3u - 3o - 2u - 2o - u - o - 4u - 3o - 2u - 4o - 2u - 2o - 2u - 2o - u$.
8. $i \le 3$: $u - 2o - 2u - 4o - 3u - 2o - u - 2o - 3u - 4o - 2u - 2o - u - 2o - 4u - 3o - 3u - 4o - 3u - 2o - 2u - 2o - u$.
9. $i \le 3$: $u - 2o - 2u - 4o - 3u - 2o - u - 2o - 3u - 4o - 2u - 2o - u - 2o - 4u - 3o - 3u - 4o - 3u - 2o - 2u - 2o - u$.
10. $i \le 4$: $2u - 2o - 2u - 4o - 4u - 2o - u - 2o - 4u - 4o - 2u - 2o - 2u - 2o - 4u - 4o - 3u - 4o - 4u - 2o - 2u - 2o - u$.

Besides the above combination in Fig. 596 derived from the knots in Figs. 594 & 595, several other symmetrical and balanced combinations can be made, one of which is shown in Fig. 597. The half-cycle braiding algorithms for the interbraided knots X and Z in Fig. 597 are as follows:

Braiding knot X:

1. : Free run.
2. $i = 0$: $o - u - o - 2u$.
3. $i = 0$: $o - u - o - 2u$.

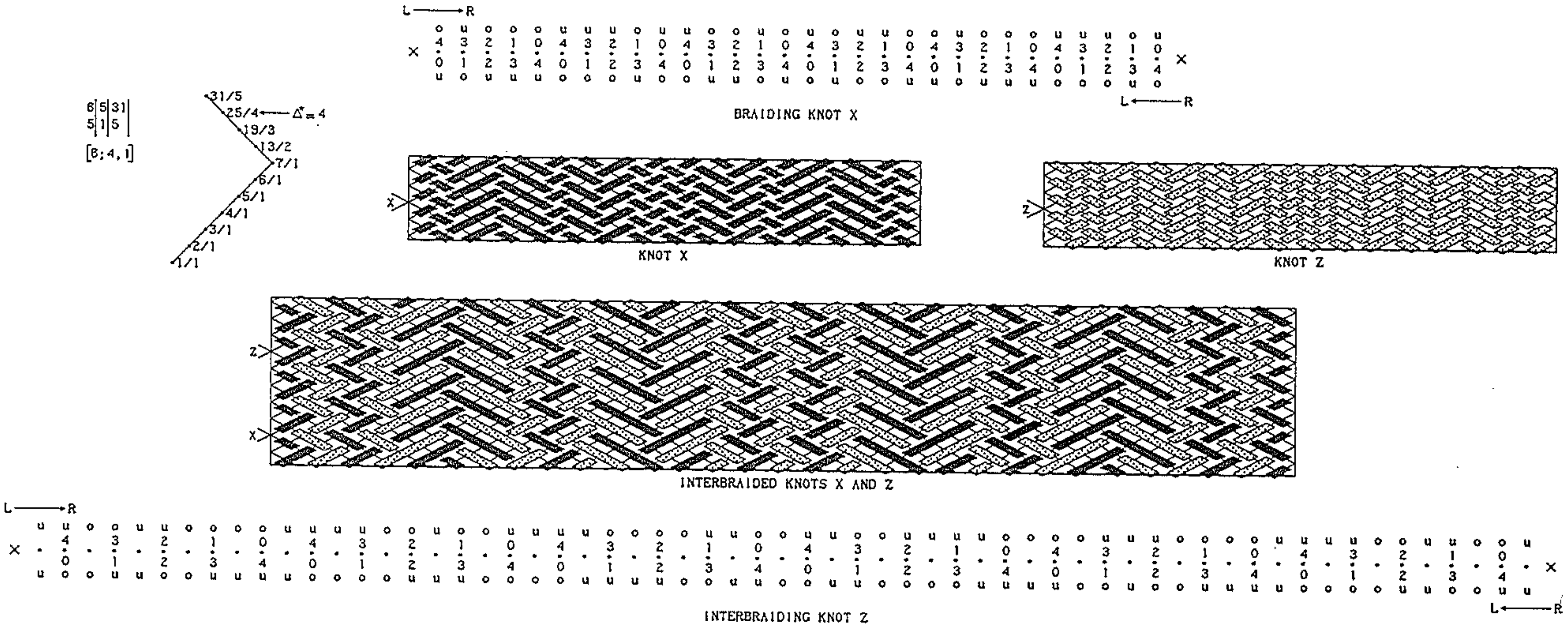

Fig. 596 — A knot derived by combining parts of the knots in Figs. 594 & 595.

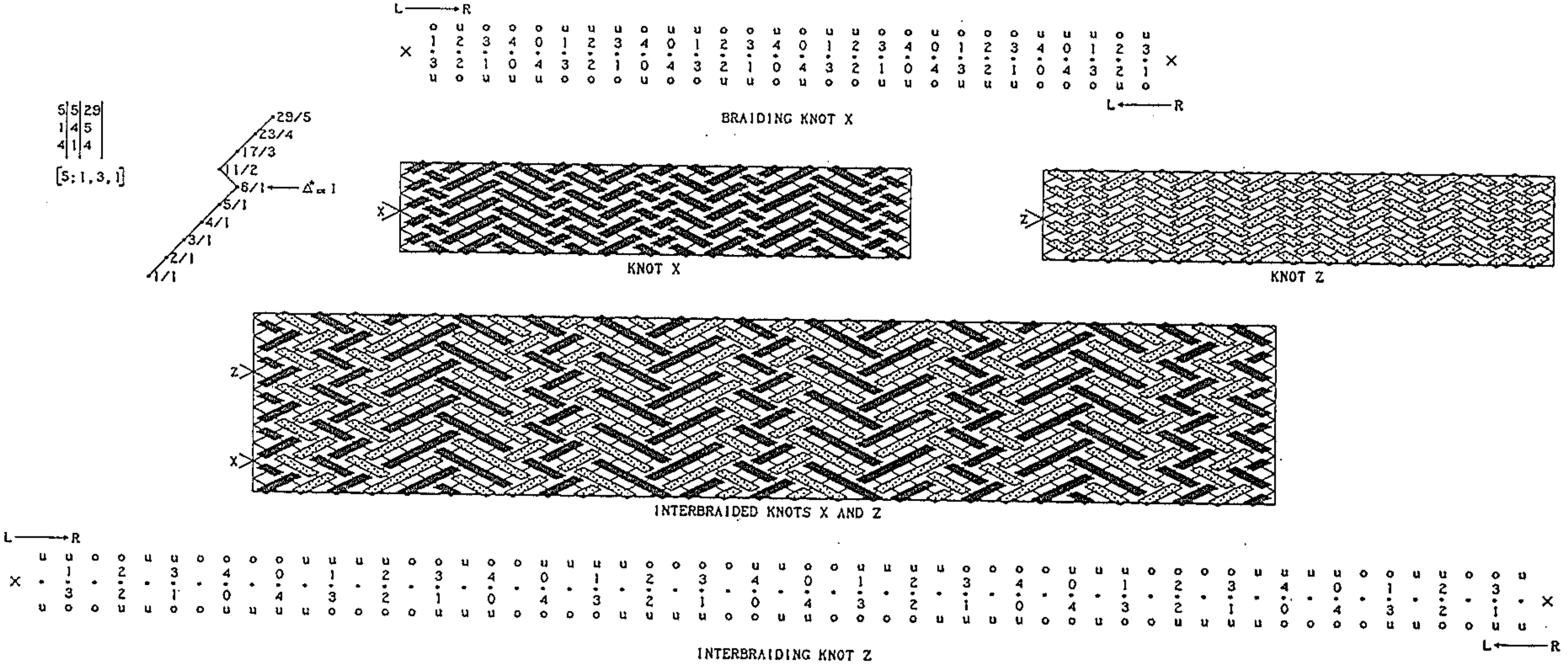

Fig. 597 — A knot derived by combining parts of the knots in Figs. 594 & 595.

4. $i \leq 1$: $2o - 3u - o - 2u - o - 2u$.
5. $i \leq 1$: $2o - 3u - o - 2u - o - 2u$.
6. $i \leq 2$: $o - u - o - 4u - 2o - 3u - 2o - 2u - o$.
7. $i \leq 2$: $o - u - o - 4u - 2o - 3u - 2o - 2u - o$.
8. $i \leq 3$: $o - u - 2o - 5u - 3o - 2u - o - u - 3o - 2u - o - u$.
9. $i \leq 3$: $o - u - 2o - 5u - 3o - 2u - o - u - 3o - 2u - o - u$.
10. $i \leq 4$: $o - u - 3o - 3u - o - 2u - 2o - u - o - 2u - 2o - u - 3o - 3u - o - u$.

Interbraiding knot Z :

1. : $u - o - u - 2o - 2u - o - u - o - 2u - 2o - u - o - 2u - 2o - u - 2o - 2u - o - u - o - u$.
2. $i = 0$: $u - o - u - 3o - 2u - o - u - o - 3u - 2o - u - 2o - 2u - 2o - 2u - 2o - 3u - o - u - o - u$.
3. $i = 0$: $u - o - u - 3o - 2u - o - u - o - 3u - 2o - u - 2o - 2u - 2o - 2u - 2o - 3u - o - u - o - u$.
4. $i \leq 1$: $2u - o - u - 3o - 3u - o - u - o - 4u - 2o - u - 2o - 3u - 2o - 3u - 2o - 3u - 2o - u - o - u$.
5. $i \leq 1$: $2u - o - u - 3o - 3u - o - u - o - 4u - 2o - u - 2o - 3u - 2o - 3u - 2o - 3u - 2o - u - o - u$.
6. $i \leq 2$: $2u - 2o - u - 3o - 4u - o - u - o - 4u - 3o - u - 2o - 4u - 2o - 3u - 3o - 3u - 2o - 2u - o - u$.
7. $i \leq 2$: $2u - 2o - u - 3o - 4u - o - u - o - 4u - 3o - u - 2o - 4u - 2o - 3u - 3o - 3u - 2o - 2u - o - u$.
8. $i \leq 3$: $2u - 2o - 2u - 3o - 4u - 2o - u - o - 4u - 4o - u - 2o - 4u - 3o - 3u - 4o - 3u - 2o - 2u - 2o - u$.
9. $i \leq 3$: $2u - 2o - 2u - 3o - 4u - 2o - u - o - 4u - 4o - u - 2o - 4u - 3o - 3u - 4o - 3u - 2o - 2u - 2o - u$.
10. $i \leq 4$: $2u - 2o - 2u - 4o - 4u - 2o - u - 2o - 4u - 4o - 2u - 2o - 4u - 4o - 3u - 4o - 4u - 2o - 2u - 2o - u$.

When we require the Interbraided Cylindrical Knot to have constricting ends, we can modify, as before, the Regular Cylindrical Braid to a Regular Nested Cylindrical Braid (a Nested Cylindrical Braid in general). The Interbraided Regular Cylindrical Knot of Fig. 592 has been modified to the Interbraided Regular Nested Cylindrical Knot of Fig. 598.

First we braid knot X; its left bight-boundary is 1 and its right bight-boundary is 3 in the final interbraid of the knots X, Y and Z. Then we interbraid knot Y; its left bight-boundary is 3 and its right bight-boundary is 1 in the final interbraid of the knots X, Y and Z. Finally we interbraid knot Z; its left bight-boundary is 2 and its right bight-boundary is 2 in the final interbraid of the knots X, Y and Z. Note that the coding of knot Z in Fig. 598 is identical to the coding of knot Z in Fig. 592, but that the codings of knots X and Y in Fig. 598 differ from their respective codings in Fig. 592. The half-cycle braiding algorithms for the respective braiding stages may be obtained from the algorithm diagrams in Fig. 598.

Braiding knot X :

1. : Free run.
2. $i = 0$: $2o - u$.
3. $i = 0$: $3o$.

4. $i \leq 1$: $u - o - u - o - 2u$.
5. $i \leq 1$: $u - o - u - 3o$.
6. $i \leq 2$: $o - u - 2o - u - o - 3u - o$.
7. $i \leq 2$: $2u - 2o - u - o - u - 2o - u$.
8. $i \leq 3$: $o - 2u - 2o - u - 2o - 2u - o - u - o$.
9. $i \leq 3$: $2u - 3o - u - 2o - u - 3o - u$.
10. $i \leq 4$: $o - 3u - 2o - 2u - 2o - 3u - o - u - o$.

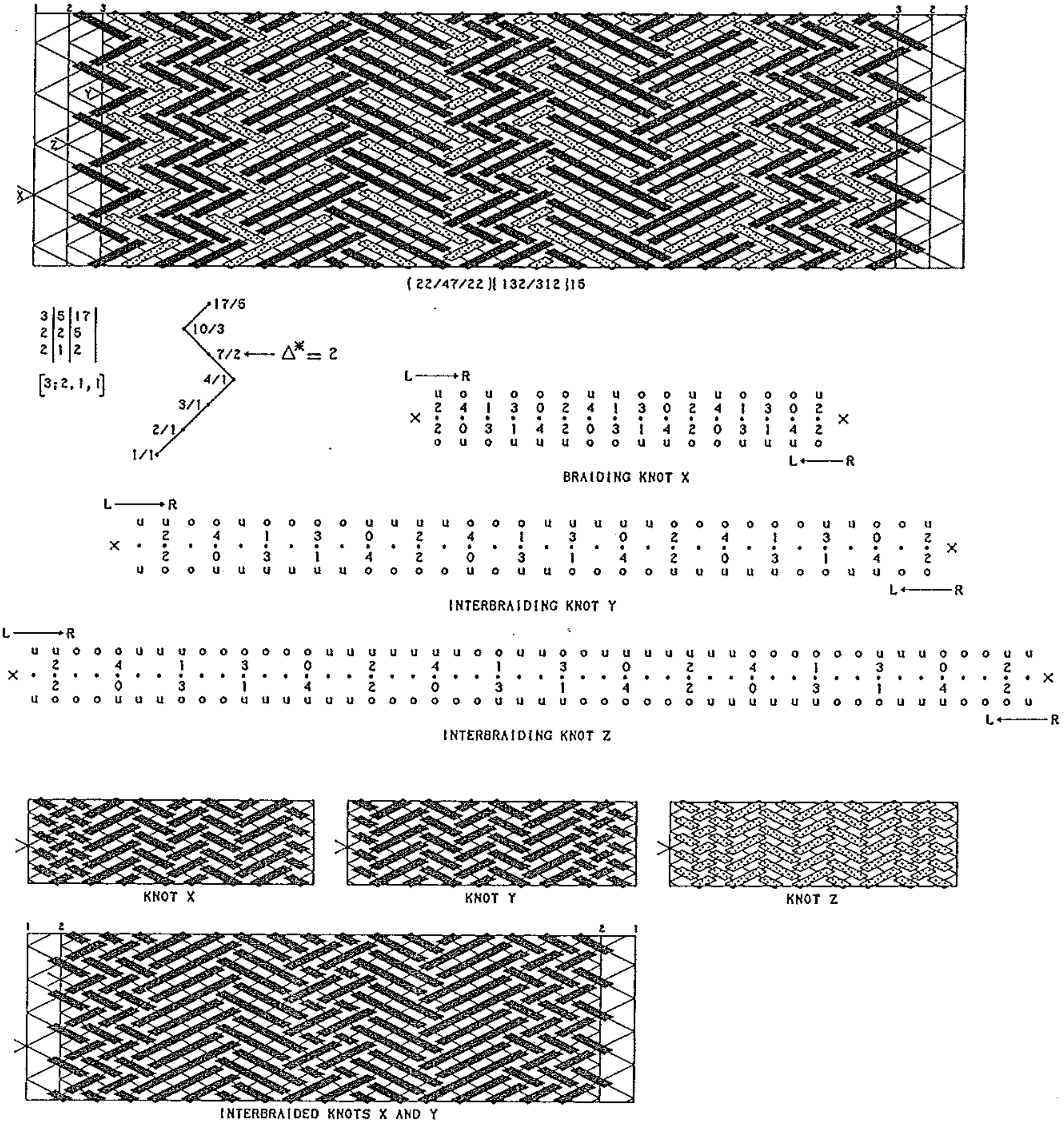

Fig. 598 — The Regular Nested interbraid of knots X, Y and Z.

Interbraiding knot Y:

1. : $u - o - u - 2o - 2u - o - 3u - 3o - u - o$.
2. $i = 0$: $o - u - o - 3u - 2o - u - o - u - 2o - 4u - o - u$.
3. $i = 0$: $u - o - u - 2o - 3u - o - 4u - 3o - u - 2o$.

4. $i \leq 1$: $o - u - 2o - 3u - 3o - u - o - u - 2o - 5u - o - u$.
5. $i \leq 1$: $u - o - u - 3o - 3u - 2o - 4u - 4o - u - 2o$.
6. $i \leq 2$: $2o - u - 2o - 4u - 3o - u - o - u - 3o - 5u - 2o - u$.
7. $i \leq 2$: $2u - o - u - 3o - 4u - 2o - 4u - 5o - u - 2o - u$.
8. $i \leq 3$: $2o - u - 2o - 5u - 3o - 2u - o - u - 3o - 6u - 2o - u$.
9. $i \leq 3$: $2u - o - u - 4o - 4u - 2o - 5u - 5o - 2u - 2o - u$.
10. $i \leq 4$: $2o - 2u - 2o - 5u - 4o - 2u - o - u - 4o - 6u - 2o - u$.

Interbraiding knot Z:

1. : $u - 2o - 2u - 4o - 5u - o - 2u - o - 5u - 4o - 2u - 2o - u$.
2. $i = 0$: $u - 2o - 2u - 2o - 5u - 4o - 2u - 5o - 4u - 2o - 3u - 2o - u$.
3. $i = 0$: $u - 2o - 2u - 5o - 5u - o - 2u - o - 6u - 4o - 2u - 3o - u$.
4. $i \leq 1$: $u - 2o - 2u - 3o - 5u - 4o - 3u - 5o - 5u - 2o - 3u - 2o - u$.
5. $i \leq 1$: $u - 2o - 3u - 5o - 5u - 2o - 2u - o - 6u - 5o - 2u - 3o - u$.
6. $i \leq 2$: $u - 3o - 2u - 3o - 5u - 5o - 3u - 6o - 5u - 2o - 3u - 3o - u$.
7. $i \leq 2$: $2u - 2o - 3u - 5o - 6u - 2o - 2u - o - 7u - 5o - 2u - 3o - 2u$.
8. $i \leq 3$: $u - 3o - 2u - 3o - 6u - 5o - 4u - 6o - 5u - 3o - 3u - 3o - u$.
9. $i \leq 3$: $2u - 2o - 3u - 6o - 6u - 2o - 2u - 2o - 7u - 5o - 3u - 3o - 2u$.
10. $i \leq 4$: $u - 3o - 3u - 3o - 6u - 6o - 4u - 6o - 6u - 3o - 3u - 3o - u$.

The Regular Nested interbraid of knots X and Y gives us also a useful symmetrical knot.

The Regular Nested interbraid of knots X and Z, depicted by the uppermost grid-diagram in Fig. 599, does not give us a useful knot, which is of course not surprising since knot X has no symmetrical coding-pattern whereas knot Z does have a symmetrical coding-pattern. We can again readily make two changes: one which does neither affect the coding of knot X nor the coding of knot Z, but only the coding of the interbraid, and one which extends knot X by two parts to the right in order to enable us to make its coding-pattern symmetrical (see in Fig. 599 knot X^*). The Δ^*-value of knot X^* is 1, and since the string-run of knot Z does not change, its Δ^*-value does not change either, hence remains equal to 2. The grid-diagram of the Regular Nested interbraid of knots X^* and Z is depicted in Fig. 599. First we braid knot X^* and next we interbraid it with knot Z. The associated half-cycle braiding algorithms are read from the respective algorithm diagrams in Fig. 599.

Braiding knot X^*:

1. : Free run.
2. $i = 0$: $3u$.
3. $i = 0$: $3o$.
4. $i \leq 1$: $o - 3u - o - u - o$.
5. $i \leq 1$: $u - 3o - u - o - u$.
6. $i \leq 2$: $o - 3u - o - u - 2o - u - o - u$.
7. $i \leq 2$: $u - 3o - u - o - 2u - o - u - o$.
8. $i \leq 3$: $o - u - o - 2u - 2o - u - 2o - 2u - o - u - o$.
9. $i \leq 3$: $u - o - u - 2o - 2u - o - 2u - 2o - u - o - u$.
10. $i \leq 4$: $o - u - o - 3u - 2o - 2u - 2o - 3u - o - u - o$.

Interbraiding knot Z:

1. : $u - o - u - 2o - 2u - o - u - o - 2u - 2o - u - o - u$.
2. $i = 0$: $u - o - u - o - 3u - 2o - u - 3o - 2u - o - 2u - o - u$.
3. $i = 0$: $u - o - u - 3o - 2u - o - u - o - 3u - 2o - u - 2o - u$.

4. $i \le 1:$ $u - o - u - 2o - 3u - 2o - 2u - 3o - 3u - o - 2u - o - u\,.$
5. $i \le 1:$ $u - o - 2u - 3o - 2u - 2o - u - o - 3u - 3o - u - 2o - u\,.$
6. $i \le 2:$ $u - 2o - u - 2o - 3u - 3o - 2u - 4o - 3u - o - 2u - 2o - u\,.$
7. $i \le 2:$ $2u - o - 2u - 3o - 3u - 2o - u - o - 4u - 3o - u - 2o - 2u\,.$
8. $i \le 3:$ $u - 2o - u - 2o - 4u - 3o - 3u - 4o - 3u - 2o - 2u - 2o - u\,.$
9. $i \le 3:$ $2u - o - 2u - 4o - 3u - 2o - u - 2o - 4u - 3o - 2u - 2o - 2u\,.$
10. $i \le 4:$ $u - 2o - 2u - 2o - 4u - 4o - 3u - 4o - 4u - 2o - 2u - 2o - u\,.$

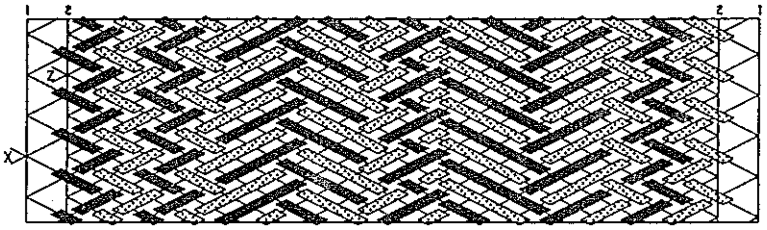

INTERBRAIDED KNOTS X AND Z

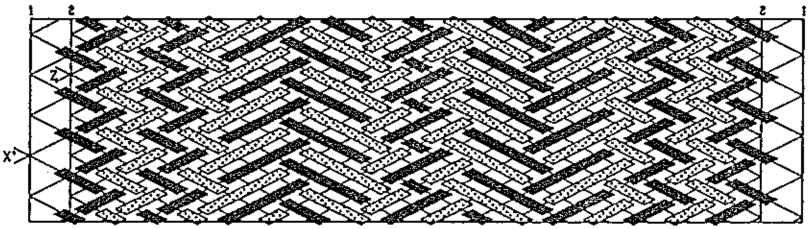

INTERBRAIDED KNOTS X* AND Z

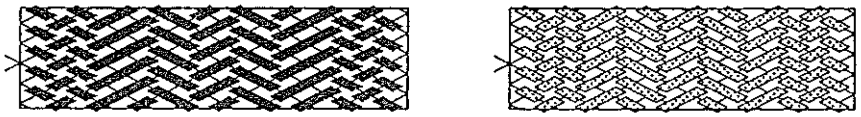

KNOT X*   KNOT Z

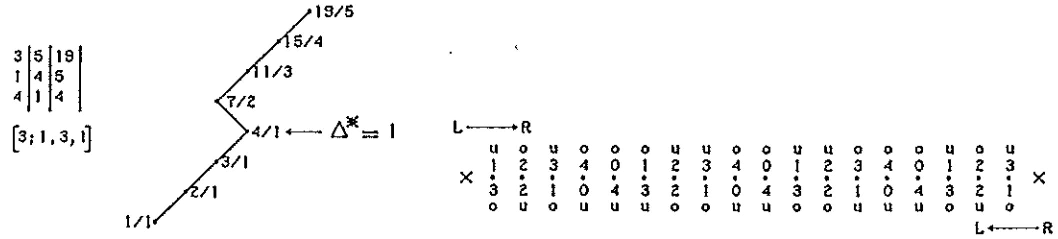

BRAIDING KNOT X*

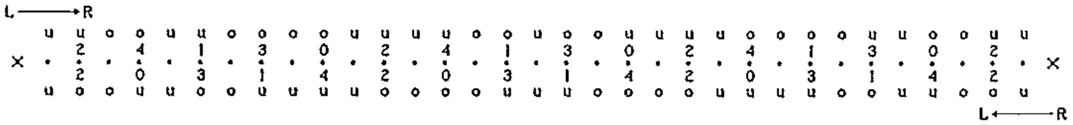
L → R
u u o o u u o o o o u u u u o o u o o u u u u o o o o u u o o u u
2 4 1 3 0 2 4 1 3 0 2 4 1 3 0 2
X X
2 0 3 1 4 2 0 3 1 4 2 0 3 1 4 2
u o o u u o o u u u u o o o o u u u o o o o u u u u o o u u o o u
L ← R

INTERBRAIDING KNOT Z

Fig. 599 — The Regular Nested interbraids of knots X^* and Z.

Two further Regular Nested interbraids of knots X^* and Z are depicted in Fig. 600. The half-cycle braiding algorithms for knot X^* are for both interbraids in Fig. 600 the half-cycle braiding algorithms for knot X^* on pg. 751.

The half-cycle braiding algorithms for interbraiding knot Z as in the uppermost interbraid of Fig. 600 are read from the uppermost algorithm diagram in Fig. 600.

Interbraiding knot Z :

1. : $u - o - u - 2o - 2u - 3o - 2u - 2o - u - o - u\,.$
2. $i = 0:$ $u - o - u - o - 3u - 2o - u - 3o - 2u - o - 2u - o - u\,.$

3. $i=0$: $u-o-u-3o-2u-3o-3u-2o-u-2o-u$.
4. $i\leq 1$: $u-o-u-2o-3u-2o-2u-3o-3u-o-2u-o-u$.
5. $i\leq 1$: $u-o-2u-3o-2u-4o-3u-3o-u-2o-u$.
6. $i\leq 2$: $u-2o-u-2o-3u-3o-2u-4o-3u-o-2u-2o-u$.
7. $i\leq 2$: $2u-o-2u-3o-3u-4o-4u-3o-u-2o-2u$.
8. $i\leq 3$: $u-2o-u-2o-4u-3o-3u-4o-3u-2o-2u-2o-u$.
9. $i\leq 3$: $2u-o-2u-4o-3u-5o-4u-3o-2u-2o-2u$.
10. $i\leq 4$: $u-2o-2u-2o-4u-4o-3u-4o-4u-2o-2u-2o-u$.

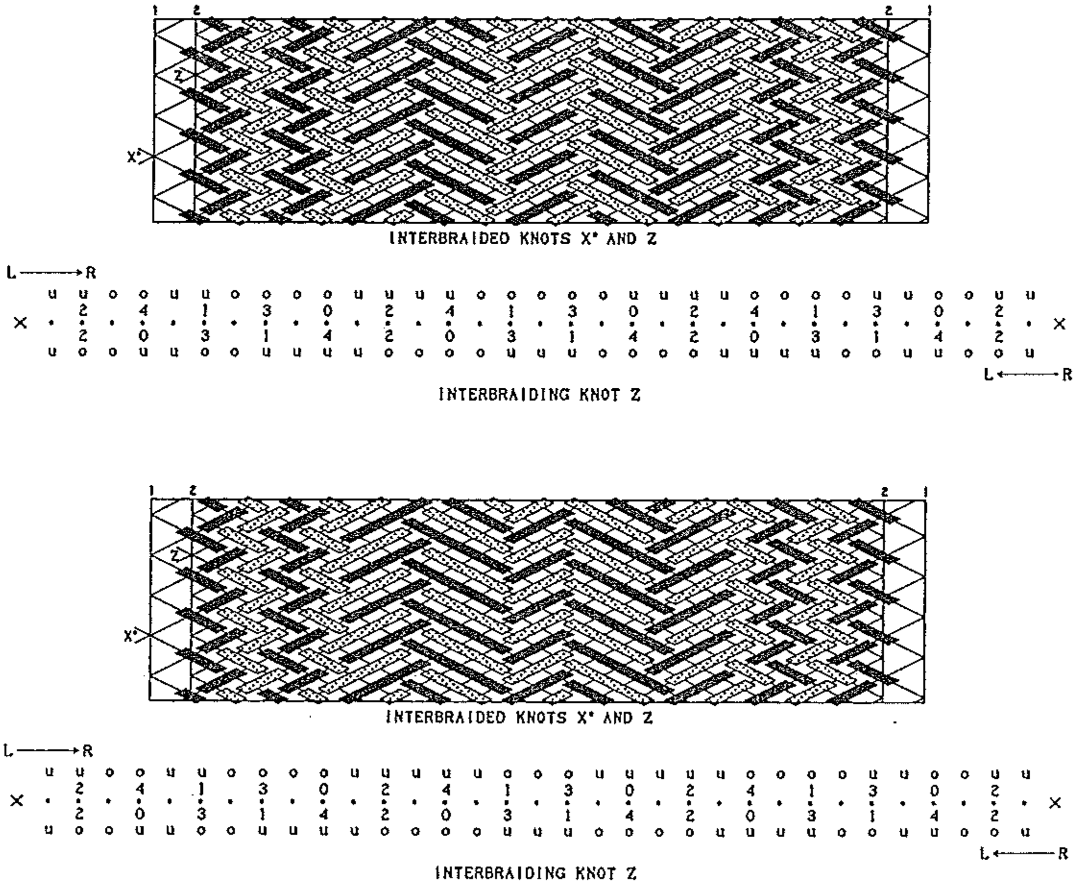

Fig. 600 — Two further Regular Nested interbraids of knots X^* and Z.

The half-cycle braiding algorithms for interbraiding knot Z as in the lowermost interbraid of Fig. 600 are read from the lowermost algorithm diagram in Fig. 600.

Interbraiding knot Z:

1. : $u-o-u-2o-3u-o-3u-2o-u-o-u$.
2. $i=0$: $u-o-u-o-3u-2o-u-3o-2u-o-2u-o-u$.
3. $i=0$: $u-o-u-3o-3u-o-4u-2o-u-2o-u$.
4. $i\leq 1$: $u-o-u-2o-3u-2o-2u-3o-3u-o-2u-o-u$.
5. $i\leq 1$: $u-o-2u-3o-3u-2o-4u-3o-u-2o-u$.
6. $i\leq 2$: $u-2o-u-2o-3u-3o-2u-4o-3u-o-2u-2o-u$.
7. $i\leq 2$: $2u-o-2u-3o-4u-2o-5u-3o-u-2o-2u$.
8. $i\leq 3$: $u-2o-u-2o-4u-3o-3u-4o-3u-2o-2u-2o-u$.
9. $i\leq 3$: $2u-o-2u-4o-4u-3o-5u-3o-2u-2o-2u$.
10. $i\leq 4$: $u-2o-2u-2o-4u-4o-3u-4o-4u-2o-2u-2o-u$.

We can of course also derive useful Regular Cylindrical interbraids from the Regular Nested Cylindrical interbraids. For example, from the Regular Nested Cylindrical interbraids in Figs. 599 & 600 we readily derive the Regular Cylindrical interbraids of Fig. 601. The half-cycle braiding algorithm for knot X^{**} are read from its algorithm diagram. Note that the respective algorithm diagrams for interbraiding knot Z do not change, hence their respective associated half-cycle braiding algorithms don't change.

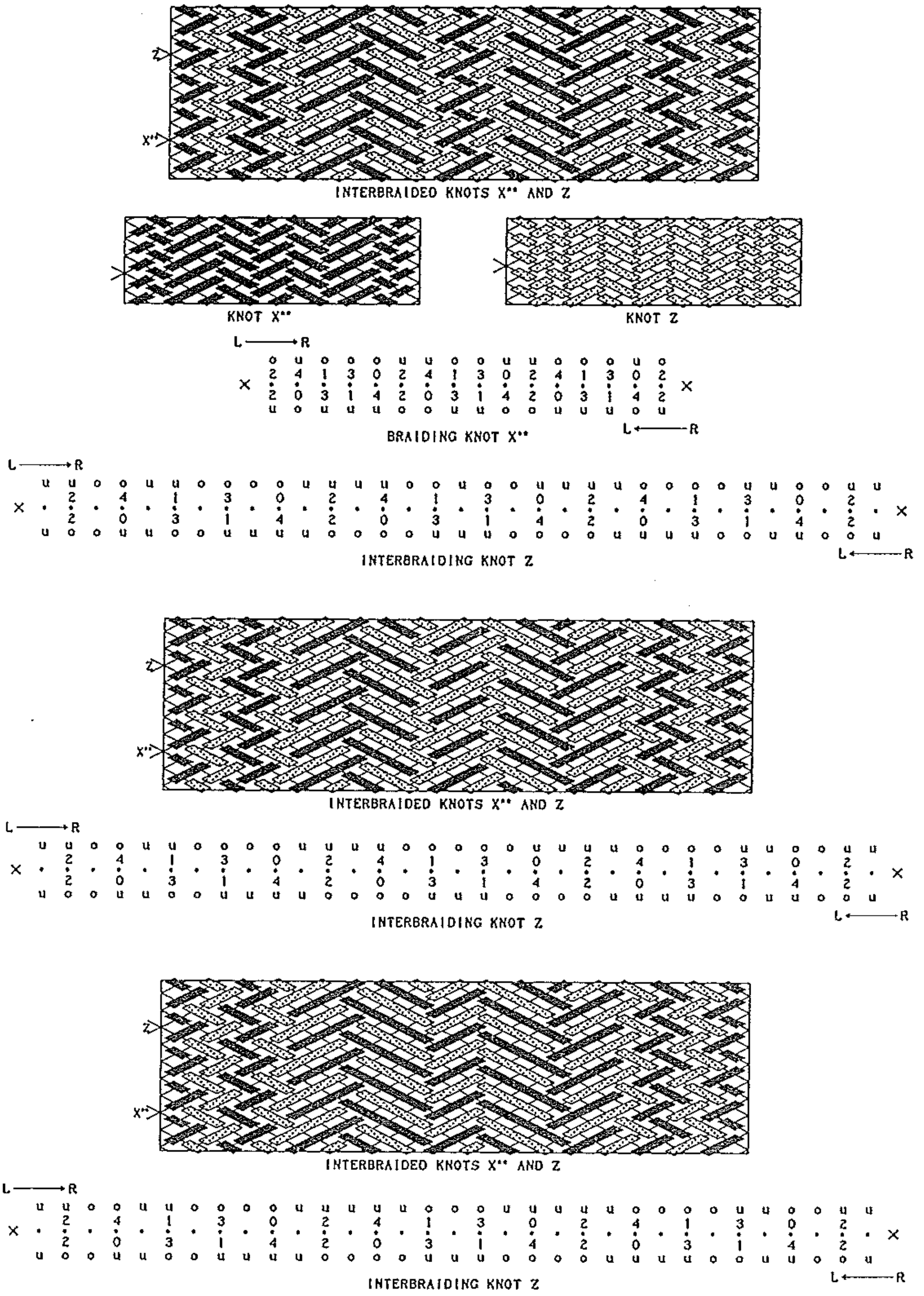
Z
X**
INTERBRAIDED KNOTS X** AND Z
KNOT X**
KNOT Z
L → R
o u o o o u u o o u u o o o u o
X 2 4 1 3 0 2 4 1 3 0 2 4 1 3 0 2 X
2 0 3 1 4 2 0 3 1 4 2 0 3 1 4 2
u o u u u o o u u o o u u u o u
L ← R
BRAIDING KNOT X**
L → R
u u o o u u o o o o u u u u o o u o o u u u u o o o o u u o o u u
X 2 4 1 3 0 2 4 1 3 0 2 4 1 3 0 2 X
2 0 3 1 4 2 0 3 1 4 2 0 3 1 4 2
u o o u u o o u u u u o o o o u u u o o o o u u u u o o u u o o u
L ← R
INTERBRAIDING KNOT Z
Z
X**
INTERBRAIDED KNOTS X** AND Z
L → R
INTERBRAIDING KNOT Z
L ← R
Z
X**
INTERBRAIDED KNOTS X** AND Z
L → R
INTERBRAIDING KNOT Z
L ← R

Fig. 601 — Interbraided Regular Knots derived from the interbraids in Figs. 599 & 600.

The Braider

APPENDIX 2002

CONTENTS

pg.

Leading Braiders up the Garden Path .... *i*

Errata — *The Braider* .... *iv*

A quarterly publication
for
the braiding artisan

Resale of this publication or copies thereof
is strictly prohibited

Copyright ©2002 by:

A.G. Schaake; 21 Sundown Cresc.; Hamilton; New Zealand.
D. Van Tassel; Box 335; Craig, Co 81626-0335; U.S.A.
F.J.M. Masurel; Ganzenzijde 4; 2317XG Leiden; Nederland.

All rights reserved. No part of this publication may be reproduced, stored in a retrieval system, or transmitted, in any form or by any means, electronic, mechanical, photo-copying, recording, or otherwise, without prior written permission.

This publication is available to braiding artisans only.

Copies may be obtained from:

A.G. Schaake,
21 Sundown Cresc.,
Hamilton,
New Zealand.

SEE NOTE BELOW.

No. 31

NOTE: the first Fig. number in this Issue is 554, but should have been 584 instead. Hence the Fig. numbers 554 - 583 not only appear in *The Braider*, Issue No. 30, but the numbers 554 - 574 appear again in *The Braider*, Issue No. 31 and the numbers 575 - 583 appear again in *The Braider*, Issue No. 32. This was noted too late for rectification.

No. 32

See NOTE under No. 31 above.

Leading Braiders up the Garden Path

We received four pages of instructions of *How to Braid a Four Strand Leather Rope Braid* which were obtained from an internet web site apparently associated with W. J. Budd from 779 Cessna Ct., Spring Creek, NV 89815, U.S.A. The braiding instructions are accompanied by eight photographs. The top of the four strands of uniform width were left attached and this attached top-part piece of leather, after dampening it slightly, was folded in half so that two strands were on the front-side and two strands were on the back-side with the skin side out and the flesh side in. The presented constructional procedure is depicted in Fig. 1.

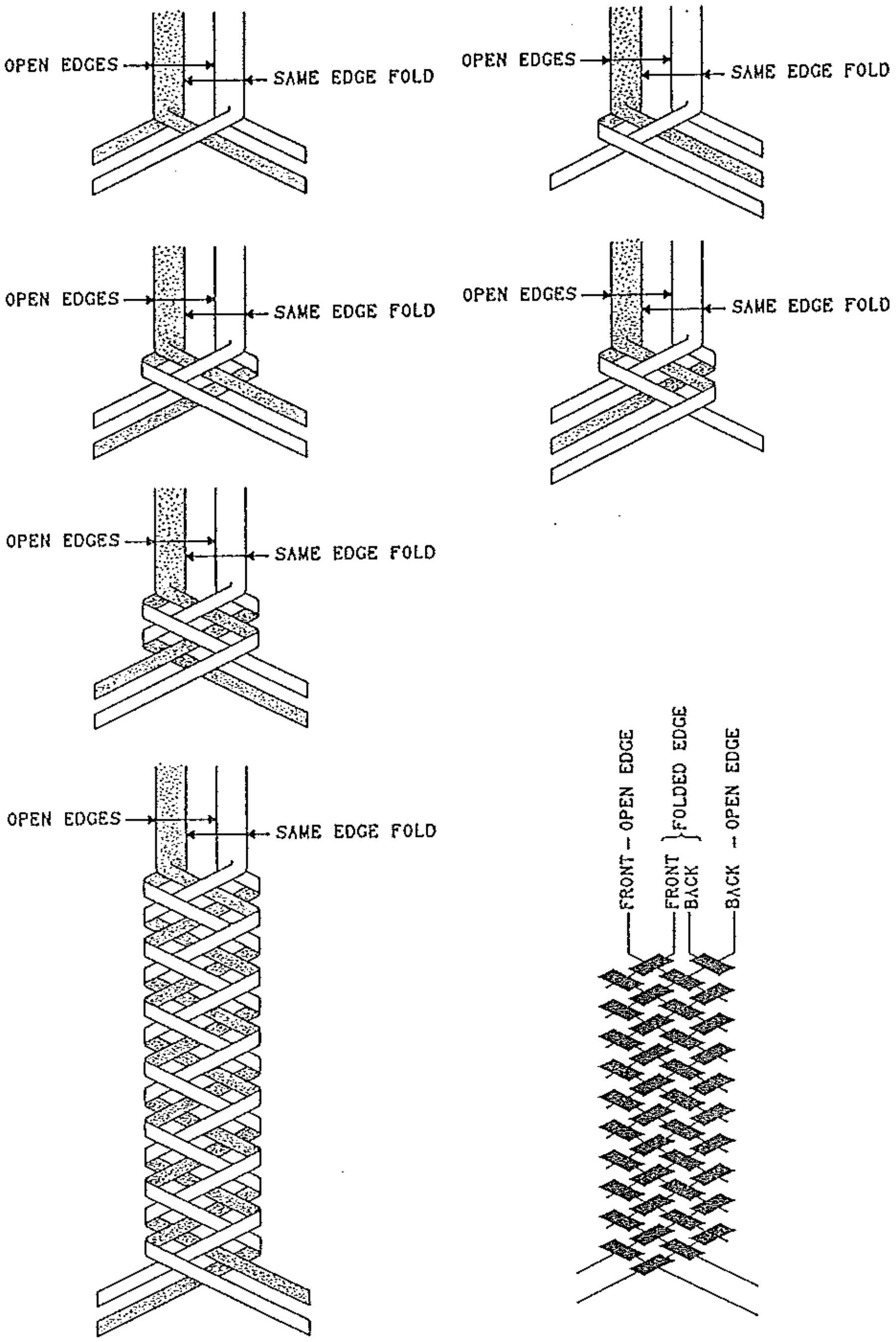

Fig. 1 — The constructional procedure presented on the internet web site.

The second sentence of the presented instruction (depicted by the uppermost left figure in Fig. 1): *Cross the strands on both sides, always keep the skin side out and the flesh side in. Take the strand on the right and go over, on the back take the one on the right and go under.*, is wrong and should have been replaced by: *Take (on the front) the strand on the right and go over (the strand on the left); on the back take the one on the* **left** *and go* **under** *(the one on the right).* The grid-diagram of the presented constructional procedure (see lowermost right figure in Fig. 1) shows clearly the error in the presented constructional procedure.

However, even with the correction of this error, the resulting constructional procedure should not be followed. Instead either the constructional procedure depicted in Fig. 2 or depicted in Fig. 3 should be adopted.

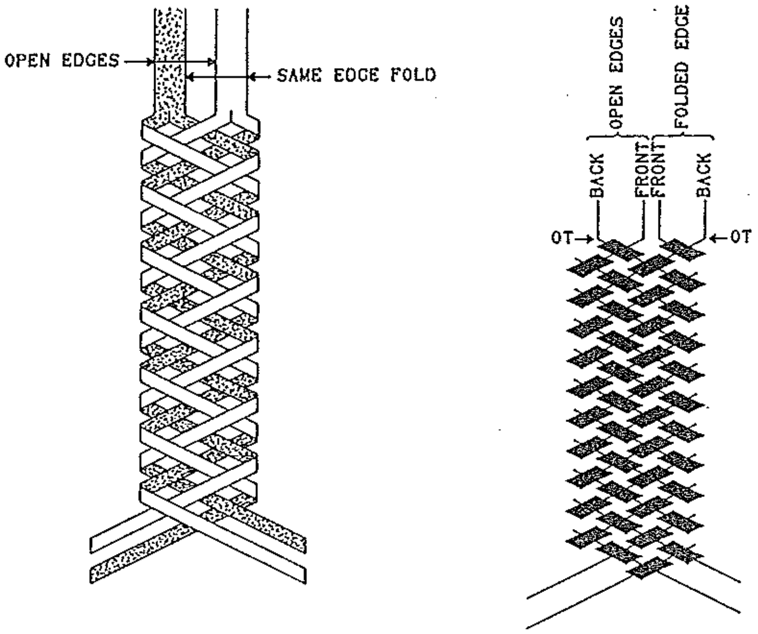

Fig. 2 — A correct constructional procedure.

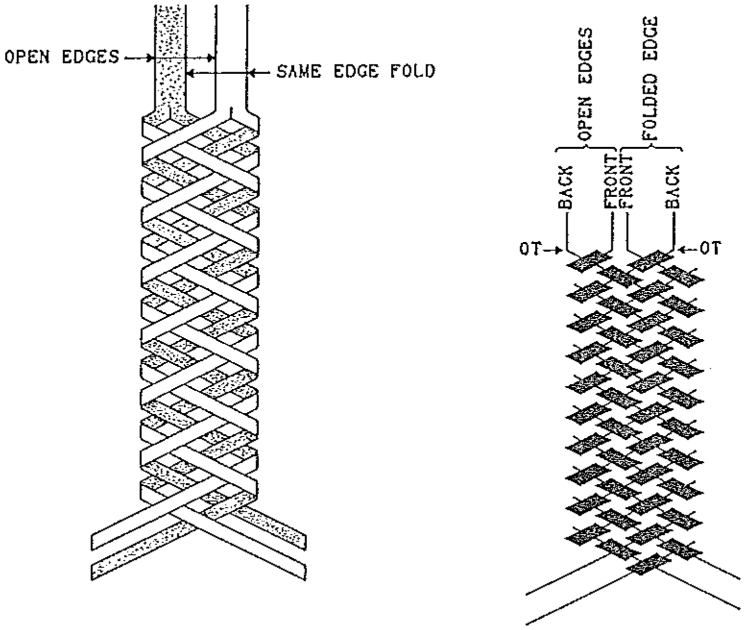

Fig. 3 — A correct constructional procedure.

On page 687, Example 5, it states: "From Fig. 562 we observe that a period consists of 7 consecutive bights, …". Fig. 562 could be confusing and should therefore be replaced by the Figure below.

Furthermore on the bottom of page 687, it states: "Thus for $B_c = 35$, for example, we obtain a single string Cylindrical Braid". This has been depicted in the diagram below.

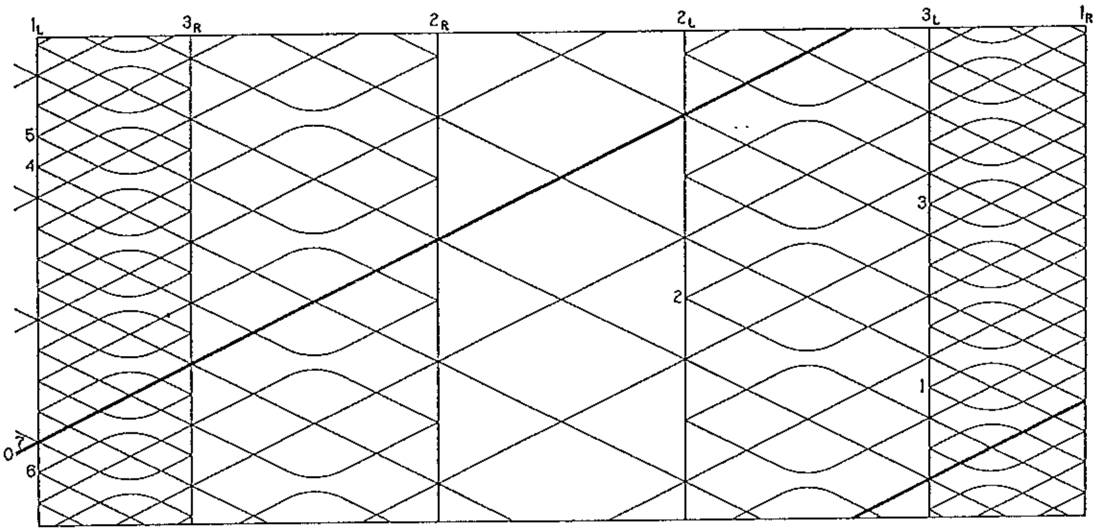

A PERIOD CONSISTS OF THE BIGHTS IN THE FIRST-RETURN STRING-RUN; HENCE CONSISTS OF α CONSECUTIVE BIGHTS

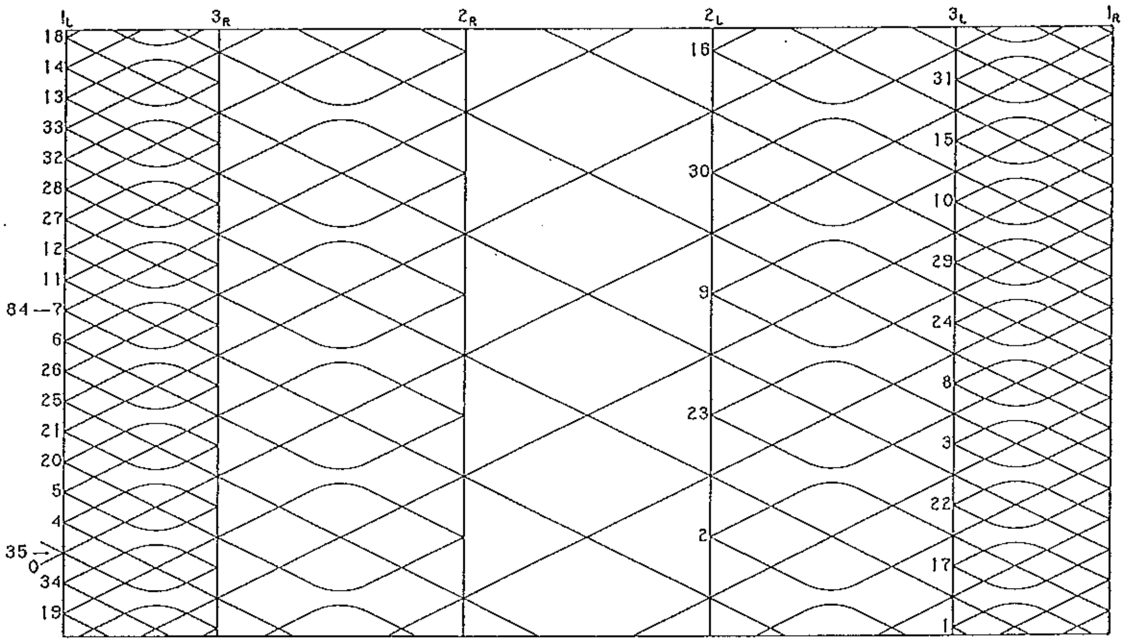

ERRATA—*THE BRAIDER*

The list below lists the typing errors which were noted in at least some copies of the following Issues of *The Braider.*

No. 1

pg. 3, line 9 — **it is**
pg. 3, line 10 — **unnecessarily**
pg. 3, line 17 — in order **to** present
pg. 12, line 5 under "An Introduction to Flat Braids" — Four pages are devoted **to**
pg. 16, line 9 under "Reviews" — **instructor**

No. 2

pg. 21, line 2 — delete **that**
pg. 28, line 6 — However, **a** one colour
pg. 38, line 18 under "Reviews" — **they** are first class

No. 3

pg. 42, line 2 — Naturally, **queries** not directly

No. 4

pg. 76, line 5 — **phenomenon**
pg. 81, line 16 — **phenomenon**

No. 5

pg. 87, line 3 from bottom of page — **exclude**
pg. 106, line 11 — **locality**

No. 6

pg. 129, line 15 — 2-**colour**

No. 7

No. 8

pg. 158, line 3 — Hence **the** number of bights
pg. 161, line 12 — In Fig. 144 are depicted the **parts-raising** processes

No. 9

No. 10

pg. 213, line 2 — **choose**

No. 11

pg. 232, line 17 — in **general**
pg. 245, line 8 — in **general**

No. 12

pg. 257, line 6 — or $B = \{(2m+2)(\alpha+1)-1\}N-(\alpha+1)$ bights
pg. 257, line 7 — Those with $B = \{(2m+2)(\alpha+1)-1\}N-(\alpha+1)$ bights
pg. 257, line 9 — $b = \{(2m+2)\alpha-1\}N-\alpha$ bights. Those with $B = \{(2m+2)(\alpha+1)-1\}N+(\alpha+1)$ bights
pg. 257, line 10 & 11 — with $p = \{(2m+2)\alpha-1$ parts and $b = \{(2m+2)\alpha-1\}N+\alpha$ bights
pg. 257, line 7 from bottom — delete **thinspace**

No. 13

pg. 276, line 7 — in **general**

No. 14

pg. 308, line 3 — in **general**

No. 15

pg. 338, line 1 — **independent**

No. 16

pg. 347, line 3 — $P = 2m(\alpha+1)+1$
pg. 353, line 16 — **screw**
pg. 356, line 3 — **two**
pg. 359, line 5 under Fig. 310 — **boundary**
pg. 361, line 3 from bottom — **Headhunter's**-coded
pg. 366, line 30 — **braided**

No. 17

pg. 369, line 12 — **mathematical**
pg. 372, lines 8, 9, 10, 13 — **positive**
pg. 383, line 13 — Figs. **326–328**
pg. 387, line 2 below Fig. 332 — in **general**
pg. 387, line 13 below Fig. 332 — **cases**

No. 18

pg. 393, the right-hand brace } immediately before the second equal sign is missing in the three lines above the upper .... line, and the right-hand brace } immediately before the third equal sign is missing in the first line below the upper .... line.
pg. 395, line 4 — **additionally**
pg. 396, bottom line — in **general**
pg. 397, line 4 from bottom — in **general**
pg. 412, Fig. 345 immediately below the sixth diagram — change $o-u-o-u$ to $u-o-u-o$.
pg. 413, Fig. 346 leftmost diagram in second row of diagrams: the two non coded crossing points should have been provided with an under coding each for the braiding direction indicated.

No. 19

pg. 419, lines 2 & 3 from bottom — in **general**
pg. 420, last line — $\Delta_{r_i} = 0$ for $r_i = 4$.
pg. 421, line 2 — $(12/19/113)\{1_1 1_2 2_4 3_3/1_1 1_2 3_3 1_4 4_5 2_6\}24$
pg. 430, lines 3 & 5 — in **general**

No. 20

pg. 446, line 14 — A few **simple** examples
pg. 446, line 3 from bottom — in **general**
pg. 447, Footnote — **These** are the
pg. 450, last line — delete **thinspace**
pg. 464, line 20 — Brion Toss

No. 21

pg. 465, line 16 — in **general**

No. 22

pg. 493, second line under "Question on pg. 479" — **appliqué**

No. 23

pg. 516, line 3 — **categorisation**
pg. 523, line 14 — **Fig. 445**

No. 24

pg. 537, line 2 — **arises**
pg. 537, line 14 — **actual**
pg. 545, line 1 — read as: greater than or equal to 2 and less than p

No. 25

pg. 563, line 19 — read as: greater than or equal to 2 and less than p

No. 26

pg. 593, line 6 — delete parenthesis after half-cycle

No. 27

pg. 631, line 18 — **Herringbone**
pg. 633, line 33 — **Herringbone**
pg. 634, line 3 — **Herringbone**

No. 28

pg. 640, line 2 — **algorithms**
pg. 647, lines 11 & 20 below Fig. 517 — **finished**
pg. 648, lines 1, 10, 19, 28, 37 & 46 — **finished**
pg. 649, lines 8 & 17 — **finished**
pg. 650, line 4 — read as: greater than 1 and less than or equal to 17
pg. 650, lines 5 & 6 — read as: greater than or equal to 3 and less than or equal to 17
pg. 650, line 4 below Fig. 519 — read as: greater than 1 and less than or equal to 23

pg. 650, line 6 below Fig. 519 — read as: greater than or equal to 3 and less than or equal to 23
pg. 651, line 3 — read as: greater than or equal to 2 and less than or equal to 8
pg. 651, line 4 below Fig. 521 — read as: greater than or equal to 2 and less than or equal to 12

No. 29

pg. 677, next to last line — usual

No. 30

pg. 704, line 9 from bottom — can be made

No. 31

NOTE: the first Fig. number in this Issue is 554, but should have been 584 instead. Hence the Fig. numbers 554 - 583 not only appear in *The Braider*, Issue No. 30, but the numbers 554 - 574 appear again in *The Braider*, Issue No. 31 and the numbers 575 - 583 appear again in *The Braider*, Issue No. 32. This was noted too late for rectification.

No. 32

See NOTE under No. 31 above.

No. 33

pg. 757, lines 1 and 5 — Any one
pg. 761, line 21 — delete parenthesis after half-cycle
pg. 768, line 1 — reality
pg. 782, line 4 — misrepresentation
pg. 782, line 29 — whereas

No. 34

pg. 793, line 2 — any one
pg. 794, lines 19 and 23 — Any one
pg. 797, line 3 from bottom — (see pg. 794)
pg. 797, line 4 from bottom and last line — the nest-index number
pg. 800, line 3 from bottom — crossings between the right-hand

No. 35

No. 36

Cover sheet — Hobbles
pg. 831, lines 1 and 2 — Hobbles
pg. 831, line 6 — knuckles
pg. 831, line 7 twice, 11, 13, 15, 21 — hobbles
pg. 831, line 19 — approximately
pg. 832, line 7 — hobbles

THE BRAIDER

No.33 **FEBRUARY 2003.**

CONTENTS

pg.

Nested Cylindrical Braids 755

Designing Interbraided Knots 767

Historical events and their fictitious renderings 782

A quarterly publication for the braiding artisan

Resale of this publication or copies thereof is strictly prohibited

Copyright ©2003 by :

A.G. Schaake; 21 Sundown Cresc.; Hamilton; New Zealand.
D. Van Tassel; Box 335; Craig, Co 81626-0335; U.S.A.
F.J.M. Masurel; Ganzenzijde 4; 2317XG Leiden; Nederland.

All rights reserved. No part of this publication may be reproduced, stored in a retrieval system, or transmitted, in any form or by any means, electronic, mechanical, photo-copying, recording, or otherwise, without prior written permission.

This publication is available to braiding artisans only.

Copies may be obtained from :

A.G. Schaake,
21 Sundown Cresc.,
Hamilton,
New Zealand.

Nested Cylindrical Braids

The Asymmetric Regular Nested Cylindrical Braids:

The Asymmetric Regular Nested Cylindrical Braids have the bight-boundary position specifications $222\cdots$ with $\mathcal{K}_l = A_l$ and $\mathcal{K}_r = A_r$. Their respective left and right sequence sets are:

$$1A_l(A_l-1)(A_l-2)(A_l-3)\cdots 432\,, \text{ and}$$
$$k|k+1|_{A_r}|k+2|_{A_r}|k+3|_{A_r}\cdots A_r123\cdots|k-2|_{A_r}|k-1|_{A_r}\,,$$

where $1 \le k \le A_r$ and $A_r \ne A_l$.

Due to these sequence sets there is no need to carry the ranking numbers, and consequently we obtain for a general left and right cycle (see Fig. 602):

$$l_{i+1} = |l_i + 2A_r + x - 2(l_i + r_i)|_{A_l}\,.$$
$$r_{i+1} = |r_i + 2A_l + x - 2(r_i + l_{i+1})|_{A_r}\,.$$

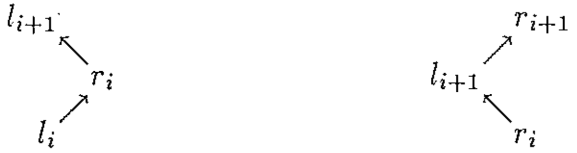

Fig. 602 — A general left and right cycle associated with the Asymmetric Regular Nested Cylindrical Braids.

The further formulae on pg. 417 modify to:

$$B_l^* = \text{number of periods at left bight-edge}.$$
$$B_r^* = \text{number of periods at right bight-edge}.$$
$$B_{total} = A_l B_l^* = A_r B_r^* = A^{**}B^{**}\,.$$
$$d = \text{g.c.d.}(A_l\,,\, A_r)\,.$$
$$A^{**} = \frac{B_{total}}{B^{**}} = \frac{A_l \cdot A_r}{d}\,.$$
$$B^{**} = \frac{B_{total} \cdot d}{A_l \cdot A_r} = \frac{B_l^* \cdot d}{A_r} = \frac{B_r^* \cdot d}{A_l}\,.$$
$$\alpha = \text{number of bights in first-return string-run}.$$
$$P_{component} = \frac{\alpha \cdot x + 2\alpha(A_l + A_r) - 2\sum(l_i + r_i)}{A^{**}}\,.$$
$$P_{total} = \sum P_{component} = A_l + A_r + x - 2\,.$$

$$\left.\begin{array}{r}\text{number of}\\ \text{components}\end{array}\right\} = \text{number of first-return string-runs}.$$

$$\left.\begin{array}{r}\text{number of}\\ \text{sub-components}\\ \text{in a component}\end{array}\right\} = \text{g.c.d.}(P_{component}\,, B^{**})\,.$$

$$\left.\begin{array}{r}\text{total number of}\\ \text{essential strings}\end{array}\right\} = \sum \text{sub-components}\,.$$

Example :

Let $A_l = 5$; $A_r = 3$; $x = 13$; $B = B_{total} = 30$; $l_1 = 1$; $r_1 = k = 1$. Consequently the string-run specification of this Asymmetric Regular Nested Cylindrical Braid is (2222/13/22){15432/123}30 . Hence:

$$B_l^* = \frac{B}{A_l} = \frac{30}{5} = 6 .$$

$$B_r^* = \frac{B}{A_r} = \frac{30}{3} = 10 .$$

$$d = \text{g.c.d.}\,(A_l\,,\ A_r) = \text{g.c.d.}\,(5\,,\ 3) = 1 .$$

$$A^{**} = \frac{A_l \cdot A_r}{d} = \frac{5 \cdot 3}{1} = 15 .$$

$$B^{**} = \frac{B_{total} \cdot d}{A_l \cdot A_r} = \frac{30 \cdot 1}{5 \cdot 3} = 2 .$$

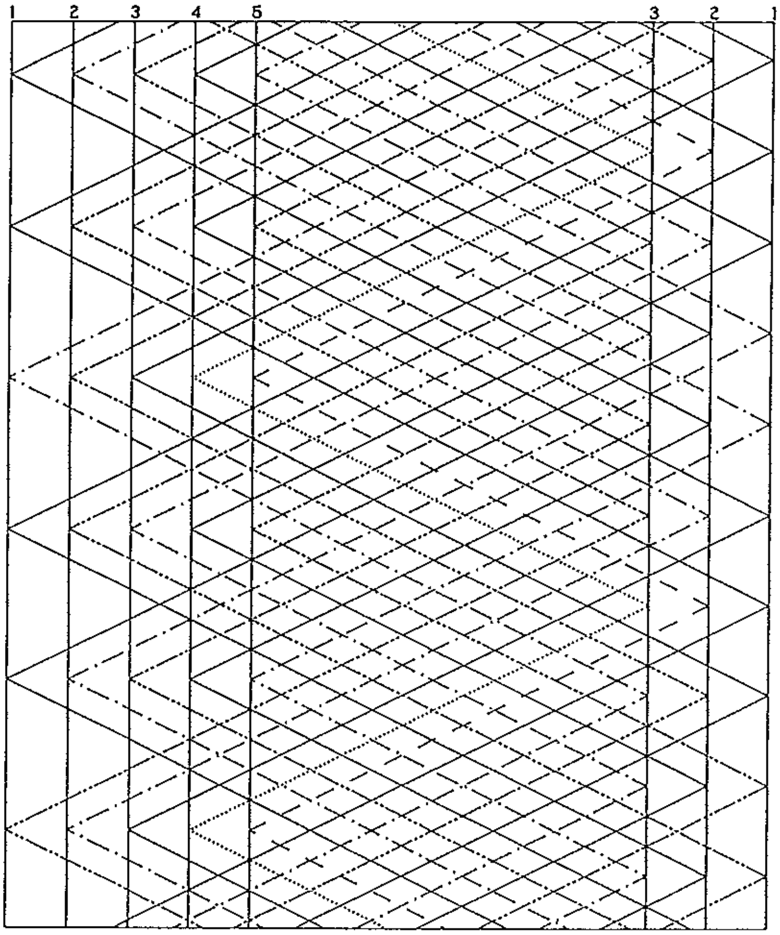

Fig. 603 — The string-run diagram of our Example.

From the given Asymmetric Regular Nested Cylindrical Braid specification we can read the lower-left to upper-right half-cycle types:

$1 \longrightarrow 1$
$2 \longrightarrow 2$
$3 \longrightarrow 1$
$4 \longrightarrow 3$
$5 \longrightarrow 2$

$1 \longrightarrow 2$
$2 \longrightarrow 1$
$3 \longrightarrow 3$
$4 \longrightarrow 2$
$5 \longrightarrow 1$

$1 \longrightarrow 3$
$2 \longrightarrow 3$
$3 \longrightarrow 2$
$4 \longrightarrow 1$
$5 \longrightarrow 3$

Anyone of these listed types may be taken as the first lower-left to upper-right half-cycle in the 1^{st} first-return string-run, but normally we take the first listed one. Every lower-left to upper-right half-cycle encountered in this 1^{st} first-return string-run gets deleted from the type-list.

Anyone of the remaining types in the type-list may be taken as the first lower-left to upper-right half-cycle in the 2^{nd} first-return string-run, and again every lower-left to upper-right half-cycle encountered in this 2^{nd} first-return string-run gets deleted from the remaining type-list.

This process is carried on until all the lower-left to upper-right half-cycle types have been deleted from the type-list.

For the first-return string-runs we thus obtain:

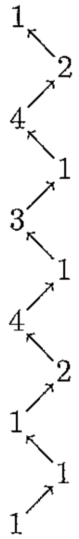

$$\begin{aligned}
l_1 &= 1 \longrightarrow 1 = r_1 &&\rightarrow\ l_2 = |1+6+13-2(1+1)|_5 = 1\,.\\
l_2 &= 1 \longleftarrow 1 = r_1 &&\rightarrow\ r_2 = |1+10+13-2(1+1)|_3 = 2\,.\\
l_2 &= 1 \longrightarrow 2 = r_2 &&\rightarrow\ l_3 = |1+6+13-2(1+2)|_5 = 4\,.\\
l_3 &= 4 \longleftarrow 2 = r_2 &&\rightarrow\ r_3 = |2+10+13-2(2+4)|_3 = 1\,.\\
l_3 &= 4 \longrightarrow 1 = r_3 &&\rightarrow\ l_4 = |4+6+13-2(4+1)|_5 = 3\,.\\
l_4 &= 3 \longleftarrow 1 = r_3 &&\rightarrow\ r_4 = |1+10+13-2(1+3)|_3 = 1\,.\\
l_4 &= 3 \longrightarrow 1 = r_4 &&\rightarrow\ l_5 = |3+6+13-2(3+1)|_5 = 4\,.\\
l_5 &= 4 \longleftarrow 1 = r_4 &&\rightarrow\ r_5 = |1+10+13-2(1+4)|_3 = 2\,.\\
l_5 &= 4 \longrightarrow 2 = r_5 &&\rightarrow\ l_6 = |4+6+13-2(4+2)|_5 = 1\,.\\
l_6 &= 1 \longleftarrow 2 = r_5 &&\rightarrow\ r_6 = |2+10+13-2(2+1)|_3 = 1\,.
\end{aligned}$$

$$P_c = \frac{\alpha x + 2\alpha(A_l + A_r) - 2\sum(l_i + r_i)}{A^{**}} =$$
$$\frac{5\cdot 13 + 2\cdot 5(5+3) - 2\{(1+1+4+3+4)+(1+2+1+1+2)\}}{15} = 7\,.$$

g.c.d. $(P_c\,,\,B^{**}) =$ g.c.d. $(7\,,\,2) = 1\,.$

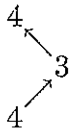

$$\begin{aligned}
l_1 &= 4 \longrightarrow 3 = r_1 &&\rightarrow\ l_2 = |4+6+13-2(4+3)|_5 = 4\,.\\
l_2 &= 4 \longleftarrow 3 = r_1 &&\rightarrow\ r_2 = |3+10+13-2(3+4)|_3 = 3\,.
\end{aligned}$$

$$P_c = \frac{\alpha x + 2\alpha(A_l + A_r) - 2\sum(l_i + r_i)}{A^{**}} = \frac{1\cdot 13 + 2\cdot 1(5+3) - 2\{(4)+(3)\}}{15} = 1\,.$$

g.c.d. $(P_c\,,\,B^{**}) =$ g.c.d. $(1\,,\,2) = 1\,.$

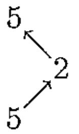

$$\begin{aligned}
l_1 &= 5 \longrightarrow 2 = r_1 &&\rightarrow\ l_2 = |5+6+13-2(5+2)|_5 = 5\,.\\
l_2 &= 5 \longleftarrow 2 = r_1 &&\rightarrow\ r_2 = |2+10+13-2(2+5)|_3 = 3\,.
\end{aligned}$$

$$P_c = \frac{\alpha x + 2\alpha(A_l + A_r) - 2\sum(l_i + r_i)}{A^{**}} = \frac{1\cdot 13 + 2\cdot 1(5+3) - 2\{(5)+(2)\}}{15} = 1\,.$$

g.c.d. $(P_c\,,\,B^{**}) =$ g.c.d. $(1\,,\,2) = 1\,.$

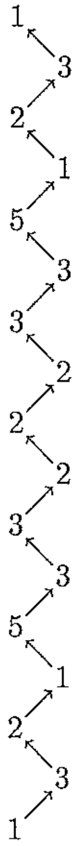

$$\begin{array}{lcl}
l_1 = 1 \longrightarrow 3 = r_1 & \to & l_2 = |1+6+13-2(1+3)|_5 = 2\,. \\
l_2 = 2 \longleftarrow 3 = r_1 & \to & r_2 = |3+10+13-2(3+2)|_3 = 1\,. \\
l_2 = 2 \longrightarrow 1 = r_2 & \to & l_3 = |2+6+13-2(2+1)|_5 = 5\,. \\
l_3 = 5 \longleftarrow 1 = r_2 & \to & r_3 = |1+10+13-2(1+5)|_3 = 3\,. \\
l_3 = 5 \longrightarrow 3 = r_3 & \to & l_4 = |5+6+13-2(5+3)|_5 = 3\,. \\
l_4 = 3 \longleftarrow 3 = r_3 & \to & r_4 = |3+10+13-2(3+3)|_3 = 2\,. \\
l_4 = 3 \longrightarrow 2 = r_4 & \to & l_5 = |3+6+13-2(3+2)|_5 = 2\,. \\
l_5 = 2 \longleftarrow 2 = r_4 & \to & r_5 = |2+10+13-2(2+2)|_3 = 2\,. \\
l_5 = 2 \longrightarrow 2 = r_5 & \to & l_6 = |2+6+13-2(2+2)|_5 = 3\,. \\
l_6 = 3 \longleftarrow 2 = r_5 & \to & r_6 = |2+10+13-2(2+3)|_3 = 3\,. \\
l_6 = 3 \longrightarrow 3 = r_6 & \to & l_7 = |3+6+13-2(3+3)|_5 = 5\,. \\
l_7 = 5 \longleftarrow 3 = r_6 & \to & r_7 = |3+10+13-2(3+5)|_3 = 1\,. \\
l_7 = 5 \longrightarrow 1 = r_7 & \to & l_8 = |5+6+13-2(5+1)|_5 = 2\,. \\
l_8 = 2 \longleftarrow 1 = r_7 & \to & r_8 = |1+10+13-2(1+2)|_3 = 3\,. \\
l_8 = 2 \longrightarrow 3 = r_8 & \to & l_9 = |2+6+13-2(2+3)|_5 = 1\,. \\
l_9 = 1 \longleftarrow 3 = r_8 & \to & r_9 = |3+10+13-2(3+1)|_3 = 3\,.
\end{array}$$

$$P_c = \frac{\alpha x + 2\alpha(A_l + A_r) - 2\sum(l_i + r_i)}{A^{**}} =$$

$$\frac{8\cdot 13 + 2\cdot 8(5+3) - 2\{(1+2+5+3+2+3+5+2)+(3+1+3+2+2+3+1+3)\}}{15} = 10\,.$$

g.c.d. $(P_c\,,\, B^{**})$ = g.c.d. $(10\,,\,2) = 2\,.$

Hence:

$$P_{total} = \sum P_{component} = 7 + 1 + 1 + 10 = 19\,.$$

$$\left.\begin{array}{r}\text{number of}\\ \text{components}\end{array}\right\} = \text{number of first-return string-runs} = 4\,.$$

$$\left.\begin{array}{r}\text{total number of}\\ \text{essential strings}\end{array}\right\} = \sum \text{sub-components} = 1 + 1 + 1 + 2 = 5\,.$$

Note that we can also calculate P_{total} by means of the formula $P_{total} = A_l + A_r + x - 2$.

The above calculations are the very basic ones for the string-run and are carried out without using the string-run diagram. The string-run diagram can of course readily be drawn up by using the string-run specification, which is in case of our Example: (2222/13/22){15432/123}30. From the general layout, or the actual layout, of the string-run we can also readily determine the first-return string-runs and the essential string-number conditions of the components by using the general law of the common divisor[†]. In order to show here the use of the general law of the common divisor, we have drawn in Fig. 604 the actual layout of the string-run (a page-length would be too short for a general layout in which none of the half-cycles of any first-return string-run cross each other). The string-run of each component has been drawn in a separate diagram and is depicted by solidly drawn half-cycles; in each diagram the half-cycles in bold depict the first-return string-run of the component.

[†] Refer to *The Braider*, Issues No. 29 & 30, where this law has been discussed.

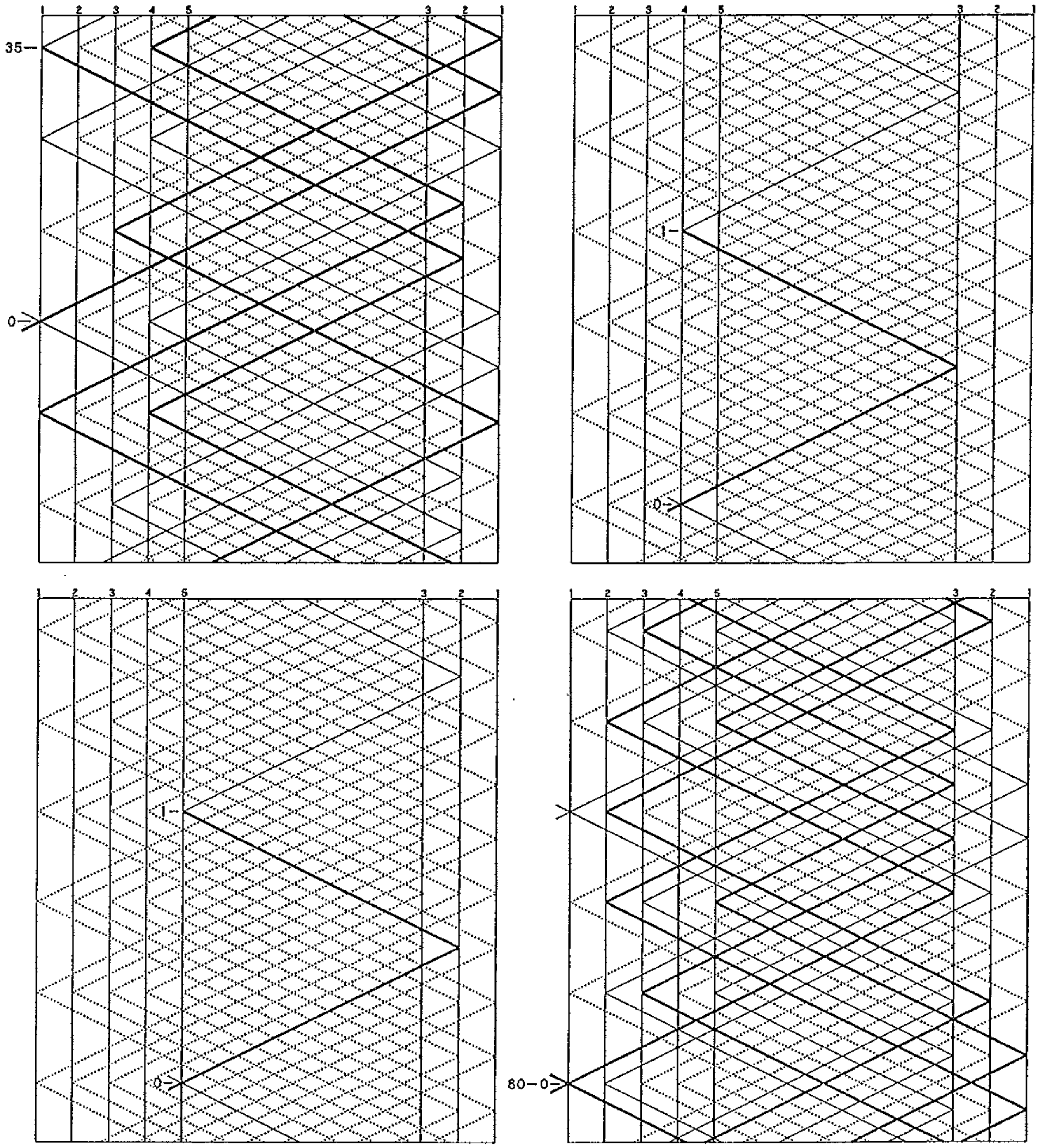

Fig. 604 — The first-return string-runs in the actual string-run diagram.

For the component in the top-left diagram the value of β (the number of bights spanned by the first-return string-run) is equal to 35, while the value of α (the number of bights of the first-return string-run) is equal to 5. Hence g.c.d. $\left(\frac{\beta}{\alpha}, \frac{B_c}{\alpha}\right) =$

g.c.d. $\left(\frac{35}{5}, \frac{10}{5}\right) = \text{g.c.d.}\,(7\,,\,2) = 1 = \lambda$, where λ is the number of essential strings in the component.

For the component in the top-right diagram the value of β (the number of bights spanned by the first-return string-run) is equal to 1, while the value of α (the number of bights of the first-return string-run) is also equal to 1. Hence g.c.d. $\left(\frac{\beta}{\alpha}, \frac{B_c}{\alpha}\right) =$ g.c.d. $\left(\frac{1}{1}, \frac{2}{1}\right) = \text{g.c.d.}\,(1\,,\,2) = 1 = \lambda$, where λ is the number of essential strings in the component.

For the component in the bottom-left diagram the value of β (the number of bights spanned by the first-return string-run) is equal to 1, while the value of α (the number of bights of the first-return string-run) is also equal to 1. Hence g.c.d. $\left(\frac{\beta}{\alpha}, \frac{B_c}{\alpha}\right) =$ g.c.d. $\left(\frac{1}{1}, \frac{2}{1}\right) = \text{g.c.d.}\,(1\,,\,2) = 1 = \lambda$, where λ is the number of essential strings in the component.

For the component in the bottom-right diagram the value of β (the number of bights spanned by the first-return string-run) is equal to 80, while the value of α (the number of bights of the first-return string-run) is equal to 8. Hence g.c.d. $\left(\frac{\beta}{\alpha}, \frac{B_c}{\alpha}\right) =$ g.c.d. $\left(\frac{80}{8}, \frac{16}{8}\right) = \text{g.c.d.}\,(10\,,\,2) = 2 = \lambda$, where λ is the number of essential strings in the component.

Note that $\frac{\beta}{\alpha} = P_c$, and that $\frac{B_c}{\alpha} = B^{**}$.

Similarly as with the Regular Nested Cylindrical Braids, we attach to the bight-boundary number of a bight of an Asymmetric Regular Nested Cylindrical Braid the **nest-index number** of the nest to which the bight belongs[†].

Let the initial Standing End half-cycle, running from lower-left to upper-right, start at the left-hand bight-boundary l_1 and end at the right-hand bight-boundary r_1. The nest, to which its left-hand bight-point belongs, receives the nest-index number $I_L = I_{L_1} = 0$, and the nest, to which its right-hand bight-point belongs, receives the nest-index number $I_R = I_{R_1} = 0$. The left-hand bight-point of this Standing End half-cycle is indicated by $I_L/l_1 = I_{L_1}/l_1 = 0/l_1$, and the right-hand bight-point of this Standing End half-cycle is indicated by $r_1/I_R = r_1/I_{R_1} = r_1/0$.

The next half-cycle (the second half-cycle), running from lower-right to upper-left, starts at the right-hand bight-point $r_1/0$ and ends at the left-hand bight-boundary l_2. The nest, to which its bight-point on the left-hand bight-boundary l_2 belongs, receives the nest-index number $I_L = I_{L_2} = |I_{L_1} + 2(A_l + A_r) + x - (l_1 + l_2 + 2r_1)|_B$. The left-hand bight-point of the second half-cycle is indicated by $I_L/l_2 = I_{L_2}/l_2$.

The next half-cycle (the third half-cycle), running from lower-left to upper-right, starts at the left-hand bight-point I_{L_2}/l_2 and ends at the right-hand bight-boundary r_2. The nest, to which its bight-point on the right-hand bight-boundary r_2 belongs, receives the nest-index number $I_R = I_{R_2} = |I_{R_1} + 2(A_l + A_r) + x - (r_1 + r_2 + 2l_2)|_B$. The right-hand bight-point of the third half-cycle is indicated by r_2/I_{R_2}.

[†] Refer to *The Braider*, Issue No. 26, pg. 592.

The next half-cycle (the fourth half-cycle), running from lower-right to upper-left, starts at the right-hand bight-point r_2/I_{R_2} and ends at the left-hand bight-boundary l_3. The nest, to which its bight-point on the left-hand bight-boundary l_3 belongs, receives the nest-index number $I_L = I_{L_3} = |I_{L_2} + 2(A_l + A_r) + x - (l_2 + l_3 + 2r_2)|_B$. The left-hand bight-point of the fourth half-cycle is indicated by $I_L/l_3 = I_{L_3}/l_3$.

The next half-cycle (the fifth half-cycle), running from lower-left to upper-right, starts at the left-hand bight-point I_{L_3}/l_3 and ends at the right-hand bight-boundary r_3. The nest, to which its bight-point on the right-hand bight-boundary r_3 belongs, receives the nest-index number $I_R = I_{R_3} = |I_{R_2} + 2(A_l + A_r) + x - (r_2 + r_3 + 2l_3)|_B$. The right-hand bight-point of the fifth half-cycle is indicated by r_3/I_{R_3}.

And so on.

In general:

The $(2n)^{th}$ half-cycle, where $n = 1, 2, 3, \cdots$, running from lower-right to upper-left, starts at right-hand bight-point r_n/I_{R_n} and ends at the left-hand bight-boundary l_{n+1}. The nest, belonging to this bight-point on the left-hand bight-boundary l_{n+1}, receives the nest-index number $I_L = I_{L_{n+1}} = |I_{L_n} + 2(A_l + A_r) + x - (l_n + l_{n+1} + 2r_n)|_B$. The left-hand bight-point of the $(2n)^{th}$ half-cycle, where $n = 1, 2, 3, \cdots$, is indicated by $I_L/l_{n+1} = I_{L_{n+1}}/l_{n+1}$.

The $(2n+1)^{th}$ half-cycle), running from lower-left to upper-right, starts at the left-hand bight-point $I_{L_{n+1}}/l_{n+1}$ and ends at the right-hand bight-boundary r_{n+1}. The nest, to which its bight-point on the right-hand bight-boundary r_{n+1} belongs, receives the nest-index number $I_R = I_{R_{n+1}} = |I_{R_n} + 2(A_l + A_r) + x - (r_n + r_{n+1} + 2l_{n+1})|_B$. The right-hand bight-point of the $(2n+1)^{th}$ half-cycle is indicated by $r_{n+1}/I_{R_{n+1}}$.

For our Example, the Standing Ends of the five essential strings are indicated in Fig. 605. The 4^{th} component consists of two sub-components with respectively the essential strings 4 & 5.

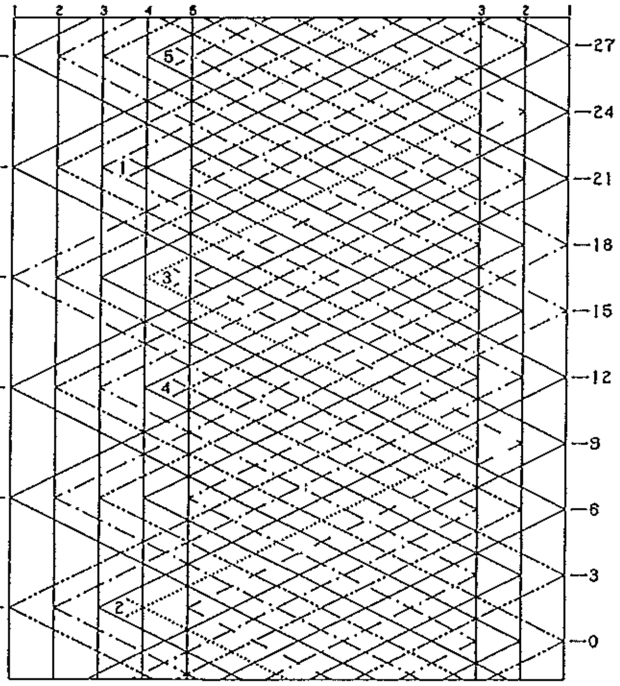

Fig. 605 — The string-runs of the five essential strings.

Thus the first-return string-runs of the four components are:

$$\begin{tikzcd}[column sep=tiny, row sep=tiny]
15/4 & \\
& 1/27 \arrow[ul] \\
25/3 \arrow[ur] & \\
& 1/6 \arrow[ul] \\
5/4 \arrow[ur] & \\
& 2/18 \arrow[ul] \\
15/1 \arrow[ur] & \\
& 1/24 \arrow[ul] \\
20/1 \arrow[ur] & \\
& 2/0 \arrow[ul] \\
0/4 \arrow[ur] &
\end{tikzcd}$$

$$\begin{aligned}
I_L = I_1 &= 0\,. \\
I_R = I_{1'} &= 0\,. \\
I_L = I_2 &= |I_1 + 2(A_l + A_r) + x - (l_1 + l_2 + 2r_1)|_B = \\
&\quad |0 + 2 \times 8 + 13 - (4 + 1 + 2 \times 2)|_{30} = 20\,. \\
I_R = I_{2'} &= |I_{1'} + 2(A_l + A_r) + x - (r_1 + r_2 + 2l_2)|_B = \\
&\quad |0 + 2 \times 8 + 13 - (2 + 1 + 2 \times 1)|_{30} = 24\,. \\
I_L = I_3 &= |I_2 + 2(A_l + A_r) + x - (l_2 + l_3 + 2r_2)|_B = \\
&\quad |20 + 2 \times 8 + 13 - (1 + 1 + 2 \times 1)|_{30} = 15\,. \\
I_R = I_{3'} &= |I_{2'} + 2(A_l + A_r) + x - (r_2 + r_3 + 2l_3)|_B = \\
&\quad |24 + 2 \times 8 + 13 - (1 + 2 + 2 \times 1)|_{30} = 18\,. \\
I_L = I_4 &= |I_3 + 2(A_l + A_r) + x - (l_3 + l_4 + 2r_3)|_B = \\
&\quad |15 + 2 \times 8 + 13 - (1 + 4 + 2 \times 2)|_{30} = 5\,. \\
I_R = I_{4'} &= |I_{3'} + 2(A_l + A_r) + x - (r_3 + r_4 + 2l_4)|_B = \\
&\quad |18 + 2 \times 8 + 13 - (2 + 1 + 2 \times 4)|_{30} = 6\,. \\
I_L = I_5 &= |I_4 + 2(A_l + A_r) + x - (l_4 + l_5 + 2r_4)|_B = \\
&\quad |5 + 2 \times 8 + 13 - (4 + 3 + 2 \times 1)|_{30} = 25\,. \\
I_R = I_{5'} &= |I_{4'} + 2(A_l + A_r) + x - (r_4 + r_5 + 2l_5)|_B = \\
&\quad |6 + 2 \times 8 + 13 - (1 + 1 + 2 \times 3)|_{30} = 27\,. \\
I_L = I_6 &= |I_5 + 2(A_l + A_r) + x - (l_5 + l_6 + 2r_5)|_B = \\
&\quad |25 + 2 \times 8 + 13 - (3 + 4 + 2 \times 1)|_{30} = 15\,.
\end{aligned}$$

$$\begin{tikzcd}[column sep=tiny, row sep=tiny]
20/5 & \\
& 1/3 \arrow[ul] \\
0/2 \arrow[ur] & \\
& 3/12 \arrow[ul] \\
10/1 \arrow[ur] & \\
& 3/21 \arrow[ul] \\
20/2 \arrow[ur] & \\
& 1/0 \arrow[ul] \\
0/5 \arrow[ur] & \\
& 3/15 \arrow[ul] \\
15/3 \arrow[ur] & \\
& 2/27 \arrow[ul] \\
25/2 \arrow[ur] & \\
& 2/6 \arrow[ul] \\
5/3 \arrow[ur] & \\
& 3/18 \arrow[ul] \\
20/5 \arrow[ur] &
\end{tikzcd}$$

$$\begin{aligned}
I_L = I_1''' &= 20\,. \\
I_R = I_{1'}''' &= |I_1''' + (l_1 + r_1) - (l_1''' + r_1''')|_B = \\
&\quad |20 + (4 + 2) - (5 + 3)|_B = |20 + 6 - 8|_{30} = 18\,. \\
I_L = I_2''' &= |I_1''' + 2(A_l + A_r) + x - (l_1''' + l_2''' + 2r_1''')|_B = \\
&\quad |20 + 2 \times 8 + 13 - (5 + 3 + 2 \times 3)|_{30} = 5\,. \\
I_R = I_{2'}''' &= |I_1''' + 2(A_l + A_r) + x - (r_1''' + r_2''' + 2l_2''')|_B = \\
&\quad |18 + 2 \times 8 + 13 - (3 + 2 + 2 \times 3)|_{30} = 6\,. \\
I_L = I_3''' &= |I_2''' + 2(A_l + A_r) + x - (l_2''' + l_3''' + 2r_2''')|_B = \\
&\quad |5 + 2 \times 8 + 13 - (3 + 2 + 2 \times 2)|_{30} = 25\,. \\
I_R = I_{3'}''' &= |I_2''' + 2(A_l + A_r) + x - (r_2''' + r_3''' + 2l_3''')|_B = \\
&\quad |6 + 2 \times 8 + 13 - (2 + 2 + 2 \times 2)|_{30} = 27\,. \\
I_L = I_4''' &= |I_3''' + 2(A_l + A_r) + x - (l_3''' + l_4''' + 2r_3''')|_B = \\
&\quad |25 + 2 \times 8 + 13 - (2 + 3 + 2 \times 2)|_{30} = 15\,. \\
I_R = I_{4'}''' &= |I_3''' + 2(A_l + A_r) + x - (r_3''' + r_4''' + 2l_4''')|_B = \\
&\quad |27 + 2 \times 8 + 13 - (2 + 3 + 2 \times 3)|_{30} = 15\,. \\
I_L = I_5''' &= |I_4''' + 2(A_l + A_r) + x - (l_4''' + l_5''' + 2r_4''')|_B = \\
&\quad |15 + 2 \times 8 + 13 - (3 + 5 + 2 \times 3)|_{30} = 0\,. \\
I_R = I_{5'}''' &= |I_4''' + 2(A_l + A_r) + x - (r_4''' + r_5''' + 2l_5''')|_B = \\
&\quad |15 + 2 \times 8 + 13 - (3 + 1 + 2 \times 5)|_{30} = 0\,. \\
I_L = I_6''' &= |I_5''' + 2(A_l + A_r) + x - (l_5''' + l_6''' + 2r_5''')|_B = \\
&\quad |0 + 2 \times 8 + 13 - (5 + 2 + 2 \times 1)|_{30} = 20\,. \\
I_R = I_{6'}''' &= |I_5''' + 2(A_l + A_r) + x - (r_5''' + r_6''' + 2l_6''')|_B = \\
&\quad |0 + 2 \times 8 + 13 - (1 + 3 + 2 \times 2)|_{30} = 21\,. \\
I_L = I_7''' &= |I_6''' + 2(A_l + A_r) + x - (l_6''' + l_7''' + 2r_6''')|_B = \\
&\quad |20 + 2 \times 8 + 13 - (2 + 1 + 2 \times 3)|_{30} = 10\,. \\
I_R = I_{7'}''' &= |I_6''' + 2(A_l + A_r) + x - (r_6''' + r_7''' + 2l_7''')|_B =
\end{aligned}$$

$$\begin{aligned}
&|21+2\times 8+13-(3+3+2\times 1)|_{30}=12\,.\\
I_L=I_8'''=\;&|I_7'''+2(A_l+A_r)+x-(l_7'''+l_8'''+2r_7''')|_B=\\
&|10+2\times 8+13-(1+2+2\times 3)|_{30}=0\,.\\
I_R=I_{8'}'''=\;&|I_7'''+2(A_l+A_r)+x-(r_7'''+r_8'''+2l_8''')|_B=\\
&|12+2\times 8+13-(3+1+2\times 2)|_{30}=3\,.\\
I_L=I_9'''=\;&|I_8'''+2(A_l+A_r)+x-(l_8'''+l_9'''+2r_8''')|_B=\\
&|0+2\times 8+13-(2+5+2\times 1)|_{30}=20\,.
\end{aligned}$$

$$\begin{tikzcd}
25/4 & \\
& 3/9 \arrow[ul] \\
10/4 \arrow[ur] &
\end{tikzcd}$$

$$\begin{aligned}
I_L=I_1'=\;&10\,.\\
I_R=I_{1'}'=\;&|I_1'+(l_1+r_1)-(l_1'+r_1')|_B=\\
&|10+(4+2)-(4+3)-A|_B=|10+6-7|_{30}=9\,.\\
I_L=I_2'=\;&|I_1'+2(A_l+A_r)+x-(l_1'+l_2'+2r_1')|_B=\\
&|10+2\times 8+13-(4+4+2\times 3)|_{30}=25\,.
\end{aligned}$$

$$\begin{tikzcd}
10/5 & \\
& 2/24 \arrow[ul] \\
25/5 \arrow[ur] &
\end{tikzcd}$$

$$\begin{aligned}
I_L=I_1''=\;&25\,.\\
I_R=I_{1'}''=\;&|I_1''+(l_1+r_1)-(l_1''+r_1'')|_B=\\
&|25+(4+2)-(5+2)|_B=|25+6-7|_{30}=24\,.\\
I_L=I_2''=\;&|I_1''+2(A_l+A_r)+x-(l_1''+l_2''+2r_1'')|_B=\\
&|25+2\times 8+13-(5+5+2\times 2)|_{30}=10\,.
\end{aligned}$$

Let's assume that we braid the essential strings in their sequential numbered order (see Fig. 605). The above calculated data can then be assembled in the half-cycle pattern depicted in Fig. 606. The number of crossings on a half-cycle from lower-left to upper-right are calculated with the formula $(A_l+A_r)+x-1-(l_i+r_i)$ for such a half-cycle running from left-hand bight-boundary l_i to right-hand bight-boundary r_i, and the number of crossings on a half-cycle from lower-right to upper-left are calculated with the formula $(A_l+A_r)+x-1-(r_i+l_{i+1})$ for such a half-cycle running from right-hand bight-boundary r_i to left-hand bight-boundary l_{i+1}. In Fig. 606 the number of crossings on a half-cycle are indicated below the half-cycle number.

1	2	3	4	5	
$\frac{57}{16}$	$\frac{33}{16}$	$\frac{9}{16}$	$\frac{23}{13}$	$\frac{25}{13}$	—25
$\frac{3}{18}$	$\frac{39}{15}$	$\frac{47}{15}$	$\frac{17}{15}$	$\frac{29}{12}$	—20
$\frac{5}{17}$	$\frac{59}{17}$	$\frac{35}{14}$	$\frac{11}{14}$	$\frac{53}{14}$	—15
$\frac{41}{16}$	$\frac{49}{16}$	$\frac{19}{16}$	$\frac{21}{13}$	$\frac{27}{13}$	—10
$\frac{13}{18}$	$\frac{55}{15}$	$\frac{31}{15}$	$\frac{7}{15}$	$\frac{45}{12}$	—5
$\frac{15}{17}$	$\frac{43}{17}$	$\frac{51}{14}$	$\frac{1}{14}$	$\frac{37}{14}$	—0

	3	2	1
27—	$\frac{58}{15}$	$\frac{34}{15}$	$\frac{10}{15}$
24—	$\frac{24}{13}$	$\frac{26}{13}$	$\frac{4}{18}$
21—	$\frac{40}{16}$	$\frac{48}{16}$	$\frac{18}{16}$
18—	$\frac{30}{14}$	$\frac{6}{14}$	$\frac{60}{14}$
15—	$\frac{36}{12}$	$\frac{12}{17}$	$\frac{54}{17}$
12—	$\frac{42}{15}$	$\frac{50}{15}$	$\frac{20}{15}$
9—	$\frac{22}{13}$	$\frac{28}{13}$	$\frac{14}{18}$
6—	$\frac{56}{16}$	$\frac{32}{16}$	$\frac{8}{16}$
3—	$\frac{46}{14}$	$\frac{16}{14}$	$\frac{44}{14}$
0—	$\frac{52}{12}$	$\frac{2}{17}$	$\frac{38}{17}$

Fig. 606 — The half-cycle pattern associated with our Example.

Let the coding, superimposed on the string-run, be as depicted in Fig. 607. Then from the half-cycle pattern in Fig. 606 we assemble the half-cycle tables in Figs. 608 & 609 for respectively the lower-left to upper-right and the lower-right to upper-left half-cycles.

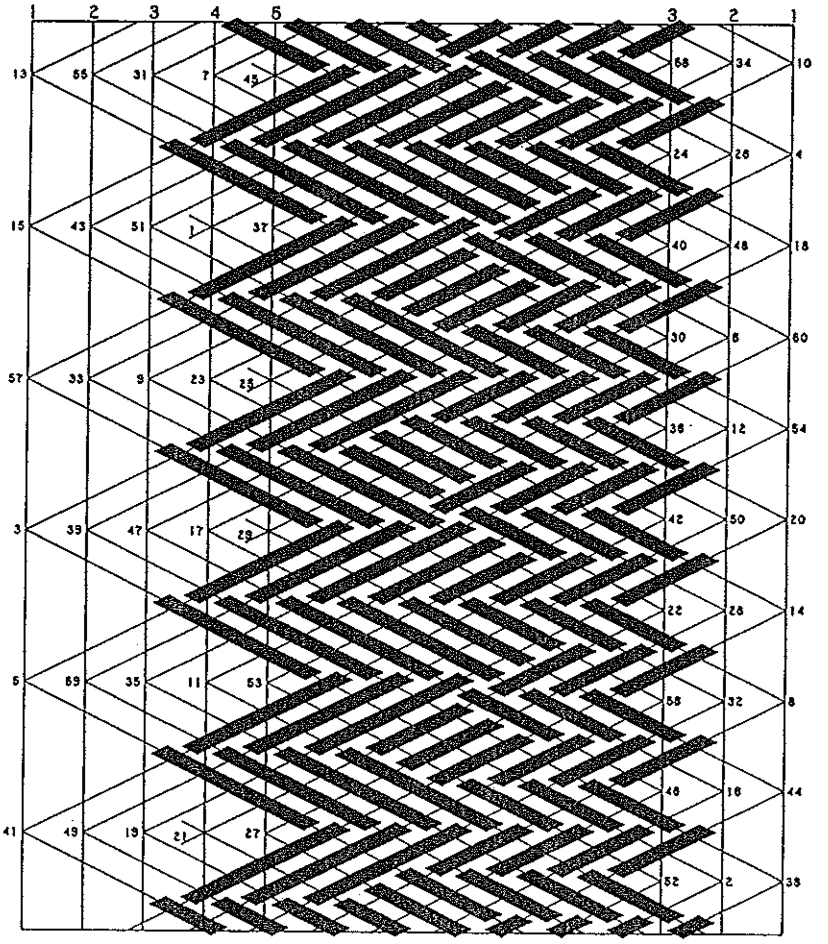

Fig. 607 — The string-run with the superimposed coding.

15	43	51	1*	37	13	55	31	7	45***	41	49	19	21**	27	5	59	35						
5	59	35	11	53	3	39	47	17	29**	57	33	9	23	25*	15	43	51						
57	33	9	23	25	15	43	51	1*	37	13	55	31	7	45**	41	49	19						
41	49	19	21	27	5	59	35	11	53	3	39	47	17	29*	57	33	9						
3	39	47	17	29**	57	33	9	23	25	15	43	51	1*	37	13	55	31						
13	55	31	7	45*	41	49	19	21	27	5	59	35	11	53	3	39	47						
u	o	o	o	o	o	u	u	u	u	u	u	u	o	o	o	u		15	5*				
u	u	o	o	o	o	o	u	o	o	o	u	u	u	o	o	o		43	59				
u	u	u	o	o	o	o	o	u	o	o	o	u	u					51*	35**				
u	u	u	u	o	o	o	o	u	u	o	o	o	u					1	11*				
u	u	u	u	u	o	o	o	u	u	u	o	o	o					37	53				
u	o	o	o	o	o	u	u	u	o	o	o	u	u	u	o	o	o			13	3*		
u	u	o	o	o	o	o	u	u	u	o	o	o	u	u						55	39		
u	u	u	o	o	o	o	o	u	u	u	o	o	o	u						31*	47**		
u	u	u	u	u	u	o	o	o	u	u	u	o	o	o						7	17*		
u	u	u	u	u	u	u	o	o	o	u	u									45	29		
u	o	o	o	o	o	u	u	u	u	u	o	o	o	u	u							41**	57***
u	u	o	o	o	o	o	u	u	u	u	u	o	o	o	u							49	33
u	u	u	o	o	o	o	o	u	u	u	u	u	o	o	o							19	9*
u	u	u	u	o	o	o	u	o	o	o	u	u										21	23**
u	u	u	u	o	o	o	u	u	o	o	o	u										27*	25

Fig. 608 — The half-cycle table for the lower-left to upper-right half-cycles.

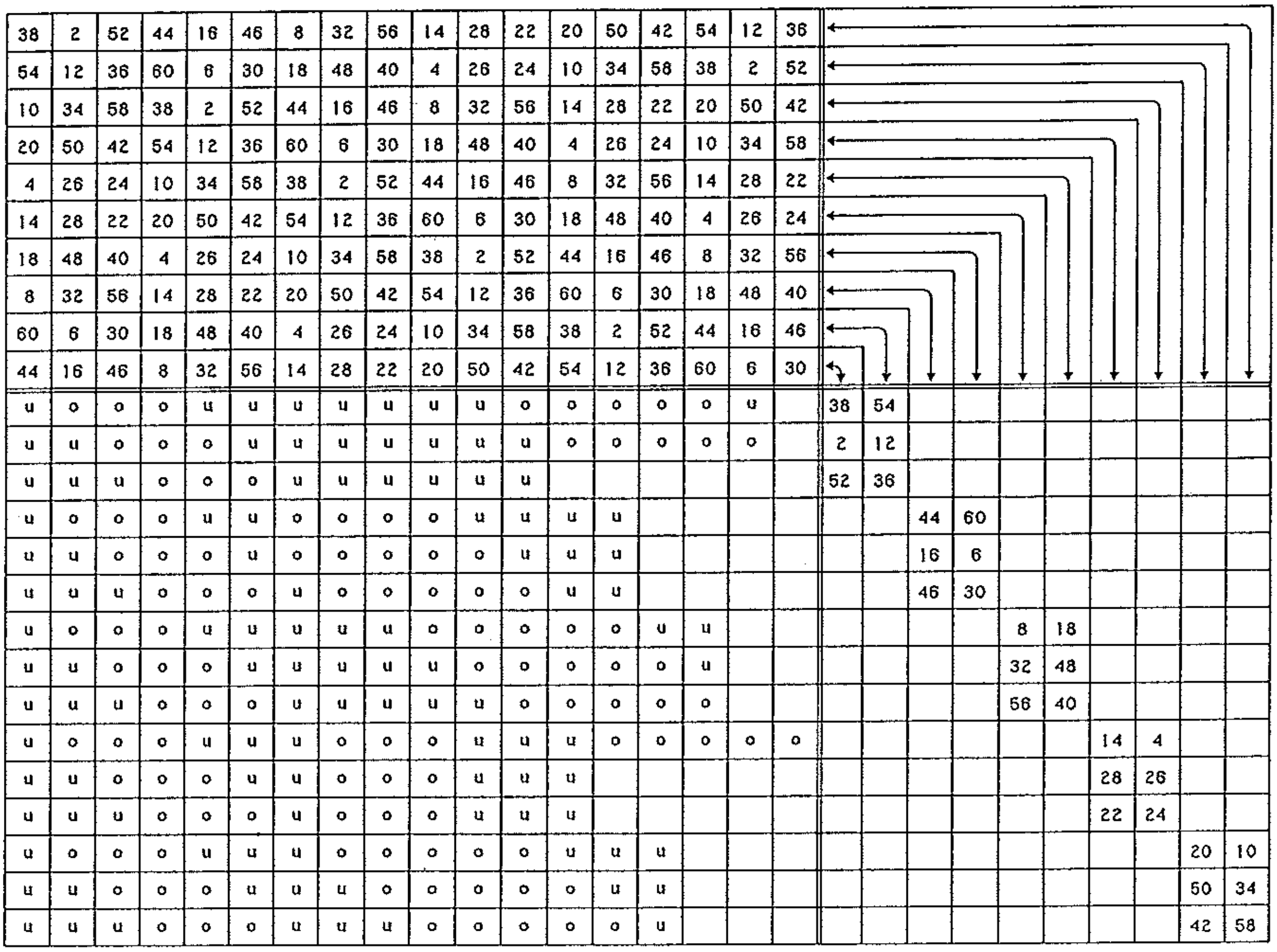

38	2	52	44	16	46	8	32	56	14	28	22	20	50	42	54	12	36										
54	12	36	60	6	30	18	48	40	4	26	24	10	34	58	38	2	52										
10	34	58	38	2	52	44	16	46	8	32	56	14	28	22	20	50	42										
20	50	42	54	12	36	60	6	30	18	48	40	4	26	24	10	34	58										
4	26	24	10	34	58	38	2	52	44	16	46	8	32	56	14	28	22										
14	28	22	20	50	42	54	12	36	60	6	30	18	48	40	4	26	24										
18	48	40	4	26	24	10	34	58	38	2	52	44	16	46	8	32	56										
8	32	56	14	28	22	20	50	42	54	12	36	60	6	30	18	48	40										
60	6	30	18	48	40	4	26	24	10	34	58	38	2	52	44	16	46										
44	16	46	8	32	56	14	28	22	20	50	42	54	12	36	60	6	30										
u	o	o	o	u	u	u	u	u	u	u	o	o	o	o	o	u		38	54								
u	u	o	o	o	u	u	u	u	u	u	u	o	o	o	o	o		2	12								
u	u	u	o	o	o	u	u	u	u	u	u							52	36								
u	o	o	o	u	u	o	o	o	o	u	u	u	u							44	60						
u	u	o	o	o	u	o	o	o	o	o	u	u	u							16	6						
u	u	u	o	o	o	u	o	o	o	o	o	u	u							46	30						
u	o	o	o	u	u	u	u	u	o	o	o	o	o	u	u							8	18				
u	u	o	o	o	u	u	u	u	u	o	o	o	o	o	u							32	48				
u	u	u	o	o	o	u	u	u	u	u	o	o	o	o	o							56	40				
u	o	o	o	u	u	u	o	o	o	u	u	u	o	o	o	o	o							14	4		
u	u	o	o	o	u	u	o	o	o	u	u	u												28	26		
u	u	u	o	o	o	u	o	o	o	u	u	u												22	24		
u	o	o	o	u	u	u	o	o	o	o	o	u	u	u												20	10
u	u	o	o	o	u	u	u	o	o	o	o	o	u	u												50	34
u	u	u	o	o	o	u	u	u	o	o	o	o	o	u												42	58

Fig. 609 — The half-cycle table for the lower-right to upper-left half-cycles.

From the half-cycle tables we read then the half-cycle braiding algorithms for the Asymmetric Regular Nested Cylindrical Braid. Note that in the table of the odd-numbered half-cycles some of these half-cycles have one or more stars attached to them. When a half-cycle in the rightmost table-section has one or more star(s) then in its associated row of half-cycles (in the uppermost table-section) only those half-cycle numbers, equal to or smaller than the half-cycle number in the rightmost table-section, with an identical number of stars are neglected[†].

Thus from the half-cycle tables in Figs. 608 & 609, associated with the Asymmetric Regular Nested Cylindrical Braid depicted in Fig. 607, we read the following half-cycle braiding algorithms:

1. $4 \longrightarrow 2$: Free run.
2. $1 \longleftarrow 2$: Free run.
3. $1 \longrightarrow 1$: Free run.
4. $1 \longleftarrow 1$: *u*.
5. $1 \longrightarrow 2$: *u*.

[†] The half-cycle numbers in the uppermost table-section are for crossing purposes associated with their immediately preceding even-numbered half-cycle, hence the starred half-cycle numbers in the uppermost table-section are for crossing purposes associated with the **final** (even-numbered) half-cycle of an essential string.

6. $4 \longleftarrow 2$: $2o$.
7. $4 \longrightarrow 1$: $2u$.
8. $3 \longleftarrow 1$: $o - u$.
9. $3 \longrightarrow 1$: $u - o$.
10. $4 \longleftarrow 1$: $o - u$.
11. $4 \longrightarrow 2$: $u - o$.
12. $1 \longleftarrow 2$: $3u - o$.
13. $1 \longrightarrow 1$: $o - u - 2o$.
14. $1 \longleftarrow 1$: $u - o - u - o$.
15. $1 \longrightarrow 2$: $u - o - u - 2o$.
16. $4 \longleftarrow 2$: $u - 2o - u$.
17. $4 \longrightarrow 1$: $3u - o$.
18. $3 \longleftarrow 1$: $u - o - u - 2o - u$.
19. $3 \longrightarrow 1$: $u - 2o - 2u - o$.
20. $4 \longleftarrow 1$: $o - 2u - o - u$.

21. $4 \longrightarrow 3$: $2u - 2o - u$.
22. $4 \longleftarrow 3$: $u - 3o - u$.
23. $4 \longrightarrow 3$: $2u - 2o - u$.
24. $4 \longleftarrow 3$: $u - 3o - u$.

25. $5 \longrightarrow 2$: $2u - o - 2u$.
26. $5 \longleftarrow 2$: $u - 3o - u$.
27. $5 \longrightarrow 2$: $2u - o - 2u$.
28. $5 \longleftarrow 2$: $u - 3o - u$.

29. $5 \longrightarrow 3$: $4u - o - u$.
30. $3 \longleftarrow 3$: $u - 3o - u - o - u$.
31. $3 \longrightarrow 2$: $u - 3o - 2u - 3o - u$.
32. $2 \longleftarrow 2$: $2u - 2o - u - 3o - u$.
33. $2 \longrightarrow 2$: $u - 2o - 2u - 3o - u$.
34. $3 \longleftarrow 2$: $u - o - 2u - 4o$.
35. $3 \longrightarrow 3$: $u - 3o - u - 2o - u$.
36. $5 \longleftarrow 3$: $2u - o - 5u$.
37. $5 \longrightarrow 1$: $3u - o - 3u - 2o$.
38. $2 \longleftarrow 1$: $2o - 5u - 2o - u$.
39. $2 \longrightarrow 3$: $u - 4o - 2u - 2o - u$.
40. $1 \longleftarrow 3$: $3u - 2o - 3u - 3o$.
41. $1 \longrightarrow 3$: $u - 3o - 2u - 3o - 2u$.
42. $2 \longleftarrow 3$: $2u - 2o - 2u - 5o$.
43. $2 \longrightarrow 1$: $u - 3o - u - 3o - 2u - 2o$.
44. $5 \longleftarrow 1$: $u - 2o - 2u - 2o - 3u$.

45. $5 \longrightarrow 3$: $5u - 2o - 2u$.
46. $3 \longleftarrow 3$: $2u - 3o - u - 3o - u$.
47. $3 \longrightarrow 2$: $2u - 4o - 3u - 2o$.
48. $2 \longleftarrow 2$: $2u - 3o - 3u - 4o - u$.
49. $2 \longrightarrow 2$: $u - 4o - 4u - 3o - u$.

50. $3 \longleftarrow 2$: $u - 2o - 3u - 5o - u$.
51. $3 \longrightarrow 3$: $2u - 4o - u - 2o - 2u$.
52. $5 \longleftarrow 3$: $3u - 2o - 6u$.
53. $5 \longrightarrow 1$: $5u - 2o - 3u - 3o$.
54. $2 \longleftarrow 1$: $3o - 7u - 4o - u$.
55. $2 \longrightarrow 3$: $2u - 4o - 3u - 3o - 2u$.
56. $1 \longleftarrow 3$: $3u - 3o - 4u - 5o$.
57. $1 \longrightarrow 3$: $u - 5o - 4u - 3o - 2u$.
58. $2 \longleftarrow 3$: $3u - 3o - 3u - 5o - u$.
59. $2 \longrightarrow 1$: $2u - 5o - u - 3o - 3u - 3o$.
60. $5 \longleftarrow 1$: $u - 3o - 2u - 4o - 4u$.

Some braiders might find it easier to work with separate half-cycle tables for each essential string, hence similar to the procedures discussed in *The Braider*, Issue No. 31. This certainly makes the reading of the half-cycle braiding algorithms from these tables quicker and easier.

It will have been noticed that the calculation procedures for obtaining the half-cycle braiding algorithms for the Asymmetric Regular Nested Cylindrical Braids are similar to the calculation procedures of the half-cycle braiding algorithms for the Perfect and Semi-Perfect Regular Nested Cylindrical Braids (see *The Braider*, Issue No. 28 and Issue No. 29). Although these calculation procedures are very simple, they are somewhat lengthy and hence here is where suitable computer software can play an important and valuable role. Some braiders may say that the half-cycle braiding algorithms can directly be obtained (with or without the assistance of a computer) from the grid-diagram. This is certainly true, but it is easy to make mistakes without the assistance of a computer and much more cumbersome to check whether or not the obtained half-cycle braiding algorithms are correct.

Designing Interbraided Knots

The Spanish Ring Knot is one of the most commonly encountered knots in a braiding project. Generally their braid is made of a single string and hence consists of a single colour, however two colour work where V's of one colour are regularly interspersed between the V's of the other colour will in many cases enliven the braided project.

A Ring Knot can have two coding arrangements: one in which the V's point up, and one in which the V's point down. These are each others complementary coding forms (see Fig. 610).

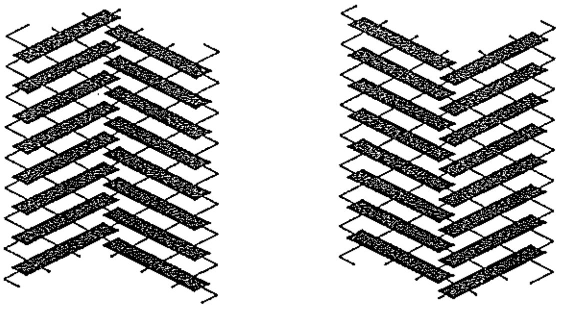

Fig. 610 — The complementary coding forms.

They are in reallity identical since a rotation through 180° of a knot having one of these coding forms produces the knot with its complementary coding form. However, since we normally start braiding from left to right and in the upwards direction, we will have to look at both the above mentioned coding forms. Each of the above mentioned coding forms provides for two ways of incorporating V's with a contrasting colour (see for example Fig. 611 where the sequence of the two sets of V's is 1 : 1).

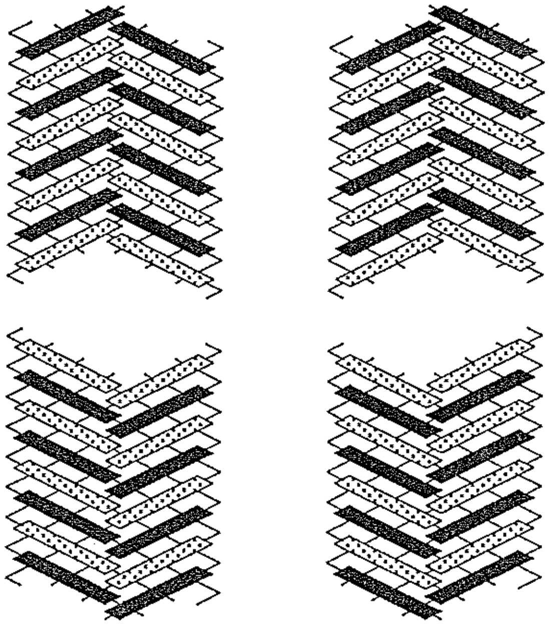

Fig. 611 — Incorporating coloured V's with the sequence 1 : 1.

It will be readily apparent from the diagrams in Fig. 611 that the string-run cannot exactly be as depicted since the coding-patterns would require the string(s) to change in colour at certain positions.

In order to obtain the pattern of V's depicted in the uppermost left-hand diagram of Fig. 611 we require the string-run and the coding to be as shown in the rightmost diagram of Fig. 612. Observe how this string-run and coding is obtained from the string-run and coding shown in the second diagram from the left, and hence how its string-run is associated with the string-run depicted in the leftmost diagram. From this leftmost string-run in Fig. 612 we can thus determine with the aid of the generalised law of the greatest common divisor[†] $\lambda = \text{g.c.d.}\left(\frac{\beta}{\alpha}, \frac{B_c}{\alpha}\right)$ the properties of the actual string-run belonging to the pattern of V's in the uppermost left-hand diagram of Fig. 611.

This leftmost string-run in Fig. 612 consists of two components; their first-return string-runs are drawn in thick heavy lines. In these first-return string-runs the bights are numbered on the right, and the bights which these first-return string-runs span in their components are numbered on the left. Hence for the lowermost first-return string-run we obtain $\alpha = 1$ and $\beta = 4$, while for the uppermost first-return string-run we obtain $\alpha = 1$ and $\beta = 3$. Let the number of bights B_c of the component associated with the lowermost first-return string-run be equal to B, then the number of bights B_c of the component associated with the uppermost first-return string-run is also equal to B. Thus for the component with the lowermost first-return string-run the number of sub-components $\lambda = \text{g.c.d.}(4, B)$, while for the component with the uppermost first-return string-run the number of sub-components λ = g.c.d.$(3, B)$. Hence for both λ-values to be equal to 1, the value of B must be coprime with 4 and 3.

[†] See *The Braider*, Issue No. 29, pg. 682, and Issue No. 30, pp. 683–690.

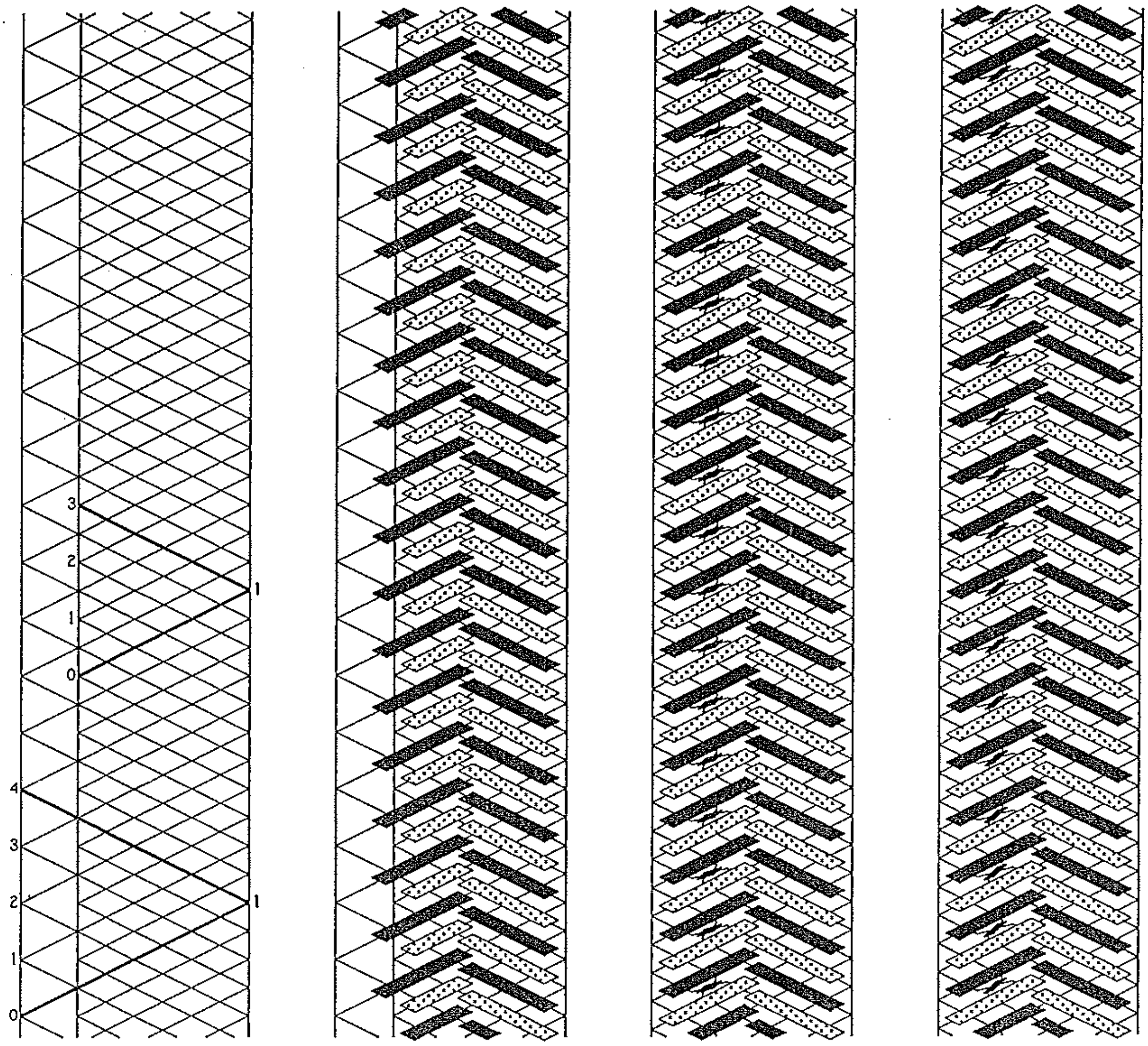

Fig. 612 — The development of the actual string-run and coding for the uppermost left-hand V pattern in Fig. 611.

If, for example, we take $B = 7$, hence the knot has 14 bights in total, we obtain the construction details shown in Fig. 613. The upper two left grid-diagrams depict respectively the foundation knot $p/b = 4/7$ and the interbraid $p'/b' = 3/7$. The foundation knot with its ultimate string-run is depicted by the uppermost right-hand grid-diagram. In the lowermost row of diagrams the three diagrams on the left depict the development of the ultimate knot depicted by the lower rightmost grid-diagram.

First we braid the foundation knot; its half-cycle braiding algorithms, read from its associated algorithm diagram, are as follows:

1. : Free run.
2. $i = 0$: Free run.
3. $i = 0$: Free run.
4. $i = 1$: u.
5. $i = 1$: u.

6. $i = 2$: u.
7. $i = 2$: u.
8. $i = 3$: $2u$.
9. $i = 3$: $o - u$.
10. $i = 4$: $2u$.
11. $i = 4$: $o - u$.
12. $i = 5$: $o - 2u$.
13. $i = 5$: $2o - u$.
14. $i = 6$: $o - 2u$.

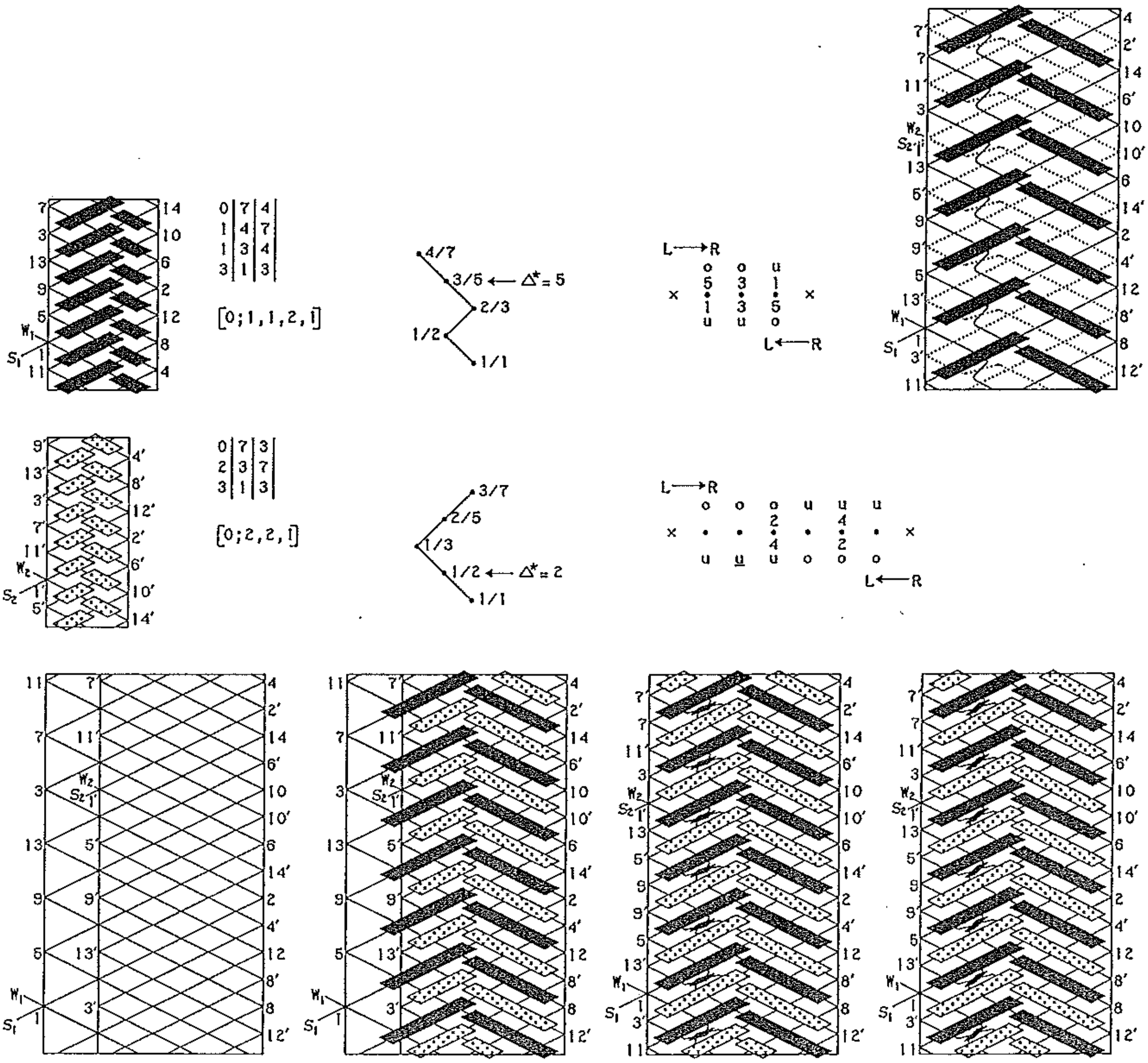

Fig. 613 — The construction details for the interbraid $p'/b' = 3/7$ with $p/b = 4/7$.

Next we interbraid the knot $p'/b' = 3/7$; its half-cycle braiding algorithms, read from its associated algorithm diagram, are as follows:

1′. : $2o - 2u$.
2′. $i = 0$: $2o - \underline{u} - u$.
3′. $i = 0$: $2o - 2u$.
4′. $i = 1$: $2o - \underline{u} - u$.

5′. $i = 1$: $2o - 2u$.
6′. $i = 2$: $3o - \underline{u} - u$.
7′. $i = 2$: $3o - 2u$.
8′. $i = 3$: $3o - \underline{u} - u$.
9′. $i = 3$: $3o - 2u$.
10′. $i = 4$: $3o - u - \underline{u} - u$.
11′. $i = 4$: $3o - 3u$.
12′. $i = 5$: $3o - u - \underline{u} - u$.
13′. $i = 5$: $3o - 3u$.
14′. $i = 6$: $3o - u - \underline{u} - u$.

For the other three V patterns the interbraiding development and the interbraiding procedures are shown in Figs. 614, 615, and 616.

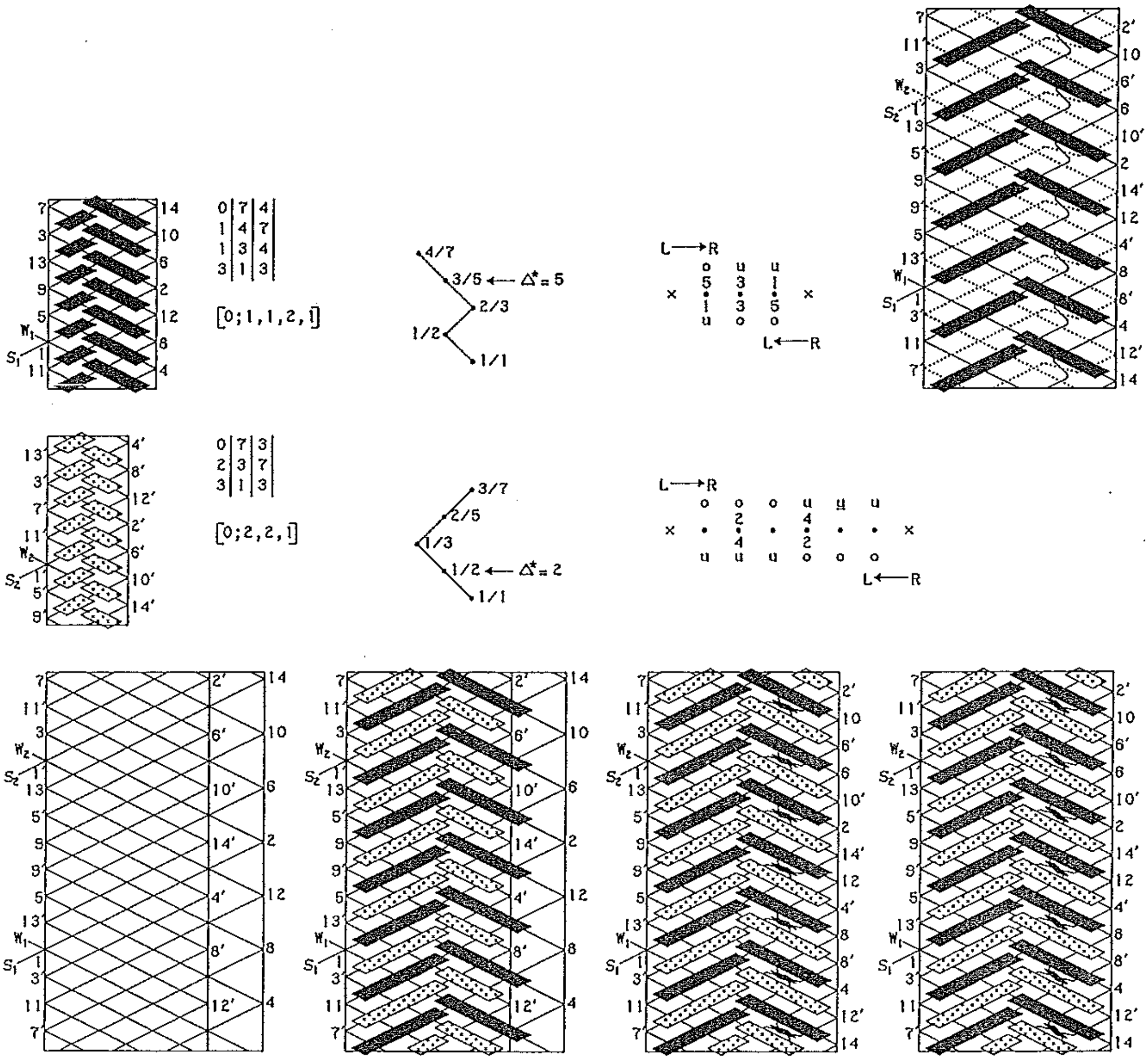

Fig. 614 — The construction details for the interbraid $p'/b' = 3/7$ with $p/b = 4/7$.

The half-cycle braiding algorithms associated with the interbraid in Fig. 614 are as follows:

1. : Free run.
2. $i = 0$: Free run.
3. $i = 0$: Free run.
4. $i = 1$: u .
5. $i = 1$: u .
6. $i = 2$: u .
7. $i = 2$: u .
8. $i = 3$: $o - u$.
9. $i = 3$: $2u$.
10. $i = 4$: $o - u$.
11. $i = 4$: $2u$.
12. $i = 5$: $2o - u$.
13. $i = 5$: $o - 2u$.
14. $i = 6$: $2o - u$.

1′. : $2o - \underline{u} - u$.
2′. $i = 0$: $2o - 2u$.
3′. $i = 0$: $2o - \underline{u} - u$.
4′. $i = 1$: $2o - 2u$.
5′. $i = 1$: $2o - \underline{u} - u$.
6′. $i = 2$: $3o - 2u$.
7′. $i = 2$: $3o - \underline{u} - u$.
8′. $i = 3$: $3o - 2u$.
9′. $i = 3$: $3o - \underline{u} - u$.
10′. $i = 4$: $3o - 3u$.
11′. $i = 4$: $3o - u - \underline{u} - u$.
12′. $i = 5$: $3o - 3u$.
13′. $i = 5$: $3o - u - \underline{u} - u$.
14′. $i = 6$: $3o - 3u$.

The half-cycle braiding algorithms associated with the interbraid in Fig. 615 are as follows:

1. : Free run.
2. $i = 0$: Free run.
3. $i = 0$: Free run.
4. $i = 1$: o .
5. $i = 1$: o .
6. $i = 2$: o .
7. $i = 2$: o .
8. $i = 3$: $u - o$.
9. $i = 3$: $2o$.
10. $i = 4$: $u - o$.
11. $i = 4$: $2o$.
12. $i = 5$: $2u - o$.
13. $i = 5$: $u - 2o$.
14. $i = 6$: $2u - o$.

1′. : $2u - 2o$.

$2'.\quad i=0 \quad : \quad u-\underline{u}-2o.$
$3'.\quad i=0 \quad : \quad 2u-2o.$
$4'.\quad i=1 \quad : \quad u-\underline{u}-2o.$
$5'.\quad i=1 \quad : \quad 2u-2o.$
$6'.\quad i=2 \quad : \quad u-\underline{u}-u-2o.$
$7'.\quad i=2 \quad : \quad 3u-2o.$
$8'.\quad i=3 \quad : \quad u-\underline{u}-u-2o.$
$9'.\quad i=3 \quad : \quad 3u-2o.$
$10'.\quad i=4 \quad : \quad u-\underline{u}-u-3o.$
$11'.\quad i=4 \quad : \quad 3u-3o.$
$12'.\quad i=5 \quad : \quad u-\underline{u}-u-3o.$
$13'.\quad i=5 \quad : \quad 3u-3o.$
$14'.\quad i=6 \quad : \quad u-\underline{u}-u-3o.$

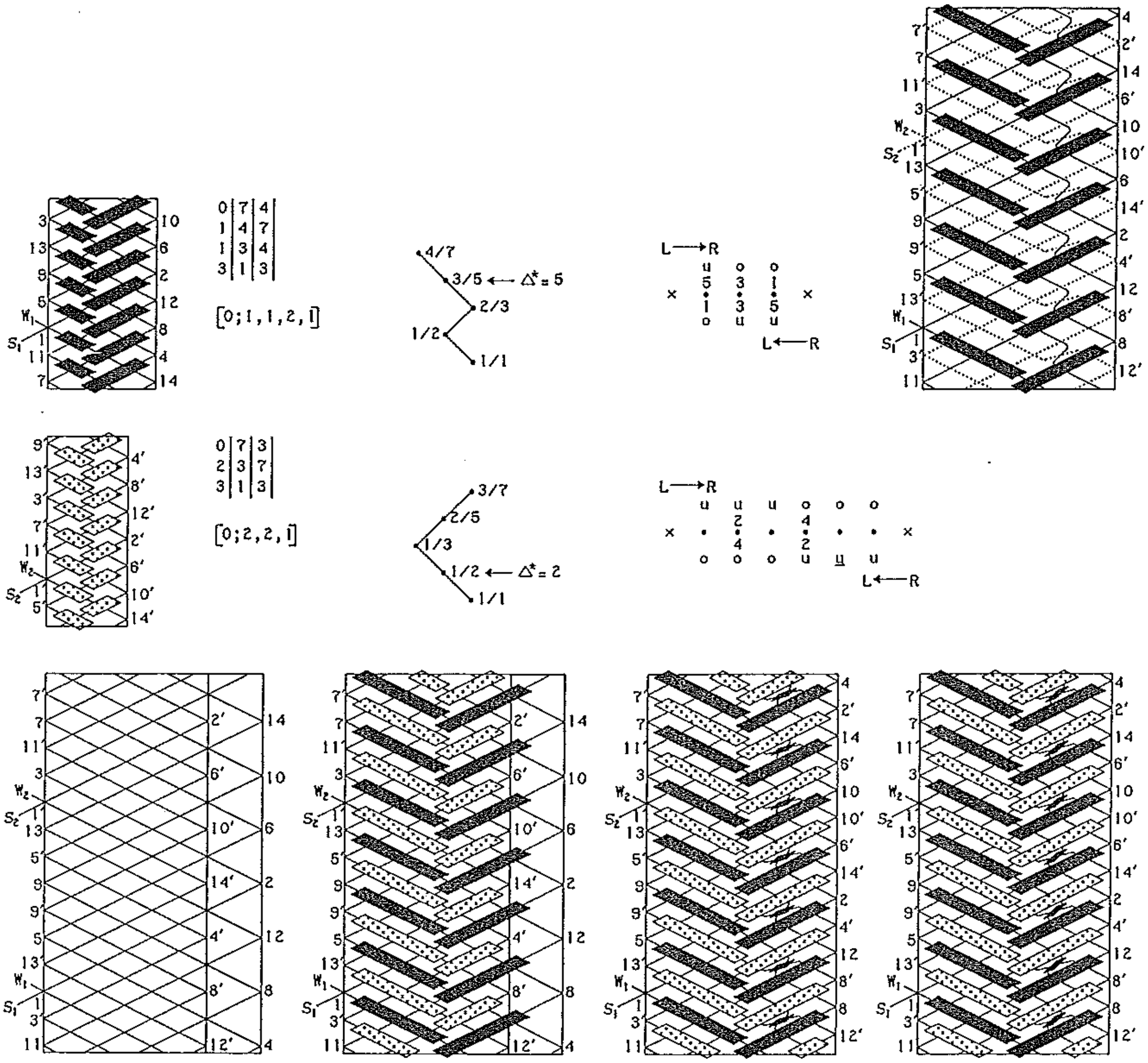

Fig. 615 — The construction details for the interbraid $p'/b' = 3/7$ with $p/b = 4/7$.

The half-cycle braiding algorithms associated with the interbraid in Fig. 616 are as follows:

1. : Free run.
2. $i = 0$: Free run.
3. $i = 0$: Free run.
4. $i = 1$: o.
5. $i = 1$: o.
6. $i = 2$: o.
7. $i = 2$: o.
8. $i = 3$: $2o$.
9. $i = 3$: $u - o$.
10. $i = 4$: $2o$.
11. $i = 4$: $u - o$.
12. $i = 5$: $u - 2o$.
13. $i = 5$: $2u - o$.
14. $i = 6$: $u - 2o$.

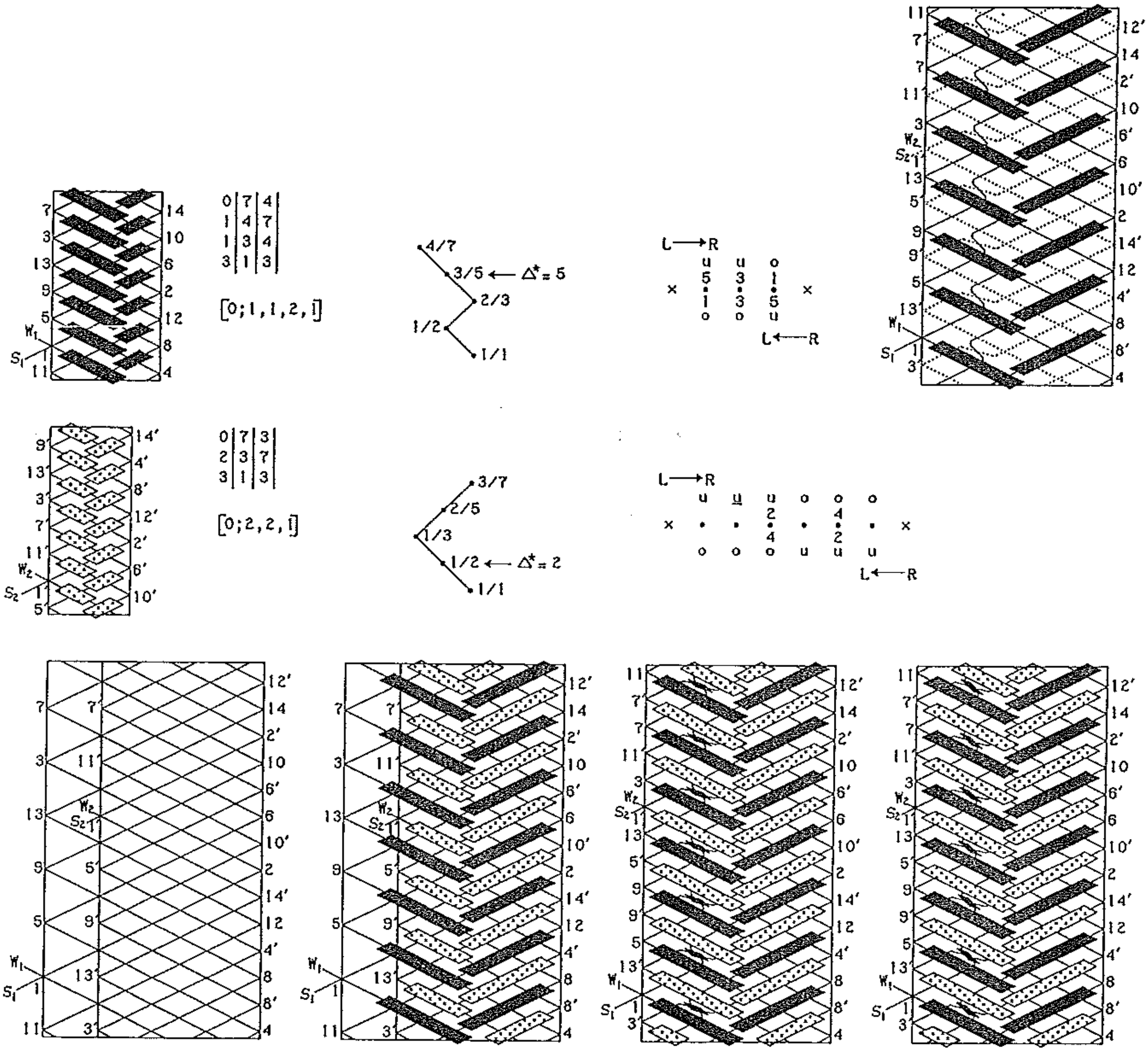

Fig. 616 — The construction details for the interbraid $p'/b' = 3/7$ with $p/b = 4/7$.

1′. : $u - \underline{u} - 2o$.

$2'.$ $i = 0$: $2u - 2o.$
$3'.$ $i = 0$: $u - \underline{u} - 2o.$
$4'.$ $i = 1$: $2u - 2o.$
$5'.$ $i = 1$: $u - \underline{u} - 2o.$
$6'.$ $i = 2$: $3u - 2o.$
$7'.$ $i = 2$: $u - \underline{u} - u - 2o.$
$8'.$ $i = 3$: $3u - 2o.$
$9'.$ $i = 3$: $u - \underline{u} - u - 2o.$
$10'.$ $i = 4$: $3u - 3o.$
$11'.$ $i = 4$: $u - \underline{u} - u - 3o.$
$12'.$ $i = 5$: $3u - 3o.$
$13'.$ $i = 5$: $u - \underline{u} - u - 3o.$
$14'.$ $i = 6$: $3u - 3o.$

Let's now have a look at the case where the sequence of two sets of V's is 2 : 1.

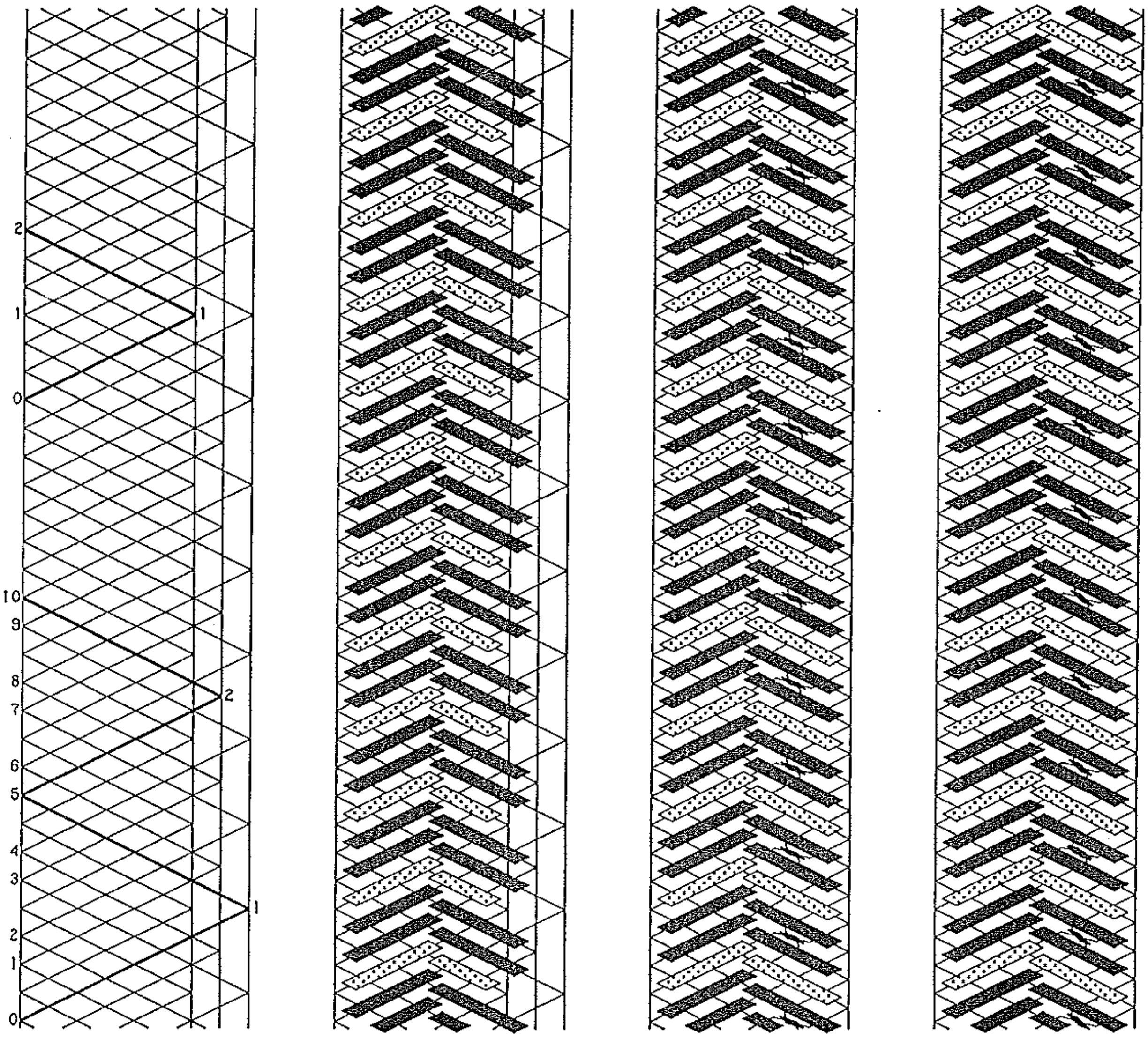

Fig. 617 — The development of the actual string-run and coding for a V pattern sequence 2 : 1.

Note again how this string-run and coding is obtained from the string-run and coding shown in the second diagram from the left, and hence how its string-run is associated with the string-run depicted in the leftmost diagram. From this leftmost string-run in Fig. 617 we can thus determine with the aid of the generalised law of the greatest common divisor $\lambda = \text{g.c.d.}\left(\dfrac{\beta}{\alpha}, \dfrac{B_c}{\alpha}\right)$ the properties of the actual string-run belonging to the pattern of V's in the rightmost diagram of Fig. 617.

This leftmost string-run in Fig. 617 consists of two components; their first-return string-runs are drawn in thick heavy lines. In these first-return string-runs the bights are numbered on the right, and the bights which these first-return string-runs span in their components are numbered on the left. Hence for the lowermost first-return string-run we obtain $\alpha = 2$ and $\beta = 10$, while for the uppermost first-return string-run we obtain $\alpha = 1$ and $\beta = 2$. Let the number of bights B_c of the component associated with the lowermost first-return string-run be equal to B, then the number of bights B_c of the component associated with the uppermost first-return string-run is equal to $\frac{B}{2}$. Thus for the component with the lowermost first-return string-run the number of sub-components $\lambda = \text{g.c.d.}(5, \frac{B}{2})$, while for the component with the uppermost first-return string-run the number of sub-components $\lambda = \text{g.c.d.}(2, \frac{B}{2})$. Hence for both λ-values to be equal to 1, the value of $\frac{B}{2}$ must be coprime with 5 and 2.

If, for example, we take $B = 6$, hence the knot has 9 bights in total, we obtain the construction details shown in Fig. 618.

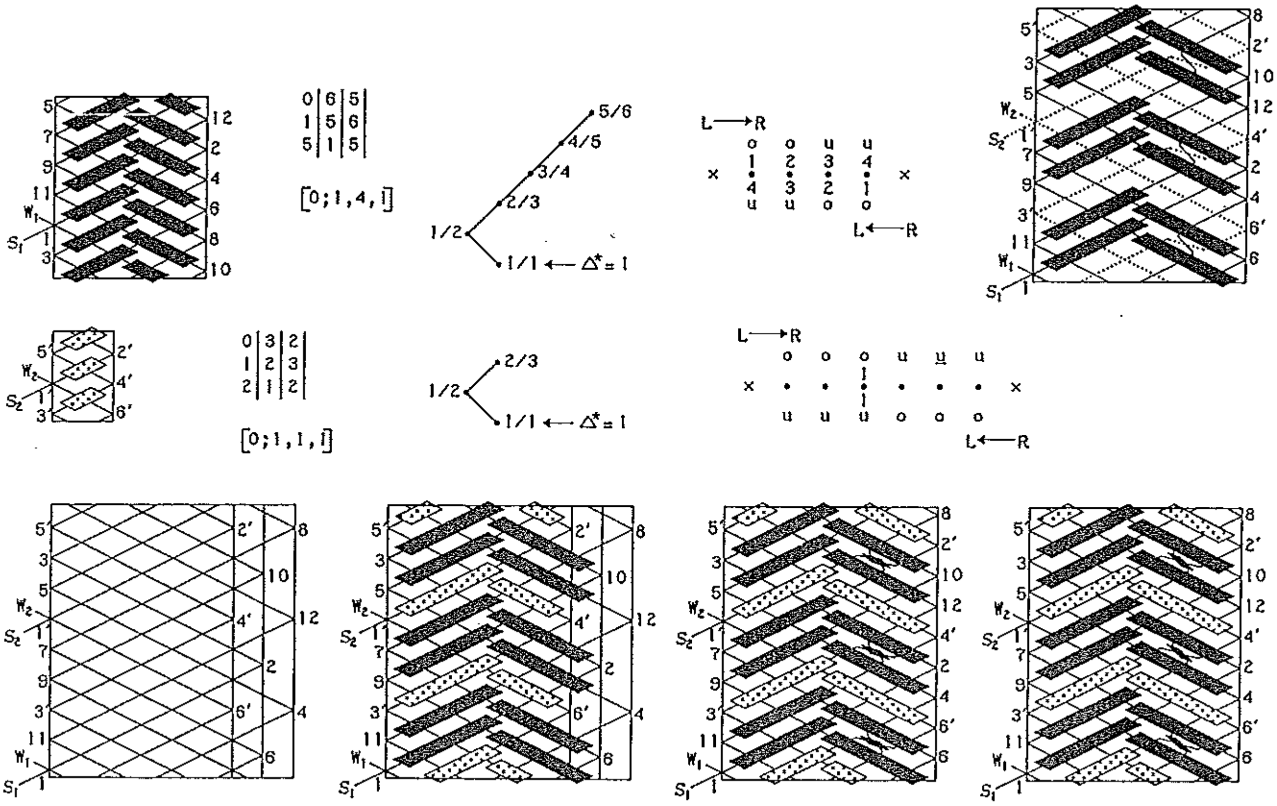

Fig. 618 — The construction details for the interbraid $p'/b' = 2/3$ with $p/b = 5/6$.

The upper two left grid-diagrams depict respectively the foundation knot $p/b = 5/6$ and the interbraid $p'/b' = 2/3$. The foundation knot with its ultimate string-run is depicted by the uppermost right-hand grid-diagram. In the lowermost row of diagrams the three diagrams on the left depict the development of the ultimate knot depicted by the lower rightmost grid-diagram.

The construction details associated with interbraiding $p/b = 5/6$ and $p'/b' = 2/3$ for the other three V patterns are shown in Figs. 619, 620, and 621.

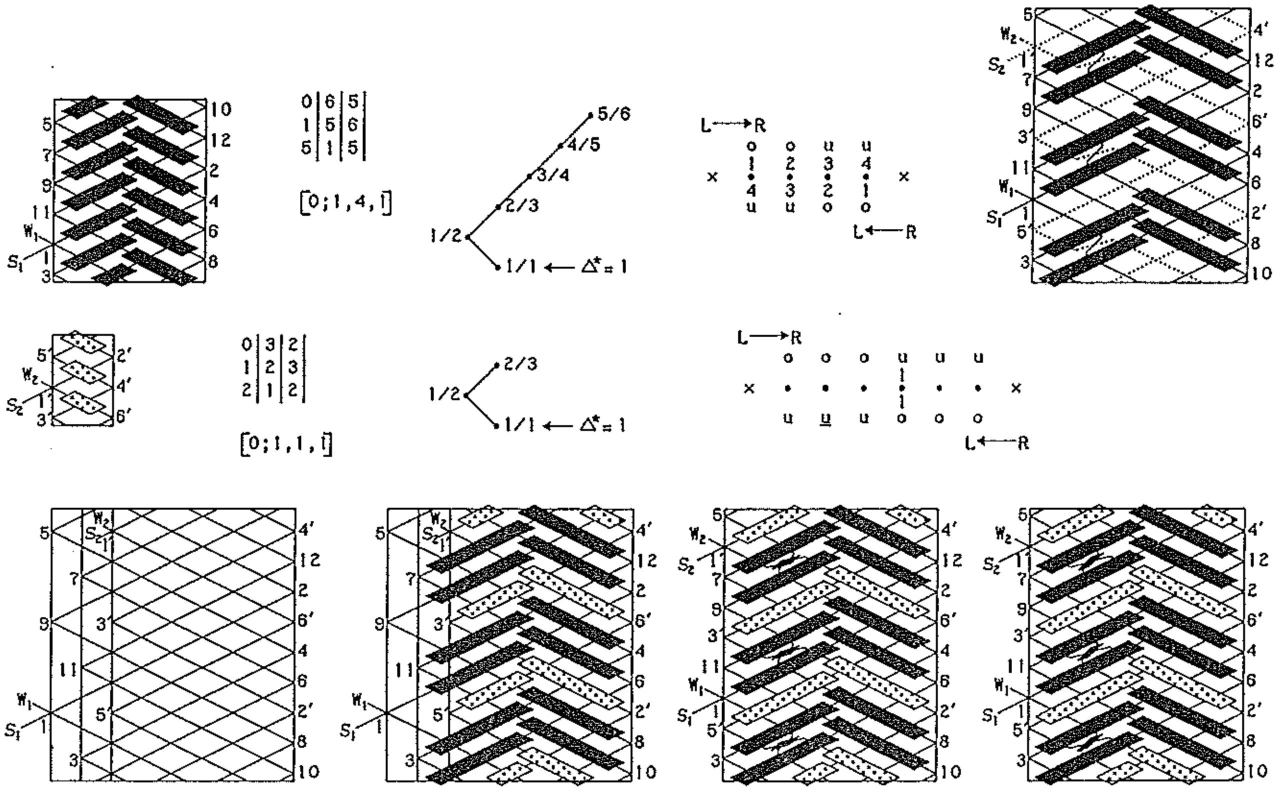

Fig. 619 — The construction details for the interbraid $p'/b' = 2/3$ with $p/b = 5/6$.

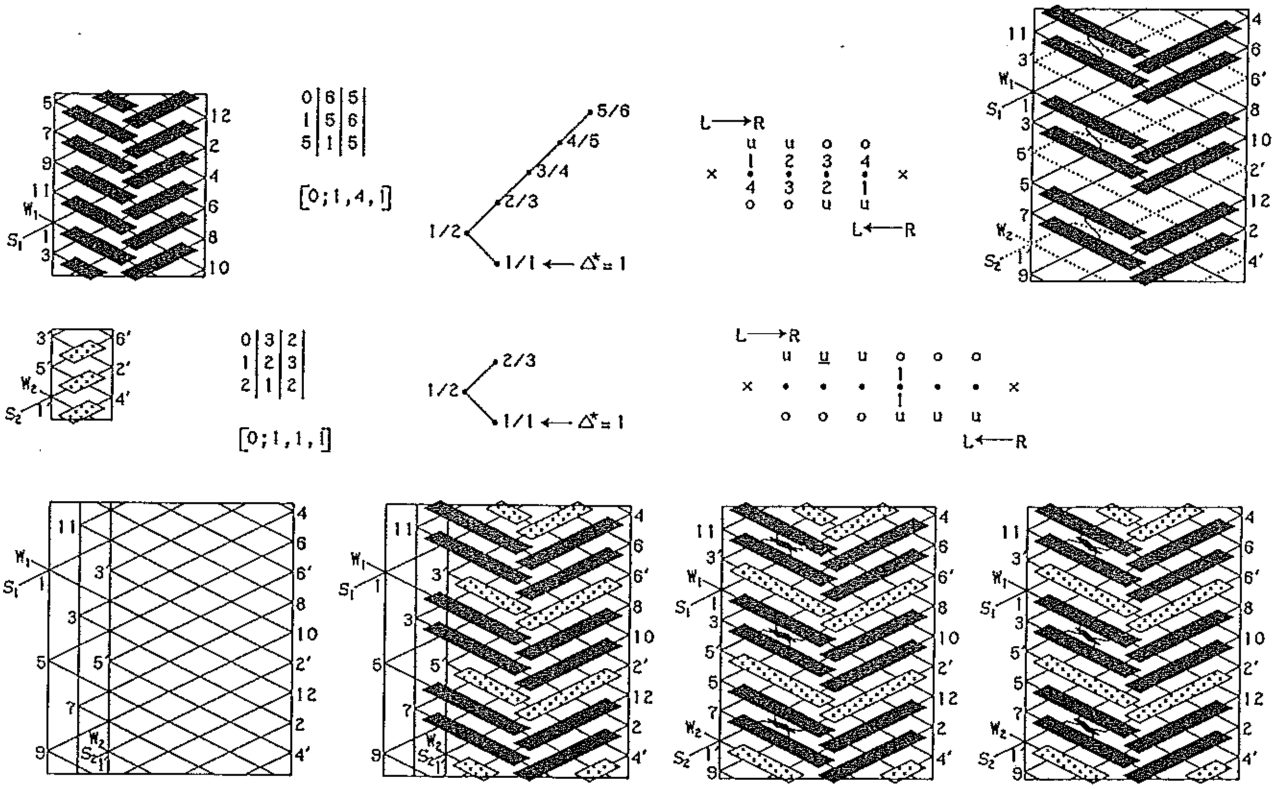

Fig. 620 — The construction details for the interbraid $p'/b' = 2/3$ with $p/b = 5/6$.

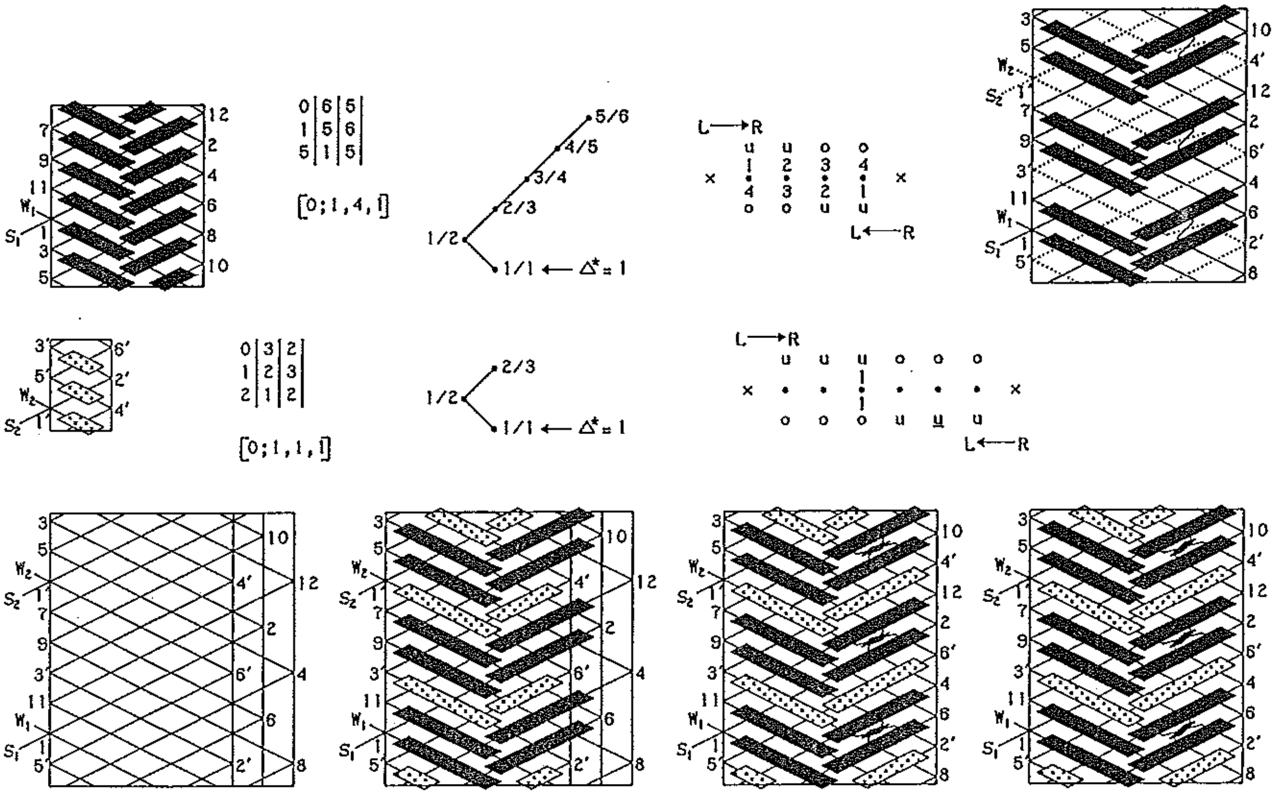

Fig. 621 — The construction details for the interbraid $p'/b' = 2/3$ with $p/b = 5/6$.

First we braid the foundation knots $p/b = 5/6$; their half-cycle braiding algorithms are again read from their associated algorithm diagrams. Note that these are 2-pass Spanish Ring Knots. Then we interbraid the knots $p'/b' = 2/3$; their half-cycle braiding algorithms are again read from their associated algorithm diagrams.

⋆⋆ *A commonly encountered 2-pass Spanish Ring Knot is the one with* $p/b = 5/8$. *Say we want to interbraid such a Spanish Ring Knot with a contrasting set of V's. Give for the four V patterns the construction details for doing this.*

In Fig. 622 we have shown the development of the actual string-run and coding for a V pattern sequence 3 : 1. In the leftmost string-run we have again drawn the two first-return string-runs in thick heavy lines, and as before, in these first-return string-runs the bights are numbered on the right, and the bights which these first-return string-runs span in their components are numbered on the left. Hence for the lowermost first-return string-run we obtain $\alpha = 1$ and $\beta = 2$, while for the uppermost first-return string-run we obtain $\alpha = 3$ and $\beta = 15$. Let the number of bights B_c of the component associated with the uppermost first-return string-run be equal to B, then the number of bights B_c of the component associated with the lowermost first-return string-run is equal to $\frac{B}{3}$. Thus for the component with the uppermost first-return string-run the number of sub-components $\lambda = \text{g.c.d.}(5\,,\,\frac{B}{3})$, while for the component with the lowermost first-return string-run the number of sub-components $\lambda = \text{g.c.d.}(2\,,\,\frac{B}{3})$. Hence for both λ-values to be equal to 1, the value of $\frac{B}{3}$ must be coprime with 5 and 2.

If, for example, we take $B = 9$, hence the knot has 12 bights in total, we obtain the construction details shown in Fig. 623.

Note that the component $p/b = 5/9$ is a 2-pass Spanish Ring Knot.

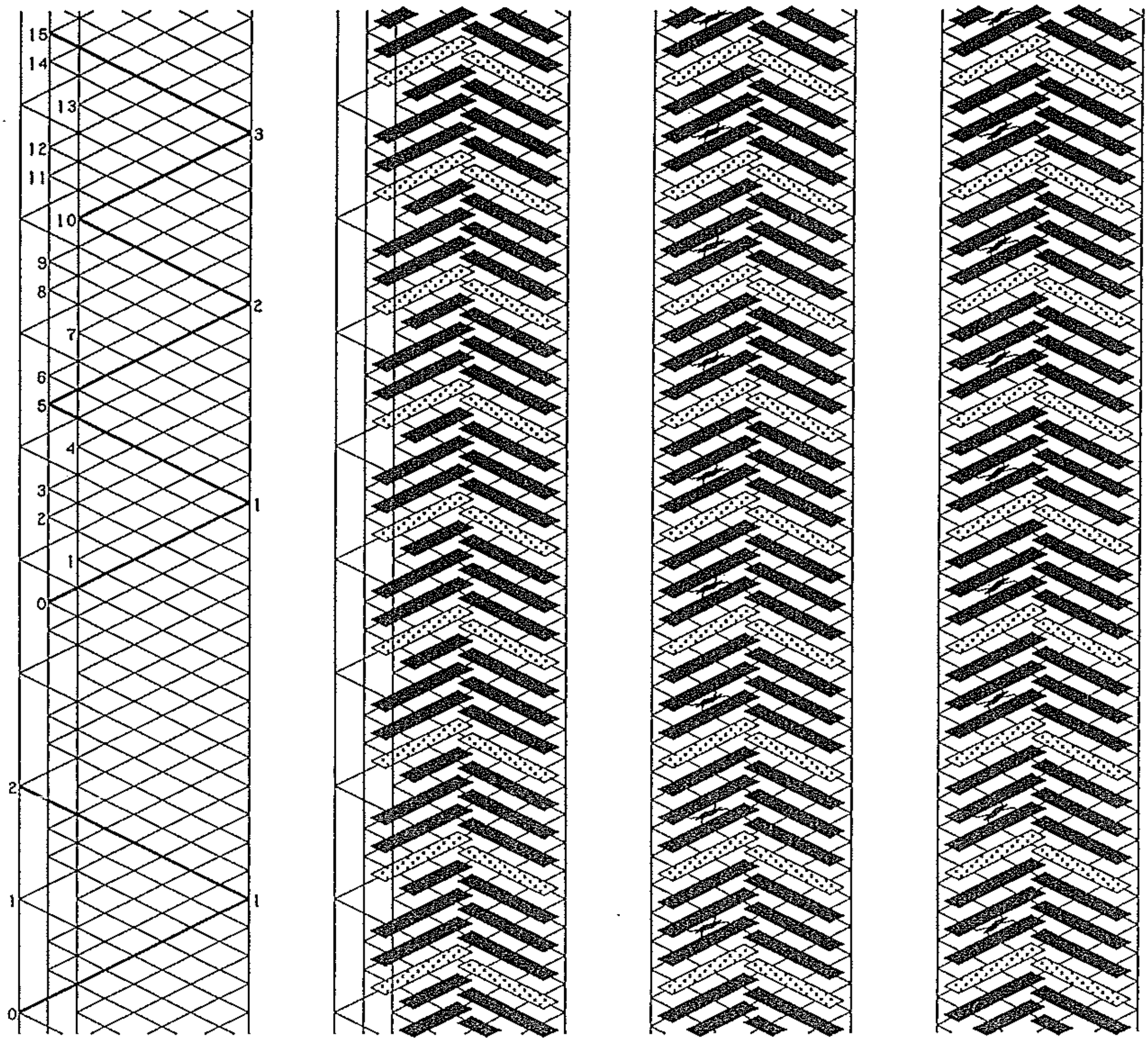

Fig. 622 — The development of the actual string-run and coding for a V pattern sequence 3 : 1.

The construction details for the other three V patterns with a V pattern sequence of 3 : 1 are shown in Figs. 624, 625, and 626.

The half-cycle braiding algorithms are again read from the associated algorithm diagrams.

When Spanish Ring Knots with contrasting interwoven V's are employed in braiding projects it is important to ensure that the correct symmetry and/or balance is obtained.[†] Hence it is necessary to be able to braid any one of the four V patterns which have the same V pattern sequence. This symmetry and/or balance aspect is very important for a high braiding standard. It is therefore unfortunate that many braiders tend to neglect it. This neglect is nearly always due to a lack in braiding skills.

[†] The balance and/or symmetry of similar components in a project depends on the configuration of the project, hence is project specific. It is therefore not possible to give here general guidelines for symmetry and/or balance.

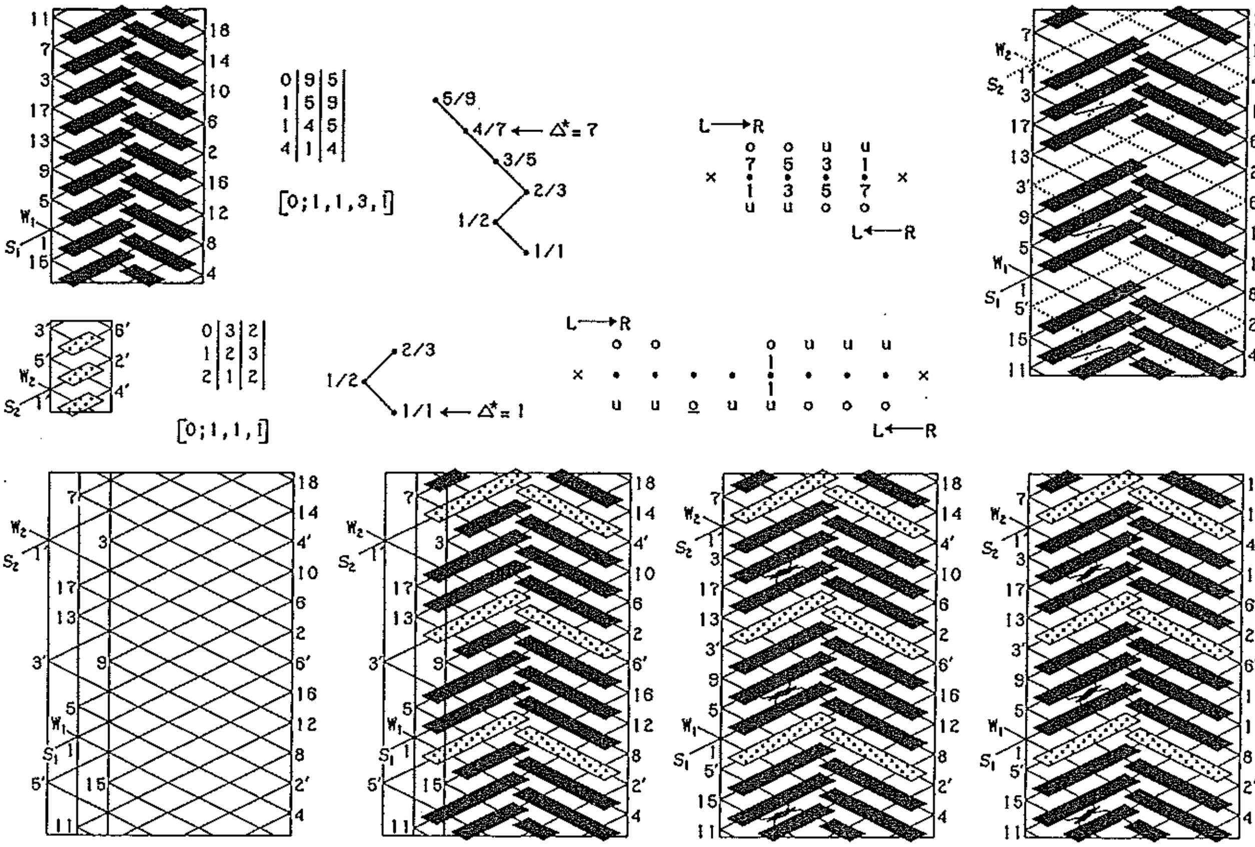

Fig. 623 — The construction details for the interbraid $p'/b' = 2/3$ with $p/b = 5/9$.

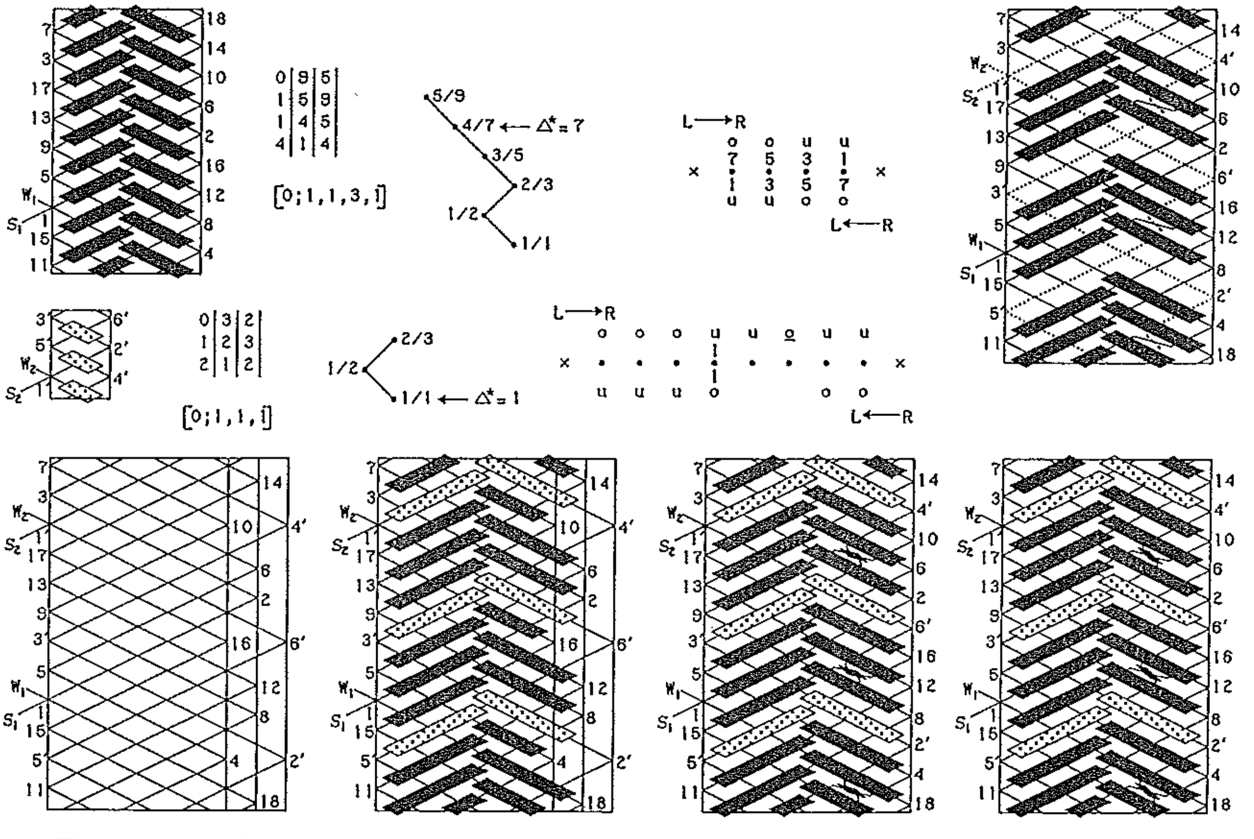

Fig. 624 — The construction details for the interbraid $p'/b' = 2/3$ with $p/b = 5/9$.

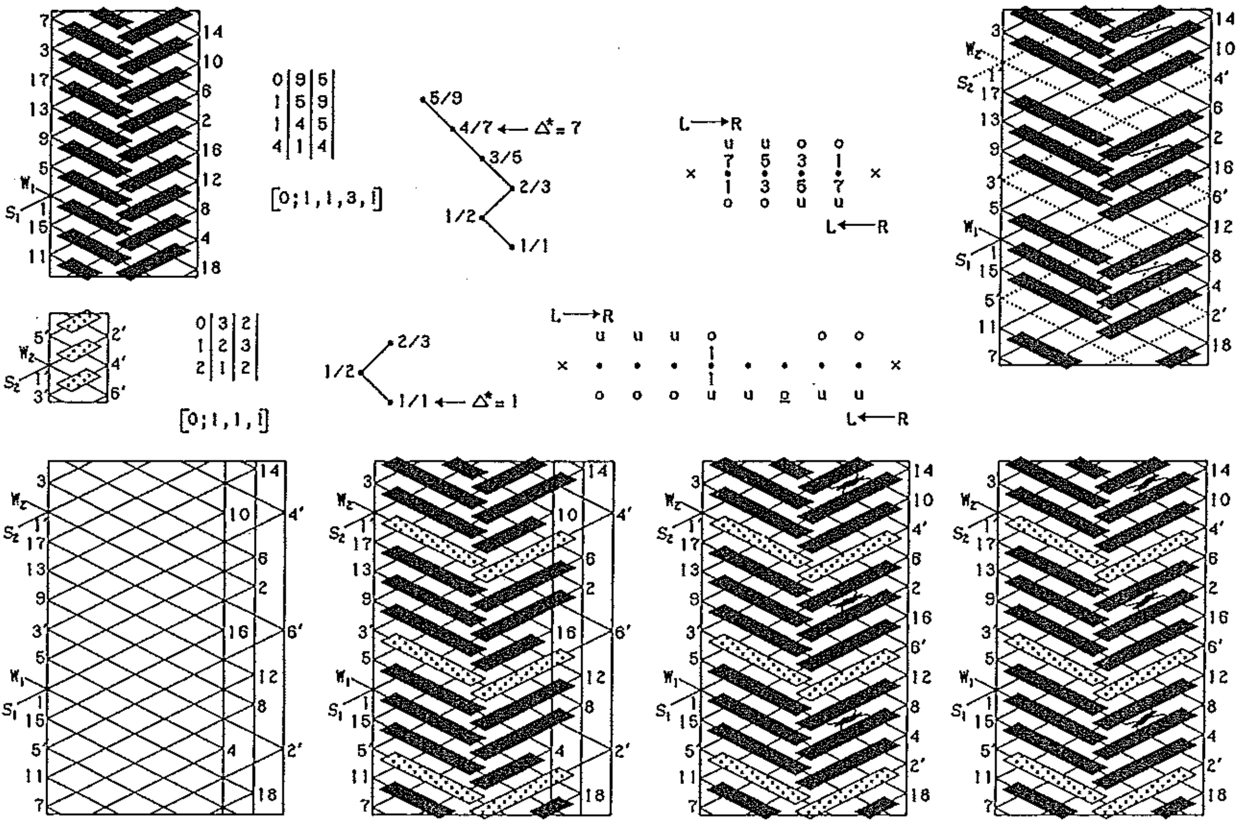

Fig. 625 — The construction details for the interbraid $p'/b' = 2/3$ with $p/b = 5/9$.

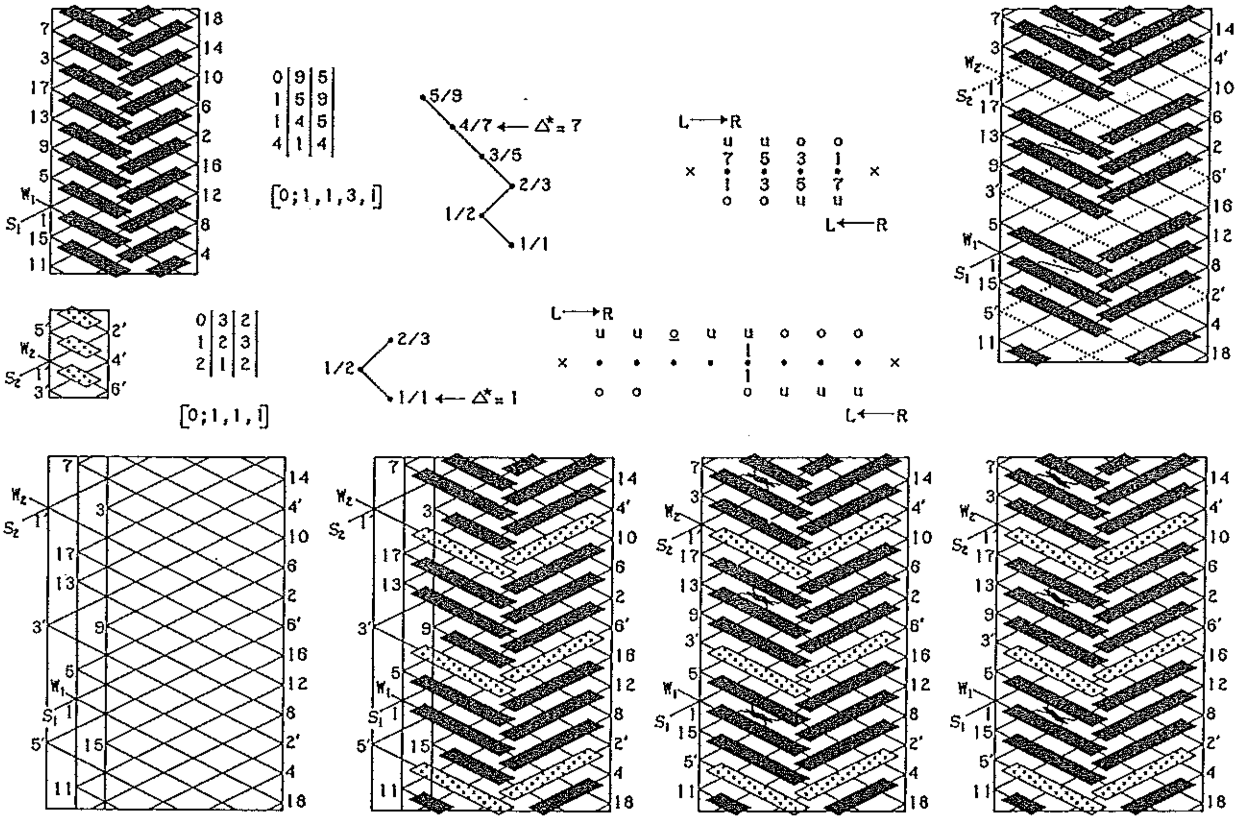

Fig. 626 — The construction details for the interbraid $p'/b' = 2/3$ with $p/b = 5/9$.

Historical events and their fictitious renderings.

In the last decade or so we have seen many fictitious renderings of historical events. Fictitious renderings of historical events are often difficult if not impossible to be recognised as such since the lapsed timespan between the event and the present may be too great, but in some circles the misrepresentsation of facts has become a habit with the result that the magnitude of lapsed timespans are neglected; this then enables us to identify such circles and file their stories in the garbage bin.

A few years ago (1998) we found on the World Wide Web (WWW) "Het Knoopeknauwertje's Homepage" with, amongst others, **The Head Hunter Ring** by Dean Westervelt. The story of **The Head Hunter Ring** by Dean Westervelt reads quite different to its translation in *Het Knoopeknauwertje*, Issue No. 9, pp. 4-5 (the more a story gets retold, the more it changes). The translation in *Het Knoopeknauwertje* reads:

> In 1948 I visited the renowned Ripley's Believe It or Not Museum. There, a descendant of a headhunter tribe was tying a ring from two strands. After returning home, I puzzled a little while over the way he did it. In due course I found the procedure. Years later I found in The Encyclopedia of Knots and Fancy Ropework by Graumont and Hensel a similar ring with the name Head hunter Ring (pg. 526, Fig. 428). They gave, however, no method for tying it since this was a secret. Below is my method which is now no secret any longer. Take two strands of equal length. Preferably of two different colours A and B. Secure the starting-ends with a rubber band and follow the drawings, the algorithm below or a combination of both.

The text on the Web-site reads:

> In 1948 I visited the famous Believe It or Not Museum in New York City. There, a descendant of a Phillipine Headhunter Tribe was tying finger rings using two strands of split bamboo. The ring was woven in a coding pattern of over-three, under-three, over three. I puzzled over this very attractive knot for several months before I discovered a procedure for tying it. The cryptic text accompanying a photo of this same knot in Graumont and Hensel's Encyclopedia of Knots and Fancy Rope Work (page 524,-5, plate 286, No. 428) was of little help.

According to the Web-site text it is clear that Dean did possess the quoted Encyclopedia by Graumont and Hensel before he solved the construction procedure, but it did not make him any wiser. In the Web-site version we cannot find 'the algorithm below', wheras it is present on pg. 4 in Het Knoopeknauwertje. There is little doubt however that the method employed by the descendant of the Headhunter Tribe was not the original tying method, but rather a 'stage act' to impress the audience. It should be noted that the 3-pass Headhunters knots $p/b = 10/12$ and $10/22$ are interweaves of respectively two over–under coded $p/b = 5/6$ Regular Knots and two over–under coded $p/b = 5/11$ Regular Knots. The $p/b = 5/6$ over–under coded Regular Knot is the 1^{st} order Method II enlargement of the over–under coded $p/b = 3/4$ Regular Knot. The $p/b = 5/11$ over–under coded Regular Knot is the 1^{st} order Method II enlargement of the over–under coded $p/b = 3/7$ Regular Knot which is easily obtained from the over–under coded $p/b = 3/4$ Regular Knot. It should be noted that a 3-pass Headhunters knot $p/b = 10/(10n + 2)$ is the interweave of two over–under coded $p/b = 5/(5n + 1)$ over–under coded Regular Knots. Hence the foundation knot of such a Headhunters knot is the 1^{st} order Method II enlargement of the over–under coded $p/b = 3/(3n + 1)$ Regular Knot. Furthermore, observe that such a foundation knot and the associated 3-pass Headhunters knot are knots of the "braiding to pattern" variety. Hence it is more likely that the original tying method was via the over–under coded $p/b = 3/(3n + 1)$ Regular Knots together with the "braiding to pattern" construction method.

THE BRAIDER

No.34 MAY 2003.

CONTENTS

pg.

The separate half-cycle tables for each essential string in the Example on pp. 756-767 783

Solution to the Question in Issue No.33 785

Nested Cylindrical Braids 790

Toggle Knots at the end of a 4-string Round Braid 806

A quarterly publication
for
the braiding artisan

Resale of this publication or copies thereof is strictly prohibited

Copyright ©2003 by:

A.G. Schaake; 21 Sundown Cresc.; Hamilton; New Zealand.
D. Van Tassel; Box 335; Craig, Co 81626-0335; U.S.A.
F.J.M. Masurel; Ganzenzijde 4; 2317XG Leiden; Nederland.

All rights reserved. No part of this publication may be reproduced, stored in a retrieval system, or transmitted, in any form or by any means, electronic, mechanical, photo-copying, recording, or otherwise, without prior written permission.

This publication is available to braiding artisans only.

Copies may be obtained from:

A.G. Schaake,
21 Sundown Cresc.,
Hamilton,
New Zealand.

The separate half-cycle tables for each essential string in the Example on pp. 756–767

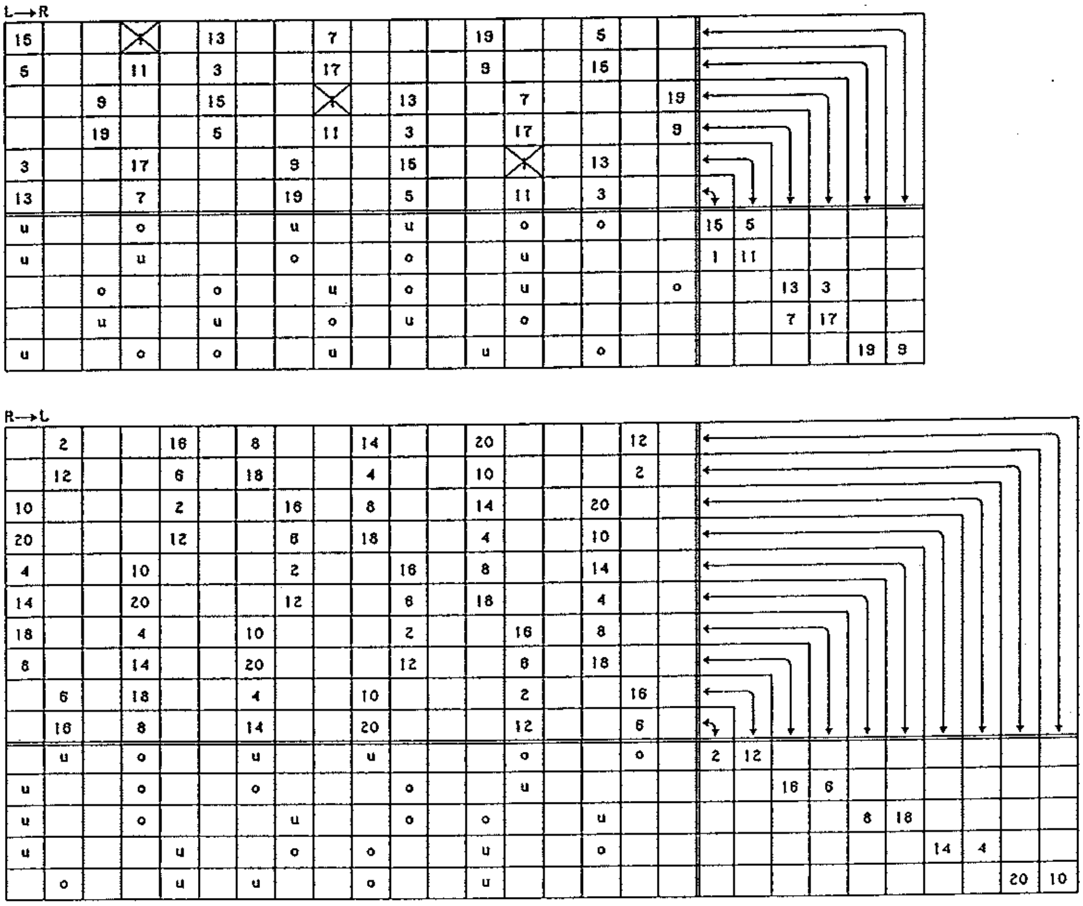

Fig. 627 — Essential string with half-cycles 1–20.

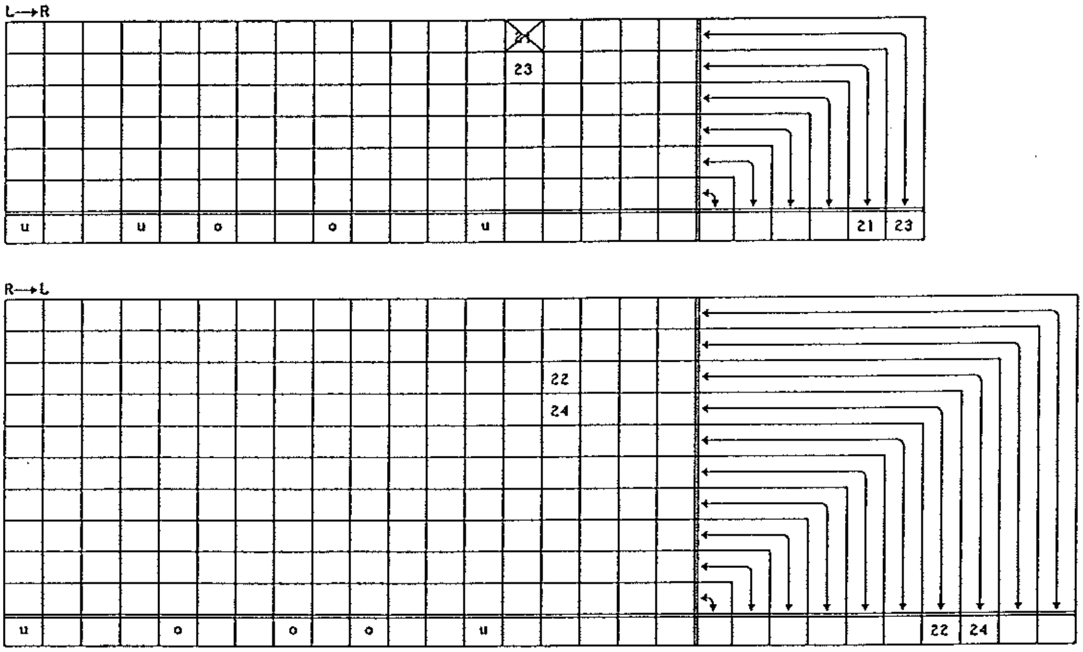

Fig. 628 — Essential string with half-cycles 21–24.

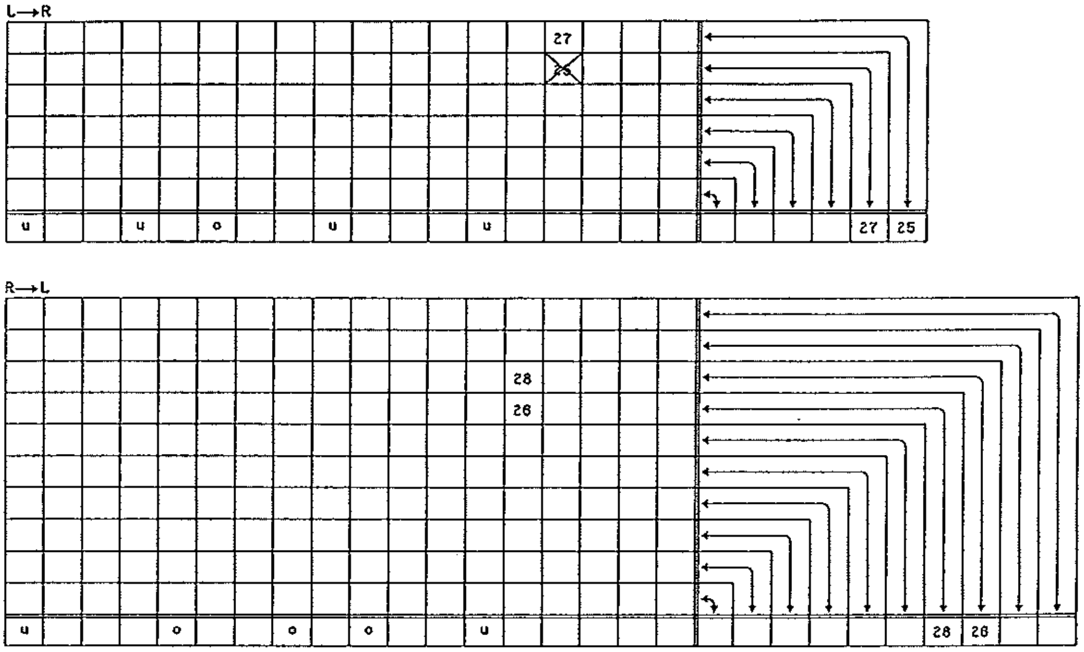

Fig. 629 — Essential string with half-cycles 25–28.

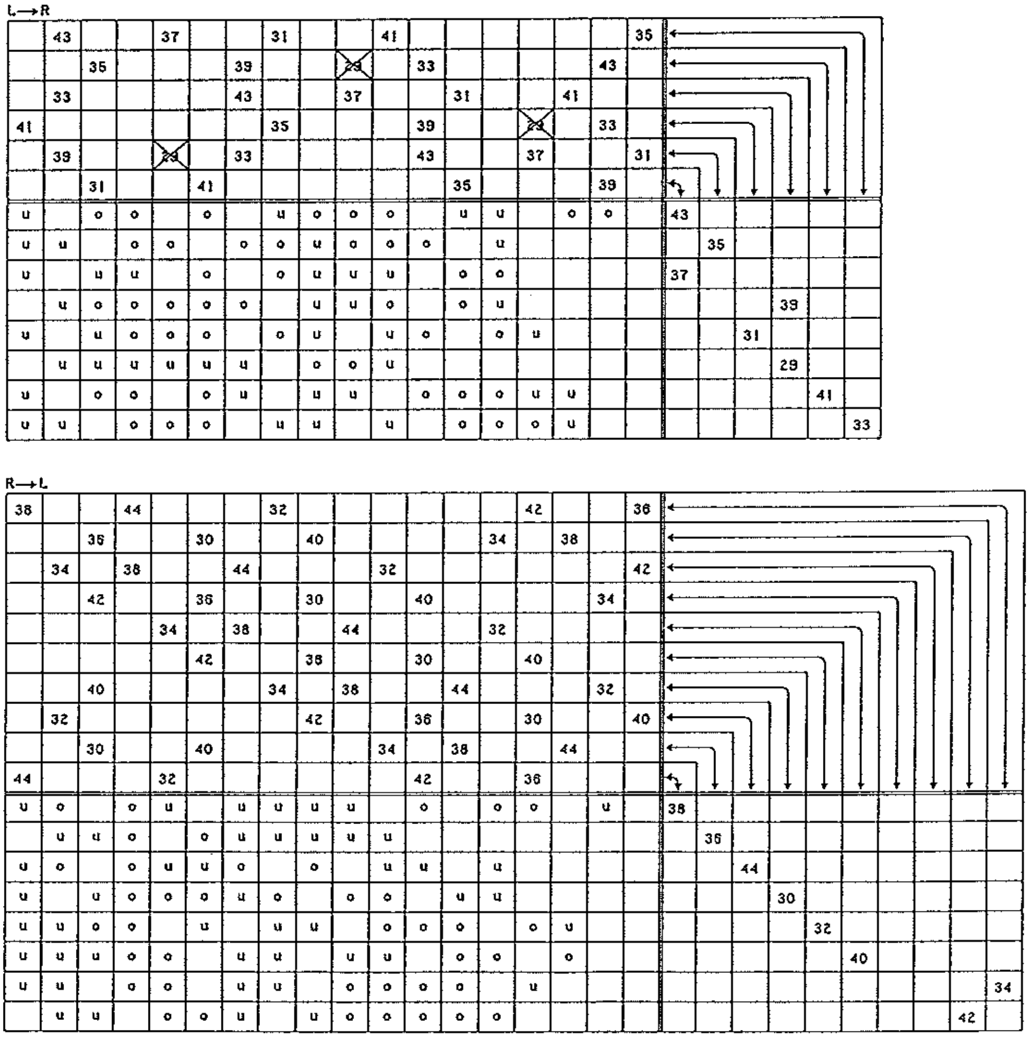

Fig. 630 — Essential string with half-cycles 29–44.

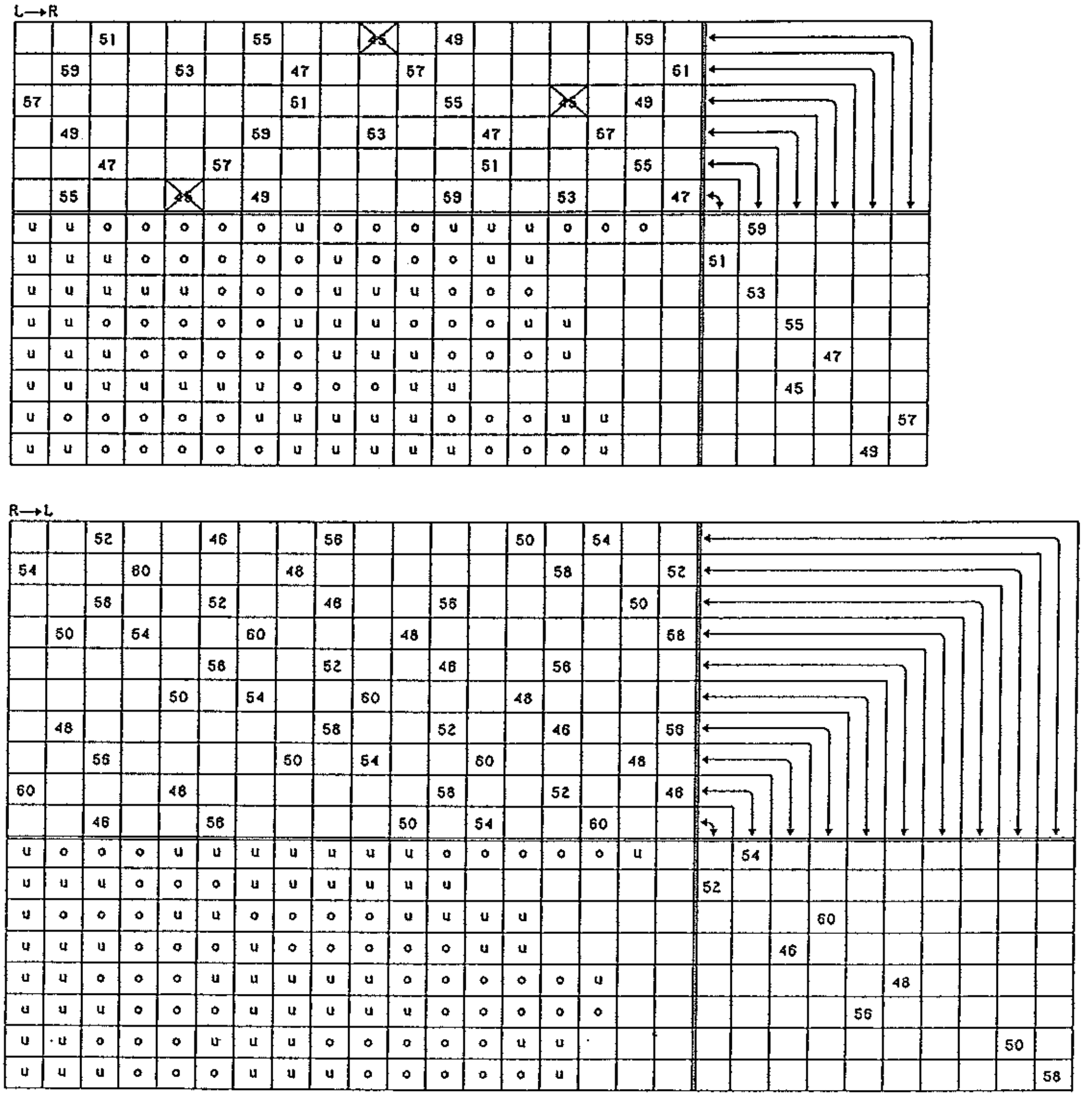

Fig. 631 — Essential string with half-cycles 45–60.

Solution to the Question in Issue No. 33

Refer to Fig. 617, pg. 775, and to pg. 776.

For the component with the lowermost first-return string-run in Fig. 617 the number of sub-components $\lambda = \text{g.c.d.}(5, \frac{B}{2})$, hence for $B = 8$, consequently $\frac{B}{2} = 4$, we obtain $\lambda = \text{g.c.d.}(5, \frac{B}{2}) = \text{g.c.d.}(5, 4) = 1$, while for the component with the uppermost first-return string-run in Fig. 617 the number of sub-components $\lambda = \text{g.c.d.}(2, \frac{B}{2}) = \text{g.c.d.}(2, 4) = 2$. We thus require two essential strings for the interbraiding of the coloured V's. The two respective interbraids with Standing-Ends S_2 and S_3 have each one part and two bights.

The construction details for interbraiding the two $p/b = 1/2$ Regular Knots with the 2-pass Spanish Ring Knot $p/b = 5/8$, are for the four V patterns depicted in respectively Fig. 632, Fig. 633, Fig. 634 and Fig. 635.

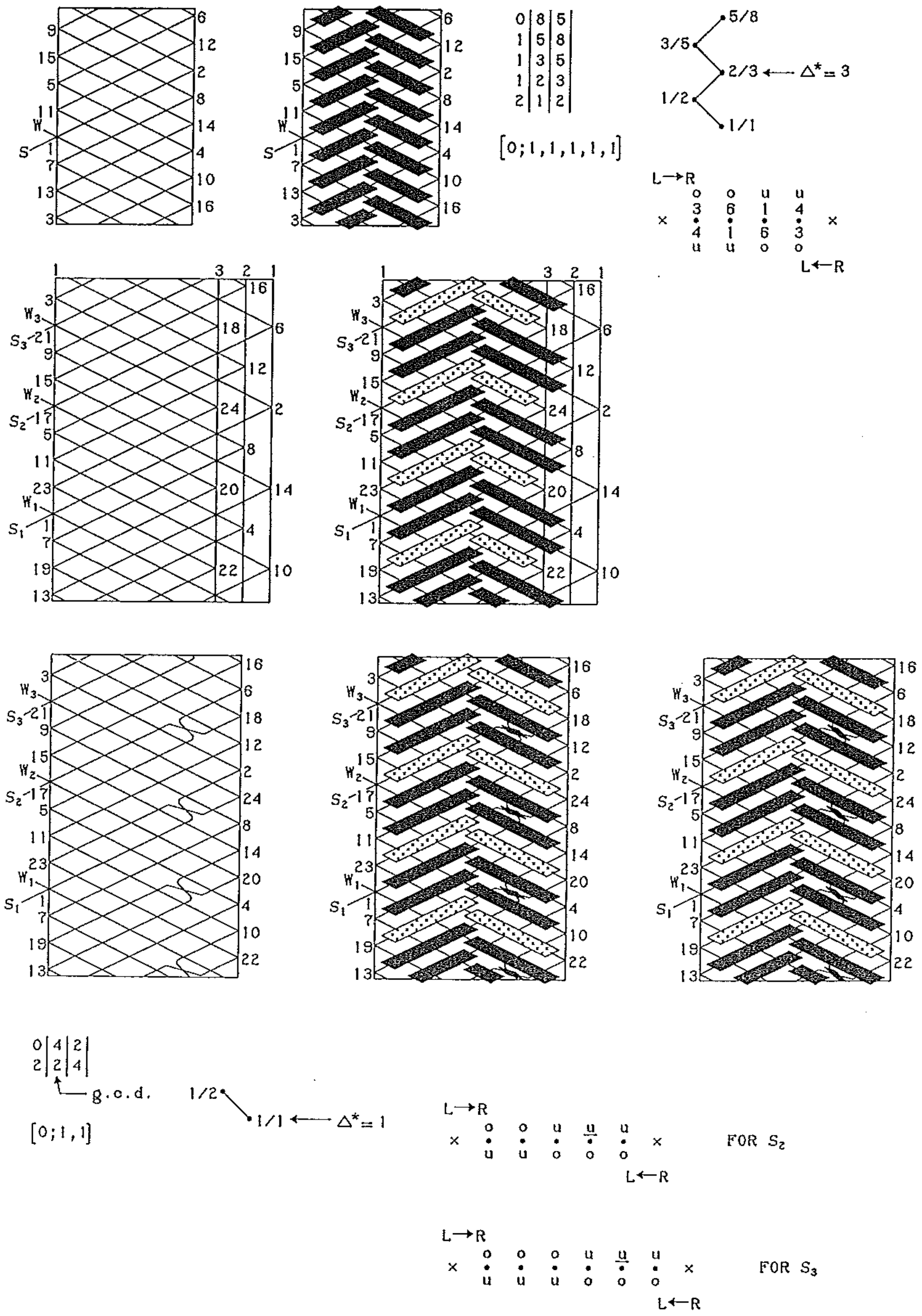

Fig. 632 — Construction details for the two interbraids $p'/b' = 1/2$ with $p/b = 5/8$.

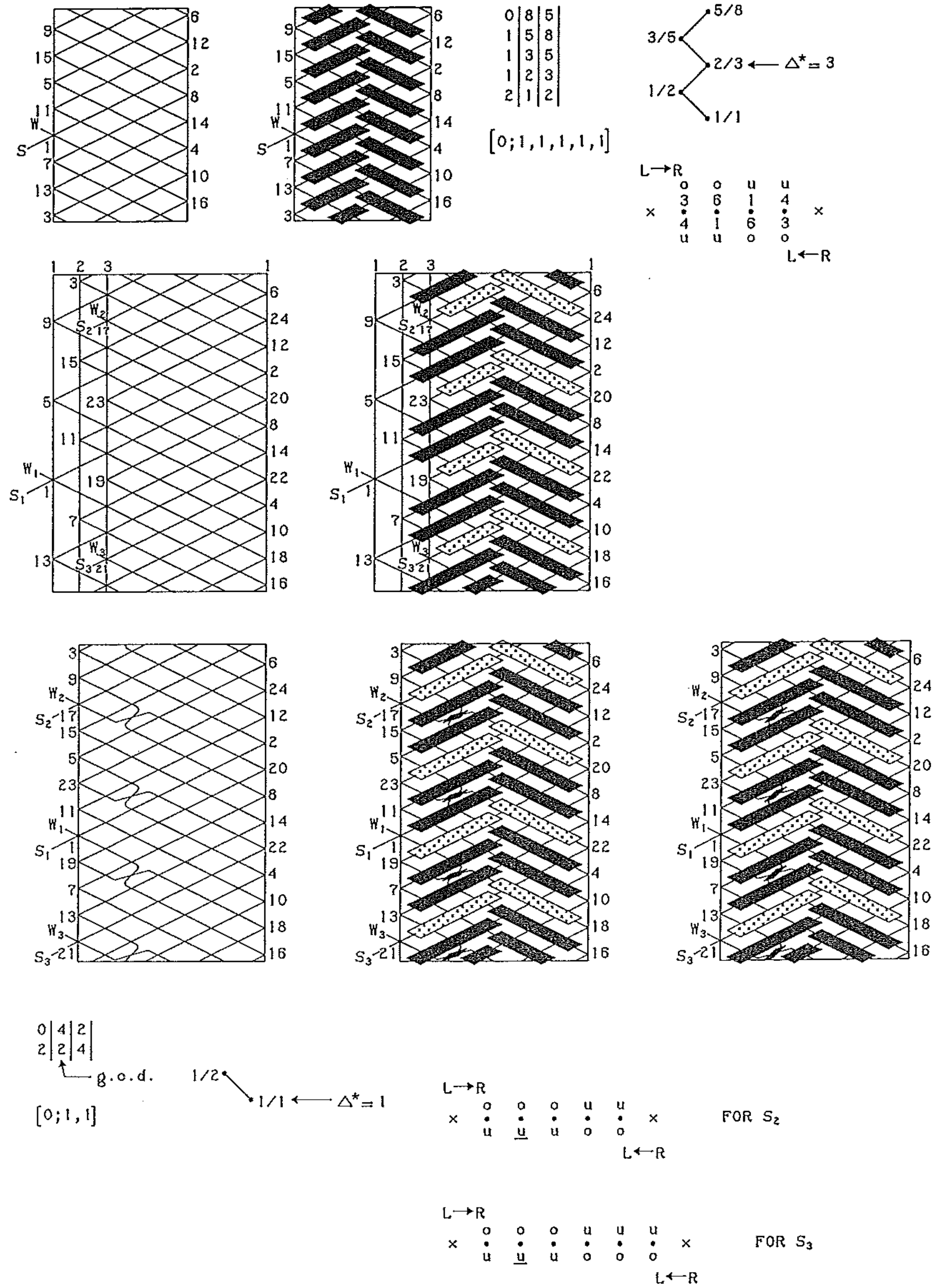

Fig. 633 — Construction details for the two interbraids $p'/b' = 1/2$ with $p/b = 5/8$.

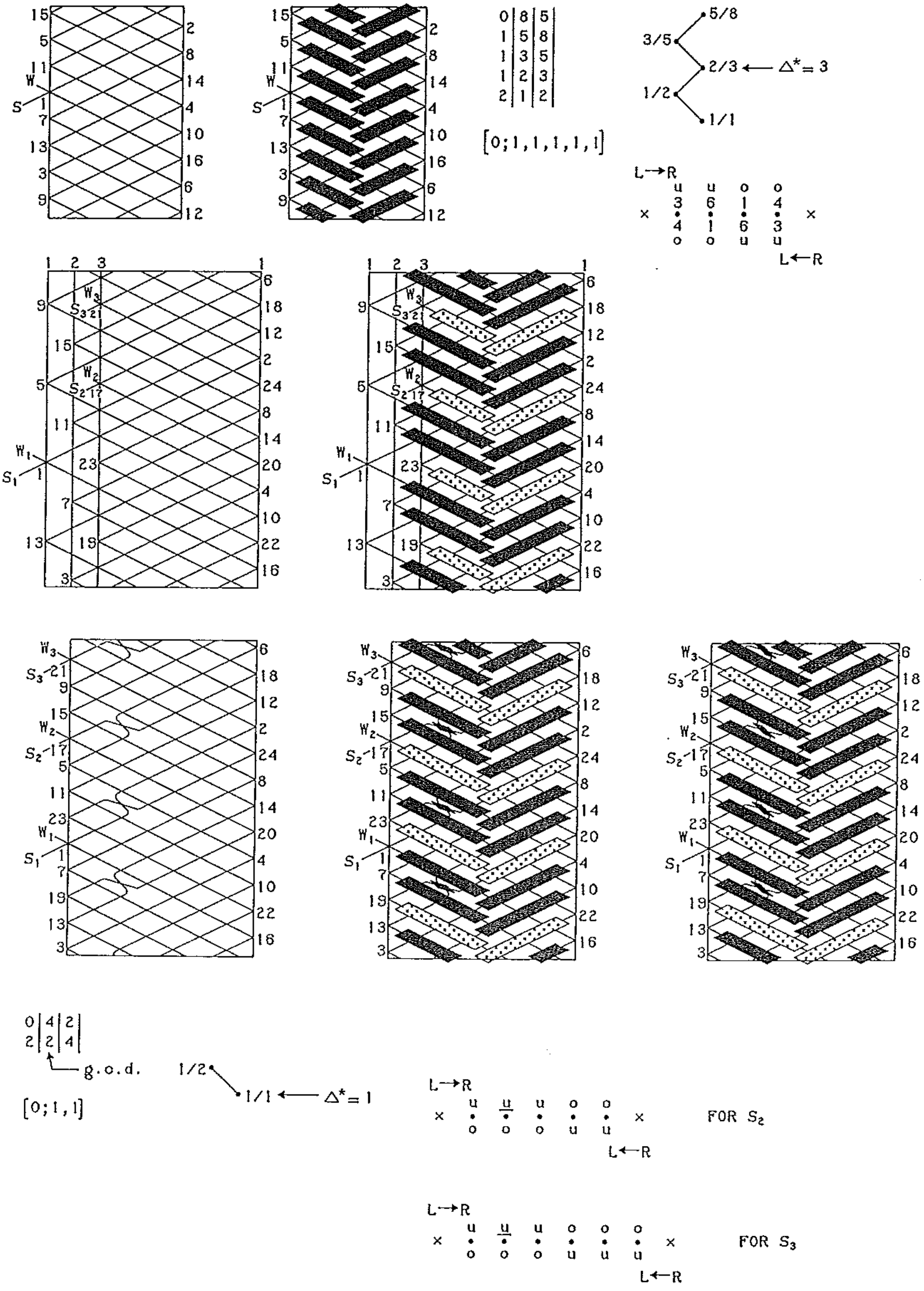

Fig. 634 — Construction details for the two interbraids $p'/b' = 1/2$ with $p/b = 5/8$.

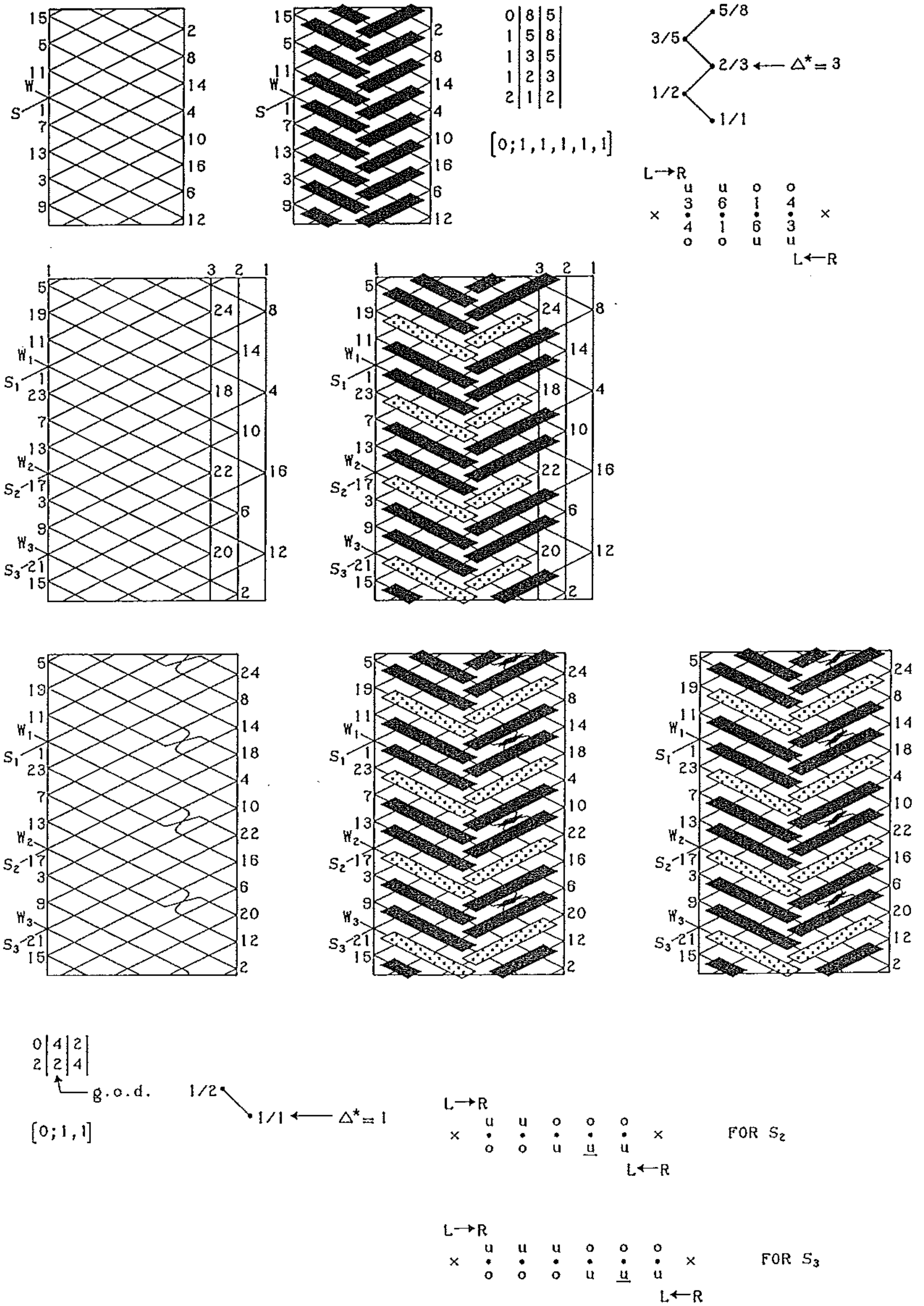

Fig. 635 — Construction details for the two interbraids $p'/b' = 1/2$ with $p/b = 5/8$.

Nested Cylindrical Braids

The Periodic Regular Nested Cylindrical Braids:

Let the left **nesting-number**(see *The Braider*, Issue No. 19, pp. 415-419) A_l being made-up of two **sub-nesting-numbers** A_{l_1} and A_{l_2}, thus $A_l = A_{l_1} + A_{l_2}$. Similarly let the right **nesting-number** A_r being made-up of two **sub-nesting-numbers** A_{r_1} and A_{r_2}, thus $A_r = A_{r_1} + A_{r_2}$. Furthermore, let $A_{l_1} > A_{l_2}$ and $A_{r_1} > A_{r_2}$.

Note that in this general case are contained the following two special cases:

1). The nesting-number on one bight-edge is made-up of two sub-nesting-numbers, and the nesting-number on the other bight-edge is made-up of only **one** sub-nesting-number.

2). The nesting-number on one bight-edge is made-up of two sub-nesting-numbers, and the nesting-number on the other bight-edge is made-up of only **one** sub-nesting-number which is equal to 1 (hence this latter bight-edge consists of one bight-boundary only).

For the left bight-edge and for the right bight-edge there are two types of bight-edges when the nesting-number of the bight-edge is made-up of two sub-nesting-numbers with the following **bight-boundary position specifications** and **bight-boundary sequence specifications**:

For the left bight-edge:

1). The two sub-nesting-numbers A_{l_1} and A_{l_2} do have the same parity.

The left bight-boundary position specification is then:

$$\underbrace{222\cdots2}_{(A_{l_1}-1)\text{ elements}}$$

While the left bight-boundary sequence specification is then:

$$1_1(z)_{(A_{l_1}+A_{l_2})}(z-1)_{(A_{l_1}+A_{l_2}-1)}(z-2)_{(A_{l_1}+A_{l_2}-2)}\cdots$$
$$(z-A_{l_2}+1)_{(A_{l_1}+1)}(A_{l_1})_{(A_{l_1})}(A_{l_1}-1)_{(A_{l_1}-1)}\cdots2_2\,.$$

Where $z = \dfrac{A_{l_1}+A_{l_2}}{2}$.

2). The two sub-nesting-numbers A_{l_1} and A_{l_2} do not have the same parity.

The left bight-boundary position specification is then:

$$\underbrace{222\cdots2}_{\substack{z-2A_{l_2}\\ \text{elements}}}\underbrace{111\cdots1}_{\substack{2A_{l_2}\\ \text{elements}}}\underbrace{222\cdots2}_{\substack{A_l-z-1\\ \text{elements}}}$$

Note that $A_l - z - 1 = z - 2A_{l_2}$.

While the left bight-boundary sequence specification is then:

i). For $A_{l_1} = A_{l_2} + 1$:

$$1_1(z)_{(A_{l_1}+A_{l_2})}(z-2)_{(A_{l_1}+A_{l_2}-1)}(z-4)_{(A_{l_1}+A_{l_2}-2)}\cdots$$
$$2_{(A_{l_1}+1)}(z+1)_{(z+1-A_{l_2})}(z-1)_{(z-A_{l_2})}(z-3)_{(z-1-A_{l_2})}\cdots3_2\,.$$

Where $z = \dfrac{A_{l_1}+A_{l_2}-1}{2} + A_{l_2} = 2A_{l_2}$.

ii). For $A_{l_1} \geq A_{l_2} + 3$:

$$1_1(z)_{(A_{l_1}+A_{l_2})}(z-2)_{(A_{l_1}+A_{l_2}-1)}(z-4)_{(A_{l_1}+A_{l_2}-2)}\cdots$$
$$(z+2-2A_{l_2})_{(A_{l_1}+1)}(A_{l_1}+A_{l_2})_{(A_{l_1})}(A_{l_1}+A_{l_2}-1)_{(A_{l_1}-1)}(A_{l_1}+A_{l_2}-2)_{(A_{l_1}-2)}\cdots$$
$$(z+1)_{(z+1-A_{l_2})}(z-1)_{(z-A_{l_2})}(z-3)_{(z-1-A_{l_2})}\cdots$$
$$(z+1-2A_{l_2})_{(z+1-2A_{l_2})}(z-2A_{l_2})_{(z-2A_{l_2})}(z-1-2A_{l_2})_{(z-1-2A_{l_2})}\cdots2_2\,.$$

Where $z = \dfrac{A_{l_1}+A_{l_2}-1}{2} + A_{l_2}$.

⋆⋆ Determine for the four left-hand bight-edges in Fig. 636 the left bight-boundary position specification and the left bight-boundary sequence set with ranking-numbers.

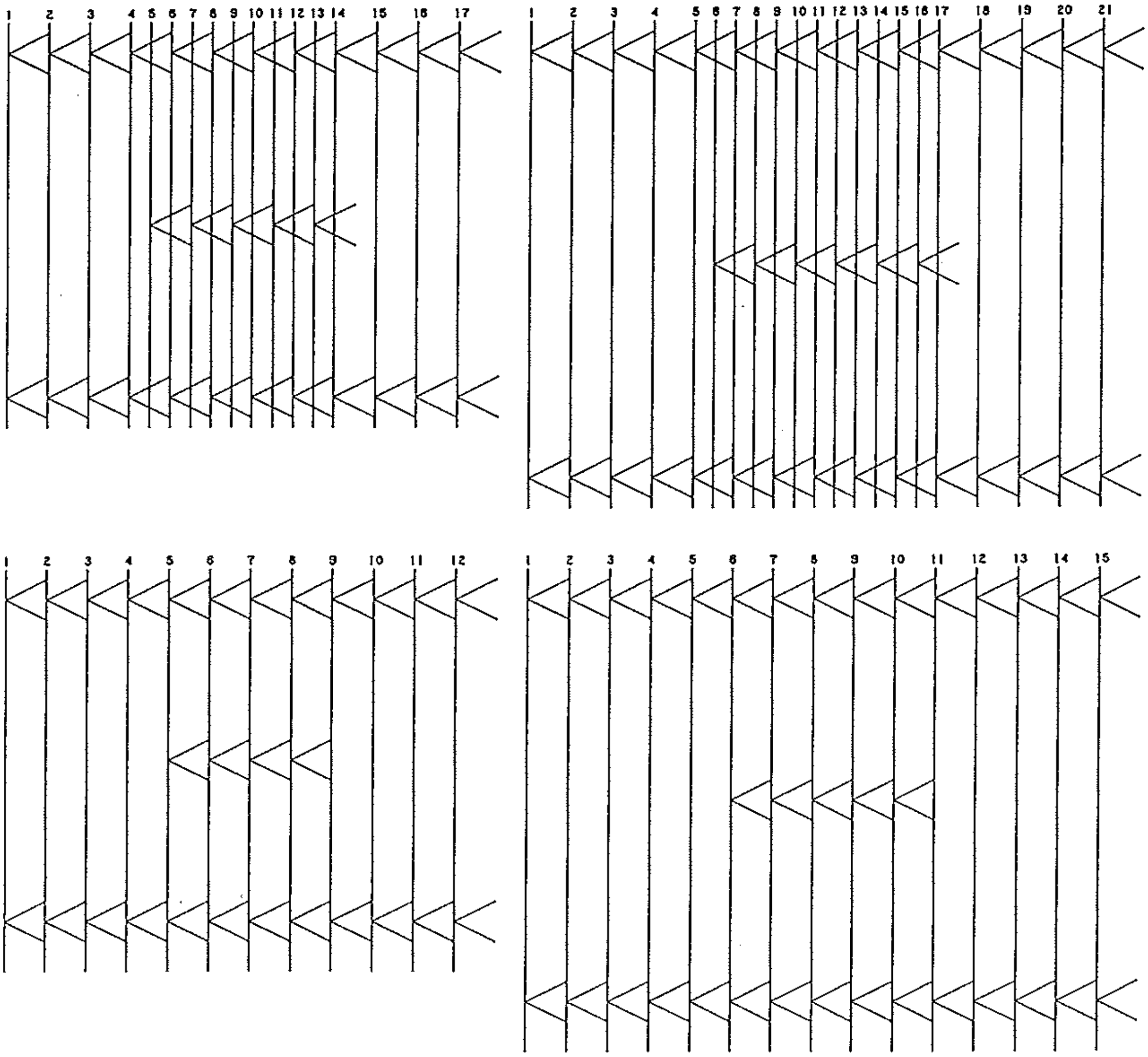

Fig. 636 — Examples of sub-nesting numbers A_{l_1} and A_{l_2}.

For the right bight-edge:

1). The two sub-nesting-numbers A_{r_1} and A_{r_2} do have the same parity:

The right bight-boundary position specification is then:

$$\underbrace{222\cdots 2}_{(A_{r_1}-1)\text{ elements}}$$

While the right bight-boundary sequence specification is then:

$$123\cdots(A_{r_1})(z+1-A_{r_2})(z+2-A_{r_2})(z+3-A_{r_2})\cdots z\,.$$

Where $z = \dfrac{A_{r_1}+A_{r_2}}{2}$.

2). The two sub-nesting-numbers A_{r_1} and A_{r_2} do not have the same parity:

The right bight-boundary position specification is then:

$$\underbrace{222\cdots 2}_{\substack{A_r-z-1\\ \text{elements}}}\underbrace{111\cdots 1}_{\substack{2A_{r_2}\\ \text{elements}}}\underbrace{222\cdots 2}_{\substack{z-2A_{r_2}\\ \text{elements}}}$$

Note that $A_r - z - 1 = z - 2A_{r_2}$.

While the right bight-boundary sequence specification is then:

i). For $A_{r_1} = A_{r_2} + 1$:
$135 \cdots (z+1) 246 \cdots z$.

Where $z = \dfrac{A_{r_1} + A_{r_2} - 1}{2} + A_{r_2} = 2A_{r_2}$.

ii). For $A_{r_1} \geq A_{r_2} + 3$:
$123 \cdots (z+1-2A_{r_2})(z+3-2A_{r_2})(z+5-2A_{r_2}) \cdots (z+1)(z+2)(z+3) \cdots$
$(A_{r_1} + A_{r_2})(z+2-2A_{r_2})(z+4-2A_{r_2})(z+6-2A_{r_2}) \cdots z$.

Where $z = \dfrac{A_{r_1} + A_{r_2} - 1}{2} + A_{r_2}$.

⋆⋆ *Determine for the four right-hand bight-edges in Fig. 637 the right bight-boundary position specification and in general terms the right bight-boundary sequence set.*

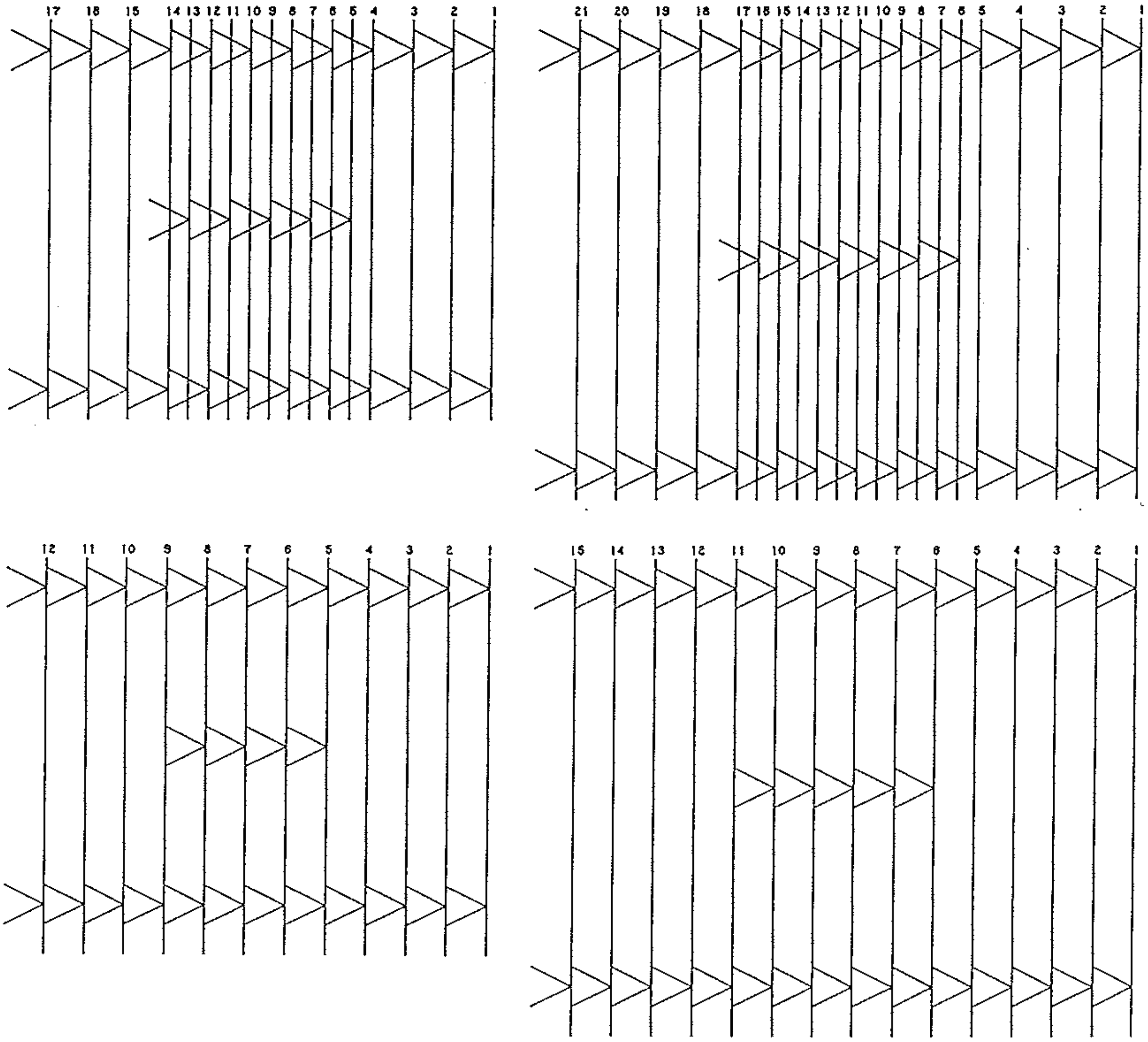

Fig. 637 — Examples of sub-nesting numbers A_{r_1} and A_{r_2}.

Note that for the left bight-edge we have used for the first lower-left to upper-right half-cycle the conventional start at left bight-boundary 1. Consequently we could fully specify in general terms the bight-boundary sequence specification (the bight-boundary sequence with their ranking-numbers). For the right bight-edge we can only specify in general terms the cyclic sequence of the bight-boundaries since the first lower-left to upper-right half-cycle can be made to end at anyone of the right bight-boundaries which then receives the ranking-number 1. The sequential order of the ranking-numbers $23\cdots(A_{r_1}+A_{r_2})$ follows then the further cyclic sequence of the bight-boundaries. For example, when $A_{r_1}=9$ and $A_{r_2}=4$, the cyclic sequence of the right bight-boundaries will be $123579(11)(12)(13)468(10)$. Say that the first lower-left to upper-right half-cycle ends at right bight-boundary 7, then the right bight-boundary sequence specification with its ranking-numbers becomes $7_1 9_2 11_3 12_4 13_5 4_6 6_7 8_8 10_9 1_{10} 2_{11} 3_{12} 5_{13}$.

Although there is a distinct calculation procedure associated with each of the two types of bight-edges, it is, however, more convenient to use a single, more universal, calculation procedure for both types. With the aid of the following Example we will run through this more universal calculation process.

Example 1.:

Let $A_{l_1}=5$; $A_{l_2}=2$; $A_{r_1}=4$; $A_{r_2}=2$ $x=11$.
Hence:

$$A_l = A_{l_1}+A_{l_2}=5+2=7.$$

$$A_r = A_{r_1}+A_{r_2}=4+2=6.$$

$$B_{total}=B_l^*\cdot A_l = B_l^*\cdot 7 = B_r^*\cdot A_r = B_r^*\cdot 6\,,$$

let B_{total} be equal to 42, then

$$B_l^*=6 \text{ and } B_r^*=7\,.$$

$$d=\text{g.c.d.}\,(A_l,A_r)=\text{g.c.d.}\,(7,6)=1\,.$$

$$A^{**}=\frac{A_l\cdot A_r}{d}=\frac{7\cdot 6}{1}=42\,.$$

$$B^{**}=\frac{B_{total}}{A^{**}}=\frac{42}{42}=1\,.$$

The left bight-boundary position specification is 211112,
hence $\mathcal{K}_l=7$.

The left bight-boundary sequence specification is $1_1 5_7 3_6 7_5 6_4 4_3 2_2$.

The right bight-boundary position specification is 222,
hence $\mathcal{K}_r=4$.

The right bight-boundary sequence specification is $1_1 2_2 3_3 4_4 2_5 3_6$.

Hence the string-run specification of this Periodic Regular Nested Cylindrical Braid is $(211112/11/222)\{1_1 5_7 3_6 7_5 6_4 4_3 2_2/1_1 2_2 3_3 4_4 2_5 3_6\}42$.

We can now readily calculate the Δ_{l_i} and the Δ_{r_i} values:

$$\begin{array}{llll}
\Delta_{l_i}=8 & \text{for } l_i=1\,. & \Delta_{r_i}=6 & \text{for } r_i=1\,.\\
\Delta_{l_i}=6 & \text{for } l_i=2\,. & \Delta_{r_i}=4 & \text{for } r_i=2\,.\\
\Delta_{l_i}=5 & \text{for } l_i=3\,. & \Delta_{r_i}=2 & \text{for } r_i=3\,.\\
\Delta_{l_i}=4 & \text{for } l_i=4\,. & \Delta_{r_i}=0 & \text{for } r_i=4\,.\\
\Delta_{l_i}=3 & \text{for } l_i=5\,. & & \\
\Delta_{l_i}=2 & \text{for } l_i=6\,. & & \\
\Delta_{l_i}=0 & \text{for } l_i=7\,. & &
\end{array}$$

Each lower-left to upper-right half-cycle type in a Nested Cylindrical Braid occurs only once in all the first-return string-runs of such a braid. Hence we can read the lower-left to upper-right half-cycle types from the Periodic Regular Nested Cylindrical Braid specification $(211112/11/222)\{1_1 5_7 3_6 7_5 6_4 4_3 2_2 / 1_1 2_2 3_3 4_4 2_5 3_6\}42$:

$1_1 \longrightarrow 1_1$
$5_7 \longrightarrow 2_2$
$3_6 \longrightarrow 3_3$
$7_5 \longrightarrow 4_4$
$6_4 \longrightarrow 2_5$
$4_3 \longrightarrow 3_6$
$2_2 \longrightarrow 1_1$
$1_1 \longrightarrow 2_2$
$5_7 \longrightarrow 3_3$
$3_6 \longrightarrow 4_4$
$7_5 \longrightarrow 2_5$
$6_4 \longrightarrow 3_6$
$4_3 \longrightarrow 1_1$
$2_2 \longrightarrow 2_2$

$1_1 \longrightarrow 3_3$
$5_7 \longrightarrow 4_4$
$3_6 \longrightarrow 2_5$
$7_5 \longrightarrow 3_6$
$6_4 \longrightarrow 1_1$
$4_3 \longrightarrow 2_2$
$2_2 \longrightarrow 3_3$
$1_1 \longrightarrow 4_4$
$5_7 \longrightarrow 2_5$
$3_6 \longrightarrow 3_6$
$7_5 \longrightarrow 1_1$
$6_4 \longrightarrow 2_2$
$4_3 \longrightarrow 3_3$
$2_2 \longrightarrow 4_4$

$1_1 \longrightarrow 2_5$
$5_7 \longrightarrow 3_6$
$3_6 \longrightarrow 1_1$
$7_5 \longrightarrow 2_2$
$6_4 \longrightarrow 3_3$
$4_3 \longrightarrow 4_4$
$2_2 \longrightarrow 2_5$
$1_1 \longrightarrow 3_6$
$5_7 \longrightarrow 1_1$
$3_6 \longrightarrow 2_2$
$7_5 \longrightarrow 3_3$
$6_4 \longrightarrow 4_4$
$4_3 \longrightarrow 2_5$
$2_2 \longrightarrow 3_6$

Anyone of these listed types may be taken as the first lower-left to upper-right half-cycle in the 1st first-return string-run, but normally we take the first listed one. Every lower-left to upper-right half-cycle encountered in this 1st first-return string-run gets deleted from the type-list.

Anyone of the remaining types in the type-list may be taken as the first lower-left to upper-right half-cycle in the 2nd first-return string-run, and again every lower-left to upper-right half-cycle encountered in this 2nd first-return string-run gets deleted from the remaining type-list.

This process is carried on till all the lower-left to upper-right half-cycle types have been deleted from the type-list.

For the first-return string-runs we thus obtain:

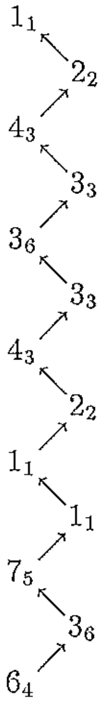

$$l_{1_{j_l}} = 1_1 \longrightarrow 1_1 = r_{1_{j_r}} \quad \rightarrow \quad j'_l = |1+8+11+6|_7 = 5 \quad \rightarrow \quad l_{2_{j'_l}} = 7_5\,.$$
$$l_{2_{j'_l}} = 7_5 \longleftarrow 1_1 = r_{1_{j_r}} \quad \rightarrow \quad j'_r = |1+6+11+0|_6 = 6 \quad \rightarrow \quad r_{2_{j'_r}} = 3_6\,.$$
$$l_{2_{j_l}} = 7_5 \longrightarrow 3_6 = r_{2_{j'_r}} \quad \rightarrow \quad j'_l = |5+0+11+2|_7 = 4 \quad \rightarrow \quad l_{3_{j'_l}} = 6_4\,.$$
$$l_{3_{j'_l}} = 6_4 \longleftarrow 3_6 = r_{2_{j_r}} \quad \rightarrow \quad j'_r = |6+2+11+2|_6 = 3 \quad \rightarrow \quad r_{3_{j'_r}} = 3_3\,.$$
$$l_{3_{j_l}} = 6_4 \longrightarrow 3_3 = r_{3_{j'_r}} \quad \rightarrow \quad j'_l = |4+2+11+2|_7 = 5 \quad \rightarrow \quad l_{4_{j'_l}} = 7_5\,.$$
$$l_{4_{j'_l}} = 7_5 \longleftarrow 3_3 = r_{3_{j_r}} \quad \rightarrow \quad j'_r = |3+2+11+0|_6 = 4 \quad \rightarrow \quad r_{4_{j'_r}} = 4_4\,.$$
$$l_{4_{j_l}} = 7_5 \longrightarrow 4_4 = r_{4_{j'_r}} \quad \rightarrow \quad j'_l = |5+0+11+0|_7 = 2 \quad \rightarrow \quad l_{5_{j'_l}} = 2_2\,.$$
$$l_{5_{j'_l}} = 2_2 \longleftarrow 4_4 = r_{4_{j_r}} \quad \rightarrow \quad j'_r = |4+0+11+6|_6 = 3 \quad \rightarrow \quad r_{5_{j'_r}} = 3_3\,.$$
$$l_{5_{j_l}} = 2_2 \longrightarrow 3_3 = r_{5_{j'_r}} \quad \rightarrow \quad j'_l = |2+6+11+2|_7 = 7 \quad \rightarrow \quad l_{6_{j'_l}} = 5_7\,.$$
$$l_{6_{j'_l}} = 5_7 \longleftarrow 3_3 = r_{5_{j_r}} \quad \rightarrow \quad j'_r = |3+2+11+3|_6 = 1 \quad \rightarrow \quad r_{6_{j'_r}} = 1_1\,.$$
$$l_{6_{j_l}} = 5_7 \longrightarrow 1_1 = r_{6_{j'_r}} \quad \rightarrow \quad j'_l = |7+3+11+6|_7 = 6 \quad \rightarrow \quad l_{7_{j'_l}} = 3_6\,.$$

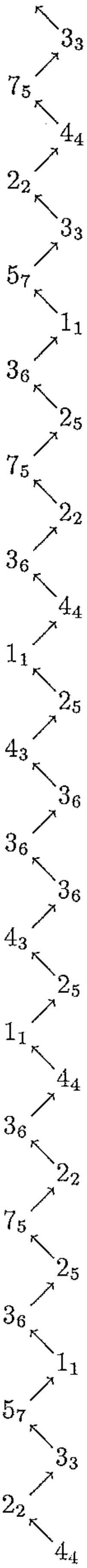

$$l_{7_{j_l'}} = 3_6 \longleftarrow 1_1 = r_{6_{j_r}} \rightarrow j_r' = |1+6+11+5|_6 = 5 \rightarrow r_{7_{j_r'}} = 2_5 .$$
$$l_{7_{j_l}} = 3_6 \longrightarrow 2_5 = r_{7_{j_r'}} \rightarrow j_l' = |6+5+11+4|_7 = 5 \rightarrow l_{8_{j_l'}} = 7_5 .$$
$$l_{8_{j_l'}} = 7_5 \longleftarrow 2_5 = r_{7_{j_r}} \rightarrow j_r' = |5+4+11+0|_6 = 2 \rightarrow r_{8_{j_r'}} = 2_2 .$$
$$l_{8_{j_l}} = 7_5 \longrightarrow 2_2 = r_{8_{j_r'}} \rightarrow j_l' = |5+0+11+4|_7 = 6 \rightarrow l_{9_{j_l'}} = 3_6 .$$
$$l_{9_{j_l'}} = 3_6 \longleftarrow 2_2 = r_{8_{j_r}} \rightarrow j_r' = |2+4+11+5|_6 = 4 \rightarrow r_{9_{j_r'}} = 4_4 .$$
$$l_{9_{j_l}} = 3_6 \longrightarrow 4_4 = r_{9_{j_r'}} \rightarrow j_l' = |6+5+11+0|_7 = 1 \rightarrow l_{10_{j_l'}} = 1_1 .$$
$$l_{10_{j_l'}} = 1_1 \longleftarrow 4_4 = r_{9_{j_r}} \rightarrow j_r' = |4+0+11+8|_6 = 5 \rightarrow r_{10_{j_r'}} = 2_5 .$$
$$l_{10_{j_l}} = 1_1 \longrightarrow 2_5 = r_{10_{j_r'}} \rightarrow j_l' = |1+8+11+4|_7 = 3 \rightarrow l_{11_{j_l'}} = 4_3 .$$
$$l_{11_{j_l'}} = 4_3 \longleftarrow 2_5 = r_{10_{j_r}} \rightarrow j_r' = |5+4+11+4|_6 = 6 \rightarrow r_{11_{j_r'}} = 3_6 .$$
$$l_{11_{j_l}} = 4_3 \longrightarrow 3_6 = r_{11_{j_r'}} \rightarrow j_l' = |3+4+11+2|_7 = 6 \rightarrow l_{12_{j_l'}} = 3_6 .$$
$$l_{12_{j_l'}} = 3_6 \longleftarrow 3_6 = r_{11_{j_r}} \rightarrow j_r' = |6+2+11+5|_6 = 6 \rightarrow r_{12_{j_r'}} = 3_6 .$$
$$l_{12_{j_l}} = 3_6 \longrightarrow 3_6 = r_{12_{j_r'}} \rightarrow j_l' = |6+5+11+2|_7 = 3 \rightarrow l_{13_{j_l'}} = 4_3 .$$
$$l_{13_{j_l'}} = 4_3 \longleftarrow 3_6 = r_{12_{j_r}} \rightarrow j_r' = |6+2+11+4|_6 = 5 \rightarrow r_{13_{j_r'}} = 2_5 .$$
$$l_{13_{j_l}} = 4_3 \longrightarrow 2_5 = r_{13_{j_r'}} \rightarrow j_l' = |3+4+11+4|_7 = 1 \rightarrow l_{14_{j_l'}} = 1_1 .$$
$$l_{14_{j_l'}} = 1_1 \longleftarrow 2_5 = r_{13_{j_r}} \rightarrow j_r' = |5+4+11+8|_6 = 4 \rightarrow r_{14_{j_r'}} = 4_4 .$$
$$l_{14_{j_l}} = 1_1 \longrightarrow 4_4 = r_{14_{j_r'}} \rightarrow j_l' = |1+8+11+0|_7 = 6 \rightarrow l_{15_{j_l'}} = 3_6 .$$
$$l_{15_{j_l'}} = 3_6 \longleftarrow 4_4 = r_{14_{j_r}} \rightarrow j_r' = |4+0+11+5|_6 = 2 \rightarrow r_{15_{j_r'}} = 2_2 .$$
$$l_{15_{j_l}} = 3_6 \longrightarrow 2_2 = r_{15_{j_r'}} \rightarrow j_l' = |6+5+11+4|_7 = 5 \rightarrow l_{16_{j_l'}} = 7_5 .$$
$$l_{16_{j_l'}} = 7_5 \longleftarrow 2_2 = r_{15_{j_r}} \rightarrow j_r' = |2+4+11+0|_6 = 5 \rightarrow r_{16_{j_r'}} = 2_5 .$$
$$l_{16_{j_l}} = 7_5 \longrightarrow 2_5 = r_{16_{j_r'}} \rightarrow j_l' = |5+0+11+4|_7 = 6 \rightarrow l_{17_{j_l'}} = 3_6 .$$
$$l_{17_{j_l'}} = 3_6 \longleftarrow 2_5 = r_{16_{j_r}} \rightarrow j_r' = |5+4+11+5|_6 = 1 \rightarrow r_{17_{j_r'}} = 1_1 .$$
$$l_{17_{j_l}} = 3_6 \longrightarrow 1_1 = r_{17_{j_r'}} \rightarrow j_l' = |6+5+11+6|_7 = 7 \rightarrow l_{18_{j_l'}} = 5_7 .$$
$$l_{18_{j_l'}} = 5_7 \longleftarrow 1_1 = r_{17_{j_r}} \rightarrow j_r' = |1+6+11+3|_6 = 3 \rightarrow r_{18_{j_r'}} = 3_3 .$$
$$l_{18_{j_l}} = 5_7 \longrightarrow 3_3 = r_{18_{j_r'}} \rightarrow j_l' = |7+3+11+2|_7 = 2 \rightarrow l_{19_{j_l'}} = 2_2 .$$
$$l_{19_{j_l'}} = 2_2 \longleftarrow 3_3 = r_{18_{j_r}} \rightarrow j_r' = |3+2+11+6|_6 = 4 \rightarrow r_{19_{j_r'}} = 4_4 .$$
$$l_{19_{j_l}} = 2_2 \longrightarrow 4_4 = r_{19_{j_r'}} \rightarrow j_l' = |2+6+11+0|_7 = 5 \rightarrow l_{20_{j_l'}} = 7_5 .$$
$$l_{20_{j_l'}} = 7_5 \longleftarrow 4_4 = r_{19_{j_r}} \rightarrow j_r' = |4+0+11+0|_6 = 3 \rightarrow r_{20_{j_r'}} = 3_3 .$$
$$l_{20_{j_l}} = 7_5 \longrightarrow 3_3 = r_{20_{j_r'}} \rightarrow j_l' = |5+0+11+2|_7 = 4 \rightarrow l_{21_{j_l'}} = 6_4 .$$
$$l_{21_{j_l'}} = 6_4 \longleftarrow 3_3 = r_{20_{j_r}} \rightarrow j_r' = |3+2+11+2|_6 = 6 \rightarrow r_{21_{j_r'}} = 3_6 .$$
$$l_{21_{j_l}} = 6_4 \longrightarrow 3_6 = r_{21_{j_r'}} \rightarrow j_l' = |4+2+11+2|_7 = 5 \rightarrow l_{22_{j_l'}} = 7_5 .$$
$$l_{22_{j_l'}} = 7_5 \longleftarrow 3_6 = r_{21_{j_r}} \rightarrow j_r' = |6+2+11+0|_6 = 1 \rightarrow r_{22_{j_r'}} = 1_1 .$$
$$l_{22_{j_l}} = 7_5 \longrightarrow 1_1 = r_{22_{j_r'}} \rightarrow j_l' = |5+0+11+6|_7 = 1 \rightarrow l_{23_{j_l'}} = 1_1 .$$
$$l_{23_{j_l'}} = 1_1 \longleftarrow 1_1 = r_{22_{j_r}} \rightarrow j_r' = |1+6+11+8|_6 = 2 \rightarrow r_{23_{j_r'}} = 2_2 .$$
$$l_{23_{j_l}} = 1_1 \longrightarrow 2_2 = r_{23_{j_r'}} \rightarrow j_l' = |1+8+11+4|_7 = 3 \rightarrow l_{24_{j_l'}} = 4_3 .$$
$$l_{24_{j_l'}} = 4_3 \longleftarrow 2_2 = r_{23_{j_r}} \rightarrow j_r' = |2+4+11+4|_6 = 3 \rightarrow r_{24_{j_r'}} = 3_3 .$$
$$l_{24_{j_l}} = 4_3 \longrightarrow 3_3 = r_{24_{j_r'}} \rightarrow j_l' = |3+4+11+2|_7 = 6 \rightarrow l_{25_{j_l'}} = 3_6 .$$
$$l_{25_{j_l'}} = 3_6 \longleftarrow 3_3 = r_{24_{j_r}} \rightarrow j_r' = |3+2+11+5|_6 = 3 \rightarrow r_{25_{j_r'}} = 3_3 .$$

$$\begin{tikzcd}
 & {} \\
7_5 \arrow[ur] & \\
 & 3_3 \arrow[ul] \\
6_4 \arrow[ur] & \\
 & 3_6 \arrow[ul] \\
7_5 \arrow[ur] & \\
 & 1_1 \arrow[ul] \\
1_1 \arrow[ur] &
\end{tikzcd}$$

$$\begin{array}{llll}
l_{25_{j_l}} = 3_6 \longrightarrow 3_3 = r_{25_{j'_r}} & \to\ j'_l = |6+5+11+2|_7 = 3 & \to & l_{26_{j'_l}} = 4_3\,. \\
l_{26_{j'_l}} = 4_3 \longleftarrow 3_3 = r_{25_{j_r}} & \to\ j'_r = |3+2+11+4|_6 = 2 & \to & r_{26_{j'_r}} = 2_2\,. \\
l_{26_{j_l}} = 4_3 \longrightarrow 2_2 = r_{26_{j'_r}} & \to\ j'_l = |3+4+11+4|_7 = 1 & \to & l_{27_{j'_l}} = 1_1\,. \\
l_{27_{j'_l}} = 1_1 \longleftarrow 2_2 = r_{26_{j_r}} & \to\ j'_r = |2+4+11+8|_6 = 1 & \to & r_{27_{j'_r}} = 1_1\,.
\end{array}$$

$P_c = \frac{\alpha\cdot x+\sum(\Delta_{l_i}+\Delta_{r_i})}{A^{**}} = \frac{26\cdot 11+(4\cdot 8+2\cdot 6+6\cdot 5+4\cdot 4+2\cdot 3+2\cdot 2+6\cdot 0)+(4\cdot 6+8\cdot 4+10\cdot 2+4\cdot 0)}{42} = 11\,.$
g.c.d. $(P_c\,,\,B^{**}) =$ g.c.d. $(11\,,\,1) = 1\,.$

$$\begin{tikzcd}
1_1 & \\
 & 3_6 \arrow[ul] \\
1_1 \arrow[ur] & \\
 & 3_3 \arrow[ul] \\
1_1 \arrow[ur] &
\end{tikzcd}$$

$$\begin{array}{llll}
l_{1_{j_l}} = 1_1 \longrightarrow 3_3 = r_{1_{j_r}} & \to\ j'_l = |1+8+11+2|_7 = 1 & \to & l_{2_{j'_l}} = 1_1\,. \\
l_{2_{j'_l}} = 1_1 \longleftarrow 3_3 = r_{1_{j_r}} & \to\ j'_r = |3+2+11+8|_6 = 6 & \to & r_{2_{j'_r}} = 3_6\,. \\
l_{2_{j_l}} = 1_1 \longrightarrow 3_6 = r_{2_{j'_r}} & \to\ j'_l = |1+8+11+2|_7 = 1 & \to & l_{3_{j'_l}} = 1_1\,. \\
l_{3_{j'_l}} = 1_1 \longleftarrow 3_6 = r_{2_{j_r}} & \to\ j'_r = |6+2+11+8|_6 = 3 & \to & r_{3_{j'_r}} = 3_3\,.
\end{array}$$

$P_c = \frac{\alpha\cdot x+\sum(\Delta_{l_i}+\Delta_{r_i})}{A^{**}} = \frac{2\cdot 11+(2\cdot 8)+(2\cdot 2)}{42} = 1\,.$
g.c.d. $(P_c\,,\,B^{**}) =$ g.c.d. $(1\,,\,1) = 1\,.$

$$\begin{tikzcd}
2_2 & \\
 & 2_2 \arrow[ul] \\
2_2 \arrow[ur] & \\
 & 2_5 \arrow[ul] \\
2_2 \arrow[ur] &
\end{tikzcd}$$

$$\begin{array}{llll}
l_{1_{j_l}} = 2_2 \longrightarrow 2_5 = r_{1_{j_r}} & \to\ j'_l = |2+6+11+4|_7 = 2 & \to & l_{2_{j'_l}} = 2_2\,. \\
l_{2_{j'_l}} = 2_2 \longleftarrow 2_5 = r_{1_{j_r}} & \to\ j'_r = |5+4+11+6|_6 = 2 & \to & r_{2_{j'_r}} = 2_2\,. \\
l_{2_{j_l}} = 2_2 \longrightarrow 2_2 = r_{2_{j'_r}} & \to\ j'_l = |2+6+11+4|_7 = 2 & \to & l_{3_{j'_l}} = 2_2\,. \\
l_{3_{j'_l}} = 2_2 \longleftarrow 2_2 = r_{2_{j_r}} & \to\ j'_r = |2+4+11+6|_6 = 5 & \to & r_{3_{j'_r}} = 2_5\,.
\end{array}$$

$P_c = \frac{\alpha\cdot x+\sum(\Delta_{l_i}+\Delta_{r_i})}{A^{**}} = \frac{2\cdot 11+(2\cdot 6)+(2\cdot 4)}{42} = 1\,.$
g.c.d. $(P_c\,,\,B^{**}) =$ g.c.d. $(1\,,\,1) = 1\,.$

$$\begin{tikzcd}
6_4 & \\
 & 4_4 \arrow[ul] \\
4_3 \arrow[ur] & \\
 & 1_1 \arrow[ul] \\
4_3 \arrow[ur] & \\
 & 4_4 \arrow[ul]
\end{tikzcd}$$

$$\begin{array}{llll}
l_{1_{j_l}} = 6_4 \longrightarrow 2_5 = r_{1_{j_r}} & \to\ j'_l = |4+2+11+4|_7 = 7 & \to & l_{2_{j'_l}} = 5_7\,. \\
l_{2_{j'_l}} = 5_7 \longleftarrow 2_5 = r_{1_{j_r}} & \to\ j'_r = |5+4+11+3|_6 = 5 & \to & r_{2_{j'_r}} = 2_5\,. \\
l_{2_{j_l}} = 5_7 \longrightarrow 2_5 = r_{2_{j'_r}} & \to\ j'_l = |7+3+11+4|_7 = 4 & \to & l_{3_{j'_l}} = 6_4\,. \\
l_{3_{j'_l}} = 6_4 \longleftarrow 2_5 = r_{2_{j_r}} & \to\ j'_r = |5+4+11+2|_6 = 4 & \to & r_{3_{j'_r}} = 4_4\,. \\
l_{3_{j_l}} = 6_4 \longrightarrow 4_4 = r_{3_{j'_r}} & \to\ j'_l = |4+2+11+0|_7 = 3 & \to & l_{4_{j'_l}} = 4_3\,.
\end{array}$$

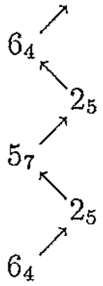

$$\begin{aligned}
&l_{4_{j_l'}} = 4_3 \longleftarrow 4_4 = r_{3_{j_r}} &&\to j_r' = |4+0+11+4|_6 = 1 &&\to r_{4_{j_r'}} = 1_1\,.\\
&l_{4_{j_l}} = 4_3 \longrightarrow 1_1 = r_{4_{j_r'}} &&\to j_l' = |3+4+11+6|_7 = 3 &&\to l_{5_{j_l'}} = 4_3\,.\\
&l_{5_{j_l'}} = 4_3 \longleftarrow 1_1 = r_{4_{j_r}} &&\to j_r' = |1+6+11+4|_6 = 4 &&\to r_{5_{j_r'}} = 4_4\,.\\
&l_{5_{j_l}} = 4_3 \longrightarrow 4_4 = r_{5_{j_r'}} &&\to j_l' = |3+4+11+0|_7 = 4 &&\to l_{6_{j_l'}} = 6_4\,.\\
&l_{6_{j_l'}} = 6_4 \longleftarrow 4_4 = r_{5_{j_r}} &&\to j_r' = |4+0+11+2|_6 = 5 &&\to r_{6_{j_r'}} = 2_5\,.
\end{aligned}$$

$P_c = \frac{\alpha\cdot x+\sum(\Delta_{l_i}+\Delta_{r_i})}{A^{**}} = \frac{5\cdot 11+(2\cdot 2+1\cdot 3+2\cdot 4)+(2\cdot 4+2\cdot 0+1\cdot 6)}{42} = 2\,.$
g.c.d. $(P_c\,,\, B^{**}) =$ g.c.d. $(2\,,\,1) = 1\,.$

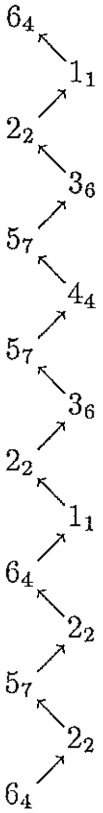

$$\begin{aligned}
&l_{1_{j_l}} = 6_4 \longrightarrow 2_2 = r_{1_{j_r}} &&\to j_l' = |4+2+11+4|_7 = 7 &&\to l_{2_{j_l'}} = 5_7\,.\\
&l_{2_{j_l'}} = 5_7 \longleftarrow 2_2 = r_{1_{j_r}} &&\to j_r' = |2+4+11+3|_6 = 2 &&\to r_{2_{j_r'}} = 2_2\,.\\
&l_{2_{j_l}} = 5_7 \longrightarrow 2_2 = r_{2_{j_r'}} &&\to j_l' = |7+3+11+4|_7 = 4 &&\to l_{3_{j_l'}} = 6_4\,.\\
&l_{3_{j_l'}} = 6_4 \longleftarrow 2_2 = r_{2_{j_r}} &&\to j_r' = |2+4+11+2|_6 = 1 &&\to r_{3_{j_r'}} = 1_1\,.\\
&l_{3_{j_l}} = 6_4 \longrightarrow 1_1 = r_{3_{j_r'}} &&\to j_l' = |4+2+11+6|_7 = 2 &&\to l_{4_{j_l'}} = 2_2\,.\\
&l_{4_{j_l'}} = 2_2 \longleftarrow 1_1 = r_{3_{j_r}} &&\to j_r' = |1+6+11+6|_6 = 6 &&\to r_{4_{j_r'}} = 3_6\,.\\
&l_{4_{j_l}} = 2_2 \longrightarrow 3_6 = r_{4_{j_r'}} &&\to j_l' = |2+6+11+2|_7 = 7 &&\to l_{5_{j_l'}} = 5_7\,.\\
&l_{5_{j_l'}} = 5_7 \longleftarrow 3_6 = r_{4_{j_r}} &&\to j_r' = |6+2+11+3|_6 = 4 &&\to r_{5_{j_r'}} = 4_4\,.\\
&l_{5_{j_l}} = 5_7 \longrightarrow 4_4 = r_{5_{j_r'}} &&\to j_l' = |7+3+11+0|_7 = 7 &&\to l_{6_{j_l'}} = 5_7\,.\\
&l_{6_{j_l'}} = 5_7 \longleftarrow 4_4 = r_{5_{j_r}} &&\to j_r' = |4+0+11+3|_6 = 6 &&\to r_{6_{j_r'}} = 3_6\,.\\
&l_{6_{j_l}} = 5_7 \longrightarrow 3_6 = r_{6_{j_r'}} &&\to j_l' = |7+3+11+2|_7 = 2 &&\to l_{7_{j_l'}} = 2_2\,.\\
&l_{7_{j_l'}} = 2_2 \longleftarrow 3_6 = r_{6_{j_r}} &&\to j_r' = |6+2+11+6|_6 = 1 &&\to r_{7_{j_r'}} = 1_1\,.\\
&l_{7_{j_l}} = 2_2 \longrightarrow 1_1 = r_{7_{j_r'}} &&\to j_l' = |2+6+11+6|_7 = 4 &&\to l_{8_{j_l'}} = 6_4\,.\\
&l_{8_{j_l'}} = 6_4 \longleftarrow 1_1 = r_{7_{j_r}} &&\to j_r' = |1+6+11+2|_6 = 2 &&\to r_{8_{j_r'}} = 2_2\,.
\end{aligned}$$

$P_c = \frac{\alpha\cdot x+\sum(\Delta_{l_i}+\Delta_{r_i})}{A^{**}} = \frac{7\cdot 11+(2\cdot 2+3\cdot 3+2\cdot 6)+(2\cdot 4+2\cdot 6+2\cdot 2)+1\cdot 0}{42} = 3\,.$
g.c.d. $(P_c\,,\, B^{**}) =$ g.c.d. $(3\,,\,1) = 1\,.$

Although the calculation process is simple, it is nevertheless a bit tedious, and hence a suitable computer program will be advantageous.

In order to obtain an overview of the actual positions of the bights on the left-hand and right-hand bight-edges we attach to the bight-boundary number with ranking-number of a bight the nest-index number of the nest to which the bight belongs. We can obtain the nest-index number which belongs to a bight-boundary number with ranking-number from the list of lower-left to upper-right half-cycle types (see pg. 794) after we have indicated in this list the nest-index numbers associated with the left-hand and right-hand bight-points, or we can obtain the nest-index number which belongs to a bight-boundary number with ranking-number by means of a calculation. The first method is the quickest and simplest, and hence will be one we shall use.

For our Example the list of lower-left to upper-right half-cycle types with the nest-index numbers will be as shown in Fig. 638.

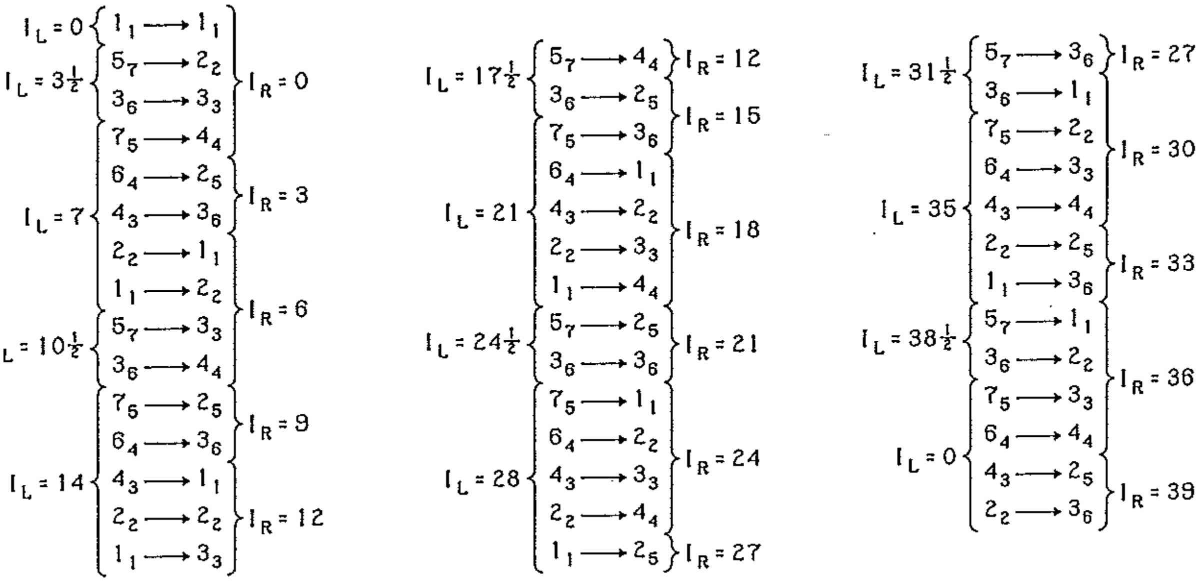
$I_L = 0$ { $1_1 \to 1_1$
$I_L = 3\frac{1}{2}$ { $5_7 \to 2_2$, $3_6 \to 3_3$
$I_L = 7$ { $7_5 \to 4_4$, $6_4 \to 2_5$, $4_3 \to 3_6$, $2_2 \to 1_1$, $1_1 \to 2_2$
$I_L = 10\frac{1}{2}$ { $5_7 \to 3_3$, $3_6 \to 4_4$
$I_L = 14$ { $7_5 \to 2_5$, $6_4 \to 3_6$, $4_3 \to 1_1$, $2_2 \to 2_2$, $1_1 \to 3_3$
$I_R = 0$
$I_R = 3$
$I_R = 6$
$I_R = 9$
$I_R = 12$
$I_L = 17\frac{1}{2}$ { $5_7 \to 4_4$, $3_6 \to 2_5$
$I_L = 21$ { $7_5 \to 3_6$, $6_4 \to 1_1$, $4_3 \to 2_2$, $2_2 \to 3_3$, $1_1 \to 4_4$
$I_L = 24\frac{1}{2}$ { $5_7 \to 2_5$, $3_6 \to 3_6$
$I_L = 28$ { $7_5 \to 1_1$, $6_4 \to 2_2$, $4_3 \to 3_3$, $2_2 \to 4_4$, $1_1 \to 2_5$
$I_R = 12$
$I_R = 15$
$I_R = 18$
$I_R = 21$
$I_R = 24$
$I_R = 27$
$I_L = 31\frac{1}{2}$ { $5_7 \to 3_6$, $3_6 \to 1_1$
$I_L = 35$ { $7_5 \to 2_2$, $6_4 \to 3_3$, $4_3 \to 4_4$, $2_2 \to 2_5$, $1_1 \to 3_6$
$I_L = 38\frac{1}{2}$ { $5_7 \to 1_1$, $3_6 \to 2_2$
$I_L = 0$ { $7_5 \to 3_3$, $6_4 \to 4_4$, $4_3 \to 2_5$, $2_2 \to 3_6$
$I_R = 27$
$I_R = 30$
$I_R = 33$
$I_R = 36$
$I_R = 39$

Fig. 638 — The lower-left to upper-right half-cycle types.

The nest-index number interval between adjacent sets of half-cycle types is for the left-hand bight-edge equal to $\frac{A_{l_1}+A_{l_2}}{2} = \frac{A_l}{2}$, and is for the right-hand bight-edge equal to $\frac{A_{r_1}+A_{r_2}}{2} = \frac{A_r}{2}$.

The first-return string-runs in which the bight-boundary numbers with ranking-numbers are provided with their associated nest-index numbers are then as follows:

$$\begin{array}{ll}
0/1_1 & \\
\nwarrow & \\
 & 2_2/18 \\
\nearrow & \\
21/4_3 & \\
\nwarrow & \\
 & 3_3/0 \\
\nearrow & \\
3\frac{1}{2}/3_6 & \\
\nwarrow & \\
 & 3_3/24 \\
\nearrow & \\
28/4_3 & \\
\nwarrow & \\
 & 2_2/6 \\
\nearrow & \\
7/1_1 & \\
\nwarrow & \\
 & 1_1/24 \\
\nearrow & \\
28/7_5 & \\
\nwarrow & \\
 & 3_6/9 \\
\nearrow & \\
14/6_4 & \\
\nwarrow & \\
 & 3_3/36
\end{array}$$

$$\begin{tikzcd}
 & \\
0/7_5 \arrow[ur] & \\
 & 4_4/24 \arrow[ul] \\
28/2_2 \arrow[ur] & \\
 & 3_3/6 \arrow[ul] \\
10\tfrac{1}{2}/5_7 \arrow[ur] & \\
 & 1_1/30 \arrow[ul] \\
31\tfrac{1}{2}/3_6 \arrow[ur] & \\
 & 2_5/9 \arrow[ul] \\
14/7_5 \arrow[ur] & \\
 & 2_2/36 \arrow[ul] \\
38\tfrac{1}{2}/3_6 \arrow[ur] & \\
 & 4_4/18 \arrow[ul] \\
21/1_1 \arrow[ur] & \\
 & 2_5/39 \arrow[ul] \\
0/4_3 \arrow[ur] & \\
 & 3_6/21 \arrow[ul] \\
24\tfrac{1}{2}/3_6 \arrow[ur] & \\
 & 3_6/3 \arrow[ul] \\
7/4_3 \arrow[ur] & \\
 & 2_5/27 \arrow[ul] \\
28/1_1 \arrow[ur] & \\
 & 4_4/6 \arrow[ul] \\
10\tfrac{1}{2}/3_6 \arrow[ur] & \\
 & 2_2/30 \arrow[ul] \\
35/7_5 \arrow[ur] & \\
 & 2_5/15 \arrow[ul] \\
17\tfrac{1}{2}/3_6 \arrow[ur] & \\
 & 1_1/36 \arrow[ul] \\
38\tfrac{1}{2}/5_7 \arrow[ur] & \\
 & 3_3/18 \arrow[ul] \\
21/2_2 \arrow[ur] &
\end{tikzcd}$$

$$\begin{tikzcd}
7/6_4 & \\
 & 4_4/30 \arrow[ul] \\
35/4_3 \arrow[ur] &
\end{tikzcd}$$

$$\begin{tikzcd}
28/6_4 & \\
 & 1_1/6 \arrow[ul] \\
7/2_2 \arrow[ur] & \\
 & 3_6/27 \arrow[ul] \\
31\tfrac{1}{2}/5_7 \arrow[ur] & \\
 & 4_4/12 \arrow[ul] \\
17\tfrac{1}{2}/5_7 \arrow[ur] &
\end{tikzcd}$$

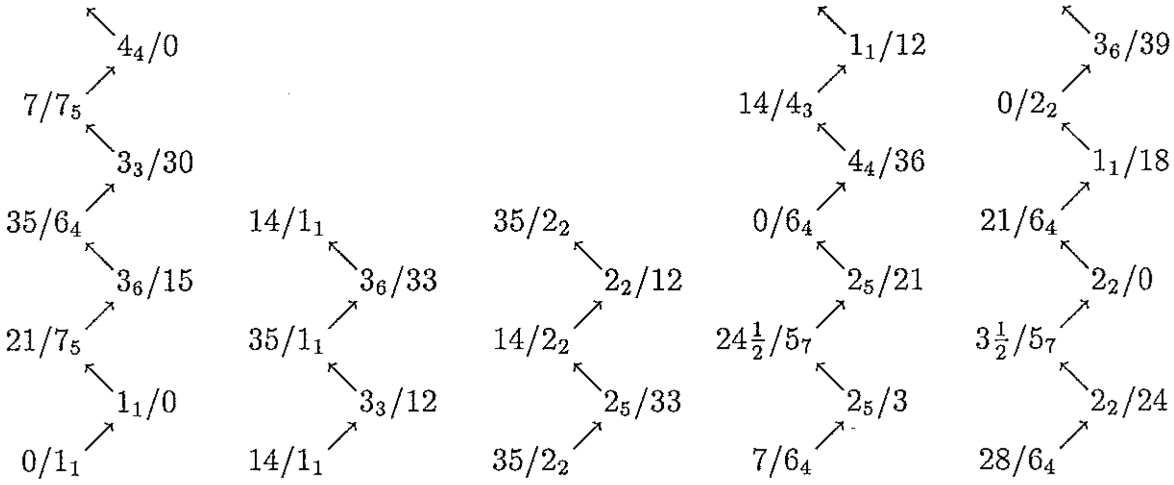

We can now construct the half-cycle pattern of the first-return string-runs (see Fig. 639).

1	2	3	4	5	6	7	
		$\frac{29}{16}$		$\frac{11}{16}$			— $38\frac{1}{2}$
$\frac{55}{16}$	$\frac{57}{16}$		$\frac{69}{12}$		$\frac{5}{12}$	$\frac{15}{12}$	— 35
		$\frac{33}{17}$		$\frac{81}{15}$			— $31\frac{1}{2}$
$\frac{19}{17}$	$\frac{37}{13}$		$\frac{47}{13}$		$\frac{71}{13}$	$\frac{43}{13}$	— 28
		$\frac{23}{16}$		$\frac{63}{16}$			— $24\frac{1}{2}$
$\frac{27}{14}$	$\frac{9}{14}$		$\frac{51}{14}$		$\frac{75}{14}$	$\frac{3}{12}$	— 21
		$\frac{13}{17}$		$\frac{79}{13}$			— $17\frac{1}{2}$
$\frac{53}{15}$	$\frac{59}{15}$		$\frac{67}{15}$		$\frac{41}{13}$	$\frac{31}{13}$	— 14
		$\frac{17}{14}$		$\frac{35}{14}$			— $10\frac{1}{2}$
$\frac{45}{16}$	$\frac{83}{16}$		$\frac{21}{14}$		$\frac{61}{14}$	$\frac{7}{10}$	— 7
		$\frac{49}{15}$		$\frac{73}{15}$			— $3\frac{1}{2}$
$\frac{1}{17}$	$\frac{77}{15}$		$\frac{25}{15}$		$\frac{65}{11}$	$\frac{39}{11}$	— 0

	4	3	2	1
39 —		$\frac{78}{15}$	$\frac{26}{17}$	
36 —	$\frac{66}{12}$	$\frac{40}{12}$	$\frac{30}{12}$	$\frac{12}{17}$
33 —		$\frac{56}{16}$	$\frac{58}{16}$	
30 —	$\frac{70}{11}$	$\frac{6}{11}$	$\frac{16}{16}$	$\frac{34}{16}$
27 —		$\frac{82}{15}$	$\frac{20}{15}$	
24 —	$\frac{38}{10}$	$\frac{48}{15}$	$\frac{72}{15}$	$\frac{44}{17}$
21 —		$\frac{24}{14}$	$\frac{64}{14}$	
18 —	$\frac{28}{14}$	$\frac{10}{14}$	$\frac{52}{16}$	$\frac{76}{16}$
15 —		$\frac{4}{13}$	$\frac{14}{13}$	
12 —	$\frac{80}{13}$	$\frac{54}{15}$	$\frac{60}{15}$	$\frac{68}{15}$
9 —		$\frac{42}{12}$	$\frac{32}{17}$	
6 —	$\frac{18}{14}$	$\frac{36}{14}$	$\frac{46}{14}$	$\frac{84}{14}$
3 —		$\frac{22}{16}$	$\frac{62}{16}$	
0 —	$\frac{8}{13}$	$\frac{50}{13}$	$\frac{74}{13}$	$\frac{2}{13}$

Fig. 639 — The half-cycle pattern of the first-return string-runs.

The number of crossings on a half-cycle are again indicated below the half-cycle number (see *The Braider*, Issue No. 33, pg. 763). The number of crossings on a half-cycle are calculated as the sum of three sets of crossings:

i). The number of crossings between the left-hand bight-boundary 1 up to and including the innermost left-hand bight-boundary.
ii). The number of crossings between the innermost left-hand bight-boundary and the innermost right-hand bight-boundary; hence equal to $(x-1)$.
iii). The number of crossings between the right-hand bight-boundary 1 up to and including the innermost right-hand bight-boundary.

The general scheme for the number of crossings under **i)** is as follows:

a). The two sub-nesting numbers A_{l_1} and A_{l_2} do have the same parity.

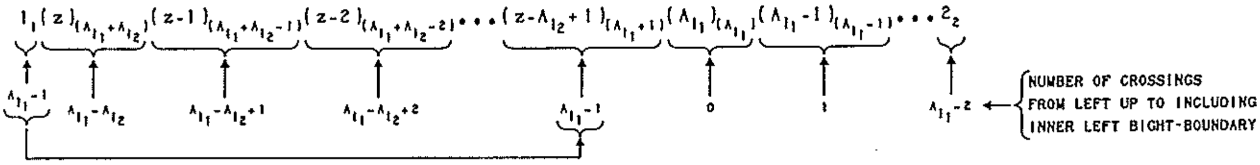
$1_1(z)_{(A_{l_1}+A_{l_2})}(z-1)_{(A_{l_1}+A_{l_2}-1)}(z-2)_{(A_{l_1}+A_{l_2}-2)}\dots(z-A_{l_2}+1)_{(A_{l_1}+1)}(A_{l_1})_{(A_{l_1})}(A_{l_1}-1)_{(A_{l_1}-1)}\dots 2_2$
$A_{l_1}-1$
$A_{l_1}-A_{l_2}$
$A_{l_1}-A_{l_2}+1$
$A_{l_1}-A_{l_2}+2$
$A_{l_1}-1$
0
1
$A_{l_1}-2$
NUMBER OF CROSSINGS FROM LEFT UP TO INCLUDING INNER LEFT BIGHT-BOUNDARY

b). The two sub-nesting numbers A_{l_1} and A_{l_2} do not have the same parity.

1). For $A_{l_1} = A_{l_2} + 1$:

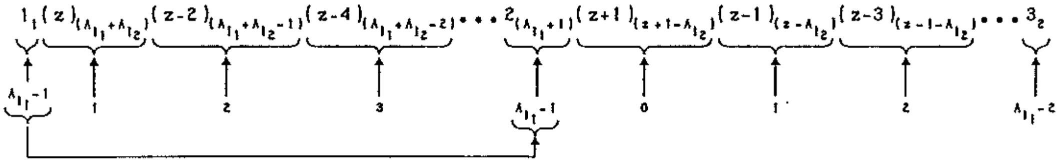
$1_1(z)_{(A_{l_1}+A_{l_2})}(z-2)_{(A_{l_1}+A_{l_2}-1)}(z-4)_{(A_{l_1}+A_{l_2}-2)}\dots 2_{(A_{l_1}+1)}(z+1)_{(z+1-A_{l_2})}(z-1)_{(z-A_{l_2})}(z-3)_{(z-1-A_{l_2})}\dots 3_2$
$A_{l_1}-1$
1
2
3
$A_{l_1}-1$
0
1
2
$A_{l_1}-2$

2). For $A_{l_1} \geq A_{l_2} + 3$:

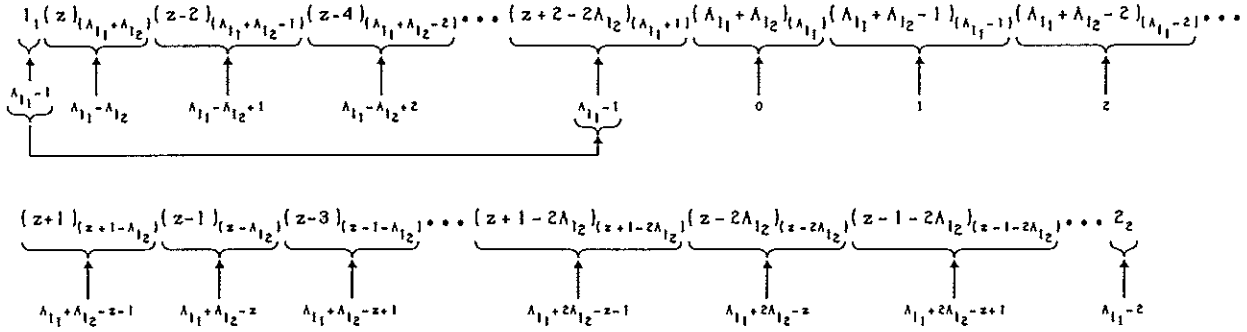
$1_1(z)_{(A_{l_1}+A_{l_2})}(z-2)_{(A_{l_1}+A_{l_2}-1)}(z-4)_{(A_{l_1}+A_{l_2}-2)}\dots(z+2-2A_{l_2})_{(A_{l_1}+1)}(A_{l_1}+A_{l_2})_{(A_{l_1})}(A_{l_1}+A_{l_2}-1)_{(A_{l_1}-1)}(A_{l_1}+A_{l_2}-2)_{(A_{l_1}-2)}\dots$
$A_{l_1}-1$
$A_{l_1}-A_{l_2}$
$A_{l_1}-A_{l_2}+1$
$A_{l_1}-A_{l_2}+2$
$A_{l_1}-1$
0
1
2
$(z+1)_{(z+1-A_{l_2})}(z-1)_{(z-A_{l_2})}(z-3)_{(z-1-A_{l_2})}\dots(z+1-2A_{l_2})_{(z+1-2A_{l_2})}(z-2A_{l_2})_{(z-2A_{l_2})}(z-1-2A_{l_2})_{(z-1-2A_{l_2})}\dots 2_2$
$A_{l_1}+A_{l_2}-z-1$
$A_{l_1}+A_{l_2}-z$
$A_{l_1}+A_{l_2}-z+1$
$A_{l_1}+2A_{l_2}-z-1$
$A_{l_1}+2A_{l_2}-z$
$A_{l_1}+2A_{l_2}-z+1$
$A_{l_1}-2$

The general scheme for the number of crossings under **iii)** is as follows:

a). The two sub-nesting numbers A_{r_1} and A_{r_2} do have the same parity.

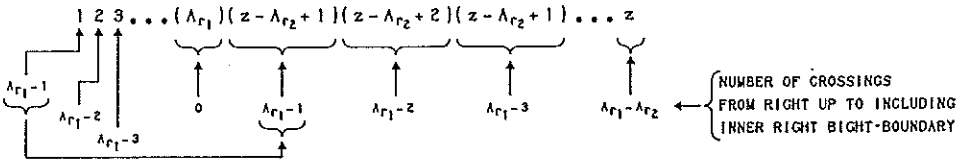
$1\ 2\ 3\dots(A_{r_1})(z-A_{r_2}+1)(z-A_{r_2}+2)(z-A_{r_2}+1)\dots z$
$A_{r_1}-1$
$A_{r_1}-2$
$A_{r_1}-3$
0
$A_{r_1}-1$
$A_{r_1}-2$
$A_{r_1}-3$
$A_{r_1}-A_{r_2}$
NUMBER OF CROSSINGS FROM RIGHT UP TO INCLUDING INNER RIGHT BIGHT-BOUNDARY

b). The two sub-nesting numbers A_{r_1} and A_{r_2} do not have the same parity.

1). For $A_{r_1} = A_{r_2} + 1$:

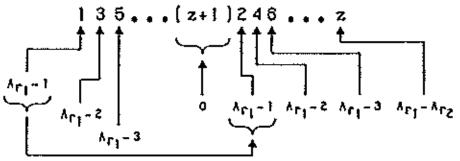

2). For $A_{r_1} \geq A_{r_2} + 3$:

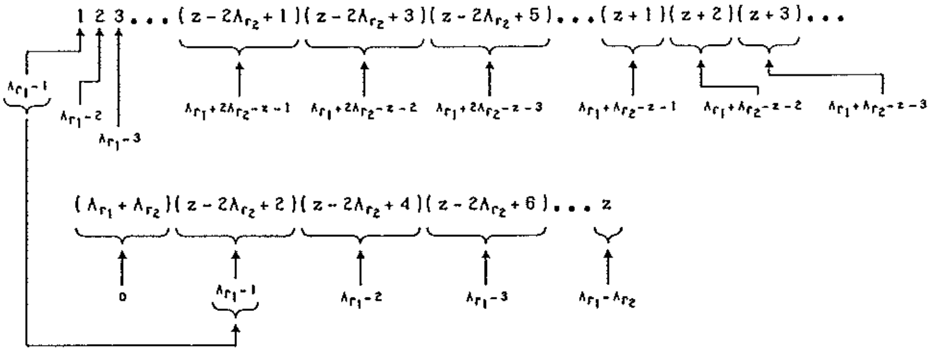

Thus for our Example we obtain:

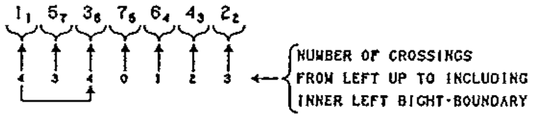

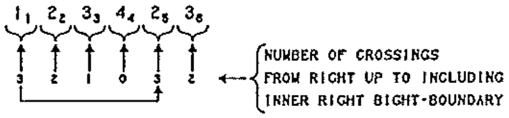

Since in our Example $B^{**} = 1$ we know that the string-run of each component consists of only one first-return string-run of that component, hence in the half-cycle pattern of Fig. 639 all bight-points are occupied.

Say we superimpose on the string-run of our Example an under–over coding, then we can now assemble the half-cycle tables for the components; Fig. 640 presents the table for the odd-numbered half-cycles (the half-cycles from lower-left to upper-right), and Fig. 641 presents the even-numbered half-cycles (the half-cycles from lower-right to upper left). Note that in the table of the odd-numbered half-cycles (see Fig. 640) some of the half-cycle numbers have one or more stars attached to them. When a half-cycle number in the rightmost section of this table has one or more star(s), then in its associated row of half-cycles in the uppermost section of this table only those half-cycle numbers equal to or smaller than the half-cycle number in the rightmost table-section with an identical number of stars are neglected[†].

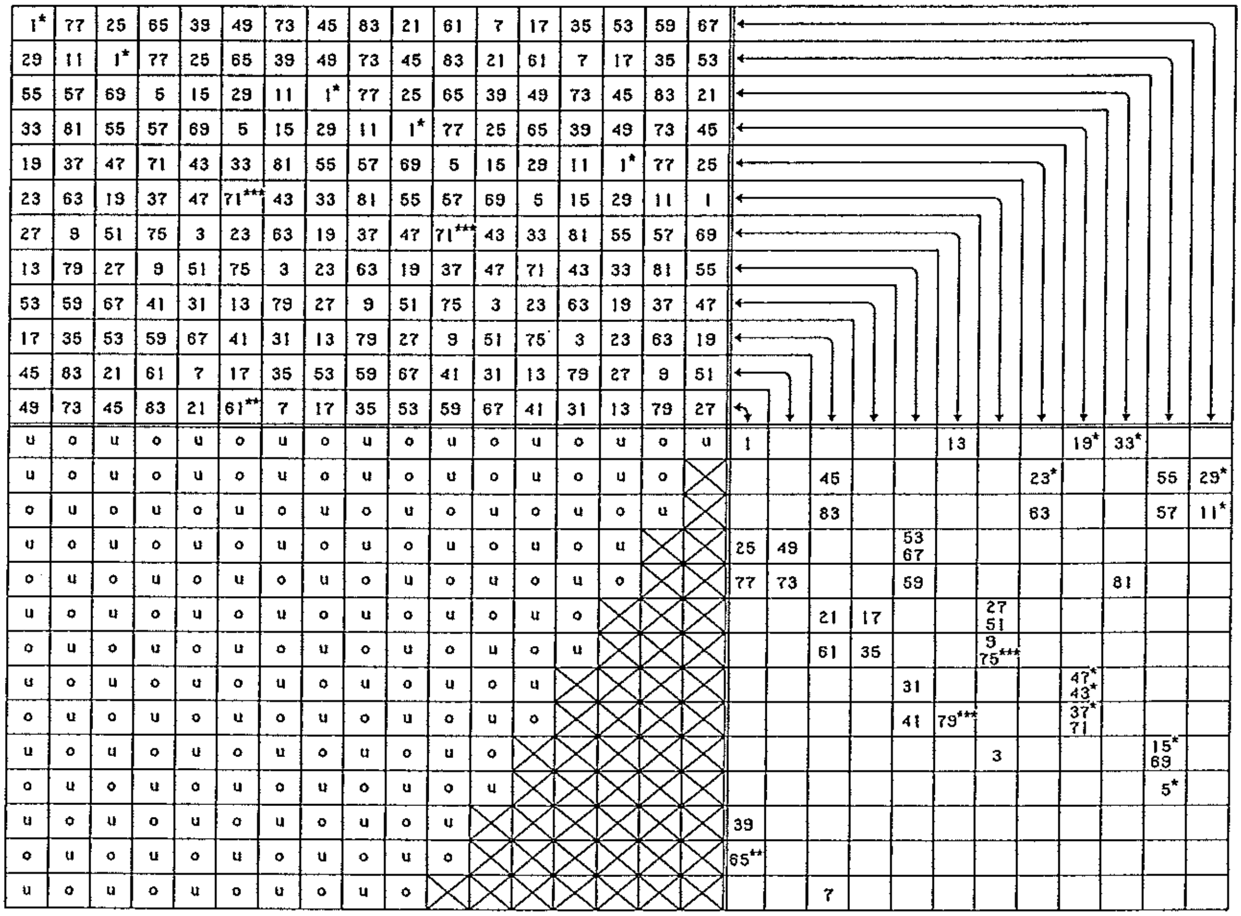

1*	77	25	65	39	49	73	45	83	21	61	7	17	35	53	59	67	←											
29	11	1*	77	25	65	39	49	73	45	83	21	61	7	17	35	53	←											
55	57	69	5	15	29	11	1*	77	25	65	39	49	73	45	83	21	←											
33	81	55	57	69	5	15	29	11	1*	77	25	65	39	49	73	45	←											
19	37	47	71	43	33	81	55	57	69	5	15	29	11	1*	77	25	←											
23	63	19	37	47	71***	43	33	81	55	57	69	5	15	29	11	1	←											
27	9	51	75	3	23	63	19	37	47	71***	43	33	81	55	57	69	←											
13	79	27	9	51	75	3	23	63	19	37	47	71	43	33	81	55	←											
53	59	67	41	31	13	79	27	9	51	75	3	23	63	19	37	47	←											
17	35	53	59	67	41	31	13	79	27	9	51	75	3	23	63	19	←											
45	83	21	61	7	17	35	53	59	67	41	31	13	79	27	9	51	←											
49	73	45	83	21	61**	7	17	35	53	59	67	41	31	13	79	27	↰											
u	o	u	o	u	o	u	o	u	o	u	o	u	o	u	o	u	1					13			19*	33*		
u	o	u	o	u	o	u	o	u	o	u	o	u	o	u	o	☒			45					23*			55	29*
o	u	o	u	o	u	o	u	o	u	o	u	o	u	o	u	☒			83					63			57	11*
u	o	u	o	u	o	u	o	u	o	u	o	u	o	u	☒	☒	25	49			53 67							
o	u	o	u	o	u	o	u	o	u	o	u	o	u	o	☒	☒	77	73			59					81		
u	o	u	o	u	o	u	o	u	o	u	o	u	o	☒	☒	☒			21	17			27 51					
o	u	o	u	o	u	o	u	o	u	o	u	o	u	☒	☒	☒			61	35			9 75***					
u	o	u	o	u	o	u	o	u	o	u	o	u	☒	☒	☒	☒					31				47* 43*			
o	u	o	u	o	u	o	u	o	u	o	u	o	☒	☒	☒	☒					41	79***			37* 71			
u	o	u	o	u	o	u	o	u	o	u	o	☒	☒	☒	☒	☒							3				15* 69	
o	u	o	u	o	u	o	u	o	u	o	u	☒	☒	☒	☒	☒											5*	
u	o	u	o	u	o	u	o	u	o	u	☒	☒	☒	☒	☒	☒	39											
o	u	o	u	o	u	o	u	o	u	o	☒	☒	☒	☒	☒	☒	65**											
u	o	u	o	u	o	u	o	u	o	☒	☒	☒	☒	☒	☒	☒			7									

Fig. 640 — The half-cycle table for the lower-left to upper-right half-cycles.

The half-cycle braiding algorithms are subsequently being read from these half-cycle tables.

[†] See *The Braider*, Issue No. 33, pp. 764-765.

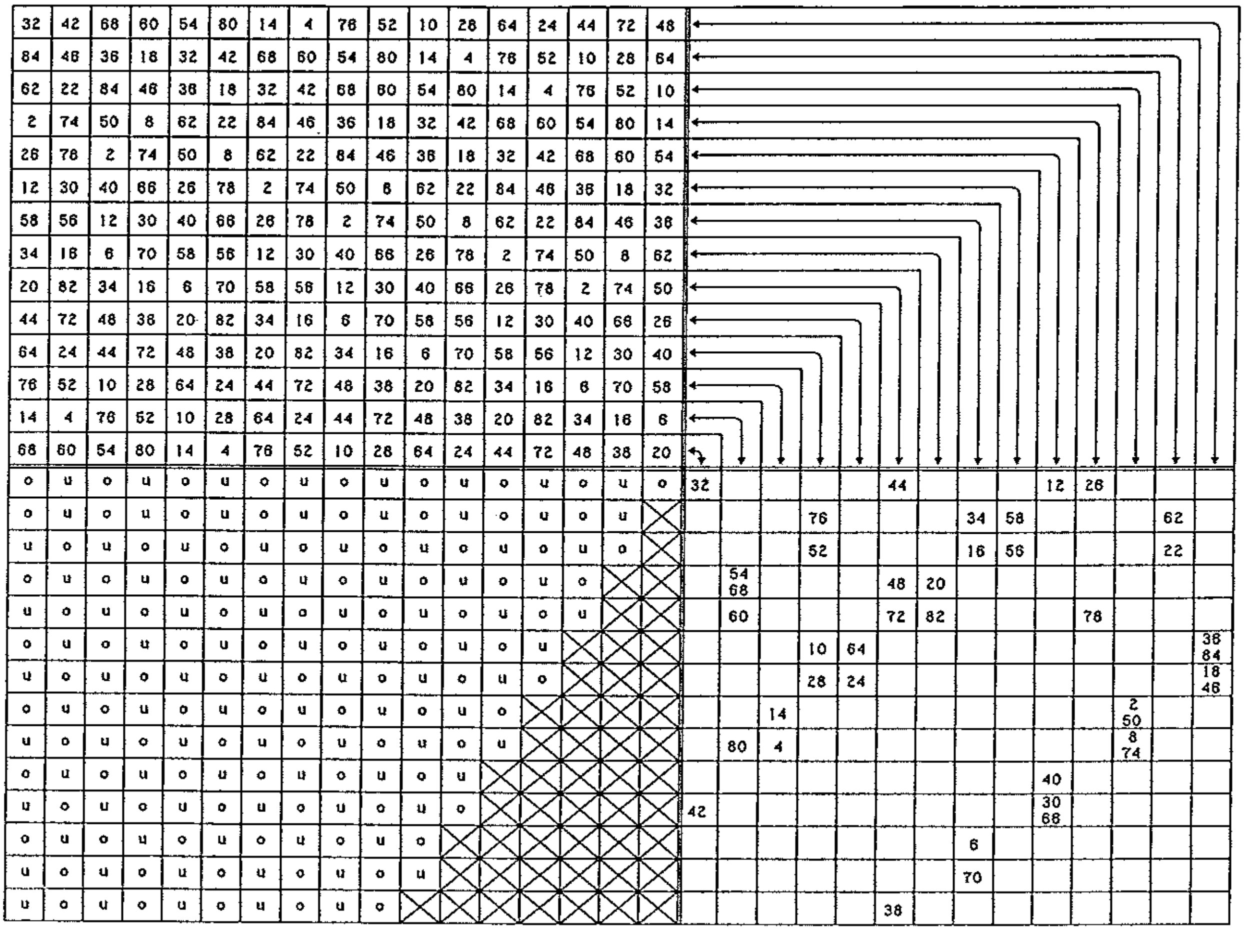

Fig. 641 — The half-cycle table for the lower-right to upper-left half-cycles.

The braiding half-cycle algorithms are as follows:

1. $1_1 \longrightarrow 1_1$: Free run.
2. $7_5 \longleftarrow 1_1$: Free run.
3. $7_5 \longrightarrow 3_6$: Free run.
4. $6_4 \longleftarrow 3_6$: Free run.
5. $6_4 \longrightarrow 3_3$: Free run.
6. $7_5 \longleftarrow 3_3$: o
7. $7_5 \longrightarrow 4_4$: Free run.
8. $2_2 \longleftarrow 4_4$: Free run.
9. $2_2 \longrightarrow 3_3$: o.
10. $5_7 \longleftarrow 3_3$: o.
11. $5_7 \longrightarrow 1_1$: u.
12. $3_6 \longleftarrow 1_1$: $o - u$.
13. $3_6 \longrightarrow 2_5$: $o - u$.
14. $7_5 \longleftarrow 2_5$: o.
15. $7_5 \longrightarrow 2_2$: o.
16. $3_6 \longleftarrow 2_2$: $2u - o$.
17. $3_6 \longrightarrow 4_4$: $o - u - o$.
18. $1_1 \longleftarrow 4_4$: $u - o - u$.
19. $1_1 \longrightarrow 2_5$: $o - 2u$.
20. $4_3 \longleftarrow 2_5$: $u - 3o$.

21. $4_3 \longrightarrow 3_6$: $u - o - u - o$.
22. $3_6 \longleftarrow 3_6$: $o - u - o - u$.
23. $3_6 \longrightarrow 3_6$: $2u - 2o$.
24. $4_3 \longleftarrow 3_6$: $u - o - 2u$.
25. $4_3 \longrightarrow 2_5$: $2u - o - u$.
26. $1_1 \longleftarrow 2_5$: $o - 3u - o$.
27. $1_1 \longrightarrow 4_4$: $3u - o$.
28. $3_6 \longleftarrow 4_4$: $o - u - o - u$.
29. $3_6 \longrightarrow 2_2$: $u - 2o - u$.
30. $7_5 \longleftarrow 2_2$: $2u - 3o$.
31. $7_5 \longrightarrow 2_5$: $2u - o - u - 2o$.
32. $3_6 \longleftarrow 2_5$: $o - u - o - 2u - o$.
33. $3_6 \longrightarrow 1_1$: $o - u - o - u - o - u$.
34. $5_7 \longleftarrow 1_1$: $o - u - 2o - 2u$.
35. $5_7 \longrightarrow 3_3$: $o - 2u - o - u - o$.
36. $2_2 \longleftarrow 3_3$: $2o - u - o - 2u$.
37. $2_2 \longrightarrow 4_4$: $o - u - o - u - o - u$.
38. $7_5 \longleftarrow 4_4$: $2u - o - 2u - o$.
39. $7_5 \longrightarrow 3_3$: $2u - o - u$.
40. $6_4 \longleftarrow 3_3$: $2o - 2u - o - u$.
41. $6_4 \longrightarrow 3_6$: $2o - u - o - 2u - o$.
42. $7_5 \longleftarrow 3_6$: $u - o - u - 2o$.
43. $7_5 \longrightarrow 1_1$: $u - o - u - o - u - o$.
44. $1_1 \longleftarrow 1_1$: $2o - u - 2o - u - 3o$.
45. $1_1 \longrightarrow 2_2$: $u - 2o - u - 2o - u - o - u$.
46. $4_3 \longleftarrow 2_2$: $u - o - u - o - u - 2o$.
47. $4_3 \longrightarrow 3_3$: $u - o - u - o - u - o$.
48. $3_6 \longleftarrow 3_3$: $2o - u - 2o - u - 3o$.
49. $3_6 \longrightarrow 3_3$: $3u - o - 2u - o - 2u$.
50. $4_3 \longleftarrow 3_3$: $2u - o - u - o - u - o$.
51. $4_3 \longrightarrow 2_2$: $2u - o - 2u - o - u - o$.
52. $1_1 \longleftarrow 2_2$: $o - 2u - o - 2u - o - 2u - o$.

---

53. $1_1 \longrightarrow 3_3$: $2u - o - 2u - 2o - u - 2o - u$.
54. $1_1 \longleftarrow 3_3$: $o - 2u - o - 2u - 2o - u - 2o$.
55. $1_1 \longrightarrow 3_6$: $u - o - 3u - 4o - u - o$.
56. $1_1 \longleftarrow 3_6$: $u - o - 4u - 3o - u - o$.

---

57. $2_2 \longrightarrow 2_5$: $o - u - 3o - 4u - o - u$.
58. $2_2 \longleftarrow 2_5$: $o - u - 4o - 3u - o - u$.
59. $2_2 \longrightarrow 2_2$: $2o - u - 2o - 2u - o - 2u - o$.
60. $2_2 \longleftarrow 2_2$: $u - 2o - u - 2o - 2u - o - 2u$.

---

61. $6_4 \longrightarrow 2_5$: $o - u - o - 2u - o - 2u - o - 2u$.
62. $5_7 \longleftarrow 2_5$: $u - o - u - o - 2u - 2o - 2u - o - u$.
63. $5_7 \longrightarrow 2_5$: $o - u - 2o - 2u - 2o - u - o - u - o$.
64. $6_4 \longleftarrow 2_5$: $2o - u - 2o - u - 2o - u - o - u$.
65. $6_4 \longrightarrow 4_4$: $4o - u - o - u - o$.

66. $4_3 \longleftarrow 4_4$: $3u - o - u - 2o - u - o$.
67. $4_3 \longrightarrow 1_1$: $2u - o - 2u - o - u - o - u - 2o - u$.
68. $4_3 \longleftarrow 1_1$: $o - 2u - o - u - o - u - 2o - u - 2o$.
69. $4_3 \longrightarrow 4_4$: $u - o - 2u - o - u - 3o$.
70. $6_4 \longleftarrow 4_4$: $u - o - u - o - u - o - 3u$.

71. $6_4 \longrightarrow 2_2$: $2o - u - o - u - o - u - o - 2u - o$.
72. $5_7 \longleftarrow 2_2$: $2u - o - u - o - u - o - u - o - u - o - 2u$.
73. $5_7 \longrightarrow 2_2$: $2o - u - o - u - o - u - o - u - o - u - 2o$.
74. $6_4 \longleftarrow 2_2$: $u - 2o - u - o - u - o - u - o - 2u$.
75. $6_4 \longrightarrow 1_1$: $o - u - o - u - 2o - 2u - o - u - o - u$.
76. $2_2 \longleftarrow 1_1$: $o - u - o - u - o - u - 2o - u - o - u - o - u - o - u$.
77. $2_2 \longrightarrow 3_6$: $o - u - 2o - u - o - u - o - u - o - u - o - u - o$.
78. $5_7 \longleftarrow 3_6$: $u - o - u - o - u - 2o - u - o - u - o - u - o - u$.
79. $5_7 \longrightarrow 4_4$: $o - u - o - u - o - u - o - u - o - 2u - o$.
80. $5_7 \longleftarrow 4_4$: $u - o - u - o - u - o - u - o - u - o - u - o - u$.
81. $5_7 \longrightarrow 3_6$: $o - u - o - u - o - u - o - u - o - u - o - u - o - u - o$.
82. $2_2 \longleftarrow 3_6$: $u - o - u - o - u - o - u - o - u - o - u - o - u - o - u$.
83. $2_2 \longrightarrow 1_1$: $o - u - o - u - o - u - o - u - o - u - o - u - o - u - o - u$.
84. $6_4 \longleftarrow 1_1$: $o - u - o - u - o - u - o - u - o - u - o - u - o - u$.

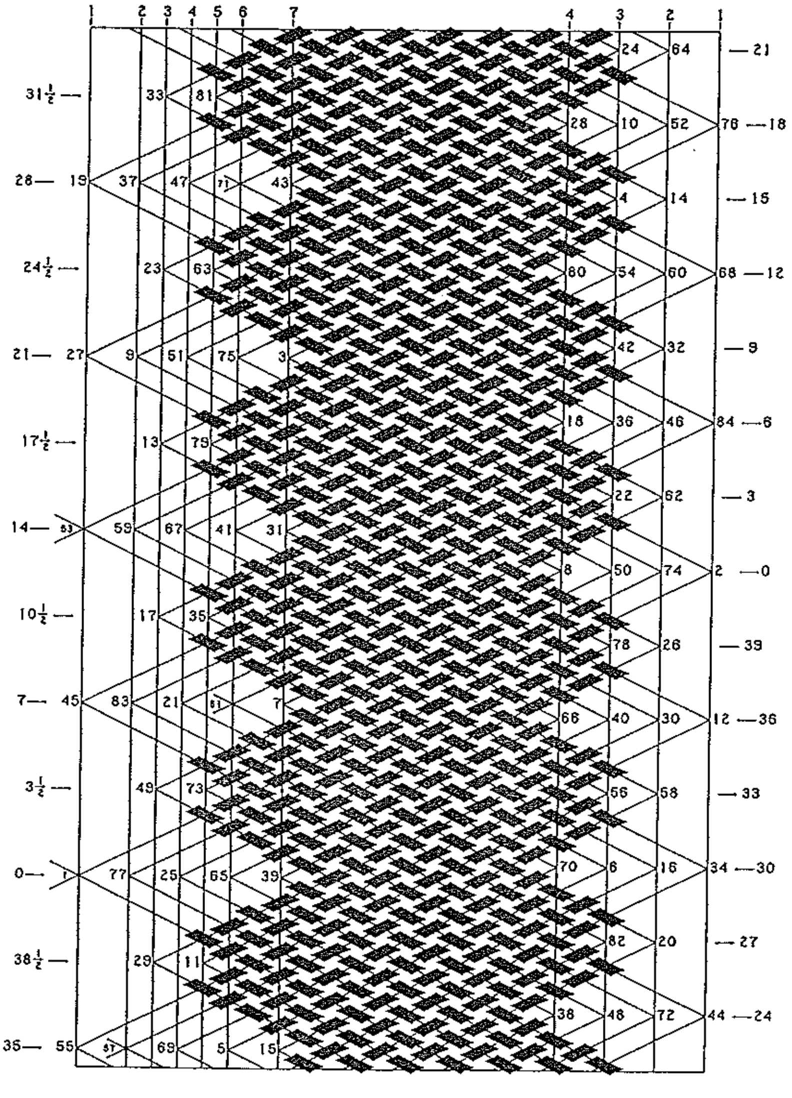

Fig. 642 — The grid-diagram of Example 1.

It is generally more convenient to read the half-cycle braiding algorithms for each component (and in case a component consists of more than one sub-component, for each sub-component) from its two own specific half-cycle tables (one for the odd-numbered half-cycles and one for the even-numbered half-cycles). Although the calculation procedures are simple, there are many to be performed and consequently mistakes are easily made. Hence in practice it will be advantageous to make use of a suitable software program which will enable a computer not only to do these calculations, but also will enable it to produce all the various associated lists, tables, and of course the grid-diagram.

Toggle Knots at the end of a 4-string Round Braid

Fig. 643 depicts two toggle knots; each toggle knot forms an integral part with a 4-string round braid. The end of the 4-string round braid is indicated by A, C, G, I.

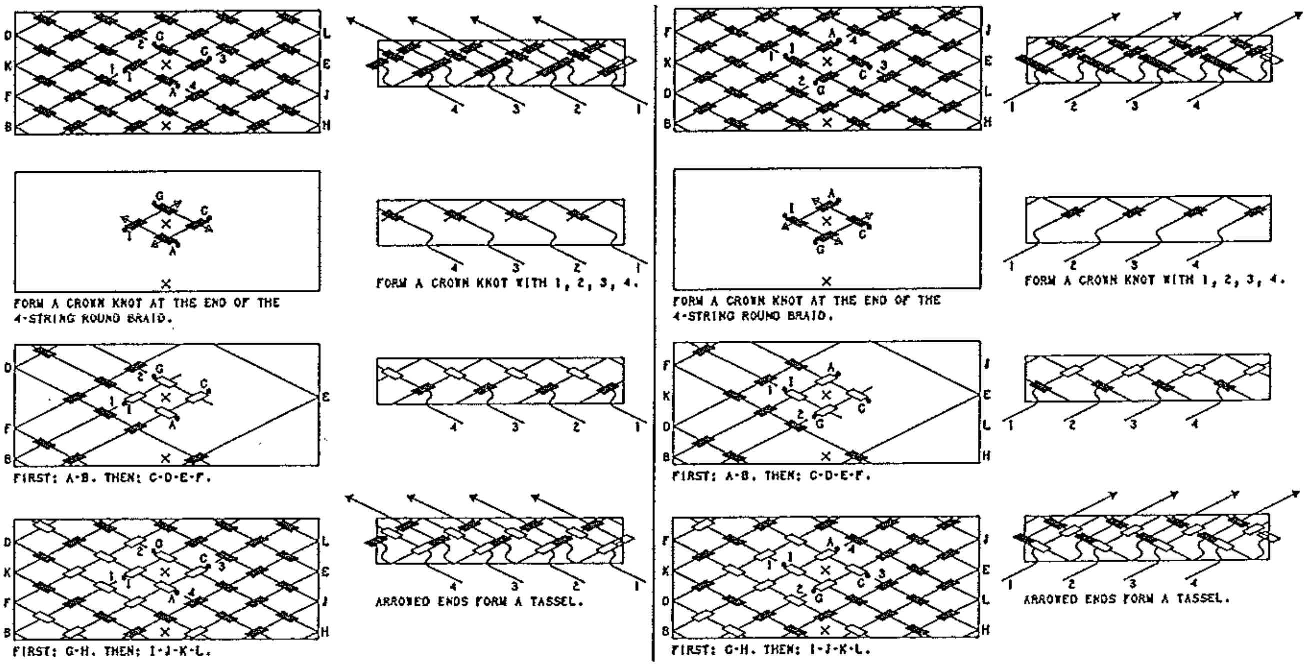

FORM A CROWN KNOT AT THE END OF THE 4-STRING ROUND BRAID.

FORM A CROWN KNOT WITH 1, 2, 3, 4.

FIRST: A-B. THEN: C-D-E-F.

FIRST: G-H. THEN: I-J-K-L.

ARROWED ENDS FORM A TASSEL.

FORM A CROWN KNOT AT THE END OF THE 4-STRING ROUND BRAID.

FORM A CROWN KNOT WITH 1, 2, 3, 4.

FIRST: A-B. THEN: C-D-E-F.

FIRST: G-H. THEN: I-J-K-L.

ARROWED ENDS FORM A TASSEL.

Fig. 643 — Toggle Knots at the end of a 4-string Round Braid.

Braiding procedure:

Form a Crown Knot with the string-ends A, C, G and I by crowning as indicated.

Lay down the rest of A : Free run.
B : Free run. Ends at 1.
Lay down the rest of C : u.
D : $o-u$.
E : $o-u-o$.
F : $o-2u$. Ends at 2.
Lay down the rest of G : u.
H : o. Ends at 3.
Lay down the rest of I : $2u$.
J : $2o-u-2o-u-o$.
K : $u-o-u-o-2u-o-u$.
L : $o-u-o-u$. Ends at 4.

Form a Crown Knot with the string-ends 1, 2, 3 and 4 by crowning as indicated. Then finish off as further depicted in the subsequent diagrams.

THE BRAIDER

No.35 **AUGUST 2003.**

CONTENTS

pg.

Solutions to the Questions in Issue No.34 807

A Hanger (Lanyard) with colourful knots 808

Nested Cylindrical Braids 810

An Integrated Pineapple Knot for an 8-string
2u-2o Round Braid 829

A quarterly publication for the braiding artisan

Resale of this publication or copies thereof is strictly prohibited

Copyright ©2003 by:

A.G. Schaake; 21 Sundown Cresc.; Hamilton; New Zealand.
D. Van Tassel; Box 335; Craig, Co 81626-0335; U.S.A.
F.J.M. Masurel; Ganzenzijde 4; 2317XG Leiden; Nederland.

All rights reserved. No part of this publication may be reproduced, stored in a retrieval system, or transmitted, in any form or by any means, electronic, mechanical, photo-copying, recording, or otherwise, without prior written permission.

This publication is available to braiding artisans only.

Copies may be obtained from:

A.G. Schaake,
21 Sundown Cresc.,
Hamilton,
New Zealand.

Solutions to the Questions in Issue No. 34

Question on pg.791.

For determining the left bight-boundary position specification and the left bight-boundary sequence set with ranking-numbers we can use for the **Periodic Regular Nested Cylindrical Braids** the general fundamental calculation procedures as discussed in *The Braider*, Issue No. 19, pp. 415-416, or we can use their general forms as shown in *The Braider*, Issue No. 34, pg. 790.

The bight-boundary position specification and the bight-boundary sequence set with ranking-numbers for the left bight-edge depicted at the upper left in Fig. 636 is then with $A_{l_1} = 12$ and $A_{l_2} = 5$, hence $z = 13$:

$$(22211111111111222)\{1_1(13)_{17}(11)_{16}9_{15}7_{14}5_{13}(17)_{12}(16)_{11}(15)_{10}(14)_9(12)_8(10)_7 8_6 6_5 4_4 3_3 2_2\}\,.$$

The bight-boundary position specification and the bight-boundary sequence set with ranking-numbers for the left bight-edge depicted at the upper right in Fig. 636 is then with $A_{l_1} = 15$ and $A_{l_2} = 6$, hence $z = 16$:

$$(222211111111111112222)\{1_1(16)_{21}(14)_{20}(12)_{19}(10)_{18}8_{17}6_{16}(21)_{15}(20)_{14}(19)_{13}(18)_{12}(17)_{11}(15)_{10}(13)_9(11)_8 9_7 7_6 5_5 4_4 3_3 2_2\}\,.$$

The bight-boundary position specification and the bight-boundary sequence set with ranking-numbers for the left bight-edge depicted at the lower left in Fig. 636 is then with $A_{l_1} = 12$ and $A_{l_2} = 4$, hence $z = 8$:

$$(22222222222)\{1_1 8_{16}7_{15}6_{14}5_{13}(12)_{12}(11)_{11}(10)_{10}9_9 8_8 7_7 6_6 5_5 4_4 3_3 2_2\}\,.$$

The bight-boundary position specification and the bight-boundary sequence set with ranking-numbers for the left bight-edge depicted at the lower right in Fig. 636 is then with $A_{l_1} = 15$ and $A_{l_2} = 5$, hence $z = 10$:

$$(22222222222222)\{1_1(10)_{20}9_{19}8_{18}7_{17}6_{16}(15)_{15}(14)_{14}(13)_{13}(12)_{12}(11)_{11}(10)_{10}9_9 8_8 7_7 6_6 5_5 4_4 3_3 2_2\}\,.$$

Question on pg.792.

For determining the right bight-boundary position specification and the right bight-boundary sequence set with ranking-numbers in nominal cyclic form (since the RRHC[†] is not known) we can use for the **Periodic Regular Nested Cylindrical Braids** the general fundamental procedures as discussed in *The Braider*, Issue No. 19, pg. 415, or we can use their general forms as shown in *The Braider*, Issue No. 34, pp. 791-792.

The bight-boundary position specification and the bight-boundary sequence set for the right bight-edge depicted at the upper left in Fig. 637 is then with $A_{r_1} = 12$ and $A_{r_2} = 5$, hence $z = 13$:

(22211111111111222){123468(10)(12)(14)(15)(16)(17)579(11)(13)}.

The bight-boundary position specification and the bight-boundary sequence set for the right bight-edge depicted at the upper right in Fig. 637 is then with $A_{r_1} = 15$ and $A_{r_2} = 6$, hence $z = 16$:

(222211111111111112222){1234579(11)(13)(15)(17)(18)(19)(20)(21)68(10)(12)(14)(16)}.

The bight-boundary position specification and the bight-boundary sequence set for the right bight-edge depicted at the lower left in Fig. 637 is then with $A_{r_1} = 12$ and $A_{r_2} = 4$, hence $z = 8$:

(22222222222){123456789(10)(11)(12)5678}.

The bight-boundary position specification and the bight-boundary sequence set for the right bight-edge depicted at the lower right in Fig. 637 is then with $A_{r_1} = 15$ and $A_{r_2} = 5$, hence $z = 10$:

[†] See *The Braider*, Issue No. 19, pg. 415.

(22222222222222){123456789(10)(11)(12)(13)(14)(15)6789(10)}.

A Hanger (Lanyard) with colourful knots

In early 1999 we received from Gene Ulrich[†] a hanger decorated with a number of colourful knots. Fig. 644 shows schematically the hanger with the various knots. Two seven feet, white cotton, round braided, strands of $\frac{5}{32}$in diameter were used. Half the length of one strand was dyed blue. The other strand was dyed red for half its length, and dyed black for the other half of its length.

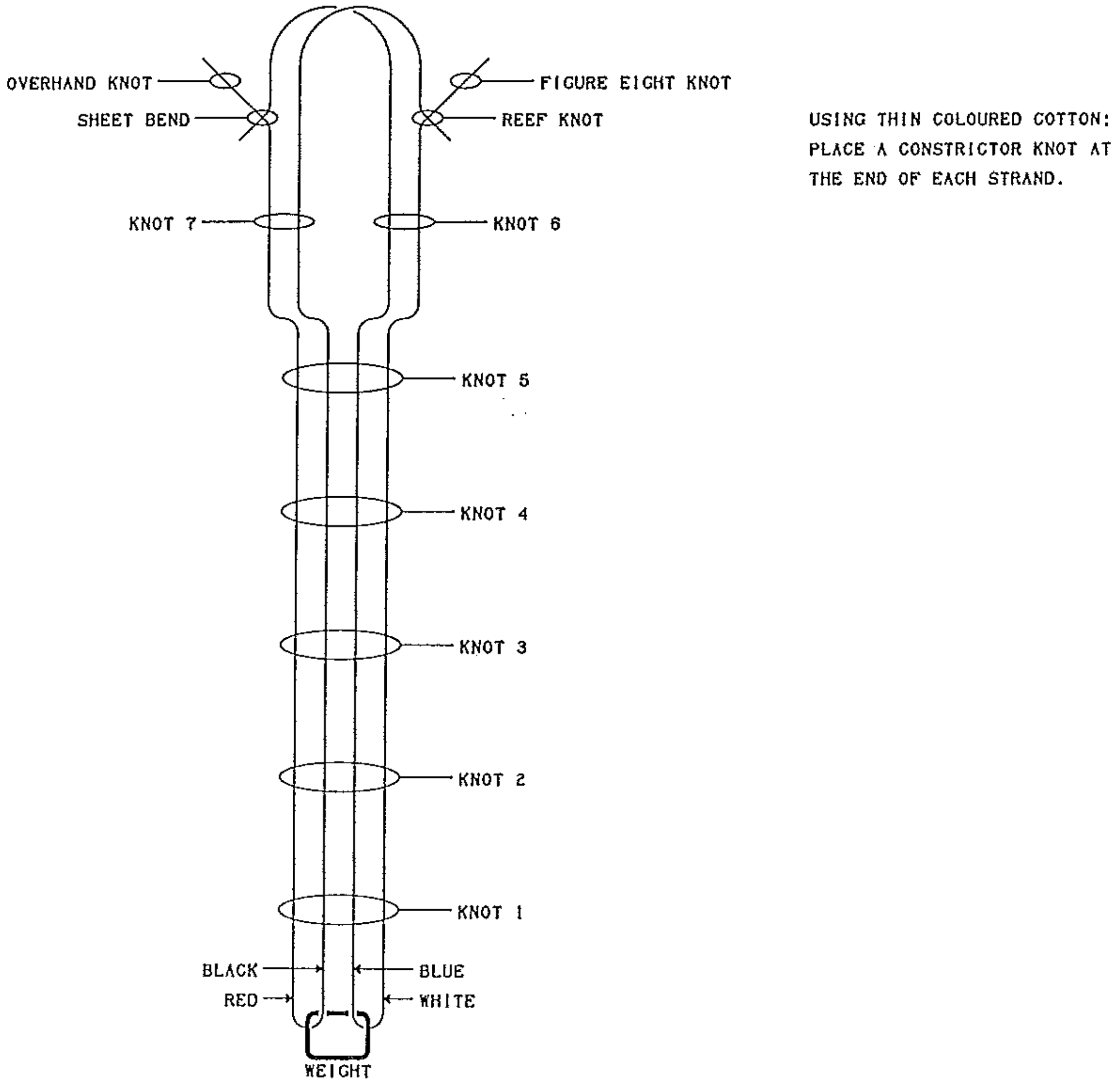

Fig. 644 — The schematic layout of the hanger with its knots.

The grid-diagrams of the knots #1 to #7 are shown in Fig. 645. Knot #1 is a 2-ply form of a **footrope knot**[‡], which is a 4-string **Crown knot** with a 4-string **Wall knot** under it and feeding the string-ends through the crown (knot #4).

[†] See *The Braider*, Issue No. 26, pg. 599.

[‡] See *The Braider*, Issue No. 5, pg. 97, Fig. 81; pg. 99, Fig. 83; pg. 106.

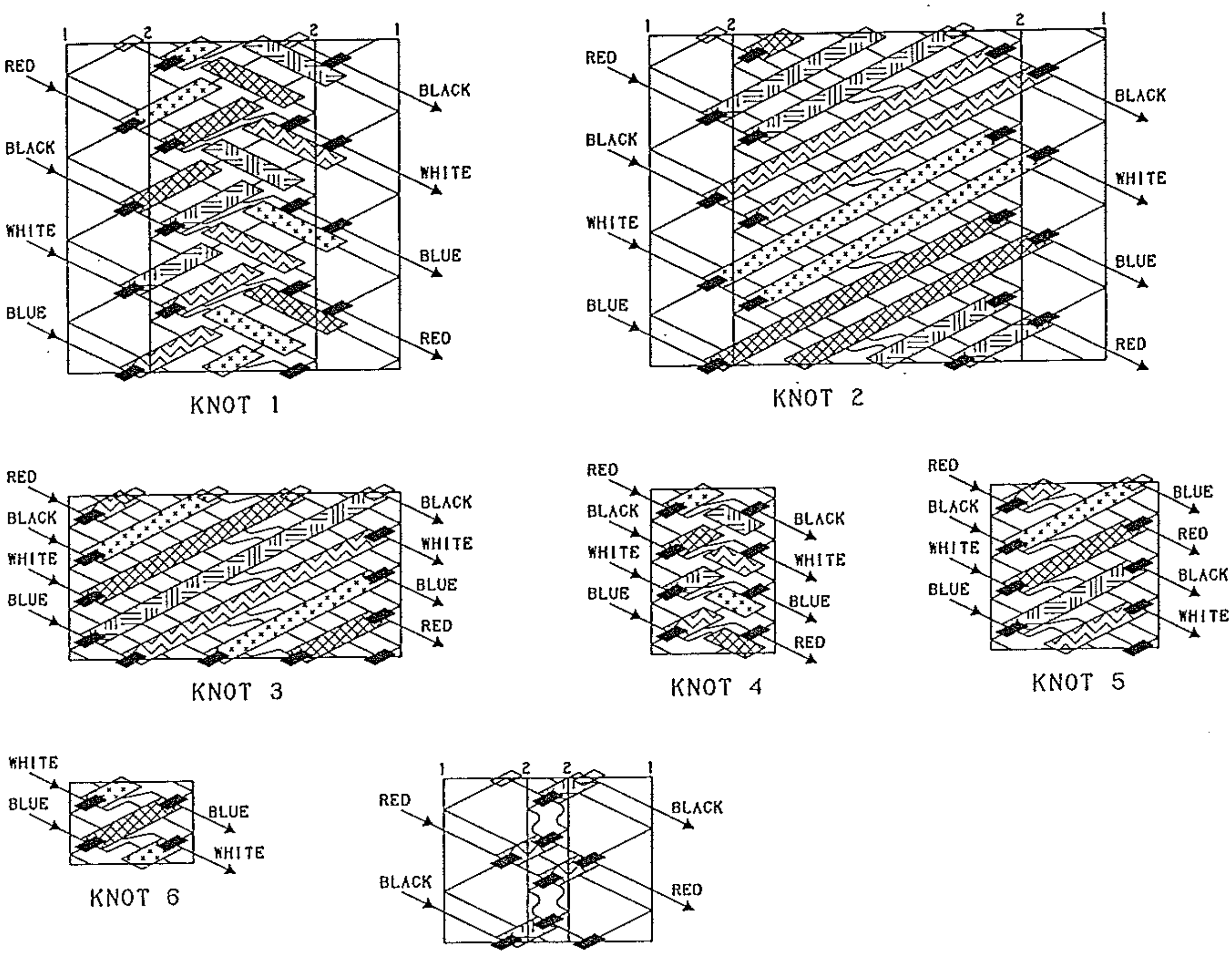

KNOT 1 KNOT 2 KNOT 3 KNOT 4 KNOT 5 KNOT 6 KNOT 7

Fig. 645 — The grid-diagrams of the knots #1 to #7.

Knot #2 is a 2-ply form of a $p/b = 5/4$ (5-parts/4-bights) Matthew Walker Knot.[†]

Knot #3 is a $p/b = 8/4$ Matthew Walker Knot.

Knot #4 is a $p/b = 3/4$ Footrope Knot.

Knot #5 is a $p/b = 4/4$ Matthew Walker Knot.

Knot #6 is a $p/b = 3/2$ Matthew Walker Knot.

Knot #7 is a 2-ply form of a $p/b = 2/2$ Matthew Walker Knot (which is a $p/b = 2/2$ Wall Knot). We can draw the grid-diagram of knot #7 in Fig. 645 also as in Fig. 646.

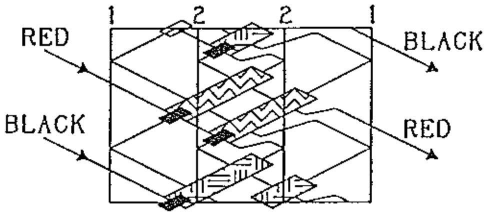

Fig. 646 — Knot #7; alternative drawing of its grid-diagram in Fig. 645.

[†] We have discussed this 2-ply form in *The Braider*, Issue No. 26, pg. 600, Fig. 488 lower right.

There are always two 2-ply forms of a Regular Cylindrical Braid; for example in Fig. 647 we have depicted the other 2-ply form of the $p/b = 5/4$ Matthew Walker Knot on which knot #2 is based. If the colour, shape and texture of all the four strings are identical, then knot #2 and the knot in Fig. 647 would look exactly the same, although they are, of course, not the same.

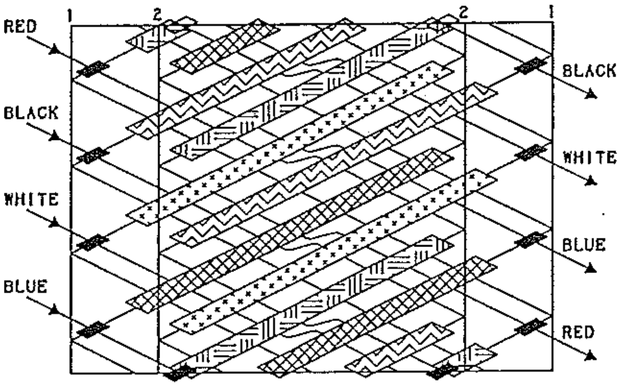

Fig. 647 — The other 2-ply form associated with the knot on which knot #2 is based.

If one would continue braiding knot #5 as the knot in Fig. 647, one would get the same colour-pattern as in knot #2, but the knot is a bit shorter of course. With the aid of grid-diagrams we can readily find the longer 2-ply Matthew Walker Knots which have the same colour-pattern.

Nested Cylindrical Braids

In *The Braider*, Issue No. 33, we discussed for the **Asymmetric Regular Nested Cylindrical Braids** the basic calculation procedures leading to their half-cycle braiding algorithms. Let's now have a further look at their first-return string-runs. We shall use as convention $A_l > A_r$.

There are two basic complementary forms associated with a first-return string-run:

1. The basic complementary form 1 first-return string-run is the mirror-image of a first-return string-run.

Example 1: $(A_l = 10\ ;\ A_r = 6\ ;\ x = 33)$

$$\begin{tikzcd}
2 & & & 2 & \\
& 5 \arrow[ul] & & & 2 \arrow[ul] \\
3 \arrow[ur] & & & 9 \arrow[ur] & \\
& 6 \arrow[ul] & & & 3 \arrow[ul] \\
10 \arrow[ur] & & \longrightarrow & 10 \arrow[ur] & \\
& 3 \arrow[ul] & & & 6 \arrow[ul] \\
9 \arrow[ur] & & & 3 \arrow[ur] & \\
& 2 \arrow[ul] & & & 5 \arrow[ul] \\
2 \arrow[ur] & & & 2 \arrow[ur] &
\end{tikzcd}$$

2. The basic complementary form 2 first-return string-run involves the half-cycle complements with respect to A_l and A_r (the (A_l, A_r)-complement,

where the complement of l_i is equal to $(A_l + 1 - l_i)$ and the complement of r_i is equal to $(A_r + 1 - r_i)$).

Example 2: $(A_l = 10\,;\ A_r = 6\,;\ x = 33)$

$$\begin{tikzcd}
2 & & & 9 & & & 1 & \\
& 5 \arrow[ul] & & & 2 \arrow[ul] & & & 4 \arrow[ul] \\
3 \arrow[ur] & & & 8 \arrow[ur] & & & 2 \arrow[ur] & \\
& 6 \arrow[ul] & & & 1 \arrow[ul] & & & 5 \arrow[ul] \\
10 \arrow[ur] & & \longrightarrow & 1 \arrow[ur] & & = & 9 \arrow[ur] & \\
& 3 \arrow[ul] & & & 4 \arrow[ul] & & & 2 \arrow[ul] \\
9 \arrow[ur] & & & 2 \arrow[ur] & & & 8 \arrow[ur] & \\
& 2 \arrow[ul] & & & 5 \arrow[ul] & & & 1 \arrow[ul] \\
2 \arrow[ur] & & & 9 \arrow[ur] & & & 1 \arrow[ur] &
\end{tikzcd}$$

The combination of these two basic complementary first-return string-run forms results in a compound-complementary first-return string-run which is the mirror-imaged (A_l, A_r)-complement of the given first-return string-run.

Example 3: $(A_l = 10\,;\ A_r = 6\,;\ x = 33)$

$$\begin{tikzcd}
2 & & & 9 & & & 1 & & & 1 & \\
& 5 \arrow[ul] & & & 2 \arrow[ul] & & & 4 \arrow[ul] & & & 1 \arrow[ul] \\
3 \arrow[ur] & & & 8 \arrow[ur] & & & 2 \arrow[ur] & & & 8 \arrow[ur] & \\
& 6 \arrow[ul] & & & 1 \arrow[ul] & & & 5 \arrow[ul] & & & 2 \arrow[ul] \\
10 \arrow[ur] & & \longrightarrow & 1 \arrow[ur] & & = & 9 \arrow[ur] & & \longrightarrow & 9 \arrow[ur] & \\
& 3 \arrow[ul] & & & 4 \arrow[ul] & & & 2 \arrow[ul] & & & 5 \arrow[ul] \\
9 \arrow[ur] & & & 2 \arrow[ur] & & & 8 \arrow[ur] & & & 2 \arrow[ur] & \\
& 2 \arrow[ul] & & & 5 \arrow[ul] & & & 1 \arrow[ul] & & & 4 \arrow[ul] \\
2 \arrow[ur] & & & 9 \arrow[ur] & & & 1 \arrow[ur] & & & 1 \arrow[ur] &
\end{tikzcd}$$

It should be noted that the given first-return string-run

$$\begin{tikzcd}
2 & \\
& 5 \arrow[ul] \\
3 \arrow[ur] & \\
& 6 \arrow[ul] \\
10 \arrow[ur] & \\
& 3 \arrow[ul] \\
9 \arrow[ur] & \\
& 2 \arrow[ul] \\
2 \arrow[ur] &
\end{tikzcd}$$

in the above examples is not the only first-return string-run in the Asymmetric Regular Nested Cylindrical Braid with $A_l = 10$; $A_r = 6$; $x = 33$ and a lower-left to upper-right half-cycle from left bight-boundary 2 to right bight-boundary 2.

An Asymmetric Regular Nested Cylindrical Braid has in general more than one distinct y-value associated with its first-return string-run(s). In fact, when an Asymmetric Regular Nested Cylindrical Braid has only one distinct y-value, the g.c.d. (A_l, A_r) must be A_r as we shortly shall see. When an Asymmetric Regular Nested Cylindrical Braid has more than one distinct y-value and more than one first-return string-run, then each first-return string-run is not necessarily associated with all the distinct y-values of the braid.

In Fig. 648 is depicted a section of an Asymmetric Regular Nested Cylindrical Braid. The y-values (in general not all distinct) associated with a first-return string-run are calculated with the formula

$$y_i = |2A_l + x - 2(l_i + r_i)|_{2A_r} ,$$

whereas the distinct y_m-values associated with the Asymmetric Regular Nested Cylindrical Braid are calculated from any y_n-value with the formula

$$y_m = |y_n + 2n'A_l|_{2A_r} , \quad \text{where } n' = 0 , 1 , 2 , 3 , \cdots , (\frac{A_r}{d} - 1) .$$

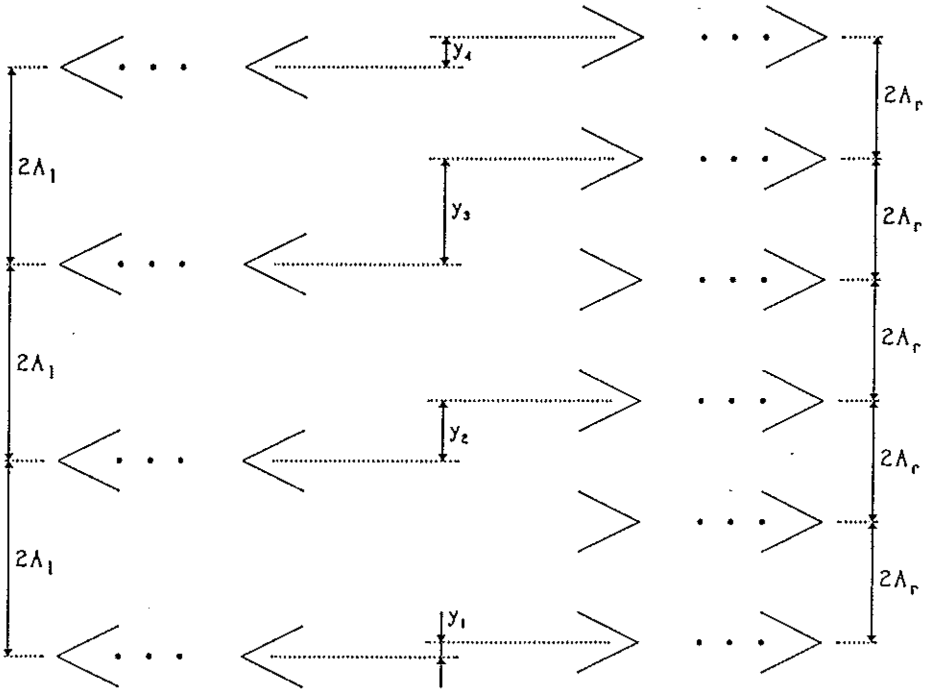

Fig. 648 — A section of an Asymmetric Regular Nested cylindrical Braid.

$$|2n'A_l|_{2A_r} = \left|2n'd\frac{A_l}{d}\right|_{2d\frac{A_r}{d}} = 2d\left|n'\frac{A_l}{d}\right|_{\frac{A_r}{d}} = 2md , \quad \text{where}$$

$m = 0 , 1 , 2 , 3 , \cdots , (\frac{A_r}{d} - 1)$. Hence $y_m = |y_n + 2md|_{2A_r}$. It thus follows that $y_{\min} = |y_n|_{2d} = |y_m|_{2d}$, and $y_m = |y_n|_{2d} + 2md$.

The various distinct y_m-values associated with an Asymmetric Regular Nested Cylindrical Braid for which the g.c.d. $(A_l, A_r) = d$ are indicated by × in the left-hand diagram of Fig. 649.

When we take the mirror-image of this Asymmetric Regular Nested Cylindrical Braid (mirror-image from "top" to "bottom" in order to keep the A_l bight-edge on the left-hand side and the A_r bight-edge on the right-hand side), then the distinct y_m-values associated with this mirror-imaged Asymmetric Regular Nested Cylindrical Braid are indicated by $\star$ in the right-hand diagram of Fig. 649. Hence the lines $y = md$, where $m = 0, 1, 2, 3, \cdots, (2\frac{A_r}{d} - 1)$, are lines of symmetry for mirror-imaged Asymmetric Regular Nested Cylindrical Braids having the same x-value.

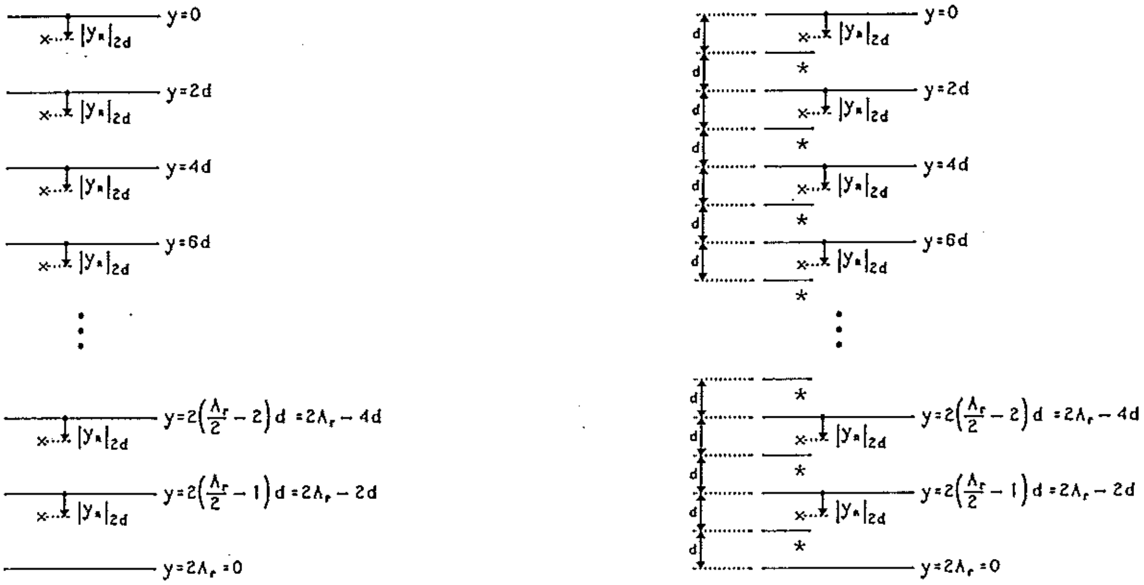
y=0
y=2d
y=4d
y=6d
$y=2(\frac{A_r}{2}-2)d=2A_r-4d$
$y=2(\frac{A_r}{2}-1)d=2A_r-2d$
$y=2A_r=0$
$|y_n|_{2d}$
x
d
*

Fig. 649 — The distinct y_m-values associated with an Asymmetric Regular Nested Cylindrical Braid with g.c.d.$(A_l, A_r) = d$ and with its mirror-imaged complementary Asymmetric Regular Nested Cylindrical Braid.

Note that for $\frac{A_r}{d} =$ **even**, y_m and $|A_r + y_m|_{2A_r}$ are both distinct y-values of the same Asymmetric Regular Nested Cylindrical Braid, and that for $\frac{A_r}{d} =$ **odd**, y_m and $|A_r + y_m - d|_{2A_r}$ are both distinct y-values of the same Asymmetric Regular Nested Cylindrical Braid.

On pg. 812 we mentioned that when an Asymmetric Regular Nested Cylindrical Braid has only one distinct y_m-value, the g.c.d.(A_l, A_r) must be A_r. This follows immediately from the formula $y_m = |y_n|_{2d} + 2md$, where $m = 0, 1, 2, 3, \cdots, (\frac{A_r}{d} - 1)$, since m can then only be equal to 0, hence $(\frac{A_r}{d} - 1) = 0$. This requires $d = A_r$.

From the left-hand diagram in Fig. 649 we saw that an Asymmetric Regular Nested Cylindrical Braid having nesting-numbers A_l and A_r with g.c.d.$(A_l, A_r) = d$ has the following $\frac{A_r}{d}$ distinct y_m-values:

$$|y_n|_{2d} + 2md, \text{ where } m = 0, 1, 2, 3, \cdots, (\frac{A_r}{d} - 1).$$

We shall indicate this set of $\frac{A_r}{d}$ distinct y_m-values as the $|y_n|_{2d}$-set of distinct y_m-values.

For the Asymmetric Regular Nested Cylindrical Braids with nesting-numbers A_l and A_r, hence having g.c.d.$(A_l, A_r) = d$, we thus have $2d$ distinct $|y_n|_{2d}$-sets each of

$\frac{A_r}{d}$ distinct y_m-values. In the y_m-x tables we repeat the $|y_n|_{2d} = 0$-set of distinct y_m-values as the $|y_n|_{2d} = 2d$-set of distinct y_m-values. Hence in the y_m-x tables we have $(2d+1)$ rows of $|y_n|_{2d}$-sets with the row for the set $|y_n|_{2d} = d$ being the mirror-imaging row.

The minimum x-value associated with a $|y_n|_{2d}$-set of distinct y_m-values depends on the minimum y_m-value in this set, hence depends on $|y_n|_{2d}$. The minimum x-value associated with the $|y_n|_{2d}$-set is expressed by the formula:

$$x_{\min} = 2 - |y_n|_d \, .$$

Braid with $x = x_1$:

$$\begin{tikzcd} l_{i+1} & \\ & r_i \arrow[ul] \\ l_i \arrow[ur] & \end{tikzcd}$$

$$\Delta l_i = |l_{i+1} - l_i|_{A_l} \, .$$

$$\Delta l_i = |2A_r + x_1 - 2(l_i + r_i)|_{A_l} \, .$$

$$\begin{tikzcd} & r_{j+1} \\ l_j \arrow[ur] & \\ & r_j \arrow[ul] \end{tikzcd}$$

$$\Delta r_j = |r_{j+1} - r_j|_{A_r} \, .$$

$$\Delta r_j = |2A_l + x_1 - 2(r_j + l_j)|_{A_r} \, .$$

Complementary form (2); braid with $x = x_2$:

$$\begin{tikzcd} |A_l + 1 - l_{i+1}|_{A_l} & \\ & |A_r + 1 - r_i|_{A_r} \arrow[ul] \\ |A_l + 1 - l_i|_{A_l} \arrow[ur] & \end{tikzcd}$$

$$\Delta l_i^* = |l_i - l_{i+1}|_{A_l} \, .$$

$$\Delta l_i^* = |2A_r + x_2 - 2(A_l + A_r + 2 - (l_i + r_i))|_{A_l} \, .$$

$$\begin{tikzcd} & |A_r + 1 - r_{j+1}|_{A_r} \\ |A_l + 1 - l_j|_{A_l} \arrow[ur] & \\ & |A_r + 1 - r_j|_{A_r} \arrow[ul] \end{tikzcd}$$

$$\Delta r_j^* = |r_j - r_{j+1}|_{A_r} \, .$$

$$\Delta r_j^* = |2A_l + x_2 - 2(A_l + A_r + 2 - (r_j + l_j))|_{A_r} \, .$$

For Δl_i^* to be $|l_i - l_{i+1}|_{A_l} = |-\Delta l_i|_{A_l}$ and Δr_i^* to be $|r_i - r_{i+1}|_{A_r} = |-\Delta r_i|_{A_r}$, we must have the condition $x_2 = 2n^*A^{**} - 2(A_l + A_r - 2) - x_1$, where $|2n^*A^{**}|_{A_l} = |2n^*A^{**}|_{A_r} = 0$. Hence the x_c-lines (the lines about which (A_l, A_r) complementary/compound complementary symmetry takes place) are the lines $x = \frac{x_1 + x_2}{2} = n^*A^{**} + 2 - (A_l + A_r)$.

Since $|2n^*A^{**}|_{A_l} = |2n^*A^{**}|_{A_r} = 0$ (hence $2n^*\frac{A_r}{d}$ must be a *whole number* and $2n^*\frac{A_l}{d}$ must be a *whole number*), and since g.c.d. $(\frac{A_l}{d}, \frac{A_r}{d}) = 1$ (consequently $\frac{A_l}{d}$ and $\frac{A_l}{d}$ cannot both be *even*) it follows that $2n^*$ must be a *whole number*). However, since $x \geq 2 - |y_n|_d$, we therefore require n^*A^{**} to be a *natural number* such that $\{n^*A^{**} + 2 - (A_l + A_r)\} \geq \{2 - d\}$. Hence n^* is a positive integer such that $\{n^*A^{**} + 2 - (A_l + A_r)\} \geq \{2 - d\}$.

Let $|y_n|_{2d} = y_1$ be the y_m-set associated with x_1. Then:

$$y_1 = |2A_l + x_1 - 2(l_i + r_i)|_{2d} \,.$$

Thus for the Asymmetric Regular Nested Cylindrical Braid associated with x_1 the y_m-values are $y_1 + 2md$, where $m = 0, 1, 2, 3, \cdots, (\frac{A_r}{d} - 1)$. Consequently, when $\frac{A_r}{d} = \mathit{even}$ and y_1 is a y_m-value associated with the Asymmetric Regular Nested Cylindrical Braid, then also $y_1 + A_r$ is another y_m-value associated with the same braid.

Let $|y_n|_{2d} = y_2$ be the y_m-set associated with x_2. Then:

$$\begin{aligned} y_2 &= |2A_l + x_2 - 2(l_i^* + r_i^*)|_{2d} \\ &= |2A_l + 2n^*A^{**} - 2(A_l + A_r - 2) - x_1 - 2(A_l + A_r + 2 - (l_i + r_i))|_{2d} \\ &= |2n^*A^{**} - 2A_l + 2(l_i + r_i) - x_1|_{2d} \\ &= |2n^*A^{**} - y_1|_{2d} \,. \end{aligned}$$

$|2n^*A^{**}|_{2d} = 0$ for $y_2 = |-y_1|_{2d}$.

Hence for $|y_2|_{2d} = |-y_1|_{2d}$: (the Asymmetric Regular Nested Cylindrical braids associated with x_1 and x_2 are (A_l, A_r)-complements of each other)

When $\frac{A_l}{d} =$ **even**: (note that $A^{**} = \mathit{even}$ and $\frac{A_r}{d}$ is *odd*)

$2n^*$ has to be a **positive** integer such that $\{n^*A^{**} + 2 - (A_l + A_r)\} \geq \{2 - d\}$.

When $\frac{A_r}{d} =$ **even**: (note that $A^{**} = \mathit{even}$ and $\frac{A_l}{d}$ is *odd*)

$2n^*$ has to be a **positive** integer such that $\{n^*A^{**} + 2 - (A_l + A_r)\} \geq \{2 - d\}$.

When $\frac{A_l}{d} =$ **odd** and $\frac{A_r}{d} =$ **odd**: (note that $A^{**} = \mathit{even}$ or *odd*)

n^* has to be a **positive** integer such that $\{n^*A^{**} + 2 - (A_l + A_r)\} \geq \{2 - d\}$.

Since $y_2 = |-y_1|_{2d}$ for the above conditions, the row associated with the y_m-set $|y_n|_{2d} = d$ is for those conditions the row of symmetry for the (A_l, A_r)-complements associated with any of the y_m-sets. The row associated with the y_m-set $|y_n|_{2d} = d$ is also the row of symmetry for the mirror-complements associated with any y_m-set.

$|2n^*A^{**}|_{2d} = d$ for $y_2 = |d - y_1|_{2d}$.

Hence for $|y_2|_{2d} = |d - y_1|_{2d}$: (the Asymmetric Regular Nested Cylindrical braids associated with x_1 and x_2 are (A_l, A_r)-complements of each other)

$\frac{A_l}{d} =$ **odd**, $\frac{A_r}{d} =$ **odd** and $A^{**} =$ **even** (hence $d = \mathit{even}$):

$2n^*$ has to be a **positive odd** integer such that $\{n^*A^{**} + 2 - (A_l + A_r)\} \geq \{2 - d\}$.

Since $y_2 = |d - y_1|_{2d}$ for $\frac{A_l}{d} =$ **odd**, $\frac{A_r}{d} =$ **odd**, $A^{**} =$ **even** (hence $d = \mathit{even}$) and $2n^*$ a **positive odd** integer such that $\{n^*A^{**} + 2 - (A_l + A_r)\} \geq \{2 - d\}$, the row associated with the y_m-set $|y_n|_{2d} = \frac{d}{2}$ is the row of symmetry for the (A_l, A_r)-complements associated with the y_m-sets $|y_n|_{2d} \leq d$, while the row associated with the y_m-set $|y_n|_{2d} = \frac{3d}{2}$ is the row of symmetry for the (A_l, A_r)-complements associated with the y_m-sets $|y_n|_{2d} \geq d$.

The row associated with the y_m-set $|y_n|_{2d} = d$ is the row of symmetry for the mirror-complements associated with any y_m-set.

$\frac{A_l}{d}$ = **odd**, $\frac{A_r}{d}$ = **odd** and A^{**} = **odd** (hence $d = odd$):

When $2n^*$ is a **positive odd** integer then $2\{n^*A^{**} + 2 - (A_l + A_r)\}$ is **odd**, hence $\{n^*A^{**} + 2 - (A_l + A_r)\} = \left\{\frac{2n'' + 1}{2}A^{**} + 2 - (A_l + A_r)\right\}$, where n'' is a whole number such that $\left\{\frac{2n'' + 1}{2}A^{**} + 2 - (A_l + A_r)\right\} \geq \{2 - d\}$. These x_c-values are *mixed numbers*, hence are not real x-values. The lines representing them fall between the real x-values $\left\{\frac{3 + (2n'' + 1)A^{**}}{2} - (A_l + A_r)\right\}$ and $\left\{\frac{5 + (2n'' + 1)A^{**}}{2} - (A_l + A_r)\right\}$.

Since $y_2 = |d - y_1|_{2d}$ for $\frac{A_l}{d}$ = **odd**, $\frac{A_r}{d}$ = **odd**, A^{**} = **odd** (hence $d = odd$) and $2n^*$ a **positive odd** integer such that $\{n^*A^{**} + 2 - (A_l + A_r)\} \geq \{2 - d\}$, the values of $|y_n|_{2d} = \frac{d}{2}$ and $|y_n|_{2d} = \frac{3d}{2}$ are *mixed numbers*, hence not real $|y_n|_{2d}$-values. The line representing the $\frac{d}{2}$-value is the line of symmetry for the (A_l, A_r)-complements associated with the y_m-sets $|y_n|_{2d} \leq d$, while the line representing the $\frac{3d}{2}$-value is the line of symmetry for the (A_l, A_r)-complements associated with the y_m-sets $|y_n|_{2d} \geq d$.

The row associated with the y_m-set $|y_n|_{2d} = d$ is the row of symmetry for the mirror-complements associated with any y_m-set.

Thus:

For Asymmetric Regular Nested Cylindrical Braids with $\frac{A_l}{d} = \text{odd}$, $\frac{A_r}{d} = \text{odd}$, $A^{**} = \text{odd}$, the general y_m-x table layout is as in Fig. 650. The vertical bold x_c-lines are associated with the values $\left\{\frac{2n'' + 1}{2}A^{**} + 2 - (A_l + A_r)\right\}$, and the horizontal bold lines are associated with the values $\frac{d}{2}$ and $\frac{3d}{2}$.

For Asymmetric Regular Nested Cylindrical Braids with $\frac{A_l}{d} = \text{odd}$, $\frac{A_r}{d} = \text{odd}$, $A^{**} = \text{even}$, the general y_m-x table layout is as in Fig. 651.

For Asymmetric Regular Nested Cylindrical Braids with $\frac{A_l}{d} = \text{even}$, $\frac{A_r}{d} = \text{odd}$, or with $\frac{A_l}{d} = \text{odd}$, $\frac{A_r}{d} = \text{even}$, the general y_m-x table layout is as in Fig. 652.

The first-return string-runs belonging to cell F_1 and cell F_2 are the mirror-image of each other.

The first-return string-runs belonging to cell F_3 and cell F_4 are the mirror-image of each other.

The first-return string-runs belonging to cell F_1 and cell F_3 are the mirror-imaged (A_l, A_r)-complements of each other.

The first-return string-runs belonging to cell F_2 and cell F_4 are the mirror-imaged (A_l, A_r)-complements of each other.

The first-return string-runs belonging to cell F_1 and cell F_4 are the (A_l, A_r)-complements of each other.

The first-return string-runs belonging to cell F_2 and cell F_3 are the (A_l, A_r)-complements of each other.

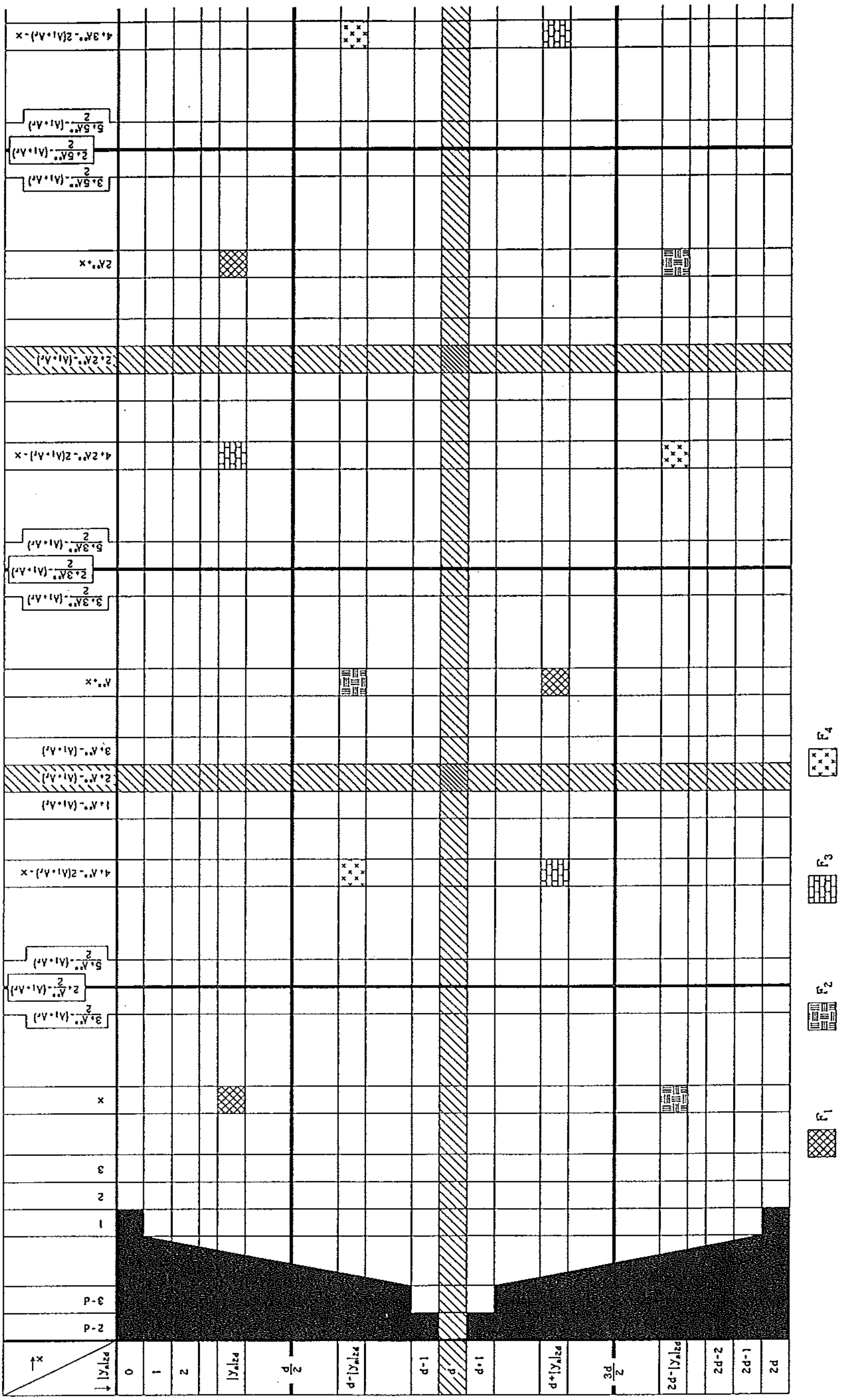

Fig. 650 — General y_m-x table layout when $\dfrac{A_l}{d} = \text{odd}$, $\dfrac{A_r}{d} = \text{odd}$, $A^{**} = \text{odd}$.

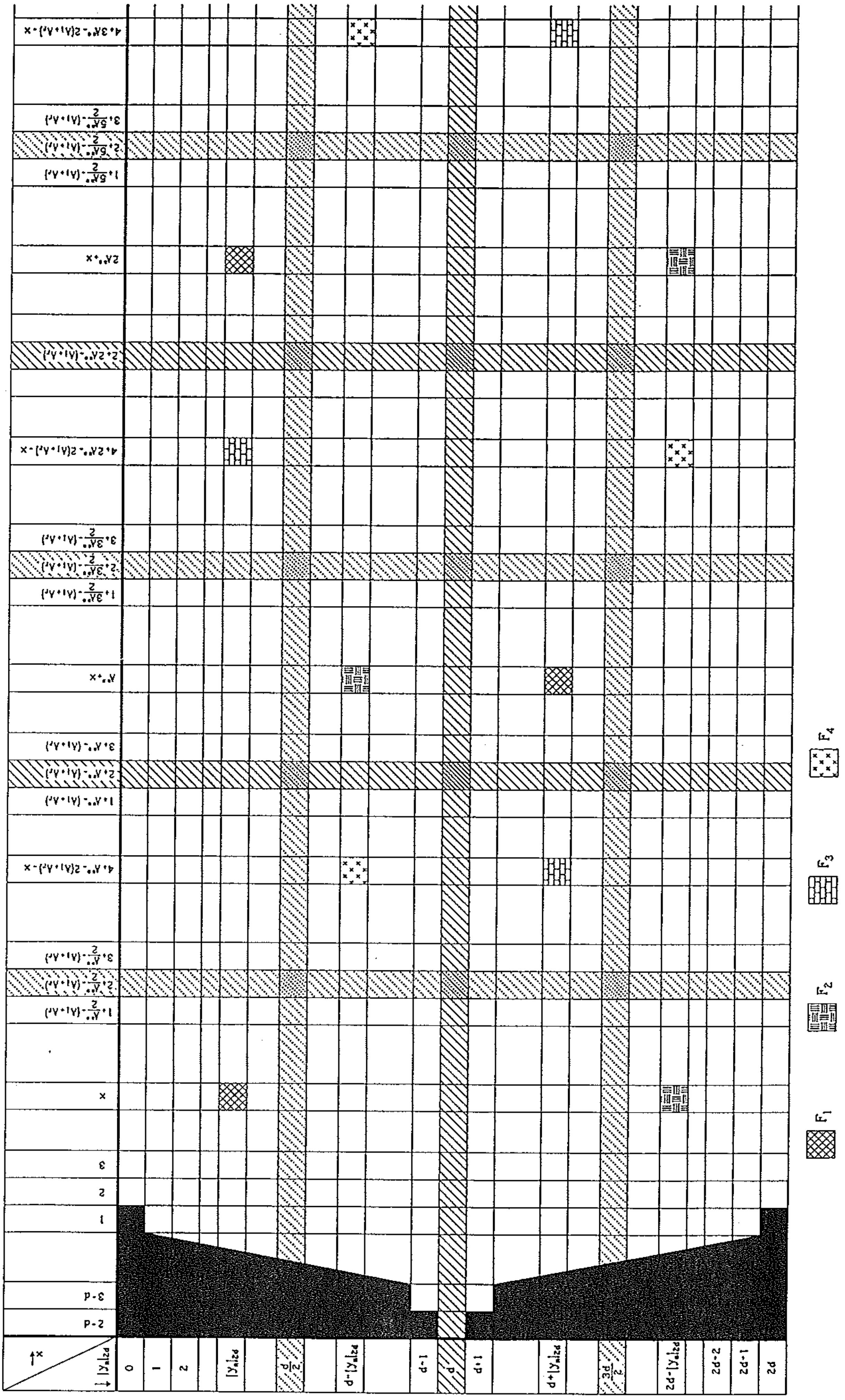

Fig. 651 — General y_m-x table layout when $\frac{A_l}{d} = \text{odd}$, $\frac{A_r}{d} = \text{odd}$, $A^{**} = \text{even}$.

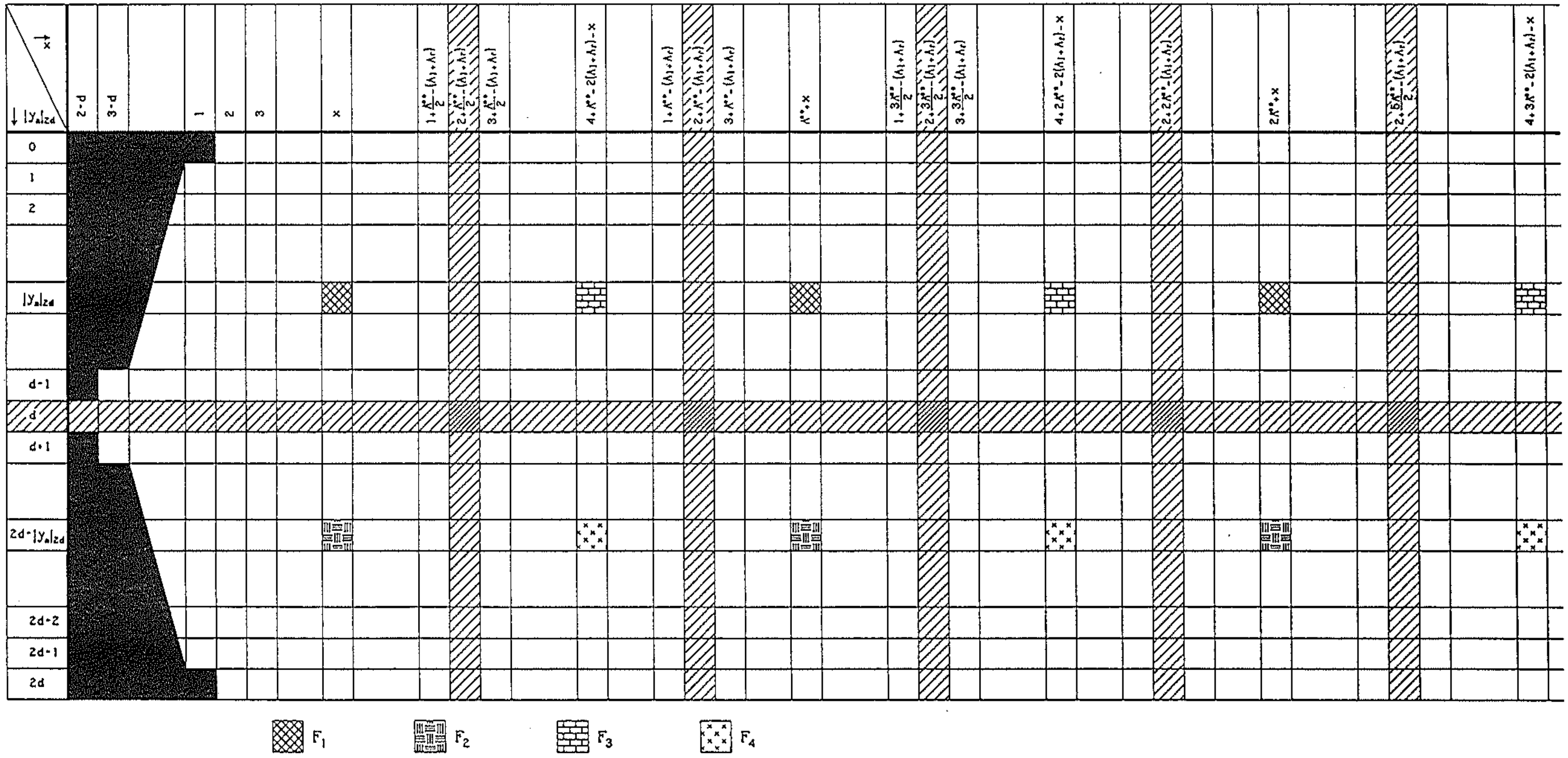

Fig. 652 — General y_m-x table layout when $\dfrac{A_l}{d} = \text{even}$, or $\dfrac{A_r}{d} = \text{even}$.

Hence:

In the x/y-tables for $\frac{A_l}{d} = odd$, $\frac{A_r}{d} = odd$, and $A^{**} = odd$, cells in the same $|y_n|_{2d}$-row (hence belonging to the same $|y_n|_{2d}$-set) at equiperpendicular distance from a compound complementary x_c-column equal to $n^*A^{**} + 2 - (A_l + A_r)$, where n^* is a positive integer such that $n^*A^{**} + 2 - (A_l + A_r) \geq 2 - d$, where $d = \text{g.c.d.}(A_l, A_r)$, belong to Asymmetric Regular Nested Cylindrical Braids whose first-return string-runs are compound complementary. See Fig. 650.

In the x/y-tables for $\frac{A_l}{d} = odd$, $\frac{A_r}{d} = odd$, and $A^{**} = even$, cells in the same $|y_n|_{2d}$-row (hence belonging to the same $|y_n|_{2d}$-set) at equiperpendicular distance from a compound complementary x_c-column equal to $n^*A^{**} + 2 - (A_l + A_r)$, where n^* is a positive integer such that $n^*A^{**} + 2 - (A_l + A_r) \geq 2 - d$, where $d = \text{g.c.d.}(A_l, A_r)$) belong to Asymmetric Regular Nested Cylindrical Braids whose first-return string-runs are compound complementary. See Fig. 651.

In the x/y-tables for $\frac{A_l}{d} = even$ or $\frac{A_r}{d} = even$, cells in the same $|y_n|_{2d}$-row (hence belonging to the same $|y_n|_{2d}$-set) at equiperpendicular distance from a compound complementary x_c-column equal to $n^*A^{**} + 2 - (A_l + A_r)$, where $2n^*$ is a positive integer such that $n^*A^{**} + 2 - (A_l + A_r) \geq 2 - d$, where $d = \text{g.c.d.}(A_l, A_r)$) belong to Asymmetric Regular Nested Cylindrical Braids whose first-return string-runs are compound complementary. See Fig. 652.

Example 4:

$A_l = 15$, $A_r = 9$. Hence $\text{g.c.d.}(A_l, A_r) = d = 3$ and $A^{**} = 45$. Take for braid 1: $x_1 = 13$, $y_1 = 1$, $l_1 = 1$. The set of y_m-values is then 1, $1 + 2d = 7$, $1 + 4d = 13$.

For calculating the first-return string-run(s) we use the general formulae:

$$r_i = \left| A_l + \frac{x - y_i - 2l_i}{2} \right|_{A_r} .$$

$$l_{i+1} = |2A_r + x - (l_i + 2r_i)|_{A_l} .$$

$$r_{j+1} = |2A_l + x - (r_j + 2l_j)|_{A_r} .$$

$$y_i = |2A_l + x - 2(l_i + r_i)|_{A_r} .$$

Hence for $A_l = 15$, $A_r = 9$, $x = 13$, $y_1 = 1$, $l_1 = 1$ we obtain:

$$r_1 = \left| 15 + \frac{13 - 1 - 2}{2} \right|_9 = 2 .$$

$$y_i = |30 + 13 - 2(l_i + r_i)|_{18} = |43 - 2(l_i + r_i)|_{18} .$$

$$l_{i+1} = |18 + 13 - (l_i + 2r_i)|_{15} = |31 - (l_i + 2r_i)|_{15} .$$

$$r_{j+1} = |30 + 13 - (r_j + 2l_j)|_9 = |43 - (r_j + 2l_j)|_9 .$$

As we shall see below, the first-return string-run of which the first half-cycle runs from left bight-boundary 1 to right bight-boundary 2 consists of 18 half-cycles. There are thus another $2A^{**} - 18 = 72$ further half-cycles which are contained in one or more further first-return string-runs. Since we have the half-cycle from left bight-boundary 1 to right bight-boundary 2, we also have the half-cycle from left bight-boundary 1 to right bight boundary $2 + d = 5$ and the half-cycle from left bight-boundary 1 to right bight boundary $2+2d=8$. The first-return string-run which consists of 18 half-cycle contains the half-cycle from left bight-boundary 1 to right bight-boundary 2 only, hence the second first-return string-run can start with the half-cycle from left bight-boundary 1 to right bight-boundary 5. As we shall see below, the second first-return string-run consists of 72 half-cycles. There are thus no further first-return string-runs.

$$\begin{tikzcd}
1 & & \\
& 9 \arrow[ul] & y_i = 1 \\
12 \arrow[ur] & & \\
& 1 \arrow[ul] & y_i = 1 \\
2 \arrow[ur] & & \\
& 2 \arrow[ul] & y_i = 1 \\
10 \arrow[ur] & & \\
& 3 \arrow[ul] & y_i = 7 \\
15 \arrow[ur] & & \\
& 1 \arrow[ul] & y_i = 13 \\
14 \arrow[ur] & & \\
& 5 \arrow[ul] & y_i = 1 \\
7 \arrow[ur] & & \\
& 6 \arrow[ul] & y_i = 7 \\
12 \arrow[ur] & & \\
& 4 \arrow[ul] & y_i = 13 \\
11 \arrow[ur] & & \\
& 8 \arrow[ul] & y_i = 1 \\
4 \arrow[ur] & & \\
& 9 \arrow[ul] & y_i = 7 \\
9 \arrow[ur] & & \\
& 7 \arrow[ul] & y_i = 13 \\
8 \arrow[ur] & & \\
& 2 \arrow[ul] & y_i = 13 \\
4 \arrow[ur] & & \\
& 6 \arrow[ul] & y_i = 1 \\
15 \arrow[ur] & & \\
& 7 \arrow[ul] & y_i = 7 \\
2 \arrow[ur] & & \\
& 5 \arrow[ul] & y_i = 7 \\
4 \arrow[ur] & &
\end{tikzcd}$$

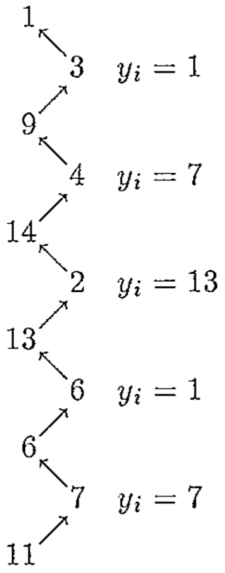
1
3 $y_i = 1$
9
4 $y_i = 7$
14
2 $y_i = 13$
13
6 $y_i = 1$
6
7 $y_i = 7$
11

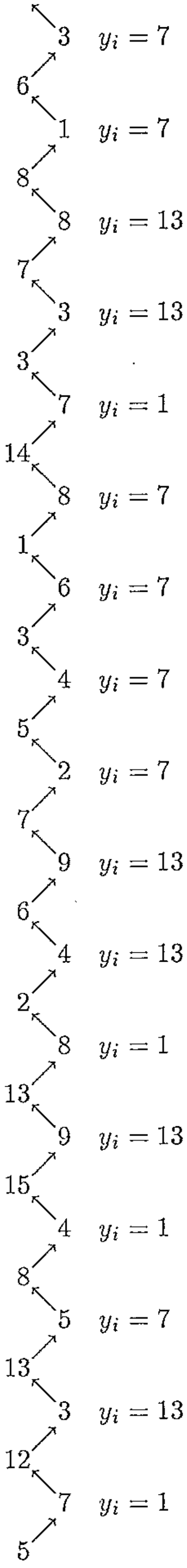
3 $y_i = 7$
6
1 $y_i = 7$
8
8 $y_i = 13$
7
3 $y_i = 13$
3
7 $y_i = 1$
14
8 $y_i = 7$
1
6 $y_i = 7$
3
4 $y_i = 7$
5
2 $y_i = 7$
7
9 $y_i = 13$
6
4 $y_i = 13$
2
8 $y_i = 1$
13
9 $y_i = 13$
15
4 $y_i = 1$
8
5 $y_i = 7$
13
3 $y_i = 13$
12
7 $y_i = 1$
5

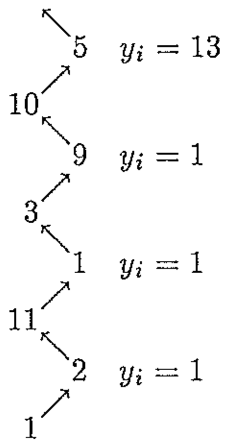

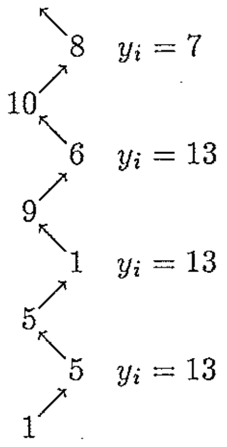

The (A_l, A_r)-complements of these two first-return string-runs can now readily be derived from them, and for convenience we start with their respective half-cycles from left bight-boundary 14 to right bight-boundary 4 and from left bight-boundary 15 to right bight-boundary 9. Hence the (A_l, A_r)-complementary first-return string-runs start respectively with the half-cycles from left bight-boundary 2 to right bight-boundary 6 and from left bight-boundary 1 to right bight-boundary 1. The indicated y_i-values associated with these (A_l, A_r)-complementary first-return string-runs have been calculated with the general formulae on pg. 825.

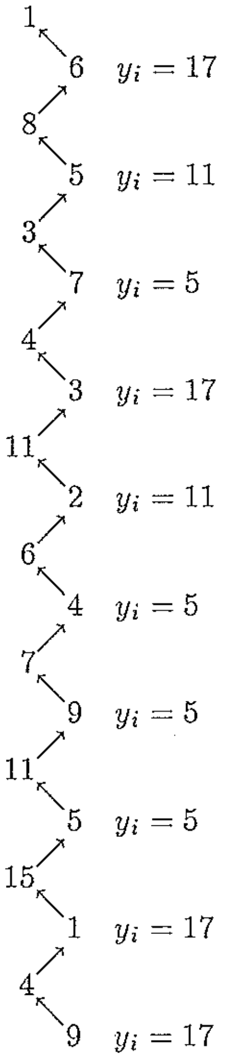

$$\begin{tikzcd}
 & {} & \\
14 \arrow[ur] & & \\
 & 8 \arrow[ul] & y_i = 17 \\
6 \arrow[ur] & & \\
 & 7 \arrow[ul] & y_i = 11 \\
1 \arrow[ur] & & \\
 & 9 \arrow[ul] & y_i = 5 \\
2 \arrow[ur] & & \\
 & 5 \arrow[ul] & y_i = 17 \\
9 \arrow[ur] & & \\
 & 4 \arrow[ul] & y_i = 11 \\
4 \arrow[ur] & & \\
 & 6 \arrow[ul] & y_i = 5 \\
5 \arrow[ur] & & \\
 & 2 \arrow[ul] & y_i = 17 \\
12 \arrow[ur] & & \\
 & 1 \arrow[ul] & y_i = 11 \\
7 \arrow[ur] & & \\
 & 3 \arrow[ul] & y_i = 5 \\
8 \arrow[ur] & & \\
 & 8 \arrow[ul] & y_i = 5 \\
12 \arrow[ur] & & \\
 & 4 \arrow[ul] & y_i = 17 \\
1 \arrow[ur] & & \\
 & 3 \arrow[ul] & y_i = 11 \\
14 \arrow[ur] & & \\
 & 5 \arrow[ul] & y_i = 11 \\
12 \arrow[ur] & & \\
 & 7 \arrow[ul] & y_i = 11 \\
10 \arrow[ur] & & \\
 & 9 \arrow[ul] & y_i = 11 \\
8 \arrow[ur] & & \\
 & 2 \arrow[ul] & y_i = 5 \\
9 \arrow[ur] & & \\
 & 7 \arrow[ul] & y_i = 5
\end{tikzcd}$$

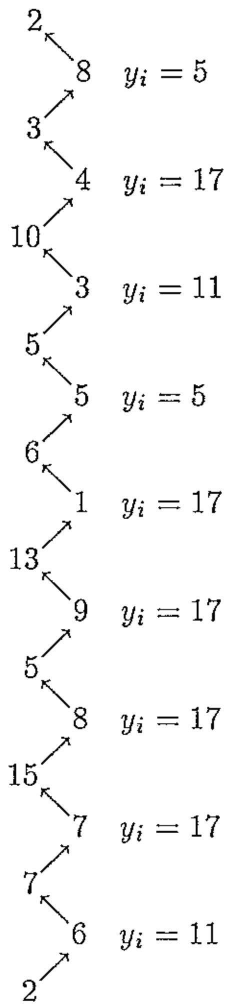

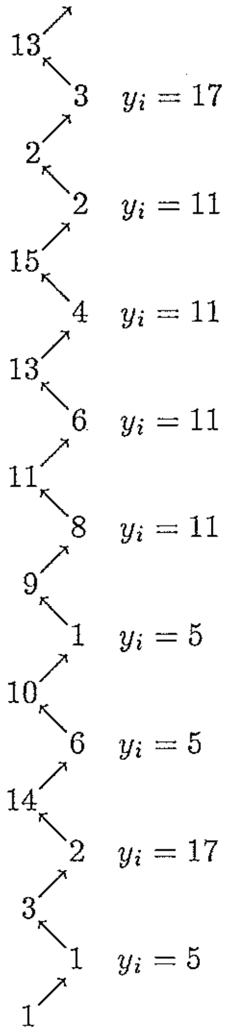

From the general formulae on pg. 820 we readily derive the following general formulae:

$$\begin{aligned} n_l A_l &= n_r A_r + (\Delta l_i + \Delta r_i) - 2(A_l - A_r)\,. \\ x &= n_l A_l + l_i + l_{i+1} + 2r_i - 2A_r\,. \\ &= n_r A_r + r_j + r_{j+1} + 2l_j - 2A_l\,. \\ y_i &= |(n_l + 2)A_l + \Delta l_i|_{2A_r}\,. \\ |y_i|_{2d} &= |\Delta l_i + n_l A_l|_{2d}\,. \end{aligned}$$

Hence for the above (A_l, A_r)-complementary first-return string-runs we obtain with $l_i = 1$, $r_i = 1$, $l_{i+1} = 3$, $r_{i+1} = 2$:

$$\begin{aligned} n_l A_l &= n_r A_r + (\Delta l_i + \Delta r_i) - 2(A_l - A_r) \\ 15 n_l &= 9 n_r + (2 + 1) - 2(15 - 9) \\ 5 n_l &= 3 n_r - 3\,. \end{aligned}$$

$n_r = 6 \quad \rightarrow \quad n_l = 3 \quad \rightarrow \quad x = 33 \quad \rightarrow \quad |y_n|_{2d} = 5\,.$
$n_r = 11 \quad \rightarrow \quad n_l = 6 \quad \rightarrow \quad x = 78 \quad \rightarrow \quad |y_n|_{2d} = 2\,.$
$n_r = 16 \quad \rightarrow \quad n_l = 9 \quad \rightarrow \quad x = 123 \quad \rightarrow \quad |y_n|_{2d} = 5\,.$
$n_r = 21 \quad \rightarrow \quad n_l = 12 \quad \rightarrow \quad x = 168 \quad \rightarrow \quad |y_n|_{2d} = 2\,.$
$n_r = 26 \quad \rightarrow \quad n_l = 15 \quad \rightarrow \quad x = 213 \quad \rightarrow \quad |y_n|_{2d} = 5\,.$
$n_r = 31 \quad \rightarrow \quad n_l = 18 \quad \rightarrow \quad x = 258 \quad \rightarrow \quad |y_n|_{2d} = 2\,.$
$n_r = 36 \quad \rightarrow \quad n_l = 21 \quad \rightarrow \quad x = 303 \quad \rightarrow \quad |y_n|_{2d} = 5\,.$

For the original first-return string-runs (the string-runs on pg. 823 → 822 → 821) we obtain with $l_i = 1$, $r_i = 2$, $l_{i+1} = 11$, $r_{i+1} = 1$:

$$\begin{aligned} n_l A_l &= n_r A_r + (\Delta l_i + \Delta r_i) - 2(A_l - A_r) \\ 15 n_l &= 9 n_r + (10 - 1) - 2(15 - 9) \\ 5 n_l &= 3 n_r - 1 . \end{aligned}$$

$$\begin{array}{lllllll} n_r = 2 & \rightarrow & n_l = 1 & \rightarrow & x = 13 & \rightarrow & |y_n|_{2d} = 1 . \\ n_r = 7 & \rightarrow & n_l = 4 & \rightarrow & x = 58 & \rightarrow & |y_n|_{2d} = 4 . \\ n_r = 12 & \rightarrow & n_l = 7 & \rightarrow & x = 103 & \rightarrow & |y_n|_{2d} = 1 . \\ n_r = 17 & \rightarrow & n_l = 10 & \rightarrow & x = 148 & \rightarrow & |y_n|_{2d} = 4 . \\ n_r = 22 & \rightarrow & n_l = 13 & \rightarrow & x = 193 & \rightarrow & |y_n|_{2d} = 1 . \\ n_r = 27 & \rightarrow & n_l = 16 & \rightarrow & x = 238 & \rightarrow & |y_n|_{2d} = 4 . \\ n_r = 32 & \rightarrow & n_l = 19 & \rightarrow & x = 283 & \rightarrow & |y_n|_{2d} = 1 . \end{array}$$

The positions in the y_m-x table of these and their (A_l, A_r)-complementary Asymmetric Regular Nested Cylindrical Braids are depicted in Fig. 653.

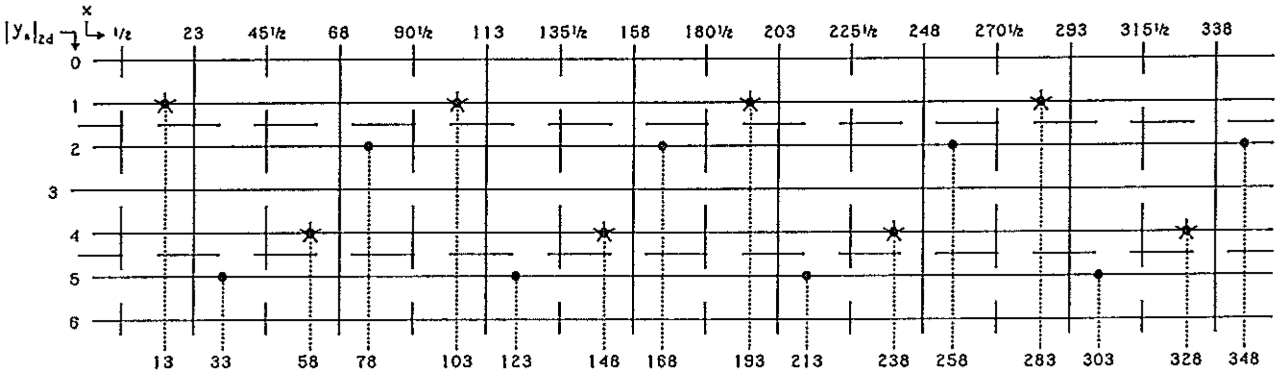

Fig. 653 — The y_m-x table associated with Example 4.

Example 5:

$A_l = 12$, $A_r = 8$. Hence g.c.d.$(A_l, A_r) = d = 4$ and $A^{**} = 24$. Take for braid 1: $x_1 = 26$, $y_1 = 6$, $l_1 = 1$. The set of y_m-values is then 6, $1 + 2d = 14$.

For calculating the first-return string-run(s) we use the general formulae on pg. 820: Hence for $A_l = 12$, $A_r = 8$, $x = 26$, $y_1 = 6$, $l_1 = 1$ we obtain:

$$\begin{aligned} r_1 &= \left| 12 + \frac{26 - 6 - 2}{2} \right|_8 = 5 . \\ y_i &= |24 + 26 - 2(l_i + r_i)|_{16} = |50 - 2(l_i + r_i)|_{16} . \\ l_{i+1} &= |16 + 26 - (l_i + 2r_i)|_{12} = |42 - (l_i + 2r_i)|_{12} . \\ r_{j+1} &= |24 + 26 - (r_j + 2l_j)|_8 = |50 - (r_j + 2l_j)|_8 . \end{aligned}$$

When there is a half-cycle from left bight-boundary 1 to right bight-boundary 5, then there is a half-cycle from left bight-boundary 1 to right bight-boundary $|5 + d|_{A_r} = |5 + 4|_8 = 1$. As we shall see, there are two first-return string-runs. Say we start the first one of these with the half-cycle from left bight-boundary 1 to right bight-boundary 1. As we shall see, there is in this first-return string-run no half-cycle from left bight-boundary 2 to a right bight-boundary, hence we can start the second first-return string-run with such a half-cycle. Since there is a half-cycle from left bight-boundary 1 to right bight-boundary 1 (in the first first-return string-run), there must exist a half-cycle from left bight-boundary 2 to right bight-boundary $A_r = 8$, hence there must be a half-cycle from left bight-boundary 2 to right bight-boundary $|8+d|_{A_r} = |8+4|_8 = 4$. Say we start the second first-return string-run with the half-cycle from left bight-boundary 2 to right bight-boundary 4. The following two first-return string-runs are then obtained:

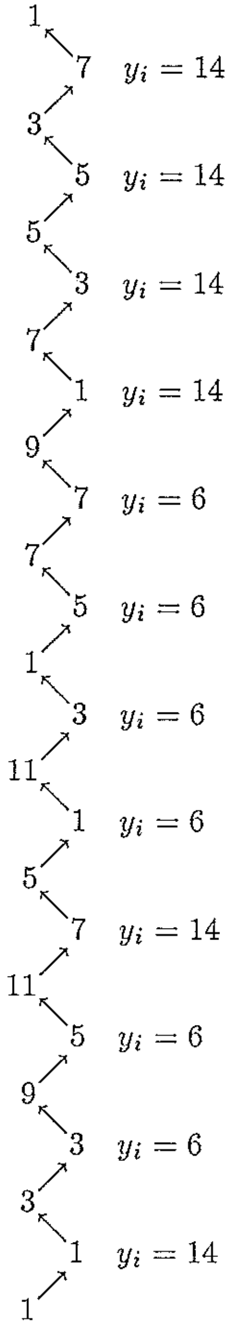

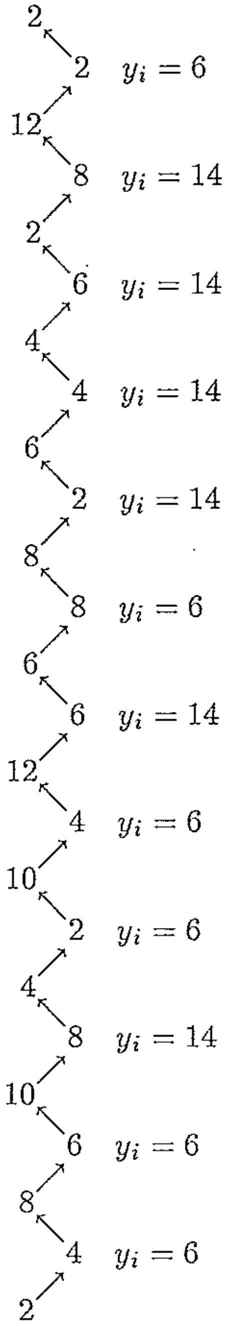

The (A_l, A_r)-complements of these two first-return string-runs can again readily be derived from them, and for convenience we start with their respective half-cycles from left bight-boundary 11 to right bight-boundary 7 and from left bight-boundary 12 to right bight-boundary 6. Hence the (A_l, A_r)-complementary first-return string-runs start respectively with the half-cycles from left bight-boundary 2 to right bight-boundary 2 and from left bight-boundary 1 to right bight-boundary 3. The indicated y_i-values associated with these (A_l, A_r)-complementary first-return string-runs have again been calculated with the general formulae on pg. 825.

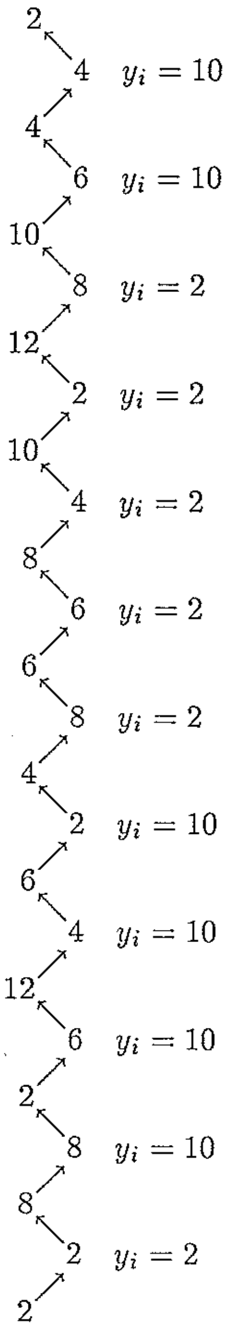

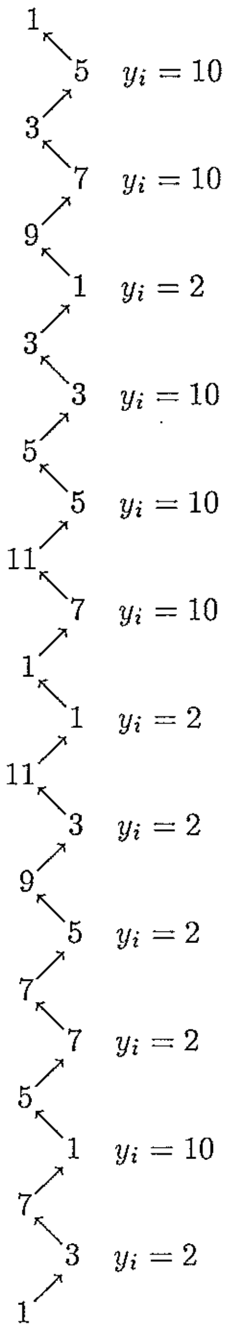

With the general formulae on pg. 825 we obtain for these (A_l, A_r)-complementary first-return string-runs with $l_i = 2\,,\ r_i = 2\,,\ l_{i+1} = 8\,,\ r_{i+1} = 8$:

$$\begin{aligned} n_l A_l &= n_r A_r + (\Delta l_i + \Delta r_i) - 2(A_l - A_r) \\ 12 n_l &= 8 n_r + (6+6) - 2(12-8) \\ 3 n_l &= 2 n_r + 1\,. \end{aligned}$$

$$\begin{array}{lclclcl}
n_r = 1 & \longrightarrow & n_l = 1 & \longrightarrow & x = 10 & \longrightarrow & |y_n|_{2d} = 2\,. \\
n_r = 4 & \longrightarrow & n_l = 3 & \longrightarrow & x = 34 & \longrightarrow & |y_n|_{2d} = 2\,. \\
n_r = 7 & \longrightarrow & n_l = 5 & \longrightarrow & x = 58 & \longrightarrow & |y_n|_{2d} = 2\,. \\
n_r = 10 & \longrightarrow & n_l = 7 & \longrightarrow & x = 82 & \longrightarrow & |y_n|_{2d} = 2\,. \\
n_r = 13 & \longrightarrow & n_l = 9 & \longrightarrow & x = 106 & \longrightarrow & |y_n|_{2d} = 2\,. \\
n_r = 16 & \longrightarrow & n_l = 11 & \longrightarrow & x = 130 & \longrightarrow & |y_n|_{2d} = 2\,. \\
n_r = 19 & \longrightarrow & n_l = 13 & \longrightarrow & x = 154 & \longrightarrow & |y_n|_{2d} = 2\,.
\end{array}$$

For the original first-return string-runs (the string-runs on pg. 827) we obtain with $l_i = 1$, $r_i = 1$, $l_{i+1} = 3$, $r_{i+1} = 3$:

$$\begin{aligned} n_l A_l &= n_r A_r + (\Delta l_i + \Delta r_i) - 2(A_l - A_r) \\ 12 n_l &= 8 n_r + (2+2) - 2(12-8) \\ 3 n_l &= 2 n_r - 1 . \end{aligned}$$

$$\begin{array}{lllllllll} n_r = 2 & \rightarrow & n_l = 1 & \rightarrow & x = 2 & \rightarrow & |y_n|_{2d} = 6 . \\ n_r = 5 & \rightarrow & n_l = 3 & \rightarrow & x = 26 & \rightarrow & |y_n|_{2d} = 6 . \\ n_r = 8 & \rightarrow & n_l = 5 & \rightarrow & x = 50 & \rightarrow & |y_n|_{2d} = 6 . \\ n_r = 11 & \rightarrow & n_l = 7 & \rightarrow & x = 74 & \rightarrow & |y_n|_{2d} = 6 . \\ n_r = 14 & \rightarrow & n_l = 9 & \rightarrow & x = 98 & \rightarrow & |y_n|_{2d} = 6 . \\ n_r = 17 & \rightarrow & n_l = 11 & \rightarrow & x = 122 & \rightarrow & |y_n|_{2d} = 6 . \\ n_r = 20 & \rightarrow & n_l = 13 & \rightarrow & x = 146 & \rightarrow & |y_n|_{2d} = 6 . \end{array}$$

The positions in the y_m-x table of these and their (A_l, A_r)-complementary Asymmetric Regular Nested Cylindrical Braids are depicted in Fig. 654.

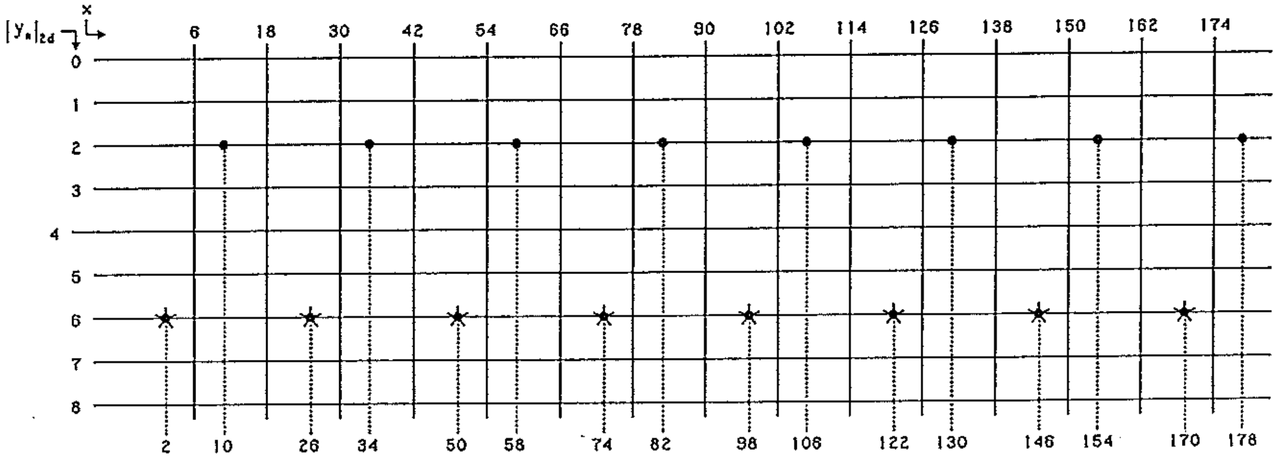

Fig. 654 — The y_m-x table associated with Example 5.

An Integrated Pineapple Knot for an 8-string 2u-2o Round Braid.

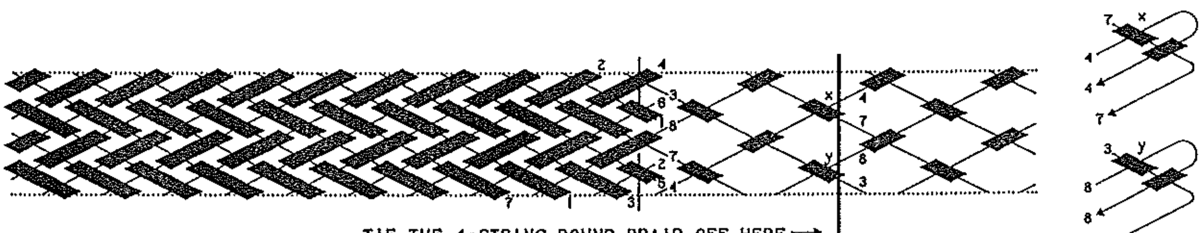

TIE THE 4-STRING ROUND BRAID OFF HERE ⟶
WITH A CONSTRICTOR KNOT AND UNBRAID THE
RIGHT-HAND PART OF THE 4-THONG ROUND BRAID

Fig. 655 — Preparing the Round Braid for the integrated Pineapple Knot.

The consecutive braiding steps for the integrated Pineapple Knot are depicted in Fig. 656.

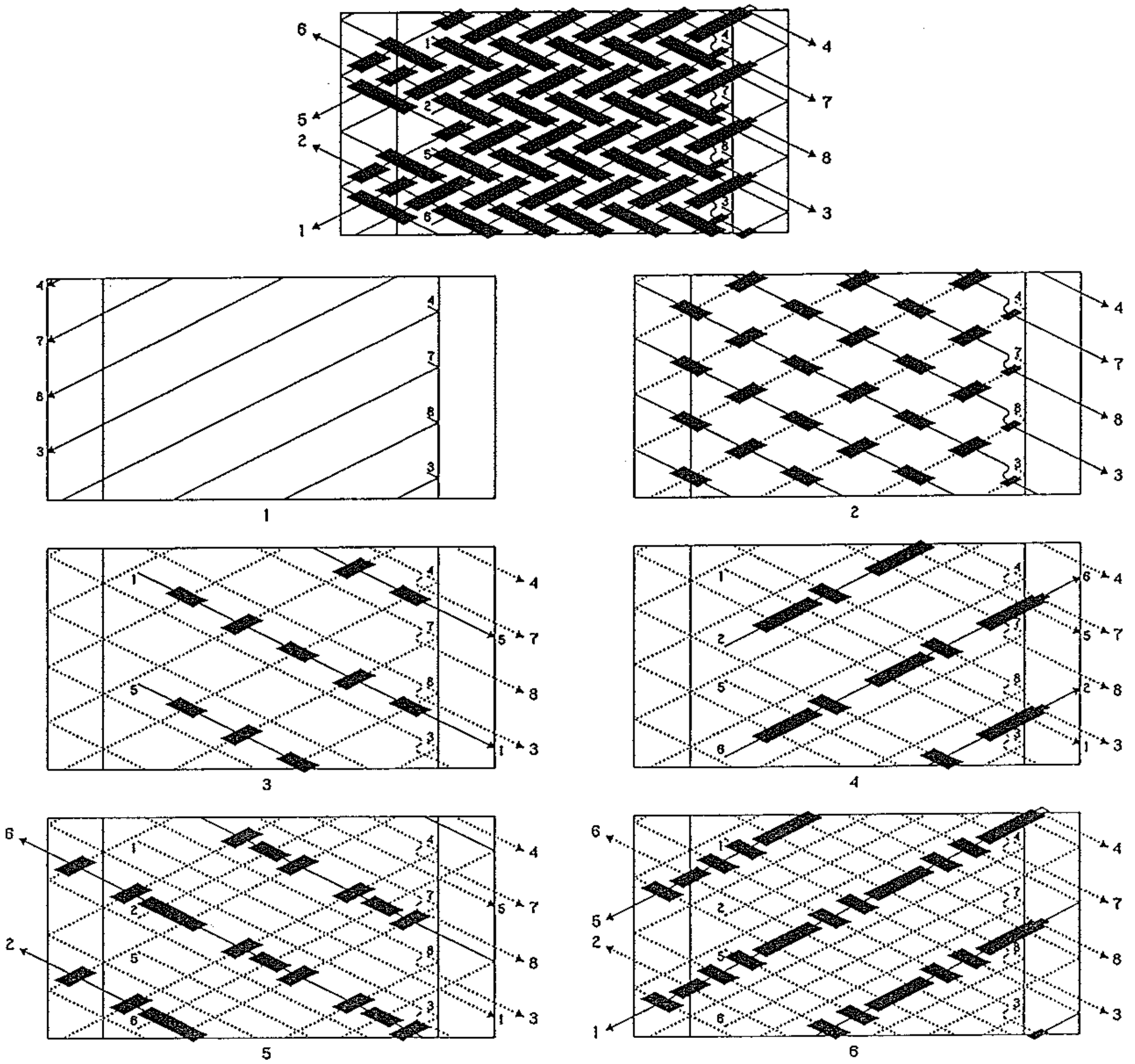

Fig. 656 — The consecutive braiding steps for the integrated Pineapple Knot.

This integrated Pineapple Knot can be closed completely on the right-hand side.

As Fig. 657 shows, a good colour pattern is obtained when in the 8-string round braid the strings 1, 2, 5, 6 all have the same colour and the strings 3, 4, 7, 8 all have the same but a different colour. In this case the colour pattern of the 8-string round braid is as depicted by the upper-right grid-diagrams on pp. 219 and 221 in *The Braider* No. 10.

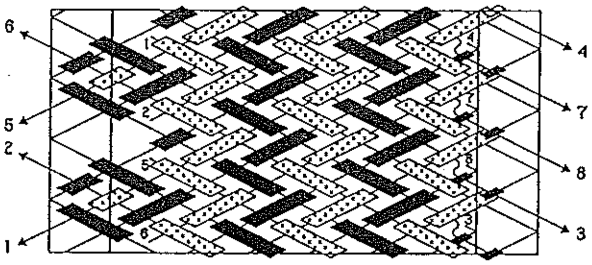

Fig. 657 — A good colour pattern for the integrated Pineapple Knot.

THE BRAIDER

No.36 **NOVEMBER 2003.**

CONTENTS

pg.

A pair of South American Hobbels 831

Nested Cylindrical Braids 845

A quarterly publication for the braiding artisan

Resale of this publication or copies thereof is strictly prohibited

Copyright ©2003 by:

A.G. Schaake; 21 Sundown Cresc.; Hamilton; New Zealand.
D. Van Tassel; Box 335; Craig, Co 81626-0335; U.S.A.
F.J.M. Masurel; Ganzenzijde 4; 2317XG Leiden; Nederland.

All rights reserved. No part of this publication may be reproduced, stored in a retrieval system, or transmitted, in any form or by any means, electronic, mechanical, photo-copying, recording, or otherwise, without prior written permission.

This publication is available to braiding artisans only.

Copies may be obtained from:

A.G. Schaake,
21 Sundown Cresc.,
Hamilton,
New Zealand.

A pair of South American Hobbels

Hobbels are used to immobilise a horse by restraining either the front legs or the back legs. They generally consist of two cuffs joined by a centrepiece. In some publications it has been stated that their measurements are usually determined as follows: a man's fist should just fit through the cuff when it is buttoned closed and the distance between the cuffs should be that of the width of the hand at the height of the knuckels if the hobbels are to be used on the front legs, and about double that if the hobbels are to be used on the back legs. It may well be true that their measurements are determined that way in some quarters, but the obvious question would be: does men with small hands ride small horses and men with big hands big horses?

The pair of hobbels we are discussing here, are owned by a fellow in Wyoming who lent them to Doug Van Tassel who in turn unravelled their construction. According to the owner, the hobbels were made by an Argentinian or Chilean (he referred to the maker twice as an Argentinian and once as a Chilean) working on one of the ranches. The hobbels were braided from quite heavy rawhide; the straps and strands being all hand cut to width and not split by machine to a uniform thickness (as Doug states, this being very common for nearly all the South American equipment seen on the ranches around here), however, this did not adversely affect their appearance.

The strands in the four strand round centrepiece braid are approxmately $^5/_8$" or slightly less in width. This braid is about $^3/_4$" in diameter and $5\,^1/_4$" in length. The method of construction used for the hobbels is similar to the method described by Bruce Grant in his book *Encyclopedia of Rawhide and Leather Braiding*, Plate 141 on pg. 349, except that each strap has only two strands cut on one end so the centrepiece braid is a four strand Round Braid. A closed cuff is very slightly more than 3" in diameter. The hair-side of the rawhide is on the inside of the cuff against the horse's leg. The hair-side of the rawhide is also to the outside on the centrepiece braid.

The drawings in Plate 141 are misleading. In drawing Fig. 2 the flesh-side is uppermost. Fig. 3 would then indicate that the flesh-side also becomes outermost on the centrepiece braid. However, Fig. 7 indicates that the cuffs have been rolled closed as the centrepiece braid was being braided. This would then normally cause the flesh-side to be on the inside of the cuffs, hence against the horse's legs, while the hair-side to be on the outside of the cuffs as well as being outermost on the centrepiece braid. This is what appears to be the case for both samples in the lower photo on pg. 344 of Bruce Grant's *Encyclopedia of Rawhide and Leather Braiding.*

In order to get the hair-side on the inside of the cuffs and on the outside of the centrepiece braid, the braid can be made as shown in Fig. 658. Here, *A* represents a cuff-end which has been slit into two braiding-strands, showing the first crossing. *B* shows a cheater-strap with one end being slit into two braiding-strands. This cheater-strap can be braided from left to right together with the two braiding-strands of *A* to make a four strand round centrepiece braid. The cheater-strap is introduced into the cuff-strap as indicated by the arrow. Once the braid has been done to the desired length, the cheater-strands can be removed a little at a time and replaced with the two braiding strands of the other cuff-strap in a right to left braiding direction. The result is that the two buttons shown in Fig. 1 on pg. 349 of Bruce Grant's *Encyclopedia of Rawhide and Leather Braiding* are on the hair-side of the cuffs.

Once the cheater-strap has been replaced by the strands of the second cuff-strap, we would then have the two cuffs joined by a centrepiece four-strand Round Braid. The two braiding-strands of either cuff will exit on the other cuff's hair-side where this other cuff was split to form its braiding-strands. At each cuff, the two emerging braiding-strands are each split into two strings in order to obtain at each cuff four knotting-strings of about $^1/_4$" wide each. Each of these four knotting-strings are braided into a terminal knot to serve as the cuff's closure knot. In addition to these closure knots, there are two woven knots, one at each end of the centrepiece, covering the Round Braid.

So, the hobbels have overall nothing unusual in their construction.

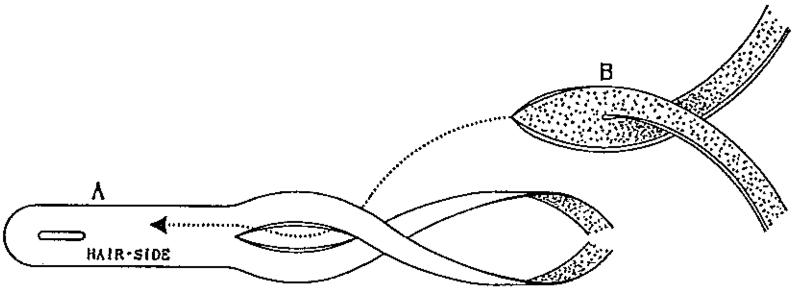

Fig. 658 — The left cuff-strap and the cheater-strap.

The two woven knots, one at each end of the centrepiece four strand Round Braid, have the general appearance of Regular Cylindrical Braids with the nominal column-coding $4u - 3o - 3u - 4o$. If this would be the actual coding of a Regular Cylindrical Braid, then the number of parts would be $\{1 + (4 + 3 + 3 + 4)\} = 15$, and since these braids appear to have each 12 bights, the number of strings required would be g.c.d.$(15, 12) = 3$. However, these woven knots are each made with two strings and the quite noticeable glitch in the braid clearly indicates that there must be an irregularity in the braid. The grid-diagram of the actual braid is depicted by the leftmost diagram in Fig. 659.

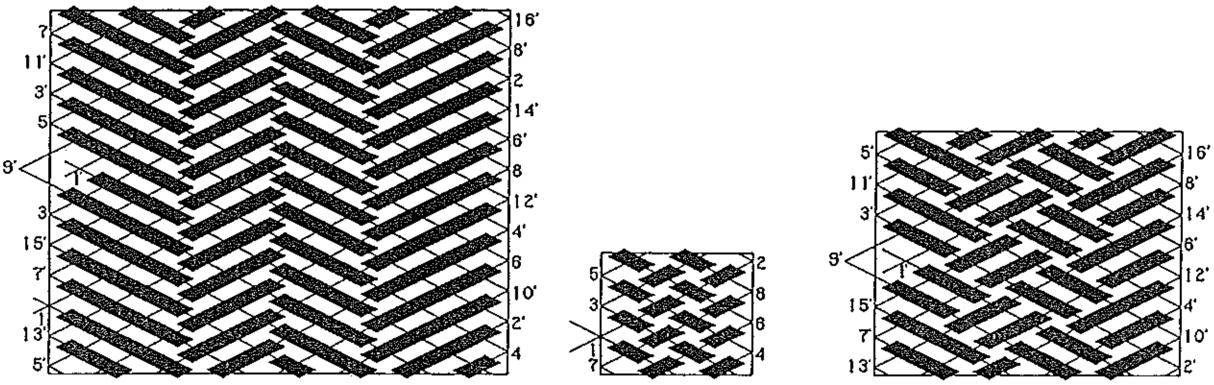

Fig. 659 — The actual woven knots at the ends of the centrepiece braid.

A Regular Cylindrical Braid with $P/B = 15/12$ would be an interbraid of three Regular Knots, each with $p/b = 5/4$. Fig. 660 depicts the three stages of braiding an interbraided $P/B = 15/12$ Regular Cylindrical Braid. It follows from the columns $3, 6, 9, 12$ in the rightmost diagram of Fig. 660 that when the $P/B = 15/12$ Regular Cylindrical Braid has to be column-coded, the three $p/b = 5/4$ Regular Knots must be identical column-coded Regular Knots. In the interbraid of two of these $p/b = 5/4$ Regular Knots, the additional columns $1, 3, 5, 7, 9$ have been created.

In order to obtain a column-coding for a Regular Cylindrical Braid, produced by interbraiding two identical Regular Knots, these Regular Knots must be column-coded. Let each of the two identical column-coded Regular Knots have p-parts and b-bights:

1.) $p = 2n + 1$, where $n = 1, 2, 3, \cdots$.

$2^{(2n+1)}$ different column-coded $2p/2b$ Regular Cylindrical Braids can be created by interbraiding these two identical column-coded Regular Knots if for their column-coding the condition {coding of column x} = {coding of column $(2n + 1 - x)$}, where $x = 1, 2, 3, \cdots, n$, does not apply for at least one x-value. If for their column-coding the condition {coding of column x} = {coding of column $(2n + 1 - x)$}, where $x = 1, 2, 3, \cdots, n$, does apply, then $2^n (2^n + 1)$ different column-coded $2p/2b$ Regular Cylindrical Braids can be created by interbraiding these two identical column-coded Regular Knots, and $2^{(n+1)}$ of these interbraided $P/B = 2p/2b$ Regular Cylindrical Braids have then a balanced column-coding.

2.) $p = 2n$, where $n = 1, 2, 3, \cdots$.

$2^{(2n)}$ different column-coded $2p/2b$ Regular Cylindrical Braids can be created by interbraiding these two identical column-coded Regular Knots if for their column-coding the condition {coding of column x} = {coding of column $(2n - x)$}, where $x = 1, 2, 3, \cdots, (n - 1)$, does not apply for at least one x-value. If for their column-coding the condition {coding of column x} = {coding of column $(2n - x)$}, where $x = 1, 2, 3, \cdots, (n - 1)$, does apply, then $2^{(n-1)} (2^n + 1)$ different column-coded $2p/2b$ Regular Cylindrical Braids can be created by interbraiding these two identical column-coded Regular Knots, and 2^n of these interbraided $P/B = 2p/2b$ Regular Cylindrical Braids have then a balanced column-coding.

Note that when the two identical p/b column-coded Regular Knots have an over-under coding, a balanced column-coding for the interbraided $P/B = 2p/2b$ Regular Cylindrical Braid can only be created when p is *even*.

⋆⋆ *Prove the above relationships for interbraided $P/B = 2p/2b$ column-coded Regular Cylindrical Braids.*

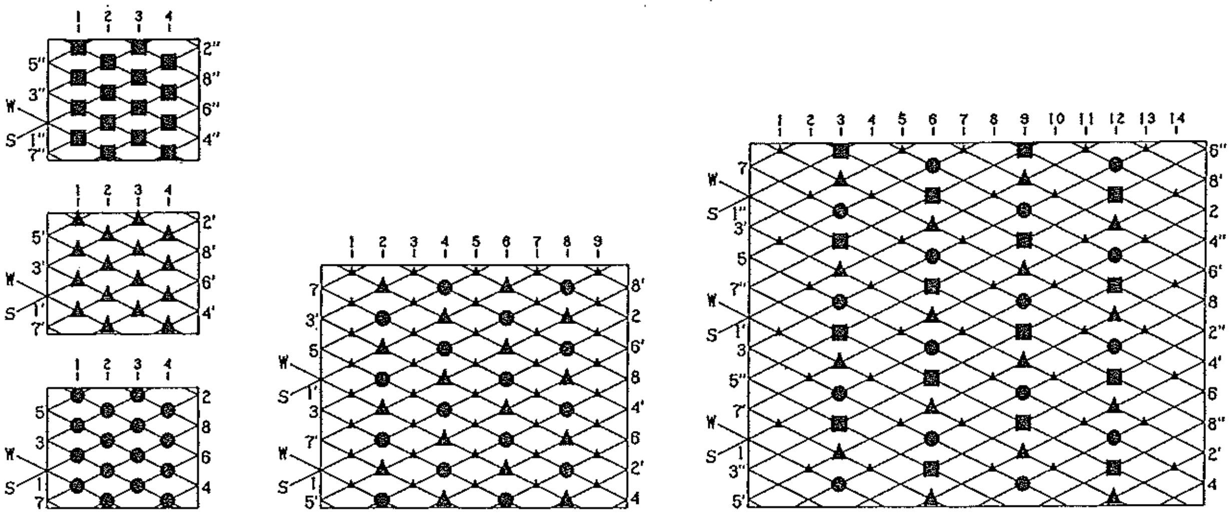

Fig. 660 — The three stages of braiding an interbraided $P/B = 15/12$ Regular Cylindrical Braid.

When a $P/B = 2p/2b = 10/8$ Regular Cylindrical Braid has to be column-coded, we can create $2^5 = 32$ different column-coded Regular Cylindrical Braids by interbraiding two identical $p/b = 5/4$ column-coded Regular Knots if for their column-coding the condition {coding of column x} = {coding of column $(5 - x)$}, where $x = 1, 2,$

does not apply for at least one x-value. If for their column-coding the condition $\{\text{coding of column } x\} = \{\text{coding of column } (5-x)\}$, where $x = 1, 2$, does apply, then $2^2\left(2^2+1\right) = 20$ different column-coded $P/B = 2p/2b$ Regular Cylindrical Braids can be created by interbraiding these two identical column-coded Regular Knots, and $2^{(2+1)} = 8$ of these interbraided $P/B = 2p/2b = 10/8$ Regular Cylindrical Braids have then a balanced column-coding. Note that when the two identical $p/b = 5/4$ column-coded Regular Knots have an over-under coding, the $P/B = 10/8$ interbraided Regular Cylindrical Braids cannot have a balanced column-coding.

From the rightmost diagram in Fig. 660 we see that by interbraiding three Regular Knots, each with the same p/b-values, these Regular knots must have an identical column-coding to enable the interbraided Regular Cylindrical Braid to be column-coded. We furthermore see that by interbraiding the third one of the three Regular Knots, each of the columns $1, 3, 5, 7, 9$ in the central diagram splits into two columns. Hence when the interbraided Regular Cylindrical Braids depicted by the central and rightmost diagrams in Fig. 660 are both to be column-coded, then in the rightmost diagram the columns 1 and 2 must have the same coding, the columns 4 and 5 must have the same coding, the columns 7 and 8 must have the same coding, the columns 10 and 11 must have the same coding, the columns 13 and 14 must have the same coding. Consequently the same relationships with regards column-coding as the ones we formulated earlier for the interbraided $P/B = 2p/2b$ Regular Cylindrical Braids must then also apply to the interbraided $P/B = 3p/3b$ Regular Cylindrical Braids. Thus in this case when the three identical p/b Regular Knots have an over-under coding, a balanced column-coding for the interbraided $P/B = 3p/3b$ Regular Cylindrical Braid can only exist when p is *even*, hence not for $p = 5$. Consequently a balanced column-coding for the interbraided $P/B = 3p/3b$ Regular Cylindrical Braid, when the three identical p/b Regular Knots have an over-under coding with p *odd*, tells us that the interbraided $P/B = 2p/2b$ Regular Cylindrical Braid cannot be column-coded (the columns $\frac{3p-1}{2}$ and $\frac{3p+1}{2}$ in the interbraided $P/B = 3p/3b$ Regular Cylindrical Braid cannot have an identical coding, hence the column p in the interbraided $P/B = 2p/2b$ Regular Cylindrical Braid cannot be column-coded).

Let's have a look at column-coded interbraided $P/B = 3p/3b$ Regular Cylindrical Braids without worrying about the coding arrangements in the interbraided $P/B = 2p/2b$ Regular Cylindrical Braids. We have already seen that in order to obtain a column-coding for a Regular Cylindrical Braid, produced by interbraiding three identical Regular Knots, these Regular Knots must be column-coded. Let each of the three identical column-coded Regular Knots have p-parts and b-bights:

1.) $p = 2n+1$, where $n = 1, 2, 3, \cdots$.

$2^{(4n+2)}$ different column-coded $3p/3b$ Regular Cylindrical Braids can be created by interbraiding these three identical column-coded Regular Knots if for their column-coding the condition $\{\text{coding of column } x\} = \{\text{coding of column } (2n+1-x)\}$, where $x = 1, 2, 3, \cdots, n$, does not apply for at least one x-value. If for their column-coding the condition $\{\text{coding of column } x\} = \{\text{opposite coding of column } (2n+1-x)\}$, where $x = 1, 2, 3, \cdots, n$, applies, then $2^{(2n+1)}$ of these interbraided $P/B = 3p/3b$ Regular Cylindrical Braids have a balanced column-coding.

If for their column-coding the condition $\{\text{coding of column } x\} = \{\text{coding of column } (2n+1-x)\}$, where $x = 1, 2, 3, \cdots, n$, does apply, then $2^{2n}\left(2^{(2n+1)}+1\right)$ different column-coded $3p/3b$ Regular Cylindrical Braids can be created by interbraiding these three identical column-coded Regular Knots, and $2^{(2n+1)}$ of these interbraided $P/B = 3p/3b$ Regular Cylindrical Braids have then a balanced column-coding.

2.) $p = 2n$, where $n = 1, 2, 3, \cdots$.

$2^{(4n)}$ different column-coded $3p/3b$ Regular Cylindrical Braids can be created by interbraiding these three identical column-coded Regular Knots if for their column-coding the condition $\{\text{coding of column } x\} = \{\text{coding of column } (2n - x)\}$, where $x = 1, 2, 3, \cdots, (n-1)$, does not apply for at least one x-value. If for their column-coding the condition $\{\text{coding of column } x\} = \{\text{coding of column } (2n - x)\}$, where $x = 1, 2, 3, \cdots, (n-1)$, does apply, then $2^{(2n-1)}\left(2^{2n} + 1\right)$ different column-coded $3p/3b$ Regular Cylindrical Braids can be created by interbraiding these three identical column-coded Regular Knots, and 2^{2n} of these interbraided $P/B = 3p/3b$ Regular Cylindrical Braids have then a balanced column-coding.

Note that when the three identical p/b column-coded Regular Knots have an over-under coding, a balanced column-coding for the interbraided $P/B = 3p/3b$ Regular Cylindrical Braid can be created for both p is *odd* and p is *even*. For p is *odd* we have the condition $\{\text{coding of column } x\} = \{\text{opposite coding of column } (2n+1-x)\}$, where $x = 1, 2, 3, \cdots, n$, and for p is *even* we have the condition $\{\text{coding of column } x\} = \{\text{coding of column } (2n - x)\}$, where $x = 1, 2, 3, \cdots, (n-1)$.

⋆⋆ *Prove the above relationships for interbraided $P/B = 3p/3b$ column-coded Regular Cylindrical Braids.*

When a $P/B = 3p/3b = 15/12$ Regular Cylindrical Braid has to be column-coded, we can create $2^{10} = 1024$ different ones of such column-coded Regular Cylindrical Braids by interbraiding three identical $p/b = 5/4$ column-coded Regular Knots if for their column-coding the condition $\{\text{coding of column } x\} = \{\text{coding of column } (5-x)\}$, where $x = 1, 2$, does not apply for at least one x-value. If for their column-coding the condition $\{\text{coding of column } x\} = \{\text{opposite coding of column } (2n+1-x)\}$, where $x = 1, 2, 3, \cdots, n$, applies, then $2^{(4+1)} = 32$ of these interbraided $P/B = 3p/3b = 15/12$ Regular Cylindrical Braids have a balanced column-coding.

If for their column-coding the condition $\{\text{coding of column } x\} = \{\text{coding of column } (5 - x)\}$, where $x = 1, 2$, does apply, then $2^4\left(2^5 + 1\right) = 528$ different column-coded $P/B = 3p/3b$ Regular Cylindrical Braids can be created by interbraiding these three identical column-coded Regular Knots, and $2^{(4+1)} = 32$ of these interbraided $P/B = 3p/3b = 15/12$ Regular Cylindrical Braids have then a balanced column-coding.

Note that for three identical $p/b = 5/4$ over-under coded Regular Knots the condition $\{\text{coding of column } x\} = \{\text{coding of column } (2n + 1 - x)\}$, where $x = 1, 2, 3, \cdots, n$, does not apply, but the condition $\{\text{coding of column } x\} = \{\text{opposite coding of column } (2n + 1 - x)\}$, where $x = 1, 2, 3, \cdots, n$, does apply, hence of the 1024 different column-coded $P/B = 3p/3b = 15/12$ Regular Cylindrical Braids 32 have a balanced column-coding. These 32 balanced column-coding forms are depicted in Fig. 661.

Note that the nominal coding-form used in the woven knots at each end of the centrepiece is No. 26 in Fig. 661, and that this coding-form with the coding-form of No. 30 in Fig. 661 are the nearest balanced coding-forms obtainable that superficially somewhat look like a Gaucho-coding. As we shall see shortly, one is just as easy to braid as the other one, however No. 26 resembles in appearance a Gaucho-coding a little closer and in the way the knot has been braided, the glitch created may not be quite as pronounced.

1	/	\	\	\	\	/	\	/	\	/	/	/	/	\
2	\	\	\	\	\	/	\	/	\	/	/	/	/	/
3	/	/	\	\	\	/	\	/	\	/	/	/	\	\
4	\	/	\	\	\	/	\	/	\	/	/	/	\	/
5	/	\	\	/	\	/	\	/	\	/	\	/	/	\
6	\	\	\	/	\	/	\	/	\	/	\	/	/	/
7	/	/	\	/	\	/	\	/	\	/	\	/	\	\
8	\	/	\	/	\	/	\	/	\	/	\	/	\	/
9	/	\	\	\	/	/	\	/	\	\	/	/	/	\
10	\	\	\	\	/	/	\	/	\	\	/	/	/	/
11	/	/	\	\	/	/	\	/	\	\	/	/	\	\
12	\	/	\	\	/	/	\	/	\	\	/	/	\	/
13	/	\	\	/	/	/	\	/	\	\	\	/	/	\
14	\	\	\	/	/	/	\	/	\	\	\	/	/	/
15	/	/	\	/	/	/	\	/	\	\	\	/	\	\
16	\	/	\	/	/	/	\	/	\	\	\	/	\	/
17	/	\	\	\	\	/	/	\	\	/	/	/	/	\
18	\	\	\	\	\	/	/	\	\	/	/	/	/	/
19	/	/	\	\	\	/	/	\	\	/	/	/	\	\
20	\	/	\	\	\	/	/	\	\	/	/	/	\	/
21	/	\	\	/	\	/	/	\	\	/	\	/	/	\
22	\	\	\	/	\	/	/	\	\	/	\	/	/	/
23	/	/	\	/	\	/	/	\	\	/	\	/	\	\
24	\	/	\	/	\	/	/	\	\	/	\	/	\	/
25	/	\	\	\	/	/	/	\	\	\	/	/	/	\
26	\	\	\	\	/	/	/	\	\	\	/	/	/	/
27	/	/	\	\	/	/	/	\	\	\	/	/	\	\
28	\	/	\	\	/	/	/	\	\	\	/	/	\	/
29	/	\	\	/	/	/	/	\	\	\	\	/	/	\
30	\	\	\	/	/	/	/	\	\	\	\	/	/	/
31	/	/	\	/	/	/	/	\	\	\	\	/	\	\
32	\	/	\	/	/	/	/	\	\	\	\	/	\	/

Fig. 661 — The balanced coding-forms.

Fig. 662 shows the relevant details and construction steps of an interbraided Regular Cylindrical Braid with the coding-pattern No. 26 of Fig. 661. Note the consecutive half-cycle braiding algorithms for the consecutive components. Braiding half-cycle n', where $n' = 2', 3', \cdots, 8'$, can be obtained by adding braiding half-cycle n, where $n = 2, 3, \cdots, 8$, to braiding half-cycle $1'$; similarly, braiding half-cycle n'', where $n'' = 2'', 3'', \cdots, 8''$, can be obtained by adding braiding half-cycle n, where $n = 2, 3, \cdots, 8$, to braiding half-cycle $1''$. Observe how braiding half-cycle $1'$ relates to braiding half-cycle 8, and how braiding half-cycle 1″ relates to braiding half-cycle 8′.

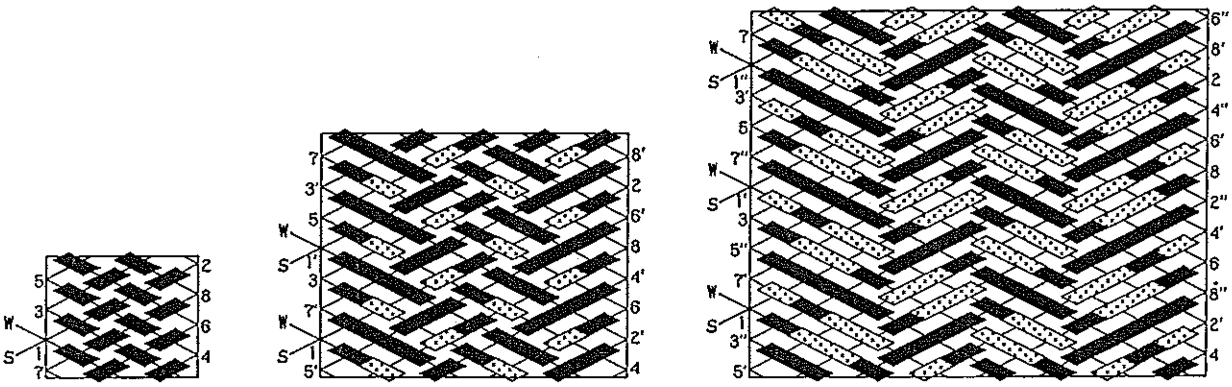

1. : FREE RUN
2. $l=0$: o.
3. $l=0$: o.
4. $l=1$: u-o.
5. $l=1$: u-o.
6. $l=2$: o-u-o.
7. $l=2$: o-u-o.
8. $l=3$: u-o-u-o.

1′. A : u-o-u-2o.
2′. $l=0$, A : u-o-u-3o.
3′. $l=0$, A : u-o-u-3o.
4′. $l=1$, A : u-o-2u-3o.
5′. $l=1$, A : u-o-2u-3o.
6′. $l=2$, A : u-2o-2u-3o.
7′. $l=2$, A : u-2o-2u-3o.
8′. $l=3$, A : 2u-2o-2u-3o.

1″. A,B : 3u-2o-2u-3o.
2″. $l=0$, A,B : 3u-2o-2u-4o.
3″. $l=0$, A,B : 3u-2o-2u-4o.
4″. $l=1$, A,B : 3u-2o-3u-4o.
5″. $l=1$, A,B : 3u-2o-3u-4o.
6″. $l=2$, A,B : 3u-3o-3u-4o.
7″. $l=2$, A,B : 3u-3o-3u-4o.
8″. $l=3$, A,B : 4u-3o-3u-4o.

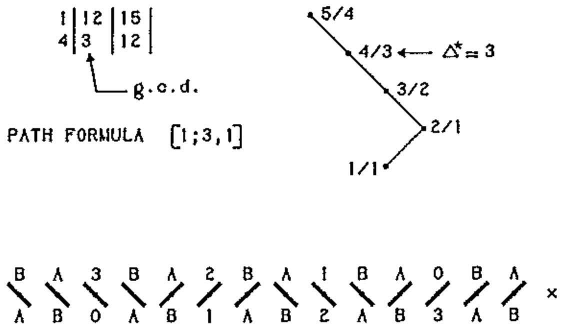

Fig. 662 — The relevant details and construction steps for an interbraided Regular Cylindrical Braid with the coding-pattern No. 26 of Fig. 661.

Fig. 663 shows the relevant details and construction steps of an interbraided Regular Cylindrical Braid with the coding-pattern No. 30 of Fig. 661. Note again the consecutive half-cycle braiding algorithms for the consecutive components. Braiding half-cycle n', where $n' = 2', 3', \cdots, 8'$, can be obtained by adding braiding half-cycle n, where $n = 2, 3, \cdots, 8$, to braiding half-cycle 1′; similarly, braiding half-cycle n'', where $n'' = 2'', 3'', \cdots, 8''$, can be obtained by adding braiding half-cycle n, where $n = 2, 3, \cdots, 8$, to braiding half-cycle 1″. Observe how braiding half-cycle 1′ relates to braiding half-cycle 8, and how braiding half-cycle 1″ relates to braiding half-cycle 8′.

On pg. 832 we showed in Fig. 659 the actual construction of the woven knots, at the ends of the centrepiece four strand Round Braid, which have the nominal coding-pattern No. 26 in Fig. 661. In these woven knots, two components of the final interbraid in Fig. 662 have been combined into one, depicted by the rightmost grid-diagram in Fig. 659. Observe that the construction of this knot is in essence the same as the construction of the knot depicted by the uppermost second grid-diagram from the left in Fig. 456, pg. 547 in *The Braider*, Issue No. 24. Observe that the sequential half-cycle braiding algorithms for the actual woven knots at the ends of the centrepiece (see the leftmost sequential half-cycle braiding algorithms in Fig. 664) are only with the exception of half-cycle 16′ identical to the sequential half-cycle braiding algorithms for the interbraided $P/B = 15/12$ Regular Cylindrical Braid of Fig. 662.

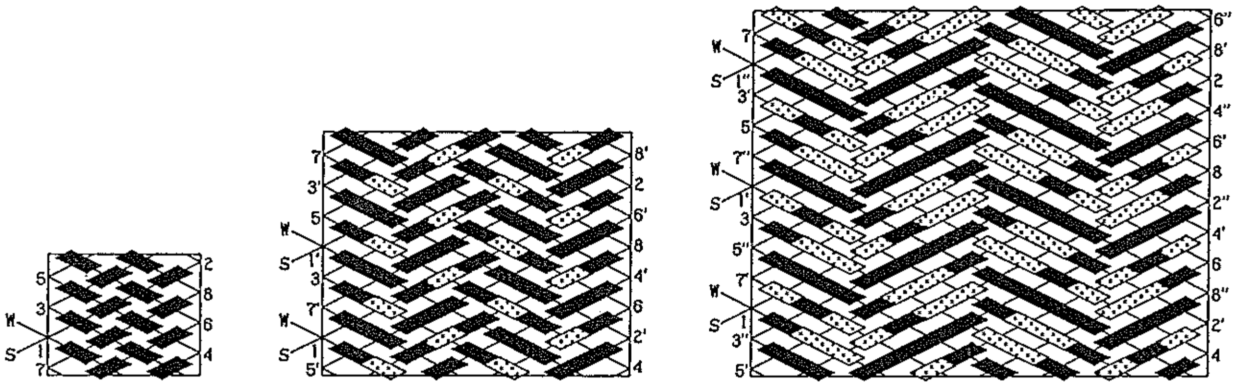

1. : FREE RUN
2. $\ell=0$: o.
3. $\ell=0$: o.
4. $\ell=1$: u-o.
5. $\ell=1$: u-o.
6. $\ell=2$: o-u-o.
7. $\ell=2$: o-u-o.
8. $\ell=3$: u-o-u-o.

1′. A : u-o-2u-o.
2′. $\ell=0$, A : u-o-2u-2o.
3′. $\ell=0$, A : u-o-2u-2o.
4′. $\ell=1$, A : u-o-3u-2o.
5′. $\ell=1$, A : u-o-3u-2o.
6′. $\ell=2$, A : u-2o-3u-2o.
7′. $\ell=2$, A : u-2o-3u-2o.
8′. $\ell=3$, A : 2u-2o-3u-2o.

1″. A, B : 2u-3o-3u-2o.
2″. $\ell=0$, A, B : 2u-3o-3u-3o.
3″. $\ell=0$, A, B : 2u-3o-3u-3o.
4″. $\ell=1$, A, B : 2u-3o-4u-3o.
5″. $\ell=1$, A, B : 2u-3o-4u-3o.
6″. $\ell=2$, A, B : 2u-4o-4u-3o.
7″. $\ell=2$, A, B : 2u-4o-4u-3o.
8″. $\ell=3$, A, B : 3u-4o-4u-3o.

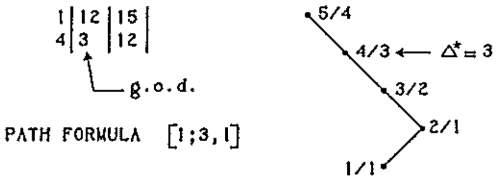

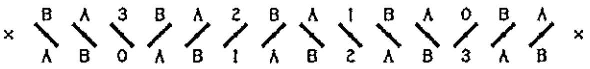

Fig. 663 — The relevant details and construction steps for an interbraided Regular Cylindrical Braid with the coding-pattern No. 30 of Fig. 661.

The glitch in the braid of these actual interwoven knots can readily be avoided by constructing them as depicted by the lowermost left grid-diagram in Fig. 664 with the aid of the associated sequential half-cycle braiding algorithms at the lower right-hand side. This construction method, compared with the construction method actually employed, requires a change in the half-cycle braiding algorithms for half-cycles 8′ and 16′.

The uppermost left grid-diagram in Fig. 665 depicts for the nominal coding-pattern No. 30 in Fig. 661 the construction of the interwoven knots by the same method as used for the actual interwoven knots at the ends of the centrepiece. The lower left-hand associated half-cycle braiding algorithms are, with the exception of only half-cycle 16′, identical to the sequential half-cycle braiding algorithms for the interbraided $P/B = 15/12$ Regular Cylindrical Braid of Fig. 663. The glitch in the braid of such interwoven knots can readily be avoided by constructing them as depicted by the lowermost left grid-diagram in Fig. 665 with the aid of the associated sequential half-cycle braiding algorithms at the lower right-hand side. This construction method, compared with the construction method depicted by the uppermost right-hand grid-diagram requires a change in the half-cycle braiding algorithms for half-cycles 8′ and 16′.

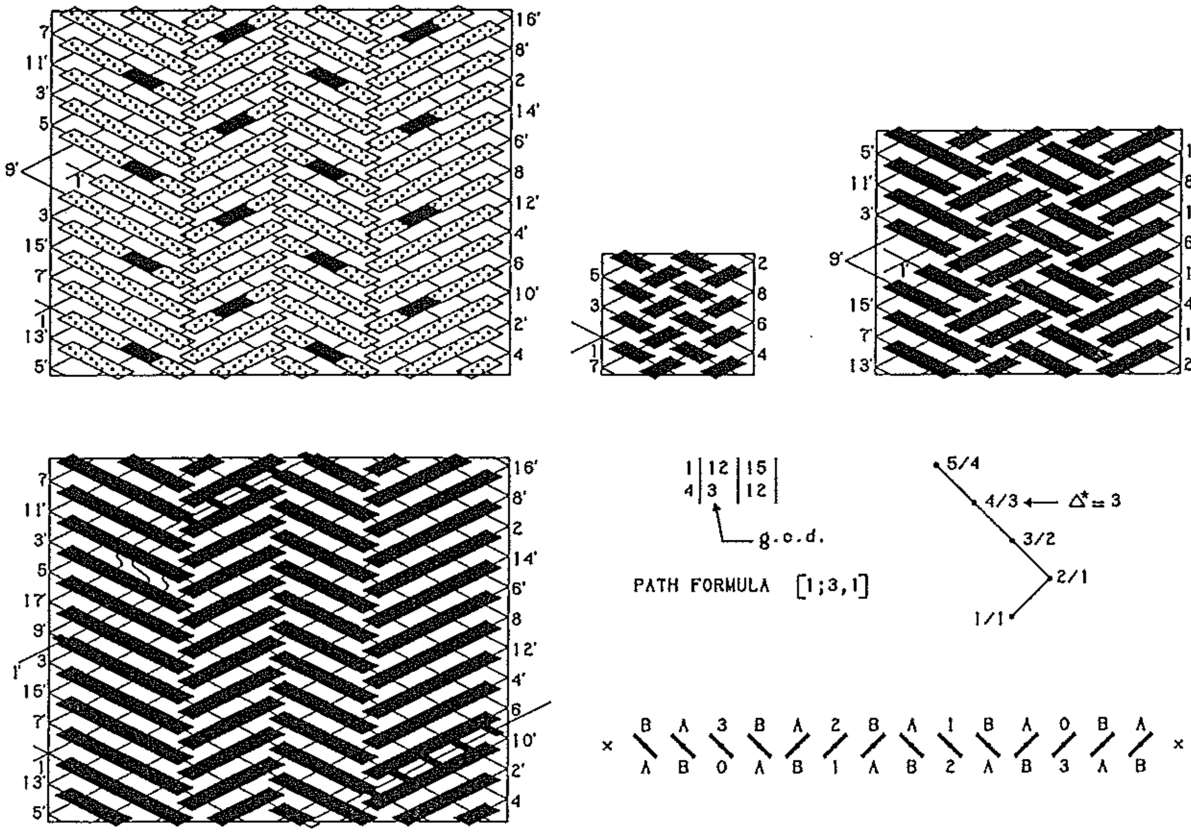

1.	:	FREE RUN
2.	$\ell=0$:	o.
3.	$\ell=0$:	o.
4.	$\ell=1$:	u-o.
5.	$\ell=1$:	u-o.
6.	$\ell=2$:	o-u-o.
7.	$\ell=2$:	o-u-o.
8.	$\ell=3$:	u-o-u-o.
1'.	A :	u-o-u-2o.
2'.	$\ell=0$,A :	u-o-u-3o.
3'.	$\ell=0$,A :	u-o-u-3o.
4'.	$\ell=1$,A :	u-o-2u-3o.
5'.	$\ell=1$,A :	u-o-2u-3o.
6'.	$\ell=2$,A :	u-2o-2u-3o.
7'.	$\ell=2$,A :	u-2o-2u-3o.
8'.	$\ell=3$,A :	2u-2o-2u-3o.
9'.	A,B :	3u-2o-2u-3o.
10'.	$\ell=0$,A,B :	3u-2o-2u-4o.
11'.	$\ell=0$,A,B :	3u-2o-2u-4o.
12'.	$\ell=1$,A,B :	3u-2o-3u-4o.
13'.	$\ell=1$,A,B :	3u-2o-3u-4o.
14'.	$\ell=2$,A,B :	3u-3o-3u-4o.
15'.	$\ell=2$,A,B :	3u-3o-3u-4o.
16'.	$\ell=3$,A,B :	4u-3o-3u-3o. (NEGLECT LAST A POSITION)

1.	:	FREE RUN
2.	$\ell=0$:	o.
3.	$\ell=0$:	o.
4.	$\ell=1$:	u-o.
5.	$\ell=1$:	u-o.
6.	$\ell=2$:	o-u-o.
7.	$\ell=2$:	o-u-o.
8.	$\ell=3$:	u-o-u-o.
1'.	A :	u-o-u-2o.
2'.	$\ell=0$,A :	u-o-u-3o.
3'.	$\ell=0$,A :	u-o-u-3o.
4'.	$\ell=1$,A :	u-o-2u-3o.
5'.	$\ell=1$,A :	u-o-2u-3o.
6'.	$\ell=2$,A :	u-2o-2u-3o.
7'.	$\ell=2$,A :	u-2o-2u-3o.
8'.	$\ell=3$,A :	2u-2o-2u-4o.
9'.	A,B :	3u-2o-2u-3o.
10'.	$\ell=0$,A,B :	3u-2o-2u-4o.
11'.	$\ell=0$,A,B :	3u-2o-2u-4o.
12'.	$\ell=1$,A,B :	3u-2o-3u-4o.
13'.	$\ell=1$,A,B :	3u-2o-3u-4o.
14'.	$\ell=2$,A,B :	3u-3o-3u-4o.
15'.	$\ell=2$,A,B :	3u-3o-3u-4o.
16'.	$\ell=3$,A,B :	4u-3o-3u-5o.
17'.	:	15u.

Fig. 664 — The relevant details and construction steps for an interbraided Regular Cylindrical Braid with the nominal coding-pattern No. 26 of Fig. 661.

We see here once again the importance of using grid-diagrams. They readily enable us to modify construction methods which may have been found by experimental ways, but contain irregularities. Sometimes an experimentally found construction method may be correct, but not be the simplest or most preferable method when it has superfluous braiding movements which are not obviously visible. We will meet a typical example of this with the terminal knots which are intended to serve as the closure knots of the cuffs.

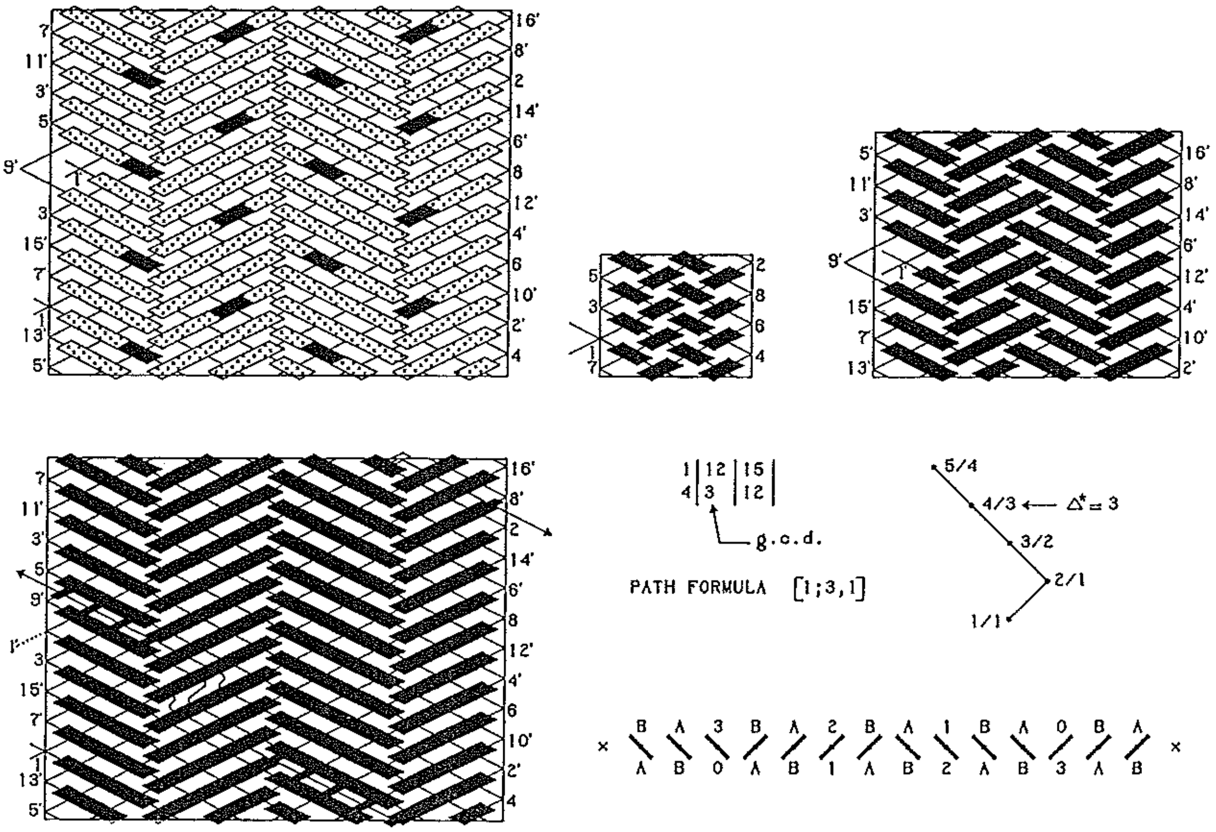

1. : FREE RUN
2. ℓ=0 : o.
3. ℓ=0 : o.
4. ℓ=1 : u-o.
5. ℓ=1 : u-o.
6. ℓ=2 : o-u-o.
7. ℓ=2 : o-u-o.
8. ℓ=3 : u-o-u-o.

1'. A : u-o-2u-o.
2'. ℓ=0,A : u-o-2u-3o.
3'. ℓ=0,A : u-o-2u-3o.
4'. ℓ=1,A : u-o-3u-2o.
5'. ℓ=1,A : u-o-3u-2o.
6'. ℓ=2,A : u-2o-3u-2o.
7'. ℓ=2,A : u-2o-3u-2o.
8'. ℓ=3,A : 2u-2o-3u-2o.

9'. A,B : 2u-3o-3u-2o.
10'. ℓ=0,A,B : 2u-3o-3u-3o.
11'. ℓ=0,A,B : 2u-3o-3u-3o.
12'. ℓ=1,A,B : 2u-3o-4u-3o.
13'. ℓ=1,A,B : 2u-3o-4u-3o.
14'. ℓ=2,A,B : 2u-4o-4u-3o.
15'. ℓ=2,A,B : 2u-4o-4u-3o.
16'. ℓ=3,A,B : 3u-4o-4u-2o. (NEGLECT LAST A POSITION)

1. : FREE RUN
2. ℓ=0 : o.
3. ℓ=0 : o.
4. ℓ=1 : u-o.
5. ℓ=1 : u-o.
6. ℓ=2 : o-u-o.
7. ℓ=2 : o-u-o.
8. ℓ=3 : u-o-u-o.

1'. A : u-o-2u-o.
2'. ℓ=0,A : u-o-2u-2o.
3'. ℓ=0,A : u-o-2u-2o.
4'. ℓ=1,A : u-o-3u-2o.
5'. ℓ=1,A : u-o-3u-2o.
6'. ℓ=2,A : u-2o-3u-2o.
7'. ℓ=2,A : u-2o-3u-2o.
8'. ℓ=3,A : 2u-2o-4u-2o.

9'. A,B : 2u-3o-3u-2o.
10'. ℓ=0,A,B : 2u-3o-3u-3o.
11'. ℓ=0,A,B : 2u-3o-3u-3o.
12'. ℓ=1,A,B : 2u-3o-4u-3o.
13'. ℓ=1,A,B : 2u-3o-4u-3o.
14'. ℓ=2,A,B : 2u-4o-4u-3o.
15'. ℓ=2,A,B : 2u-4o-4u-3o.
16'. ℓ=3,A,B : 3u-4o-8u.
17'/1'. : 3o-12u.

Fig. 665 — The relevant details and construction steps for an interbraided Regular Cylindrical Braid with the nominal coding-pattern No. 30 of Fig. 661.

The grid-diagram, and hence the construction method, of the terminal knots for closing the cuffs can be presented as depicted by the uppermost left-hand diagram in Fig. 666. This diagram, however, is equivalent to the uppermost right-hand diagram in Fig. 666, but instead of using this simplified uppermost right-hand grid-diagram, it is much more convenient to use the lowermost diagram in Fig. 666. The convenience of using this lowermost diagram in Fig. 666 is that after the initial crowning and walling operation, the actual braiding sequence is "*o*–*u*" for each half-cycle in a set of identical half-cycles, except for the last set of identical half-cycles for which the actual sequence is all *unders* (see the solid black codings in diagrams 3, 4, 5 of Fig. 667, hence the codings as depicted under "A" below (codings actually laid down during previous half-cycles are indicated as under "B" below, and codings as indicated under "C" below are not actually laid down during these half-cycles)).

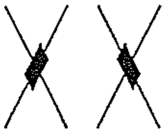
A

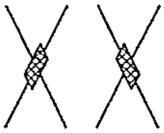
B

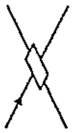
C

Fig. 667 depicts the construction of the lowermost knot in Fig. 666, which is the uppermost right-hand knot in Fig. 667.

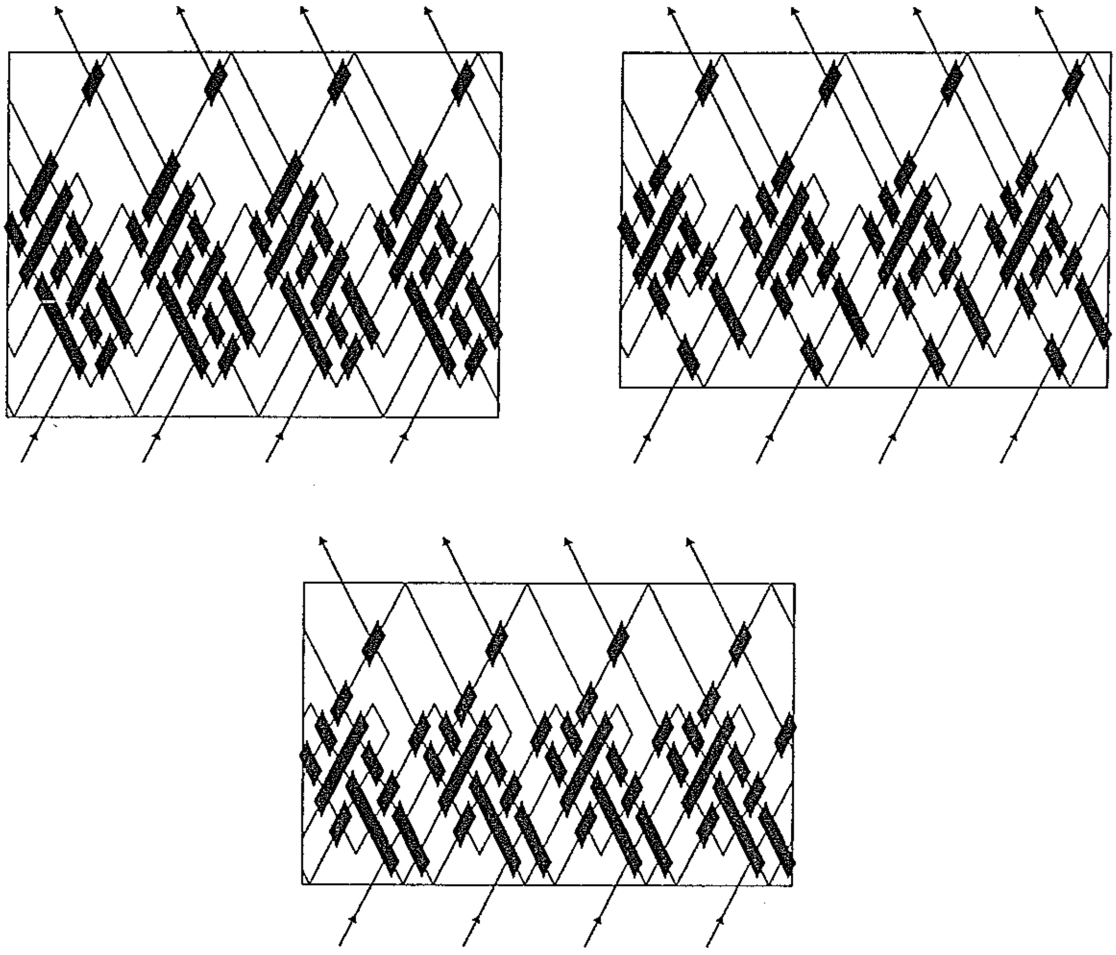

Fig. 666 — Three equivalent grid-diagrams depicting the terminal knots which are used for closing the cuffs.

It should be noted that for good braidwork the terminal knots used for closing the cuffs should be complementary. The grid-diagrams and construction steps for the complementary terminal knot are shown in Fig. 668.

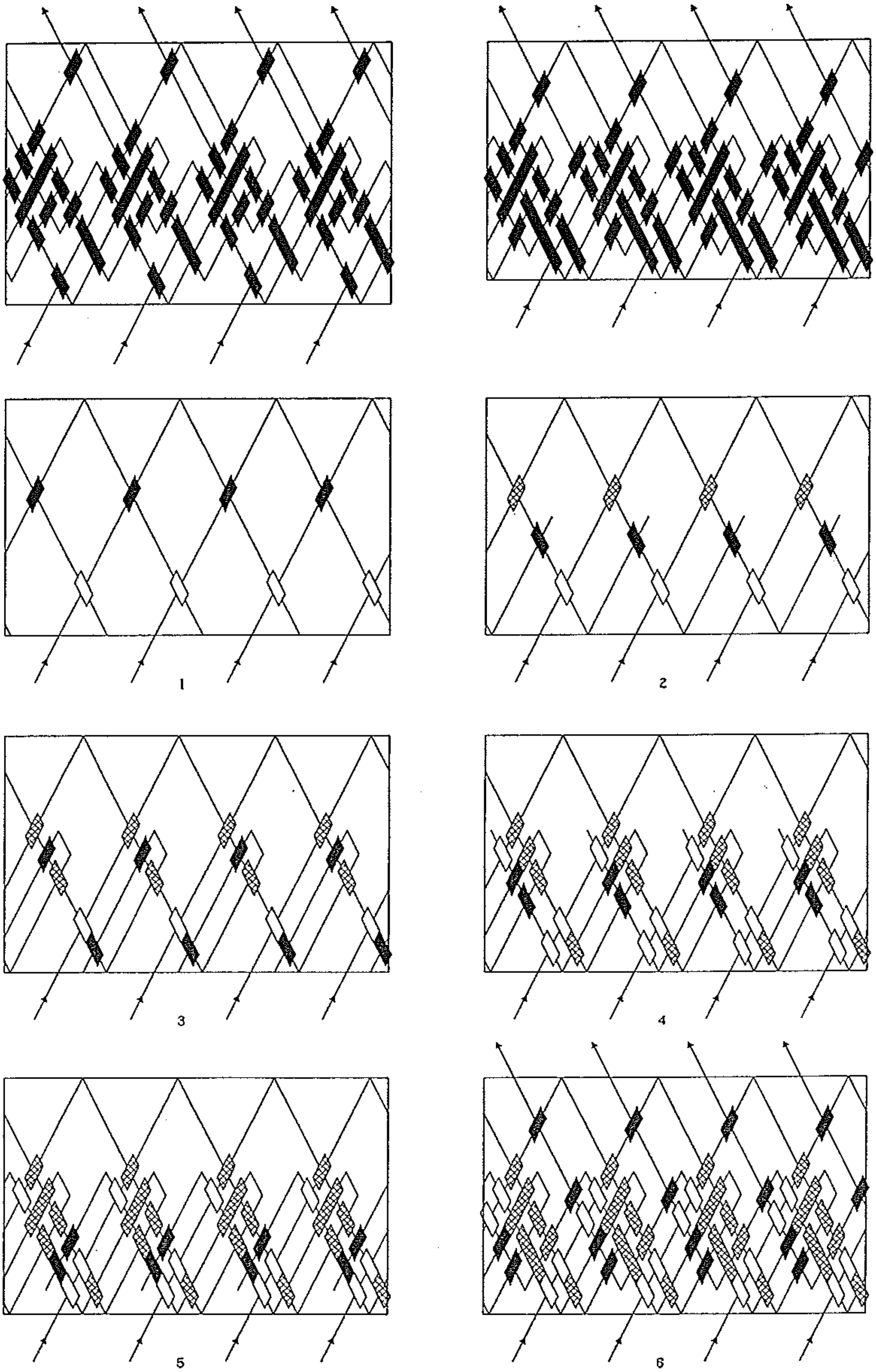

Fig. 667 — The terminal knot in Fig. 666 and its construction steps.

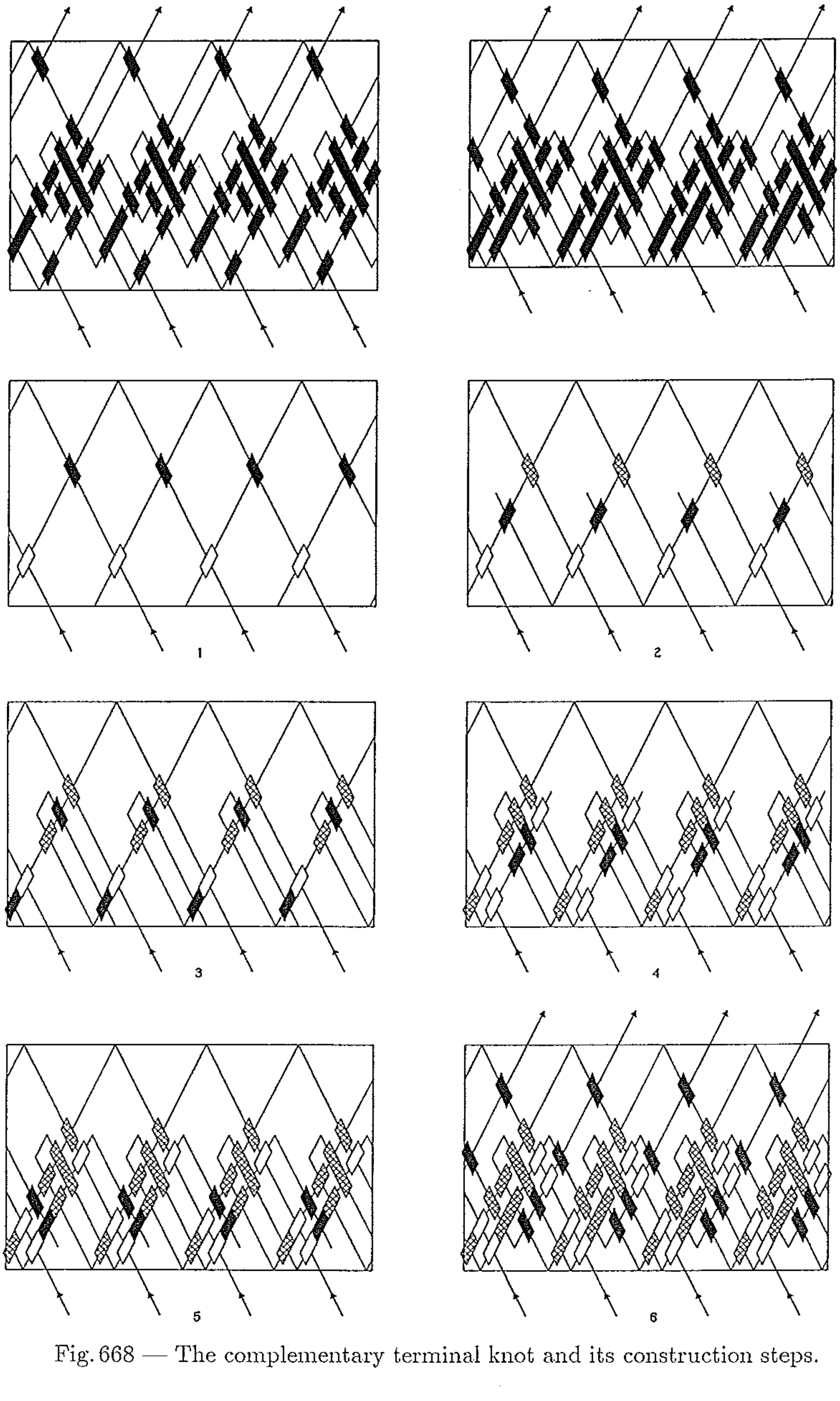

Fig. 668 — The complementary terminal knot and its construction steps.

The construction of the terminal knot in Fig. 668 is, apart from the crowning operation, the same as the construction of the "Boton de ocho tientos (redondo)" in the book *Trenzas Gauchas*, pp. 152 - 155 by Mario A. Lopez Osornio[†].

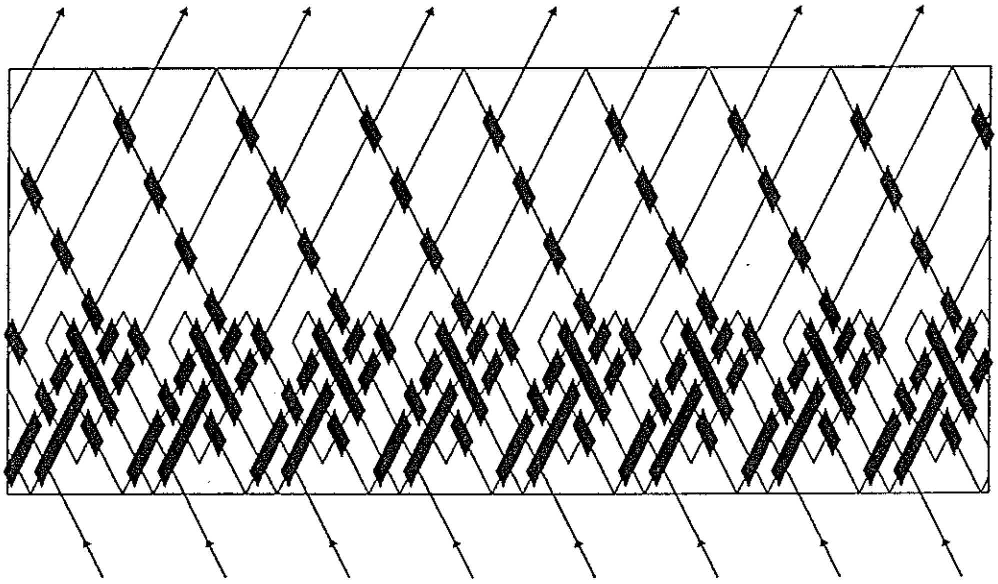

BOTON DE OCHO TIENTOS (REDONDO)
IN TRENZAS GAUCHAS BY MARIO A. LOPEZ OSORNIO ; PP. 152-155

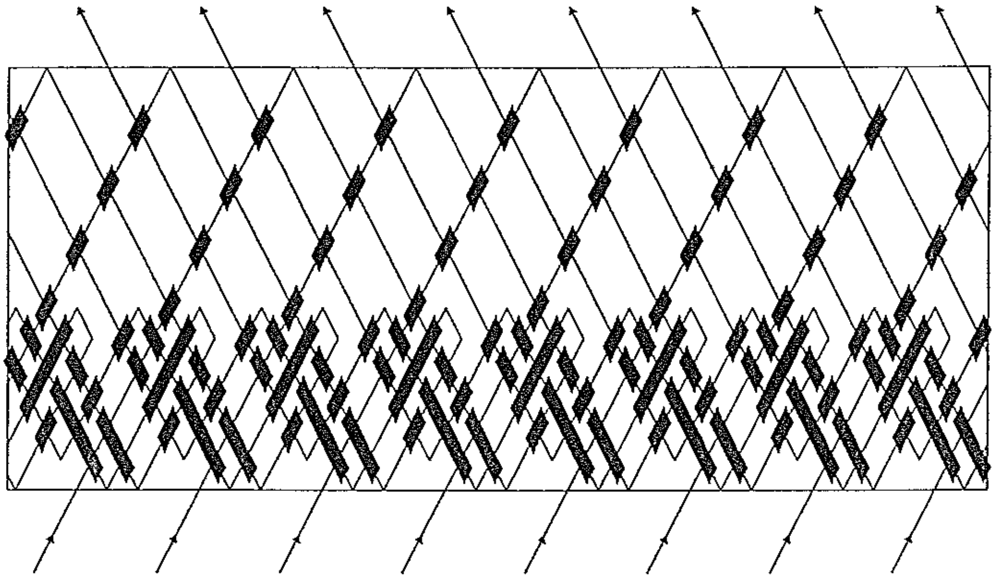

Fig. 669 — Boton de ocho tientos (redondo).

[†] The book *Trenzas Gauchas* by Mario A. Lopez Osornio was published in 1934 and has had very many reprints (17 up to and including 1995). It is interesting to observe that much in Bruce Grant's *Encyclopedia of Rawhide and Leather Braiding* seems to come from the book *Trenzas Gauchas*, sometimes, but not always, with the identical mistakes. Since the first edition of Grant's *Encyclopedia of Rawhide and Leather Braiding* was published in 1972, one wonders why he left some of the knots in *Trenzas Gauchas* out. The reason could have been that the errors in the drawings by Mario A. Lopez Osornio fooled him in braiding those knots.

The drawings in the book *Trenzas Gauchas* are very poor and it should be noted that he made two mistakes in the case of the "Boton de ocho tientos (redondo)": one in Fig. N° 203 and one in Fig. N° 204. These mistakes are readily picked up by drawing the grid-diagrams. The two complementary grid-diagrams of these knots (but without the mistakes) are depicted in Fig. 669.

Nested Cylindrical Braids

In *The Braider*, Issue No. 35, we met on pg. 820 the formula $r_i = \left|A_l + \frac{x-y_i-2l_i}{2}\right|_{A_r}$. For a specified x-value and $|y_n|_{2d}$-set of distinct y_m-values, this formula enables us to calculate the set of $\frac{A_r}{d}$ r_i-values associated with an l_i-value. Since we are dealing here with the Asymmetric Regular Nested Cylindrical Braids, the set of r_i-values associated with an l_i-value other than 1 follows directly from the set of r_i-values associated with $l_i = 1$.[†] It therefore suffices to know for the various $(|y_n|_{2d}, x)$-values the r_i-set associated with $l_i = 1$. The general module of these r_i-sets associated with $(|y_n|_{2d}, x)$-values, which readily can be derived from the formula $r_i = \left|A_l + \frac{x-y_i-2l_i}{2}\right|_{A_r}$, is displayed in Fig. 671. A short initial section of the y_m - x table for $A_l = 10$ and $A_r = 6$ with the r_i-sets for $l_i = 1$ is shown in Fig. 670.

$\rightarrow x$ $\lvert y_n\rvert_{2d}\downarrow$	0	1	2	3	4	5	6	7	8
0			$1 \longrightarrow 2$ $1 \longrightarrow 4$ $1 \longrightarrow 6$		$1 \longrightarrow 1$ $1 \longrightarrow 3$ $1 \longrightarrow 5$		$1 \longrightarrow 2$ $1 \longrightarrow 4$ $1 \longrightarrow 6$		$1 \longrightarrow 1$ $1 \longrightarrow 3$ $1 \longrightarrow 5$
1		$1 \longrightarrow 1$ $1 \longrightarrow 3$ $1 \longrightarrow 5$		$1 \longrightarrow 2$ $1 \longrightarrow 4$ $1 \longrightarrow 6$		$1 \longrightarrow 1$ $1 \longrightarrow 3$ $1 \longrightarrow 5$		$1 \longrightarrow 2$ $1 \longrightarrow 4$ $1 \longrightarrow 6$	
2	$1 \longrightarrow 2$ $1 \longrightarrow 4$ $1 \longrightarrow 6$		$1 \longrightarrow 1$ $1 \longrightarrow 3$ $1 \longrightarrow 5$		$1 \longrightarrow 2$ $1 \longrightarrow 4$ $1 \longrightarrow 6$		$1 \longrightarrow 1$ $1 \longrightarrow 3$ $1 \longrightarrow 5$		$1 \longrightarrow 2$ $1 \longrightarrow 4$ $1 \longrightarrow 6$
3		$1 \longrightarrow 2$ $1 \longrightarrow 4$ $1 \longrightarrow 6$		$1 \longrightarrow 1$ $1 \longrightarrow 3$ $1 \longrightarrow 5$		$1 \longrightarrow 2$ $1 \longrightarrow 4$ $1 \longrightarrow 6$		$1 \longrightarrow 1$ $1 \longrightarrow 3$ $1 \longrightarrow 5$	
4			$1 \longrightarrow 2$ $1 \longrightarrow 4$ $1 \longrightarrow 6$		$1 \longrightarrow 1$ $1 \longrightarrow 3$ $1 \longrightarrow 5$		$1 \longrightarrow 2$ $1 \longrightarrow 4$ $1 \longrightarrow 6$		$1 \longrightarrow 1$ $1 \longrightarrow 3$ $1 \longrightarrow 5$

Fig. 670 — The $1 \longrightarrow r_i$ sets; $A_l = 10$, $A_r = 6$.

In order to make a y_m - x table useful for practical purposes, we must in each applicable $(|y_n|_{2d}, x)$ cell enter the relevant details of its component(s) (first-return string-run(s)).

Example 1. For $A_l = 10$ and $A_r = 6$ the first-return string-run details for x-values from 0 to 16 with $|y_n|_{2d}$-values from 0 to d are presented on pp. 847 - 851. In the y_m - x table on pp. 852 - 853, 'sbb' stands for: sum of bight-boundary numbers; and 4 × 3, for example, stands for: 4 components, each with 3 parts.

[†] $r_i' = |r_i - \Delta l_i|_{A_r}$. For example, if for $A_r = 15$ and $d = 5$ we have for $l_i = 1$ the associated r_i-set 3, 8, 13, then we have for $l_i = 4$ the associated r_i-set 5, 10, 15.

$\lvert y_n\rvert_{2d}\downarrow$ \ $x\rightarrow$	$2n\Lambda_r+4-2\Lambda_l+2md$	$2n\Lambda_r+5-2\Lambda_l+2md$	$2n\Lambda_r+6-2\Lambda_l+2md$	$2n\Lambda_r+7-2\Lambda_l+2md$	$2n\Lambda_r+8-2\Lambda_l+2md$		$2n\Lambda_r+2-2\Lambda_l+(2m+2)d$	$2n\Lambda_r+3-2\Lambda_l+(2m+2)d$
0	$1\longrightarrow 1$ $1\longrightarrow 1+d$ $1\longrightarrow 1+2d$ $\vdots$ $1\longrightarrow 1+\Lambda_r-d$		$1\longrightarrow 2$ $1\longrightarrow 2+d$ $1\longrightarrow 2+2d$ $\vdots$ $1\longrightarrow 2+\Lambda_r-d$		$1\longrightarrow 3$ $1\longrightarrow 3+d$ $1\longrightarrow 3+2d$ $\vdots$ $1\longrightarrow 3+\Lambda_r-d$		$1\longrightarrow d$ $1\longrightarrow 2d$ $1\longrightarrow 3d$ $\vdots$ $1\longrightarrow \Lambda_r$	
1		$1\longrightarrow 1$ $1\longrightarrow 1+d$ $1\longrightarrow 1+2d$ $\vdots$ $1\longrightarrow 1+\Lambda_r-d$		$1\longrightarrow 2$ $1\longrightarrow 2+d$ $1\longrightarrow 2+2d$ $\vdots$ $1\longrightarrow 2+\Lambda_r-d$				$1\longrightarrow d$ $1\longrightarrow 2d$ $1\longrightarrow 3d$ $\vdots$ $1\longrightarrow \Lambda_r$
2	$1\longrightarrow d$ $1\longrightarrow 2d$ $1\longrightarrow 3d$ $\vdots$ $1\longrightarrow \Lambda_r$		$1\longrightarrow 1$ $1\longrightarrow 1+d$ $1\longrightarrow 1+2d$ $\vdots$ $1\longrightarrow 1+\Lambda_r-d$		$1\longrightarrow 2$ $1\longrightarrow 2+d$ $1\longrightarrow 2+2d$ $\vdots$ $1\longrightarrow 2+\Lambda_r-d$		$1\longrightarrow d-1$ $1\longrightarrow 2d-1$ $1\longrightarrow 3d-1$ $\vdots$ $1\longrightarrow \Lambda_r-1$	
3		$1\longrightarrow d$ $1\longrightarrow 2d$ $1\longrightarrow 3d$ $\vdots$ $1\longrightarrow \Lambda_r$		$1\longrightarrow 1$ $1\longrightarrow 1+d$ $1\longrightarrow 1+2d$ $\vdots$ $1\longrightarrow 1+\Lambda_r-d$				$1\longrightarrow d-1$ $1\longrightarrow 2d-1$ $1\longrightarrow 3d-1$ $\vdots$ $1\longrightarrow \Lambda_r-1$
4	$1\longrightarrow d-1$ $1\longrightarrow 2d-1$ $1\longrightarrow 3d-1$ $\vdots$ $1\longrightarrow \Lambda_r-1$		$1\longrightarrow d$ $1\longrightarrow 2d$ $1\longrightarrow 3d$ $\vdots$ $1\longrightarrow \Lambda_r$		$1\longrightarrow 1$ $1\longrightarrow 1+d$ $1\longrightarrow 1+2d$ $\vdots$ $1\longrightarrow 1+\Lambda_r-d$		$1\longrightarrow d-2$ $1\longrightarrow 2d-2$ $1\longrightarrow 3d-2$ $\vdots$ $1\longrightarrow \Lambda_r-2$	
2d-2	$1\longrightarrow 2$ $1\longrightarrow 2+d$ $1\longrightarrow 2+2d$ $\vdots$ $1\longrightarrow 2+\Lambda_r-d$		$1\longrightarrow 3$ $1\longrightarrow 3+d$ $1\longrightarrow 3+2d$ $\vdots$ $1\longrightarrow 3+\Lambda_r-d$		$1\longrightarrow 4$ $1\longrightarrow 4+d$ $1\longrightarrow 4+2d$ $\vdots$ $1\longrightarrow 4+\Lambda_r-d$		$1\longrightarrow 1$ $1\longrightarrow 1+d$ $1\longrightarrow 1+2d$ $\vdots$ $1\longrightarrow 1+\Lambda_r-d$	
2d-1		$1\longrightarrow 2$ $1\longrightarrow 2+d$ $1\longrightarrow 2+2d$ $\vdots$ $1\longrightarrow 2+\Lambda_r-d$		$1\longrightarrow 3$ $1\longrightarrow 3+d$ $1\longrightarrow 3+2d$ $\vdots$ $1\longrightarrow 3+\Lambda_r-d$				$1\longrightarrow 1$ $1\longrightarrow 1+d$ $1\longrightarrow 1+2d$ $\vdots$ $1\longrightarrow 1+\Lambda_r-d$
2d	$1\longrightarrow 1$ $1\longrightarrow 1+d$ $1\longrightarrow 1+2d$ $\vdots$ $1\longrightarrow 1+\Lambda_r-d$		$1\longrightarrow 2$ $1\longrightarrow 2+d$ $1\longrightarrow 2+2d$ $\vdots$ $1\longrightarrow 2+\Lambda_r-d$		$1\longrightarrow 3$ $1\longrightarrow 3+d$ $1\longrightarrow 3+2d$ $\vdots$ $1\longrightarrow 3+\Lambda_r-d$		$1\longrightarrow d$ $1\longrightarrow 2d$ $1\longrightarrow 3d$ $\vdots$ $1\longrightarrow \Lambda_r$	

Fig. 671 — The general $(\lvert y_n\rvert_{2d}, x)$ module of r_i-sets.

$\Lambda_l=10;\ \Lambda_r=6;\ d=2;\ x=0;\ \frac{\Lambda_l\Lambda_r}{d}=30;\ 2(\Lambda_l+\Lambda_r)+x=32;\ |y_x|_{2d}=d=2;\ y=2,6,10;\ l_{i+1}=|12-(l_i+2r_i)|_{10};\ r_{j+1}=|20-(r_j+2l_j)|_6.$

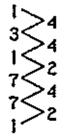

$2\sum(l_i+r_i)=70$

$\alpha=5$

$P_o=\frac{5\times32-70}{30}=3$

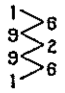

$2\sum(l_i+r_i)=66$

$\alpha=3$

$P_o=\frac{3\times32-66}{30}=1$

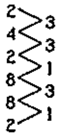

$2\sum(l_i+r_i)=70$

$\alpha=5$

$P_o=\frac{5\times32-70}{30}=3$

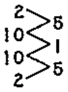

$2\sum(l_i+r_i)=66$

$\alpha=3$

$P_o=\frac{3\times32-66}{30}=1$

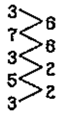

$2\sum(l_i+r_i)=68$

$\alpha=4$

$P_o=\frac{4\times32-68}{30}=2$

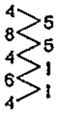

$2\sum(l_i+r_i)=68$

$\alpha=4$

$P_o=\frac{4\times32-68}{30}=2$

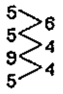

$2\sum(l_i+r_i)=66$

$\alpha=3$

$P_o=\frac{3\times32-66}{30}=1$

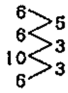

$2\sum(l_i+r_i)=66$

$\alpha=3$

$P_o=\frac{3\times32-66}{30}=1$

$\Lambda_l=10;\ \Lambda_r=6;\ d=2;\ x=1;\ \frac{\Lambda_l\Lambda_r}{d}=30;\ 2(\Lambda_l+\Lambda_r)+x=33;\ |y_x|_{2d}=1;\ y=1,3,5;\ l_{i+1}=|13-(l_i+2r_i)|_{10};\ r_{j+1}=|21-(r_j+2l_j)|_6.$

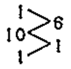

$2\sum(l_i+r_i)=36$

$\alpha=2$

$P_o=\frac{2\times33-36}{30}=1$

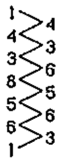

$2\sum(l_i+r_i)=108$

$\alpha=6$

$P_o=\frac{6\times33-108}{30}=3$

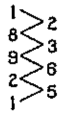

$2\sum(l_i+r_i)=72$

$\alpha=4$

$P_o=\frac{4\times33-72}{30}=2$

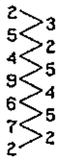

$2\sum(l_i+r_i)=108$

$\alpha=6$

$P_o=\frac{6\times33-108}{30}=3$

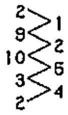

$2\sum(l_i+r_i)=72$

$\alpha=4$

$P_o=\frac{4\times33-72}{30}=2$

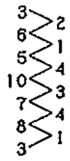

$2\sum(l_i+r_i)=108$

$\alpha=6$

$P_o=\frac{6\times33-108}{30}=3$

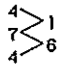

$2\sum(l_i+r_i)=36$

$\alpha=2$

$P_o=\frac{2\times33-36}{30}=1$

$\Lambda_l=10;\ \Lambda_r=6;\ d=2;\ x=2;\ \frac{\Lambda_l\Lambda_r}{d}=30;\ 2(\Lambda_l+\Lambda_r)+x=34;\ |y_x|_{2d}=0;\ y=0,4,8,12=0;\ l_{i+1}=|14-(l_i+2r_i)|_{10};\ r_{j+1}=|22-(r_j+2l_j)|_6.$

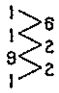

$2\sum(l_i+r_i)=42$

$\alpha=3$

$P_o=\frac{3\times34-42}{30}=2$

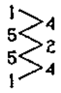

$2\sum(l_i+r_i)=42$

$\alpha=3$

$P_o=\frac{3\times34-42}{30}=2$

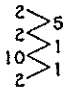

$2\sum(l_i+r_i)=42$

$\alpha=3$

$P_o=\frac{3\times34-42}{30}=2$

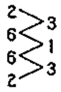

$2\sum(l_i+r_i)=42$

$\alpha=3$

$P_o=\frac{3\times34-42}{30}=2$

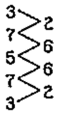

$2\sum(l_i+r_i)=76$

$\alpha=4$

$P_o=\frac{4\times34-76}{30}=2$

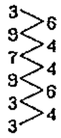

$2\sum(l_i+r_i)=110$

$\alpha=5$

$P_o=\frac{5\times34-110}{30}=2$

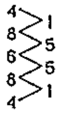

$2\sum(l_i+r_i)=76$

$\alpha=4$

$P_o=\frac{4\times34-76}{30}=2$

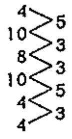

$2\sum(l_i+r_i)=110$

$\alpha=5$

$P_o=\frac{5\times34-110}{30}=2$

$\Lambda_l=10;\ \Lambda_r=6;\ d=2;\ x=2;\ \frac{\Lambda_l\Lambda_r}{d}=30;\ 2(\Lambda_l+\Lambda_r)+x=34;\ |y_x|_{2d}=2;\ y=2,6,10;\ l_{i+1}=|14-(l_i+2r_i)|_{10};\ r_{j+1}=|22-(r_j+2l_j)|_6.$

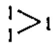

$2\sum(l_i+r_i)=4$

$\alpha=1$

$P_o=\frac{1\times34-4}{30}=1$

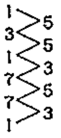

$2\sum(l_i+r_i)=80$

$\alpha=5$

$P_o=\frac{5\times34-80}{30}=3$

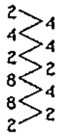

$2\sum(l_i+r_i)=80$

$\alpha=5$

$P_o=\frac{5\times34-80}{30}=3$

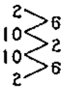

$2\sum(l_i+r_i)=72$

$\alpha=3$

$P_o=\frac{3\times34-72}{30}=1$

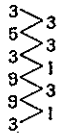

$2\sum(l_i+r_i)=80$

$\alpha=5$

$P_o=\frac{5\times34-80}{30}=3$

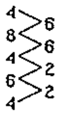

$2\sum(l_i+r_i)=76$

$\alpha=4$

$P_o=\frac{4\times34-76}{30}=2$

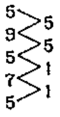

$2\sum(l_i+r_i)=76$

$\alpha=4$

$P_o=\frac{4\times34-76}{30}=2$

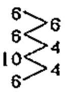

$2\sum(l_i+r_i)=72$

$\alpha=3$

$P_o=\frac{3\times34-72}{30}=1$

$\Lambda_l=10;\ \Lambda_r=6;\ d=2;\ x=3;\ \frac{\Lambda_l\Lambda_r}{d}=30;\ 2(\Lambda_l+\Lambda_r)+x=35;\ |y_x|_{2d}=1;\ y=1,5,9;\ l_{i+1}=|15-(l_i+2r_i)|_{10};\ r_{j+1}=|23-(r_j+2l_j)|_6.$

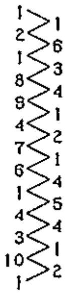

$2\sum(l_i+r_i)=180$

$\alpha=12$

$P_o=\frac{12\times35-180}{30}=8$

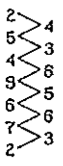

$2\sum(l_i+r_i)=120$

$\alpha=6$

$P_o=\frac{6\times35-120}{30}=3$

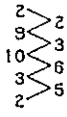

$2\sum(l_i+r_i)=80$

$\alpha=4$

$P_o=\frac{4\times35-80}{30}=2$

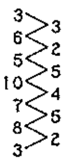

$2\sum(l_i+r_i)=120$

$\alpha=6$

$P_o=\frac{6\times35-120}{30}=3$

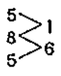

$2\sum(l_i+r_i)=40$

$\alpha=2$

$P_o=\frac{2\times35-40}{30}=1$

$\Lambda_l=10;\ \Lambda_r=6;\ d=2;\ x=4;\ \frac{\Lambda_l\Lambda_r}{d}=30;\ 2(\Lambda_l+\Lambda_r)+x=36;\ |y_s|_{2d}=0;\ y=0,4,8,12=0;\ l_{i+1}=|16-(l_i+2r_i)|_{10};\ r_{j+1}=|24-(r_j+2l_j)|_6.$

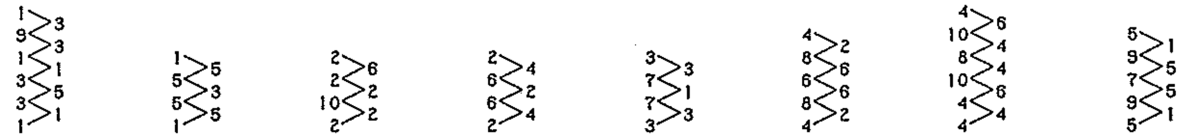

$2\sum(l_i+r_i)=60$	$2\sum(l_i+r_i)=48$	$2\sum(l_i+r_i)=48$	$2\sum(l_i+r_i)=48$	$2\sum(l_i+r_i)=48$	$2\sum(l_i+r_i)=84$	$2\sum(l_i+r_i)=120$	$2\sum(l_i+r_i)=84$
$\alpha=5$	$\alpha=3$	$\alpha=3$	$\alpha=3$	$\alpha=3$	$\alpha=4$	$\alpha=5$	$\alpha=4$
$P_0=\frac{5\times36-60}{30}=4$	$P_0=\frac{3\times36-48}{30}=2$	$P_0=\frac{3\times36-48}{30}=2$	$P_0=\frac{3\times36-48}{30}=2$	$P_0=\frac{3\times36-48}{30}=2$	$P_0=\frac{4\times36-84}{30}=2$	$P_0=\frac{5\times36-120}{30}=2$	$P_0=\frac{4\times36-84}{30}=2$

$\Lambda_l=10;\ \Lambda_r=6;\ d=2;\ x=4;\ \frac{\Lambda_l\Lambda_r}{d}=30;\ 2(\Lambda_l+\Lambda_r)+x=36;\ |y_s|_{2d}=2;\ y=2,6,10;\ l_{i+1}=|16-(l_i+2r_i)|_{10};\ r_{j+1}=|24-(r_j+2l_j)|_6.$

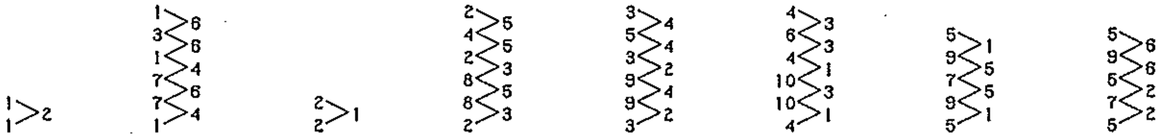

$2\sum(l_i+r_i)=6$	$2\sum(l_i+r_i)=90$	$2\sum(l_i+r_i)=6$	$2\sum(l_i+r_i)=90$	$2\sum(l_i+r_i)=90$	$2\sum(l_i+r_i)=90$	$2\sum(l_i+r_i)=84$	$2\sum(l_i+r_i)=84$
$\alpha=1$	$\alpha=5$	$\alpha=1$	$\alpha=5$	$\alpha=5$	$\alpha=5$	$\alpha=4$	$\alpha=4$
$P_0=\frac{1\times36-6}{30}=1$	$P_0=\frac{5\times36-90}{30}=3$	$P_0=\frac{1\times36-6}{30}=1$	$P_0=\frac{5\times36-90}{30}=3$	$P_0=\frac{5\times36-90}{30}=3$	$P_0=\frac{5\times36-90}{30}=3$	$P_0=\frac{4\times36-84}{30}=2$	$P_0=\frac{4\times36-84}{30}=2$

$\Lambda_l=10;\ \Lambda_r=6;\ d=2;\ x=5;\ \frac{\Lambda_l\Lambda_r}{d}=30;\ 2(\Lambda_l+\Lambda_r)+x=37;\ |y_s|_{2d}=1;\ y=1,5,9;\ l_{i+1}=|17-(l_i+2r_i)|_{10};\ r_{j+1}=|25-(r_j+2l_j)|_6.$

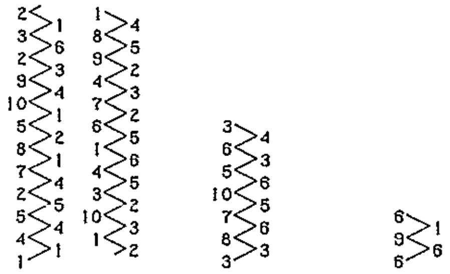

$2\sum(l_i+r_i)=364$	$2\sum(l_i+r_i)=132$	$2\sum(l_i+r_i)=44$
$\alpha=22$	$\alpha=6$	$\alpha=2$
$P_0=\frac{22\times37-364}{30}=15$	$P_0=\frac{6\times37-132}{30}=3$	$P_0=\frac{2\times37-44}{30}=1$

$\Lambda_l=10;\ \Lambda_r=6;\ d=2;\ x=6;\ \frac{\Lambda_l\Lambda_r}{d}=30;\ 2(\Lambda_l+\Lambda_r)+x=38;\ |y_s|_{2d}=0;\ y=0,4,8,12=0;\ l_{i+1}=|18-(l_i+2r_i)|_{10};\ r_{j+1}=|26-(r_j+2l_j)|_6.$

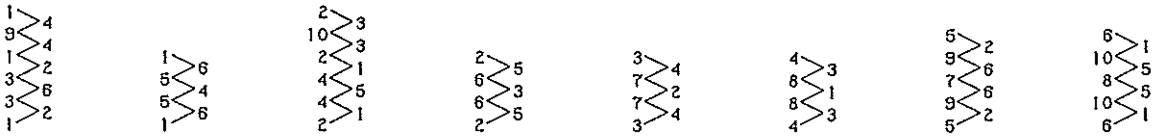

$2\sum(l_i+r_i)=70$	$2\sum(l_i+r_i)=54$	$2\sum(l_i+r_i)=70$	$2\sum(l_i+r_i)=54$	$2\sum(l_i+r_i)=54$	$2\sum(l_i+r_i)=54$	$2\sum(l_i+r_i)=92$	$2\sum(l_i+r_i)=92$
$\alpha=5$	$\alpha=3$	$\alpha=5$	$\alpha=3$	$\alpha=3$	$\alpha=3$	$\alpha=4$	$\alpha=4$
$P_0=\frac{5\times38-70}{30}=4$	$P_0=\frac{3\times38-54}{30}=2$	$P_0=\frac{5\times38-70}{30}=4$	$P_0=\frac{3\times38-54}{30}=2$	$P_0=\frac{3\times38-54}{30}=2$	$P_0=\frac{3\times38-54}{30}=2$	$P_0=\frac{4\times38-92}{30}=2$	$P_0=\frac{4\times38-92}{30}=2$

$\Lambda_l=10;\ \Lambda_r=6;\ d=2;\ x=6;\ \frac{\Lambda_l\Lambda_r}{d}=30;\ 2(\Lambda_l+\Lambda_r)+x=38;\ |y_s|_{2d}=2;\ y=2,6,10;\ l_{i+1}=|18-(l_i+2r_i)|_{10};\ r_{j+1}=|26-(r_j+2l_j)|_6.$

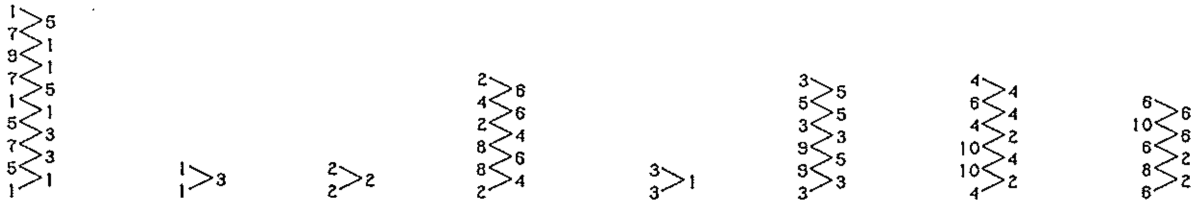

$2\sum(l_i+r_i)=124$	$2\sum(l_i+r_i)=8$	$2\sum(l_i+r_i)=8$	$2\sum(l_i+r_i)=100$	$2\sum(l_i+r_i)=8$	$2\sum(l_i+r_i)=100$	$2\sum(l_i+r_i)=100$	$2\sum(l_i+r_i)=92$
$\alpha=8$	$\alpha=1$	$\alpha=1$	$\alpha=5$	$\alpha=1$	$\alpha=5$	$\alpha=5$	$\alpha=4$
$P_0=\frac{8\times38-124}{30}=6$	$P_0=\frac{1\times38-8}{30}=1$	$P_0=\frac{1\times38-8}{30}=1$	$P_0=\frac{5\times38-100}{30}=3$	$P_0=\frac{1\times38-8}{30}=1$	$P_0=\frac{5\times38-100}{30}=3$	$P_0=\frac{5\times38-100}{30}=3$	$P_0=\frac{4\times38-92}{30}=2$

$\Lambda_l = 10;\ \Lambda_r = 6;\ d = 2;\ x = 7;\ \frac{\Lambda_l \Lambda_r}{d} = 30;\ 2(\Lambda_l + \Lambda_r) + x = 39;\ |y_s|_{2d} = 1;\ y = 1, 5, 9;\ l_{i+1} = |19 - (l_i + 2r_i)|_{10};\ r_{j+1} = |27 - (r_j + 2l_j)|_6.$

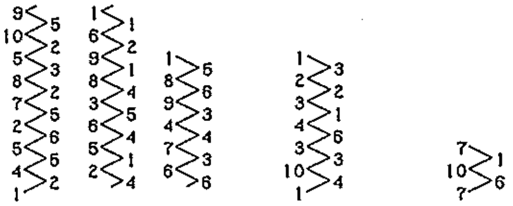

$2\sum(l_i + r_i) = 408$, $\alpha = 22$, $P_0 = \frac{22 \times 39 - 408}{30} = 15$

$2\sum(l_i + r_i) = 84$, $\alpha = 6$, $P_0 = \frac{6 \times 39 - 84}{30} = 5$

$2\sum(l_i + r_i) = 48$, $\alpha = 2$, $P_0 = \frac{2 \times 39 - 48}{30} = 1$

$\Lambda_l = 10;\ \Lambda_r = 6;\ d = 2;\ x = 8;\ \frac{\Lambda_l \Lambda_r}{d} = 30;\ 2(\Lambda_l + \Lambda_r) + x = 40;\ |y_s|_{2d} = 0;\ y = 0, 4, 8, 12 = 0;\ l_{i+1} = |20 - (l_i + 2r_i)|_{10};\ r_{j+1} = |28 - (r_j + 2l_j)|_6.$

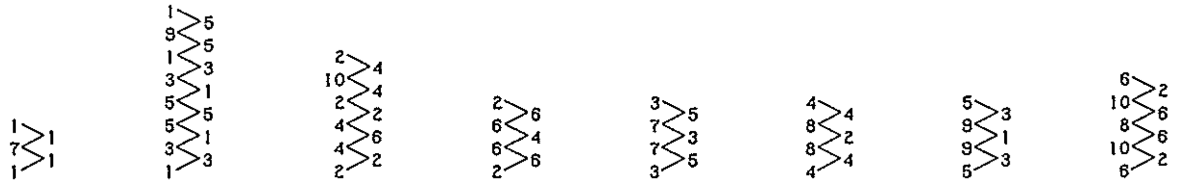

$2\sum(l_i + r_i) = 20$, $\alpha = 2$, $P_0 = \frac{2 \times 40 - 20}{30} = 2$

$2\sum(l_i + r_i) = 100$, $\alpha = 7$, $P_0 = \frac{7 \times 40 - 100}{30} = 6$

$2\sum(l_i + r_i) = 80$, $\alpha = 5$, $P_0 = \frac{5 \times 40 - 80}{30} = 4$

$2\sum(l_i + r_i) = 60$, $\alpha = 3$, $P_0 = \frac{3 \times 40 - 60}{30} = 2$

$2\sum(l_i + r_i) = 60$, $\alpha = 3$, $P_0 = \frac{3 \times 40 - 60}{30} = 2$

$2\sum(l_i + r_i) = 60$, $\alpha = 3$, $P_0 = \frac{3 \times 40 - 60}{30} = 2$

$2\sum(l_i + r_i) = 60$, $\alpha = 3$, $P_0 = \frac{3 \times 40 - 60}{30} = 2$

$2\sum(l_i + r_i) = 100$, $\alpha = 4$, $P_0 = \frac{4 \times 40 - 100}{30} = 2$

$\Lambda_l = 10;\ \Lambda_r = 6;\ d = 2;\ x = 8;\ \frac{\Lambda_l \Lambda_r}{d} = 30;\ 2(\Lambda_l + \Lambda_r) + x = 40;\ |y_s|_{2d} = 2;\ y = 2, 6, 10;\ l_{i+1} = |20 - (l_i + 2r_i)|_{10};\ r_{j+1} = |28 - (r_j + 2l_j)|_6.$

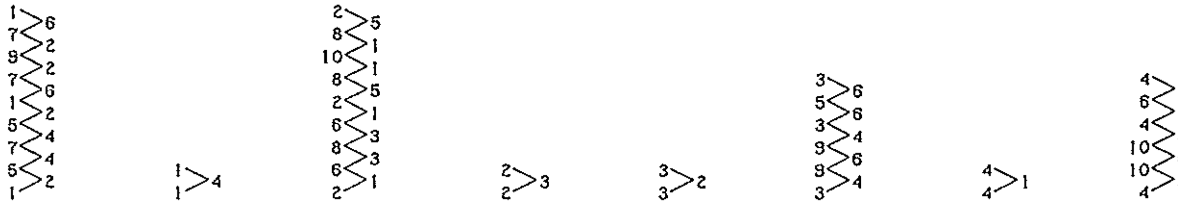

$2\sum(l_i + r_i) = 140$, $\alpha = 8$, $P_0 = \frac{8 \times 40 - 140}{30} = 6$

$2\sum(l_i + r_i) = 10$, $\alpha = 1$, $P_0 = \frac{1 \times 40 - 10}{30} = 1$

$2\sum(l_i + r_i) = 140$, $\alpha = 8$, $P_0 = \frac{8 \times 40 - 140}{30} = 6$

$2\sum(l_i + r_i) = 10$, $\alpha = 1$, $P_0 = \frac{1 \times 40 - 10}{30} = 1$

$2\sum(l_i + r_i) = 10$, $\alpha = 1$, $P_0 = \frac{1 \times 40 - 10}{30} = 1$

$2\sum(l_i + r_i) = 110$, $\alpha = 5$, $P_0 = \frac{5 \times 40 - 110}{30} = 3$

$2\sum(l_i + r_i) = 10$, $\alpha = 1$, $P_0 = \frac{1 \times 40 - 10}{30} = 1$

$2\sum(l_i + r_i) = 110$, $\alpha = 5$, $P_0 = \frac{5 \times 40 - 110}{30} = 3$

$\Lambda_l = 10;\ \Lambda_r = 6;\ d = 2;\ x = 9;\ \frac{\Lambda_l \Lambda_r}{d} = 30;\ 2(\Lambda_l + \Lambda_r) + x = 41;\ |y_s|_{2d} = 1;\ y = 1, 5, 9;\ l_{i+1} = |21 - (l_i + 2r_i)|_{10};\ r_{j+1} = |29 - (r_j + 2l_j)|_6.$

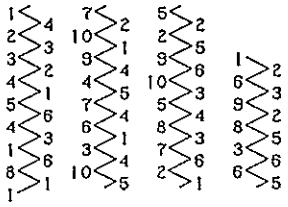

$2\sum(l_i + r_i) = 540$, $\alpha = 30$, $P_0 = \frac{30 \times 41 - 540}{30} = 23$

$\Lambda_l = 10;\ \Lambda_r = 6;\ d = 2;\ x = 10;\ \frac{\Lambda_l \Lambda_r}{d} = 30;\ 2(\Lambda_l + \Lambda_r) + x = 42;\ |y_s|_{2d} = 0;\ y = 0, 4, 8, 12 = 0;\ l_{i+1} = |22 - (l_i + 2r_i)|_{10};\ r_{j+1} = |30 - (r_j + 2l_j)|_6.$

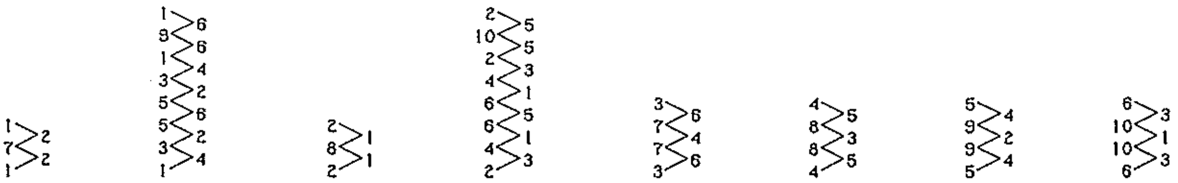

$2\sum(l_i + r_i) = 24$, $\alpha = 2$, $P_0 = \frac{2 \times 42 - 24}{30} = 2$

$2\sum(l_i + r_i) = 114$, $\alpha = 7$, $P_0 = \frac{7 \times 42 - 114}{30} = 6$

$2\sum(l_i + r_i) = 24$, $\alpha = 2$, $P_0 = \frac{2 \times 42 - 24}{30} = 2$

$2\sum(l_i + r_i) = 114$, $\alpha = 7$, $P_0 = \frac{7 \times 42 - 114}{30} = 6$

$2\sum(l_i + r_i) = 66$, $\alpha = 3$, $P_0 = \frac{3 \times 42 - 66}{30} = 2$

$2\sum(l_i + r_i) = 66$, $\alpha = 3$, $P_0 = \frac{3 \times 42 - 66}{30} = 2$

$2\sum(l_i + r_i) = 66$, $\alpha = 3$, $P_0 = \frac{3 \times 42 - 66}{30} = 2$

$2\sum(l_i + r_i) = 66$, $\alpha = 3$, $P_0 = \frac{3 \times 42 - 66}{30} = 2$

$A_l=10;\ A_r=6;\ d=2;\ x=10;\ \frac{A_lA_r}{d}=30;\ 2(A_l+A_r)+x=42;\ |y_*|_{2d}=2;\ y=2,6,10;\ l_{i+1}=|22-(l_i+2r_i)|_{10};\ r_{j+1}=|30-(r_j+2l_j)|_6.$

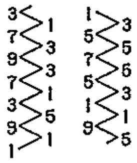

$2\sum(l_i+r_i)=204$ $\alpha=12$ $P_o=\frac{12\times42-204}{30}=10$

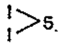

$2\sum(l_i+r_i)=12$ $\alpha=1$ $P_o=\frac{1\times42-12}{30}=1$

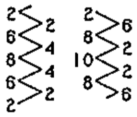

$2\sum(l_i+r_i)=156$ $\alpha=8$ $P_o=\frac{8\times42-156}{30}=6$

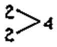

$2\sum(l_i+r_i)=12$ $\alpha=1$ $P_o=\frac{1\times42-12}{30}=1$

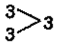

$2\sum(l_i+r_i)=12$ $\alpha=1$ $P_o=\frac{1\times42-12}{30}=1$

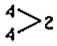

$2\sum(l_i+r_i)=12$ $\alpha=1$ $P_o=\frac{1\times42-12}{30}=1$

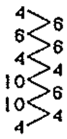

$2\sum(l_i+r_i)=120$ $\alpha=5$ $P_o=\frac{5\times42-120}{30}=3$

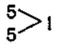

$2\sum(l_i+r_i)=12$ $\alpha=1$ $P_o=\frac{1\times42-12}{30}=1$

$A_l=10;\ A_r=6;\ d=2;\ x=11;\ \frac{A_lA_r}{d}=30;\ 2(A_l+A_r)+x=43;\ |y_*|_{2d}=1;\ y=1,5,9;\ l_{i+1}=|23-(l_i+2r_i)|_{10};\ r_{j+1}=|31-(r_j+2l_j)|_6.$

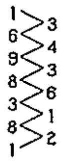

$2\sum(l_i+r_i)=108$ $\alpha=6$ $P_o=\frac{6\times43-108}{30}=5$

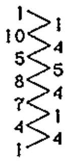

$2\sum(l_i+r_i)=108$ $\alpha=6$ $P_o=\frac{6\times43-108}{30}=5$

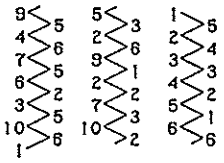

$2\sum(l_i+r_i)=324$ $\alpha=18$ $P_o=\frac{18\times43-324}{30}=15$

$A_l=10;\ A_r=6;\ d=2;\ x=12;\ \frac{A_lA_r}{d}=30;\ 2(A_l+A_r)+x=44;\ |y_*|_{2d}=0;\ y=0,4,8,12=0;\ l_{i+1}=|24-(l_i+2r_i)|_{10};\ r_{j+1}=|32-(r_j+2l_j)|_6.$

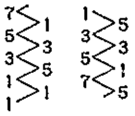

$2\sum(l_i+r_i)=112$ $\alpha=8$ $P_o=\frac{8\times44-112}{30}=8$

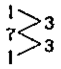

$2\sum(l_i+r_i)=28$ $\alpha=2$ $P_o=\frac{2\times44-28}{30}=2$

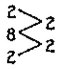

$2\sum(l_i+r_i)=28$ $\alpha=2$ $P_o=\frac{2\times44-28}{30}=2$

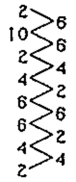

$2\sum(l_i+r_i)=128$ $\alpha=7$ $P_o=\frac{7\times44-128}{30}=6$

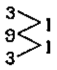

$2\sum(l_i+r_i)=28$ $\alpha=2$ $P_o=\frac{2\times44-28}{30}=2$

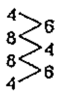

$2\sum(l_i+r_i)=72$ $\alpha=3$ $P_o=\frac{3\times44-72}{30}=2$

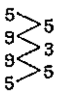

$2\sum(l_i+r_i)=72$ $\alpha=3$ $P_o=\frac{3\times44-72}{30}=2$

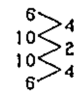

$2\sum(l_i+r_i)=72$ $\alpha=3$ $P_o=\frac{3\times44-72}{30}=2$

$A_l=10;\ A_r=6;\ d=2;\ x=12;\ \frac{A_lA_r}{d}=30;\ 2(A_l+A_r)+x=44;\ |y_*|_{2d}=2;\ y=2,6,10;\ l_{i+1}=|24-(l_i+2r_i)|_{10};\ r_{j+1}=|32-(r_j+2l_j)|_6.$

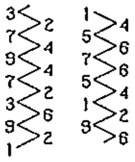

$2\sum(l_i+r_i)=228$ $\alpha=12$ $P_o=\frac{12\times44-228}{30}=10$

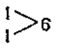

$2\sum(l_i+r_i)=14$ $\alpha=1$ $P_o=\frac{1\times44-14}{30}=1$

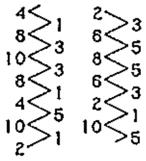

$2\sum(l_i+r_i)=228$ $\alpha=12$ $P_o=\frac{12\times44-228}{30}=10$

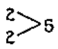

$2\sum(l_i+r_i)=14$ $\alpha=1$ $P_o=\frac{1\times44-14}{30}=1$

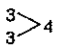

$2\sum(l_i+r_i)=14$ $\alpha=1$ $P_o=\frac{1\times44-14}{30}=1$

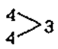

$2\sum(l_i+r_i)=14$ $\alpha=1$ $P_o=\frac{1\times44-14}{30}=1$

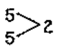

$2\sum(l_i+r_i)=14$ $\alpha=1$ $P_o=\frac{1\times44-14}{30}=1$

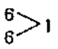

$2\sum(l_i+r_i)=14$ $\alpha=1$ $P_o=\frac{1\times44-14}{30}=1$

$A_l=10;\ A_r=6;\ d=2;\ x=13;\ \frac{A_lA_r}{d}=30;\ 2(A_l+A_r)+x=45;\ |y_*|_{2d}=1;\ y=1,5,9;\ l_{i+1}=|25-(l_i+2r_i)|_{10};\ r_{j+1}=|33-(r_j+2l_j)|_6.$

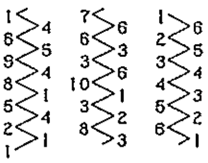

$2\sum(l_i+r_i)=300$ $\alpha=18$ $P_o=\frac{18\times45-300}{30}=17$

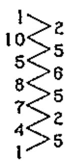

$2\sum(l_i+r_i)=120$ $\alpha=6$ $P_o=\frac{6\times45-120}{30}=5$

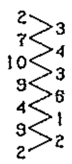

$2\sum(l_i+r_i)=120$ $\alpha=6$ $P_o=\frac{6\times45-120}{30}=5$

$\Lambda_l=10;\ \Lambda_r=6;\ d=2;\ x=14;\ \frac{\Lambda_l\Lambda_r}{d}=30;\ 2(\Lambda_l+\Lambda_r)+x=46;\ |y_s|_{2d}=0;\ y=0,4,8,12=0;\ l_{l+1}=|26-(l_l+2r_l)|_{10};\ r_{l+1}=|34-(r_l+2l_l)|_6.$

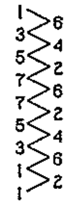

$2\sum(l_l+r_l)=128$
$\alpha=8$
$P_o=\frac{8\times46-128}{30}=8$

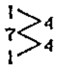

$2\sum(l_l+r_l)=32$
$\alpha=2$
$P_o=\frac{2\times46-32}{30}=2$

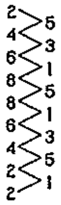

$2\sum(l_l+r_l)=128$
$\alpha=8$
$P_o=\frac{8\times46-128}{30}=8$

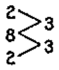

$2\sum(l_l+r_l)=32$
$\alpha=2$
$P_o=\frac{2\times46-32}{30}=2$

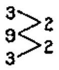

$2\sum(l_l+r_l)=32$
$\alpha=2$
$P_o=\frac{2\times46-32}{30}=2$

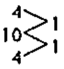

$2\sum(l_l+r_l)=32$
$\alpha=2$
$P_o=\frac{2\times46-32}{30}=2$

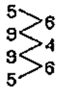

$2\sum(l_l+r_l)=78$
$\alpha=3$
$P_o=\frac{3\times46-78}{30}=2$

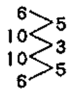

$2\sum(l_l+r_l)=78$
$\alpha=3$
$P_o=\frac{3\times46-78}{30}=2$

$\Lambda_l=10;\ \Lambda_r=6;\ d=2;\ x=14;\ \frac{\Lambda_l\Lambda_r}{d}=30;\ 2(\Lambda_l+\Lambda_r)+x=46;\ |y_s|_{2d}=2;\ y=2,6,10;\ l_{l+1}=|26-(l_l+2r_l)|_{10};\ r_{l+1}=|34-(r_l+2l_l)|_6.$

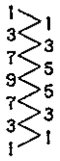

$2\sum(l_l+r_l)=96$
$\alpha=6$
$P_o=\frac{6\times46-96}{30}=6$

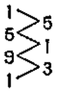

$2\sum(l_l+r_l)=48$
$\alpha=3$
$P_o=\frac{3\times46-48}{30}=3$

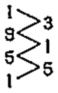

$2\sum(l_l+r_l)=48$
$\alpha=3$
$P_o=\frac{3\times46-48}{30}=3$

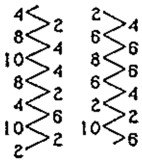

$2\sum(l_l+r_l)=252$
$\alpha=12$
$P_o=\frac{12\times46-252}{30}=10$

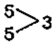

$2\sum(l_l+r_l)=16$
$\alpha=1$
$P_o=\frac{1\times46-16}{30}=1$

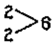

$2\sum(l_l+r_l)=16$
$\alpha=1$
$P_o=\frac{1\times46-16}{30}=1$

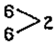

$2\sum(l_l+r_l)=16$
$\alpha=1$
$P_o=\frac{1\times46-16}{30}=1$

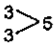

$2\sum(l_l+r_l)=16$
$\alpha=1$
$P_o=\frac{1\times46-16}{30}=1$

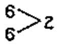

$2\sum(l_l+r_l)=16$
$\alpha=1$
$P_o=\frac{1\times46-16}{30}=1$

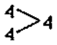

$2\sum(l_l+r_l)=16$
$\alpha=1$
$P_o=\frac{1\times46-16}{30}=1$

$\Lambda_l=10;\ \Lambda_r=6;\ d=2;\ x=15;\ \frac{\Lambda_l\Lambda_r}{d}=30;\ 2(\Lambda_l+\Lambda_r)+x=47;\ |y_s|_{2d}=1;\ y=1,5,9;\ l_{l+1}=|27-(l_l+2r_l)|_{10};\ r_{l+1}=|35-(r_l+2l_l)|_6.$

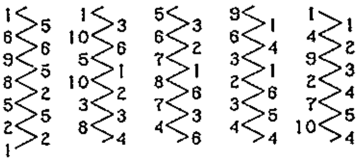

$2\sum(l_l+r_l)=540$
$\alpha=30$
$P_o=\frac{30\times47-540}{30}=29$

$\Lambda_l=10;\ \Lambda_r=6;\ d=2;\ x=16;\ \frac{\Lambda_l\Lambda_r}{d}=30;\ 2(\Lambda_l+\Lambda_r)+x=48;\ |y_s|_{2d}=0;\ y=0,4,8,12=0;\ l_{l+1}=|28-(l_l+2r_l)|_{10};\ r_{l+1}=|36-(r_l+2l_l)|_6.$

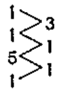

$2\sum(l_l+r_l)=24$
$\alpha=3$
$P_o=\frac{3\times48-24}{30}=4$

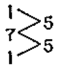

$2\sum(l_l+r_l)=36$
$\alpha=2$
$P_o=\frac{2\times48-36}{30}=2$

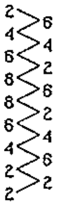

$2\sum(l_l+r_l)=144$
$\alpha=8$
$P_o=\frac{8\times48-144}{30}=8$

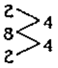

$2\sum(l_l+r_l)=36$
$\alpha=2$
$P_o=\frac{2\times48-36}{30}=2$

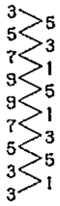

$2\sum(l_l+r_l)=144$
$\alpha=8$
$P_o=\frac{8\times48-144}{30}=8$

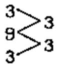

$2\sum(l_l+r_l)=36$
$\alpha=2$
$P_o=\frac{2\times48-36}{30}=2$

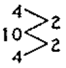

$2\sum(l_l+r_l)=36$
$\alpha=2$
$P_o=\frac{2\times48-36}{30}=2$

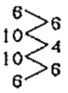

$2\sum(l_l+r_l)=84$
$\alpha=3$
$P_o=\frac{3\times48-84}{30}=2$

$\Lambda_l=10;\ \Lambda_r=6;\ d=2;\ x=16;\ \frac{\Lambda_l\Lambda_r}{d}=30;\ 2(\Lambda_l+\Lambda_r)+x=48;\ |y_s|_{2d}=2;\ y=2,6,10;\ l_{l+1}=|28-(l_l+2r_l)|_{10};\ r_{l+1}=|36-(r_l+2l_l)|_6.$

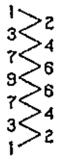

$2\sum(l_l+r_l)=108$
$\alpha=6$
$P_o=\frac{6\times48-108}{30}=6$

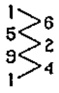

$2\sum(l_l+r_l)=54$
$\alpha=3$
$P_o=\frac{3\times48-54}{30}=3$

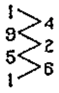

$2\sum(l_l+r_l)=54$
$\alpha=3$
$P_o=\frac{3\times48-54}{30}=3$

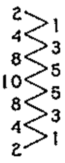

$2\sum(l_l+r_l)=108$
$\alpha=6$
$P_o=\frac{6\times48-108}{30}=6$

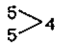

$2\sum(l_l+r_l)=18$
$\alpha=1$
$P_o=\frac{1\times48-18}{30}=1$

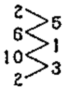

$2\sum(l_l+r_l)=54$
$\alpha=3$
$P_o=\frac{3\times48-54}{30}=3$

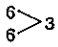

$2\sum(l_l+r_l)=18$
$\alpha=1$
$P_o=\frac{1\times48-18}{30}=1$

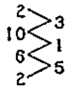

$2\sum(l_l+r_l)=54$
$\alpha=3$
$P_o=\frac{3\times48-54}{30}=3$

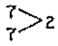

$2\sum(l_l+r_l)=18$
$\alpha=1$
$P_o=\frac{1\times48-18}{30}=1$

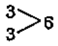

$2\sum(l_l+r_l)=18$
$\alpha=1$
$P_o=\frac{1\times48-18}{30}=1$

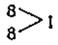

$2\sum(l_l+r_l)=18$
$\alpha=1$
$P_o=\frac{1\times48-18}{30}$

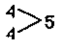

$2\sum(l_l+r_l)=18$
$\alpha=1$
$P_o=\frac{1\times48-18}{30}=1$

x $[y_n]_{2d}$	0	α	2× sbb	1	α	2× sbb	2	α	2× sbb	3	α	2× sbb	4	α	2× sbb	5	α	2× sbb	6	α	2× sbb	7	α	2× sbb	8	α	2× sbb	9	α	2× sbb	10	α	2× sbb	11	α	2× sbb	12	α	2× sbb
0							4×2 2×2 2×2	3 4 5	42 76 110				4×2 2×2 1×2 1×4	3 4 5 5	48 84 120 60				4×2 2×2 2×4	3 4 5	54 92 70				1×2 4×2 1×2 1×4 1×6	2 3 4 5 7	20 60 100 80 100				2×2 4×2 2×6	2 3 7	24 66 114				3×2 3×2 1×6 1×8	2 3 7 8	28 72 128 112
1				2×1 2×2 3×3	2 4 6	36 72 108				1×1 1×2 2×3 1×8	2 4 6 12	40 80 120 180				1×1 1×3 1×15	2 6 22	44 132 364				1×1 1×5 1×15	2 6 22	48 84 408				1×23	30	540				2×5 1×15	6 18	108 324			
2=d	4×1 2×2 2×3	3 4 5	66 68 70				1×1 2×1 2×2 3×3	1 3 4 5	4 72 76 80				2×1 2×2 4×3	1 4 5	6 84 90				3×1 1×2 3×3 1×6	1 4 5 8	8 92 100 124				4×1 2×3 2×6	1 5 8	10 110 140				5×1 1×3 1×6 1×10	1 5 8 12	12 120 156 204				6×1 2×10	1 12	14 228
3				2×1 2×2 3×3	2 4 6	36 72 108				1×1 1×2 2×3 1×8	2 4 6 12	40 80 120 180				1×1 1×3 1×15	2 6 22	44 132 364				1×1 1×5 1×15	2 6 22	48 84 408				1×23	30	540				2×5 1×15	6 18	108 324			
4=2d							4×2 2×2 2×2	3 4 5	42 76 110				4×2 2×2 1×2 1×4	3 4 5 5	48 84 120 60				4×2 2×2 2×4	3 4 5	54 92 70				1×2 4×2 1×2 1×4 1×6	2 3 4 5 7	20 60 100 80 100				2×2 4×2 2×6	2 3 7	24 66 114				3×2 3×2 1×6 1×8	2 3 7 8	28 72 128 112

x $[y_n]_{2d}$	13	α	2× sbb	14	α	2× sbb	15	α	2× sbb	16	α	2× sbb	17	α	2× sbb	18	α	2× sbb	19	α	2× sbb	20	α	2× sbb	21	α	2× sbb	22	α	2× sbb	23	α	2× sbb	24	α	2× sbb	25	α	2× sbb
0				4×2 2×2 2×8	2 3 8	32 78 128				4×2 1×2 1×4 2×8	2 3 3 8	36 84 24 144				4×2 2×4 2×8	2 3 8	40 30 160				3×2 3×4 1×8 1×8	2 3 7 8	44 36 124 176				2×2 4×4 2×8	2 3 7	48 42 138				1×2 4×4 1×6 1×6 1×8	2 3 4 5 7	52 48 44 100 152			
1	2×5 1×17	6 18	120 300				1×29	30	540				1×31	30	540				2×7 1×19	6 18	96 348				2×7 1×21	6 18	108 324				1×37	30	540				1×3 1×7 1×29	2 6 22	24 132 384
2=d				6×1 2×3 1×6 1×10	1 3 6 12	16 48 96 252				6×1 4×3 2×6	1 3 6	18 54 108				6×1 2×3 1×6 1×14	1 3 6 12	20 60 120 180				6×1 2×14	1 12	22 204				5×1 1×7 1×10 1×14	1 5 8 12	24 60 132 228				4×1 2×7 2×10	1 5 8	26 70 148			
3	2×5 1×17	6 18	120 300				1×29	30	540				1×31	30	540				2×7 1×19	6 18	96 348				2×7 1×21	6 18	108 324				1×37	30	540				1×3 1×7 1×29	2 6 22	24 132 384
4=2d				4×2 2×2 2×8	2 3 8	32 78 128				4×2 1×2 1×4 2×8	2 3 3 8	36 84 24 144				4×2 2×4 2×8	2 3 8	40 30 160				3×2 3×4 1×8 1×8	2 3 7 8	44 36 124 176				2×2 4×4 2×8	2 3 7	48 42 138				1×2 4×4 1×6 1×6 1×8	2 3 4 5 7	52 48 44 100 152			

x → ↓ $\lvert y_n\rvert_{2d}$	26	α	2× sbb	27	α	2× sbb	28	α	2× sbb	29	α	2× sbb	30	α	2× sbb	31	α	2× sbb	32	α	2× sbb	33	α	2× sbb	34	α	2× sbb	35	α	2× sbb	36	α	2× sbb	37	α	2× sbb	38	α	2× sbb
0	4×4 2×6 2×6	3 4 5	54 52 110				4×4 2×6 1×6 1×8	3 4 5 5	60 60 120 60				4×4 2×6 2×8	3 4 5	66 68 70				1×2 2×4 2×6 3×8	1 3 4 5	4 72 76 80				2×2 2×6 4×8	1 4 5	6 84 90				3×2 1×6 3×8 1×14	1 4 5 8	8 92 100 124				4×2 2×8 2×14	1 5 8	10 110 140
1				1×3 1×9 1×29	2 6 22	28 84 428				1×3 1×6 2×9 1×16	2 4 6 12	32 64 96 252				2×3 2×6 3×9	2 4 6	36 72 108				1×3 1×6 2×9 1×20	2 4 6 12	40 80 120 180				1×3 1×9 1×37	2 6 22	44 132 364				1×3 1×11 1×37	2 6 22	48 84 408			
2=d	3×1 1×6 3×7 1×10	1 4 5 8	28 52 80 104				2×1 2×6 4×7	1 4 5	30 60 90				1×1 2×5 2×6 3×7	1 3 4 5	32 36 68 100				4×5 2×6 2×7	3 4 5	42 76 110				4×5 2×6 1×7 1×9	3 4 5 5	48 84 120 60				4×5 2×6 2×9	3 4 5	54 92 70				1×4 4×5 1×6 1×9 1×13	2 3 4 5 7	20 60 100 80 100
3				1×3 1×9 1×29	2 6 22	28 84 428				1×3 1×6 2×9 1×16	2 4 6 12	32 64 96 252				2×3 2×6 3×9	2 4 6	36 72 108				1×3 1×6 2×9 1×20	2 4 6 12	40 80 120 180				1×3 1×9 1×37	2 6 22	44 132 364				1×3 1×11 1×37	2 6 22	48 84 408			
4=2d	4×4 2×6 2×6	3 4 5	54 52 110				4×4 2×6 1×6 1×8	3 4 5 5	60 60 120 60				4×4 2×6 2×8	3 4 5	66 68 70				1×2 2×4 2×6 3×8	1 3 4 5	4 72 76 80				2×2 2×6 4×8	1 4 5	6 84 90				3×2 1×6 3×8 1×14	1 4 5 8	8 92 100 124				4×2 2×8 2×14	1 5 8	10 110 140

x → ↓ $\lvert y_n\rvert_{2d}$	39	α	2× sbb	40	α	2× sbb	41	α	2× sbb	42	α	2× sbb	43	α	2× sbb	44	α	2× sbb	45	α	2× sbb	46	α	2× sbb	47	α	2× sbb	48	α	2× sbb	49	α	2× sbb	50	α	2× sbb	51	α	2× sbb
0				5×2 1×8 1×14 1×22	1 5 8 12	12 120 156 204				6×2 2×22	1 12	14 228				6×2 2×6 1×12 1×22	1 3 6 12	16 48 96 252				6×2 4×6 2×12	1 3 6	18 54 108				6×2 2×6 1×12 1×26	1 3 6 12	20 60 120 180				6×2 2×26	1 12	22 204			
1	1×53	30	540				2×11 1×33	6 18	108 324				2×11 1×35	6 18	120 300				1×59	30	540				1×61	30	540				2×13 1×37	6 18	96 348				2×13 1×39	6 18	108 324
2=d				2×4 4×5 2×13	2 3 7	24 66 114				3×4 3×5 1×13 1×16	2 3 7 8	28 72 128 112				4×4 2×5 2×16	2 3 8	32 78 128				4×4 1×5 1×7 2×16	2 3 3 8	36 84 24 144				4×4 2×7 2×16	2 3 8	40 30 160				3×4 3×7 1×15 1×16	2 3 7 8	44 36 124 176			
3	1×53	30	540				2×11 1×33	6 18	108 324				2×11 1×35	6 18	120 300				1×59	30	540				1×61	30	540				2×13 1×37	6 18	96 348				2×13 1×39	6 18	108 324
4=2d				5×2 1×8 1×14 1×22	1 5 8 12	12 120 156 204				6×2 2×22	1 12	14 228				6×2 2×6 1×12 1×22	1 3 6 12	16 48 96 252				6×2 4×6 2×12	1 3 6	18 54 108				6×2 2×6 1×12 1×26	1 3 6 12	20 60 120 180				6×2 2×26	1 12	22 204			

The first-return string-run details for x ranging from 1 to 16 and $|y_n|_{2d}$ ranging from 0 to d supply us with all the necessary information for the first-return string-runs of **all** Asymmetric Regular Nested Cylindrical Braids with $A_l = 10$ and $A_r = 6$.

Let the cells $(|y_n|_{2d}, x)$ and $(|y_n|'_{2d}, x')$ be (A_l, A_r)-complementary.

Let $\Delta x = x' - x$.

Let P_c be the number of parts associated with a first-return string-run belonging to cell $(|y_n|_{2d}, x)$ and let P'_c be the number of parts associated with its (A_l, A_r)-complementary first-return string-run belonging to cell $(|y_n|'_{2d}, x')$. Let $\Delta P_c = P'_c - P_c$.

Let $2 \times \text{sbb} = 2\sum(l_i + r_i)$ for a first-return string-run belonging to cell $(|y_n|_{2d}, x)$ and let $2 \times \text{sbb}' = 2\sum(l'_i + r'_i)$ for its (A_l, A_r)-complementary first-return string-run belonging to cell $(|y_n|'_{2d}, x')$. Then:

$$\Delta P_c = \frac{\alpha \cdot \Delta x + 2(2 \times \text{sbb}) - 2\alpha(A_l + A_r + 2)}{A^{**}}, \quad \text{where } A^{**} = \frac{A_l \cdot A_r}{d}.$$

$$2 \times \text{sbb}' = 2\alpha(A_l + A_r + 2) - 2 \times \text{sbb}.$$

Example 1(i):

Cell $(|y_n|_{2d}, x) = (2,0)$ is (A_l, A_r)-complementary to cell $(|y_n|'_{2d}, x') = (0,2)$.

components for cell $(0,2)$	$\longrightarrow$	for cell $(2,0)$
4×2 ; $\alpha = 3$; $2 \times \text{sbb} = 42$		$\Delta P_c = \frac{3(-2)+2\cdot 42-6\cdot 18}{30} = -1$; $2 \times \text{sbb}' = 6 \cdot 18 - 42 = 66$.
2×2 ; $\alpha = 4$; $2 \times \text{sbb} = 76$		$\Delta P_c = \frac{4(-2)+2\cdot 76-8\cdot 18}{30} = 0$; $2 \times \text{sbb}' = 8 \cdot 18 - 76 = 68$.
2×2 ; $\alpha = 5$; $2 \times \text{sbb} = 110$		$\Delta P_c = \frac{5(-2)+2\cdot 110-10\cdot 18}{30} = +1$; $2 \times \text{sbb}' = 10 \cdot 18 - 110 = 70$.

Example 1(ii):

Cell $(|y_n|'_{2d}, x') = (1,19)$ is (A_l, A_r)-complementary to cell $(|y_n|_{2d}, x) = (3,13)$ which in turn is the mirror image of cell $(|y_n|_{2d}, x) = (1,13)$. Hence cell $(1,19)$ is the mirror-imaged (A_l, A_r)-complement to cell $(1,13)$.

components for cell $(1,13)$	$\longrightarrow$	for cell $(1,19)$
2×5 ; $\alpha = 6$; $2 \times \text{sbb} = 120$		$\Delta P_c = \frac{6\cdot 6+2\cdot 120-12\cdot 18}{30} = +2$; $2 \times \text{sbb}' = 12 \cdot 18 - 120 = 96$.
1×17 ; $\alpha = 18$; $2 \times \text{sbb} = 300$		$\Delta P_c = \frac{18\cdot 6+2\cdot 300-36\cdot 18}{30} = +2$; $2 \times \text{sbb}' = 36 \cdot 18 - 300 = 348$.

Example 1(iii):

Cell $(|y_n|'_{2d}, x') = (1,49)$ is (A_l, A_r)-complementary to cell $(|y_n|_{2d}, x) = (3,43)$ which is the (A_l, A_r)-complement to cell $(3,19)$ which in turn is the mirror image of cell $(|y_n|_{2d}, x) = (1,19)$. Hence the first-return string-runs of cell $(1,49)$ are identical to the first-return string-run(s) of cell $(3,19)$ (apart from the y_i-values). Mirroring of a first-return string-run has no effect on its associated P_c-value and sbb-value, consequently the ΔP_c-values between the cells $(1,19)$ and $(1,49)$ are calculated with the formula:

$$\Delta P_c = \frac{\alpha \cdot \Delta x}{A^{**}}.$$

THE BRAIDER

APPENDIX 2003

CONTENTS

pg.

Errata — *The Braider* .... *i*

A quarterly publication
for
the braiding artisan

Resale of this publication or copies thereof is strictly prohibited

Copyright ©2003 by:

A.G. Schaake; 21 Sundown Cresc.; Hamilton; New Zealand.
D. Van Tassel; Box 335; Craig, Co 81626-0335; U.S.A.
F.J.M. Masurel; Ganzenzijde 4; 2317 XG Leiden; Nederland.

All rights reserved. No part of this publication may be reproduced, stored in a retrieval system, or transmitted, in any form or by any means, electronic, mechanical, photo-copying, recording, or otherwise, without prior written permission.

This publication is available to braiding artisans only.

Copies may be obtained from:

A.G. Schaake,
21 Sundown Cresc.,
Hamilton,
New Zealand.

ERRATA—*THE BRAIDER*

The list below lists the typing errors which were noted in at least some copies of the following Issues of *The Braider*.

No. 1

pg. 3, line 9 — **it** is
pg. 3, line 10 — **unnecessarily**
pg. 3, line 17 — in order **to** present
pg. 12, line 5 under "An Introduction to Flat Braids" — Four pages are devoted **to**
pg. 16, line 9 under "Reviews" — **instructor**

No. 2

pg. 21, line 2 — delete **that**
pg. 28, line 6 — However, **a** one colour
pg. 38, line 18 under "Reviews" — **they** are first class

No. 3

pg. 42, line 2 — Naturally, **queries** not directly

No. 4

pg. 76, line 5 — **phenomenon**
pg. 81, line 16 — **phenomenon**

No. 5

pg. 87, line 3 from bottom of page — **exclude**
pg. 106, line 11 — **locality**

No. 6

pg. 129, line 15 — 2-**colour**

No. 7

No. 8

pg. 158, line 3 — Hence **the** number of bights
pg. 161, line 12 — In Fig. 144 are depicted the **parts-raising** processes

No. 9

No. 10

pg. 213, line 2 — **choose**

No. 11

pg. 232, line 17 — **in general**
pg. 245, line 8 — **in general**

No. 12

pg. 257, line 6 — or $B = \{(2m+2)(\alpha+1)-1\}N - (\alpha+1)$ bights
pg. 257, line 7 — Those with $B = \{(2m+2)(\alpha+1)-1\}N - (\alpha+1)$ bights
pg. 257, line 9 — $b = \{(2m+2)\alpha - 1\}N - \alpha$ bights. Those with $B = \{(2m+2)(\alpha+1)-1\}N + (\alpha+1)$ bights
pg. 257, line 10 & 11 — with $p = \{(2m+2)\alpha - 1$ parts and $b = \{(2m+2)\alpha - 1\}N + \alpha$ bights
pg. 257, line 7 from bottom — delete **thinspace**

No. 13

pg. 276, line 7 — **in general**

No. 14

pg. 308, line 3 — **in general**

No. 15

pg. 338, line 1 — **independent**

No. 16

pg. 347, line 3 — $P = 2m(\alpha+1)+1$
pg. 353, line 16 — **screw**
pg. 356, line 3 — **two**
pg. 359, line 5 under Fig. 310 — **boundary**
pg. 361, line 3 from bottom — **Headhunter's-coded**
pg. 366, line 30 — **braided**

No. 17

pg. 369, line 12 — **mathematical**
pg. 372, lines 8, 9, 10, 13 — **positive**
pg. 383, line 13 — **Figs. 326–328**
pg. 387, line 2 below Fig. 332 — **in general**
pg. 387, line 13 below Fig. 332 — **cases**

No. 18

pg. 393, the right-hand brace } immediately before the second equal sign is missing in the three lines above the upper .... line, and the right-hand brace } immediately before the third equal sign is missing in the first line below the upper .... line.
pg. 395, line 4 — **additionally**
pg. 396, bottom line — **in general**
pg. 397, line 4 from bottom — **in general**
pg. 412, Fig. 345 immediately below the sixth diagram — change $o-u-o-u$ to $u-o-u-o$.
pg. 413, Fig. 346 leftmost diagram in second row of diagrams: the two non coded crossing points should have been provided with an under coding each for the braiding direction indicated.

No. 19

pg. 419, lines 2 & 3 from bottom — in **general**
pg. 420, last line — $\Delta_{r_i} = 0$ for $r_i = 4$.
pg. 421, line 2 — $(12/19/113)\{1_1 1_2 2_4 3_3/1_1 1_2 3_3 1_4 4_5 2_6\}24$
pg. 430, lines 3 & 5 — in **general**

No. 20

pg. 446, line 14 — A few **simple** examples
pg. 446, line 3 from bottom — in **general**
pg. 447, Footnote — **These** are the
pg. 450, last line — delete **thinspace**
pg. 464, line 20 — Brion **Toss**

No. 21

pg. 465, line 16 — in **general**

No. 22

pg. 493, second line under "Question on pg. 479" — **appliqué**

No. 23

pg. 516, line 3 — **categorisation**
pg. 523, line 14 — **Fig. 445**

No. 24

pg. 537, line 2 — **arises**
pg. 537, line 14 — **actual**
pg. 545, line 1 — read as: greater than or equal to 2 and less than p

No. 25

pg. 563, line 19 — read as: greater than or equal to 2 and less than p

No. 26

pg. 593, line 6 — delete parenthesis after half-cycle

No. 27

pg. 631, line 18 — **Herringbone**
pg. 633, line 33 — **Herringbone**
pg. 634, line 3 — **Herringbone**

No. 28

pg. 640, line 2 — **algorithms**
pg. 647, lines 11 & 20 below Fig. 517 — **finished**
pg. 648, lines 1, 10, 19, 28, 37 & 46 — **finished**
pg. 649, lines 8 & 17 — **finished**
pg. 650, line 4 — read as: greater than 1 and less than or equal to 17
pg. 650, lines 5 & 6 — read as: greater than or equal to 3 and less than or equal to 17
pg. 650, line 4 below Fig. 519 — read as: greater than 1 and less than or equal to 23

pg. 650, line 6 below Fig. 519 — read as: greater than or equal to 3 and less than or equal to 23
pg. 651, line 3 — read as: greater than or equal to 2 and less than or equal to 8
pg. 651, line 4 below Fig. 521 — read as: greater than or equal to 2 and less than or equal to 12

No. 29

pg. 666, Example 1 — half-cycle 9. $1 \nearrow 3$: $2o - 2u - 2o$.
pg. 677, next to last line — **usual**

No. 30

pg. 704, line 9 from bottom — can **be** made

No. 31

NOTE: the first Fig. number in this Issue is 554, but should have been 584 instead. Hence the Fig. numbers 554 - 583 not only appear in *The Braider*, Issue No. 30, but appear again in *The Braider*, Issue numbers 31 - 32.

No. 32

No. 33

pg. 757, lines 1 and 5 — **Any one**
pg. 761, line 21 — delete parenthesis after half-cycle
pg. 768, line 1 — **reality**
pg. 782, line 4 — **misrepresentation**
pg. 782, line 29 — **whereas**

No. 34

pg. 793, line 2 — **any one**
pg. 794, lines 19 and 23 — **Any one**
pg. 797, line 3 from bottom — (see pg. **794**)
pg. 797, line 4 from bottom and last line — the **nest-index** number
pg. 800, line 3 from bottom — crossings **between** the right-hand

No. 35

No. 36

Cover sheet — **Hobbles**
pg. 831, lines 1 and 2 — **Hobbles**
pg. 831, line 6 — **knuckles**
pg. 831, line 7 twice, 11, 13, 15, 21 — **hobbles**
pg. 831, line 19 — **approximately**
pg. 832, line 7 — **hobbles**

No. 37

No. 38

pg. 882, penultimate line — **these** are
pg. 883, line 3 — **these** are
pg. 884, 1st line of 1st footnote — delete **out**
pg. 884, line 30 — **passed**
pg. 885, line 6 and line 7 — **grid-diagram**
pg. 885, line 8 — **referred**
pg. 889, line 1 and line 7 — **these** are
pg. 898, last line — **central**

No. 39

pg. 914, line 18 — Flores **Knot**
pg. 923, text line 9 or overall line 23 — **Herringbone** Pineapple Knots

No. 40

pg. 934, line 15 — **any one**
pg. 936, line 16 — **any one**

THE BRAIDER

No.37 FEBRUARY 2004.

CONTENTS

pg.

Solutions to the Questions in Issue No.36 855

Rectangular Right Prismatic Braids 857

A quarterly publication for the braiding artisan

Resale of this publication or copies thereof is strictly prohibited

Copyright ©2004 by:

A.G. Schaake; 21 Sundown Cresc.; Hamilton; New Zealand.
D. Van Tassel; Box 335; Craig, Co 81626-0335; U.S.A.
F.J.M. Masurel; Ganzenzijde 4; 2317 XG Leiden; Nederland.

All rights reserved. No part of this publication may be reproduced, stored in a retrieval system, or transmitted, in any form or by any means, electronic, mechanical, photo-copying, recording, or otherwise, without prior written permission.

This publication is available to braiding artisans only.

Copies may be obtained from:

A.G. Schaake,
21 Sundown Cresc.,
Hamilton,
New Zealand.

Solutions to the Questions in Issue No. 36

Question on pg.833.

1). p is odd, hence $p = 2n + 1$, where $n = 1, 2, 3, \cdots$, and $P = 2p = 4n + 2$.

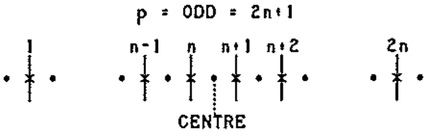

The number of new coding columns created by interbraiding two identical column-coded Regular Knots with p-parts is thus $(P - 1) - (p - 1) = (4n + 1) - (2n) = 2n + 1$. Hence the maximum number of different column-coded $P/B = 2p/2b$ Regular Cylindrical Braids which can be created is $2^{(2n+1)}$. This maximum number can only be created when for the identical column-coded Regular Knots p/b the condition $\{\text{coding of column } x\} = \{\text{coding of column } (2n + 1 - x)\}$, where $x = 1, 2, 3, \cdots, n$, does not apply for at least one x-value.

If for the column-coding of the identical column-coded Regular Knots p/b the $\{\text{coding of column } x\} = \{\text{coding of column } (2n + 1 - x)\}$, where $x = 1, 2, 3, \cdots, n$, for all x-values, then $2^{(n+1)}$ of the interbraided $P/B = 2p/2b$ Regular Cylindrical braids have a balanced column-coding (we have a choice out of two coding types for the columns $1, 3, 5, \cdots, (2n + 1)$ of the interbraided $P/B = 2p/2b$ Regular Cylindrical Braid, then the coding of column $(2n + 1 + z)$ is the coding of column $(2n + 1 - z)$, where $z = 2, 4, 6, \cdots, 2n$). There remain thus a maximum of $\left(2^{(2n+1)} - 2^{(n+1)}\right)$ column-coded interbraided $P/B = 2p/2b$ Regular Cylindrical Braids, but only half of them are different (turn one of them through 180° and the braid obtained is already among the others of the $\left(2^{(2n+1)} - 2^{(n+1)}\right)$). Hence the number of different column-coded $P/B = 2p/2b$ interbraided Regular Cylindrical Braids we obtain is equal to $\dfrac{2^{(2n+1)} - 2^{(n+1)}}{2} + 2^{(n+1)} = 2^{2n} - 2^{n} + 2^{(n+1)} = 2^{n}\left(2^{n} - 1 + 2\right) = 2^{n}\left(2^{n} + 1\right)$; of these $2^{(n+1)}$ have a balanced column-coding.

2). p is even, hence $p = 2n$, where $n = 1, 2, 3, \cdots$, and $P = 2p = 4n$.

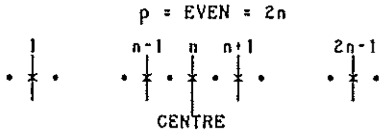

The number of new coding columns created by interbraiding two identical column-coded Regular Knots with p-parts is thus $(P - 1) - (p - 1) = (4n - 1) - (2n - 1) = 2n$. Hence the maximum number of different column-coded $P/B = 2p/2b$ Regular Cylindrical Braids which can be created is $2^{(2n)}$. This maximum number can only be created when for the identical column-coded Regular Knots p/b the condition $\{\text{coding of column } x\} = \{\text{coding of column } (2n - x)\}$, where $x = 1, 2, 3, \cdots, (n - 1)$, does not apply for at least one x-value.

If for the column-coding of the identical column-coded Regular Knots p/b the $\{\text{coding of column } x\} = \{\text{coding of column } (2n - x)\}$, where $x = 1, 2, 3, \cdots, (n - 1)$, for all x-values, then 2^{n} of the interbraided $P/B = 2p/2b$ Regular Cylindrical braids have a balanced column-coding (we have a choice out of two coding types for the columns $1, 3, 5, \cdots, (2n-1)$ of the interbraided $P/B = 2p/2b$ Regular Cylindrical Braid, then the coding of column $(2n+z)$ is the coding of column $(2n-z)$, where $z = 1, 3, 5, \cdots, (2n-1)$). There remain thus a maximum of $\left(2^{(2n)} - 2^{n}\right)$ column-coded interbraided $P/B = 2p/2b$ Regular Cylindrical Braids, but only half of them are different (turn one of them through 180° and the braid obtained is already among the others of the $\left(2^{(2n)} - 2^{n}\right)$). Hence the number of different column-coded $P/B = 2p/2b$ interbraided Regular Cylindrical Braids we obtain is equal to $\dfrac{2^{(2n)} - 2^{n}}{2} + 2^{n} = 2^{(2n-1)} - 2^{(n-1)} + 2^{n} = 2^{(n-1)}(2^{n} - 1 + 2) = 2^{(n-1)}(2^{n} + 1)$; there are 2^{n} of these which have a balanced column-coding.

Question on pg.835.

1). p is odd, hence $p = 2n+1$, where $n = 1, 2, 3, \cdots$, and $P = 3p = 6n+3$.

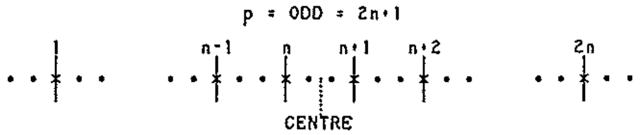

The number of new coding columns created by interbraiding three identical column-coded Regular Knots with p-parts is thus $(P-1) - (p-1) = (6n+2) - (2n) = 4n+2$. Hence the maximum number of different column-coded $P/B = 3p/3b$ Regular Cylindrical Braids which can be created is $2^{(4n+2)}$. This maximum number can only be created when for the identical column-coded Regular Knots p/b the condition $\{\text{coding of column } x\} = \{\text{coding of column } (2n+1-x)\}$, where $x = 1, 2, 3, \cdots, n$, does not apply for at least one x-value. When for the identical column-coded Regular Knots p/b the $\{\text{coding of column } x\} = \{\text{opposite coding of column } (2n+1-x)\}$, where $x = 1, 2, 3, \cdots, n$, for all x-values, then $2^{(2n+1)}$ of these interbraided $P/B = 3p/3b$ Regular Cylindrical braids have a balanced column-coding (we have a choice out of two coding types for the columns $1, 2, 4, 5, 7, 8, \cdots, (3n-2), (3n-1), (3n+1)$ of the interbraided $P/B = 3p/3b$ Regular Cylindrical Braid; the coding of column $(6n+3-z)$ is then the opposite to the coding of column z, where $z = 1, 2, 4, 5, 7, 8, \cdots, (3n-2), (3n-1), (3n+1)$).

If for the column-coding of the identical column-coded Regular Knots p/b the $\{\text{coding of column } x\} = \{\text{coding of column } (2n+1-x)\}$, where $x = 1, 2, 3, \cdots, n$, for all x-values, then $2^{(2n+1)}$ of the interbraided $P/B = 3p/3b$ Regular Cylindrical braids have a balanced column-coding (we have a choice out of two coding types for the columns $1, 2, 4, 5, 7, 8, \cdots, (3n-2), (3n-1), (3n+1)$ of the interbraided $P/B = 3p/3b$ Regular Cylindrical Braid; the coding of column $(6n+3-z)$ is then identical to the coding of column z, where $z = 1, 2, 4, 5, 7, 8, \cdots, (3n-2), (3n-1), (3n+1)$). There remain thus a maximum of $\left(2^{(4n+2)} - 2^{(2n+1)}\right)$ column-coded interbraided $P/B = 3p/3b$ Regular Cylindrical Braids, but only half of them are different (turn one of them through 180° and the braid obtained is already among the others of the $\left(2^{(4n+2)} - 2^{(2n+1)}\right)$). Hence the number of different column-coded $P/B = 3p/3b$ interbraided Regular Cylindrical Braids we obtain is equal to $\dfrac{2^{(4n+2)} - 2^{(2n+1)}}{2} + 2^{(2n+1)} = 2^{(4n+1)} - 2^{(2n)} + 2^{(2n+1)} = 2^{(2n)}\left(2^{(2n+1)} - 1 + 2\right) = 2^{(2n)}\left(2^{(2n+1)} + 1\right)$; of these $2^{(2n+1)}$ have a balanced column-coding.

2). p is even, hence $p = 2n$, where $n = 1, 2, 3, \cdots$, and $P = 3p = 6n$.

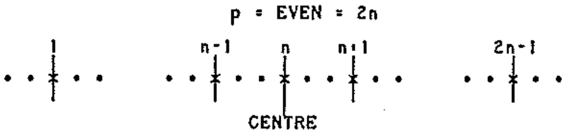

The number of new coding columns created by interbraiding three identical column-coded Regular Knots with p-parts is thus $(P-1)-(p-1) = (6n-1)-(2n-1) = 4n$. Hence the maximum number of different column-coded $P/B = 3p/3b$ Regular Cylindrical Braids which can be created is $2^{(4n)}$. This maximum number can only be created when for the identical column-coded Regular Knots p/b the condition $\{\text{coding of column } x\} = \{\text{coding of column } (2n-x)\}$, where $x = 1, 2, 3, \cdots, (n-1)$, does not apply for at least one x-value.

If for the column-coding of the identical column-coded Regular Knots p/b the $\{\text{coding of column } x\} = \{\text{coding of column } (2n-x)\}$, where $x = 1, 2, 3, \cdots, (n-1)$, for all x-values, then $2^{(2n)}$ of the interbraided $P/B = 3p/3b$ Regular Cylindrical braids have a balanced column-coding (we have a choice out of two coding types for the columns $1, 2, 4, 5, 7, 8, \cdots, (3n-2), (3n-1)$ of the interbraided $P/B = 3p/3b$ Regular Cylindrical Braid, then the coding of column $(6n-z)$ is identical to the coding of column z, where $z = 1, 2, 4, 5, 7, 8, \cdots, (3n-2), (3n-1)$). There remain thus a maximum of $\left(2^{(4n)} - 2^{(2n)}\right)$ column-coded interbraided $P/B = 3p/3b$ Regular Cylindrical Braids, but only half of them are different (turn one of them through 180° and the braid obtained is already among the others of the $\left(2^{(4n)} - 2^{(2n)}\right)$). Hence the number of different column-coded $P/B = 3p/3b$ interbraided Regular Cylindrical Braids is equal to $\dfrac{2^{(4n)} - 2^{(2n)}}{2} + 2^{(2n)} = 2^{(4n-1)} - 2^{(2n-1)} + 2^{(2n)} = 2^{(2n-1)}\left(2^{(2n)} - 1 + 2\right) = 2^{(2n-1)}\left(2^{(2n)} + 1\right)$; of these $2^{(2n)}$ have a balanced column-coding.

Rectangular Right Prismatic Braids

A Rectangular Right Prismatic Braid is a braid-form which can be used as a toggle (small sizes) or as a fender covering (large sizes). We find the description of some in *The Ashley Book of Knots* #2234, #2236, #2237, #2238, #2240.

Let's look at the braid $3 \times 4 \times 7$ mentioned under #2240:

In order to draw the grid-diagram of this braid, one most likely would develop it in the way a rectangular right prismatic box would be developed. The result is then as shown by the upper diagram in Fig. 672. Note that the "blank" codings are neglected in the braiding process since they only duplicate for clarity reasons some of the "black" codings (it are only the "black" codings which take part in the braiding process). As we shall see shortly, this type of braid-form requires at least two essential strings, and the braid $3 \times 4 \times 7$ mentioned under #2240 is a braid for which two strings suffice. In the lower string-run diagram of Fig. 672 the string-run of one of these two essential strings is depicted by the heavy line segments. This development procedure is, however, not the best for this type of braid-form.

Instead of folding the two 3×4 end-faces out in the plane containing the 4×7 top-face, we can fold half of each of these 3×4 end-faces out with the 4×7 top-face and the other half of each of these end-faces with the 4×7 bottom-face; this has been depicted by the upper grid-diagram of Fig. 673. The string-run can then be depicted as in the central string-run diagram of Fig. 673. Note that the heavy lined string-run in the central diagram of Fig. 673 is the heavy lined string-run in the lower diagram of Fig. 672.

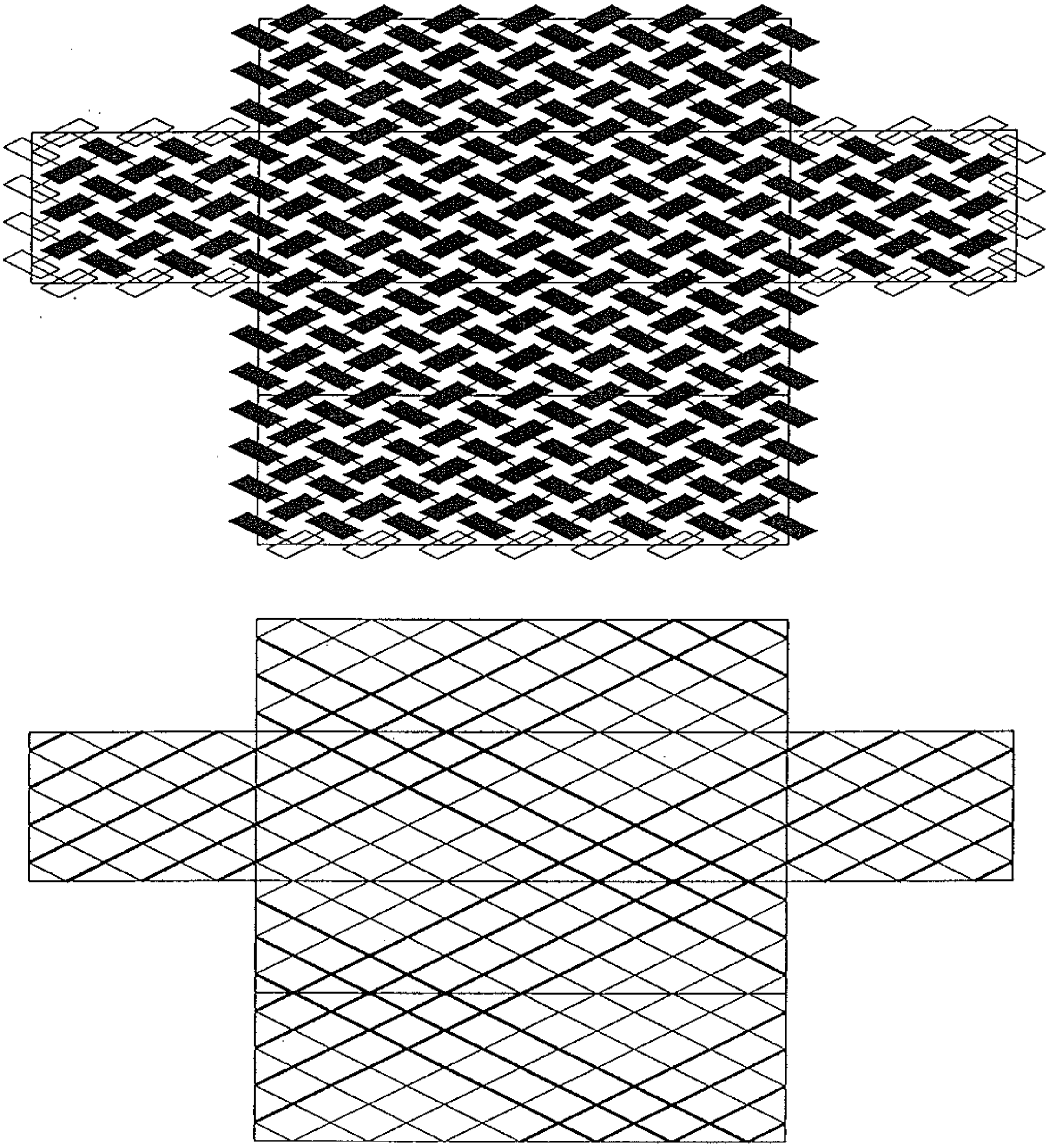

Fig. 672 — A $3 \times 4 \times 7$ over-under coded Rectangular Right Prismatic Braid.

When we now superimpose an over-under coding, we obtain the lowermost grid-diagram of this $3 \times 4 \times 7$ over-under coded Rectangular Right Prismatic Braid. The advantage of this layout (development) will immediately be obvious — fewer blank codings and a much more continuous string-run, which makes the actual braiding process much easier. To a large extent the string-run looks now like that of a Periodic Regular Nested Cylindrical Braid (there are only four points in the diagram (it are in reality only two points since the two left-hand points depict in fact only one and the same point, similarly the two right-hand points which depict in fact only one and the same point) where it deviates from a Periodic Regular Nested Cylindrical Braid).

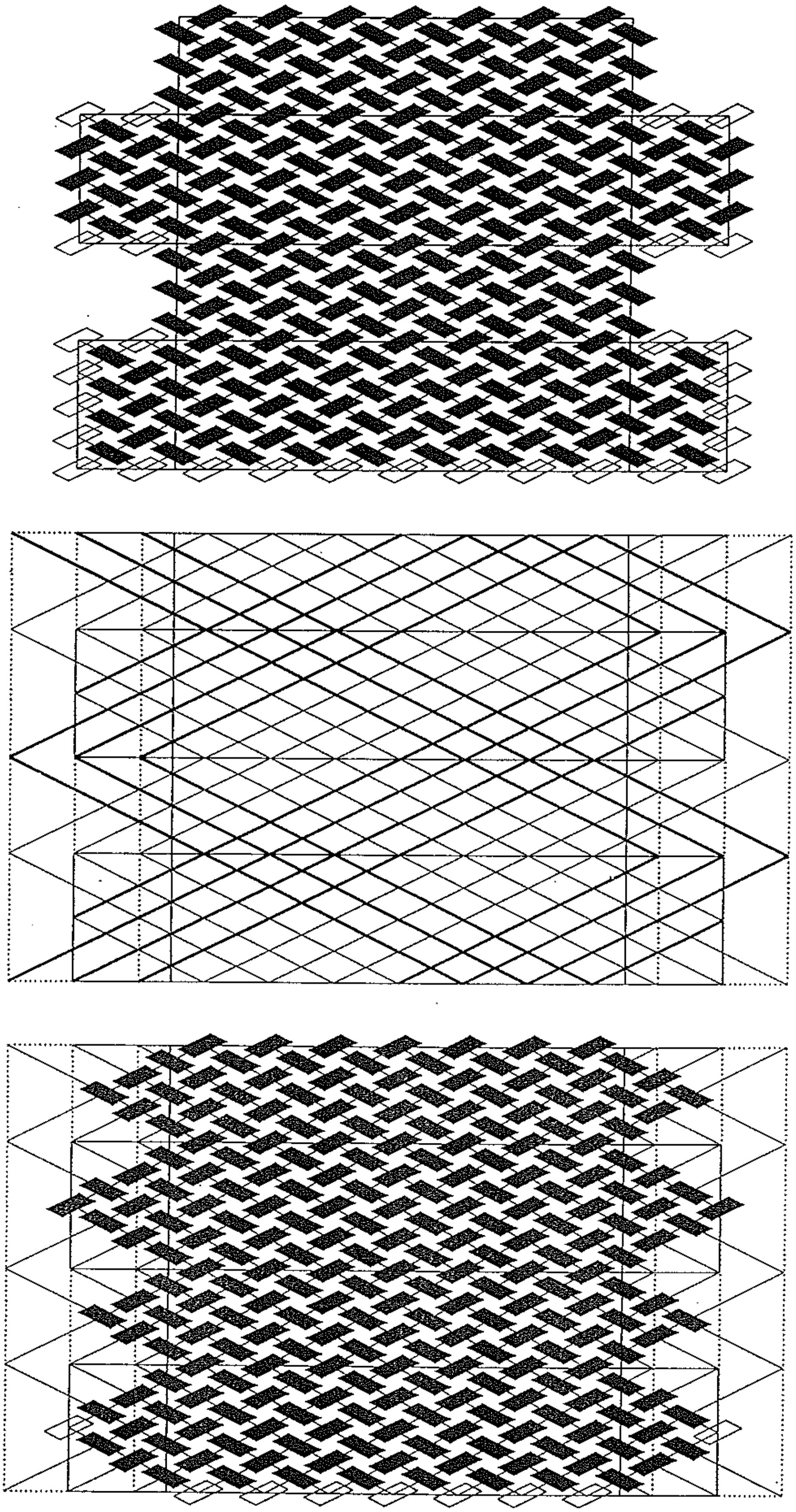

Fig. 673 — A 3 × 4 × 7 over-under coded Rectangular Right Prismatic Braid.

In order to help the reader with familiarising the reading of these diagrams, we have depicted in Figs. 674 & 675 an over-under coded $2 \times 3 \times 5$ Rectangular Right Prismatic Braid, respectively developed in the same way as the over-under coded $3 \times 4 \times 7$ Rectangular Right Prismatic Braid in Figs. 672 & 673.

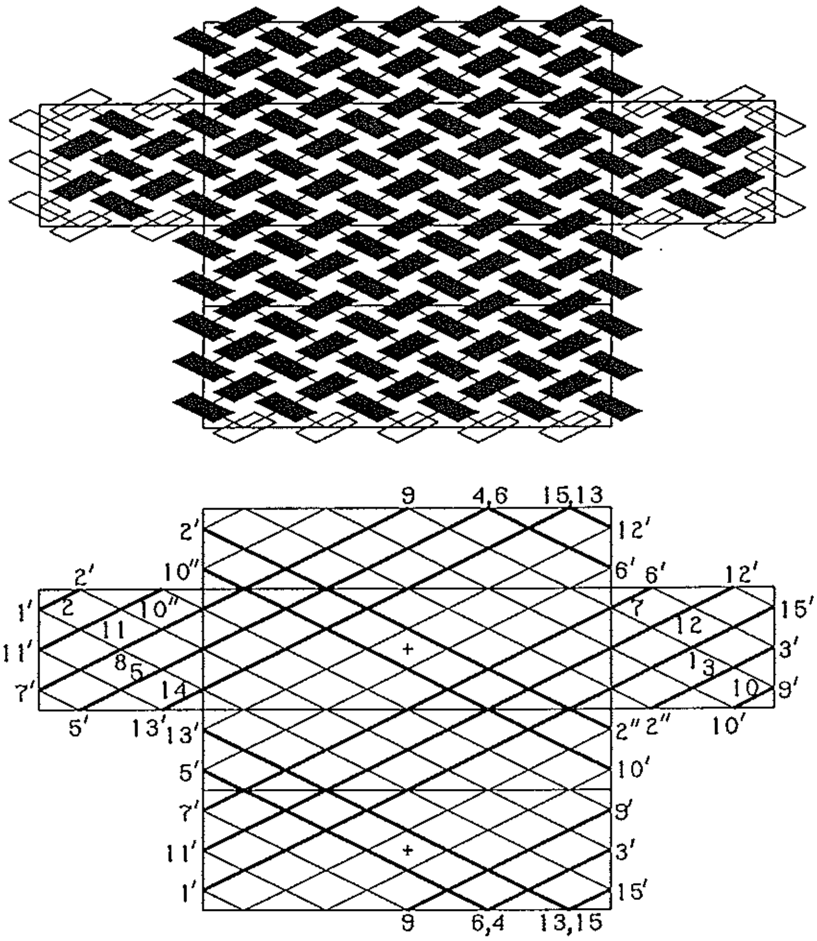

Fig. 674 — A $2 \times 3 \times 5$ over-under coded Rectangular Right Prismatic Braid.

In the lower string-run diagram of Fig. 674 the string-run of one of the two essential strings is indicated by the heavy line segments $1 - 1' - 2 - 2' - 2'' - 3 - 3' - 4 - 5 - 5' - 6 - 6' - 7 - 7' - 8 - 9 - 9' - 10 - 10' - 10'' - 11 - 11' - 12 - 12' - 13 - 13' - 14 - 15 - 15' - 1$. This string-run is depicted in Fig. 675 by the heavy line segments $1-2-3-4-5-6-7-8-9-10-11-12-13-14-15-1$ in the central string-run diagram.

The type of string-run diagrams in Figs. 673 and 675 are generalised by the upper diagram in Fig. 676, and this generalised diagram is going to tell us that the minimum number of essential strings for these type of braids is equal to two.

There are four nests of regularly stacked bights at the right and left bight-edges, and in addition we have the boundary crossing-points $A_1 = A_3$ and $A_2 = A_4$. Let each nest of bights consist of a bights, then in total we have $8a$ bights.

Let the string-run start in A_1 in the direction of arrow 1. After leaving boundary crossing-point A_1, let the first boundary crossing-point encountered by the string-run be A_1. Hence the string-run enters A_1 in the direction of arrow 2 (see diagram 1 in Fig. 676). The string then leaves boundary crossing-point $A_3\,(= A_1)$ in the direction of arrow 3. The next boundary crossing-point encountered will then be A_3 in the direction of arrow 4 and the string-run is closed. The string-run $A_1 - 1 - 2 - A_1$ and the string-run $A_3 - 3 - 4 - A_3$ can each have a maximum of $(2a - 1)$ bights, hence with the second string through the boundary crossing-points $A_2 = A_4$ the maximum number of bights through which these two strings pass is equal to $(8a - 4)$. Since the total number of bights is equal to $8a$, the braid thus requires more than two essential strings.

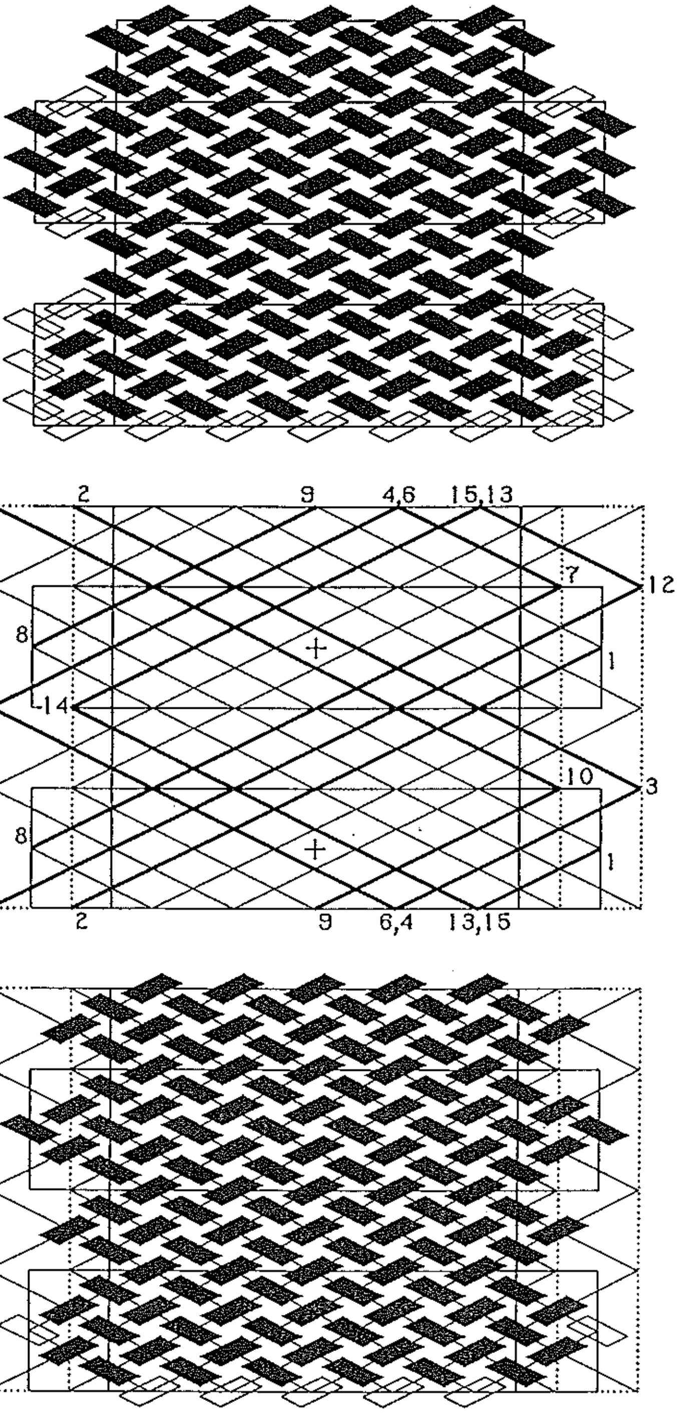

Fig. 675 — A $2 \times 3 \times 5$ over-under coded Rectangular Right Prismatic Braid.

Let the string-run start in A_1 in the direction of arrow 1. After leaving boundary crossing-point A_1 let the first boundary crossing-point encountered by the string-run be A_3. Hence the string-run enters A_3 in the direction of arrow 2 (see diagram 2 in Fig. 676). The string then leaves boundary crossing-point $A_1 (= A_3)$ in the direction of arrow 3. The next boundary crossing-point encountered will then be A_3 in the direction of arrow 4 and the string-run is closed. The string-run $A_1 - 1 - 2 - A_3$ and the string-run $A_1 - 3 - 4 - A_3$ can each have a maximum of $(2a - 1)$ bights, hence with the second string through the boundary crossing-points $A_2 = A_4$ the maximum number of bights through which these two strings pass is equal to $(8a - 4)$. Since the total number of bights is equal to $8a$, the braid thus requires more than two essential strings.

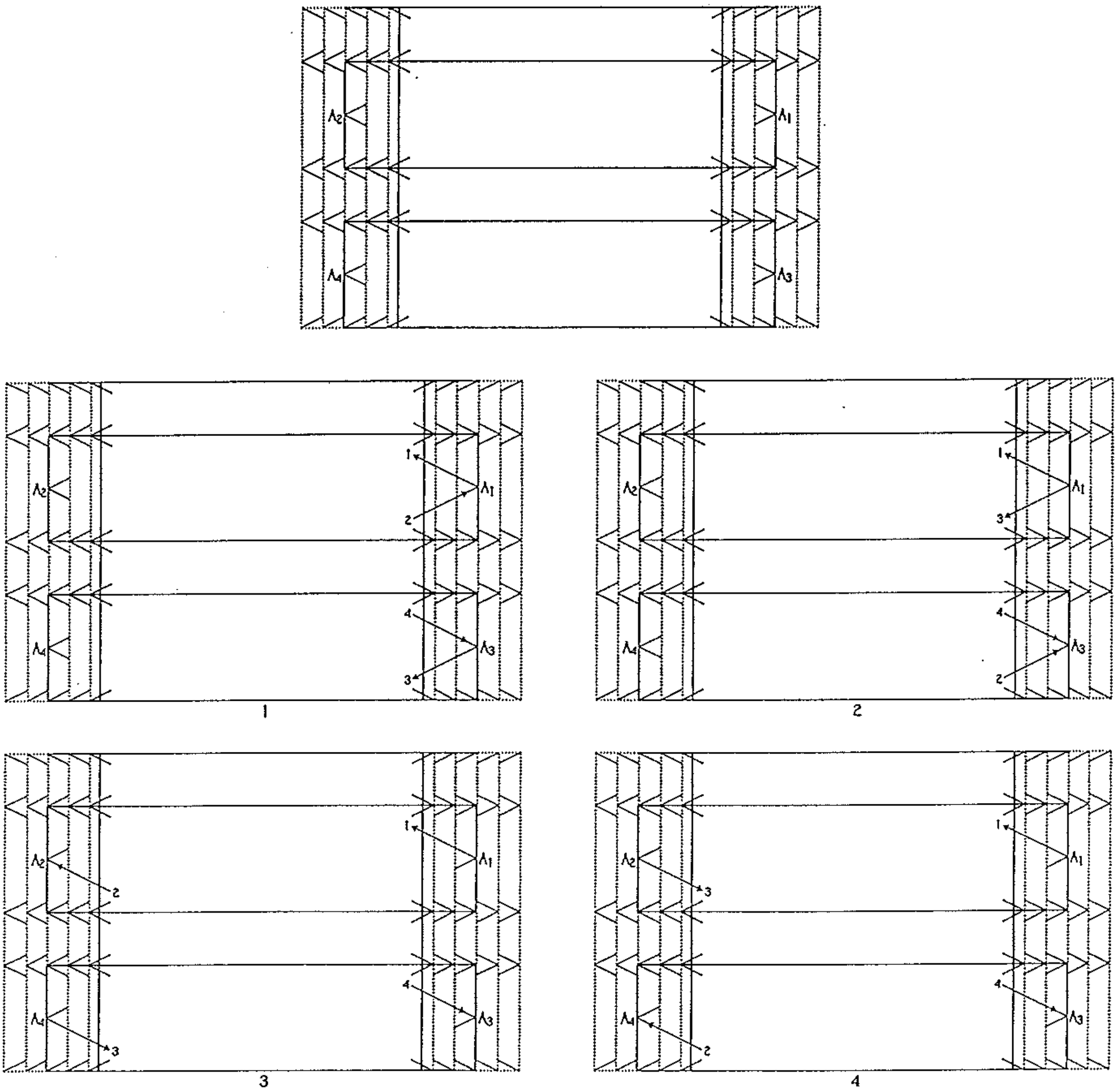

Fig. 676 — A generalised development of the string-run.

Let the string-run start in A_1 in the direction of arrow 1. After leaving boundary crossing-point A_1 let the first boundary crossing-point encountered by the string-run be A_2. Hence the string-run enters A_2 in the direction of arrow 2 (see diagram 3 in Fig. 676). The string then leaves boundary crossing-point A_4 (= A_2) in the direction of arrow 3. The next boundary crossing-point encountered will then be A_3 in the direction of arrow 4 and the string-run is closed. The string-run $A_1 - 1 - 2 - A_2$ and the string-run $A_4 - 3 - 4 - A_3$ can each have a maximum of $2a$ bights, hence with the second string through the boundary crossing-points $A_1 = A_3$ and $A_2 = A_4$ the maximum number of bights through which these two strings pass is equal to $8a$. Since the total number of bights is equal to $8a$, the braid thus requires a minimum of two essential strings.

Let the string-run start in A_1 in the direction of arrow 1. After leaving boundary crossing-point A_1 let the first boundary crossing-point encountered by the string-run be A_4. Hence the string-run enters A_4 in the direction of arrow 2 (see diagram 4 in Fig. 676). The string then leaves boundary crossing-point $A_2 (= A_4)$ in the direction of arrow 3. The next boundary crossing-point encountered will then be A_3 in the direction of arrow 4 and the string-run is closed. The string-run $A_1 - 1 - 2 - A_4$ and the string-run $A_2 - 3 - 4 - A_3$ can each have a maximum of $2a$ bights, hence with the second string through the boundary crossing-points $A_1 = A_3$ and $A_4 = A_2$ the maximum number of bights through which these two strings pass is equal to $8a$. Since the total number of bights is equal to $8a$, the braid thus requires a minimum of two essential strings.

Hence the Rectangular Right Prismatic Braids with one boundary crossing-point on each the left and the right face ($A_1 = A_3$ and $A_2 = A_4$) and requiring the minimum of two essential strings, have with regards the string-run at the boundary crossing-points a string-run diagram like diagram 3 or diagram 4 in Fig. 676.

A) The Rectangular Right Prismatic Braids

i) $(2n-1) \times (2n) \times [(2m-1)(4n-1)]$,
ii) $(2n-1) \times (2n) \times [(2m-2)(4n-1)+1]$,
iii) $(2n) \times (2n+1) \times [(2m-2)(4n+1)]$,
iv) $(2n) \times (2n+1) \times [(2m-1)(4n+1)+1]$,

where n and m are independent and have the values $1, 2, 3, \cdots$, have with regards the string-run at the boundary crossing-points a string-run diagram like diagram 3 in Fig. 676.

B) The Rectangular Right Prismatic Braids

i) $(2n-1) \times (2n) \times [(2m-1)(4n-1)+1]$,
ii) $(2n-1) \times (2n) \times [(2m-2)(4n-1)]$,
iii) $(2n) \times (2n+1) \times [(2m-2)(4n+1)+1]$,
iv) $(2n) \times (2n+1) \times [(2m-1)(4n+1)]$,

where n and m are independent and have the values $1, 2, 3, \cdots$, have with regards the string-run at the boundary crossing-points a string-run diagram like diagram 4 in Fig. 676.

Example 1 :

The two development methods for an over-under coded braid of the type A) — *i)* with $n = 1$ and $m = 1$ are depicted in Figs. 677 & 678.

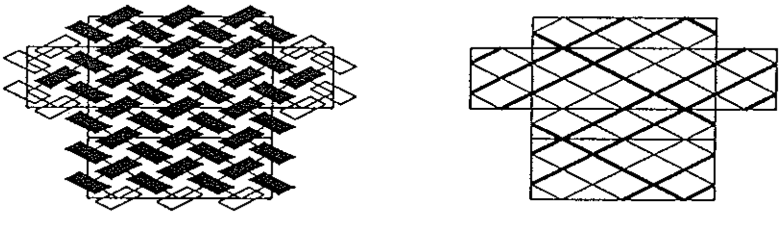

Fig. 677 — An over-under coded $1 \times 2 \times 3$ Rectangular Right Prismatic Braid.

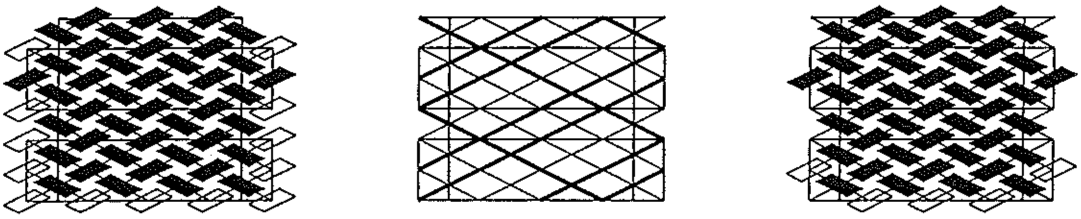

Fig. 678 — An over-under coded $1 \times 2 \times 3$ Rectangular Right Prismatic Braid.

Example 2:

The two development methods for an over-under coded braid of the type B) — *i*) with $n = 1$ and $m = 1$ are depicted in Figs. 679 & 680.

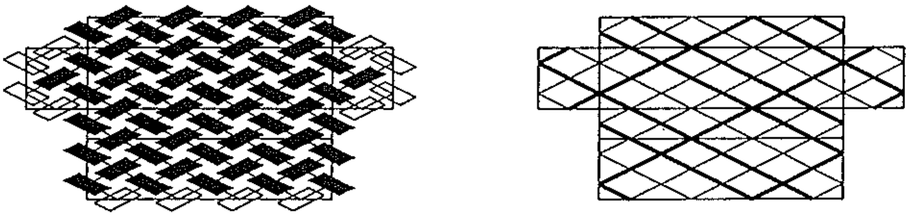

Fig. 679 — An over-under coded $1 \times 2 \times 4$ Rectangular Right Prismatic Braid.

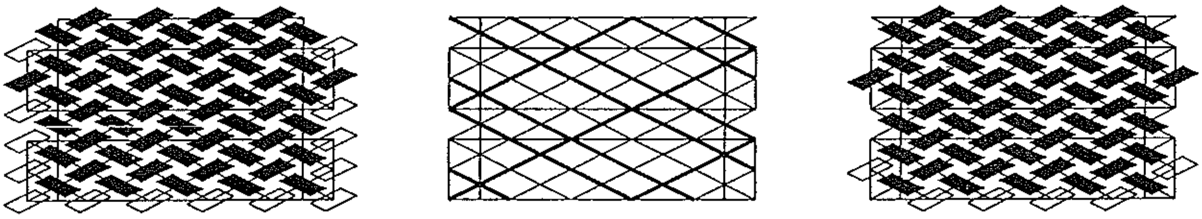

Fig. 680 — An over-under coded $1 \times 2 \times 4$ Rectangular Right Prismatic Braid.

Example 3:

The two development methods for an over-under coded braid of the type B) — *iv*) with $n = 1$ and $m = 1$ have already been depicted in Figs. 674 & 675.

Example 4:

The two development methods for an over-under coded braid of the type A) — *iv*) with $n = 1$ and $m = 1$ are depicted in Figs. 681 & 682.

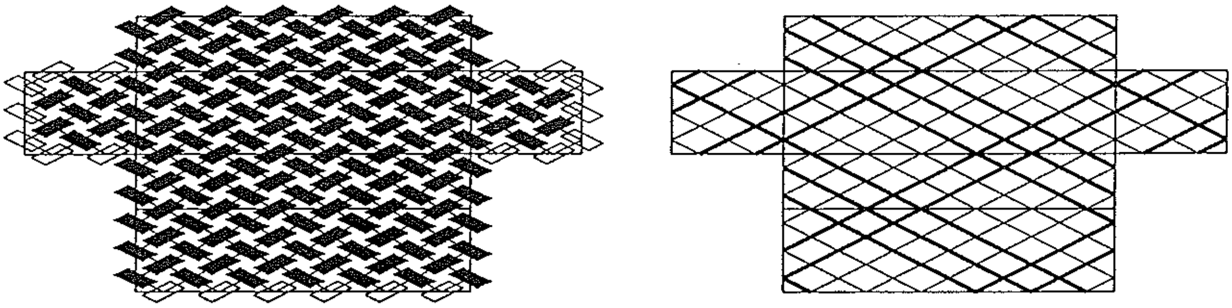

Fig. 681 — An over-under coded $2 \times 3 \times 6$ Rectangular Right Prismatic Braid.

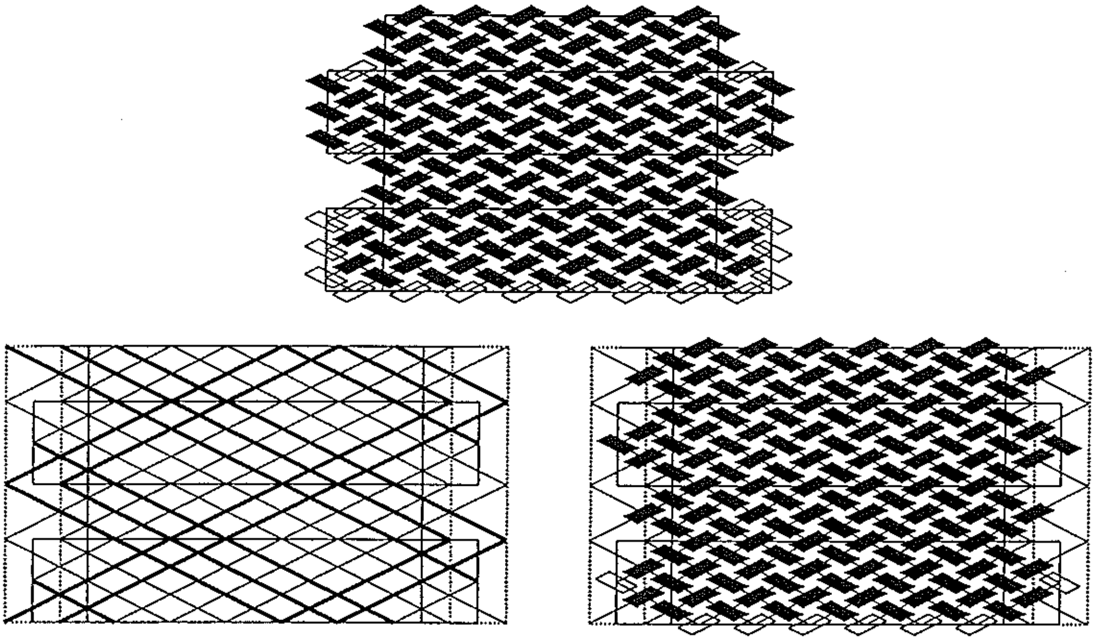

Fig. 682 — An over-under coded $2 \times 3 \times 6$ Rectangular Right Prismatic Braid.

Example 5 :

The two development methods for an over-under coded braid of the type A) — *iv*) with $n = 2$ and $m = 1$ are depicted in Figs. 683 & 684.

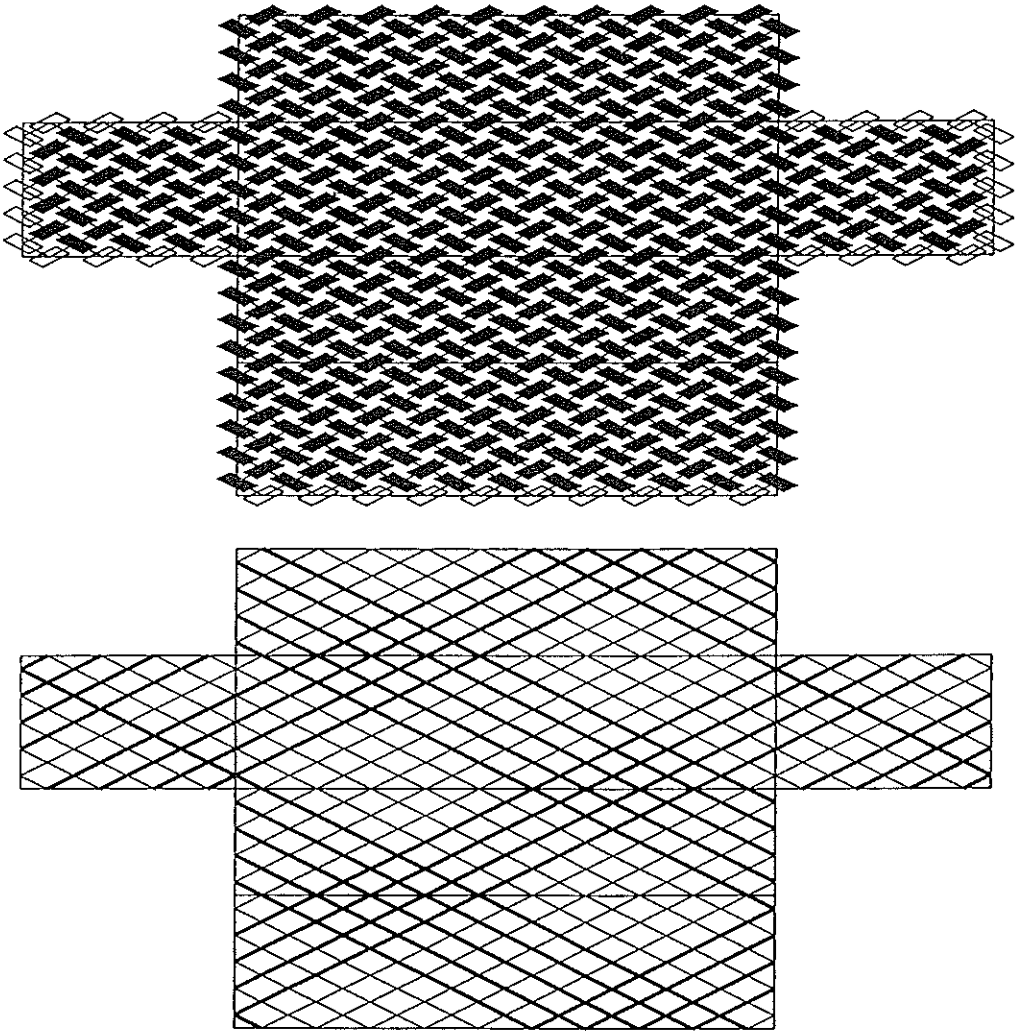

Fig. 683 — An over-under coded $4 \times 5 \times 10$ Rectangular Right Prismatic Braid.

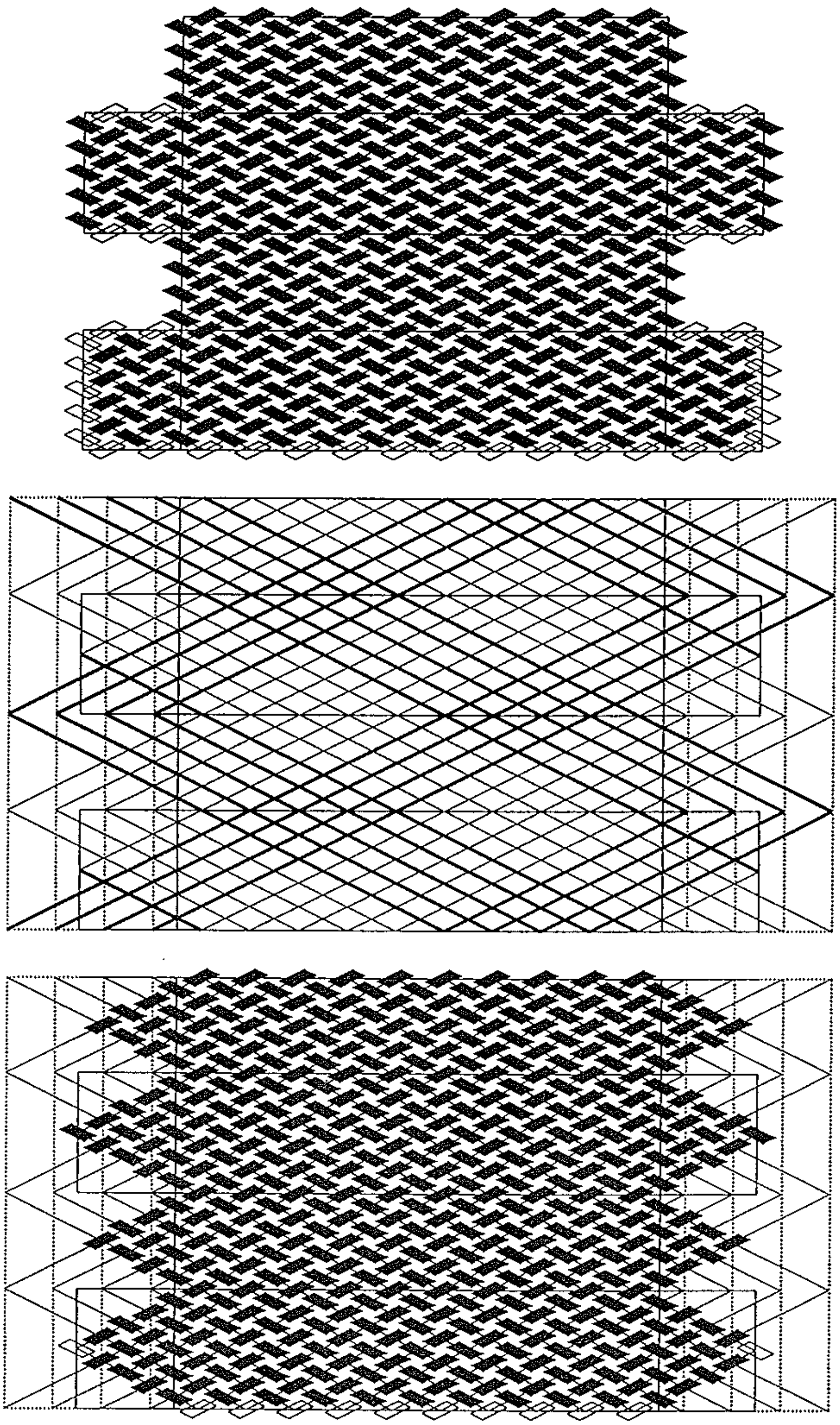

Fig. 684 — An over-under coded $4 \times 5 \times 10$ Rectangular Right Prismatic Braid.

Example 6 :

The string-run of the type A)—i) with $n = 2$ and $m = 1$, B)—ii) with $n = 2$ and $m = 2$, B)—i) with $n = 2$ and $m = 1$, A)—ii) with $n = 2$ and $m = 2$, are respectively depicted in Fig. 685.

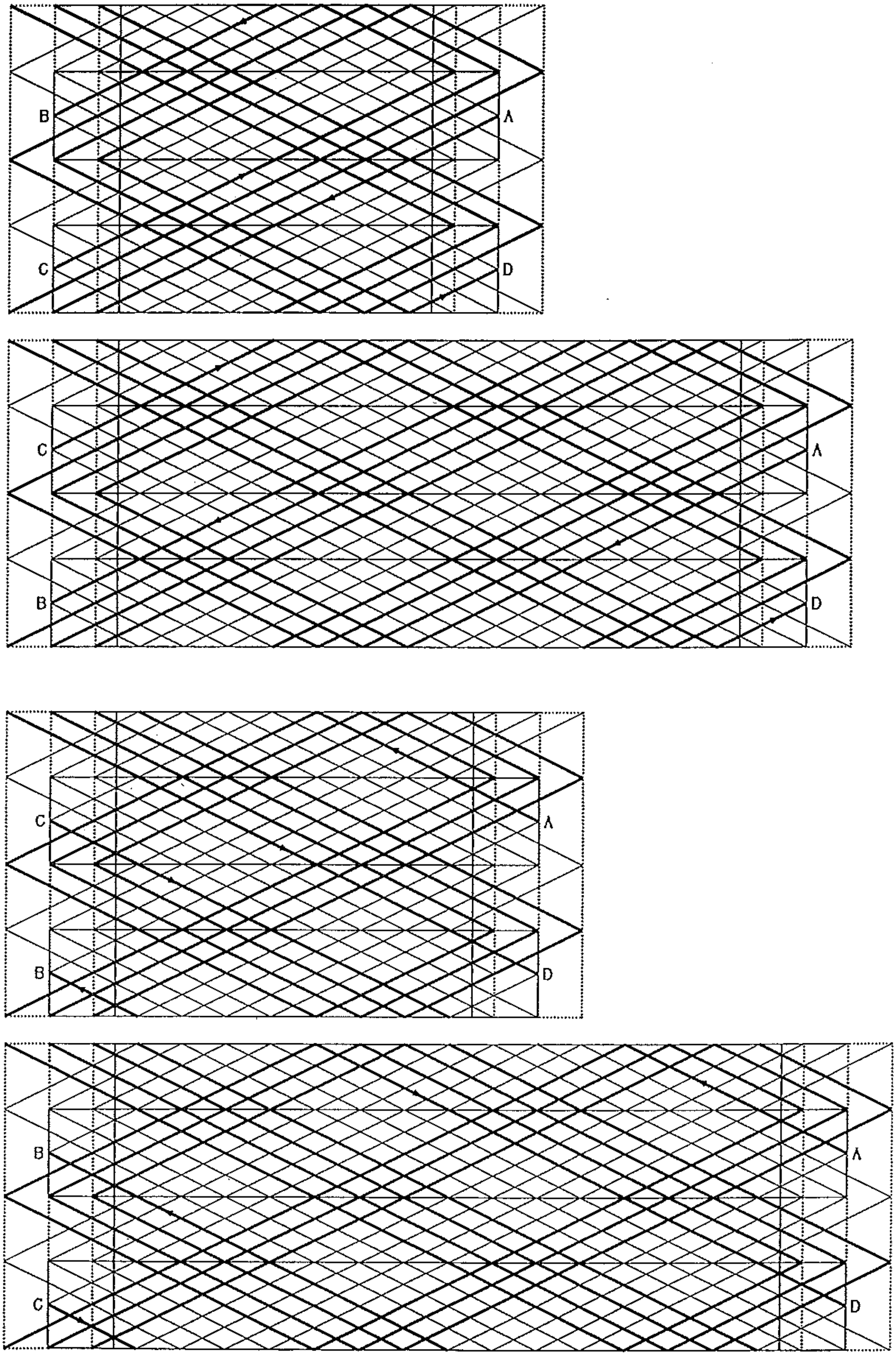

Fig. 685 — The respective string-runs of the Rectangular Right Prismatic Braids $3 \times 4 \times 7$, $3 \times 4 \times 14$, $3 \times 4 \times 8$, $3 \times 4 \times 15$.

Example 7:

The two development methods for an $1 \times 3 \times 4$ over-under coded Rectangular Right Prismatic Braid are depicted in Figs. 686 & 687.

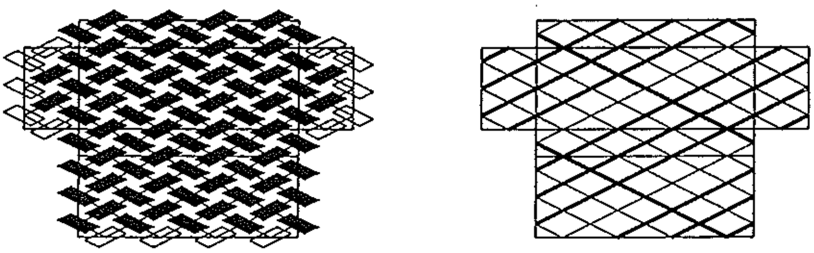

Fig. 686 — An over-under coded $1 \times 3 \times 4$ Rectangular Right Prismatic Braid.

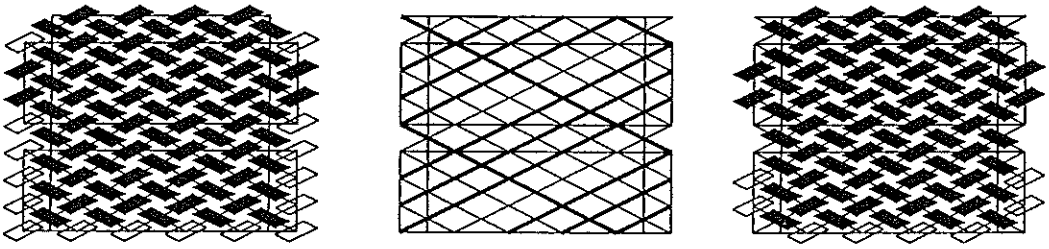

Fig. 687 — An over-under coded $1 \times 3 \times 4$ Rectangular Right Prismatic Braid.

This braid is of course identical to the identically coded $3 \times 4 \times 1$ Rectangular Right Prismatic Braid, hence its string-run is of the type A)—*ii*) with $n = 2$ and $m = 1$; its two developments are shown in Figs. 688 & 689.

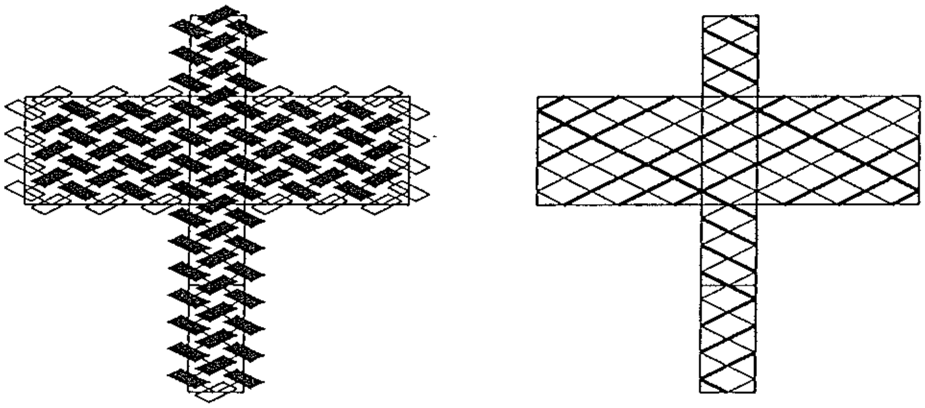

Fig. 688 — An over-under coded $3 \times 4 \times 1$ Rectangular Right Prismatic Braid.

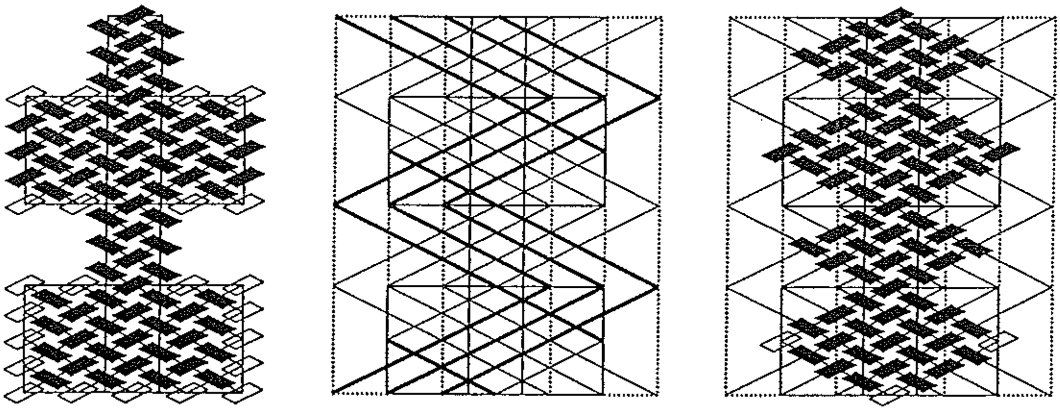

Fig. 689 — An over-under coded $3 \times 4 \times 1$ Rectangular Right Prismatic Braid.

The string-run diagrams, and hence the grid-diagrams, of the previous Examples 1-7 could be drawn with one boundary crossing-point on the left and the right bight-edge each. This will only be possible when for the Rectangular Right Prismatic Braid with sides a, b and c the difference between two of these sides is equal to 1. In the more general case, where there are no two sides which differ by 1, this will not be possible. The string-run of the over-under coded $3 \times 5 \times 8$ Rectangular Right Prismatic Braid in Example 8 requires again a minimum of two strings (the heavy lined string-run is the string-run of one of these two essential strings) but its string-run can be drawn with a minimum of two boundary crossing-points on the left and the right bight-edge each.

A rectangular box (a rectangular right prism) can be developed in six ways by the conventional development method and hence also in six ways by our special development method. For our special development method this has been shown in Example 9, Figs. 692-697, for a Rectangular Right Prismatic Braid which again requires two essential strings.

Example 8:

The two developments for an over-under coded $3\times5\times8$ Rectangular Right Prismatic Braid are depicted in Figs. 690 & 691.

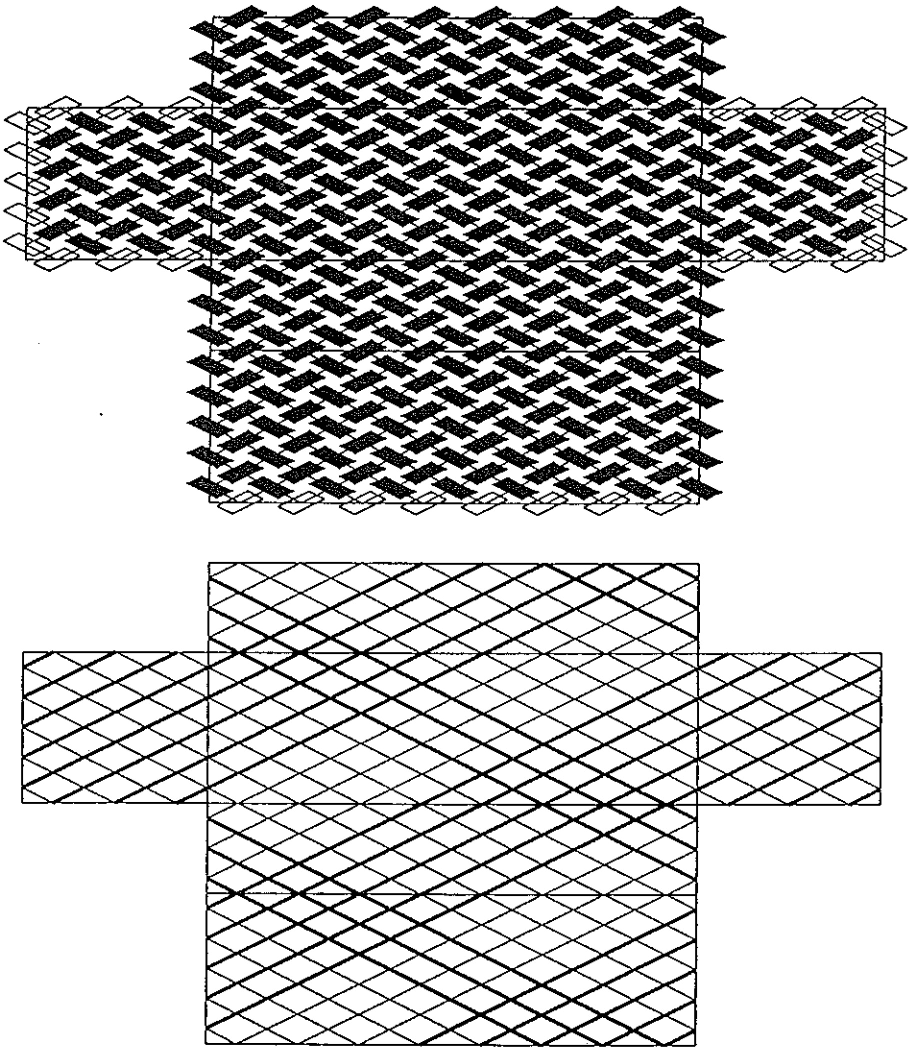

Fig. 690 — An over-under coded $3 \times 5 \times 8$ Rectangular Right Prismatic Braid.

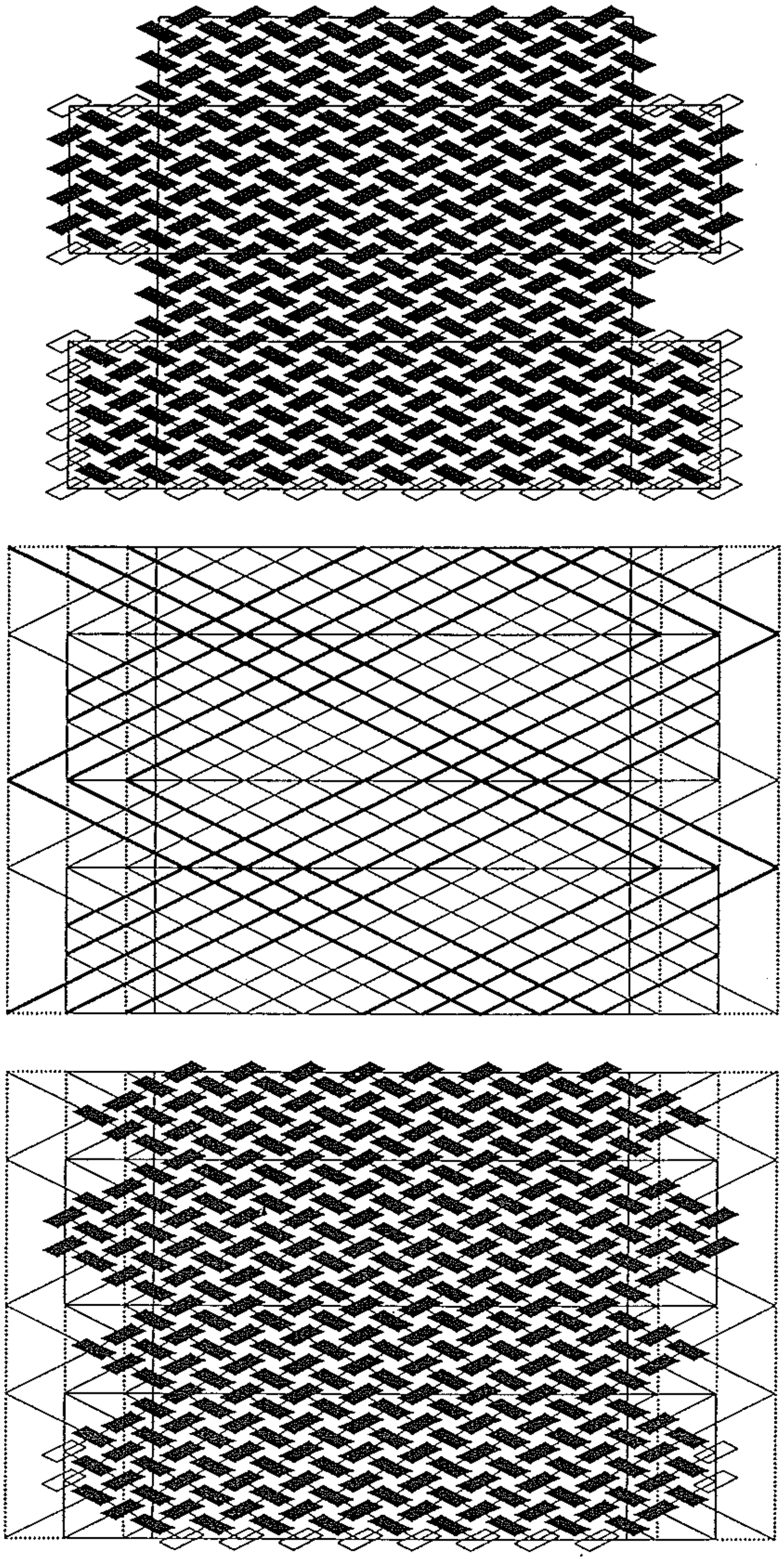

Fig. 691 — An over-under coded $3 \times 5 \times 8$ Rectangular Right Prismatic Braid.

Example 9 :

The six special developments for the string-run of a Rectangular Right Prismatic Braid with sides 3 , 8 and 11 are depicted in Figs. 692-697. Since all these six string-runs are the string-runs of the same braid, some braiders may prefer to use in the actual construction of the braid the string-run with the minimum number of boundary cossing-points, while others may prefer the string-run with the minimum number of nested bights in each nest.

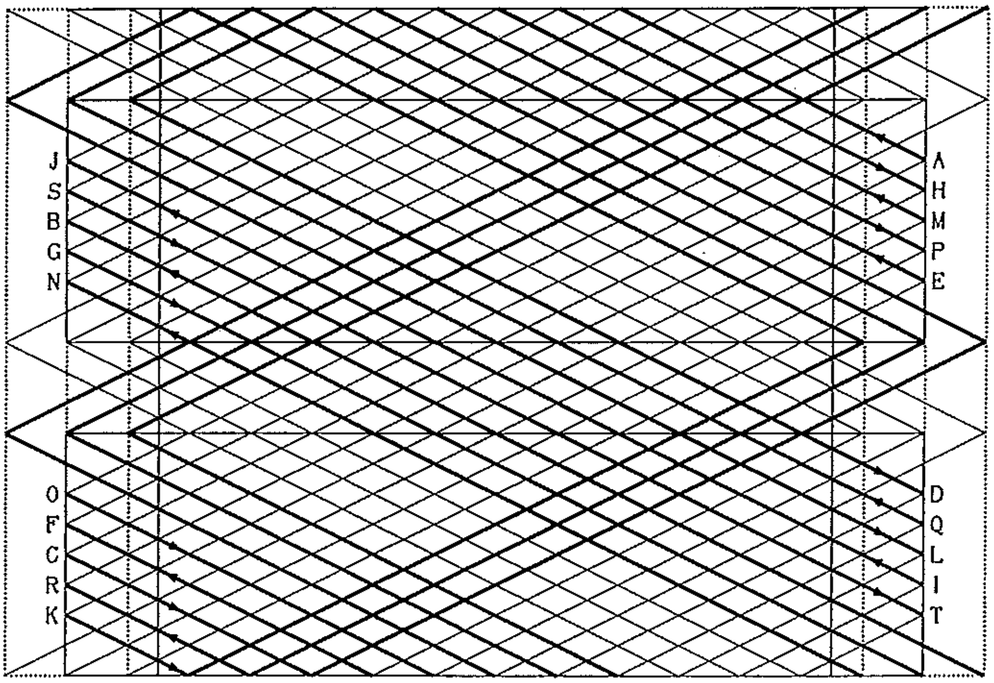

Fig. 692 — The string-run of a 3 × 8 × 11 Rectangular Right Prismatic Braid.

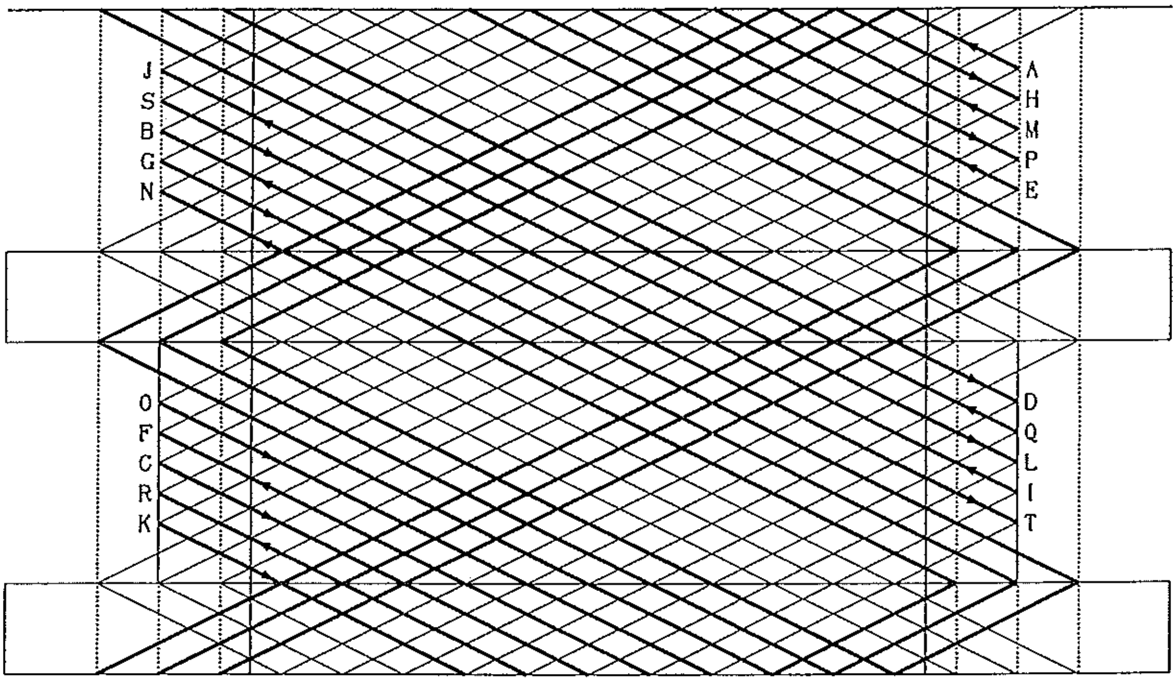

Fig. 693 — The string-run of an 8 × 3 × 11 Rectangular Right Prismatic Braid.

The string-runs in the string-run diagrams of Figs. 692 and 693 have five boundary crossing-points on the left and right bight-edge each. This number of boundary crossing-points is the absolute value of the difference between the sides 3 and 8 ($|8-3| = 5$, $|3-8| = 5$).

Note that the string-run diagrams in Figs. 692 and 693 are in fact identical and only differ in the development, and hence the position, of the rectangular surfaces of the Rectangular Right Prismatic Braid. The same applies to the string-run diagrams in Figs. 694 and 695, as well as to the string-run diagrams in Figs. 696 and 697.

Note furthermore that in the string-run diagrams of Figs. 692 and 693 the sum of **bights per nest** and **boundary crossing-points per bight-edge** equals $3 + 5 = 8$.

The three boundary crossing-points on the left and right bight-edge each in the string-run diagrams of Figs. 694 and 695 are the absolute value of the difference between the sides 8 and 11 ($|11 - 8| = 3$, $|8 - 11| = 3$).

Note that in the string-run diagrams of Figs. 694 and 695 the sum of **bights per nest** and **boundary crossing-points per bight-edge** equals $8 + 3 = 11$.

Since three boundary crossing-points on the left and right bight-edge each is the minimum number for this braid, some braiders may in the actual braiding process prefer to use the string-runs depicted in Figs. 694 and 695 for this Rectangular Right Prismatic Braid.

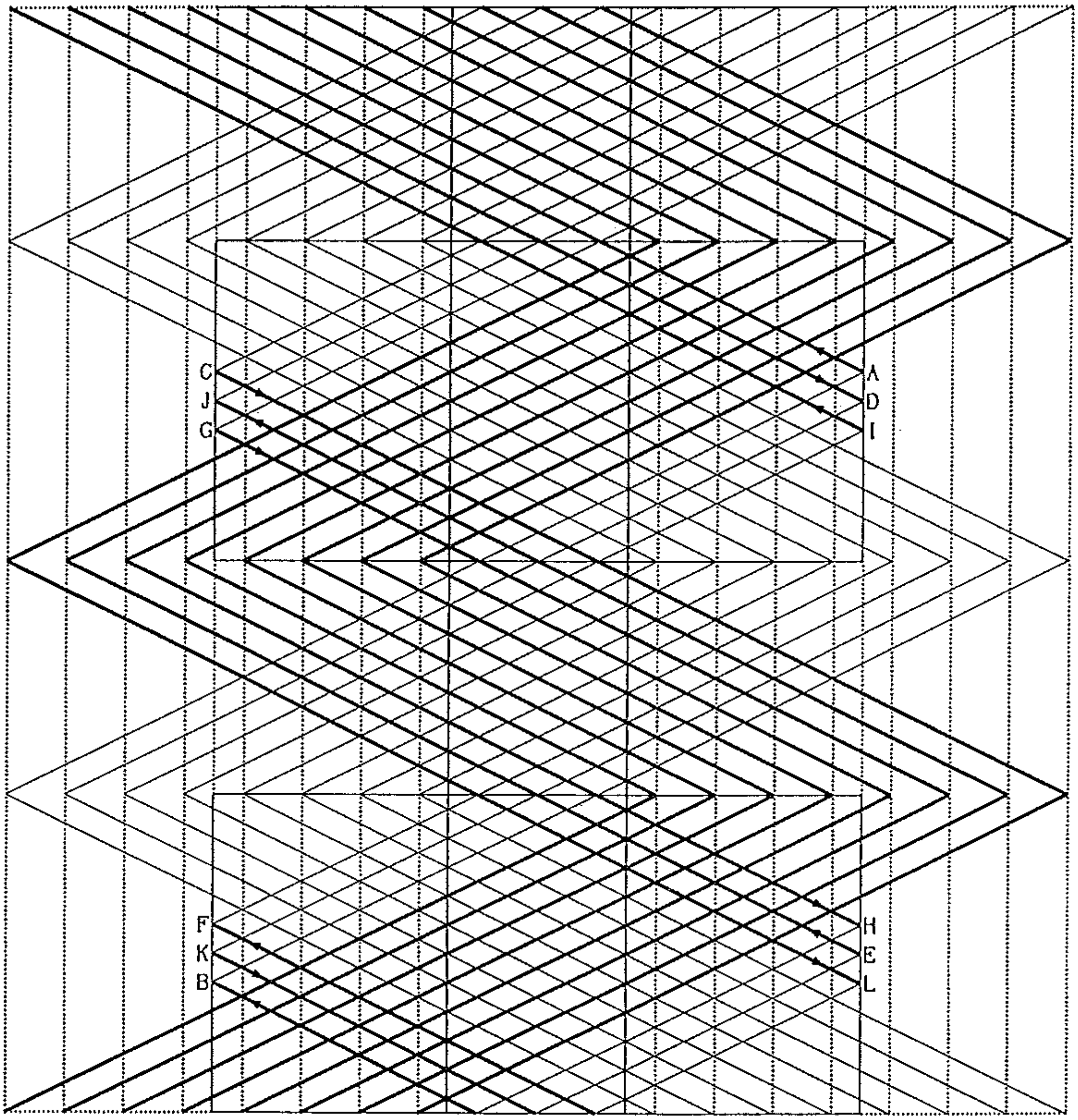

Fig. 694 — The string-run of an 8 × 11 × 3 Rectangular Right Prismatic Braid.

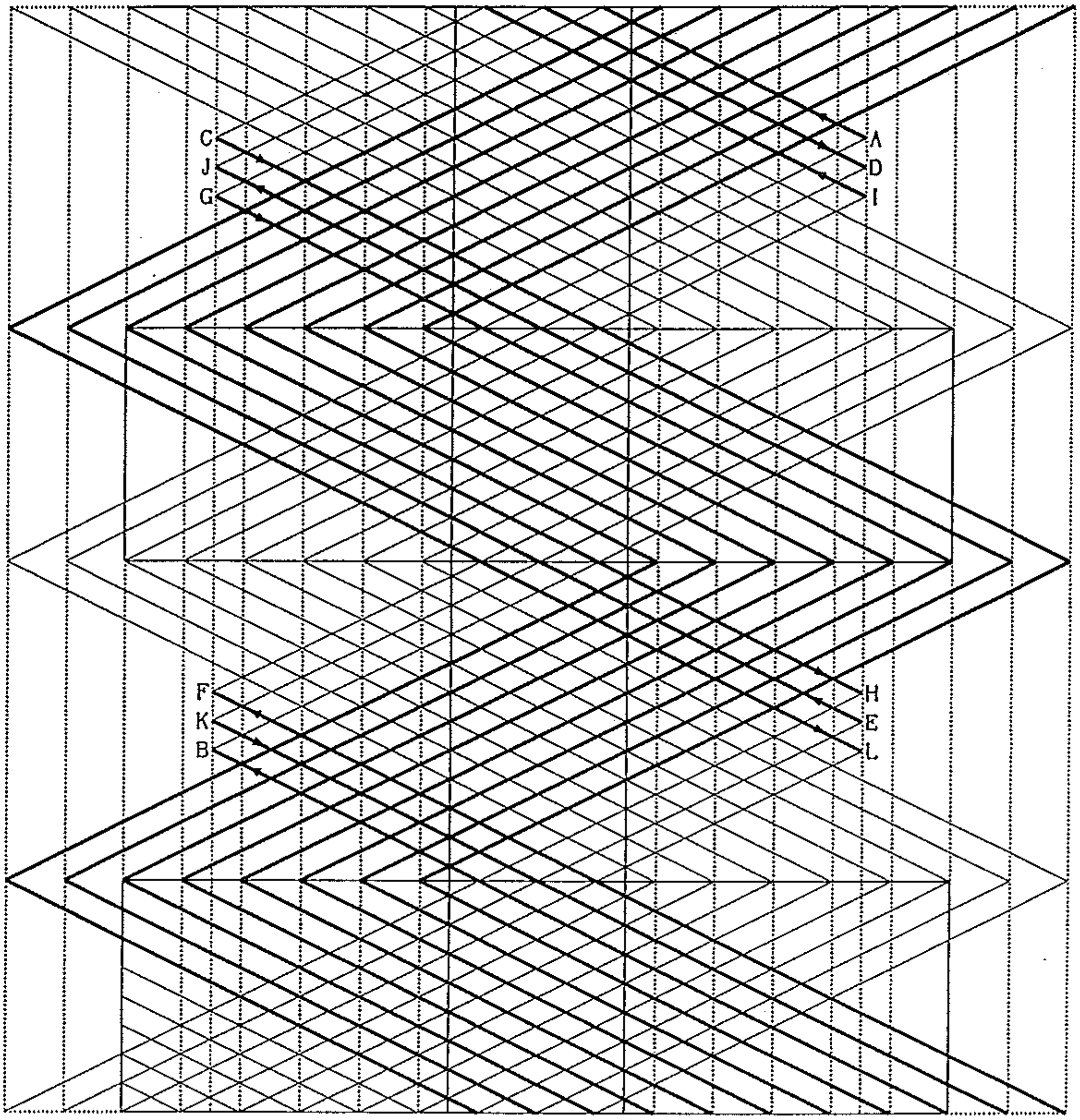

Fig. 695 — The string-run of an 11 × 8 × 3 Rectangular Right Prismatic Braid.

The eight boundary crossing-points on the left and right bight-edge each in the string-run diagrams of Figs. 696 and 697 are the absolute value of the difference between the sides 3 and 11 ($(|11-3| = 8\ ,\ |3-11| = 8)$).

Note that in the string-run diagrams of Figs. 696 and 697 the sum of **bights per nest** and **boundary crossing-points per bight-edge** equals $3 + 8 = 11$.

In the actual braiding process of this Rectangular Right Prismatic Braid we would not use the string-runs depicted in Figs. 696 and 697 since the number of bights per nest is the same as in the string-runs of Figs. 692 and 693, but the number of boundary crossing-points is eight per bight-edge against only five in the string-runs of Figs. 692 and 693.

The string-runs in Figs. 692 and 693 present a compromise between the minimum number of boundary crossing-points per bight-edge and the minimum number of bights per nest; their sum [(bights per nest) + (boundary crossing-points per bight-edge)] is a minimum.

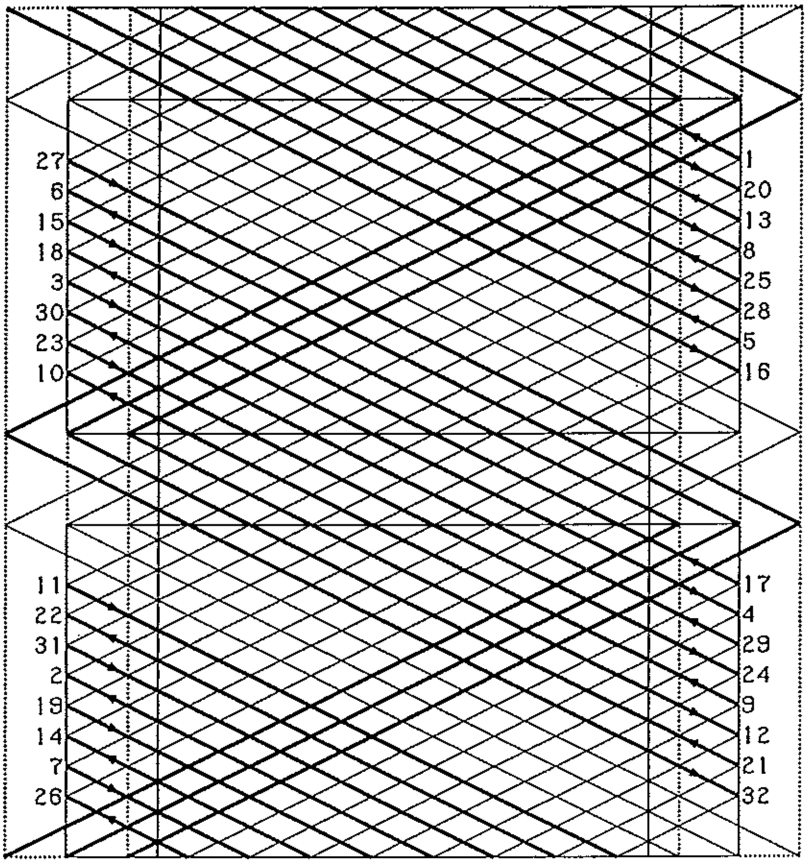

Fig. 696 — The string-run of a 3 × 11 × 8 Rectangular Right Prismatic Braid.

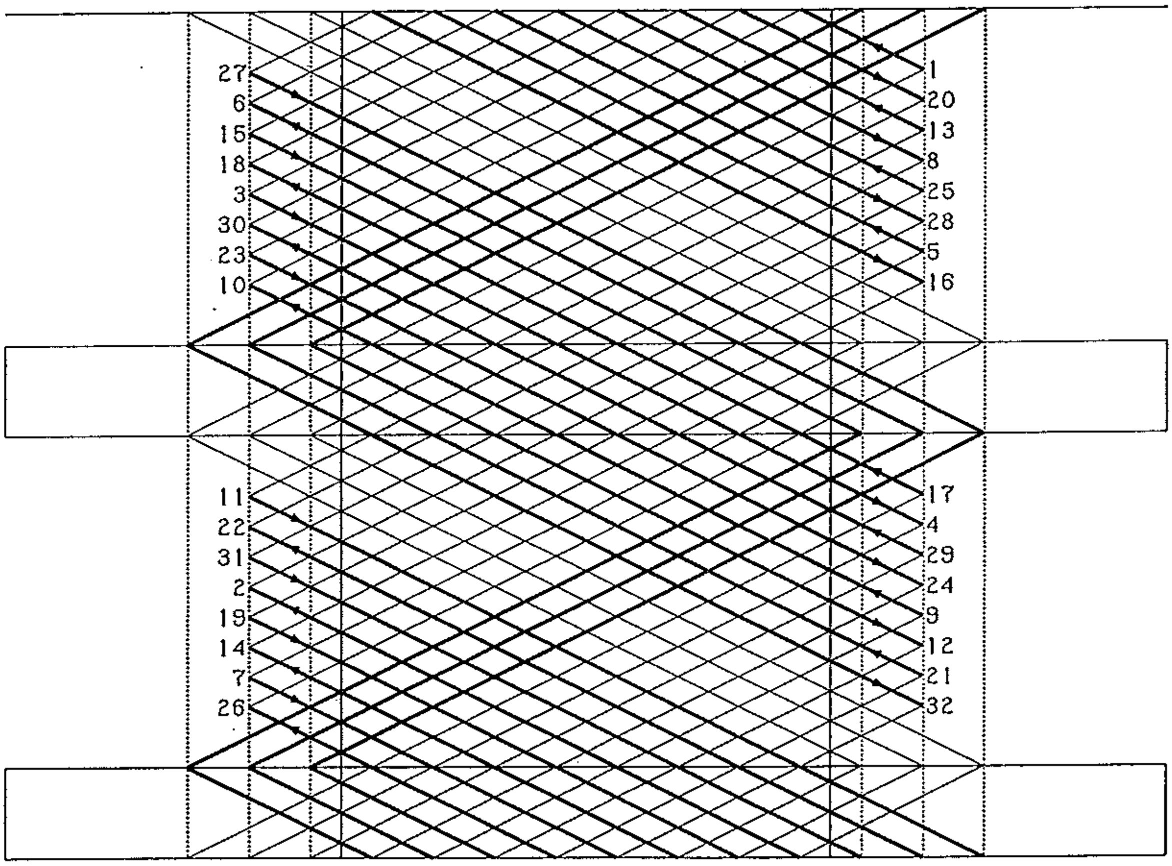

Fig. 697 — The string-run of an 11 × 3 × 8 Rectangular Right Prismatic Braid.

Special Rectangular Right Prismatic Braids are those which have two equal sides. They have a string-run diagram which can be drawn as $a \times a \times c$, as $a \times c \times a$ or as $c \times a \times a$; the last two are identical if we don't represent in these diagrams the development of the surfaces. We have already met earlier[†] the string-run diagram drawn as $a \times a \times c$ as a string-run diagram of a **Regular Nested Cylindrical Braid** with $A = a$; $x = 2c + 2$; $y = 0$; $B^* = 4$.

From the (A, x, y)-tables of these braids, it immediately follows that for $y = 0$ the only braids with a minimum of two essential strings are the braids with $A = 1$ and $x = 4n + 2$, where $n = 0, 1, 2, 3, \cdots$. Since $x = 2c + 2$, it follows that the only $a \times a \times c$ Rectangular Right Prismatic Braids with a minimum of two essential strings are the ones with $a = 1$ and $c = 2n$, where $n = 0, 1, 2, 3, \cdots$.

In order for the reader to fully understand the two types of string-run diagrams $a \times a \times c$, and $a \times c \times a$ or $c \times a \times a$, we have depicted in Figs. 698 and 699 the string-runs for respectively the $3 \times 11 \times 3$ Rectangular Right Prismatic Braid and the $3 \times 3 \times 11$ Rectangular Right Prismatic Braid. Note that these braids are of course identical and have the components 2×10 and 1×8 (which follows immediately from the $(3, x, y)$-table for $x = 2c + 2 = 24$ and $y = 0$). Since g.c.d.$(10, B^*) =$ g.c.d.$(10, 4) = 2$, the component with $P_c = 10$ requires 2 essential strings (hence the two components with $P_c = 10$ require 4 essential strings), and since g.c.d.$(8, B^*) =$ g.c.d.$(8, 4) = 4$, the component with $P_c = 8$ requires 4 essential strings (hence the one component with $P_c = 8$ requires 4 essential strings); thus in total the braid requires $4 + 4 = 8$ essential strings.

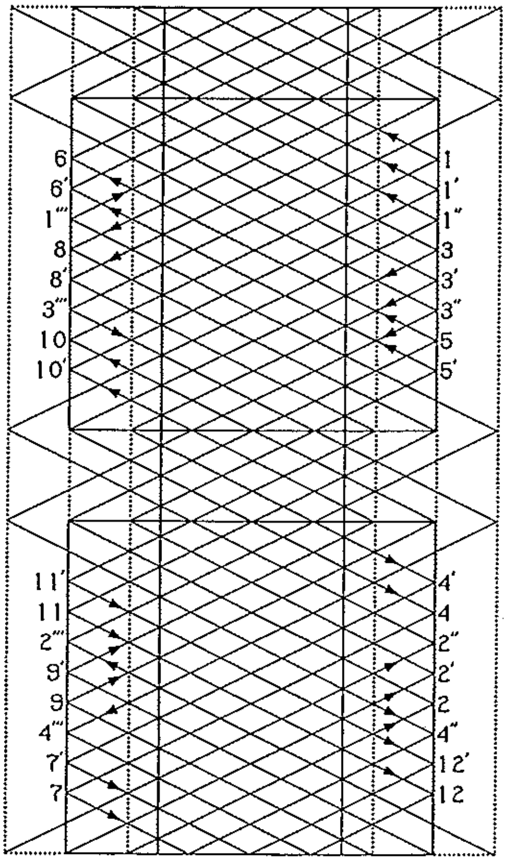

Fig. 698 — The string-run diagram of a $3 \times 11 \times 3$ Rectangular Right Prismatic Braid.

[†] See *The Braider*, Issue No. 25.

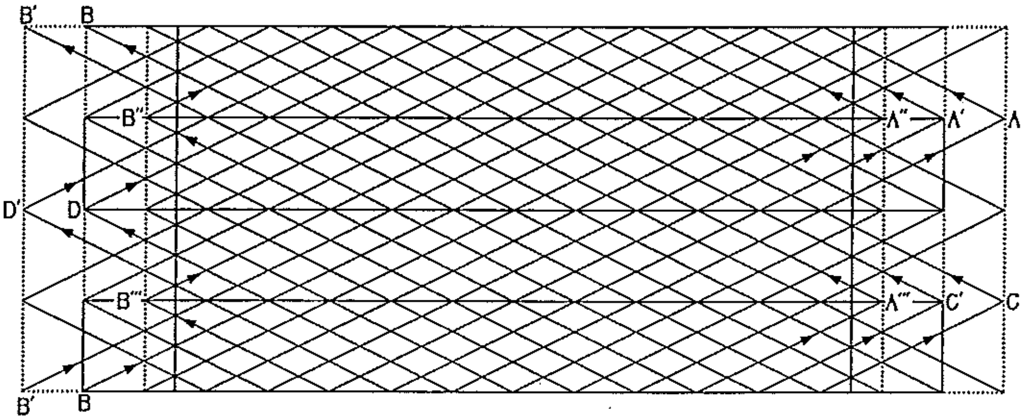

Fig. 699 — The string-run diagram of a $3 \times 3 \times 11$ Rectangular Right Prismatic Braid.

An example of the string-run diagram of a $c \times a \times a$ Rectangular Right Prismatic Braid with $a = 3$ and $c = 12$ is shown in Fig. 700. From the $(3, x, y)$-table for $x = 2c + 2 = 26$ and $y = 0$ it follows that this braid has the components 3×10 (3 components with $P_c = 10$ each), hence it requires six essential strings.

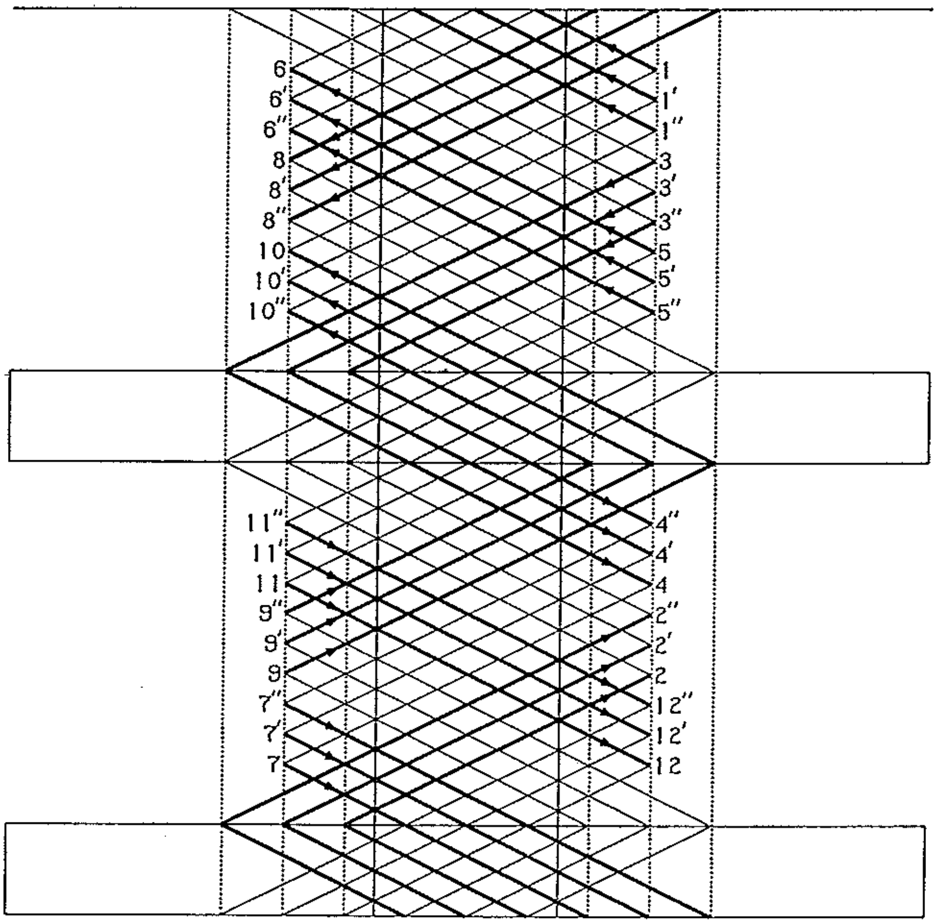

Fig. 700 — The string-run diagram of a $12 \times 3 \times 3$ Rectangular Right Prismatic Braid.

For the determination of the values a, b and c in the $a \times b \times c$ Rectangular Right Prismatic Braids, we shall restrict our further discussion here to $a \times b \times c$ Rectangular Right Prismatic Braids which require two essential strings in their construction.

From the string-run diagrams associated with our special development method it follows that if a Rectangular Right Prismatic Braid $a \times b \times c$ requires two essential strings only, then the Rectangular Right Prismatic Braid $a \times b \times \{c + n(a + b)\}$, where $n = 1, 2, 3, \cdots$, requires only two essential strings as well.

A special limit case of the $a \times b \times c$ Rectangular Right Prismatic Braid is where $c = 0$. Since the string-run of this braid is identical to the string-run of the $0 \times a \times b$ Rectangular Right Prismatic Braid, the string-run of a $0 \times a \times b$ Rectangular Right Prismatic Braid is equivalent to the string-run of an $a \times b \times 0$ Rectangular Right Prismatic Braid. The string-run in the left-hand diagram of Fig. 701 depicts an example where $a = 3$ and $b = 7$.

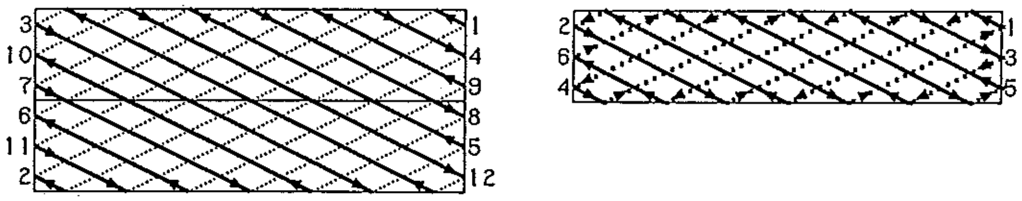

Fig. 701 — The string-run of a $0 \times 3 \times 7$ Rectangular Right Prismatic Braid.

Note that in this diagram there are no nests with bights (indicated by the lowest of the two values 0 and 3, hence 0 bights in the nests, hence no nests with bights, consequently bight-edges with no bights), and that there are $|3 - 0| = 3$ boundary crossing-points on the bight-edges with zero bights. Thus on the right-hand bight-edge point 1 is point 12, point 4 is point 5 and point 9 is point 8, while on the left-hand bight-edge point 3 is point 2, point 10 is point 11 and point 7 is point 6. In Fig. 701 crossing point 1 in the right-hand diagram is crossing-point $1 = 12$ in the left-hand diagram, crossing point 3 in the right-hand diagram is crossing-point $4 = 5$ in the left-hand diagram, crossing point 5 in the right-hand diagram is crossing-point $9 = 8$ in the left-hand diagram, crossing point 2 in the right-hand diagram is crossing-point $3 = 2$ in the left-hand diagram, crossing point 6 in the right-hand diagram is crossing-point $10 = 11$ in the left-hand diagram, crossing point 4 in the right-hand diagram is crossing-point $7 = 6$ in the left-hand diagram. Note that in Fig. 701 the heavy lines depict in the left-hand diagram half the total string-run, and that in the right-hand diagram the heavy lines together with the dotted heavy lines depict half the total string-run.

The right-hand diagram of Fig, 701 can be compared with the string-run of a **Regular Rectangular Mat.** The difference is that the number of essential strings in this right-hand diagram of Fig. 701 is twice the number of essential strings in its Regular Rectangular Mat counter part. Thus we have here a simple method for determining the number of essential stings in an $a \times b \times 0$ Rectangular Right Prismatic Braid, namely the number of essential strings in an $a \times b \times 0$ Rectangular Right Prismatic Braid is equal to twice the number of essential strings in a Regular Rectangular Mat with b bights horizontal and a bights vertical. We have seen in *The Braider*, Issue No. 10 that such a Regular Rectangular Mat can be converted into a **Regular Cylindrical Braid** with b parts and a bights. Hence for the $a \times b \times 0$ Rectangular Right Prismatic Braid to require two essential strings only, the condition $\text{g.c.d.}(a, b) = 1$ must apply; in other words: a and b must be coprime.

The string-run diagrams associated with our special development method have already disclosed that if a Rectangular Right Prismatic Braid $a \times b \times c$ requires two essential strings only, the Rectangular Right Prismatic Braid $a \times b \times \{c + n(a + b)\}$, where $n = 1, 2, 3, \cdots$, requires only two essential strings as well (see top of this page).

Furthermore, these string-run diagrams clearly show that for $|a-b|+1 \leq c \leq a+b-1$, the string-run requires more than two essential strings.

⋆⋆ *Show how this last statement is derived from these string-run diagrams.*

In order to determine whether or not an $a \times b \times c$ Rectangular Right Prismatic Braid requires only two essential strings, we can employ the following method:

Let the values for a and b be given. We have then to determine which values for c will give us a Rectangular Right Prismatic Braid which requires two essential strings only. Since we can use the relationship:
if an $a \times b \times c$ Rectangular Right Prismatic Braid requires two essential strings only, then an $a \times b \times \{c+n(a+b)\}$ Rectangular Right Prismatic Braid, where $n=1,2,3,\cdots$, also requires two essential strings only,
we can restrict our basic c-value determination to $0 \leq c \leq |a-b|$. Recall that for $|a-b|+1 \leq c \leq a+b-1$, the two essential strings only condition is not being fulfilled.

Example 10:

Does the $3 \times 11 \times 16$ Rectangular Right Prismatic Braid require two essential strings only? What are the basic values for c which would give a two essential string $3 \times 11 \times c$ Rectangular Right Prismatic Braid?

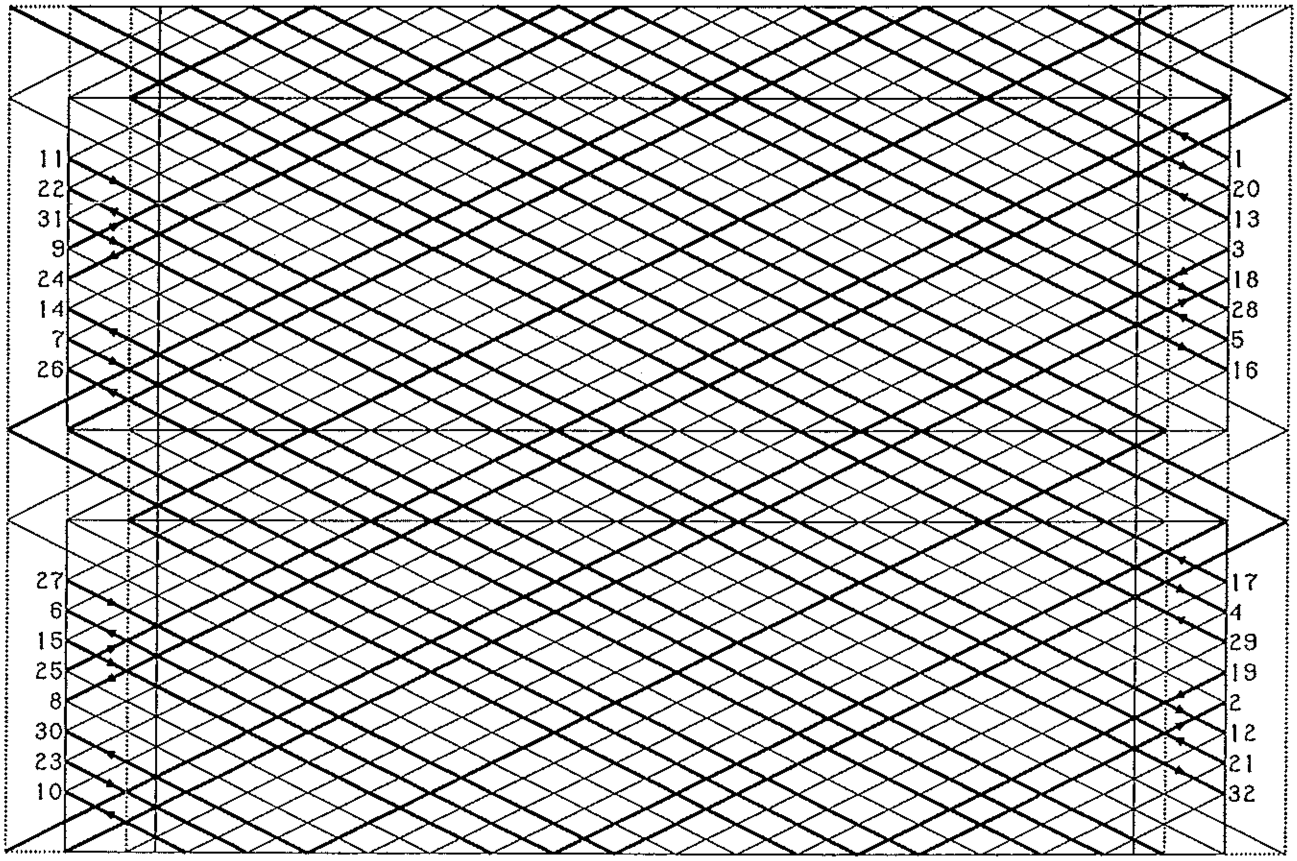

Fig. 702 — The string-run of a $3 \times 11 \times 16$ Rectangular Right Prismatic Braid.

Although we have already shown in Fig. 702 the string-run of a $3 \times 11 \times 16$ Rectangular Right Prismatic Braid, and from this string-run we can determine that it indeed requires two essential strings only, we would of course first have ensured via the calculations below, in which we can restrict the basic c-values to $0 \leq c \leq |3-11|$, hence to $0 \leq c \leq 8$, that this was the case.

3 and 11 are coprime, hence $3\times 11\times 0$ fulfills the two essential strings only condition.

$3\times 11\times 1$ is identical to $1\times 3\times 11$, which reduces to $1\times 3\times 3$ $(c-2(a+b)=11-2(1+3)=3)$. Since this braid contains two identical sides other than 1 with a third side other than 0, the braid requires more than two essential strings. Consequently, the braid $3\times 11\times 1$ does not fulfil the two essential strings only condition.

$3\times 11\times 2$ is identical to $2\times 3\times 11$, which reduces to $2\times 3\times 1$ $(c-2(a+b)=11-2(2+3)=1)$. $2\times 3\times 1$ is identical to $1\times 2\times 3$, which reduces to $1\times 2\times 0$ $(c-1(a+b)=3-1(1+2)=0)$, and since 1 and 2 are coprime, the $1\times 2\times 0$ fulfills the two essential strings only condition. Consequently, the braid $3\times 11\times 2$ fulfills the two essential strings only condition.

$3\times 11\times 3$ contains two identical sides other than 1 with a third side other than 0, hence the braid requires more than two essential strings. Hence the braid $3\times 11\times 1$ does not fulfil the two essential strings only condition.

$3\times 11\times 4$ is identical to $3\times 4\times 11$, which reduces to $3\times 4\times 4$ $(c-1(a+b)=11-1(3+4)=4)$. $3\times 4\times 4$ contains two identical sides other than 1 with a third side other than 0, hence the braid requires more than two essential strings. Hence the braid $3\times 11\times 4$ does not fulfil the two essential strings only condition.

$3\times 11\times 5$ is identical to $3\times 5\times 11$, which reduces to $3\times 5\times 3$ $(c-1(a+b)=11-1(3+5)=3)$. $3\times 11\times 3$ contains two identical sides other than 1 with a third side other than 0, hence the braid requires more than two essential strings. Hence the braid $3\times 11\times 5$ does not fulfil the two essential strings only condition.

$3\times 11\times 6$ is identical to $3\times 6\times 11$, which reduces to $3\times 6\times 2$ $(c-1(a+b)=11-1(3+6)=2)$. $3\times 6\times 2$ is identical to $2\times 3\times 6$, which reduces to $2\times 3\times 1$ $(c-1(a+b)=6-1(2+3)=1)$. $2\times 3\times 1$ is identical to $1\times 2\times 3$, which reduces to $1\times 2\times 0$ $(c-1(a+b)=3-1(1+2)=0)$, and since 1 and 2 are coprime, the $1\times 2\times 0$ fulfills the two essential strings only condition. Consequently, the braid $3\times 11\times 6$ fulfills the two essential strings only condition.

$3\times 11\times 7$ is identical to $3\times 7\times 11$, which reduces to $3\times 7\times 1$ $(c-1(a+b)=11-1(3+7)=1)$. $3\times 7\times 1$ is identical to $1\times 3\times 7$, which reduces to $1\times 3\times 3$ $(c-1(a+b)=7-1(1+3)=3)$. $1\times 3\times 3$ contains two identical sides other than 1 with a third side other than 0, hence the braid requires more than two essential strings. Hence the braid $3\times 11\times 7$ does not fulfil the two essential strings only condition.

$3\times 11\times 8$: since 3 and 8 are coprime, $3\times 8\times 0$ fulfills the two essential strings only condition and consequently so does $3\times 8\times 11$ $(c+n(a+b)=0+1(3+8)=11)$. $3\times 8\times 11$ is identical to $3\times 11\times 8$, hence $3\times 11\times 8$ fulfills the two essential strings only condition.

Since $3\times 11\times 2$ fulfills the two essential strings only condition, so does $3\times 11\times 16$ $(c+n(a+b)=2+1(3+11)=16)$ fulfil the two essential strings only condition.

The basic values for c which would give a two essential string $3\times 11\times c$ Rectangular Right Prismatic Braid are 0, 2, 6 and 8.

Example 11:

Does the $7\times 10\times 2$ Rectangular Right Prismatic Braid require two essential strings only? What are the basic values for c which would give a two essential string $7\times 10\times c$ Rectangular Right Prismatic Braid?

We can restrict the basic values for c to $0\leq c\leq |7-10|$, hence to $0\leq c\leq 3$.

7 and 10 are coprime, hence $7\times 10\times 0$ fulfills the two essential strings only condition.

$7 \times 10 \times 1$ is identical to $1 \times 7 \times 10$, which reduces to $1 \times 7 \times 2$ $(c - 1(a + b) = 10 - 1(1 + 7) = 2)$. $1 \times 7 \times 2$ is identical to $1 \times 2 \times 7$, which reduces to $1 \times 2 \times 1$ $(c - 2(a + b) = 7 - 2(1 + 2) = 1)$. $1 \times 2 \times 1$ is identical to $1 \times 1 \times 2$, which reduces to $1 \times 1 \times 0$ $(c - 1(a + b) = 2 - 1(1 + 1) = 0)$. Since this braid contains two identical sides of 1 with a third side of 0, the braid requires two essential strings only. Consequently, the braid $7 \times 10 \times 1$ fulfills the two essential strings only condition.

$7 \times 10 \times 2$ is identical to $2 \times 7 \times 10$, which reduces to $2 \times 7 \times 1$ $(c - 1(a + b) = 10 - 1(2 + 7) = 1)$. $2 \times 7 \times 1$ is identical to $1 \times 2 \times 7$, which reduces to $1 \times 2 \times 1$ $(c - 2(a + b) = 7 - 2(1 + 2) = 1)$. $1 \times 2 \times 1$ is identical to $1 \times 1 \times 2$, which reduces to $1 \times 1 \times 0$ $(c - 1(a + b) = 2 - 1(1 + 1) = 0)$. Since this braid contains two identical sides of 1 with a third side of 0, the braid requires two essential strings only. Consequently, the braid $7 \times 10 \times 2$ fulfills the two essential strings only condition.

$7 \times 10 \times 3$: since 7 and 3 are coprime, $7 \times 3 \times 0$ fulfills the two essential strings only condition and consequently so does $7 \times 3 \times 10$ $(c + n(a + b) = 0 + 1(7 + 3) = 10)$. $7 \times 3 \times 10$ is identical to $7 \times 10 \times 3$, hence $7 \times 10 \times 3$ fulfills the two essential strings only condition.

The basic values for c which would give a two essential string $7 \times 10 \times c$ Rectangular Right Prismatic Braid are 0, 1, 2 and 3.

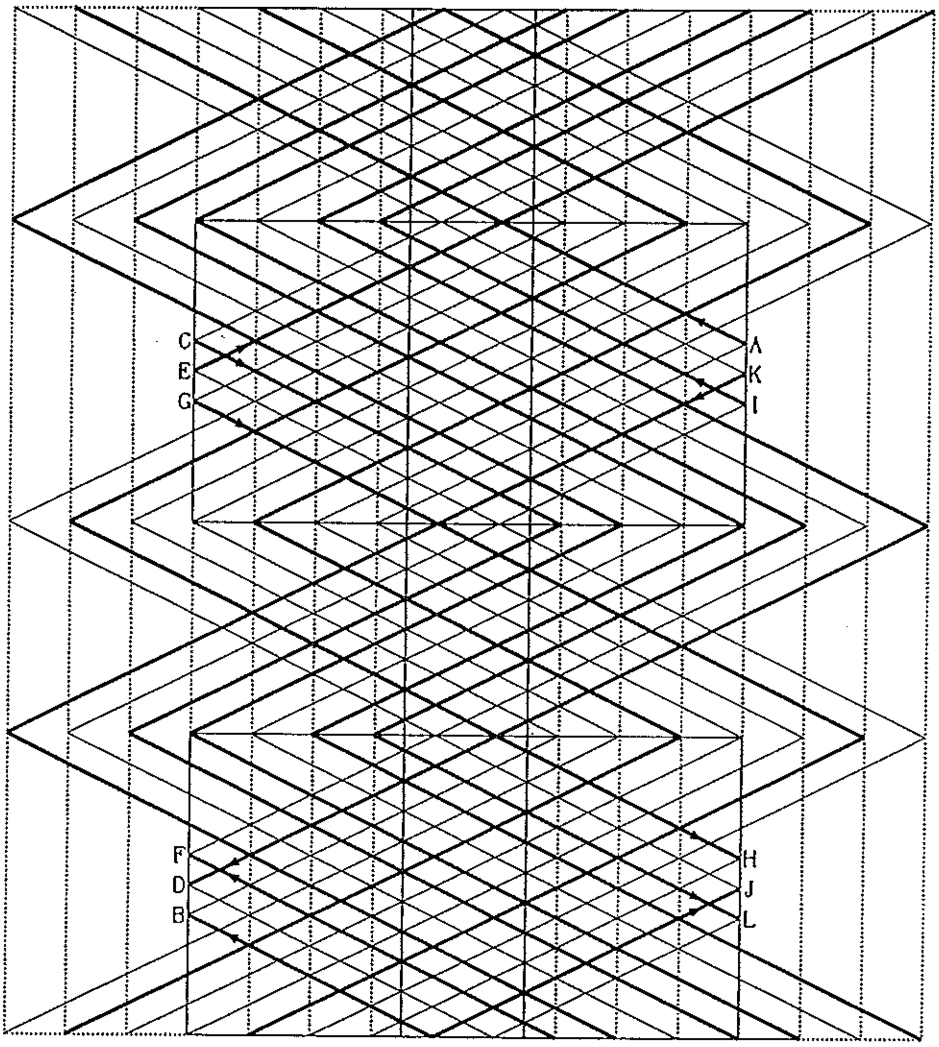

Fig. 703 — The string-run of a $7 \times 10 \times 2$ Rectangular Right Prismatic Braid.

THE BRAIDER

No.38 **MAY 2004.**

CONTENTS

pg.

Solution to the Question in Issue No.37 881

The Braider's Notebook 881

A Six Thong Round Braid Start 902

A quarterly publication
for
the braiding artisan

Resale of this publication or copies thereof
is strictly prohibited

Copyright ©2004 by:

A.G. Schaake; 21 Sundown Cresc.; Hamilton; New Zealand.
D. Van Tassel; Box 335; Craig, Co 81626-0335; U.S.A.
F.J.M. Masurel; Ganzenzijde 4; 2317XG Leiden; Nederland.

All rights reserved. No part of this publication may be reproduced, stored in a retrieval system, or transmitted, in any form or by any means, electronic, mechanical, photo-copying, recording, or otherwise, without prior written permission.

This publication is available to braiding artisans only.

Copies may be obtained from:

A.G. Schaake,
21 Sundown Cresc.,
Hamilton,
New Zealand.

Solution to the Question in Issue No. 37

Question on pg. 878.

Since the string-run of an $a\times b\times c$ Rectangular Right Prismatic Braid is equivalent to the string-run of a $b\times a\times c$ Rectangular Right Prismatic Braid with the same respective values a, b and c, we can restrict the requested proof to the string-run of an $a\times b\times c$ Rectangular Right Prismatic Braid in which $a < b$. The number of regular nested bights in each nest of bights is a, and there are $b-a$ crossing-points on each of the two bight-edges. When a Rectangular Right Prismatic Braid with a string-run containing a component whose string-run runs from a bight on one of the two bight-edges to a bight on the other bight-edge and then on to the initial bight, closing in that way the string-run of that component, must consist of more than two components, hence must require more than two essential strings. The case associated with the smallest c-value with such a string-run is depicted by the left-hand diagram in Fig. 704, and the case associated with the largest c-value with such a string-run is depicted by the right-hand diagram in Fig. 704.

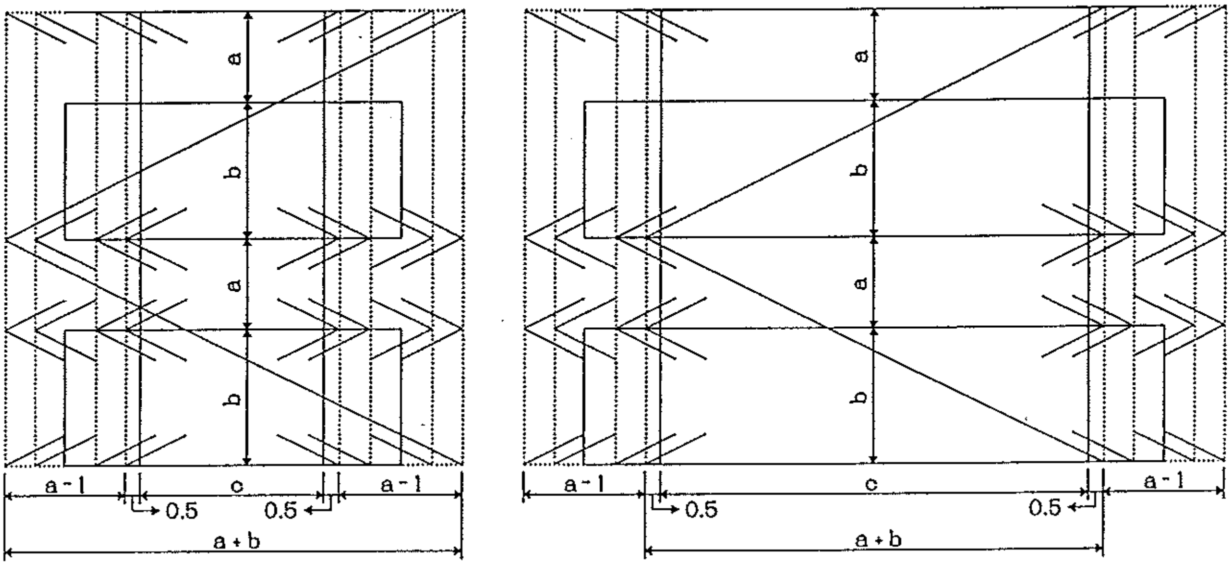

Fig. 704 — The two string-run diagrams associated with the proof.

In the left-hand diagram we see that $2a-2+1+c=a+b$, hence $c=b-a+1$. Thus in general for any $a\times b\times c$ Rectangular Right Prismatic Braid we obtain $c=|a-b|+1$.

In the right-hand diagram we see that $c+1=a+b$, hence $c=a+b-1$.

Consequently for $|a-b|+1\leq c\leq a+b-1$ an $a\times b\times c$ Rectangular Right Prismatic Braid requires more than two essential strings.

THE BRAIDER'S NOTEBOOK

In some previous issues of *The Braider* we have touched on problems concerning braid-classification attempts by some people. Such attempts can originate from a complete misunderstanding of what braids are about with the result that a **class of (braid) construction-methods** is taken to be a **class of braids**. This happened in a publication entitled '**Grant Weaves**', published in July 1995 by Pieter van de Griend.

Since **Murphy's Law**, also known as *Sod's Law*, played the upperhand in that publication, and since the weaves dealt with do **not** form a class of braids, we shall call them **Murphy Weaves**. The diagrams presented in that publication are typical braid **construction-method diagrams**, and such diagrams are often unable to tell us much about the **braidform(s)**. To investigate **braidforms** it is essential to employ grid-diagrams, and hence only grid-diagrams will be able to assist us in the classification of **braids**. It is important to stress that in general there is no connection between **braid classes** and **(braid) construction-method classes**.

We should therefor clearly keep in mind the following fundamental braiding law:

•♡• Braids of a similar string-run (structure) may be constructed by a similar construction-method, however, braids which may be constructed by a similar construction-method are not necessarily of a similar string-run (structure). Braids should therefore be classified according to their string-run (structure) and not to their construction-method as otherwise more or less unrelated braids will end up in the same braid-class.

Apart from erroneously regarding a set of braids created by a certain construction-method as a class of braids, the publication referred to above contains furthermore a fairly large number of erroneous statements and conclusions, some of them due to disregarding the most basic rule in braid investigations, namely that **flat string** only should be used.

The set of braids with which the above referred to publication tries to deal is characterised by the repetitive application of the following set of two construction sequences:

> We start with a set of n parallel strings, where n is a positive integer ≥ 2. These n strings are braided in the following manner:
>
> - Take the left-most of the n parallel strings **under** u strings towards the right. Take it up from among the strings, reverse direction to take it **over** o strings back to the left. While reversing the direction, the string should be given a full turn (right-hand screw moving down) in order for the front facing face to remain the front facing face.
> - Take the right-most of the n parallel strings **under** u strings towards the left. Take it up from among the strings, reverse direction to take it **over** o strings back to the right. While reversing the direction, the string should be given a full turn (left-hand screw moving down) in order for the front facing face to remain the front facing face.

Let's describe this braiding-method by the notation: $(n,\ u/o)$. Note that for consistency the *full-turn* movements in the definition above are also executed when $u = 0$ and when $o = 0$.

Murphy's braid construction-method falls under the 'standard' method for braiding **round braids**; it is, however, executed in a somewhat disguised way which in turn tends to mislead the braider. For this reason alone, this braid construction-method, although quite often used in the braiding literature, cannot be considered to be a good one and hence should not really be used at all.

Round braids are braids in the form of a cylinder without ends, or to put it technically a little more precise: it are braids in the form of a cylinder which has one end at minus infinity and the other end at plus infinity (Euclidian geometry), where the cylindrical braid is formed by two sets of strings: one set describes a right-hand helix while the other set desribes a left-hand helix. In the most elementary case, each set contains an equal number of strings; this are the normally encountered round braids we see. In the next case the numbers of strings in the two sets differ by 1. Let's limit ourselves to these two simple cases, and for convenience sake let's call the first case: **round braids with an even number of strings**, and the second case: **round braids with an odd number of strings.**

The 'standard' method for laying down the string-run sequence in round braids with an even number of strings is depicted in Fig. 705 by the left-most string-run diagram for an 8-string round braid.

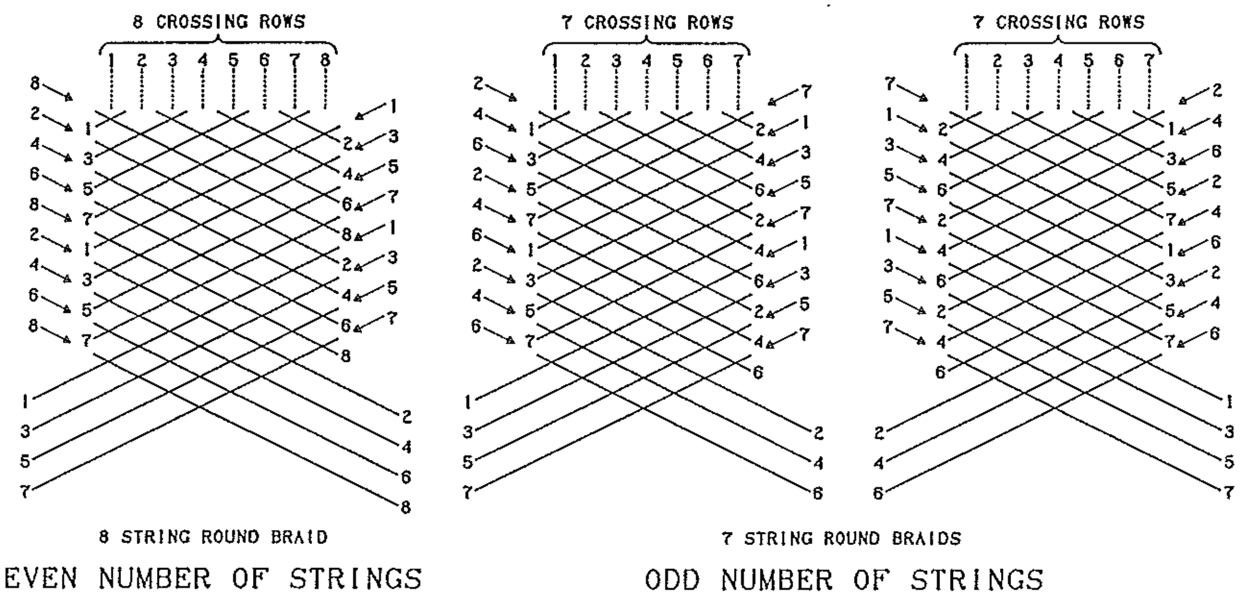

Fig. 705 — The 'standard' method for laying down the string-run in round braids.

The diagram clearly depicts the four strings which describe a right-hand helix (the strings 1, 3, 5, 7) and the four strings which describe a left-hand helix (the strings 2, 4, 6, 8). The free-ends of the strings which describe a right-hand helix point to the lower left, and the free-ends of the strings which describe a left-hand helix point to the lower right. The procedure for laying down the consecutive numbered strings is as follows:

- Take the free-end of string 1 and run it, from left to right, along the **back** of the braid; then, after giving it a full turn (right helix down), lay it down from upper-right to lower-left along the **front** of the braid, hence crossing the strings 2, 4, 6, 8 in sequence.
- Take the free-end of string 2 and run it, from right to left, along the **back** of the braid; then, after giving it a full turn (left helix down), lay it down from upper-left to lower-right along the **front** of the braid, hence crossing the strings 3, 5, 7, 1 in sequence.
- Take the free-end of string 3 and run it, from left to right, along the **back** of the braid; then, after giving it a full turn (right helix down), lay it down from upper-right to lower-left along the **front** of the braid, hence crossing the strings 4, 6, 8, 2 in sequence.
- Take the free-end of string 4 and run it, from right to left, along the **back** of the braid; then, after giving it a full turn (left helix down), lay it down from upper-left to lower-right along the **front** of the braid, hence crossing the strings 5, 7, 1, 3 in sequence.
- Take the free-end of string 5 and run it, from left to right, along the **back** of the braid; then, after giving it a full turn (right helix down), lay it down from upper-right to

lower-left along the **front** of the braid, hence crossing the strings 6, 8, 2, 4 in sequence.

- Take the free-end of string 6 and run it, from right to left, along the **back** of the braid; then, after giving it a full turn (left helix down), lay it down from upper-left to lower-right along the **front** of the braid, hence crossing the strings 7, 1, 3, 5 in sequence.
- Take the free-end of string 7 and run it, from left to right, along the **back** of the braid; then, after giving it a full turn (right helix down), lay it down from upper-right to lower-left along the **front** of the braid, hence crossing the strings 8, 2, 4, 6 in sequence.
- Take the free-end of string 8 and run it, from right to left, along the **back** of the braid; then, after giving it a full turn (left helix down), lay it down from upper-left to lower-right along the **front** of the braid, hence crossing the strings 1, 3, 5, 7 in sequence.
- Repeat the above eight steps as often as required in order to obtain the desired length of cylindrical braid.

In round braids with an odd number of strings, the set of strings with the greater number may either describe right-hand or left-hand helixes. The respective 'standard' method for laying down the string-runs is similar to the one above, and is depicted in Fig. 705 for a 7-string round braid.

It will be expedient to have a closer look at what goes on in round braids which have a set of right-hand helixes and a set of left-hand helixes[†]. It is obvious that the right-hand helixes cannot be separated from each other, and of course neither can the left-hand helixes (this will also readily be seen from Fig. 706). It will also be obvious that a right-hand helix can only be separated from the set of left-hand helixes when it is not intertwined with any of them. It therefore follows that a round braid can only be separated into two distinct parts when **none** of the right-hand helixes is intertwined with a left-hand helix, and consequently no left-hand helix is intertwined with a right-hand helix. The geometry of the round braid provides for two types of distinct separation. One type wherein the set of right-hand helixes can be totally separated from the set of left-hand helixes (**separable splitting**), and the other type wherein the one set of helixes encloses the other set of helixes (**enclosed splitting**).

From the 'general' string-run diagrams it will readily be seen that in order for each string to describe a helix on the cylindrial surface, its free-end must after having past along the back of the braid cross on the front of the braid all the strings of the opposing set. Hence in round braids with an even number of strings[‡] ($2x$ strings), the free-end of each string must at the time of its placement cross the x strings of the opposing set on the front of the braid. It will readily be seen that if the superimposed coding on these string-runs is such that for all the strings in both sets these x crossings are of an **identical** nature (hence for all the strings laid down from upper-right to lower-left as well as for the strings laid down from upper-left to lower-right either x *over*-crossings or x *under*-crossings), the braid will split into two distinct parts which can be separated totally as explained above. In fact, this necessary and sufficient condition for the coding, in order for the round braid to be splittable into two distinct parts which are totally separable, is readily to be seen from the left-most diagrams in each of the first two rows of diagrams in Fig. 706. These diagrams show the projection of a round braid with such an even number of strings. Observe that the helixes indicated by the solid lines can be lifted off the helixes indicated by the dotted lines.

[†] A round braid in which the string-run consists solely out of either right-hand helixes or left-hand helixes is called an **embrionic round braid**. Embrionic round braids and embrionic cylindrical braids are some of the most elementary braidforms, and are hence of paramount importance to physical braids. It is, for example, with the treatment of these by the Topological Knot Theory that this theory is of little or no relevance to physical braids.

[‡] As before defined with respect to the numbers of right- and left-hand helixes.

Also note that the coding in the gid-diagram second from left, central row of diagrams in Fig. 706, indicates the two totally separable parts. Hence the gid-diagram second from left, top row in Fig. 706, which depicts the upside down version of the previous refered to grid-diagram, also indicates the total separability of the round braid into two parts.

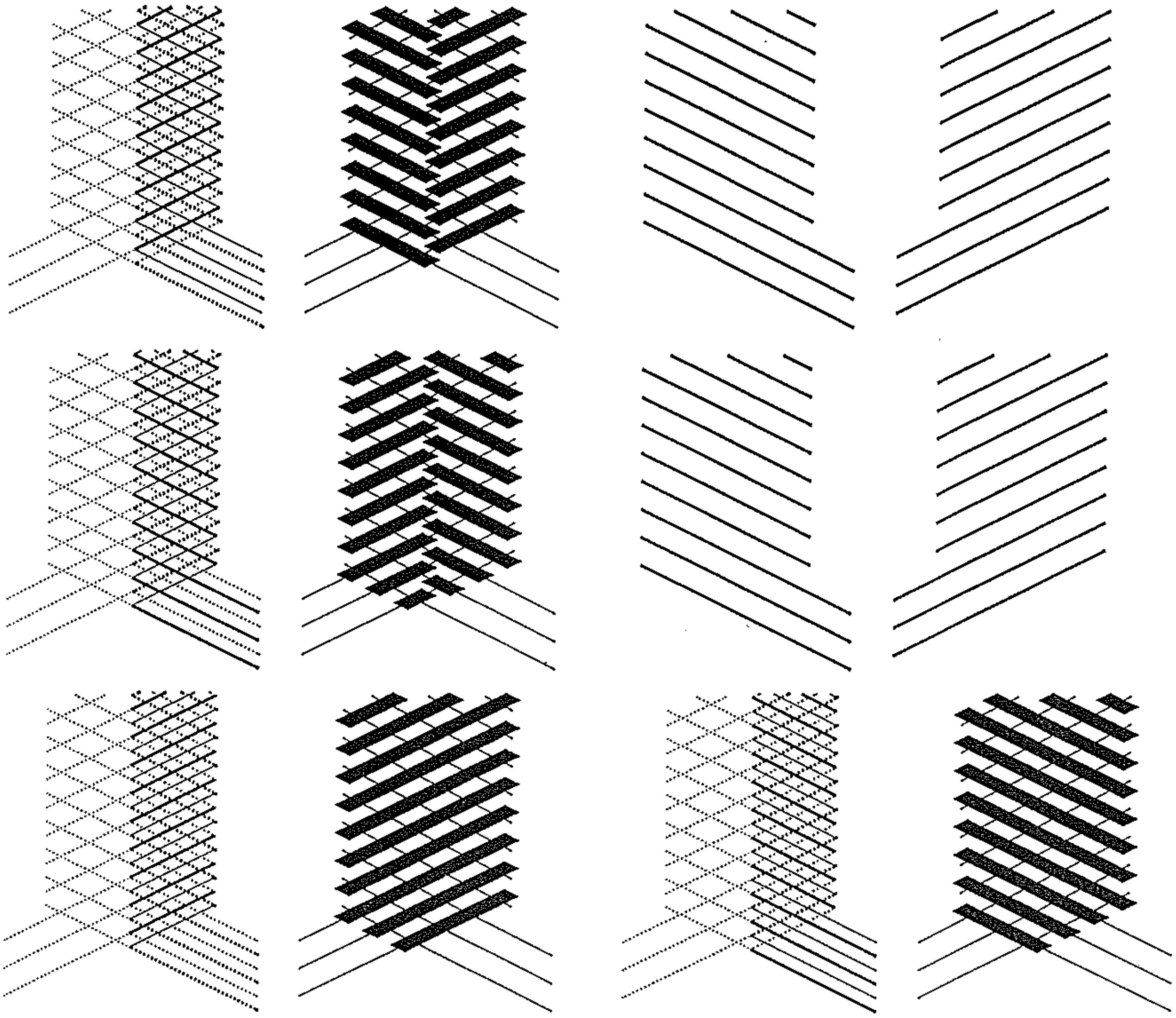

6 STRING ROUND BRAID

EVEN NUMBER OF STRINGS

THICK LINES ABOVE THIN LINES, AND SOLID LINES ABOVE DOTTED LINES OF SAME THICKNESS.

Fig. 706 — The necessary and sufficient coding requirements for splitting.

If the superimposed coding on these string-runs is such that for all the strings in one set these x crossings are of an **opposite** nature to the x crossings of the other set (hence for all the strings laid down from upper-right to lower-left x *over*-crossings while for all the strings laid down from upper-left to lower-right x *under*-crossings, or vice versa), the braid will also split into two distinct parts where the set with right-hand helixes encloses, but not intertwines, the set with left-hand helixes, or respectively vice versa (**enclosed splitting**). See Fig. 706, bottom row of diagrams.

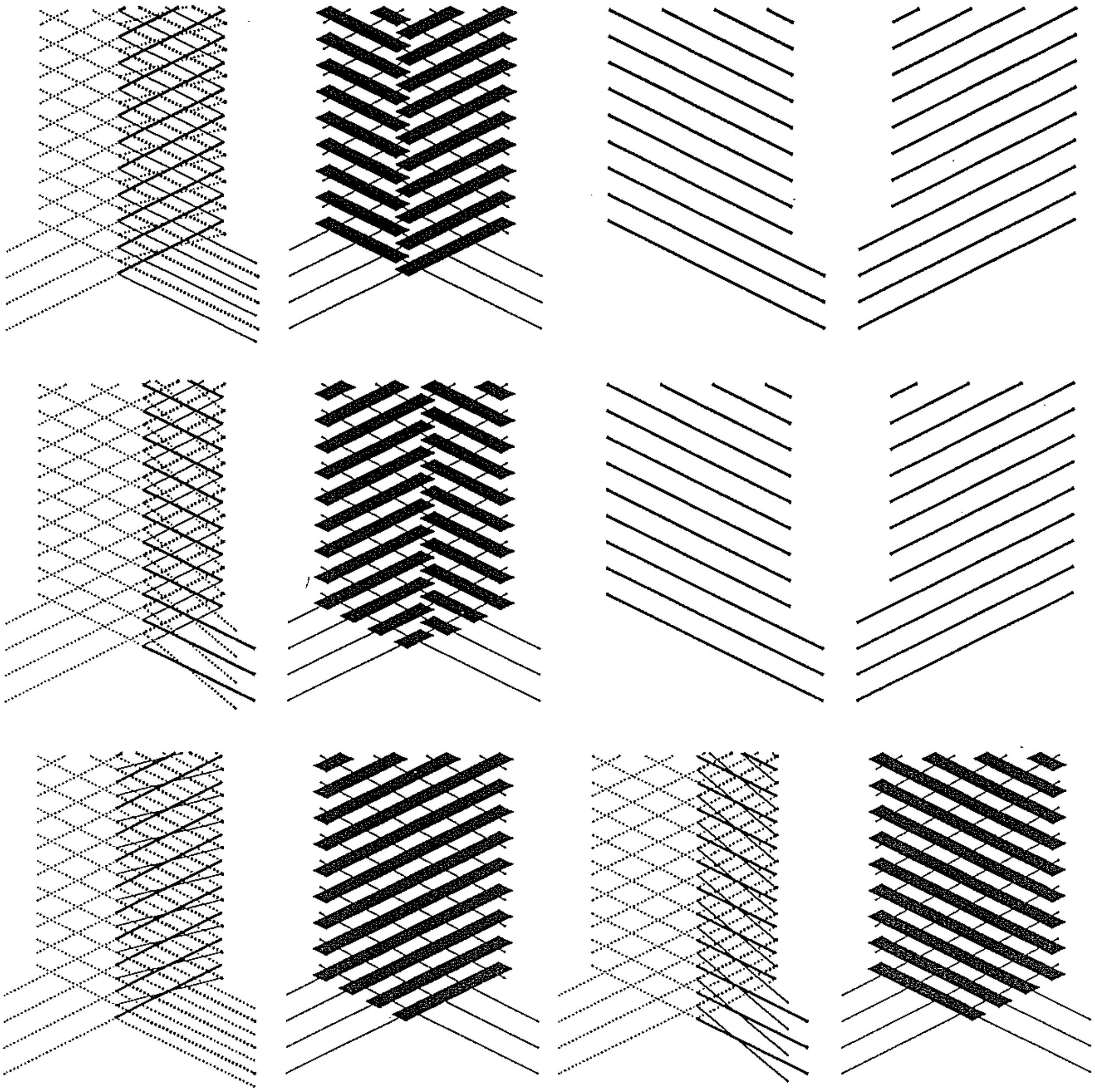

7 STRING ROUND BRAID

ODD NUMBER OF STRINGS

THICK LINES ABOVE THIN LINES, AND SOLID LINES ABOVE DOTTED LINES OF SAME THICKNESS.

Fig. 707 — The necessary and sufficient coding requirements for splitting.

In Fig. 707 we have shown the diagrams which depict the corresponding splitting in round braids with an odd number of strings[†]

[†] As before defined with respect to the numbers of right- and left-hand helixes.

Say, that instead of the 'standard' braiding-method, we use Murphy's construction-method. Then our earlier described 'standard' braiding-method for round braids with an even number of strings is identical to $\big(2x,\ u/(u+1-x)\big)$, where $(x-1) \leq u \leq (2x-1)$. Hence $o = u + 1 - x$, where $(x-1) \leq u \leq (2x-1)$. Hence when the superimposed coding is such that the braid splits into two parts (see above, and note that enclosed splitting is not possible under the the Murphy Weaves), then either $u = (x-1)$, hence $o = 0$ (central row of diagrams in Fig. 706), or $u = (2x-1)$, hence $o = x$ (top row of diagrams in Fig. 706). Note that we can't construct round braids with Murphy's construction-method which have an odd number of strings, since the two fundamental braiding steps in this method are identical with respect to the u's and o's, and hence in round braids the number of crossings which each string makes when being laid down from upper right to lower left or from upper left to lower right is equal to $(n-1-u+o)$.

It should be noted that the vertical lines through the crossing-points of the strings are rows, and that there are n rows in a round braid of n strings. When each of these rows has a constant coding, then we have a row-coded braid (when splittable into two totally separate parts, we obtain two embrionic round braids, each one without any crossing rows).

Before proceeding with the Murphy Weaves, let us first have a look at **regular flat braids** braided by the 'standard' method for round braids. After our earlier exposition of the 'standard' round braiding-method, we should not encounter any difficulties in reading the string-run diagrams in Fig. 708.

It will be needless to say that in practice nobody would contemplate braiding a regular flat braid in this manner, but as we shall see it is extensively used in Murphy's construction-method.

Note that in these diagrams the vertical lines through the crossing-points are columns and **not** rows! Also note that there are $(n-1)$ columns in a braid of n strings. When each of these columns has a constant coding, then we have a column-coded braid.

Since the two fundamental braiding steps in Murphy's construction-method are identical with respect to the u's and o's, we can't encounter with that method the "even number of strings" case, but we do encounter the "odd number of strings" case. Here for a braid with n strings we have:

$$n - 1 - u + o = \frac{n-1}{2}, \qquad \text{where } n = \text{odd}.$$

$$\text{hence:} \qquad u - o = \frac{n-1}{2}.$$

Let's summarise what we have found out so far about the Murphy Weaves.

•♡• For an **odd** number of strings n there are no Murphy Weaves which are round braids in which all the strings participate in the actual weave of the braid.

•♡• For an **odd** number of strings n there are Murphy Weaves which are regular flat braids in which all the strings participate in the actual weave of the braid. For these braids $u - o = \dfrac{n-1}{2}$.

•♡• For an **even** number of strings n there are Murphy Weaves which are round braids in which all the strings participate in the actual weave of the braid. For these braids $u - o = \dfrac{n-2}{2}$. These Murphy Weaves will split into two totally separate parts when:

(i). $o = 0$, and hence $u = \dfrac{n-2}{2}$.

(ii). $o = \dfrac{n}{2}$, and hence $u = n - 1$.

•♡• For an **even** number of strings n there are no Murphy Weaves which are regular flat braids in which all the strings participate in the actual weave of the braid.

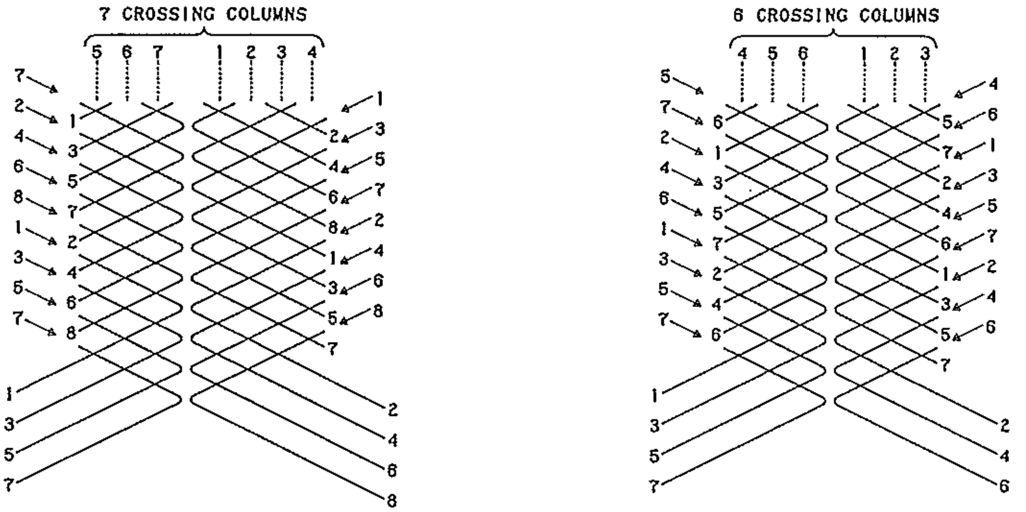

8 STRING FLAT BRAID
EVEN NUMBER OF STRINGS

7 STRING FLAT BRAID
ODD NUMBER OF STRINGS

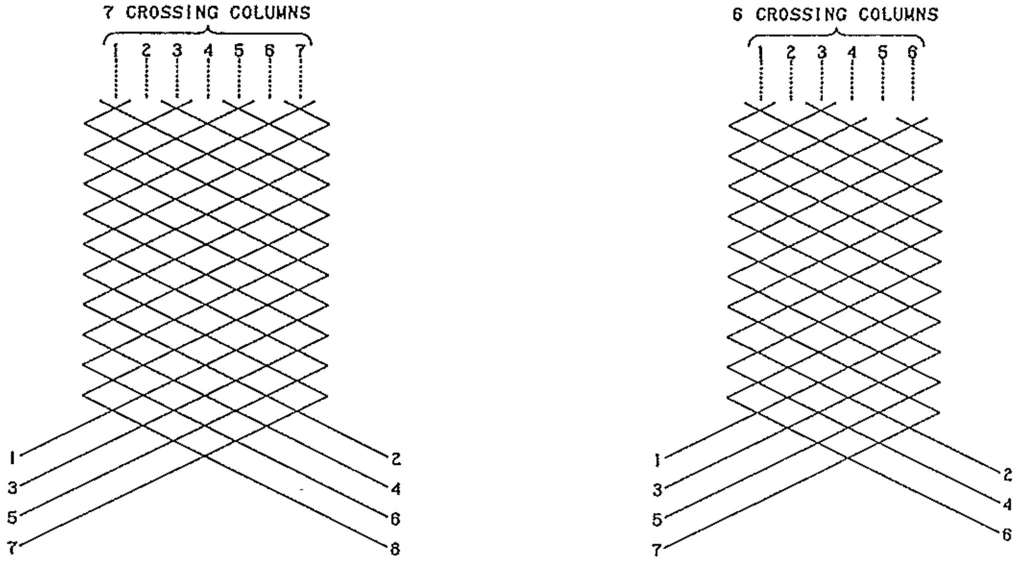

8 STRING FLAT BRAID
EVEN NUMBER OF STRINGS

7 STRING FLAT BRAID
ODD NUMBER OF STRINGS

Fig. 708 — Two different braiding-methods for regular flat braids.

When a string makes fewer than $\dfrac{n-1}{2}$ crossing-points when laid down (on the front) in a Murphy Weave with an **odd** number of strings, we see from the right-hand string-run diagrams in Fig. 708 that this Murphy Weave contains a regular flat braid. In fact we see that if this number of crossings is y, then this regular flat braid contains $(2y+1)$ strings. Hence if the Murphy Weave contains a total of n strings, it follows that $(n-2y-1)$ strings (hence an *even* number of strings) do not take part in the actual weaving; it are **passive** strings which are totally free of the regular flat braid.

When a string makes fewer than $\frac{n}{2}$ crossing-points when laid down (on the front) in a Murphy Weave with an **even** number of strings, we see from the left-hand string-run diagrams in Fig. 708 that this Murphy Weave contains a regular flat braid. In fact we see that if this number of crossings is y, then this regular flat braid contains $(2y+1)$ strings. Hence if the Murphy Weave contains a total of n strings, it follows that $(n-2y-1)$ strings (hence an *odd* number of strings) do not take part in the actual weaving; it are **passive** strings which are totally free of the regular flat braid.

Since $y = (n-1-u+o)$, it follows that for such Murphy Weaves we have the conditons:

$$u - o > \frac{n-1}{2}, \quad \text{for } n = \text{odd}, \quad \textit{with}$$

$(2n-1-2u+2o)$ strings in regular flat braid; $(2u-2o+1-n)$ passive strings.

$$u - o > \frac{n-2}{2}, \quad \text{for } n = \text{even}, \quad \textit{with}$$

$(2n-1-2u+2o)$ strings in regular flat braid; $(2u-2o+1-n)$ passive strings.

The round braids in Fig. 709 contain passive strings. We see that in order to fulfil Murphy Weave conditions, the number of passive strings must be **odd** when the total number of strings is **odd**, and the number of passive strings must be **even** when the total number of strings is **even**. The round braid itself must always have an even number of strings.

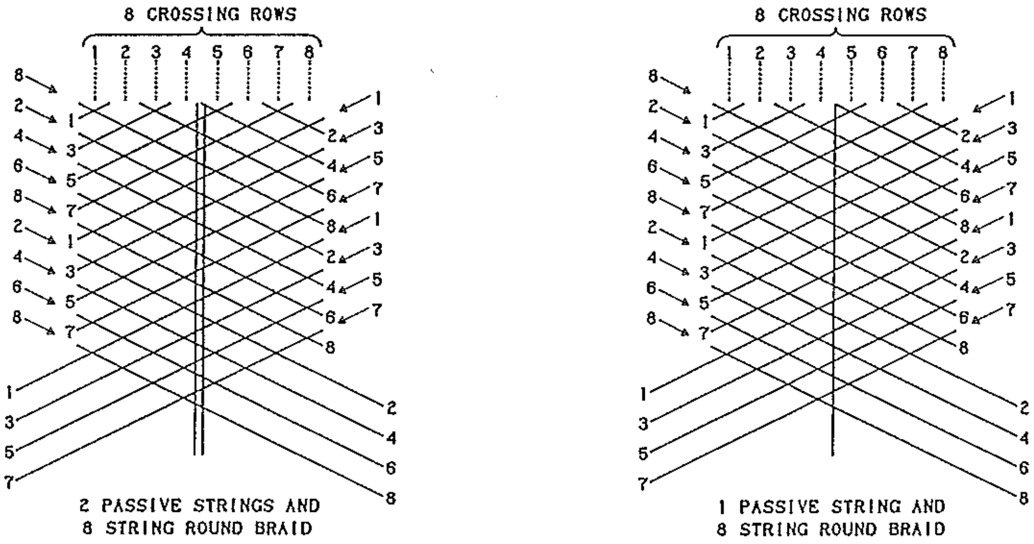

EVEN NUMBER OF STRINGS ODD NUMBER OF STRINGS

Fig. 709 — Round braids with passive strings.

When a string makes more than $\frac{n-1}{2}$ crossing-points when laid down (on the front) in a Murphy Weave with an **odd** number of strings, we see from the right-hand string-run diagram in Fig. 709 that this Murphy Weave contains a round braid with passive strings. In fact we see that if this number of crossings is y, then the number of passive strings is equal to $(2y-n)$, while the round braid itself consists of $2(n-y)$ strings.

When a string makes more than $\frac{n}{2}$ crossing-points when laid down (on the front) in a Murphy Weave with an **even** number of strings, we see from the left-hand string-run diagram in Fig. 709 that this Murphy Weave contains a round braid with passive strings. In fact we see that if this number of crossings is y, then the number of passive strings is equal to $(2y - n)$, while the round braid itself consists of $2(n - y)$ strings.

Since $y = (n - 1 - u + o)$, it follows that for such Murphy Weaves we have the conditons:

$$u - o < \frac{n-1}{2}, \quad \text{for } n = \text{odd}, \quad \textit{with}$$

$$2(u - o + 1) \text{ strings in round braid;} \quad (n - 2 - 2u + 2o) \text{ passive strings.}$$

$$u - o < \frac{n-2}{2}, \quad \text{for } n = \text{even}, \quad \textit{with}$$

$$2(u - o + 1) \text{ strings in round braid;} \quad (n - 2 - 2u + 2o) \text{ passive strings.}$$

Let's now investigate how these passive strings are positioned in these Murphy Weaves, hence how they are associated with the round braids. From Fig. 709 we observe that the passive strings are the last strings which are crossed when a string is being laid down from upper-right to lower left as well as when a string is being laid down from upper-left to lower-right. The seven different arrangement to be considered are schematically depicted in Fig. 710.

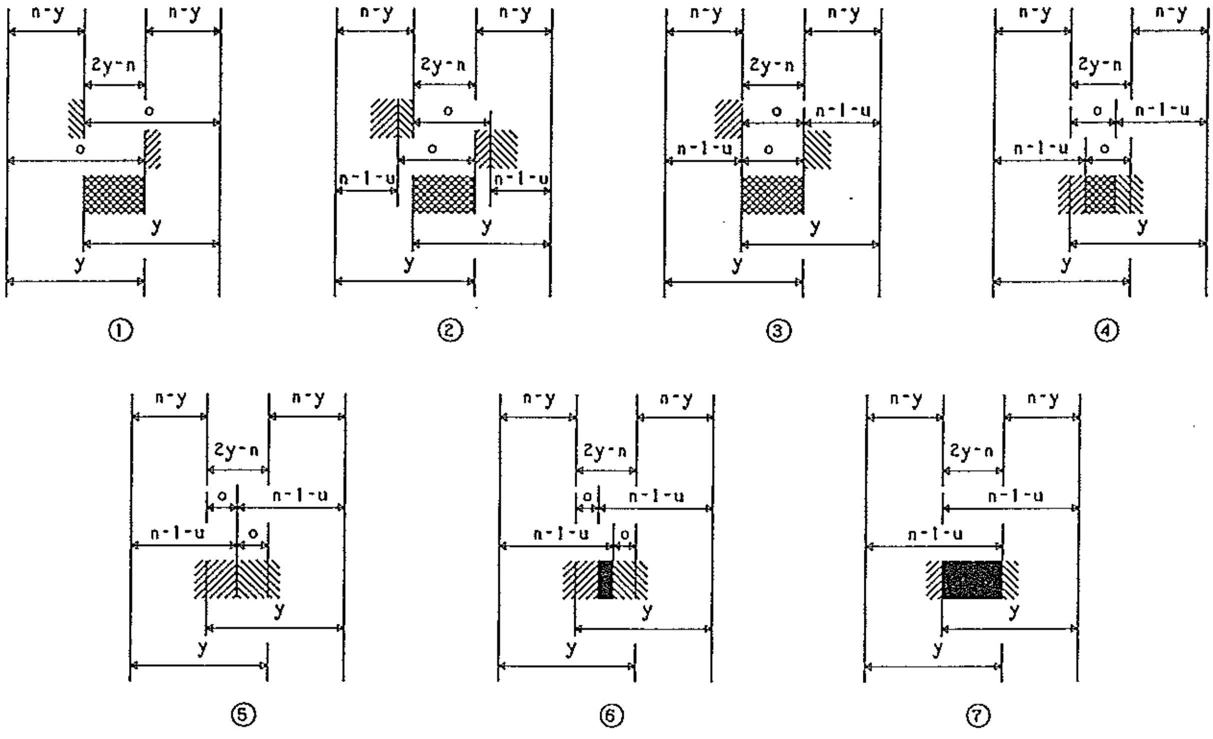

Fig. 710 — The arrangements of the passive strings.

(1). Diagram ①depicts the case where all the passive strings $(2y - n)$ are fully encircled by the round braid. When the passive strings are extracted, the round braid splits into two totally separated parts; each part being an embrionic round braid, one with a right-hand helix and the other with a left-hand helix. With the previously obtained relationships and those derived from diagram ①we obtain:

$$u - o < \frac{n-1}{2} \quad \text{for} \quad n = \text{odd},$$
$$u - o < \frac{n-2}{2} \quad \text{for} \quad n = \text{even},$$
$$u = n - 1 \quad \text{and} \quad o > \frac{n}{2},$$
$$\text{number of passive strings} = 2o - n,$$
$$\text{number of strings in each embrionic round braid} = n - o.$$

(2). Diagram ②depicts the case where all the passive strings $(2y - n)$ are fully encircled by the round braid. When the passive strings are extracted, the round braid does not split into two parts. With the previously obtained relationships and those derived from diagram ②we obtain:

$$u - o < \frac{n-1}{2} \quad \text{for} \quad n = \text{odd},$$
$$u - o < \frac{n-2}{2} \quad \text{for} \quad n = \text{even},$$
$$2u - o > n - 2 \quad \text{and} \quad u < n - 1,$$
$$\text{number of passive strings} = n - 2 - 2u + 2o,$$
$$\text{number of strings in round braid} = 2(u + 1 - o).$$

(3). Diagram ③depicts the case where all the passive strings $(2y - n)$ are fully encircled by the round braid. When the passive strings are extracted, the round braid splits into two totally separated parts; each part being an embrionic round braid, one with a right-hand helix and the other with a left-hand helix. With the previously obtained relationships and those derived from diagram ③we obtain:

$$u - o < \frac{n-1}{2} \quad \text{for} \quad n = \text{odd},$$
$$u - o < \frac{n-2}{2} \quad \text{for} \quad n = \text{even},$$
$$2u - o = n - 2,$$
$$\text{number of passive strings} = n - 2 - 2u + 2o,$$
$$\text{number of strings in each embrionic round braid} = u + 1 - o.$$

(4). Diagram ④ depicts the case where only some of the passive strings are fully encircled by the round braid; they form the central set of passive strings. The rest of the passive strings are divided into two sets with equal numbers; the left-hand set is only encircled by the set of right-hand helixes, while the right-hand set is only encircled by the left-hand helixes. The round braid splits into two totally separated parts (which are embrionic round braids, one with a right-hand helix and the other with a left-hand helix) when the central set of passive strings is extracted. Each part encircles its set of passive strings. With the previously obtained relationships and those derived from diagram ④we obtain:

$$u - o < \frac{n-1}{2} \quad \text{for} \quad n = \text{odd},$$
$$u - o < \frac{n-2}{2} \quad \text{for} \quad n = \text{even},$$
$$2u - o < n - 2 \quad \text{and} \quad u > \frac{n-2}{2},$$

number of passive strings in central set $= 2u + 2 - n$,
number of passive strings in each embrionic braid $= n - 2 - 2u + o$,
number of strings in each embrionic round braid $= u + 1 - o$.

(5). Diagram ⑤ depicts the case where the passive strings are divided into two sets with equal numbers; the left-hand set is only encircled by the set of right-hand helixes, while the right-hand set is only encircled by the left-hand helixes. The round braid splits into two totally separated parts (which are embrionic round braids, one with a right-hand helix and the other with a left-hand helix) each of which encircles its set of passive strings.

Note that this case can only exist when n is even.

With the previously obtained relationships and those derived from diagram ⑤ we obtain:

$$u - o < \frac{n-2}{2} \quad \text{for} \quad n = \text{even},$$
$$u = \frac{n-2}{2},$$

number of passive strings in each embrionic braid $= \dfrac{n - 2 - 2u + 2o}{2}$,
number of strings in each embrionic round braid $= u + 1 - o$.

(6). Diagram ⑥ depicts the case where some of the passive strings fall outside the round braid; they form the central set of passive strings. The rest of the passive strings are divided into two sets with equal numbers; the left-hand set is only encircled by the set of right-hand helixes, while the right-hand set is only encircled by the left-hand helixes. The round braid splits into two totally separated parts (which are embrionic round braids, one with a right-hand helix and the other with a left-hand helix). Each embrionic round braid encircles its set of passive strings. With the previously obtained relationships and those derived from diagram ⑥ we obtain:

$$u - o < \frac{n-1}{2} \quad \text{for} \quad n = \text{odd},$$
$$u - o < \frac{n-2}{2} \quad \text{for} \quad n = \text{even},$$
$$u < \frac{n-2}{2} \quad \text{and} \quad o > 0,$$

number of passive strings in central set $= n - 2 - 2u$,
number of passive strings in each embrionic braid $= o$,
number of strings in each embrionic round braid $= u + 1 - o$.

(7). Diagram ⑦ depicts the case where all the passive strings fall outside the round braid. The round braid splits into two totally separated parts (which are embrionic round braids, one with a right-hand helix and the other with a left-hand helix). With the previously obtained relationships and those derived from diagram ⑦ we obtain:

$$u - o < \frac{n-1}{2} \quad \text{for} \quad n = \text{odd},$$
$$u - o < \frac{n-2}{2} \quad \text{for} \quad n = \text{even},$$
$$o = 0,$$
$$\text{number of free passive strings} = n - 2 - 2u,$$
$$\text{number of strings in each embrionic round braid} = u + 1.$$

In the following two Examples, the Murphy Weaves with 6 strings and 7 strings are discussed respectively by using the above derived relationships. Although grid-diagrams with zero values for u and o are not depicted in the respective Figs. 711 and 712A & 712B, they are of course just as important as the others.

Example 1: $n = 6$.

(A). No passive strings; $u - o = \frac{n-2}{2} = \frac{6-2}{2} = 2$. Hence Murphy Weave is a round braid without passive strings.

(i). $u = 5$, hence $o = 3$; (6, 5/3).

Since in this case $u = n - 1$, the braid will split into two totally separate parts. One is an embrionic round braid with a right-hand helix and 3 strings. The other is an embrionic round braid with a left-hand helix and 3 strings.

(ii). $u = 4$, hence $o = 2$; (6, 4/2).

The round braid will not split into parts.

(iii). $u = 3$, hence $o = 1$; (6, 3/1).

The round braid will not split into parts. It can readily be seen from the grid-diagrams that (6, 3/1) is identical to (6, 4/2).

(iv). $u = 2$, hence $o = 0$; (6, 2/0).

Since in this case $o = 0$, the braid will split into two totally separate parts. One is an embrionic round braid with a right-hand helix and 3 strings. The other is an embrionic round braid with a left-hand helix and 3 strings.

(B). Passive strings; $u - o > \frac{n-2}{2}$. Hence $u - o > 2$. Murphy Weave consists of a regular flat braid and passive strings.

(i). $u = 5$, hence $o < 3$.

(6, 5/0). Number of passive strings is equal to $2u - 2o + 1 - n = 5$. Number of strings in regular flat braid is equal to $2n - 1 - 2u + 2o = 1$, hence it becomes after all also a passive string. Thus in the end no braid is formed at all, consequently all strings are passive.

(6, 5/1). Number of passive strings is equal to $2u - 2o + 1 - n = 3$. Number of strings in regular flat braid is equal to $2n - 1 - 2u + 2o = 3$.

(6, 5/2). Number of passive strings is equal to $2u - 2o + 1 - n = 1$. Number of strings in regular flat braid is equal to $2n - 1 - 2u + 2o = 5$.

(ii). $u = 4$, hence $o < 2$.

(6, 4/0). Number of passive strings is equal to $2u - 2o + 1 - n = 3$. Number of strings in regular flat braid is equal to $2n - 1 - 2u + 2o = 3$. This regular flat braid is the regular flat braid in (6, 5/1) upside down.

(6, 4/1). Number of passive strings is equal to $2u - 2o + 1 - n = 1$. Number of strings in regular flat braid is equal to $2n - 1 - 2u + 2o = 5$.

(iii). $u = 3$, hence $o < 1$.

(6, 3/0). Number of passive strings is equal to $2u - 2o + 1 - n = 1$. Number of strings in regular flat braid is equal to $2n - 1 - 2u + 2o = 5$. This regular flat braid is the regular flat braid in (6, 5/2) upside down.

(C). Passive strings; $u - o < \dfrac{n-2}{2}$, hence $u - o < 2$. Murphy Weave consists of a round braid and passive strings.

Note that the condition $u - o < 2$, hence $o > u - 2$, applies to all the cases below, and only occasionally has it been stated again in a particular case.

(1). $u = n - 1 = 5$; $o > \dfrac{n}{2}$, hence $o > 3$.

All passive strings fully encircled by round braid; round braid splits into two totally separated embrionic round braids when the passive strings are extracted.

(6, 5/4). Number of passive strings is equal to $2o - n = 2$. Number of strings in each embrionic round braid is equal to $n - o = 2$.

(6, 5/5). Number of passive strings is equal to $2o - n = 4$. Number of strings in each embrionic round braid is equal to $n - o = 1$.

(2). $2u - o > n - 2$; and $u < n - 1$. Hence $u - 2 < o < 2u - 4$; $u < 5$.

All passive strings fully encircled by round braid; round braid does not split into two parts when the passive strings are extracted.

(i). $u = 4$, hence $2 < o < 4$.

(6, 4/3). Number of passive strings is equal to $n - 2 - 2u + 2o = 2$. Number of strings in round braid is equal to $2(u + 1 - o) = 4$.

(ii). $u = 3$, hence $1 < o < 2$. No solutions for o.

(iii). $u = 2$, hence $0 < o < 0$. No solutions for o.

(3). $2u - o = n - 2$, hence $o = 2u - 4$. $u - 2 < o$.

All passive strings fully encircled by round braid; round braid splits into two totally separated embrionic round braids when the passive strings are extracted.

(i). $u = 4$, hence $o = 4$.

(6, 4/4). Number of passive strings is equal to $n - 2 - 2u + 2o = 4$. Number of strings in each embrionic round braid is equal to $u + 1 - o = 1$.

(ii). $u = 3$, hence $o = 2$.

(6, 3/2). Number of passive strings is equal to $n - 2 - 2u + 2o = 2$. Number of strings in each embrionic round braid is equal to $u + 1 - o = 2$.

(iii). $u = 2$. No solutions for o.

(4). $2u - o < n - 2$; and $u > \dfrac{n-2}{2}$. Hence $o > 2u - 4$. $u > 2$.

Only some of the passive strings are fully encircled by the round braid; they form the central set of passive strings. The rest of the passive strings are divided into two sets with equal numbers; the left-hand set is only encircled by the right-hand helixes, while the right-hand set is only encircled by the left-hand helixes. The round braid splits into two totally separate embrionic round braids when the cental set of passive strings is extracted. Each embrionic round braid encircles its set of passive strings.

(i). $u = 4$. No solutions for o.

(ii). $u = 3$. Then $o > 2$.

$(6, 3/3)$. Number of passive strings in central set is equal to $2u+2-n = 2$. Number of passive strings encircled by each embrionic round braid is equal to $n-2-2u+o = 1$. Number of strings in each embrionic round braid is equal to $u + 1 - o = 1$.

(5). $u = \dfrac{n-2}{2}$. Hence $u = 2$. $o > u - 2$, hence $o > 0$.

Passive strings are divided into two sets of equal numbers. The round braid splits into two totally separate embrionic round braids, each of which encircles its set of passive strings.

$(6, 2/1)$. Number of passive strings encircled by each embrionic round braid is equal to $\dfrac{n-2-2u+2o}{2} = 1$. Number of strings in each embrionic round braid is equal to $u + 1 - o = 2$.

$(6, 2/2)$. Number of passive strings encircled by each embrionic round braid is equal to $\dfrac{n-2-2u+2o}{2} = 2$. Number of strings in each embrionic round braid is equal to $u + 1 - o = 1$.

(6). $u < \dfrac{n-2}{2}$, hence $u < 2$. $o > 0$.

Some of the passive strings fall outside the round braid; they form the central set. The rest of the passive strings are divided into two equal sets; the left-hand set is only encircled by the set of right-hand helixes, while the right-hand set is only encircled by the left-hand helixes. The round braid splits up into two totally separated embrionic round braids, each of which encircles its set of passive strings.

$u = 1$. $o = 1$.

$(6, 1/1)$. Number of passive strings in central set is equal to $n-2-2u = 2$. Number of passive strings encircled by each embrionic round braid is equal to $o = 1$. Number of strings in each embrionic round braid is equal to $u + 1 - o = 1$.

(7). $o = 0$. $u < 2 + o$, hence $u < 2$.

All passive strings fall outside the round braid. The round braid splits up into two separated embrionic round braids, one with a right-hand helix and the other with a left-hand helix.

(i). $u = o$.

$(6,\ 0/0)$. Number of free passive strings is equal to $n - 2 - 2u = 4$. Number of strings in each embrionic round braid is equal to $u+1 = 1$. The left-most string receives a right-hand helix, and the right-most string receives a left-hand helix.

(ii). $u = 1$.

$(6,\ 1/0)$. Number of free passive strings is equal to $n - 2 - 2u = 2$. Number of strings in each embrionic round braid is equal to $u + 1 = 2$.

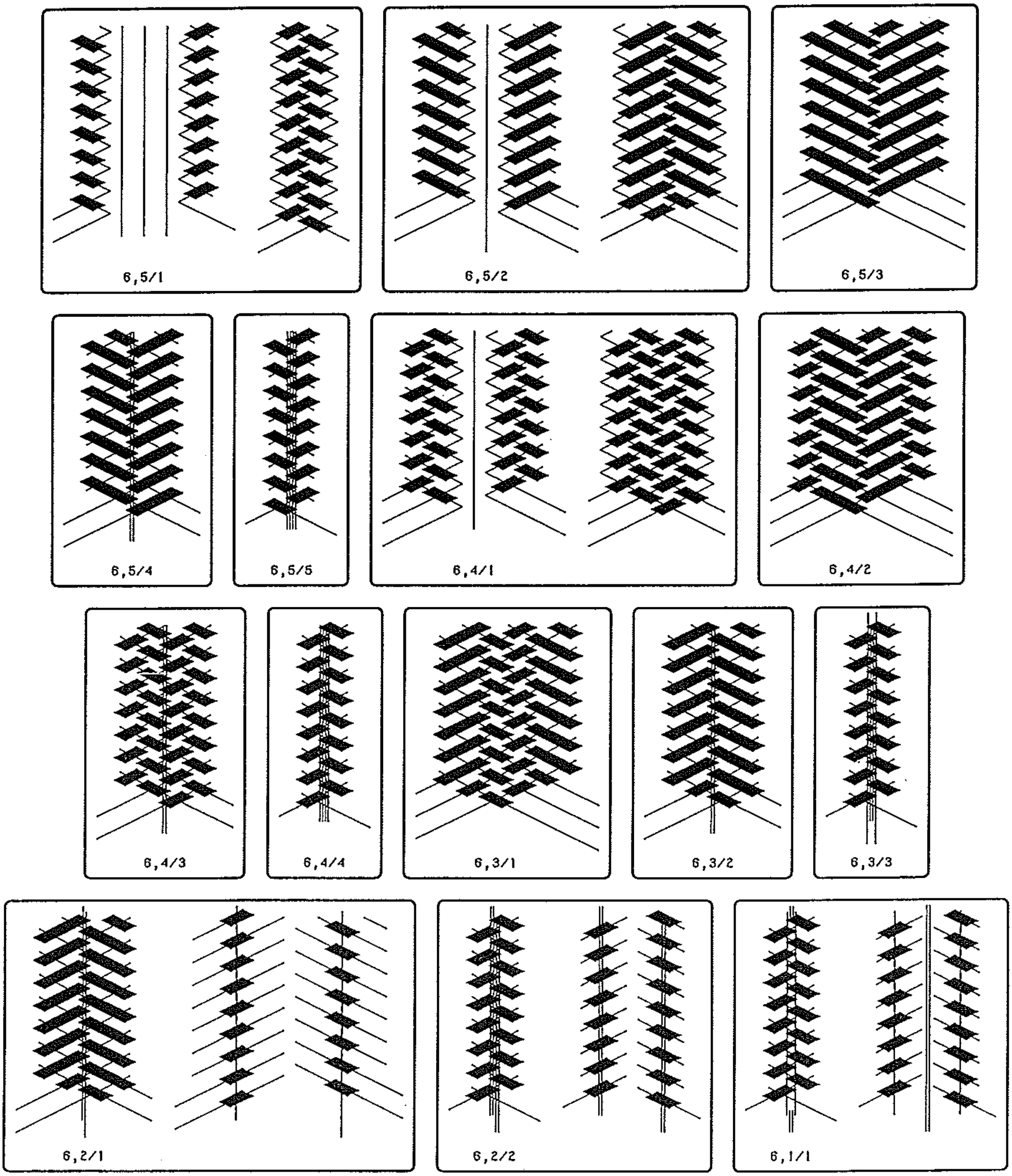

Fig. 711 — Grid-diagrams associated with Example 1.

Example 2: $n = 7$

(A). No passive strings; $u - o = \dfrac{n-1}{2} = \dfrac{7-1}{2} = 3$. Hence Murphy Weave is a regular flat braid without passive strings.

(i). $u = 6$, hence $o = 3$; (7, 6/3).

(ii). $u = 5$, hence $o = 2$; (7, 5/2).

(iii). $u = 4$, hence $o = 1$; (7, 4/1).

(iv). $u = 3$, hence $o = 0$; (7, 3/0).
This regular flat braid is identical to (7, 6/3) upside down.

(B). Passive strings; $u - o > \frac{n-1}{2}$. Hence $u - o > 3$. Murphy Weave consists of a regular flat braid and passive strings.

(i). $u = 6$, hence $o < 3$.

(7, 6/0). Number of passive strings is equal to $2u - 2o + 1 - n = 6$. Number of strings in regular flat braid is equal to $2n - 1 - 2u + 2o = 1$, hence it becomes after all also a passive string. Thus in the end no braid has been formed at all, consequently all strings are passive.

(7, 6/1). Number of passive strings is equal to $2u - 2o + 1 - n = 4$. Number of strings in regular flat braid is equal to $2n - 1 - 2u + 2o = 3$. Note also that the regular flat braid is identical to the regular flat braid in (6, 5/1).

(7, 6/2). Number of passive strings is equal to $2u - 2o + 1 - n = 2$. Number of strings in regular flat braid is equal to $2n - 1 - 2u + 2o = 5$. Note also that the regular flat braid is identical to the regular flat braid in (6, 5/2).

(ii). $u = 5$, hence $o < 2$.

(7, 5/0). Number of passive strings is equal to $2u - 2o + 1 - n = 4$. Number of strings in regular flat braid is equal to $2n - 1 - 2u + 2o = 3$. This regular flat braid is the regular flat braid in (7, 6/1) upside down. Note also that the regular flat braid is identical to the regular flat braid in (6, 4/0).

(7, 5/1). Number of passive strings is equal to $2u - 2o + 1 - n = 2$. Number of strings in regular flat braid is equal to $2n - 1 - 2u + 2o = 5$. Note also that the regular flat braid is identical to the regular flat braid in (6, 4/1).

(iii). $u = 4$, hence $o < 1$.

(7, 4/0). Number of passive strings is equal to $2u - 2o + 1 - n = 2$. Number of strings in regular flat braid is equal to $2n - 1 - 2u + 2o = 5$. This regular flat braid is the regular flat braid in (7, 6/2) upside down. Note also that the regular flat braid is identical to the regular flat braid in (6, 3/0).

(C). Passive strings; $u - o < \frac{n-1}{2}$, hence $u - o < 3$. Murphy Weave consists of a round braid and passive strings.

Note that the condition $u - o < 3$, hence $o > u - 3$, applies to all the cases below, and only occasionally has this been stated again in a particular case.

(1). $u = n - 1 = 6$; $o > \frac{n}{2}$, hence $o > 3$.

All passive strings fully encircled by round braid; round braid splits into two totally separated embrionic round braids when the passive strings are extracted.

(7, 6/4). Number of passive strings is equal to $2o - n = 1$. Number of strings in each embrionic round braid is equal to $n - o = 3$. Note that the embrionic round braids are identical to those in (6, 5/3).

(7, 6/5). Number of passive strings is equal to $2o - n = 3$. Number of strings in each embrionic round braid is equal to $n-o=2$. Note that the embrionic round braids are identical to those in (6, 5/4).

(7, 6/6). Number of passive strings is equal to $2o-n=5$. Number of strings in each embrionic round braid is equal to $n-o=1$. Note that the embrionic round braids are identical to those in (6, 5/5).

(2). $2u-o>n-2$; and $u<n-1$. Hence $u-3<o<2u-5$; $u<6$.

All passive strings fully encircled by round braid; round braid does not split into two parts when the passive strings are extracted.

(i). $u=5$, hence $2<o<5$.

(7, 5/3). Number of passive strings is equal to $n-2-2u+2o=1$. Number of strings in round braid is equal to $2(u+1-o)=6$. Note that the round braid is identical to the one in (6, 4/2).

(7, 5/4). Number of passive strings is equal to $n-2-2u+2o=3$. Number of strings in round braid is equal to $2(u+1-o)=4$. Note that the round braid is identical to the one in (6, 4/3).

(ii). $u=4$, hence $1<o<3$.

(7, 4/2). Number of passive strings is equal to $n-2-2u+2o=1$. Number of strings in round braid is equal to $2(u+1-o)=6$. Note that the round braid is identical to the one in (6, 3/1).

(iii). $u=3$, hence $0<o<1$. No solutions for o.

(3). $2u-o=n-2$, hence $o=2u-5$. $u-3<o$.

All passive strings fully encircled by round braid; round braid splits into two totally separated embrionic round braids when the passive strings are extracted.

(i). $u=5$, hence $o=5$.

(7, 5/5). Number of passive strings is equal to $n-2-2u+2o=5$. Number of strings in each embrionic round braid is equal to $u+1-o=1$. Note that (7, 5/5) is identical to (7, 6/6) upside down. Note also that the embrionic round braids are identical to those in (6, 4/4).

(ii). $u=4$, hence $o=3$.

(7, 4/3). Number of passive strings is equal to $n-2-2u+2o=3$. Number of strings in each embrionic round braid is equal to $u+1-o=2$. Note that (7, 4/3) is identical to (7, 6/5) upside down. Note also that the embrionic round braids are identical to those in (6, 3/2).

(iii). $u=3$, hence $o=1$.

(7, 3/1). Number of passive strings is equal to $n-2-2u+2o=1$. Number of strings in each embrionic round braid is equal to $u+1-o=3$. Note that (7, 3/1) is identical to (7, 6/4) upside down. Note also that the embrionic round braids are identical to those in (6, 2/0).

(4). $2u-o<n-2$; and $u>\frac{n-2}{2}$. Hence $o>2u-5$. $u>2$.

Only some of the passive strings are fully encircled by the round braid; they form the central set of passive strings. The rest of the passive strings are divided into two sets with equal numbers; the left-hand set is only encircled by the right-hand helixes, while the right-hand set is only encircled by the left-hand helixes. The round braid splits into two totally separate embrionic round braids when the cental set of passive strings is extracted. Each embrionic round braid encircles its set of passive strings.

(i). $u = 5$. No solutions for o.

(ii). $u = 4$. Then $o > 3$.

(7, 4/4). Number of passive strings in central set is equal to $2u+2-n = 3$. Number of passive strings encircled by each embrionic round braid is equal to $n-2-2u+o = 1$. Number of strings in each embrionic round braid is equal to $u+1-o = 1$. Note that the embrionic round braids are identical to those in (6, 3/3).

(iii). $u = 3$. Then $o > 1$.

(7, 3/2). Number of passive strings in central set is equal to $2u+2-n = 1$. Number of passive strings encircled by each embrionic round braid is equal to $n-2-2u+o = 1$. Number of strings in each embrionic round braid is equal to $u+1-o = 2$. Note that the embrionic round braids are identical to those in (6, 2/1).

(7, 3/3). Number of passive strings in central set is equal to $2u+2-n = 1$. Number of passive strings encircled by each embrionic round braid is equal to $n-2-2u+o = 2$. Number of strings in each embrionic round braid is equal to $u+1-o = 1$. Note that the embrionic round braids are identical to those in (6, 2/2).

(5). This case cannot exist when n is **odd**.

(6). $u < \dfrac{n-2}{2}$, hence $u < 3$. $o > 0$.

Some of the passive strings fall outside the round braid; they form the central set. The rest of the passive strings are divided into two equal sets; the left-hand set is only encircled by the set of right-hand helixes, while the right-hand set is only encircled by the left-hand helixes. The round braid splits up into two totally separated embrionic round braids, each of which encircles its set of passive strings.

(i). $u = 2$. $o > 0$.

(7, 2/1). Number of passive strings in central set is equal to $n-2-2u = 1$. Number of passive strings encircled by each embrionic round braid is equal to $o = 1$. Number of strings in each embrionic round braid is equal to $u+1-o = 2$. Note that the embrionic round braids are identical to those in (6, 2/1).

(7, 2/2). Number of passive strings in central set is equal to $n-2-2u = 1$. Number of passive strings encircled by each embrionic round braid is equal to $o = 2$. Number of strings in each embrionic round braid is equal to $u+1-o = 1$. Note that the embrionic round braids are identical to those in (6, 2/2).

(ii). $u = 1$. $o > 0$.

(7, 1/1). Number of passive strings in central set is equal to $n-2-2u = 3$. Number of passive strings encircled by each embrionic round braid is equal to $o = 1$. Number of strings in each embrionic round braid is equal to $u+1-o = 1$. Note that the embrionic round braids are identical to those in (6, 1/1).

(7). $o = 0$. $u < 3 + o$, hence $u < 3$.

All passive strings fall outside the round braid. The round braid splits up into two separated embrionic round braids, one with a right-hand helix and the other with a left-hand helix.

(i). $u = o$.

(7, 0/0). Number of free passive strings is equal to $n-2-2u = 5$. Number of strings in each embrionic round braid is equal to $u+1 = 1$. The left-most string receives a right-hand helix, and the right-most string receives a left-hand helix. Note that the embrionic round braids are identical to those in (6, 0/0).

(ii). $u = 1$.

(7, 1/0). Number of free passive strings is equal to $n - 2 - 2u = 3$. Number of strings in each embrionic round braid is equal to $u + 1 = 2$. Note that the embrionic round braids are identical to those in (6, 1/0).

(iii). $u = 2$.

(7, 2/0). Number of free passive strings is equal to $n - 2 - 2u = 1$. Number of strings in each embrionic round braid is equal to $u + 1 = 3$.

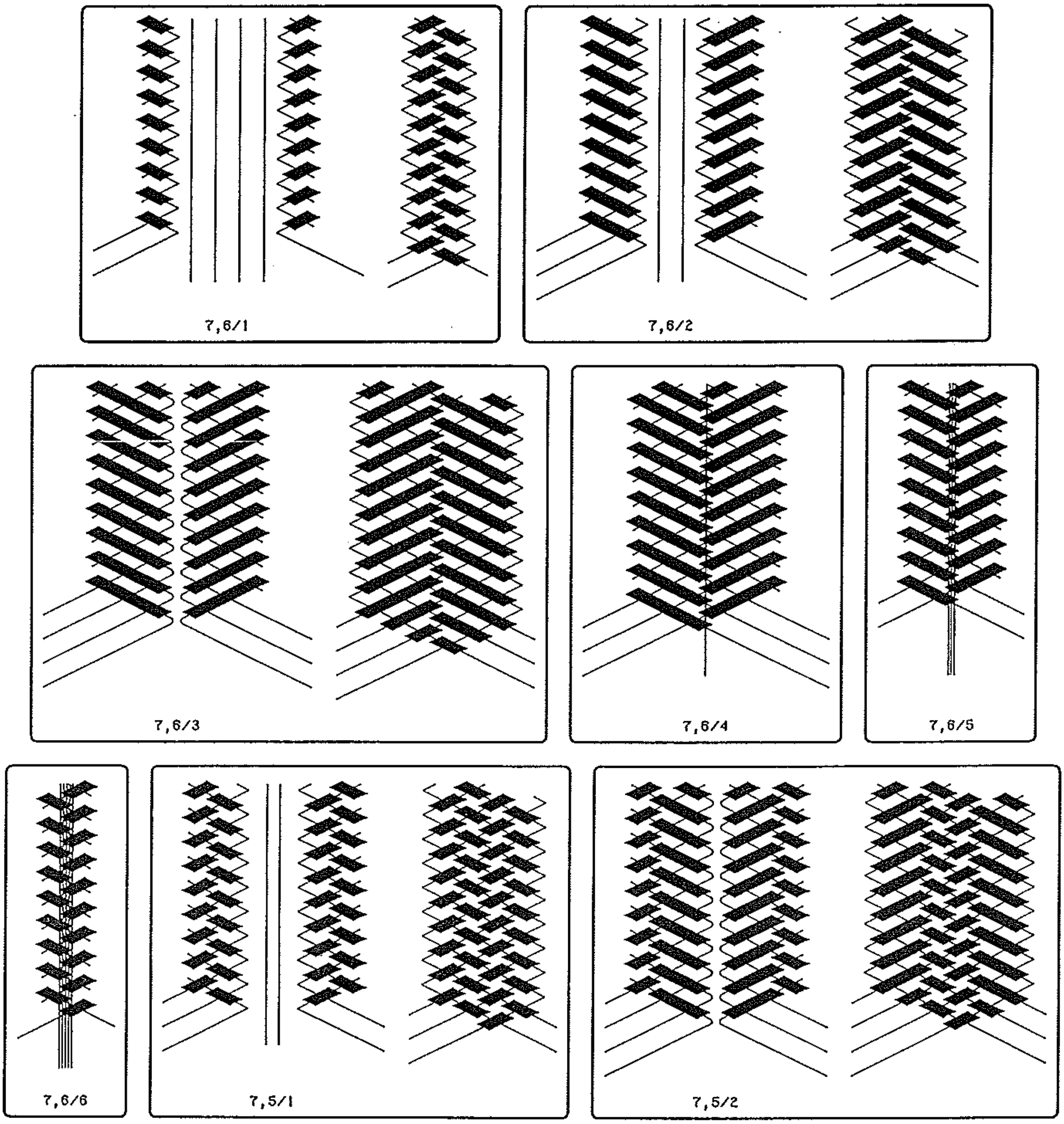

Fig. 712A — Grid-diagrams associated with Example 2.

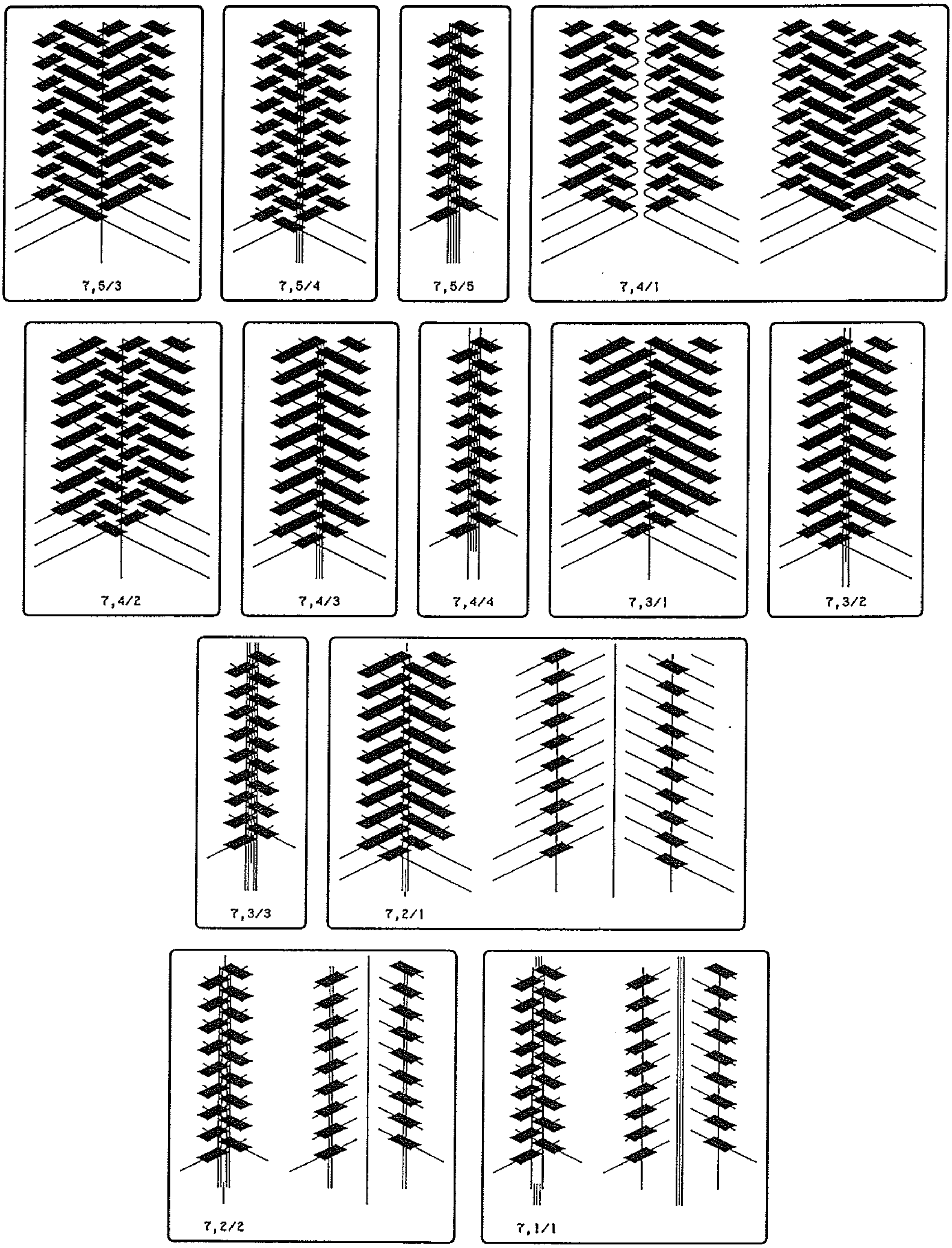

Fig. 712B — Grid-diagrams associated with Example 2.

Not only does Murphy's (braid) construction-method produce braids which do **not** belong to one braid-class, but it produces also a large number of braids which have no practical value, and in fact no theoretical value either. It is therefore a (braid) construction-method which should not be used in order not to lead a braider up the garden path.

A Six Thong Round Braid Start

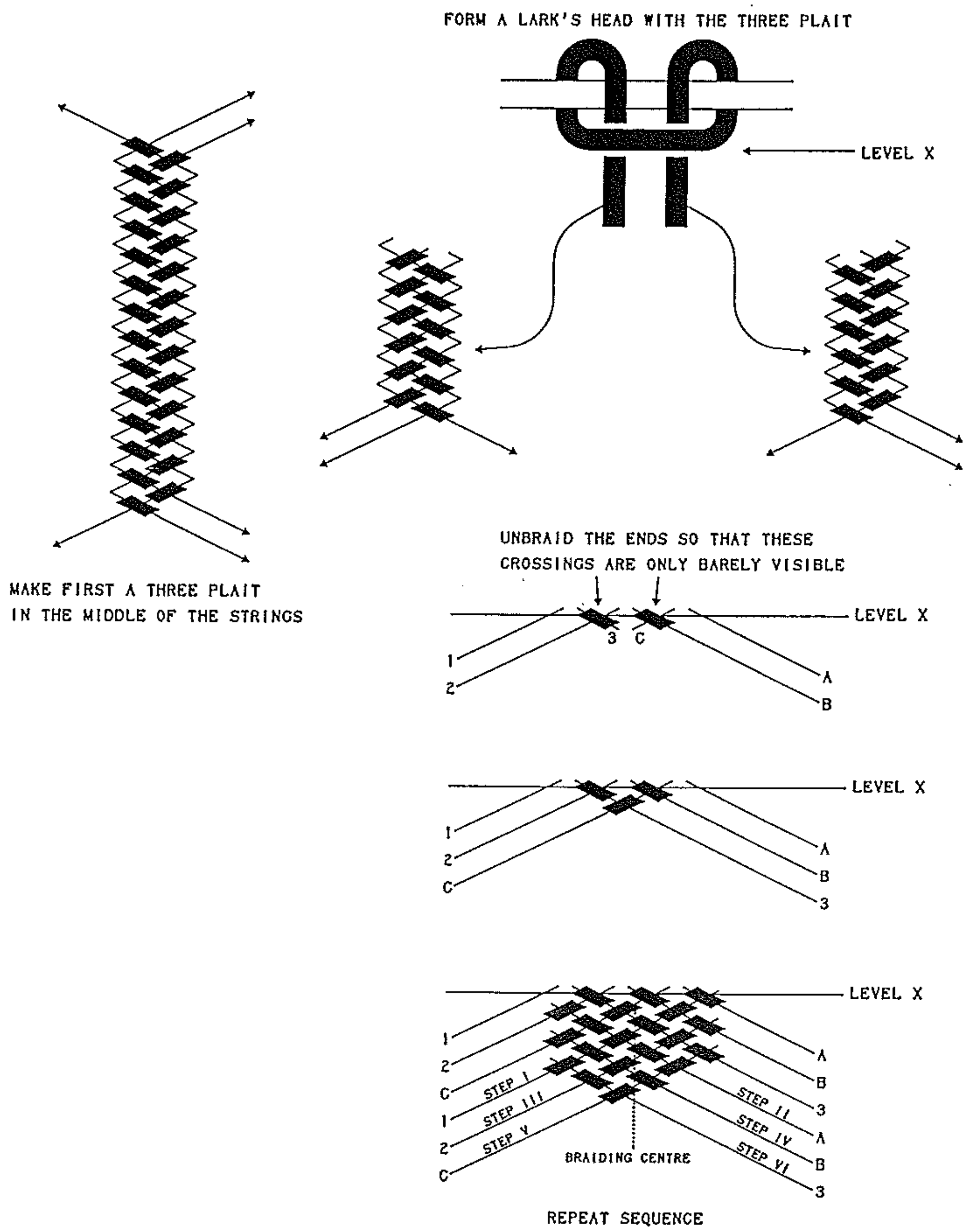

Fig. 713 — A six thong Round Braid start.

THE BRAIDER

No.39 **AUGUST 2004.**

CONTENTS

pg.

The Flores Knots 903

A quarterly publication
for
the braiding artisan

Resale of this publication or copies thereof
is strictly prohibited

Copyright ©2004 by:

A.G. Schaake; 21 Sundown Cresc.; Hamilton; New Zealand.
D. Van Tassel; Box 335; Craig, Co 81626-0335; U.S.A.
F.J.M. Masurel; Ganzenzijde 4; 2317XG Leiden; Nederland.

All rights reserved. No part of this publication may be reproduced, stored in a retrieval system, or transmitted, in any form or by any means, electronic, mechanical, photo-copying, recording, or otherwise, without prior written permission.

This publication is available to braiding artisans only.

Copies may be obtained from:

A.G. Schaake,
21 Sundown Cresc.,
Hamilton,
New Zealand.

The Flores Knots

In the *Encyclopedia of Rawhide and Leather Braiding* on pg. 424 Bruce Grant writes the following:

This beautiful little button [the Flores Button Knot] was shown to me in November 1966, in Buenos Aires by my amigo, Don Luis Alberto Flores. It illustrates a unique way to make a herringbone weave on a five-part, six-bight Turk's-head — or armadura*, as they say in the Argentine.*

From the above statement it is quite clear that it was not realised what in fact this knot was all about. Furthermore, from the three coding errors it contains, it appears that the knot was an empirical discovery (see later). The Flores Button Knot described by Bruce in the Encyclopedia is a single-string imitation of its true two-string characteristic, and since this single-string imitation of a true two-string characteristic is the usual encountered one, it contains a noticeable irregularity. Hence let's first have a look at this single-string imitation.

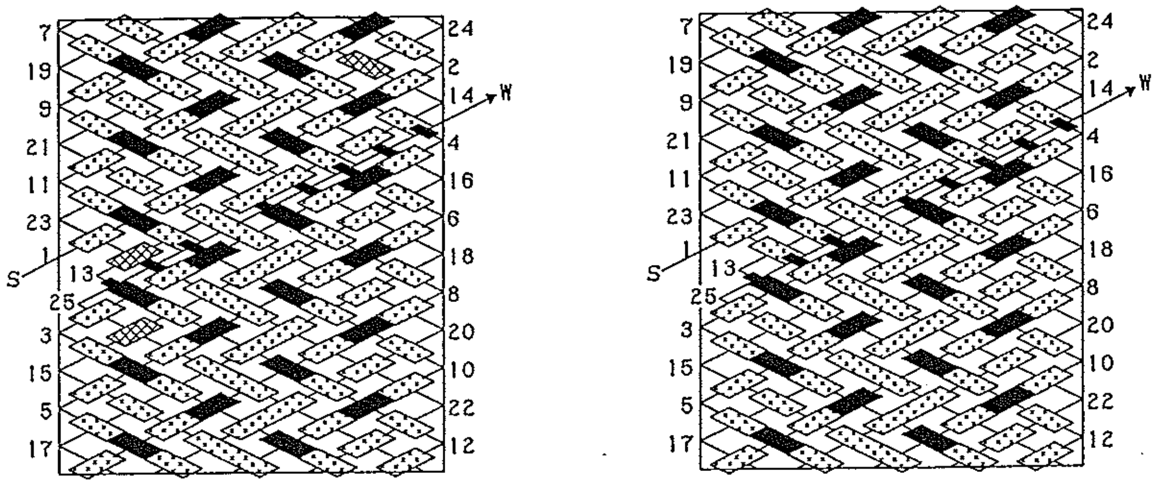

Fig. 714 — The Flores Button Knot.

The left-hand grid-diagram in Fig. 714 depicts the Flores Button Knot described by Bruce Grant. Its half-cycle braiding algorithms are as follows:

1. Free run.
2. Free run.
3. Free run.
4. u.
5. u.
6. $u - o$.
7. $u - o$.
8. $u - o - u$.
9. $u - o - u$.
10. $u - o - u - o$.
11. $u - o - u - o$.
12. $u - o - u - o$.
13. $u - o - 2u$.
14. $2u - o - 2u$.
15. $2u - o - 2u$.
16. $3u - o - 2u$.
17. $3u - o - 2u$.
18. $4u - o - 2u$.
19. $4u - o - 2u$.
20. $4u - 2o - 2u$.
21. $4u - 2o - 2u$.
22. $4u - 2o - 3u$.
23. $4u - 2o - 3u$.
24. $4u - 2o - 3u$.
25. $9u$.

Note that Bruce Grant does not work in exact half-cycles; however, it is important to work in exact half-cycles only. It is readily observed from the grid-diagram that three crossing-points are coded incorrectly: to be consistent the second and the eighth column from the left should be column-coded. The correct coding for this knot is shown by the right-hand grid-diagram of Fig. 714; its half-cycle braiding algorithms are as follows:

1. Free run.
2. Free run.
3. Free run.
4. u.
5. u.
6. $u - o$.
7. $u - o$.
8. $u - o - u$.
9. $u - o - u$.
10. $u - o - u - o$.
11. $u - o - u - o$.
12. $u - o - u - o$.
13. $u - o - 2u$.
14. $2u - o - 2u$.
15. $2u - o - 2u$.
16. $3u - o - 2u$.
17. $3u - o - 2u$.
18. $4u - o - 2u$.
19. $4u - o - 2u$.
20. $4u - 2o - 2u$.
21. $4u - 2o - 2u$.
22. $4u - 2o - u - o - u$.
23. $4u - 2o - u - o - u$.
24. $4u - 2o - u - o - u$.
25. $9u$.

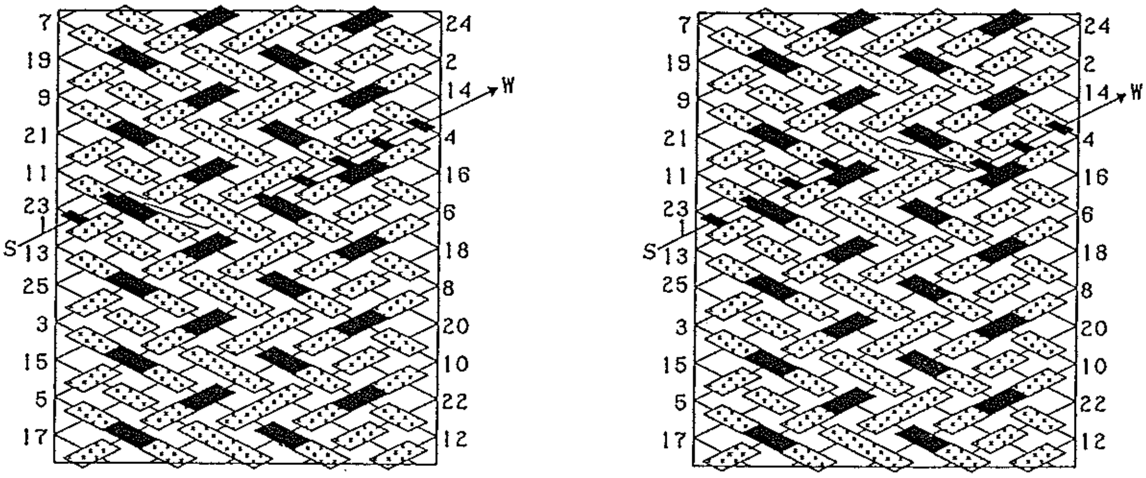

Fig. 715 — The Flores Knot without the boundary irregularity.

The already mentioned irregularity in the braid can be avoided by braiding the knot as shown by the grid-diagrams in Fig. 715 for example. The half-cycle braiding algorithms associated with the left-hand grid-diagram in Fig. 715 are as follows:

1. Free run.
2. Free run.
3. Free run.
4. u.
5. u.
6. $u - o$.
7. $u - o$.
8. $u - o - u$.
9. $u - o - u$.
10. $u - o - u - o$.
11. $u - o - u - o$.
12. $u - o - u - o$.
13. $u - o - 2u$.
14. $2u - o - 2u$.
15. $2u - o - 2u$.
16. $3u - o - 2u$.
17. $3u - o - 2u$.
18. $4u - o - 2u$.
19. $4u - o - 2u$.
20. $4u - 2o - 2u$.
21. $4u - 2o - 2u$.
22. $4u - 2o - 2u - o$.
23. $4u - 2o - u - o - u$.
24. $4u - 2o - u - o - u$.
25. $9u$.

The half-cycle braiding algorithms associated with the right-hand grid-diagram in Fig. 715 are as follows:

1. Free run.
2. Free run.
3. Free run.
4. u.
5. u.
6. $u-o$.
7. $u-o$.
8. $u-o-u$.
9. $u-o-u$.
10. $u-o-u-o$.
11. $u-o-u-o$.
12. $u-o-u-o$.
13. $u-o-2u$.
14. $2u-o-2u$.
15. $2u-o-2u$.
16. $3u-o-2u$.
17. $3u-o-2u$.
18. $3u-2o-2u$.
19. $4u-o-2u$.
20. $4u-o-u-o-u$.
21. $4u-2o-2u$.
22. $4u-2o-2u-o$.
23. $4u-2o-u-o-u$.
24. $4u-2o-u-o-u$.
25. $4u-2o-3u$.

These knots are single-string imitations of the true two-string form, hence let's call the true two-string form the Flores Knot. But what is the Flores Knot then really and what is its physical appearance?

The physical appearance of the Flores Knot is that of the Semi-Standard Herringbone Pineapple Knot with $A=2$, $x=6$, $B^*=6$ (see the left-hand grid-diagram of Fig. 716).

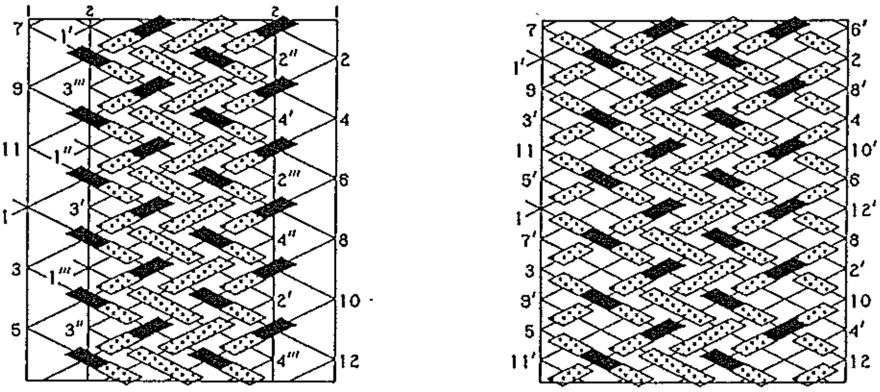

Fig. 716 — The evolution of the Flores Knot from the Semi-Standard Herringbone Pineapple Knot.

The right-hand grid-diagram in Fig. 716 shows how the Flores Knot evolves from it while retaining the physical appearance of the Semi-Standard Herringbone Pineapple knot from which it evolves. In this right-hand grid-diagram there are crossings in the second and penultimate crossing-columns which do not yet have a superimposed coding. Note that the codings of those crossings do not affect the physical appearance of the knot. Although each of those crossings can therefore be given an arbitrary coding, we limit these codings so that:

1. The **columns** to which they belong become **column-coded**.
2. The **rows** to which they belong become **row-coded**.

When we fulfil the column-coding option (option **1.** above), then the Flores Knot is depicted by the left-hand grid-diagram in Fig. 717. The Flores Knot is an interbraid of an over-under coded Regular Knot and a two-pass Spanish Ring Knot.

When we fulfil the row-coding option (option **2.** above), then the Flores Knot is depicted by the left-hand grid-diagram in Fig. 718. The Flores Knot is an interbraid of two over-under coded Regular Knots.

Note that the Flores knot requires two essential strings, whereas the Semi-Standard Herringbone Pineapple knot from which it has evolved, but to which it is identical in physical appearance, requires four essential strings.

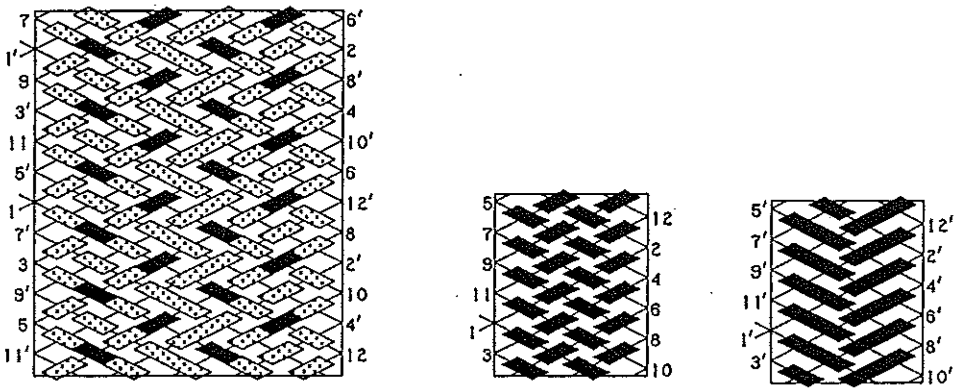

Fig. 717 — The Column-coding option.

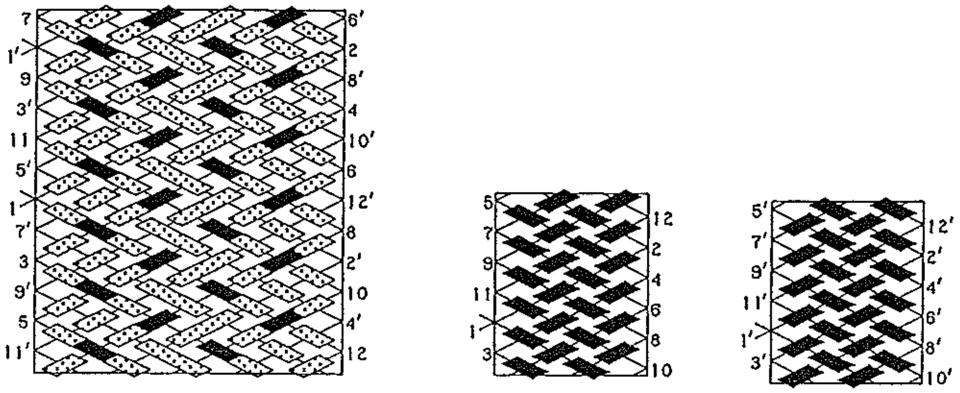

Fig. 718 — The Row-coding option.

⋆⋆ *Draw for each of the left-hand grid-diagrams in Figs. 717 & 718 the path in the RKT and from it determine their* Δ^* *values, then construct their algorithm diagrams. Read from their algorithm diagrams their half-cycle braiding algorithms.*

There is of course no reason why a Flores Knot should be restricted in having to be evolved in the above discussed manner from a two-pass Semi-Standard Herringbone Pineapple Knot. It can as well evolve in a similar manner from an A-pass Herringbone Pineapple Knot in general.

From the Standard and Semi-Standard Herringbone Pineapple Knots to the Flores Knots.

In Fig. 719 are depicted the string-runs of two Flores Knot examples: the upper diagram depicts the evolution of the string-run of a Flores Knot from the string-run of a six-pass Standard Herringbone Pineapple Knot, and the lower diagram depicts the evolution of the string-run of a Flores Knot from the string-run of a five-pass Semi-Standard Herringbone Pineapple Knot.

Since A-pass Standard and Semi-Standard Herringbone Pineapple Knots consist of A components (their string-run is such that $\left|\frac{x}{2}-(1+r_1)\right|_A = \left|\frac{x}{2}-(1+k)\right|_A = \frac{A}{2}$, hence $y = A$), the Flores Knots evolved from them also consist of A components.[†]

[†] Refer to *The Braider*, Issue No. 23, pp. 513-515, 526 and Issue No. 24, pg. 557.

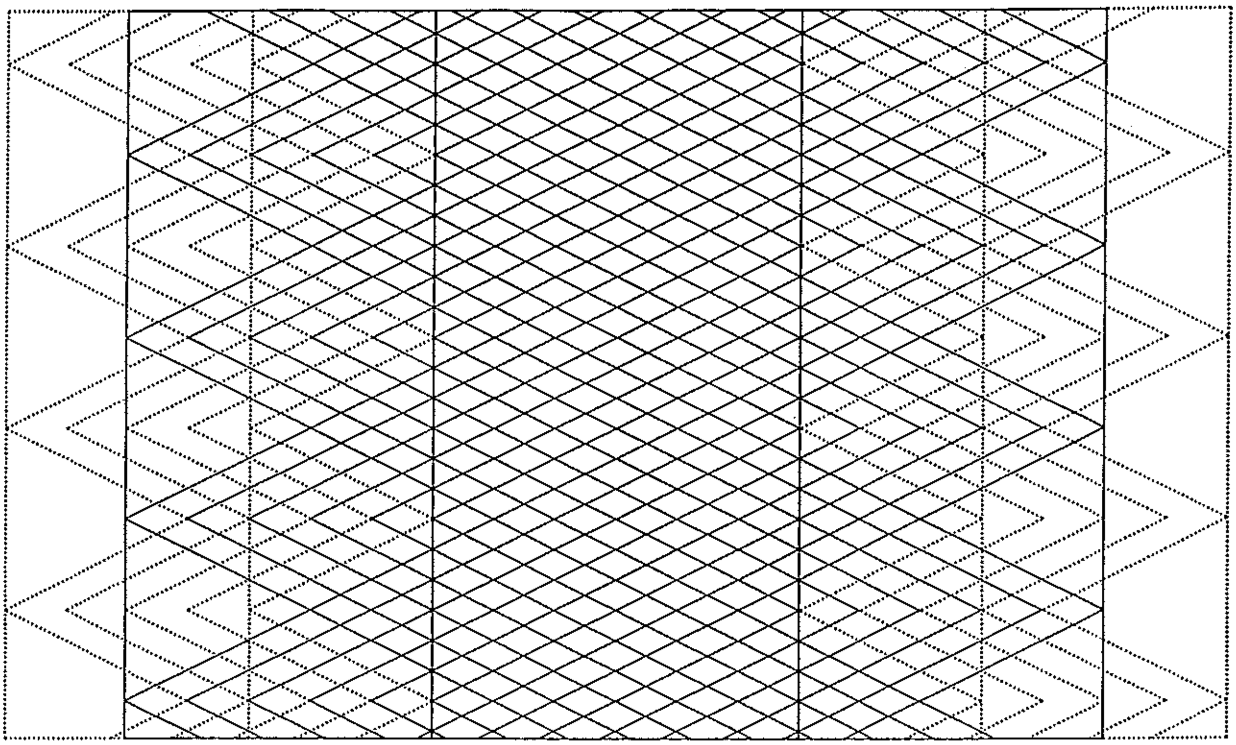

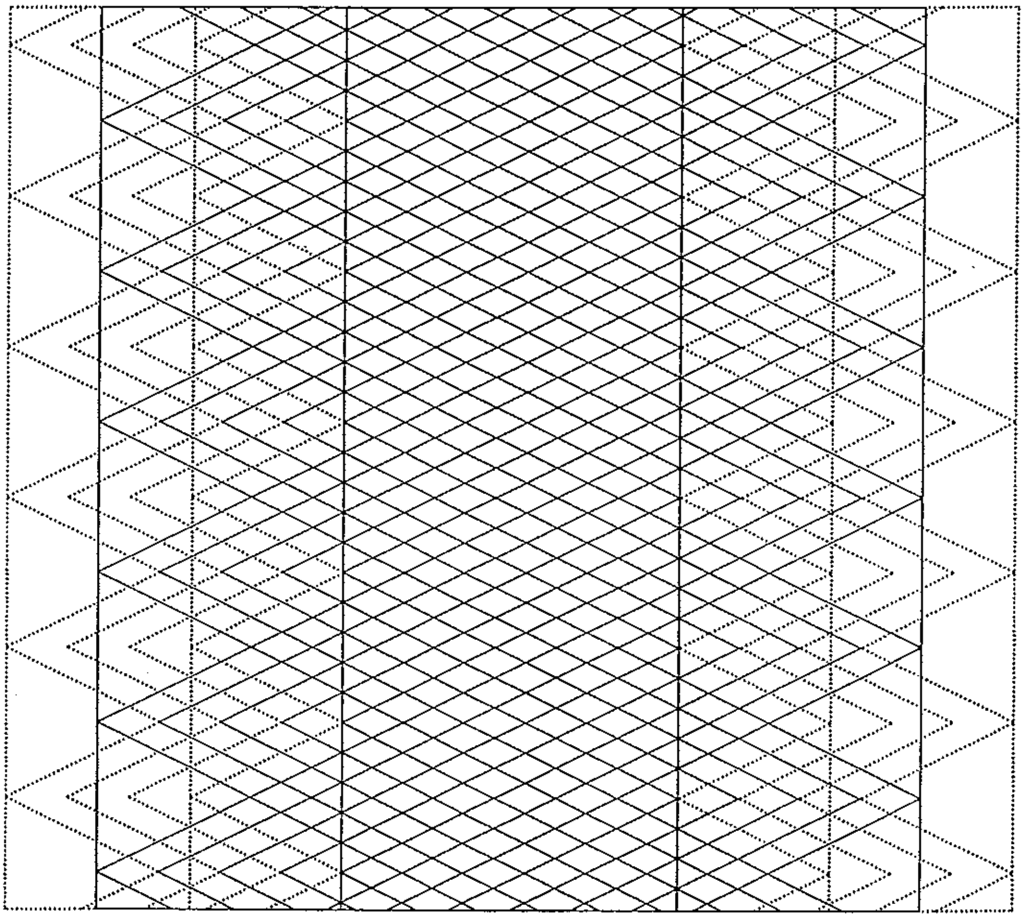

Fig. 719 — Flores Knot string-runs evolved from Standard or Semi-Standard Herringbone Pineapple Knot string-runs.

Let the number of parts of the Standard or Semi-Standard Herringbone Pineapple Knot component with the lower-left to upper-right half-cycle $l_i \longrightarrow r_i$ be P_{cP} and let the number of parts of its associated Flores knot component be P_{cF}, then the following relationships apply:

i). For $l_i = 1$ and $r_i = 1$: $P_{cF} = P_{cP}$.
ii). For $l_i = 1$ and $1 < r_i \leq A$: $P_{cF} = P_{cP} + 1$.
iii). For $1 < l_i \leq A$ and $r_i = 1$: $P_{cF} = P_{cP} + 1$.
v). For $1 < l_i \leq A$ and $1 < r_i \leq A$: $P_{cF} = P_{cP} + 2$.

Example 1.

Herringbone Pineapple Knot with $A = 6$; $x = 12$; $k = \left|\frac{x+A}{2} - 1\right|_A = 2$; $B^* = 4$. Its string-run is contained in the upper diagram of Fig. 719.

For $l_i = 1$; $r_i = k = 2$: $P_{cP} = 4 + \frac{x-2(k+1)}{A} = 5$.[†] Hence $P_{cF} = P_{cP} + 1 = 5 + 1 = 6$ for the associated Flores Knot component. The number of essential strings for the associated Flores component is thus g.c.d.$(P_{cF}, B^*) =$ g.c.d.$(6,4) = 2$.

For $l_i = 2$; $r_i = 1$: $P_{cP} = 4 + \frac{x-2(k+1)}{A} = 5$. Hence $P_{cF} = P_{cP} + 1 = 5 + 1 = 6$ for the associated Flores Knot component. The number of essential strings for the associated Flores component is thus g.c.d.$(P_{cF}, B^*) =$ g.c.d.$(6,4) = 2$.

For $l_i = 3$; $r_i = A = 6$: $P_{cP} = 2 + \frac{x-2(k+1)}{A} = 3$.[‡] Hence $P_{cF} = P_{cP} + 2 = 3 + 2 = 5$ for the associated Flores Knot component. The number of essential strings for the associated Flores component is thus g.c.d.$(P_{cF}, B^*) =$ g.c.d.$(5,4) = 1$.

For $l_i = 4$; $r_i = 5$: $P_{cP} = 2 + \frac{x-2(k+1)}{A} = 3$. Hence $P_{cF} = P_{cP} + 2 = 3 + 2 = 5$ for the associated Flores Knot component. The number of essential strings for the associated Flores component is thus g.c.d.$(P_{cF}, B^*) =$ g.c.d.$(5,4) = 1$.

For $l_i = 5$; $r_i = 4$: $P_{cP} = 2 + \frac{x-2(k+1)}{A} = 3$. Hence $P_{cF} = P_{cP} + 2 = 3 + 2 = 5$ for the associated Flores Knot component. The number of essential strings for the associated Flores component is thus g.c.d.$(P_{cF}, B^*) =$ g.c.d.$(5,4) = 1$.

For $l_i = 6$; $r_i = 3$: $P_{cP} = 2 + \frac{x-2(k+1)}{A} = 3$. Hence $P_{cF} = P_{cP} + 2 = 3 + 2 = 5$ for the associated Flores Knot component. The number of essential strings for the associated Flores component is thus g.c.d.$(P_{cF}, B^*) =$ g.c.d.$(5,4) = 1$.

Hence the total number of essential strings for the Flores Knot is 8, whereas the Herringbone Pineapple knot required 6 essential strings.

Example 2.

Herringbone Pineapple Knot with $A = 5$; $x = 11$; $k = \left|\frac{x+A}{2} - 1\right|_A = 2$; $B^* = 6$. Its string-run is contained in the lower diagram of Fig. 719.

For $l_i = 1$; $r_i = k = 2$: $P_{cP} = 4 + \frac{x-2(k+1)}{A} = 5$. Hence $P_{cF} = P_{cP} + 1 = 5 + 1 = 6$ for the associated Flores Knot component. The number of essential strings for the associated Flores component is thus g.c.d.$(P_{cF}, B^*) =$ g.c.d.$(6,6) = 6$.

For $l_i = 2$; $r_i = 1$: $P_{cP} = 4 + \frac{x-2(k+1)}{A} = 5$. Hence $P_{cF} = P_{cP} + 1 = 5 + 1 = 6$ for the associated Flores Knot component. The number of essential strings for the associated Flores component is thus g.c.d.$(P_{cF}, B^*) =$ g.c.d.$(6,6) = 6$.

[†] Refer to *The Braider*, Issue No. 23, pg. 521.

[‡] Refer to *The Braider*, Issue No. 23, pg. 521.

For $l_i = 3$; $r_i = A = 5$: $P_{cP} = 2 + \frac{x-2(k+1)}{A} = 3$. Hence $P_{cF} = P_{cP} + 2 = 3 + 2 = 5$ for the associated Flores Knot component. The number of essential strings for the associated Flores component is thus g.c.d. $(P_{cF}, B^*) =$ g.c.d. $(5,6) = 1$.

For $l_i = 4$; $r_i = 4$: $P_{cP} = 2 + \frac{x-2(k+1)}{A} = 3$. Hence $P_{cF} = P_{cP} + 2 = 3 + 2 = 5$ for the associated Flores Knot component. The number of essential strings for the associated Flores component is thus g.c.d. $(P_{cF}, B^*) =$ g.c.d. $(5,6) = 1$.

For $l_i = 5$; $r_i = 3$: $P_{cP} = 2 + \frac{x-2(k+1)}{A} = 3$. Hence $P_{cF} = P_{cP} + 2 = 3 + 2 = 5$ for the associated Flores Knot component. The number of essential strings for the associated Flores component is thus g.c.d. $(P_{cF}, B^*) =$ g.c.d. $(5,6) = 1$.

Hence the total number of essential strings for the Flores Knot is 15, whereas the Herringbone Pineapple knot required 11 essential strings.

The Flores Knots in the above two examples are only of practical value if their greater number of essential strings, as compared to the number of essential strings in the Herringbone Pineapple Knots from which they have evolved, is used for special colour effects. Such a special colour effect is shown in Fig. 720.

Although there are for Flores Knots, evolved from A-pass Standard or Semi-Standard Herringbone Pineapple Knots, two ways to superimpose on the non-coded crossings a coding so that all those near the left bight-edge are coded identically and opposite to those near the right bight-edge, note that for $A > 2$ only a row-coding for the rows to which they belong can be achieved; the columns to which they belong cannot become column-coded. Hence the row-coded case is the general one, whereas the column-coded case is specific to $A = 2$ only. Hence of the above two ways to superimpose a coding on the non-coded crossings, let's call one **the row-coding case** and the other **the non row-coding case**.

The algorithm diagrams from which we read the half-cycle braiding algorithms for the Flores knots evolved from A-pass Standard or Semi-Standard Herringbone Pineapple Knots can be derived in the following way:

Imagine that we modify the string-run of such a Flores Knot a little further so that the string-run becomes that of a Standard or Semi-Standard Herringbone Pineapple Knot again. For the above two Examples this is shown in Fig. 721. All the components (if any) which do not have a bight-boundary 1 in the grid-diagram with this modified string-run are true components of the Flores Knot (let's call these the true Flores Knot components). Hence the grid-diagram with this modified string-run has either one component (when it has a component with the left and the right bight-boundary both 1) or two components (when one component has the left bight-boundary 1, and another component has the right bight-boundary 1) which is/are not true components of the Flores Knot (let's call this/these the nontrue Flores Knot component(s)). In practice we can then first braid the true Flores Knot components (if there are any), and finally braid the reconverted nontrue Flores Knot component(s).

The row-coding case:

In the modified Flores Knot grid-diagram a lower-left to upper-right half-cycle running from l_i to r_i has the coding sequence:

$$(l_i-1)u-(A+1-l_i)o-(l_i)u-Ao-Au-\cdots-Au-Ao-(r_i-1)u-(A-r_i)o-(r_i)u\,,$$

in which each set of crossings, except the first set $(l_i-1)u$ and the two penultimate sets $(r_i-1)u-(A-r_i)o$, has one crossing belonging to string-run of the component between the bight-boundaries l_i and r_i.

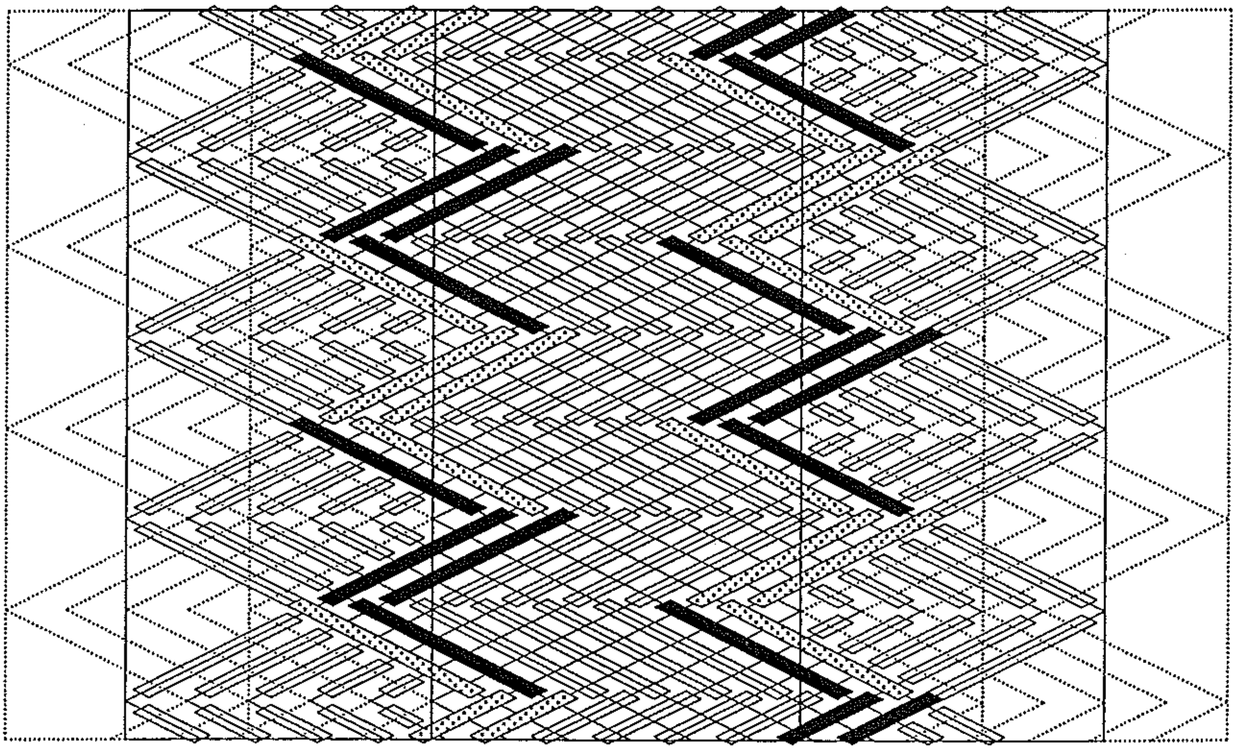

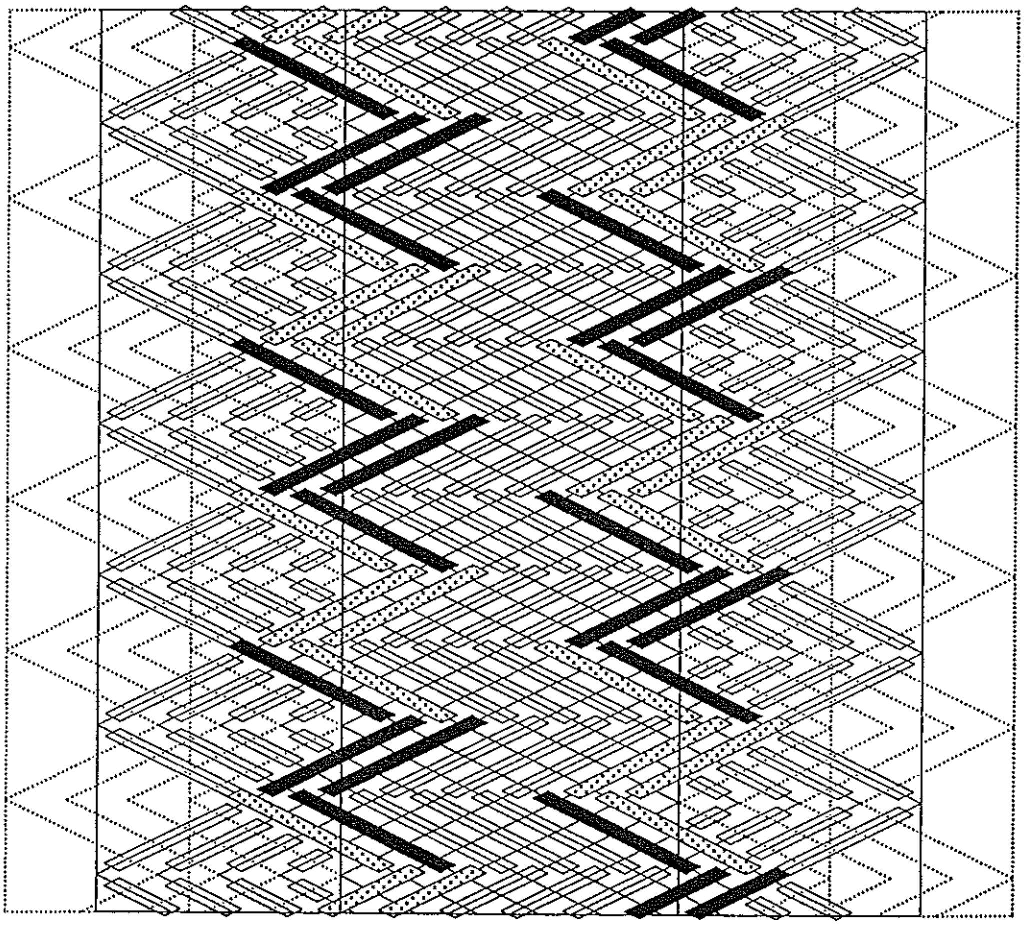

Fig. 720 — Flores Knots evolved from Standard or Semi-Standard Herringbone Pineapple Knots.

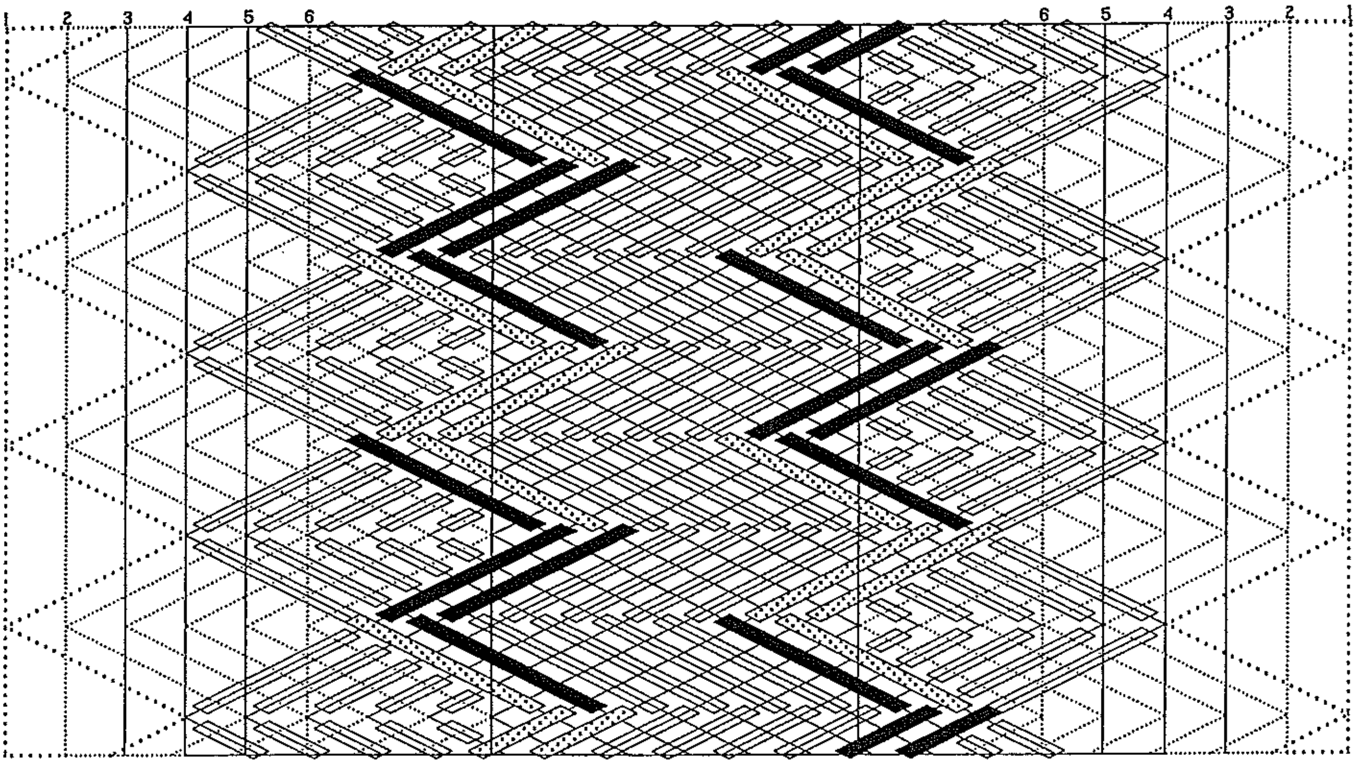

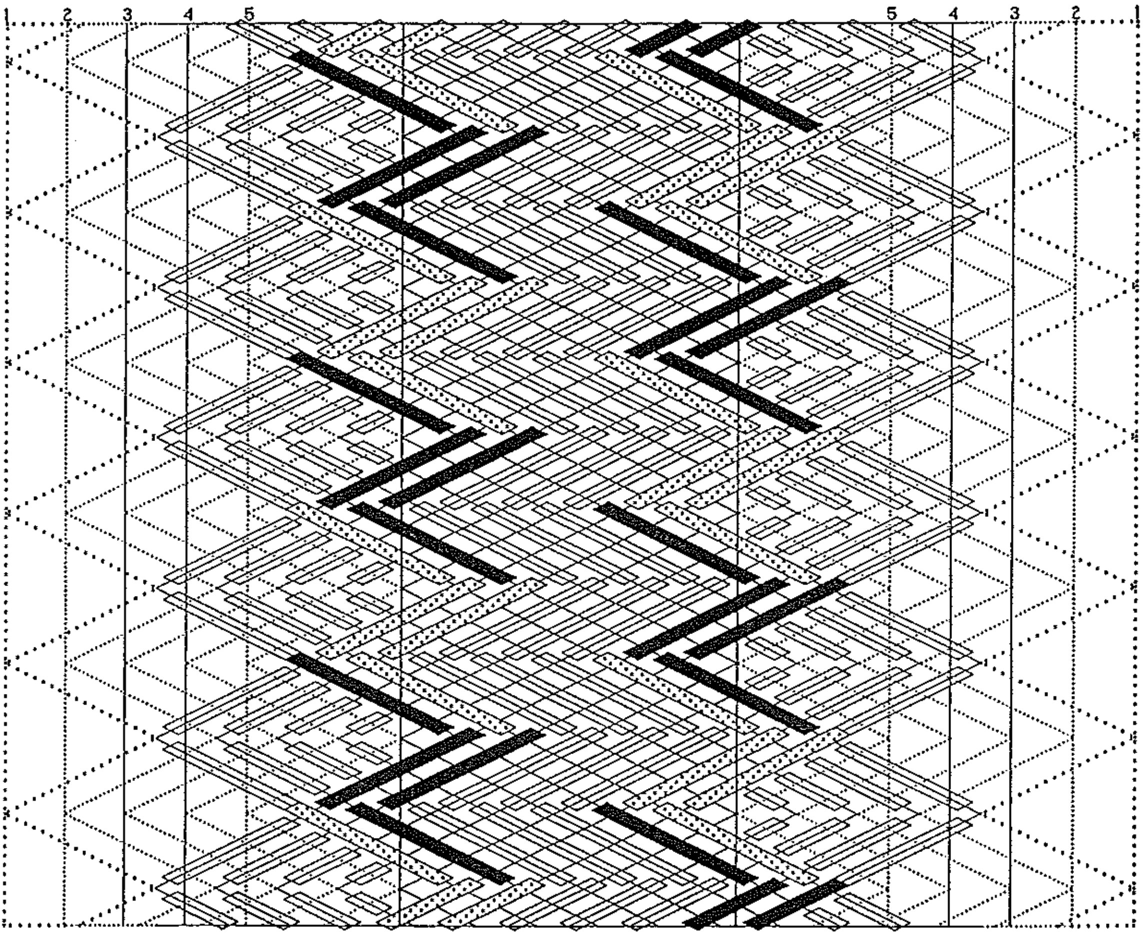

Fig. 721 — Flores Knot string-runs modified into Standard or Semi-Standard Herringbone Pineapple Knot string-runs.

In the modified Flores Knot grid-diagram a lower-right to upper-left half-cycle running from r_i to l_i has the coding sequence:

$$(r_i-1)u-(A+1-r_i)o-(r_i)u-Ao-Au-\cdots-Au-Ao-(l_i-1)u-(A-l_i)o-(l_i)u\,,$$

in which each set of crossings, except the first set $(r_i-1)u$ and the two penultimate sets $(l_i-1)u-(A-l_i)o$, has one crossing belonging to the string-run of the component between the bight-boundaries l_i and r_i.

Hence the reference half-cycle sequences, consequently the first half-cycle sequences of the components, are:

From lower-left l_i to upper-right r_i :

$$(l_i-1)u-(A-l_i)o-(l_i-1)u-(A-1)o-(A-1)u-\cdots-(A-1)u-(A-1)o-(r_i-1)u-(A-r_i)o-(r_i-1)u\,.$$

From lower-right r_i to upper-left l_i :

$$(r_i-1)u-(A-r_i)o-(r_i-1)u-(A-1)o-(A-1)u-\cdots-(A-1)u-(A-1)o-(l_i-1)u-(A-l_i)o-(l_i-1)u\,.$$

The general form of the algorithm diagram for the true Flores Knot components is thus:

$$\begin{array}{ccccccccccccc}
\longrightarrow & l_i-1 & A-l_i & l_i-1 & A-1 & A-1 & \dots & A-1 & A-1 & A-1 & r_i-1 & A-r_i & r_i-1 \\
\vdash & & \star & \star & \star & \star & \dots & \star & \star & \star & & & \star \\
/ & \backslash & / & \backslash & / & \backslash & \dots & / & \backslash & / & \backslash & / & \backslash \\
\star & & & \star & \star & \star & \dots & \star & \star & \star & \star & & \dashv \\
l_i-1 & A-l_i & l_i-1 & A-1 & A-1 & A-1 & \dots & A-1 & A-1 & r_i-1 & A-r_i & r_i-1 & \longleftarrow
\end{array}$$

The positions of the stars are occupied by the i-values of the complementary bight-number scheme associated with the component to be braided. The value above an upper star, or below a lower star, increases by 1 when its associated i-value is applicable to the half-cycle concerned. For all the lower-left to upper-right half-cycles the first entry $(l_i-1)u$ and the last two penultimate entries $(r_i-1)u-(A-r_i)o$ remain the same. Similarly, for all the lower-right to upper-left half-cycles the first entry $(r_i-1)u$ and the last two penultimate entries $(l_i-1)u-(A-l_i)o$ remain the same.

After the true Flores Knot components (if there are any) have been braided, we finally braid the reconverted nontrue Flores Knot component(s).

If there is only one nontrue Flores Knot component, then the algorithm diagram for its reconverted form (its true form) is:

$$\begin{array}{ccccccccccc}
\longrightarrow & A-l_i & l_i-1 & A-1 & A-1 & \dots & A-1 & A-1 & A-1 & r_i-1 & A-r_i \\
\vdash & & \star & \star & \star & \dots & \star & \star & \star & & \\
\backslash & / & \backslash & / & \backslash & \dots & / & \backslash & / & \backslash & / \\
 & & \star & \star & \star & \dots & \star & \star & \star & & \dashv \\
A-l_i & l_i-1 & A-1 & A-1 & A-1 & \dots & A-1 & A-1 & r_i-1 & A-r_i & \longleftarrow
\end{array}$$

The positions of the stars are occupied by the i-values of the complementary bight-number scheme associated with the reconverted component to be braided. The value above an upper star, or below a lower star, increases by 1 when its associated i-value is applicable to the half-cycle concerned. For all the lower-left to upper-right half-cycles the first entry $(A-l_i)o$ and the last two entries $(r_i-1)u-(A-r_i)o$ remain the same. Similarly, for all the lower-right to upper-left half-cycles the first entry $(A-r_i)o$ and the last two entries $(l_i-1)u-(A-l_i)o$ remain the same.

If there are two nontrue Flores Knot components, then the algorithm diagram for the reconverted form (the true form) of the nontrue Flores Knot component with left bight-boundary 1 is:

$$\begin{array}{cccccccccccc}
\longrightarrow & A-l_i & l_i-1 & A-1 & A-1 & \ldots & A-1 & A-1 & A-1 & r_i-1 & A-r_i & r_i-1 \\
\vdash & & \star & \star & \star & \ldots & \star & \star & \star & & & \star \\
\backslash & / & \backslash & / & \backslash & \cdots & / & \backslash & / & \backslash & / & \backslash \\
 & & \star & \star & \star & \ldots & \star & \star & \star & \star & & \dashv \\
A-l_i & l_i-1 & A-1 & A-1 & A-1 & \ldots & A-1 & A-1 & r_i-1 & A-r_i & r_i-1 & \longleftarrow
\end{array}$$

The positions of the stars are occupied by the i-values of the complementary bight-number scheme associated with the reconverted component to be braided. The value above an upper star, or below a lower star, increases by 1 when its associated i-value is applicable to the half-cycle concerned. For all the lower-left to upper-right half-cycles the first entry $(A-l_i)o$ and the last two penultimate entries $(r_i-1)u-(A-r_i)o$ remain the same. Similarly, for all the lower-right to upper-left half-cycles the first entry $(r_i-1)u$ and the last two entries $(l_i-1)u-(A-l_i)o$ remain the same.

The algorithm diagram for the reconverted form (the true form) of the nontrue Flores Knot component with right bight-boundary 1 is:

$$\begin{array}{cccccccccccc}
\longrightarrow & l_i-1 & A-l_i & l_i-1 & A-1 & A-1 & \ldots & A-1 & A-1 & A-1 & r_i-1 & A-r_i \\
\vdash & & \star & \star & \star & \star & \ldots & \star & \star & \star & & \\
/ & \backslash & / & \backslash & / & \backslash & \cdots & / & \backslash & / & \backslash & / \\
\star & & & \star & \star & \star & \ldots & \star & \star & \star & & \dashv \\
l_i-1 & A-l_i & l_i-1 & A-1 & A-1 & A-1 & \ldots & A-1 & A-1 & r_i-1 & A-r_i & \longleftarrow
\end{array}$$

The positions of the stars are occupied by the i-values of the complementary bight-number scheme associated with the reconverted component to be braided. The value above an upper star, or below a lower star, increases by 1 when its associated i-value is applicable to the half-cycle concerned. For all the lower-left to upper-right half-cycles the first entry $(l_i-1)u$ and the last two entries $(r_i-1)u-(A-r_i)o$ remain the same. Similarly, for all the lower-right to upper-left half-cycles the first entry $(A-r_i)o$ and the last two penultimate entries $(l_i-1)u-(A-l_i)o$ remain the same.

Example 3:

Take the Flores Knot depicted by the upper grid-diagram in Fig. 720 under the row-coding case; $A=6$; $B^*=4$; $x=24$.

Then for the string-run of a Standard or Semi-Standard Herringbone Pineapple Knot we obtain:

$$\text{For } l_1=1 \quad \longrightarrow \quad r_1=\left|\frac{x+A}{2}-1\right|_A=\left|\frac{24+6}{2}-1\right|_6=2=k\,.$$

$$n=\frac{x+A-2k-2}{2A}=\frac{24+6-2\times2-2}{2\times6}=2\,,\ \text{hence :}$$

$P_{cP}=3+2n=3+2\times2=7$ for $k=2$ components. These are nontrue Flores Knot components with the half-cycles $1\longrightarrow2$ and $2\longrightarrow1$ respectively. Hence $P_{cF}=6$ for their reconverted components.

$P'_{cP}=1+2n=1+2\times2=5$ for $A-k=6-2=4$ components. These are true Flores Knot components, hence with $P'_{cF}=5$ each.

Since $\text{g.c.d.}(P_{cF},B^*)=\text{g.c.d.}(6,4)=2$, each of the two reconverted components require two essential strings. The other four components, with $\text{g.c.d.}(P'_{cF},B^*)=\text{g.c.d.}(5,4)=1$, require one essential string each.

Say we braid the various components in the six sequential stages depicted in Fig. 722.

Stage 1. We first braid the component which in the upper diagram of Fig. 721 starts with the half-cycle which runs from lower-left to upper-right between left bight-boundary 3 and right bight-boundary 6. Then, at present, for this component the left bight-boundary is 1 and the right bight-boundary is 1.

Stage 2. Next we interbraid the component which in the upper diagram of Fig. 721 starts with the half-cycle which runs from lower-left to upper-right between left bight-boundary 4 and right bight-boundary 5. Then, at present, for this component the left bight-boundary is 2 and the right bight-boundary is 1.

Stage 3. Next we interbraid the component which in the upper diagram of Fig. 721 starts with the half-cycle which runs from lower-left to upper-right between left bight-boundary 5 and right bight-boundary 4. Then, at present, for this component the left bight-boundary is 3 and the right bight-boundary is 1.

Stage 4. Next we interbraid the component which in the upper diagram of Fig. 721 starts with the half-cycle which runs from lower-left to upper-right between left bight-boundary 6 and right bight-boundary 3. Then, at present, for this component the left bight-boundary is 4 and the right bight-boundary is 1.

This completes the braiding of the true Flores Knot components. Next we interbraid the two reconverted nontrue Flores Kot components.

Stage 5. The first one we interbraid runs in the upper diagram of Fig. 721 as a nontrue Flores Knot component between left bight-boundary 1 and right bight-boundary 2. Hence for this nontrue Flores Knot component, which results into two reconverted sub-components, the left bight-boundary is 1 and the right bight-boundary is 1.

Stage 6. Finally we interbraid the other reconverted nontrue Flores Knot component, which as a nontrue Flores Knot runs in the upper diagram of Fig. 721 as a nontrue Flores Knot component between left bight-boundary 2 and right bight-boundary 1. For this nontrue Flores Knot component, which results into two reconverted sub-components, the left bight-boundary is 2 and the right bight-boundary is 1.

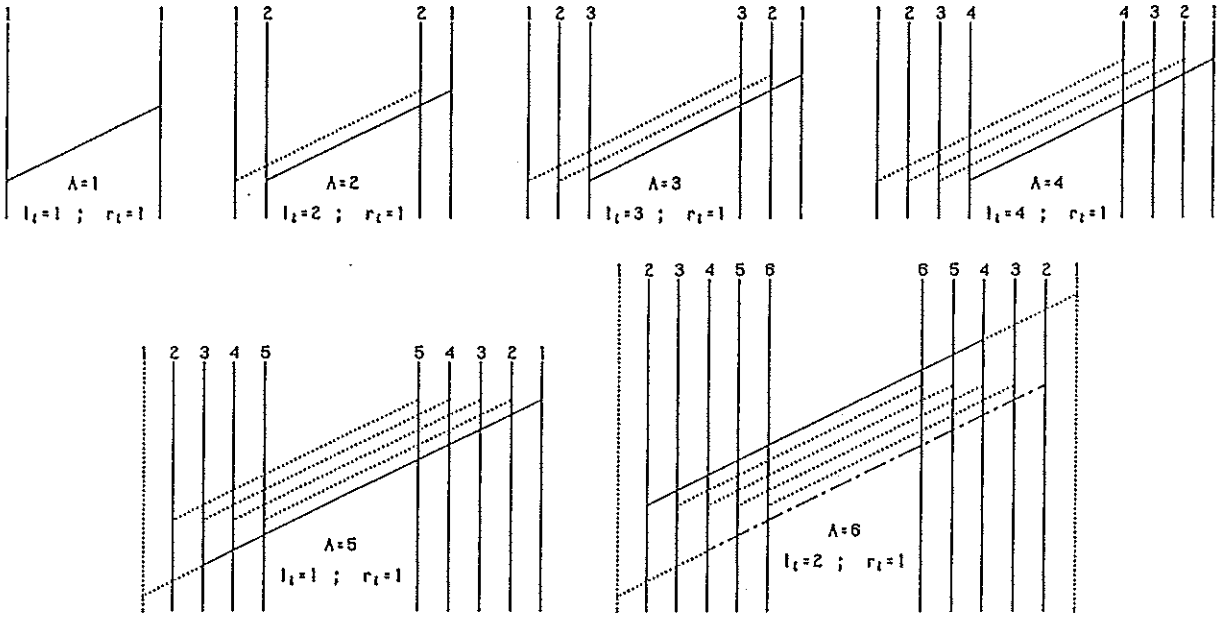

Fig. 722 — The sequence of braiding the various components.

Each of the components in the stages 1, 2, 3 and 4 require only one essential string in their construction. Each of these components is a Regular Knot with 5-parts and 4-bights, hence their Δ^*-value is equal to 3, and their generalised algorithm diagrams are as follows:

$$\begin{array}{cccccccc}
\longrightarrow & l_i-1 & A-l_i & l_i-1 & A-1 & r_i-1 & A-r_i & r_i-1 \\
\vdash & & \star & \star & \star & & & \star \\
/ & \backslash & / & \backslash & / & \backslash & / & \backslash \\
\star & & & \star & \star & \star & & \dashv \\
l_i-1 & A-l_i & l_i-1 & A-1 & r_i-1 & A-r_i & r_i-1 & \longleftarrow
\end{array}$$

The algorithm diagram for stage 1 is thus:

$$\begin{array}{cccccccc}
\longrightarrow & 0 & 0 & 0 & 0 & 0 & 0 & 0 \\
\vdash & & 3 & 2 & 1 & & & 0 \\
/ & \backslash & / & \backslash & / & \backslash & / & \backslash \\
0 & & & 1 & 2 & 3 & & \dashv \\
0 & 0 & 0 & 0 & 0 & 0 & 0 & \longleftarrow
\end{array}$$

From this algorithm diagram we read the half-cycle braiding algorithms for stage 1:

half-cycle 1 : $L_1 \longrightarrow R_1$ Free Run.
half-cycle 2 $i=0$: $L_1 \longleftarrow R_1$ u.
half-cycle 3 $i=0$: $L_1 \longrightarrow R_1$ u.
half-cycle 4 $i \leq 1$: $L_1 \longleftarrow R_1$ $o-u$.
half-cycle 5 $i \leq 1$: $L_1 \longrightarrow R_1$ $o-u$.
half-cycle 6 $i \leq 2$: $L_1 \longleftarrow R_1$ $u-o-u$.
half-cycle 7 $i \leq 2$: $L_1 \longrightarrow R_1$ $u-o-u$.
half-cycle 8 $i \leq 3$: $L_1 \longleftarrow R_1$ $o-u-o-u$.

These half-cycle braiding steps are shown in Fig. 723.

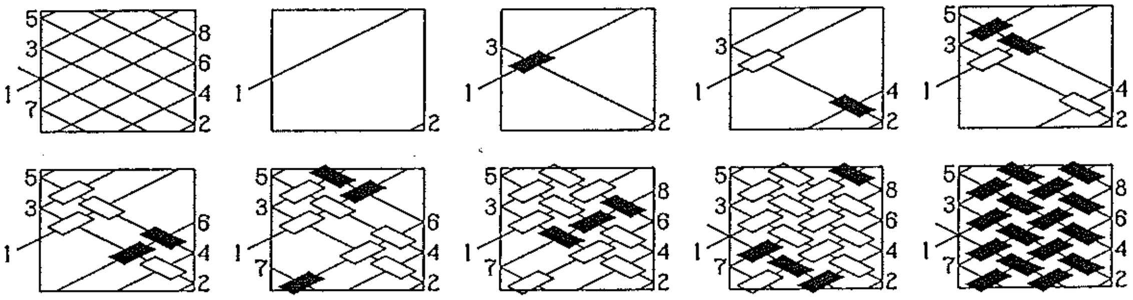

Fig. 723 — The half-cyle braiding steps for the first component.

The algorithm diagram for stage 2 is thus:

$$\begin{array}{cccccccc}
\longrightarrow & 1 & 0 & 1 & 1 & 0 & 1 & 0 \\
\vdash & & 3 & 2 & 1 & & & 0 \\
/ & \backslash & / & \backslash & / & \backslash & / & \backslash \\
0 & & & 1 & 2 & 3 & & \dashv \\
1 & 0 & 1 & 1 & 0 & 1 & 0 & \longleftarrow
\end{array}$$

From this algorithm diagram we read the half-cycle braiding algorithms for stage 2:

half-cycle 1 : $L_2 \longrightarrow R_1$ $2u-2o$.
half-cycle 2 $i=0$: $L_2 \longleftarrow R_1$ $2o-3u$.
half-cycle 3 $i=0$: $L_2 \longrightarrow R_1$ $2u-2o-u$.
half-cycle 4 $i \leq 1$: $L_2 \longleftarrow R_1$ $3o-3u$.
half-cycle 5 $i \leq 1$: $L_2 \longrightarrow R_1$ $2u-3o-u$.
half-cycle 6 $i \leq 2$: $L_2 \longleftarrow R_1$ $o-u-2o-3u$.
half-cycle 7 $i \leq 2$: $L_2 \longrightarrow R_1$ $3u-3o-u$.
half-cycle 8 $i \leq 3$: $L_2 \longleftarrow R_1$ $2o-u-2o-3u$.

These half-cycle braiding steps are shown in Fig. 724.

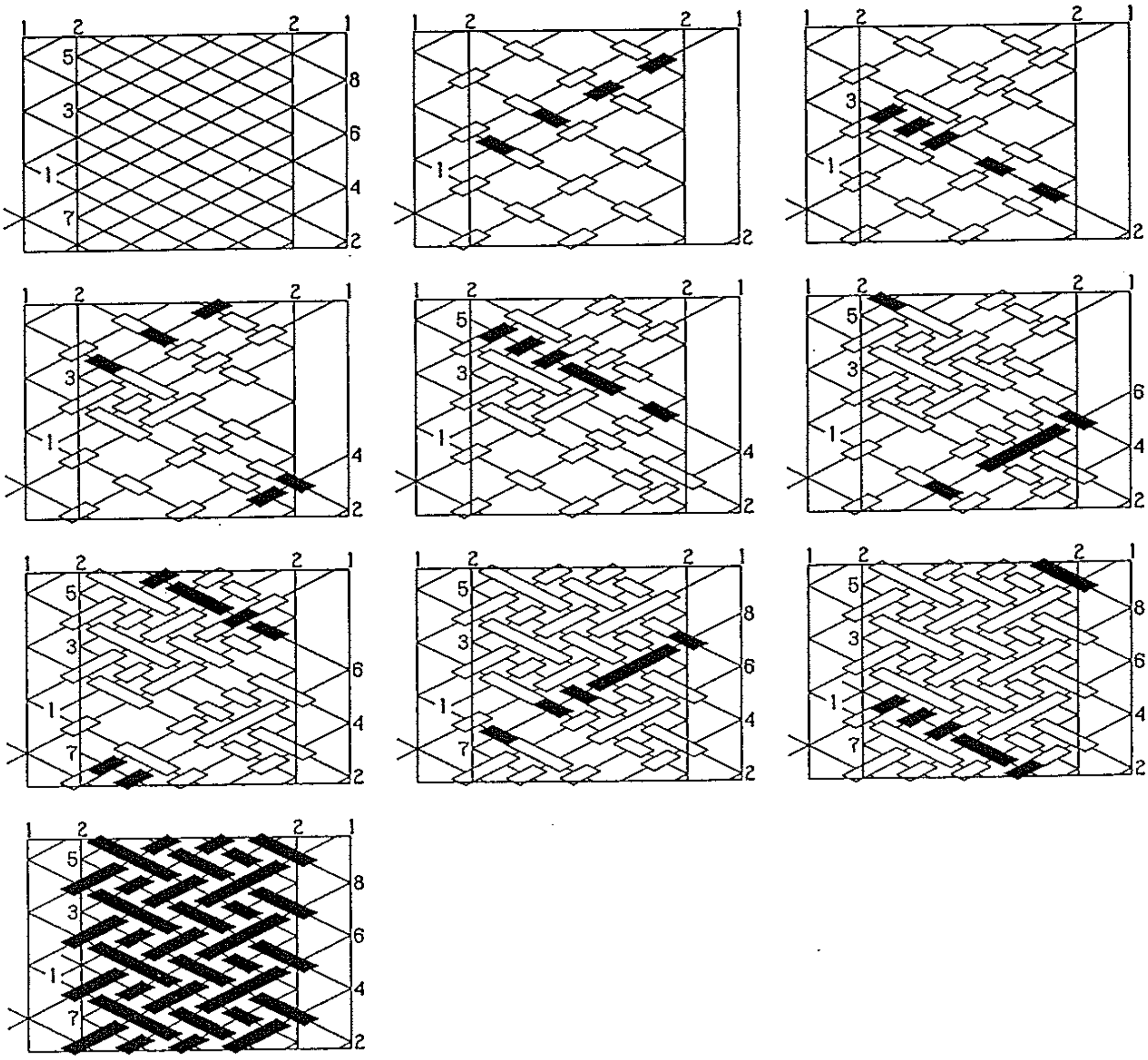

Fig. 724 — The half-cyle braiding steps for the second component.

The algorithm diagram for stage 3 is thus:

$$\begin{array}{cccccccc}
\longrightarrow & 2 & 0 & 2 & 2 & 0 & 2 & 0 \\
\vdash & & 3 & 2 & 1 & & & 0 \\
/ & \backslash & / & \backslash & / & \backslash & / & \backslash \\
0 & & & 1 & 2 & 3 & & \dashv \\
2 & 0 & 2 & 2 & 0 & 2 & 0 & \longleftarrow
\end{array}$$

From this algorithm diagram we read the half-cycle braiding algorithms for stage 3:

half-cycle 1 : $L_3 \longrightarrow R_1$ $4u - 4o$.
half-cycle 2 $i = 0$: $L_3 \longleftarrow R_1$ $4o - 5u$.
half-cycle 3 $i = 0$: $L_3 \longrightarrow R_1$ $4u - 4o - u$.
half-cycle 4 $i \leq 1$: $L_3 \longleftarrow R_1$ $5o - 5u$.
half-cycle 5 $i \leq 1$: $L_3 \longrightarrow R_1$ $4u - 5o - u$.
half-cycle 6 $i \leq 2$: $L_3 \longleftarrow R_1$ $2o - u - 3o - 5u$.
half-cycle 7 $i \leq 2$: $L_3 \longrightarrow R_1$ $5u - 5o - u$.
half-cycle 8 $i \leq 3$: $L_3 \longleftarrow R_1$ $3o - u - 3o - 5u$.

These half-cycle braiding steps are shown in Fig. 725.

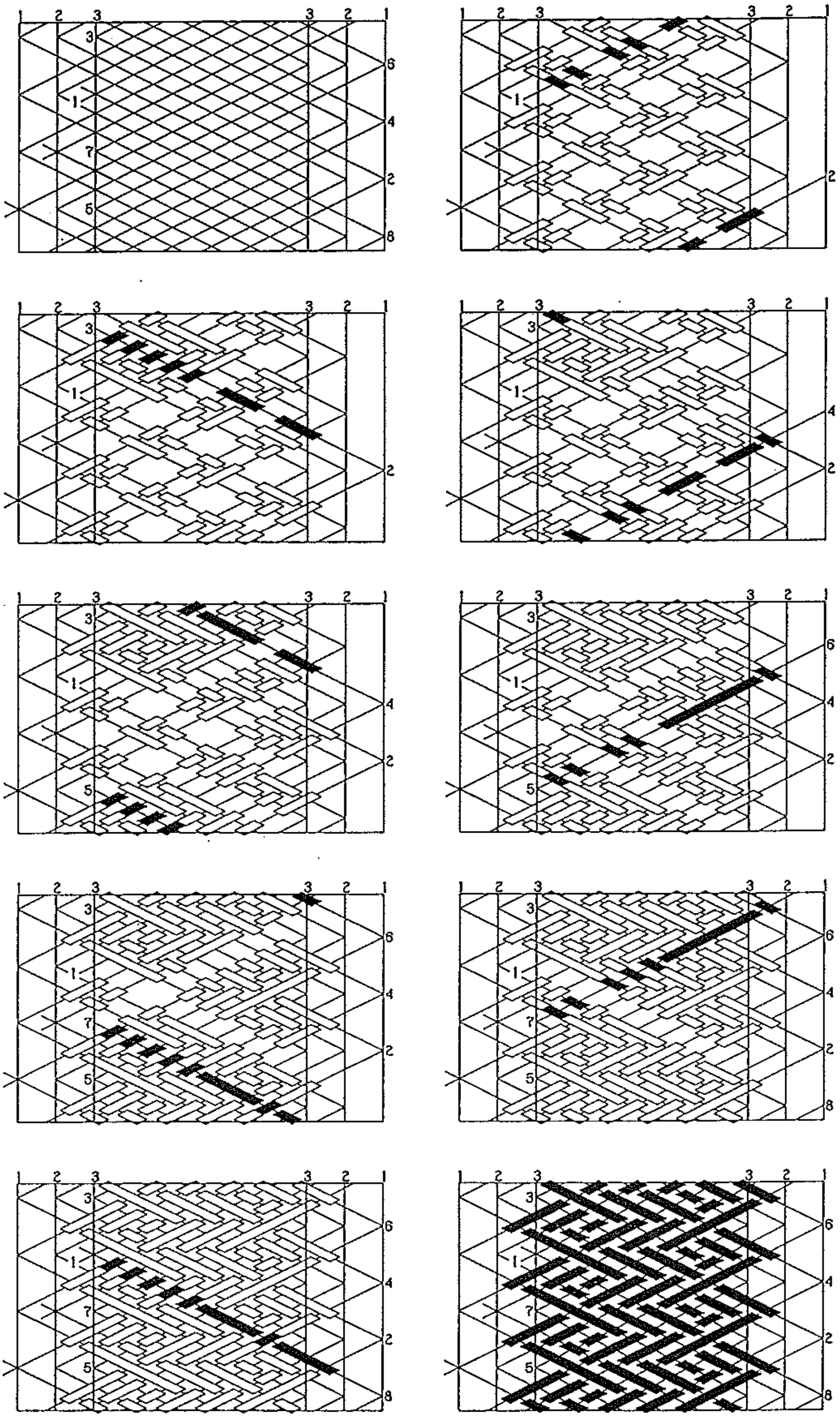

Fig. 725 — The half-cyle braiding steps for the third component.

The algorithm diagram for stage 4 is thus:

$$\begin{array}{cccccccc}
\longrightarrow & 3 & 0 & 3 & 3 & 0 & 3 & 0 \\
\vdash & & 3 & 2 & 1 & & & 0 \\
/ & \backslash & / & \backslash & / & \backslash & / & \backslash \\
0 & & & 1 & 2 & 3 & & \dashv \\
3 & 0 & 3 & 3 & 0 & 3 & 0 & \longleftarrow
\end{array}$$

From this algorithm diagram we read the half-cycle braiding algorithms for stage 4:

half-cycle 1		:	$L_4 \longrightarrow R_1$	$6u - 6o$.
half-cycle 2	$i = 0$	:	$L_4 \longleftarrow R_1$	$6o - 7u$.
half-cycle 3	$i = 0$	:	$L_4 \longrightarrow R_1$	$6u - 6o - u$.
half-cycle 4	$i \leq 1$	:	$L_4 \longleftarrow R_1$	$7o - 7u$.
half-cycle 5	$i \leq 1$	:	$L_4 \longrightarrow R_1$	$6u - 7o - u$.
half-cycle 6	$i \leq 2$	:	$L_4 \longleftarrow R_1$	$3o - u - 4o - 7u$.
half-cycle 7	$i \leq 2$	:	$L_4 \longrightarrow R_1$	$7u - 7o - u$.
half-cycle 8	$i \leq 3$	:	$L_4 \longleftarrow R_1$	$4o - u - 4o - 7u$.

These half-cycle braiding steps are shown in Fig. 726.

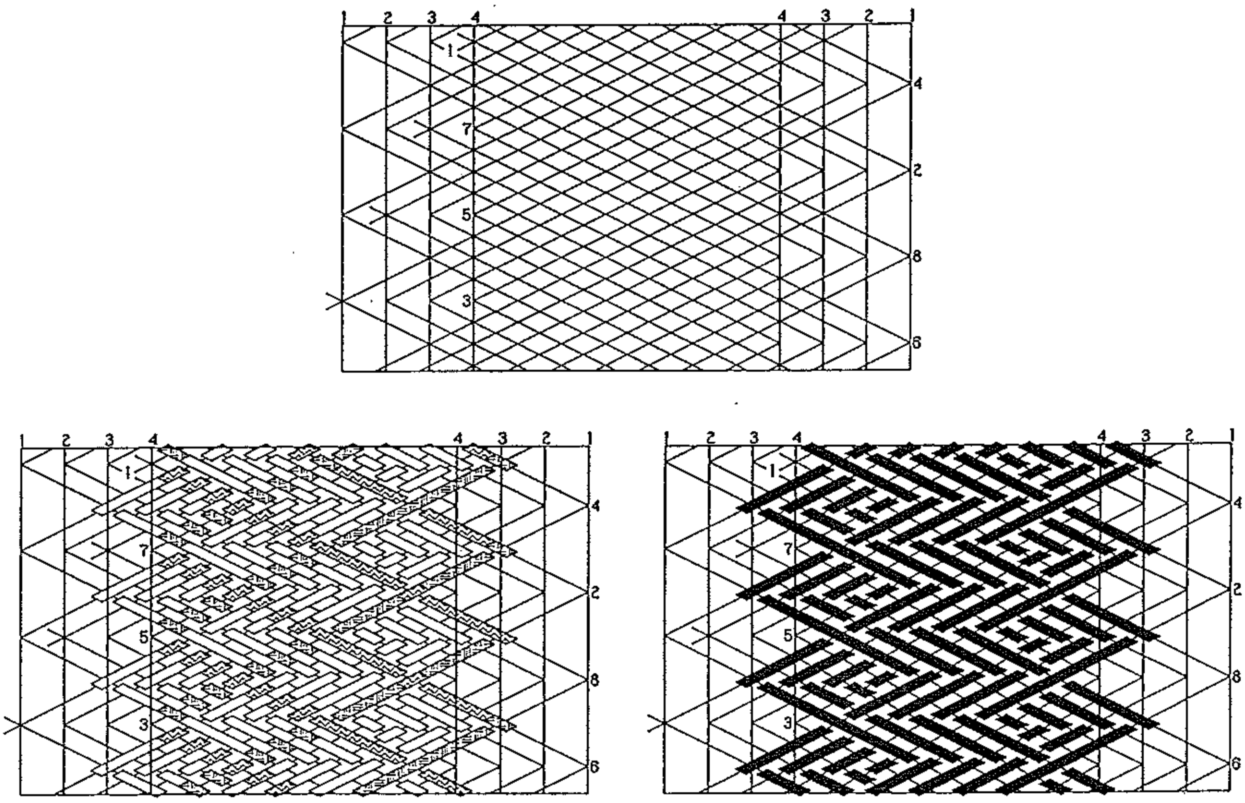

Fig. 726 — The half-cyle braiding steps for the fourth component.

The string-run of the nontrue Flores Knot component associated with stage 5 runs in Fig. 721 between left bight-boundary 1 and right bight-boundary 2. Hence the generalised algorithm diagram of the reconverted component associated with stage 5 is as follows:

$$\begin{array}{ccccccccc}
\longrightarrow & A-l_i & l_i-1 & A-1 & A-1 & A-1 & r_i-1 & A-r_i & r_i-1 \\
\vdash & & \star & \star & \star & \star & & & \star \\
\backslash & / & \backslash & / & \backslash & / & \backslash & / & \backslash \\
& & \star & \star & \star & \star & \star & & \dashv \\
A-l_i & l_i-1 & A-1 & A-1 & A-1 & r_i-1 & A-r_i & r_i-1 & \longleftarrow
\end{array}$$

The algorithm diagram for the reconverted component associated with stage 5 is thus:

$$\begin{array}{ccccccccc}
\longrightarrow & 4 & 0 & 4 & 4 & 4 & 0 & 4 & 0 \\
\vdash & & \star & \star & \star & \star & & & \star \\
\backslash & / & \backslash & / & \backslash & / & \backslash & / & \backslash \\
 & & \star & \star & \star & \star & \star & & \dashv \\
4 & 0 & 4 & 4 & 4 & 0 & 4 & 0 & \longleftarrow
\end{array}$$

The reconverted component associated with braiding stage 5 has 6-parts and 4-bights, and since $\text{g.c.d.}\,(6,4) = 2$, it requires two essential strings in its construction; hence the reconverted component consists of two sub-components. Each sub-component is a Regular Knot with 3-parts and 2-bights, hence its Δ^*-value is 1.

Since this reconverted component consists of two sub-components, the i-values for the stars are as shown in the reconverted component's algorithm diagram below:

$$\begin{array}{ccccccccc}
\longrightarrow & 4 & 0 & 4 & 4 & 4 & 0 & 4 & 0 \\
\vdash & & C & 1 & C & 0 & & & C \\
\backslash & / & \backslash & / & \backslash & / & \backslash & / & \backslash \\
 & & C & 0 & C & 1 & C & & \dashv \\
4 & 0 & 4 & 4 & 4 & 0 & 4 & 0 & \longleftarrow
\end{array}$$

This algorithm diagram gives us the following algorithm diagram for the first to be braided sub-component:

$$\begin{array}{ccccccccc}
\longrightarrow & 4 & 0 & 4 & 4 & 4 & 0 & 4 & 0 \\
\vdash & & & 1 & & 0 & & & \\
\backslash & / & \backslash & / & \backslash & / & \backslash & / & \backslash \\
 & & & 0 & & 1 & & & \dashv \\
4 & 0 & 4 & 4 & 4 & 0 & 4 & 0 & \longleftarrow
\end{array}$$

From this algorithm diagram we read the half-cycle braiding algorithms for the first to be braided sub-component associated with stage 5:

half-cycle 1 : $L \longrightarrow R_1$ $8o - 4u - 8o$.
half-cycle 2 $i = 0$: $L \longleftarrow R_1$ $8o - 5u - 8o$.
half-cycle 3 $i = 0$: $L \longrightarrow R_1$ $8o - 4u - 9o$.
half-cycle 4 $i \leq 1$: $L \longleftarrow R_1$ $4o - u - 4o - 5u - 8o$.

These half-cycle braiding steps are shown in the upper diagram of Fig. 727.

From the algorithm diagram

$$\begin{array}{ccccccccc}
\longrightarrow & 4 & 0 & 4 & 4 & 4 & 0 & 4 & 0 \\
\vdash & & C & 1 & C & 0 & & & C \\
\backslash & / & \backslash & / & \backslash & / & \backslash & / & \backslash \\
 & & C & 0 & C & 1 & C & & \dashv \\
4 & 0 & 4 & 4 & 4 & 0 & 4 & 0 & \longleftarrow
\end{array}$$

we obtain the following algorithm diagram for the next to be braided sub-component associated with stage 5:

$$\begin{array}{ccccccccc}
\longrightarrow & 4 & 1 & 4 & 5 & 4 & 0 & 4 & 1 \\
\vdash & & & 1 & & 0 & & & \\
\backslash & / & \backslash & / & \backslash & / & \backslash & / & \backslash \\
 & & & 0 & & 1 & & & \dashv \\
4 & 0 & 5 & 4 & 5 & 0 & 5 & 0 & \longleftarrow
\end{array}$$

From this algorithm diagram we read the following half-cycle braiding algorithms for the second sub-component associated with stage 5:

half-cycle 1 : $L \longrightarrow R_1$ $4o - u - 4o - 5u - 8o - u\,.$
half-cycle 2 $i = 0$: $L \longleftarrow R_1$ $10o - 5u - 9o\,.$
half-cycle 3 $i = 0$: $L \longrightarrow R_1$ $4o - u - 4o - 5u - 9o - u\,.$
half-cycle 4 $i \leq 1$: $L \longleftarrow R_1$ $5o - u - 5o - 5u - 9o\,.$

These half-cycle braiding steps are shown in the central diagram of Fig. 727.

The string-run of the nontrue Flores Knot component associated with stage 6 runs in Fig. 721 between left bight-boundary 2 and right bight-boundary 1. Hence the generalised algorithm diagram of the reconverted component associated with stage 6 is as follows:

$$\begin{array}{ccccccccc}
\longrightarrow & l_i-1 & A-l_i & l_i-1 & A-1 & A-1 & A-1 & r_i-1 & A-r_i \\
\vdash & & \star & \star & \star & \star & \star & & \\
/ & \backslash & / & \backslash & / & \backslash & / & \backslash & / \\
\star & & & \star & \star & \star & \star & & \dashv \\
l_i-1 & A-l_i & l_i-1 & A-1 & A-1 & A-1 & r_i-1 & A-r_i & \longleftarrow
\end{array}$$

The algorithm diagram for the reconverted component associated with stage 6 is thus:

$$\begin{array}{ccccccccc}
\longrightarrow & 1 & 4 & 1 & 5 & 5 & 5 & 0 & 5 \\
\vdash & & \star & \star & \star & \star & \star & & \\
/ & \backslash & / & \backslash & / & \backslash & / & \backslash & / \\
\star & & & \star & \star & \star & \star & & \dashv \\
1 & 4 & 1 & 5 & 5 & 5 & 0 & 5 & \longleftarrow
\end{array}$$

The reconverted component associated with braiding stage 6 has 6-parts and 4-bights, and since g.c.d. $(6,4) = 2$, it requires two essential strings in its construction; hence the reconverted component consists of two sub-components. Each sub-component is a Regular Knot with 3-parts and 2-bights, hence its Δ^*-value is 1.

Since this reconverted component consists of two sub-components, the i-values for the stars are as shown in the reconverted component's algorithm diagram below:

$$\begin{array}{ccccccccc}
\longrightarrow & 1 & 4 & 1 & 5 & 5 & 5 & 0 & 5 \\
\vdash & & C & 1 & C & 0 & C & & \\
/ & \backslash & / & \backslash & / & \backslash & / & \backslash & / \\
C & & & 0 & C & 1 & C & & \dashv \\
1 & 4 & 1 & 5 & 5 & 5 & 0 & 5 & \longleftarrow
\end{array}$$

This algorithm diagram gives us the following algorithm diagram for the first to be braided sub-component:

$$\begin{array}{ccccccccc}
\longrightarrow & 1 & 4 & 1 & 5 & 5 & 5 & 0 & 5 \\
\vdash & & & 1 & & 0 & & & \\
/ & \backslash & / & \backslash & / & \backslash & / & \backslash & / \\
 & & & 0 & & 1 & & & \dashv \\
1 & 4 & 1 & 5 & 5 & 5 & 0 & 5 & \longleftarrow
\end{array}$$

From this algorithm diagram we read the half-cycle braiding algorithms for the first to be braided sub-component associated with stage 6:

half-cycle 1 : $L_2 \longrightarrow R$ $u - 4o - u - 5o - 5u - 10o\,.$
half-cycle 2 $i = 0$: $L_2 \longleftarrow R$ $10o - 5u - 6o - u - 4o - u\,.$
half-cycle 3 $i = 0$: $L_2 \longrightarrow R$ $u - 4o - u - 5o - 6u - 10o\,.$
half-cycle 4 $i \leq 1$: $L_2 \longleftarrow R$ $11o - 5u - 6o - u - 4o - u\,.$

These half-cycle braiding steps are shown in the upper diagram of Fig. 728.

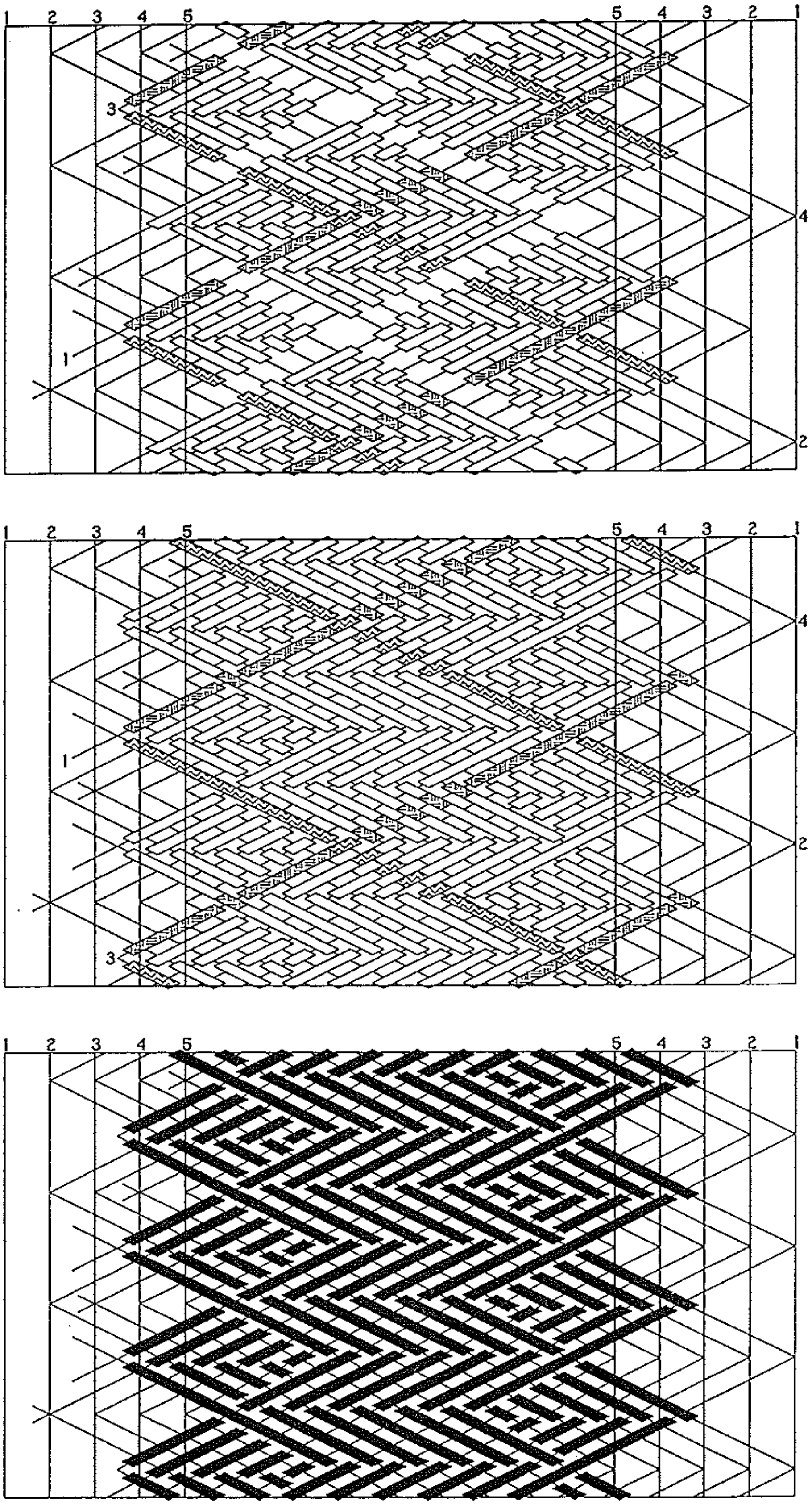

Fig. 727 — Braiding of stage 5.

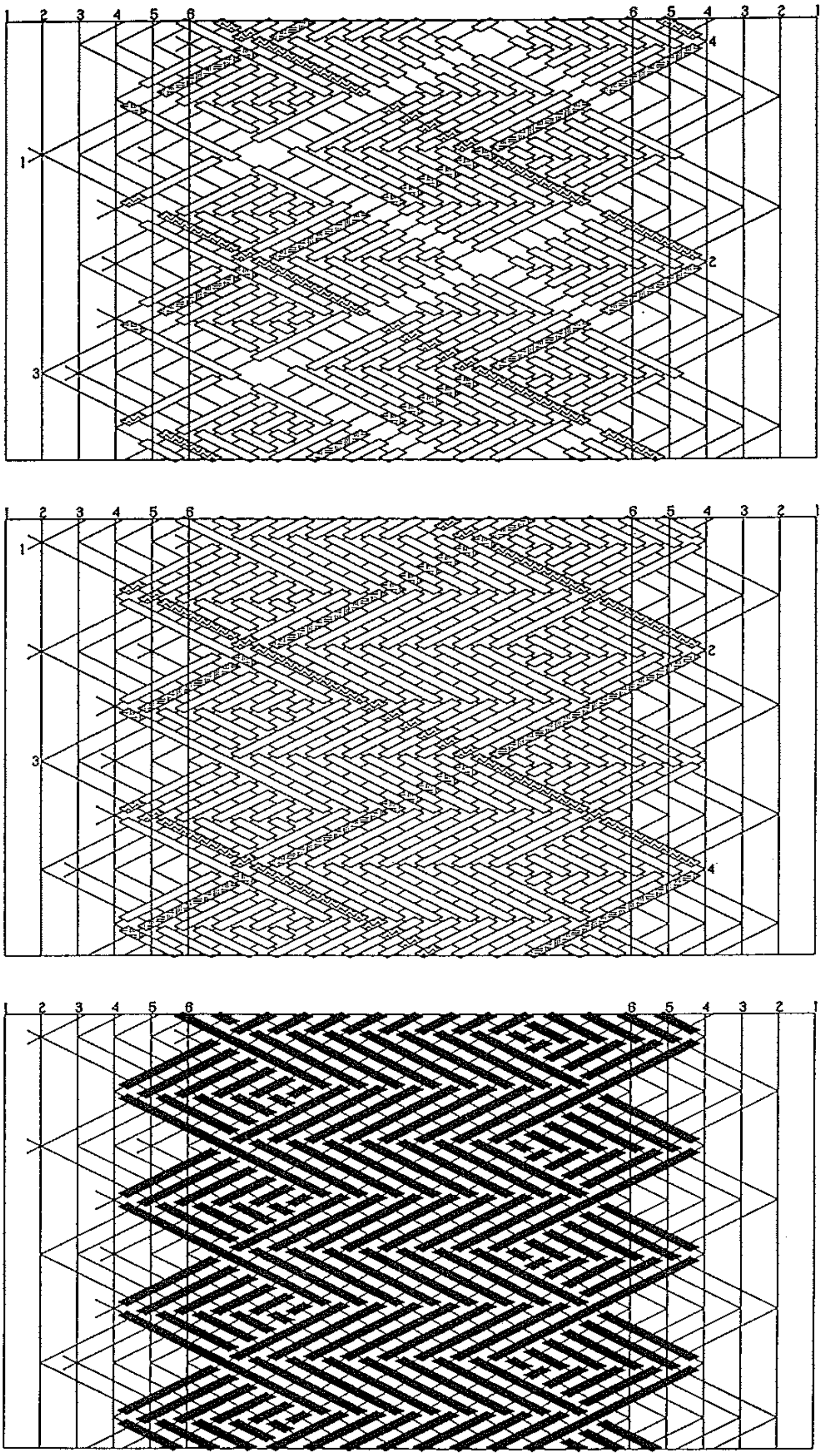

Fig. 728 — Braiding of stage 6.

From the algorithm diagram

$$\begin{array}{ccccccccc}
\longrightarrow & 1 & 4 & 1 & 5 & 5 & 5 & 0 & 5 \\
\vdash & & C & 1 & C & 0 & C & & \\
/ & \backslash & / & \backslash & / & \backslash & / & \backslash & / \\
C & & & 0 & C & 1 & C & & \dashv \\
1 & 4 & 1 & 5 & 5 & 5 & 0 & 5 & \longleftarrow
\end{array}$$

we obtain the following algorithm diagram for the next to be braided sub-component associated with stage 6:

$$\begin{array}{ccccccccc}
\longrightarrow & 1 & 5 & 1 & 6 & 5 & 6 & 0 & 5 \\
\vdash & & & 1 & & 0 & & & \\
/ & \backslash & / & \backslash & / & \backslash & / & \backslash & / \\
 & & & 0 & & 1 & & & \dashv \\
2 & 4 & 1 & 5 & 6 & 5 & 1 & 5 & \longleftarrow
\end{array}$$

From this algorithm diagram we read the following half-cycle braiding algorithms for the second sub-component associated with stage 6:

half-cycle 1 : $L_2 \longrightarrow R$ $u - 5o - u - 6o - 5u - 11o$.
half-cycle 2 $i = 0$: $L_2 \longleftarrow R$ $5o - u - 5o - 6u - 6o - u - 4o - 2u$.
half-cycle 3 $i = 0$: $L_2 \longrightarrow R$ $u - 5o - u - 6o - 6u - 11o$.
half-cycle 4 $i \leq 1$: $L_2 \longleftarrow R$ $5o - u - 6o - 6u - 6o - u - 4o - 2u$.

These half-cycle braiding steps are shown in the central diagram of Fig. 728.

Note that the components of this Flores knot can of course be braided in several different sequences, similar to braiding the components of Standard and Semi-Standard Herrinbone Pineapple Knots[†].

$A = 5$; $B^* = 6$; $x = 21$ for the Flores Knot depicted by the lower grid-diagram in Fig. 720, with $P'_{cF} = 5$ for each of the three true Flores Knot components and $P_{cF} = 6$ for the two reconverted nontrue Flores Knot components. First we braid again the three true Flores Knot components and finally the two reconverted nontrue Flores Knot components. Each of the two reconverted nontrue Flores Knot components requires six essential strings since g.c.d. $(P_{cF}, B^*) =$ g.c.d. $(6, 6) = 6$. Say that after we have braided the three true Flores Knot components we first braid the reconverted nontrue Flores Knot component of the nontrue Flores Knot component which runs between left bight-boundary 1 and right bight-boundary 2 in Fig. 729. For the braiding of this component $A = 4$; $l_i = 1$; $r_i = 1$. Say that we braid its six sub-components in the sequence shown in Fig. 729. Since each sub-component has 1-part and 1-bight, the Δ^*-value of each sub-component is equal to 0.

The generalised algorithm diagram of the reconverted component is as follows:

$$\begin{array}{ccccccccc}
\longrightarrow & A - l_i & l_i - 1 & A - 1 & A - 1 & A - 1 & r_i - 1 & A - r_i & r_i - 1 \\
\vdash & & \star & \star & \star & \star & & & \star \\
\backslash & / & \backslash & / & \backslash & / & \backslash & / & \backslash \\
 & & \star & \star & \star & \star & \star & & \dashv \\
A - l_i & l_i - 1 & A - 1 & A - 1 & A - 1 & r_i - 1 & A - r_i & r_i - 1 & \longleftarrow
\end{array}$$

The algorithm diagram for the reconverted component is thus:

[†] Refer to *The Braider*, Issue No. 23.

$$\begin{array}{ccccccccc}
\longrightarrow & 3 & 0 & 3 & 3 & 3 & 0 & 3 & 0 \\
\vdash & & \star & \star & \star & \star & & & \star \\
\backslash & / & \backslash & / & \backslash & / & \backslash & / & \backslash \\
 & & \star & \star & \star & \star & \star & & \dashv \\
3 & 0 & 3 & 3 & 3 & 0 & 3 & 0 & \longleftarrow
\end{array}$$

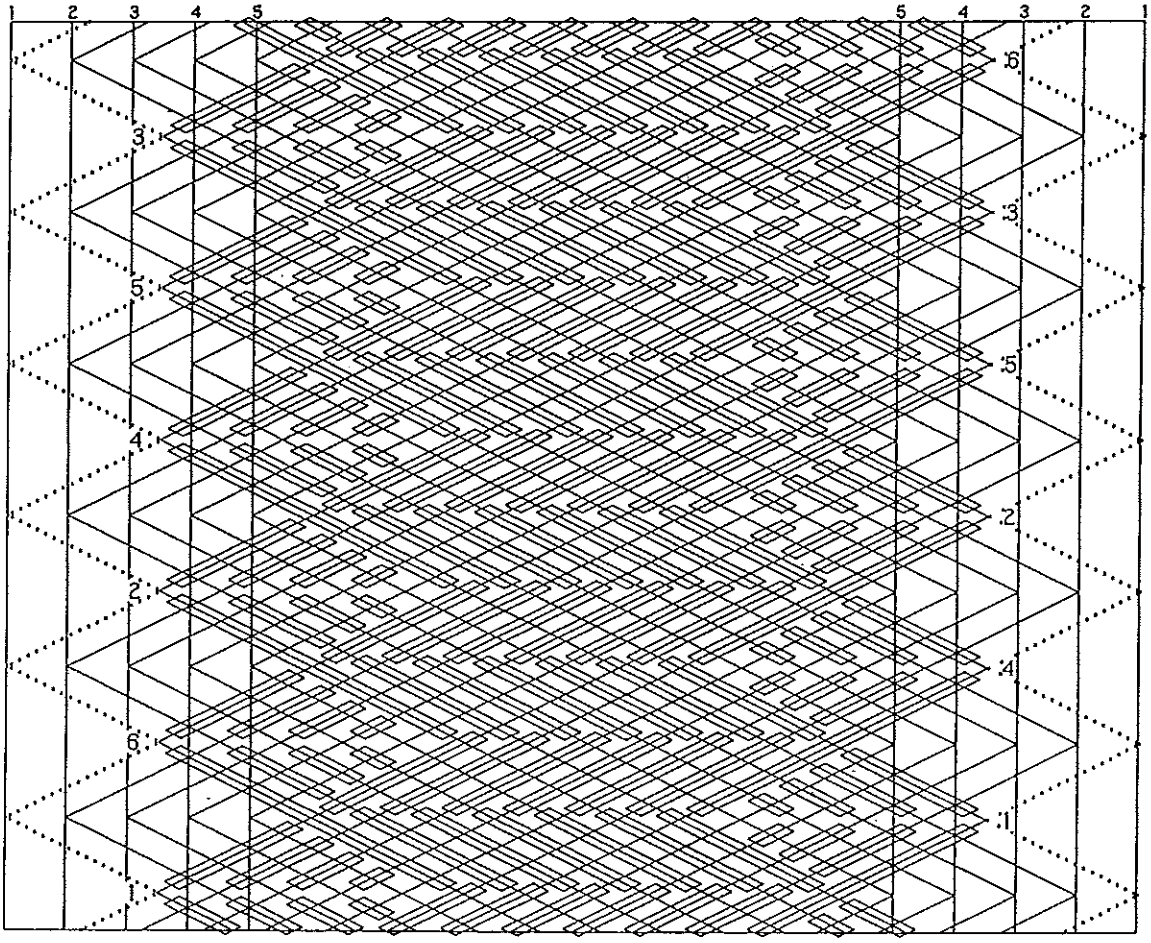

Fig. 729 — A Flores Knot with $A = 5$; $B^* = 6$; $x = 21$.

For sub-components 1 and 2 the algorithm diagram is:

$$\begin{array}{ccccccccc}
\longrightarrow & 3 & 0 & 3 & 3 & 3 & 0 & 3 & 0 \\
\vdash & & & & & C & & & \\
\backslash & / & \backslash & / & \backslash & / & \backslash & / & \backslash \\
 & & & C & & & & & \dashv \\
3 & 0 & 3 & 3 & 3 & 0 & 3 & 0 & \longleftarrow
\end{array}$$

Hence for sub-component 1 the algorithm diagram is:

$$\begin{array}{ccccccccc}
\longrightarrow & 3 & 0 & 3 & 3 & 3 & 0 & 3 & 0 \\
\vdash & & & & & & & & \\
\backslash & / & \backslash & / & \backslash & / & \backslash & / & \backslash \\
 & & & & & & & & \dashv \\
3 & 0 & 3 & 3 & 3 & 0 & 3 & 0 & \longleftarrow
\end{array}$$

From this algorithm diagram we read the following half-cycle braiding algorithms for this sub-component:

half-cycle 1 : $L \longrightarrow R_1$ $6o - 3u - 6o$.
half-cycle 2 $i = 0$: $L \longleftarrow R_1$ $6o - 3u - 6o$.

Hence for sub-component 2 the algorithm diagram is:

$$\begin{array}{ccccccccc}
\longrightarrow & 3 & 0 & 3 & 3 & 4 & 0 & 3 & 0 \\
\vdash & & & & & & & & \\
\backslash & / & \backslash & / & \backslash & / & \backslash & / & \backslash \\
 & & & & & & & & \dashv \\
3 & 0 & 3 & 4 & 3 & 0 & 3 & 0 & \longleftarrow
\end{array}$$

From this algorithm diagram we read the following half-cycle braiding algorithms for this sub-component:

half-cycle 1 : $L \longrightarrow R_1$ $6o - 3u - 7o$.
half-cycle 2 $i = 0$: $L \longleftarrow R_1$ $6o - 4u - 6o$.

For sub-component 3 the algorithm diagram is:

$$\begin{array}{ccccccccc}
\longrightarrow & 3 & 0 & 3 & 3 & 3 & 0 & 3 & 0 \\
\vdash & & C & & D & & & & \\
\backslash & / & \backslash & / & \backslash & / & \backslash & / & \backslash \\
 & & & & D & & C & & \dashv \\
3 & 0 & 3 & 3 & 3 & 0 & 3 & 0 & \longleftarrow
\end{array}$$

Hence for sub-component 3 the algorithm diagram is:

$$\begin{array}{ccccccccc}
\longrightarrow & 3 & 1 & 3 & 4 & 3 & 0 & 3 & 0 \\
\vdash & & & & & & & & \\
\backslash & / & \backslash & / & \backslash & / & \backslash & / & \backslash \\
 & & & & & & & & \dashv \\
3 & 0 & 3 & 3 & 4 & 0 & 4 & 0 & \longleftarrow
\end{array}$$

From this algorithm diagram we read the following half-cycle braiding algorithms for this sub-component:

half-cycle 1 : $L \longrightarrow R_1$ $3o - u - 3o - 4u - 6o$.
half-cycle 2 $i = 0$: $L \longleftarrow R_1$ $8o - 3u - 6o$.

For sub-component 4 the algorithm diagram is:

$$\begin{array}{ccccccccc}
\longrightarrow & 3 & 0 & 3 & 3 & 3 & 0 & 3 & 0 \\
\vdash & & & E & C & & & & D \\
\backslash & / & \backslash & / & \backslash & / & \backslash & / & \backslash \\
 & & D & & C & E & & & \dashv \\
3 & 0 & 3 & 3 & 3 & 0 & 3 & 0 & \longleftarrow
\end{array}$$

Hence for sub-component 4 the algorithm diagram is:

$$\begin{array}{ccccccccc}
\longrightarrow & 3 & 0 & 4 & 4 & 3 & 0 & 3 & 1 \\
\vdash & & & & & & & & \\
\backslash & / & \backslash & / & \backslash & / & \backslash & / & \backslash \\
 & & & & & & & & \dashv \\
3 & 0 & 4 & 3 & 4 & 1 & 3 & 0 & \longleftarrow
\end{array}$$

From this algorithm diagram we read the following half-cycle braiding algorithms for this sub-component:

half-cycle 1 : $L \longrightarrow R_1$ $7o - 4u - 6o - u$.
half-cycle 2 $i = 0$: $L \longleftarrow R_1$ $3o - u - 4o - 3u - 7o$.

For sub-components 5 and 6 the algorithm diagram is:

$$\begin{array}{ccccccccc}
\longrightarrow & 3 & 0 & 3 & 3 & 3 & 0 & 3 & 0 \\
\vdash & & E & C & G & D & & & F \\
\backslash & / & \backslash & / & \backslash & / & \backslash & / & \backslash \\
& & F & D & G & C & E & & \dashv \\
3 & 0 & 3 & 3 & 3 & 0 & 3 & 0 & \longleftarrow
\end{array}$$

Hence for sub-component 5 the algorithm diagram is:

$$\begin{array}{ccccccccc}
\longrightarrow & 3 & 1 & 4 & 3 & 4 & 0 & 3 & 1 \\
\vdash & & & & & & & & \\
\backslash & / & \backslash & / & \backslash & / & \backslash & / & \backslash \\
& & & & & & & & \dashv \\
3 & 0 & 4 & 4 & 3 & 1 & 4 & 0 & \longleftarrow
\end{array}$$

From this algorithm diagram we read the following half-cycle braiding algorithms for this sub-component:

half-cycle 1 : $L \longrightarrow R_1$ $3o - u - 4o - 3u - 7o - u$.
half-cycle 2 $i = 0$: $L \longleftarrow R_1$ $4o - u - 3o - 4u - 7o$.

Hence for sub-component 6 the algorithm diagram is:

$$\begin{array}{ccccccccc}
\longrightarrow & 3 & 1 & 4 & 4 & 4 & 0 & 3 & 1 \\
\vdash & & & & & & & & \\
\backslash & / & \backslash & / & \backslash & / & \backslash & / & \backslash \\
& & & & & & & & \dashv \\
3 & 0 & 4 & 4 & 4 & 1 & 4 & 0 & \longleftarrow
\end{array}$$

From this algorithm diagram we read the following half-cycle braiding algorithms for this sub-component:

half-cycle 1 : $L \longrightarrow R_1$ $3o - u - 4o - 4u - 7o - u$.
half-cycle 2 $i = 0$: $L \longleftarrow R_1$ $4o - u - 4o - 4u - 7o$.

In practice we wouldn't of course braid in the above sequence the six sub-components of this reconverted nontrue Flores Knot; we only took this non regular periodic sequence of construction to show the associated algorithm diagrams. Refer also to *The Braider*, Issue No. 8, pp. 173-176.

⋆⋆ *Say we finally braid the reconverted nontrue Flores Knot component of the nontrue Flores Knot component which runs between left bight-boundary 2 and right bight-boundary 1 in Fig. 729. Furthermore, say that we braid its six sub-components in the sequence shown in Fig. 729. Give the algorithm diagrams required and their associated half-cycle braiding algorithms.*

All the Flores Knots discussed here require more than one essential string and there is no real justification at all to imitate any of them by a single string construction form. If a single string braid is desired then a Flores Knot which requires only one essential string should be employed. Such Flores Knots we shall discuss in the next issue of *The Braider*.

We also like to stress that, contrary to what Bruce Grant states on pg. 424 in the *Encyclopedia of Rawhide and Leather Braiding* (see pg. 903 at the beginning of our discussion concerning the Flores Knots), the Flores Knots do **not** have a herringbone weave.

THE BRAIDER

No.40 NOVEMBER 2004.

CONTENTS

pg.

Solutions to the Questions in Issue No.39 927

The Flores Knots 931

A quarterly publication for the braiding artisan

Resale of this publication or copies thereof is strictly prohibited

Copyright ©2004 by:

A.G. Schaake; 21 Sundown Cresc.; Hamilton; New Zealand.
D. Van Tassel; Box 335; Craig, Co 81626-0335; U.S.A.
F.J.M. Masurel; Ganzenzijde 4; 2317XG Leiden; Nederland.

All rights reserved. No part of this publication may be reproduced, stored in a retrieval system, or transmitted, in any form or by any means, electronic, mechanical, photo-copying, recording, or otherwise, without prior written permission.

This publication is available to braiding artisans only.

Copies may be obtained from:

A.G. Schaake,
21 Sundown Cresc.,
Hamilton,
New Zealand.

Solutions to the Questions in Issue No. 39

Question on pg. 906.

The knots with $p/b = 10/12$, depicted by the left-hand grid-diagrams in Figs. 717 & 718, consist of two interbraided components, each with $p/b = 5/6$. The path in the RKT for these components is established as shown below:

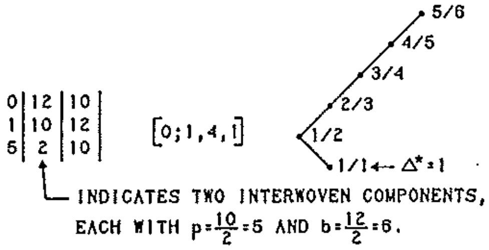
0 | 12 | 10
1 | 10 | 12
5 | 2 | 10
[0;1,4,1]
5/6
4/5
3/4
2/3
1/2
1/1 ← Δ* = 1
INDICATES TWO INTERWOVEN COMPONENTS,
EACH WITH p = 10/2 = 5 AND b = 12/2 = 6.

The general layout of the algorithm diagram for the Regular Cylindrical Braid with $p/b = 10/12$ can now be drawn up with the aid of $\Delta^* = 1$:

$$\begin{array}{ccccccccccc}
\longrightarrow &&&&&&&&&& \\
& C & 1 & C & 2 & C & 3 & C & 4 & C & \\
\vdash & \cdot & \cdot & \cdot & \cdot & \cdot & \cdot & \cdot & \cdot & \cdot & \dashv \\
& C & 4 & C & 3 & C & 2 & C & 1 & C & \\
&&&&&&&&&& \longleftarrow
\end{array}$$

Thus the algorithm diagram for the foundation knots of the knots depicted by the left-hand grid-diagrams in Figs. 717 & 718 is as follows:

$$\begin{array}{ccccccccccc}
\longrightarrow &&&&&&&&&& \\
& & 1 & & 2 & & 3 & & 4 & & \\
\vdash & \cdot & \backslash & \cdot & / & \cdot & \backslash & \cdot & / & \cdot & \dashv \\
& & 4 & & 3 & & 2 & & 1 & & \\
&&&&&&&&&& \longleftarrow
\end{array}$$

We can of course also write this algorithm diagram as follows:

$$\begin{array}{ccccccccccc}
\longrightarrow &&&&&&&&&& \\
& & 1 & & 2 & & 3 & & 4 & & \\
& & u & & o & & u & & o & & \\
\vdash & \cdot & \cdot & \cdot & \cdot & \cdot & \cdot & \cdot & \cdot & \cdot & \dashv \\
& & o & & u & & o & & u & & \\
& & 4 & & 3 & & 2 & & 1 & & \\
&&&&&&&&&& \longleftarrow
\end{array}$$

From these algorithm diagrams we read the following half-cycle braiding algorithms for the foundation knot:

half-cycle 1		:	$L \longrightarrow R$	Free Run.
half-cycle 2	$i = 0$	:	$L \longleftarrow R$	Free Run.
half-cycle 3	$i = 0$	:	$L \longrightarrow R$	Free Run.
half-cycle 4	$i \leq 1$	:	$L \longleftarrow R$	u.
half-cycle 5	$i \leq 1$	:	$L \longrightarrow R$	u.
half-cycle 6	$i \leq 2$	:	$L \longleftarrow R$	$u - o$.
half-cycle 7	$i \leq 2$	:	$L \longrightarrow R$	$u - o$.
half-cycle 8	$i \leq 3$	:	$L \longleftarrow R$	$u - o - u$.
half-cycle 9	$i \leq 3$	:	$L \longrightarrow R$	$u - o - u$.

half-cycle 10 $i \leq 4$: $L \longleftarrow R$ $u - o - u - o$.
half-cycle 11 $i \leq 4$: $L \longrightarrow R$ $u - o - u - o$.
half-cycle 12 $i \leq 5$: $L \longleftarrow R$ $u - o - u - o$.

For the knot depicted by the left-hand grid-diagram in Fig. 717, the algorithm diagram of the interbraided knot is as follows:

$$\begin{array}{ccccccccccc}
\longrightarrow & & & & & & & & & & \\
 & C & 1 & C & 2 & C & 3 & C & 4 & C & \\
 & u & u & u & u & o & o & u & o & u & \\
\vdash & \cdot & \cdot & \cdot & \cdot & \cdot & \cdot & \cdot & \cdot & \cdot & \dashv \\
 & u & o & u & o & o & u & u & u & u & \\
 & C & 4 & C & 3 & C & 2 & C & 1 & C & \\
 & & & & & & & & & & \longleftarrow
\end{array}$$

From this algorithm diagram we read the following half-cycle braiding algorithms for the interbraided knot:

half-cycle 1′ : $L \longrightarrow R$ $2u - o - 2u$.
half-cycle 2′ $i = 0$: $L \longleftarrow R$ $2u - o - 2u$.
half-cycle 3′ $i = 0$: $L \longrightarrow R$ $2u - o - 2u$.
half-cycle 4′ $i \leq 1$: $L \longleftarrow R$ $3u - o - 2u$.
half-cycle 5′ $i \leq 1$: $L \longrightarrow R$ $3u - o - 2u$.
half-cycle 6′ $i \leq 2$: $L \longleftarrow R$ $4u - o - 2u$.
half-cycle 7′ $i \leq 2$: $L \longrightarrow R$ $4u - o - 2u$.
half-cycle 8′ $i \leq 3$: $L \longleftarrow R$ $4u - 2o - 2u$.
half-cycle 9′ $i \leq 3$: $L \longrightarrow R$ $4u - 2o - 2u$.
half-cycle 10′ $i \leq 4$: $L \longleftarrow R$ $4u - 2o - u - o - u$.
half-cycle 11′ $i \leq 4$: $L \longrightarrow R$ $4u - 2o - u - o - u$.
half-cycle 12′ $i \leq 5$: $L \longleftarrow R$ $4u - 2o - u - o - u$.

For the knot depicted by the left-hand grid-diagram in Fig. 718, the algorithm diagram of the interbraided knot is as follows:

$$\begin{array}{ccccccccccc}
\longrightarrow & & & & & & & & & & \\
 & C & 1 & C & 2 & C & 3 & C & 4 & C & \\
 & u & o & u & u & o & o & u & u & u & \\
\vdash & \cdot & \cdot & \cdot & \cdot & \cdot & \cdot & \cdot & \cdot & \cdot & \dashv \\
 & u & u & u & o & o & u & u & o & u & \\
 & C & 4 & C & 3 & C & 2 & C & 1 & C & \\
 & & & & & & & & & & \longleftarrow
\end{array}$$

From this algorithm diagram we read the following half-cycle braiding algorithms for the interbraided knot:

half-cycle 1′ : $L \longrightarrow R$ $2u - o - 2u$.
half-cycle 2′ $i = 0$: $L \longleftarrow R$ $2u - o - 2u$.
half-cycle 3′ $i = 0$: $L \longrightarrow R$ $2u - o - 2u$.
half-cycle 4′ $i \leq 1$: $L \longleftarrow R$ $u - o - u - o - 2u$.
half-cycle 5′ $i \leq 1$: $L \longrightarrow R$ $u - o - u - o - 2u$.
half-cycle 6′ $i \leq 2$: $L \longleftarrow R$ $u - o - 2u - o - 2u$.
half-cycle 7′ $i \leq 2$: $L \longrightarrow R$ $u - o - 2u - o - 2u$.
half-cycle 8′ $i \leq 3$: $L \longleftarrow R$ $u - o - 2u - 2o - 2u$.
half-cycle 9′ $i \leq 3$: $L \longrightarrow R$ $u - o - 2u - 2o - 2u$.
half-cycle 10′ $i \leq 4$: $L \longleftarrow R$ $u - o - 2u - 2o - 3u$.

half-cycle 11′ $i \leq 4$: $L \longrightarrow R$ $u - o - 2u - 2o - 3u$.
half-cycle 12′ $i \leq 5$: $L \longleftarrow R$ $u - o - 2u - 2o - 3u$.

Question on pg. 926.

$A = 5$; $l_i = 2$; $r_i = 1$ for the braiding of the reconverted nontrue Flores Knot component of the nontrue Flores Knot component which runs between left bight-boundary 2 and right bight-boundary 1 in Fig. 729. Its six sub-components are braided in the sequence shown.

The generalised algorithm diagram of this reconverted component is as follows:

$$\begin{array}{ccccccccc}
\longrightarrow & l_i-1 & A-l_i & l_i-1 & A-1 & A-1 & A-1 & r_i-1 & A-r_i \\
\vdash & & \star & \star & \star & \star & \star & & \\
/ & \backslash & / & \backslash & / & \backslash & / & \backslash & / \\
\star & & & \star & \star & \star & \star & & \dashv \\
l_i-1 & A-l_i & l_i-1 & A-1 & A-1 & A-1 & r_i-1 & A-r_i & \longleftarrow
\end{array}$$

The algorithm diagram for the reconverted component associated with the final stage is thus:

$$\begin{array}{ccccccccc}
\longrightarrow & 1 & 3 & 1 & 4 & 4 & 4 & 0 & 4 \\
\vdash & & \star & \star & \star & \star & \star & & \\
/ & \backslash & / & \backslash & / & \backslash & / & \backslash & / \\
\star & & & \star & \star & \star & \star & & \dashv \\
1 & 3 & 1 & 4 & 4 & 4 & 0 & 4 & \longleftarrow
\end{array}$$

For the sub-components 1 , 2 , 3 the algorithm diagram is:

$$\begin{array}{ccccccccc}
\longrightarrow & 1 & 3 & 1 & 4 & 4 & 4 & 0 & 4 \\
\vdash & & & D & & C & & & \\
/ & \backslash & / & \backslash & / & \backslash & / & \backslash & / \\
 & & & C & & D & & & \dashv \\
1 & 3 & 1 & 4 & 4 & 4 & 0 & 4 & \longleftarrow
\end{array}$$

Hence for sub-component 1 the algorithm diagram is:

$$\begin{array}{ccccccccc}
\longrightarrow & 1 & 3 & 1 & 4 & 4 & 4 & 0 & 4 \\
\vdash & & & & & & & & \\
/ & \backslash & / & \backslash & / & \backslash & / & \backslash & / \\
 & & & & & & & & \dashv \\
1 & 3 & 1 & 4 & 4 & 4 & 0 & 4 & \longleftarrow
\end{array}$$

From this algorithm diagram we read the following half-cycle braiding algorithms for this sub-component:

half-cycle 1 : $L_2 \longleftarrow R$ $8o - 4u - 4o - u - 3o - u$.
half-cycle 2 $i = 0$: $L_2 \longrightarrow R$ $u - 3o - u - 4o - 4u - 8o$.

Hence for sub-component 2 the algorithm diagram is:

$$\begin{array}{ccccccccc}
\longrightarrow & 1 & 3 & 1 & 4 & 4 & 4 & 0 & 4 \\
\vdash & & & & & C & & & \\
/ & \backslash & / & \backslash & / & \backslash & / & \backslash & / \\
 & & & C & & & & & \dashv \\
1 & 3 & 1 & 4 & 4 & 4 & 0 & 4 & \longleftarrow
\end{array}$$

From this algorithm diagram we read the following half-cycle braiding algorithms for this sub-component:

half-cycle 1 : $L_2 \longleftarrow R$ $8o - 4u - 5o - u - 3o - u$.
half-cycle 2 $i = 0$: $L_2 \longrightarrow R$ $u - 3o - u - 4o - 5u - 8o$.

Hence for sub-component 3 the algorithm diagram is:

$$\begin{array}{ccccccccc}
\longrightarrow & 1 & 3 & 1 & 4 & 4 & 4 & 0 & 4 \\
\vdash & & & D & & C & & & \\
/ & \backslash & / & \backslash & / & \backslash & / & \backslash & / \\
 & & & C & & D & & & \dashv \\
1 & 3 & 1 & 4 & 4 & 4 & 0 & 4 & \longleftarrow
\end{array}$$

From this algorithm diagram we read the following half-cycle braiding algorithms for this sub-component:

half-cycle 1 : $L_2 \longleftarrow R$ $9o - 4u - 5o - u - 3o - u$.
half-cycle 2 $i = 0$: $L_2 \longrightarrow R$ $u - 3o - 2u - 4o - 5u - 8o$.

For the sub-components 4, 5, 6 the algorithm diagram is:

$$\begin{array}{ccccccccc}
\longrightarrow & 1 & 3 & 1 & 4 & 4 & 4 & 0 & 4 \\
\vdash & & D & G & E & F & C & & \\
/ & \backslash & / & \backslash & / & \backslash & / & \backslash & / \\
C & & & F & E & G & D & & \dashv \\
1 & 3 & 1 & 4 & 4 & 4 & 0 & 4 & \longleftarrow
\end{array}$$

Hence for sub-component 4 the algorithm diagram is:

$$\begin{array}{ccccccccc}
\longrightarrow & 1 & 3 & 1 & 4 & 4 & 4 & 0 & 4 \\
\vdash & & D & & E & & C & & \\
/ & \backslash & / & \backslash & / & \backslash & / & \backslash & / \\
C & & & & E & & D & & \dashv \\
1 & 3 & 1 & 4 & 4 & 4 & 0 & 4 & \longleftarrow
\end{array}$$

From this algorithm diagram we read the following half-cycle braiding algorithms for this sub-component:

half-cycle 1 : $L_2 \longleftarrow R$ $4o - u - 4o - 5u - 4o - u - 3o - 2u$.
half-cycle 2 $i = 0$: $L_2 \longrightarrow R$ $u - 4o - u - 5o - 4u - 9o$.

Hence for sub-component 5 the algorithm diagram is:

$$\begin{array}{ccccccccc}
\longrightarrow & 1 & 3 & 1 & 4 & 4 & 4 & 0 & 4 \\
\vdash & & D & & E & F & C & & \\
/ & \backslash & / & \backslash & / & \backslash & / & \backslash & / \\
C & & & F & E & & D & & \dashv \\
1 & 3 & 1 & 4 & 4 & 4 & 0 & 4 & \longleftarrow
\end{array}$$

From this algorithm diagram we read the following half-cycle braiding algorithms for this sub-component:

half-cycle 1 : $L_2 \longleftarrow R$ $4o - u - 4o - 5u - 5o - u - 3o - 2u$.
half-cycle 2 $i = 0$: $L_2 \longrightarrow R$ $u - 4o - u - 5o - 5u - 9o$.

Hence for sub-component 6 the algorithm diagram is:

$$\begin{array}{ccccccccc}
\longrightarrow & 1 & 3 & 1 & 4 & 4 & 4 & 0 & 4 \\
\vdash & & D & G & E & F & C & & \\
/ & \backslash & / & \backslash & / & \backslash & / & \backslash & / \\
C & & & F & E & G & D & & \dashv \\
1 & 3 & 1 & 4 & 4 & 4 & 0 & 4 & \longleftarrow
\end{array}$$

From this algorithm diagram we read the following half-cycle braiding algorithms for this sub-component:

half-cycle 1 : $L_2 \longleftarrow R$ $4o - u - 5o - 5u - 5o - u - 3o - 2u$.
half-cycle 2 $i = 0$: $L_2 \longrightarrow R$ $u - 4o - 2u - 5o - 5u - 9o$.

The Flores Knots

The Flores Knots we discussed in the previous issue (No. 39) of *The Braider* were derived from Standard and Semi-Standard Herringbone Pineapple Knots, and consequently were really multi-string knots. In the same way we can derive Flores Knots from Perfect and Semi-Perfect Herringbone Pineapple Knots. If the Perfect or Semi-Perfect Herringbone Pineapple Knot has P_P-parts (where $P_P = 2A + x_P - 2$), then the Flores Knot which evolves from it has P_F-parts (where $P_F = 2P_P - x_P = 2A + x_F - 4$) and requires g.c.d. (P_F, B^*) essential strings. Note that $x_F = x_P + 2A$, hence x_F and A are of different parity. For the same x_P-value, and hence the same P_P-value since $P_P = 2A + x_P - 2$, there are two Perfect or two Semi-Perfect Herringbone Pineapple Knots whose first-return string-runs are the mirror-image of each other.[†]

Let's first have a look at the case where A is equal to two.

The left-hand grid-diagram in Fig. 730 depicts a Perfect Herringbone Pineapple Knot (hence only one essential string is required) with $A = 2$, $x = 9$, $y = A - 1 = 1$, $B^* = 6$, hence with $P_P = 2 \times 2 + 9 - 2 = 11$. The right-hand grid-diagram in Fig. 730 shows how the Flores Knot is derived from it while retaining the physical appearance of the Perfect Herringbone Pineapple Knot. In this right-hand grid-diagram there are crossings in the second and penultimate crossing-columns which do not yet have a superimposed coding. The codings of those crossings do not affect the physical appearance of the knot. Although each of those crossings can therefore be given an arbitrary coding, we limit these codings so that:

1. The **columns** to which they belong become **column-coded.**
2. The **rows** to which they belong become **semi row-coded.**

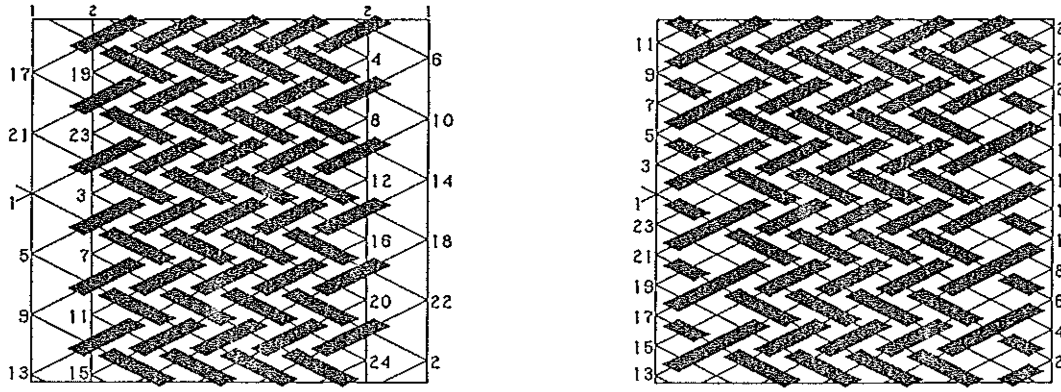

Fig. 730 — The derivation of the Flores Knot from the Perfect Herringbone Pineapple Knot.

When we fulfil the column-coding option (option **1.** above), then the Flores Knot is depicted by the left-hand grid-diagram in Fig. 731.

When we fulfil the semi row-coding option (option **2.** above), then the Flores Knot is depicted by the right-hand grid-diagram in Fig. 731.

⋆⋆ *Draw for each of the grid-diagrams in Fig. 731 the path in the RKT and from it determine their* Δ^* *values, then construct their algorithm diagrams. Read from their algorithm diagrams their half-cycle braiding algorithms.*

[†] Refer to *The Braider*, Issue No. 24, pp. 554-562, and Issue No. 28, pp. 644-645.

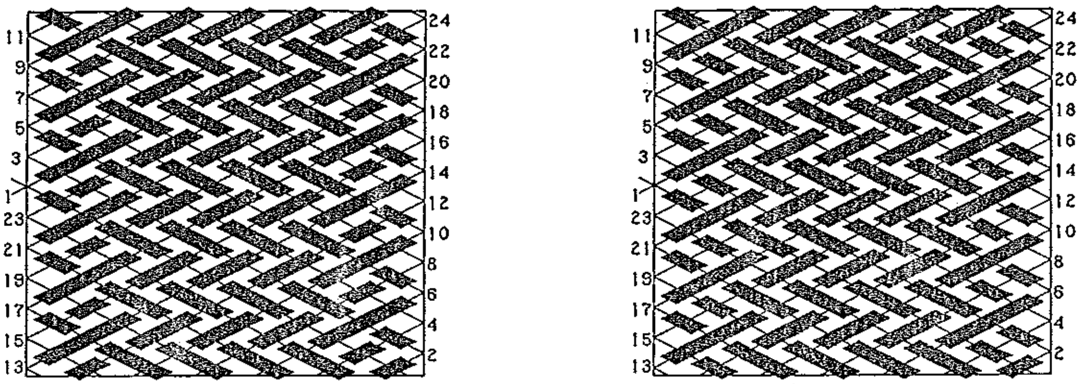

Fig. 731 — The Column-coding and semi Row-coding options.

The left-hand grid-diagram in Fig. 732 depicts a Perfect Herringbone Pineapple Knot (hence only one essential string is required) which is the mirror-image complement of the Perfect Herringbone Pineapple Knot in Fig. 730, hence with $A = 2$, $x = 9$, $y = A + 1 = 3$, $B^* = 6$. The right-hand grid-diagram in Fig. 732 shows how the Flores Knot is derived from it.

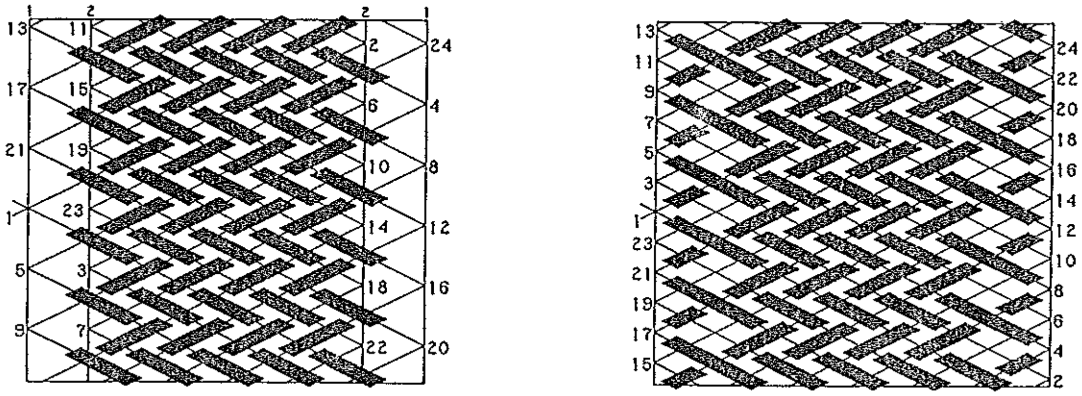

Fig. 732 — The derivation of the Flores Knot from the Perfect Herringbone Pineapple Knot.

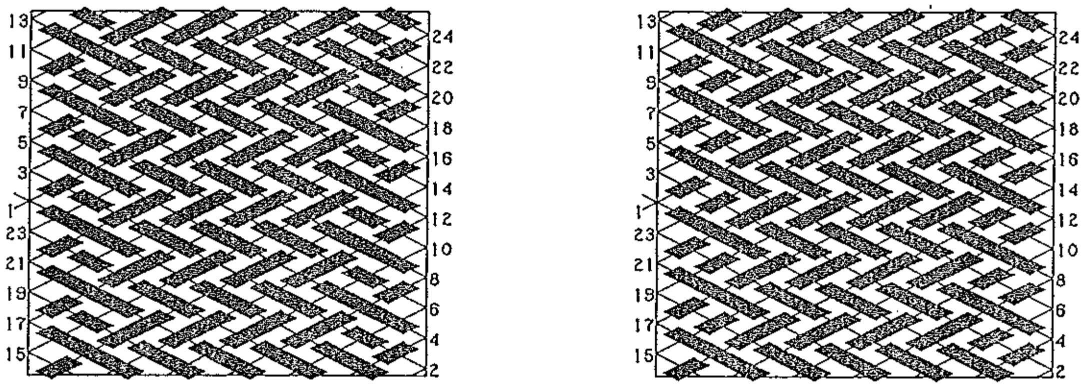

Fig. 733 — The Column-coding and semi Row-coding options.

When we fulfil the column-coding option (option **1.** above), then the Flores Knot is depicted by the left-hand grid-diagram in Fig. 733.

When we fulfil the semi row-coding option (option **2.** above), then the Flores Knot is depicted by the right-hand grid-diagram in Fig. 733.

⋆⋆ *Draw for each of the grid-diagrams in Fig. 733 the path in the RKT and from it determine their* Δ^* *values, then construct their algorithm diagrams. Read from their algorithm diagrams their half-cycle braiding algorithms.*

Since it is much simpler to determine the half-cycle braiding algorithms for a Regular Knot than for a Perfect or Semi-Perfect Herringbone Pineapple Knot, and since the physical appearance of a Perfect Herringbone Pineapple Knot, or Semi-Perfect Herringbone Pineapple Knot in which all essential strings are identical, is the same as the physical appearance of the Flores Knot derived from it, it is in practice advantageous to replace 2-pass Perfect or Semi-Perfect Herringbone Pineapple Knots which transform into single string Flores Knots (which are then Regular Knots) by those Flores Knots.

⋆⋆ *Draw for each of the Perfect Herringbone Pineapple Knots in Figs. 730 and 732 their first-return string-run, compile their half-cycle pattern and their half-cycle tables.*[†]

For the case where A is greater than 2, the two types of string-run of the Flores Knots, derived from Perfect or Semi-Perfect Herringbone Pineapple Knots, are two special string-run types of Periodic Regular Nested Cylindrical Braids with sub-nesting-numbers $A_{l_1} = A_{r_1} = A - 1$; $A_{l_2} = A_{r_2} = 1$.[‡]

We use again the conventional start where the first lower-left to upper-right half-cycle starts at left bight-boundary 1. Hence for Flores Knots with $A = \mathit{even}$, which are derived from the Perfect or Semi-Perfect Herringbone Pineapple Knots with $y = A - 1$, the first half-cycle from lower-left to upper-right is:

$$\begin{array}{lll} 1_1 \longrightarrow k-2 & \text{when } A = \mathit{even} \text{ and } A \geq \left|\frac{x-A-1}{2}\right|_A \geq 3 . \\ 1_1 \longrightarrow A-1 & \text{when } A = \mathit{even} \text{ and } \left|\frac{x-A-1}{2}\right|_A = 1 . \\ 1_1 \longrightarrow z_* & \text{when } A = \mathit{even} \text{ and } \left|\frac{x-A-1}{2}\right|_A = 2 . \end{array}$$

In these formulae $k = \left|\frac{x-A-1}{2}\right|_A$; $z = \frac{A}{2}$ while z_* is associated with A_{r_2} .

For Flores Knots with $A = \mathit{odd}$, which are derived from the Perfect or Semi-Perfect Herringbone Pineapple Knots with $y = A - 1$, the first half-cycle from lower-left to upper-right is:

$$\begin{array}{lll} 1_1 \longrightarrow k-2 & \text{when } A = \mathit{odd} \text{ and } z+1 \geq \left|\frac{x-A-1}{2}\right|_A \geq 3 . \\ 1_1 \longrightarrow k-1 & \text{when } A = \mathit{odd} \text{ and } A \geq \left|\frac{x-A-1}{2}\right|_A > z+1 . \\ 1_1 \longrightarrow A & \text{when } A = \mathit{odd} \text{ and } \left|\frac{x-A-1}{2}\right|_A = 1 . \\ 1_1 \longrightarrow z_* & \text{when } A = \mathit{odd} \text{ and } \left|\frac{x-A-1}{2}\right|_A = 2 . \end{array}$$

In these formulae $k = \left|\frac{x-A-1}{2}\right|_A$; $z = \frac{A+1}{2}$ while z_* is associated with A_{r_2} .

For Flores Knots with $A = \mathit{even}$, which are derived from the Perfect or Semi-Perfect Herringbone Pineapple Knots with $y = A + 1$, the first half-cycle from lower-left to upper-right is:

$$\begin{array}{lll} 1_1 \longrightarrow k-2 & \text{when } A = \mathit{even} \text{ and } A \geq \left|\frac{x-A-3}{2}\right|_A \geq 3 . \\ 1_1 \longrightarrow A-1 & \text{when } A = \mathit{even} \text{ and } \left|\frac{x-A-3}{2}\right|_A = 1 . \\ 1_1 \longrightarrow z_* & \text{when } A = \mathit{even} \text{ and } \left|\frac{x-A-3}{2}\right|_A = 2 . \end{array}$$

In these formulae $k = \left|\frac{x-A-3}{2}\right|_A$; $z = \frac{A}{2}$ while z_* is associated with A_{r_2} .

[†] Refer to *The Braider*, Issue No. 28, pp. 646-656.

[‡] Refer to *The Braider*, Issue No. 34, pp. 790-793.

For Flores Knots with $A = odd$, which are derived from the Perfect or Semi-Perfect Herringbone Pineapple Knots with $y = A + 1$, the first half-cycle from lower-left to upper-right is:

$$\begin{array}{lll} 1_1 \longrightarrow k-2 & \text{when } A = odd \text{ and } & z+1 \geq \left|\frac{x-A-3}{2}\right|_A \geq 3\,. \\ 1_1 \longrightarrow k-1 & \text{when } A = odd \text{ and } & A \geq \left|\frac{x-A-3}{2}\right|_A > z+1\,. \\ 1_1 \longrightarrow A & \text{when } A = odd \text{ and } & \left|\frac{x-A-3}{2}\right|_A = 1\,. \\ 1_1 \longrightarrow z_* & \text{when } A = odd \text{ and } & \left|\frac{x-A-3}{2}\right|_A = 2\,. \end{array}$$

In these formulae $k = \left|\frac{x-A-3}{2}\right|_A$; $z = \frac{A+1}{2}$ while z_* is associated with A_{r_2}.

Note that in these formulae it is irrelevant whether we take x_P or x_F for x since $x_F = x_P + 2A$; in the grid-diagram of the Flores Knot we have to use x_F of course.

By starting at left bight-boundary 1, we can again for the left bight-edge fully specify in general terms the left bight-boundary sequence specification (the left bight-boundary sequence with their ranking-numbers). For the right bight-edge we can only specify in general terms the cyclic sequence of the bight-boundaries since the first lower-left to upper-right half-cycle can be made to end at anyone of the right bight-boundaries which then receives the ranking-number 1.

The number of crossings on a half-cycle are again calculated as the sum of three sets of crossings:

i). The number of crossings between the left-hand bight-boundary 1 up to and including the innermost left-hand bight-boundary.
ii). The number of crossings between the innermost left-hand bight-boundary and the innermost right-hand bight-boundary; hence equal to $(x-1)$.
iii). The number of crossings between the right-hand bight-boundary 1 up to and including the innermost right-hand bight-boundary.

When we write the number of crossings under **i)** below the bight-boundaries in the left bight-boundary sequence specification, then the general scheme is as follows:

a). The two sub-nesting numbers A_{l_1} and A_{l_2} do have the same parity, hence $A = even$.

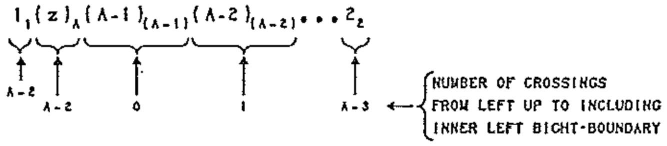
1₁ (z)_A (A-1)_(A-1) (A-2)_(A-2) • • • 2₂
A-2
A-2
0
1
A-3
NUMBER OF CROSSINGS
FROM LEFT UP TO INCLUDING
INNER LEFT BICHT-BOUNDARY

b). The two sub-nesting numbers A_{l_1} and A_{l_2} do not have the same parity, hence $A = odd$.

1). For $A_{l_1} = A_{l_2} + 1$, hence for $A = 3$:

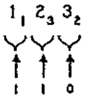

2). For $A_{l_1} \geq A_{l_2} + 3$, hence for $A \geq 5$:

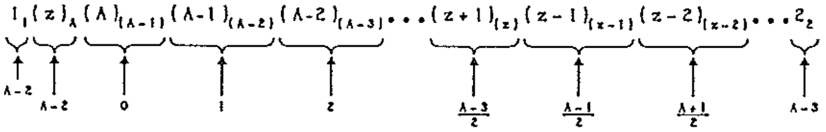
1₁ (z)_A (A)_(A-1) (A-1)_(A-2) (A-2)_(A-3) • • • (z+1)_(z) (z-1)_(z-1) (z-2)_(z-2) • • • 2₂
A-2
A-2
0
1
2
(A-3)/2
(A-1)/2
(A+1)/2
A-3

When we write the number of crossings under **iii)** below the bight-boundaries in the right cyclic bight-boundary sequence specification, then the general scheme is as follows:

a). The two sub-nesting numbers A_{r_1} and A_{r_2} do have the same parity, hence $A = even$.

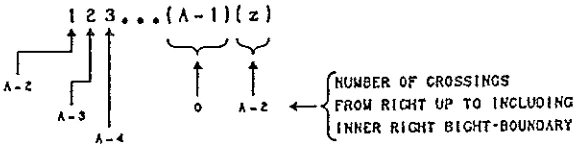
1 2 3 . . . (A−1)(z)
A−2
A−3
A−4
0
A−2
NUMBER OF CROSSINGS FROM RIGHT UP TO INCLUDING INNER RIGHT BIGHT-BOUNDARY

b). The two sub-nesting numbers A_{r_1} and A_{r_2} do not have the same parity, hence $A = odd$.

1). For $A_{r_1} = A_{r_2} + 1$, hence for $A = 3$:

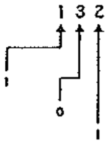

2). For $A_{r_1} \geq A_{r_2} + 3$, hence for $A \geq 5$:

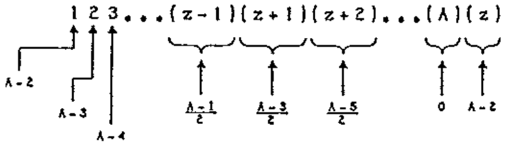

Note that these above schemes are in fact the schemes in *The Braider*, Issue No. 34, pg. 801, for $A_{l_2} = A_{r_2} = 1$.

The calculation procedures for establishing the half-cycle braiding algorithms of a Flores Knot with $A \geq 3$, derived from a Perfect or Semi-Perfect Herringbone Pineapple Knot, follow the procedures as discussed in *The Braider*, Issue No. 34, for the Periodic Regular Nested Cylindrical Braids.

Example 1.:

Let $A = 5$ hence with $A_{l_2} = A_{r_2} = 1$ we obtain $A_{l_1} = A_{r_1} = 4$. Let $x_P = 12$, hence $x_F = 12 + 2A = 22$. Let $B_{total} = 25$, hence $B^* = 5$. Let $y_P = A - 1$.

Since $A = odd$, hence $z = \frac{A+1}{2} = \frac{5+1}{2} = 3$, and $k = \left|\frac{x-A-1}{2}\right|_A = \left|\frac{22-5-1}{2}\right|_5 = 3$. Since $z+1 \geq \left|\frac{x-A-1}{2}\right|_A \geq 3$, the first lower-left to upper-right half-cycle is $1_1 \longrightarrow k-2$, hence $1_1 \longrightarrow 1$.

The left bight-boundary position specification is 2112,
hence $\mathcal{K}_l = 5$.
The left bight-boundary sequence specification is $1_1 3_5 5_4 4_3 2_2$.
The right bight-boundary position specification is 2112,
hence $\mathcal{K}_r = 5$.
The right bight-boundary sequence specification is $1_1 2_2 4_3 5_4 3_5$.

Hence the string-run specification of this Flores Knot is:

$$(2112/22/2112)\{1_1 3_5 5_4 4_3 2_2 / 1_1 2_2 4_3 5_4 3_5\}25.$$

We can now readily calculate the Δ_{l_i} and the Δ_{r_i} values:

$$\begin{array}{llll}
\Delta_{l_i} = 6 & \text{for } l_i = 1\,. & \Delta_{r_i} = 6 & \text{for } r_i = 1\,. \\
\Delta_{l_i} = 4 & \text{for } l_i = 2\,. & \Delta_{r_i} = 4 & \text{for } r_i = 2\,. \\
\Delta_{l_i} = 3 & \text{for } l_i = 3\,. & \Delta_{r_i} = 3 & \text{for } r_i = 3\,. \\
\Delta_{l_i} = 2 & \text{for } l_i = 4\,. & \Delta_{r_i} = 2 & \text{for } r_i = 4\,. \\
\Delta_{l_i} = 0 & \text{for } l_i = 5\,. & \Delta_{r_i} = 0 & \text{for } r_i = 5\,.
\end{array}$$

Each lower-left to upper-right half-cycle type in a Nested Cylindrical Braid occurs only once in all the first-return string-runs of such a braid. Hence we can read the lower-left to upper-right half-cycle types from the Flores Knot (Periodic Regular Nested Cylindrical Braid) specification $(2112/22/2112)\{1_1 3_5 5_4 4_3 2_2 / 1_1 2_2 4_3 5_4 3_5\}25$.

$$\begin{array}{l}
1_1 \longrightarrow 1_1 \\
3_5 \longrightarrow 2_2 \\
5_4 \longrightarrow 4_3 \\
4_3 \longrightarrow 5_4 \\
2_2 \longrightarrow 3_5
\end{array}$$

Anyone of these listed types may be taken as the first lower-left to upper-right half-cycle in the first-return string-run, but normally we take the first listed one.

Note that a Flores Knot which is derived from a Perfect or Semi-Perfect Herringbone Pineapple Knot has only one first-return string-run since a Perfect or Semi-Perfect Herringbone Pineapple Knot has only one first-return string-run. Hence all the listed lower-left to upper-right half-cycle types of such a Flores knot are contained in the single first-return string-run of that Flores Knot. Consequently such a Flores knot has only one component. This component consists of g.c.d.$(P_F\,,\,B^*)$ sub-components and hence requires g.c.d.$(P_F\,,\,B^*)$ essential strings.

For the first-return string-run we thus obtain:

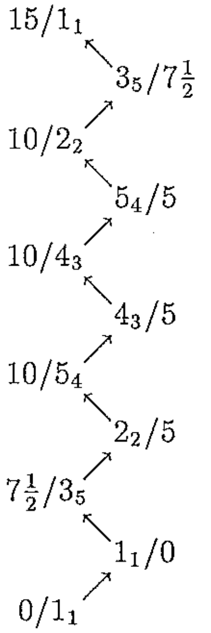

$$\begin{array}{lllll}
l_{1_{j_l}} = 1_1 \longrightarrow 1_1 = r_{1_{j_r}} & \rightarrow & j'_l = |1+6+22+6|_5 = 5 & \rightarrow & l_{2_{j'_l}} = 3_5\,. \\
l_{2_{j'_l}} = 3_5 \longleftarrow 1_1 = r_{1_{j_r}} & \rightarrow & j'_r = |1+6+22+3|_5 = 2 & \rightarrow & r_{2_{j'_r}} = 2_2\,. \\
l_{2_{j_l}} = 3_5 \longrightarrow 2_2 = r_{2_{j'_r}} & \rightarrow & j'_l = |5+3+22+4|_5 = 4 & \rightarrow & l_{3_{j'_l}} = 5_4\,. \\
l_{3_{j'_l}} = 5_4 \longleftarrow 2_2 = r_{2_{j_r}} & \rightarrow & j'_r = |2+4+22+0|_5 = 3 & \rightarrow & r_{3_{j'_r}} = 4_3\,. \\
l_{3_{j_l}} = 5_4 \longrightarrow 4_3 = r_{3_{j'_r}} & \rightarrow & j'_l = |4+0+22+2|_5 = 3 & \rightarrow & l_{4_{j'_l}} = 4_3\,. \\
l_{4_{j'_l}} = 4_3 \longleftarrow 4_3 = r_{3_{j_r}} & \rightarrow & j'_r = |3+2+22+2|_5 = 4 & \rightarrow & r_{4_{j'_r}} = 5_4\,. \\
l_{4_{j_l}} = 4_3 \longrightarrow 5_4 = r_{4_{j'_r}} & \rightarrow & j'_l = |3+2+22+0|_5 = 2 & \rightarrow & l_{5_{j'_l}} = 2_2\,. \\
l_{5_{j'_l}} = 2_2 \longleftarrow 5_4 = r_{4_{j_r}} & \rightarrow & j'_r = |4+0+22+4|_5 = 5 & \rightarrow & r_{5_{j'_r}} = 3_5\,. \\
l_{5_{j_l}} = 2_2 \longrightarrow 3_5 = r_{5_{j'_r}} & \rightarrow & j'_l = |2+4+22+3|_5 = 1 & \rightarrow & l_{6_{j'_l}} = 1_1\,. \\
l_{6_{j'_l}} = 1_1 \longleftarrow 3_5 = r_{5_{j_r}}\,. & & & &
\end{array}$$

$$I_{L_1} = 0 \quad ; \quad I_{L_{n+1}} = \left| I_{L_n} + x_F + \Delta r_i + \tfrac{\Delta l_i + \Delta l_{i+1}}{2} \right|_B .$$

$$I_{R_1} = 0 \quad ; \quad I_{R_{n+1}} = \left| I_{R_n} + x_F + \Delta l_i + \tfrac{\Delta r_i + \Delta r_{i+1}}{2} \right|_B .$$

$P_c = P_F = 2A + x_F - 4 = 10 + 22 - 4 = 28\,.$

g.c.d.$(P_F\,,\,B^*) =$ g.c.d.$(28\,,\,5) = 1$, hence the component has no sub-components, consequently this Flores Knot requires one essential string (it is a single string knot).

This single string Flores Knot was derived from the Semi-Perfect Herringbone Pineapple Knot with $A = 5$; $x_P = 12$; $y = A - 1$; $B^* = 5$; $P_P = 20$, having $\text{g.c.d.}(P_P, B^*) = \text{g.c.d.}(20, 5) = 5$, consequently this Semi-Perfect Herringbone Pineapple Knot requires five essential strings (it is a five string knot). However, the physical appearance of these two knots is the same.

In the half-cycle pattern arrangement we again indicate the number of crossings associated with a half-cycle under its half-cycle number.[†] On pp. 934-935 we discussed the calculation procedure of the number of crossings, and from the general schemes shown we obtain for our Example:

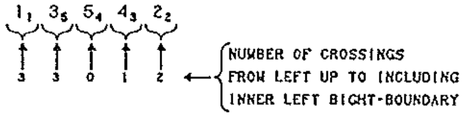
1_1 3_5 5_4 4_3 2_2
3 3 0 1 2
NUMBER OF CROSSINGS FROM LEFT UP TO INCLUDING INNER LEFT BIGHT-BOUNDARY

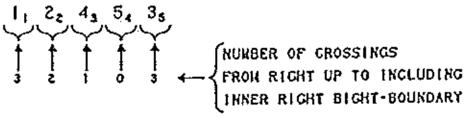
1_1 2_2 4_3 5_4 3_5
3 2 1 0 3
NUMBER OF CROSSINGS FROM RIGHT UP TO INCLUDING INNER RIGHT BIGHT-BOUNDARY

Hence the half-cycle pattern arrangement of our Flores Knot will be as shown in Fig. 734.

1	2	3	4	5		5	4	3	2	1
		$\frac{13}{26}$			— $22\frac{1}{2}$ —			$\frac{20}{27}$		
$\frac{31}{27}$	$\frac{49}{26}$		$\frac{47}{22}$	$\frac{45}{22}$	— 20 —	$\frac{18}{23}$	$\frac{16}{23}$		$\frac{14}{23}$	$\frac{32}{27}$
		$\frac{43}{26}$			— $17\frac{1}{2}$ —			$\frac{50}{27}$		
$\frac{11}{27}$	$\frac{29}{26}$		$\frac{27}{22}$	$\frac{25}{22}$	— 15 —	$\frac{48}{23}$	$\frac{46}{23}$		$\frac{44}{23}$	$\frac{12}{27}$
		$\frac{23}{26}$			— $12\frac{1}{2}$ —			$\frac{30}{27}$		
$\frac{41}{27}$	$\frac{9}{26}$		$\frac{7}{22}$	$\frac{5}{22}$	— 10 —	$\frac{28}{23}$	$\frac{26}{23}$		$\frac{24}{23}$	$\frac{42}{27}$
		$\frac{3}{26}$			— $7\frac{1}{2}$ —			$\frac{10}{27}$		
$\frac{21}{27}$	$\frac{39}{26}$		$\frac{37}{22}$	$\frac{35}{22}$	— 5 —	$\frac{8}{23}$	$\frac{6}{23}$		$\frac{4}{23}$	$\frac{22}{27}$
		$\frac{33}{26}$			— $2\frac{1}{2}$ —			$\frac{40}{27}$		
$\frac{1}{27}$	$\frac{19}{26}$		$\frac{17}{22}$	$\frac{15}{22}$	— 0 —	$\frac{38}{23}$	$\frac{36}{23}$		$\frac{34}{23}$	$\frac{2}{27}$

Fig. 734 — The half-cycle pattern of the Flores Knot in Example 1.

For the superimposed coding we can follow the semi row-coding arrangement as discussed for $A = 2$ on pp. 931-932, or we can follow its counter part which we shall call the non semi row-coding arrangement.

For the pattern of unders and overs associated with a particular half-cycle type, we can make use of the coding-patterns in:

Fig. 737 for Flores Knots with the semi-row coding arrangement, derived from Perfect or Semi-Perfect Herringbone Pineapple Knots with $y = A - 1$,

Fig. 738 for Flores Knots with the non semi row-coding arrangement, derived from Perfect or Semi-Perfect Herringbone Pineapple Knots with $y = A - 1$,

Fig. 739 for Flores Knots with the semi-row coding arrangement, derived from Perfect or Semi-Perfect Herringbone Pineapple Knots with $y = A + 1$,

Fig. 740 for Flores Knots with the non semi row-coding arrangement, derived from Perfect or Semi-Perfect Herringbone Pineapple Knots with $y = A + 1$.

[†] See *The Braider*, Issue No. 34, pg. 800.

These Figs. depict on the lower-left to upper-right half-cycles and on the lower-right to upper-left half-cycles the initial and final consecutive sets of over and under codings which do not follow the '*A*-over — *A*-under' pattern.

The initial consecutive sets of coding which end with a set of over-codings is followed by $Au - Ao - \cdots$, and which end with a set of under-codings is followed by $Ao - Au - \cdots$.

The final consecutive sets of coding which begin with a set of over-codings is preceded by $\cdots - Ao - Au$, and which begin with a set of under-codings is preceded by $\cdots - Au - Ao$.

Say that in our example we use the semi row-coding arrangement. Then with the aid of Fig. 737 (case $A = 5$) and the number of crossings on the half-cycles we can in the half-cycle tables for the lower-left to upper-right half-cycles and the lower-right to upper-left half-cycles enter the coding sequences (see Figs. 735 and 736).

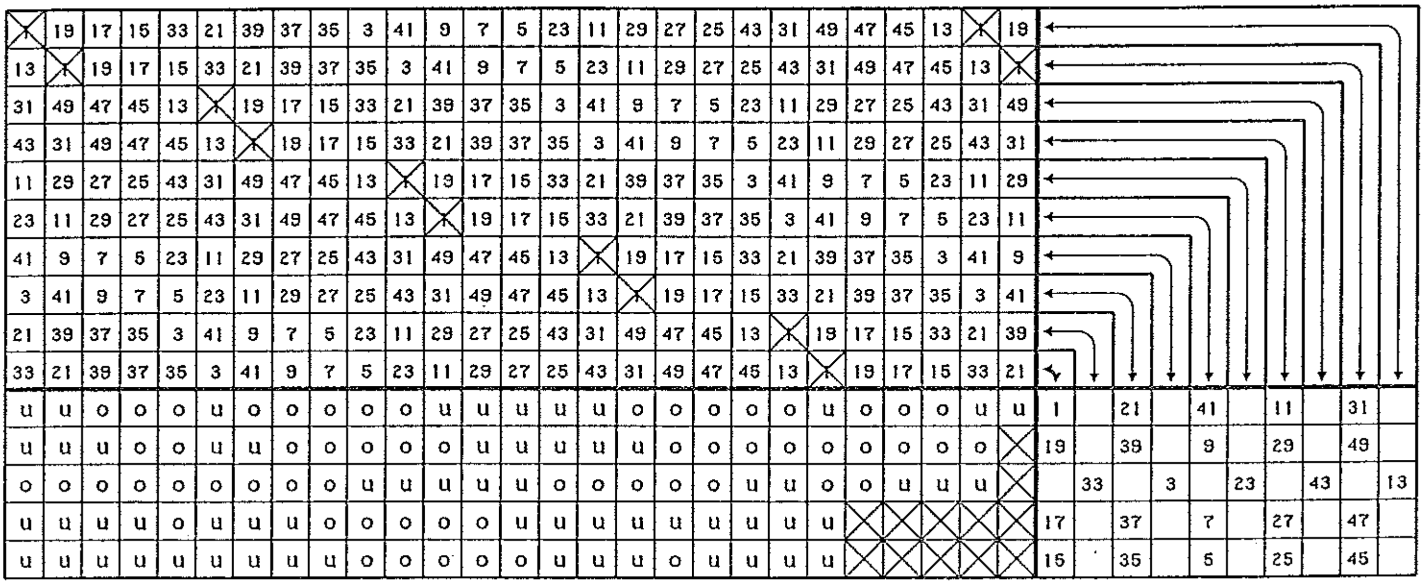

☒	19	17	15	33	21	39	37	35	3	41	9	7	5	23	11	29	27	25	43	31	49	47	45	13	☒	19										
13	☒	19	17	15	33	21	39	37	35	3	41	9	7	5	23	11	29	27	25	43	31	49	47	45	13	☒										
31	49	47	45	13	☒	19	17	15	33	21	39	37	35	3	41	9	7	5	23	11	29	27	25	43	31	49										
43	31	49	47	45	13	☒	19	17	15	33	21	39	37	35	3	41	9	7	5	23	11	29	27	25	43	31										
11	29	27	25	43	31	49	47	45	13	☒	19	17	15	33	21	39	37	35	3	41	9	7	5	23	11	29										
23	11	29	27	25	43	31	49	47	45	13	☒	19	17	15	33	21	39	37	35	3	41	9	7	5	23	11										
41	9	7	5	23	11	29	27	25	43	31	49	47	45	13	☒	19	17	15	33	21	39	37	35	3	41	9										
3	41	9	7	5	23	11	29	27	25	43	31	49	47	45	13	☒	19	17	15	33	21	39	37	35	3	41										
21	39	37	35	3	41	9	7	5	23	11	29	27	25	43	31	49	47	45	13	☒	19	17	15	33	21	39										
33	21	39	37	35	3	41	9	7	5	23	11	29	27	25	43	31	49	47	45	13	☒	19	17	15	33	21										
u	u	o	o	o	u	o	o	o	o	o	u	u	u	u	u	o	o	o	o	o	u	o	o	o	u	u	1		21		41		11		31	
u	u	u	o	o	u	u	o	o	o	o	o	u	u	u	u	u	o	o	o	o	o	o	o	o	o	☒	19		39		9		29		49	
o	o	o	o	o	o	o	o	o	u	u	u	u	u	o	o	o	o	o	u	u	o	o	u	u	u	☒		33		3		23		43		13
u	u	u	u	o	u	u	u	o	o	o	o	o	u	u	u	u	u	u	u	u	u	☒	☒	☒	☒	☒	17		37		7		27		47	
u	u	u	u	u	u	u	u	u	o	o	o	o	o	o	u	u	u	o	u	u	u	u	☒	☒	☒	☒	☒	15		35		5		25		45	

Fig. 735 — The half-cycle table for the lower-left to upper-right half-cycles.

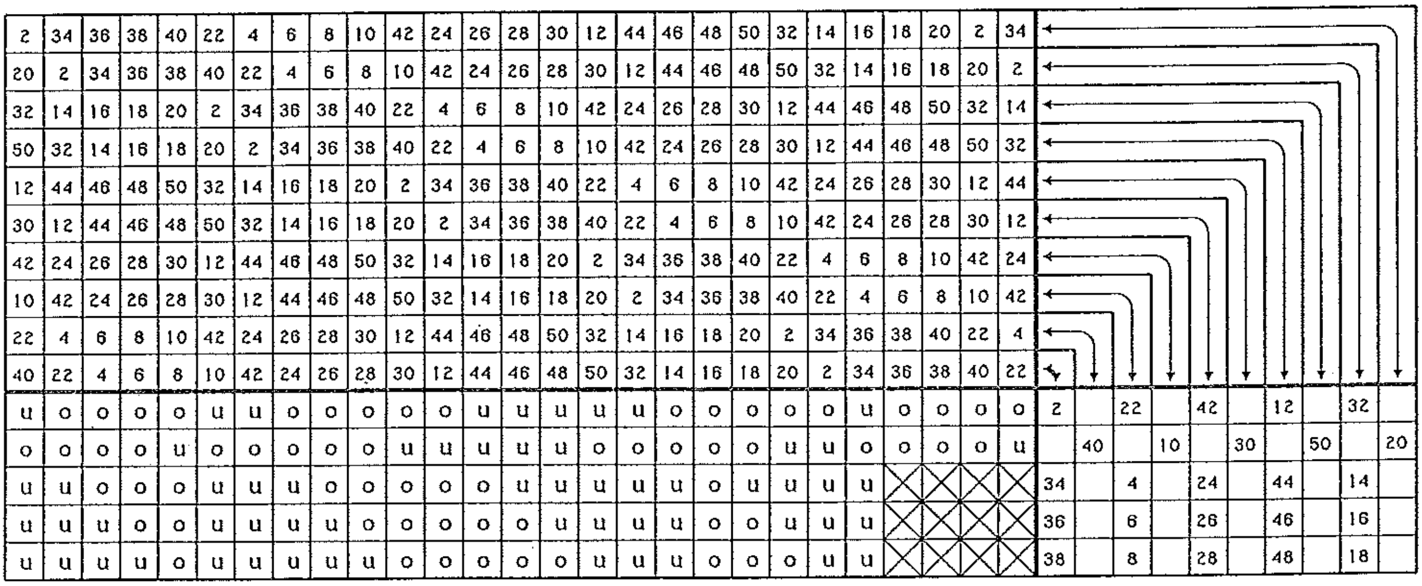

2	34	36	38	40	22	4	6	8	10	42	24	26	28	30	12	44	46	48	50	32	14	16	18	20	2	34										
20	2	34	36	38	40	22	4	6	8	10	42	24	26	28	30	12	44	46	48	50	32	14	16	18	20	2										
32	14	16	18	20	2	34	36	38	40	22	4	6	8	10	42	24	26	28	30	12	44	46	48	50	32	14										
50	32	14	16	18	20	2	34	36	38	40	22	4	6	8	10	42	24	26	28	30	12	44	46	48	50	32										
12	44	46	48	50	32	14	16	18	20	2	34	36	38	40	22	4	6	8	10	42	24	26	28	30	12	44										
30	12	44	46	48	50	32	14	16	18	20	2	34	36	38	40	22	4	6	8	10	42	24	26	28	30	12										
42	24	26	28	30	12	44	46	48	50	32	14	16	18	20	2	34	36	38	40	22	4	6	8	10	42	24										
10	42	24	26	28	30	12	44	46	48	50	32	14	16	18	20	2	34	36	38	40	22	4	6	8	10	42										
22	4	6	8	10	42	24	26	28	30	12	44	46	48	50	32	14	16	18	20	2	34	36	38	40	22	4										
40	22	4	6	8	10	42	24	26	28	30	12	44	46	48	50	32	14	16	18	20	2	34	36	38	40	22										
u	o	o	o	o	u	u	o	o	o	o	o	u	u	u	u	u	o	o	o	o	o	u	o	o	o	o	2		22		42		12		32	
o	o	o	o	u	o	o	o	o	o	u	u	u	u	u	o	o	o	o	o	u	u	o	o	o	o	u		40		10		30		50		20
u	u	o	o	o	u	u	u	o	o	o	o	o	u	u	u	u	u	o	u	u	u	u	☒	☒	☒	☒	34		4		24		44		14	
u	u	u	o	o	u	u	u	u	o	o	o	o	o	u	u	u	u	o	o	u	u	u	☒	☒	☒	☒	36		6		26		46		16	
u	u	u	u	o	u	u	u	u	u	o	o	o	o	o	u	u	u	o	o	o	u	u	☒	☒	☒	☒	38		8		28		48		18	

Fig. 736 — The half-cycle table for the lower-right to upper-left half-cycles.

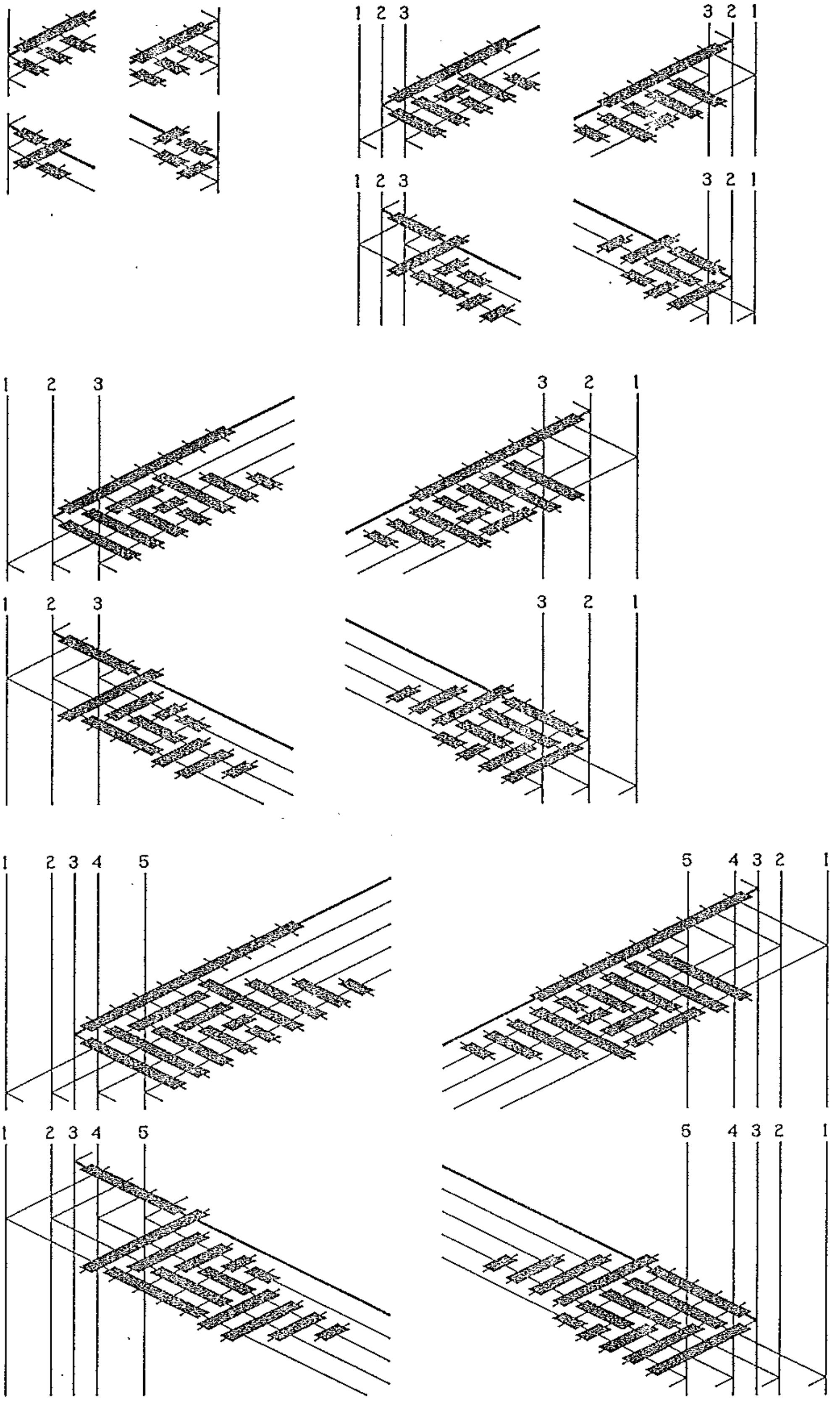

Fig. 737 — The initial and final half-cycle coding sets. (semi row-coding; $y_P = A - 1$).

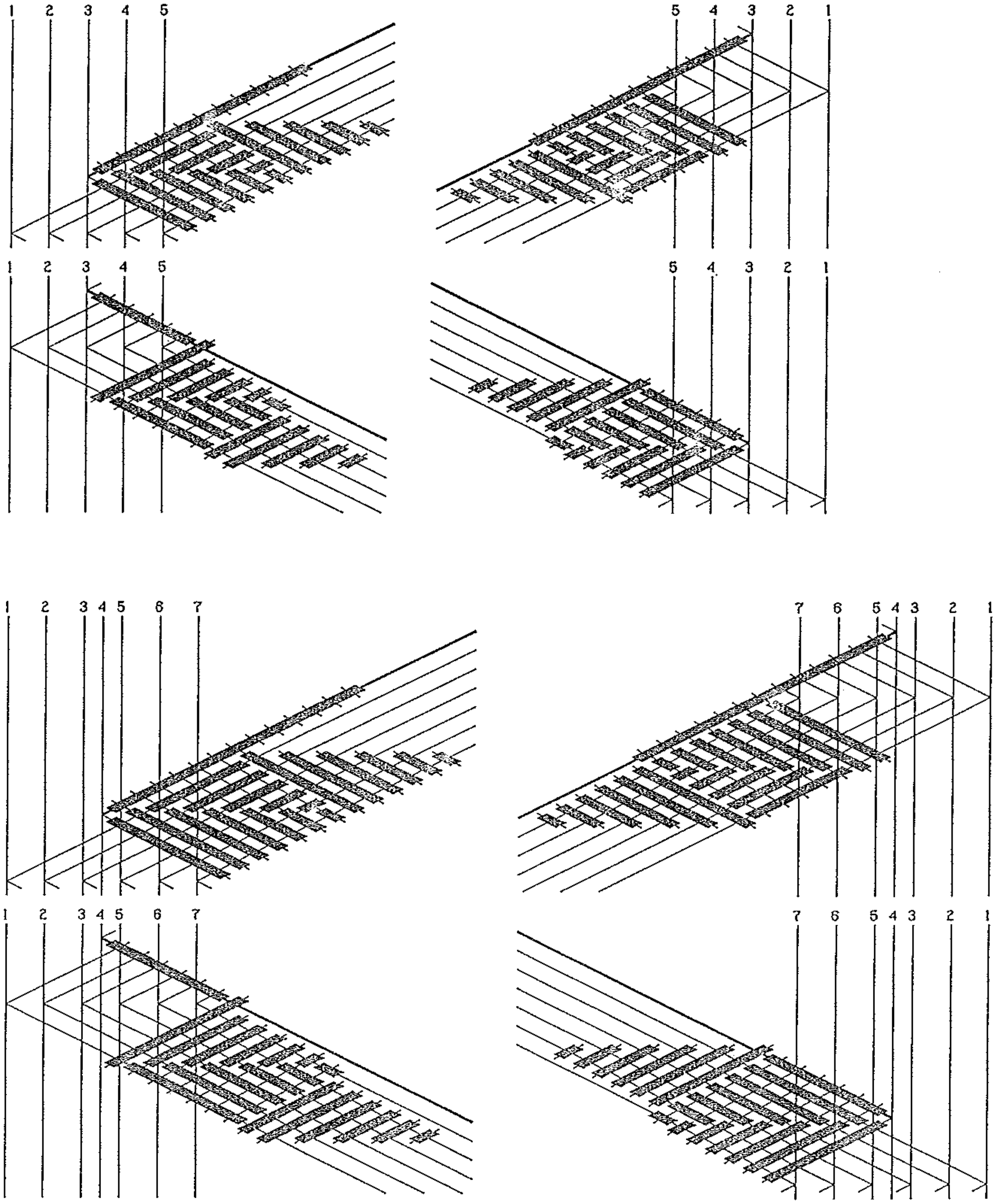

Fig. 737 Cont. — The initial and final half-cycle coding sets. (semi row-coding; $y_P = A - 1$).

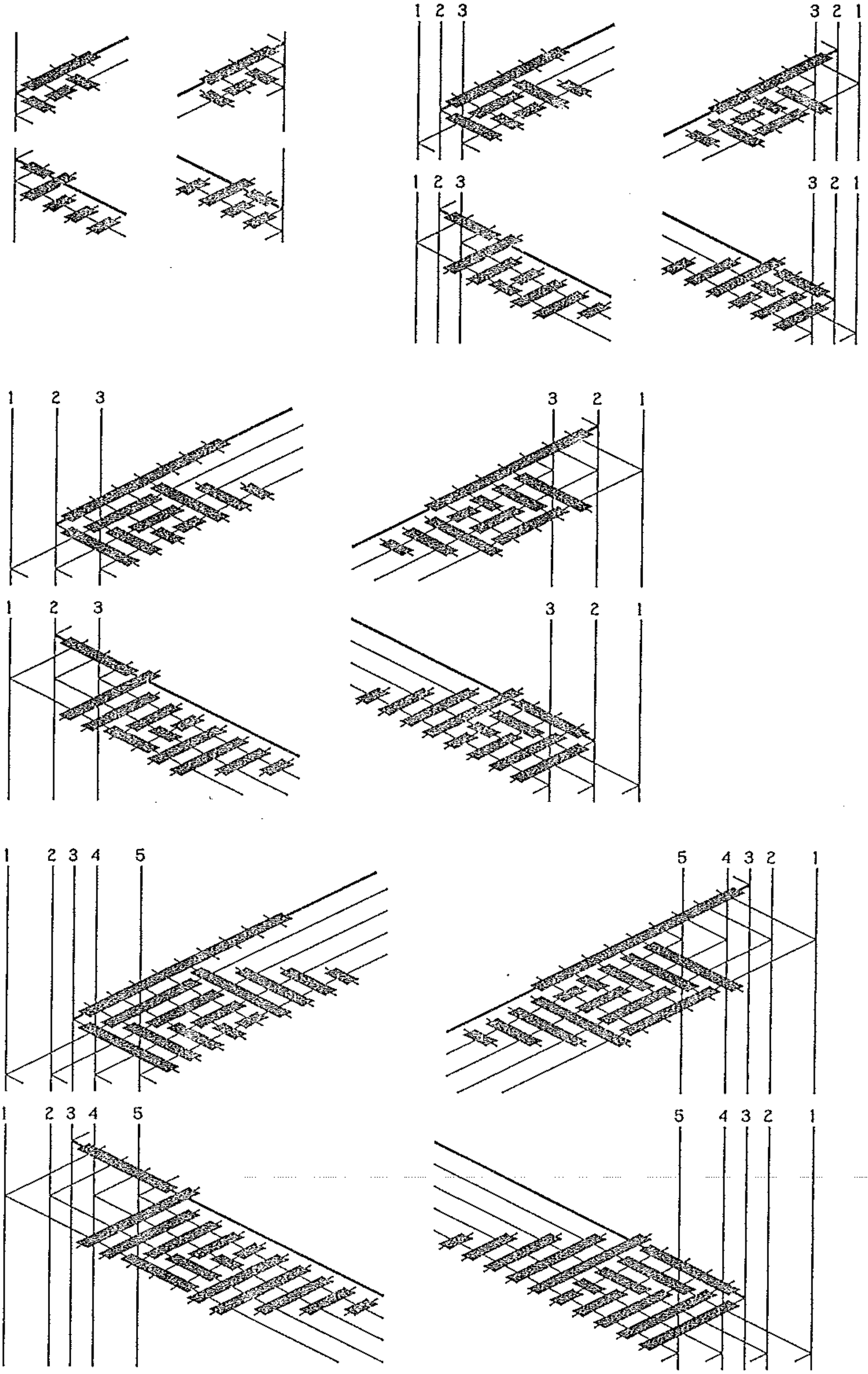

Fig. 738 — The initial and final half-cycle coding sets. (non semi row-coding; $y_P = A - 1$).

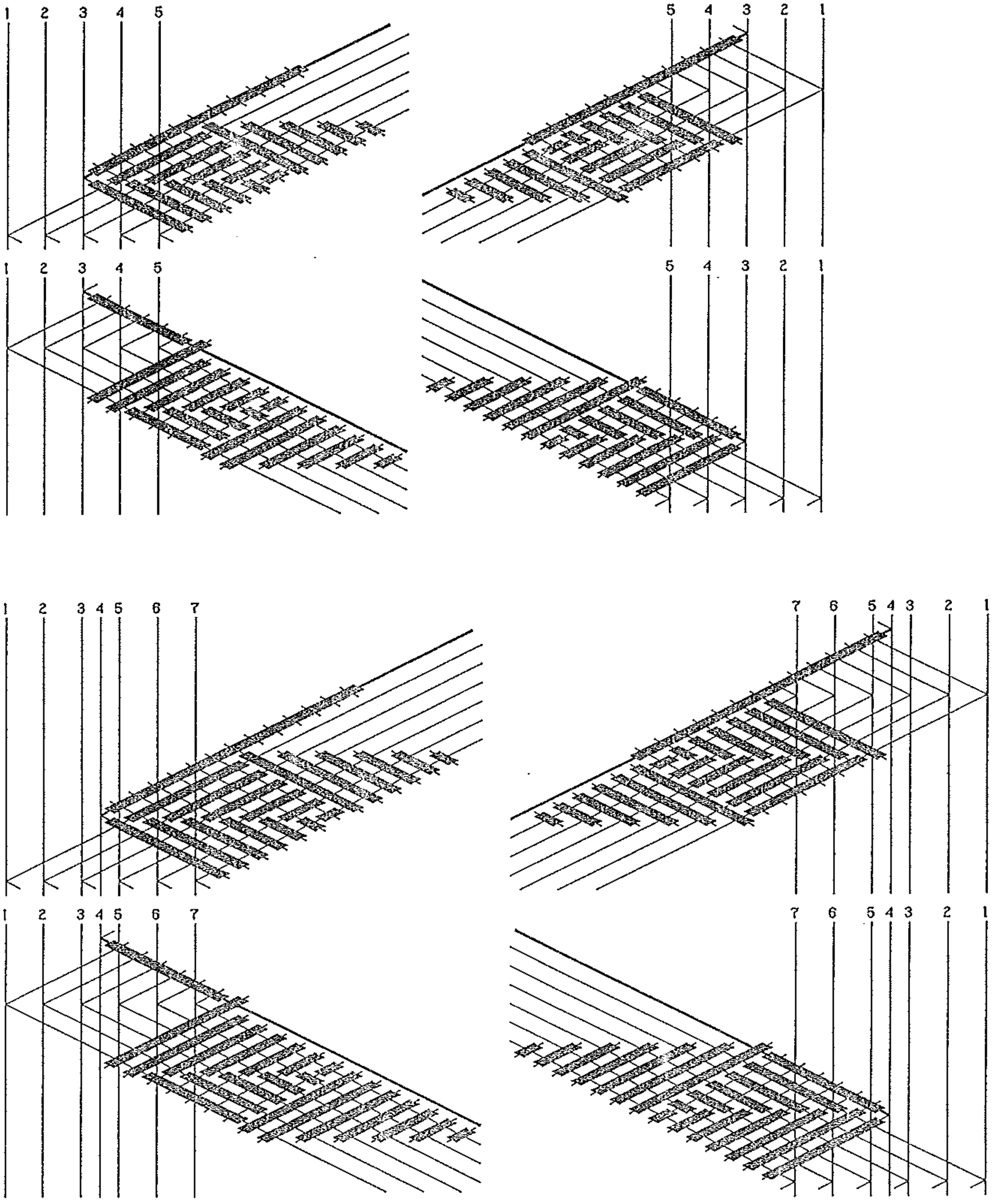

Fig. 738 Cont. — The initial and final half-cycle coding sets.
(non semi row-coding; $y_P = A - 1$).

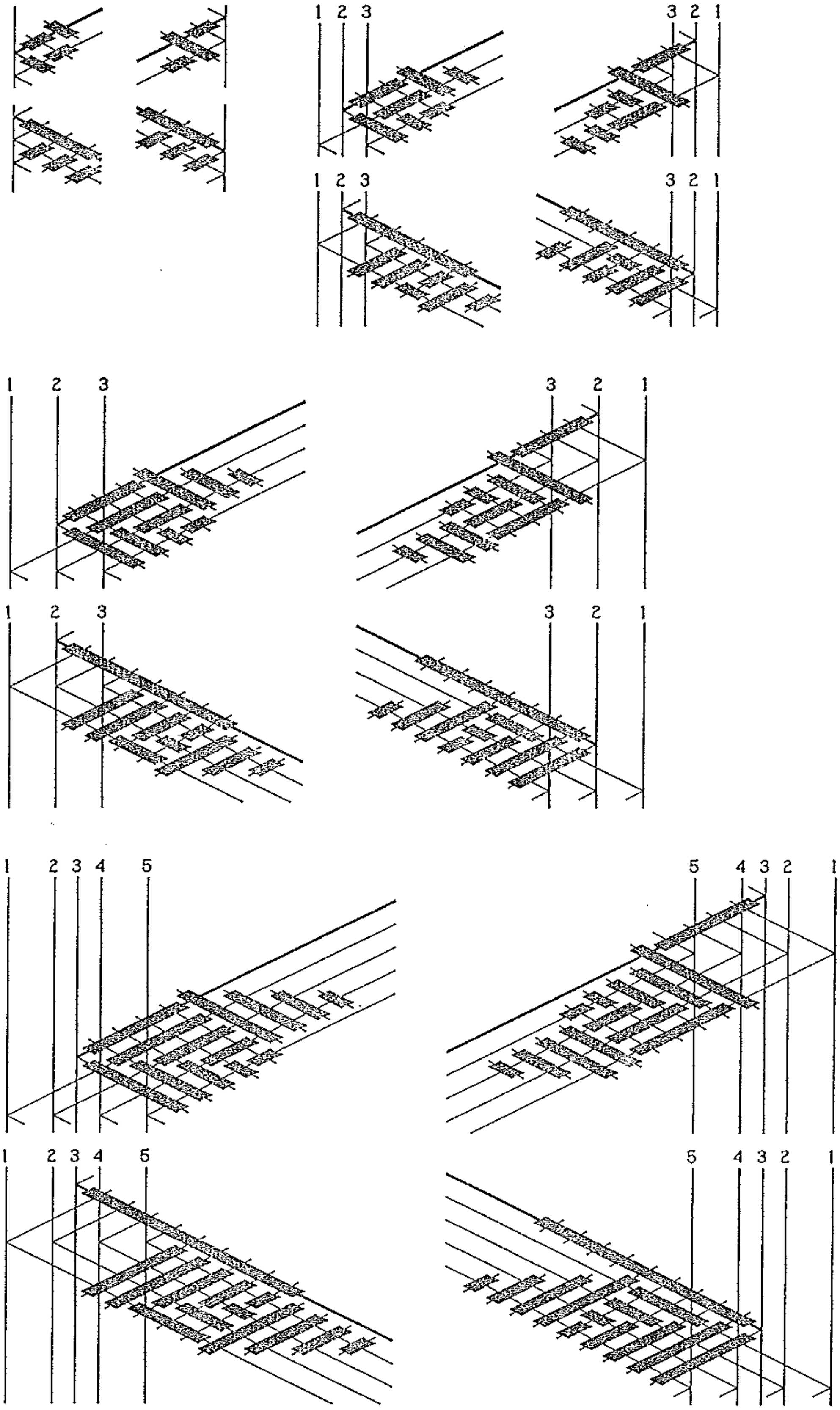

Fig. 739 — The initial and final half-cycle coding sets. (semi row-coding; $y_P = A + 1$).

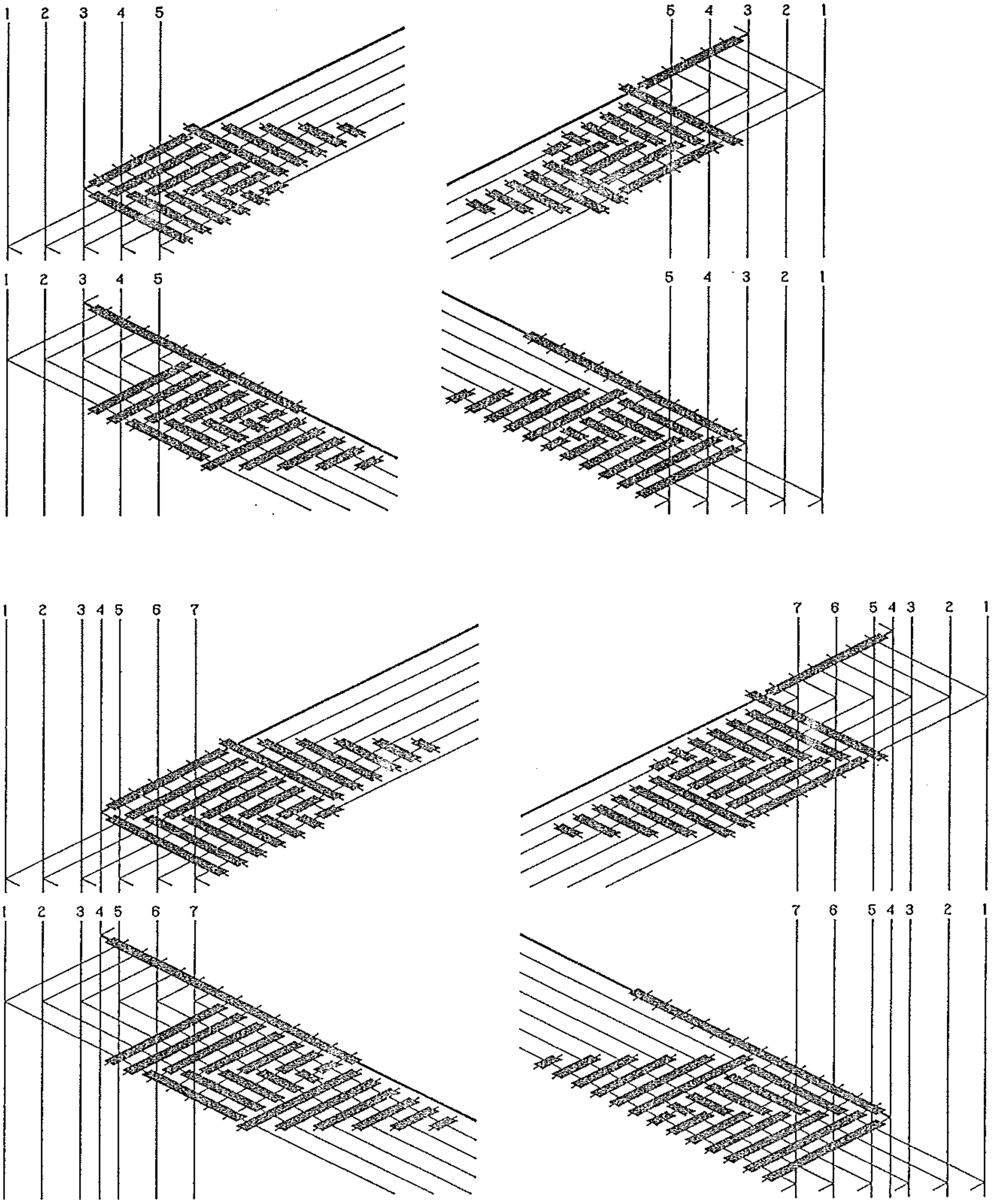

Fig. 739 Cont. — The initial and final half-cycle coding sets. (semi row-coding; $y_P = A + 1$).

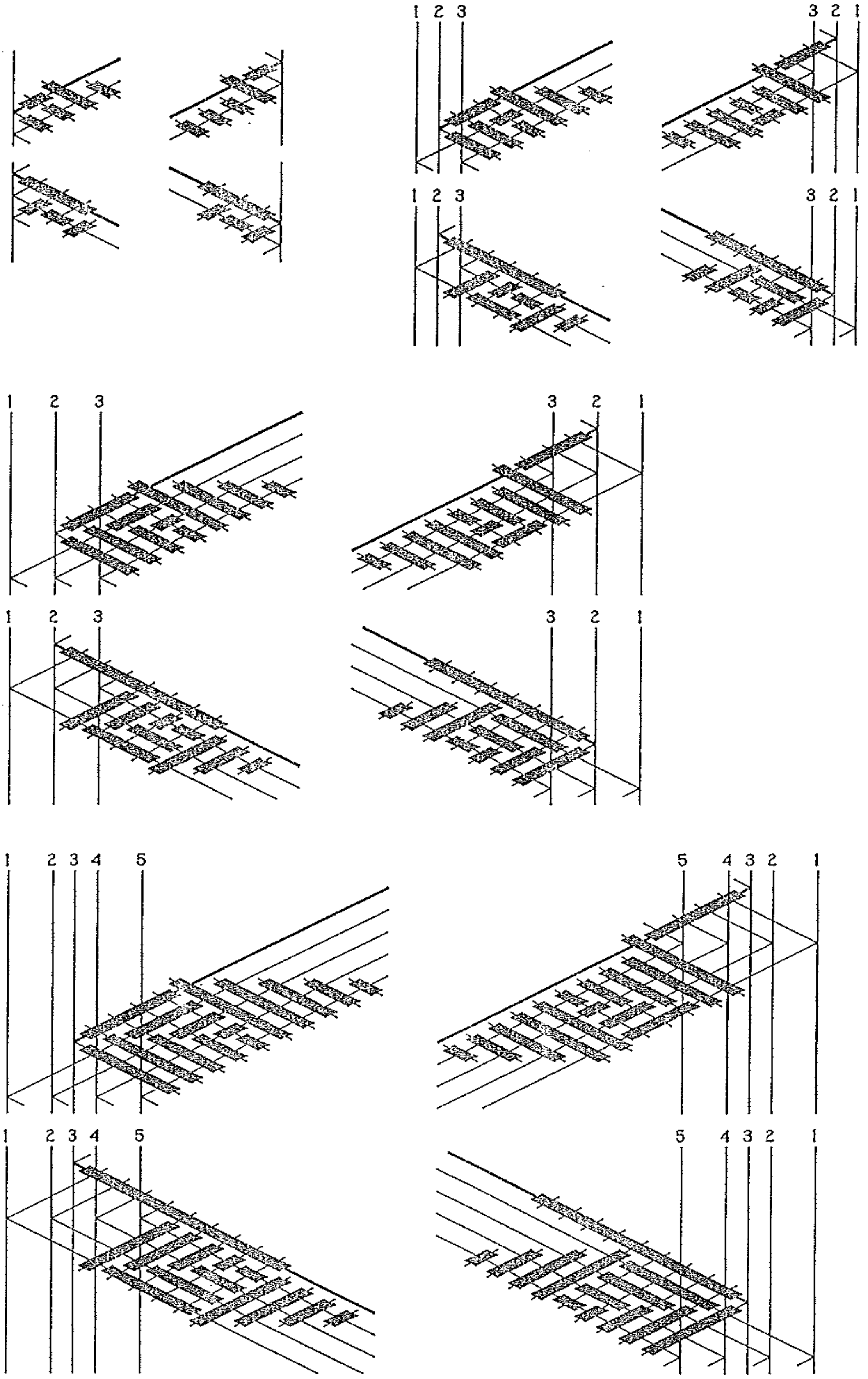

Fig. 740 — The initial and final half-cycle coding sets. (non semi row-coding; $y_P = A + 1$).

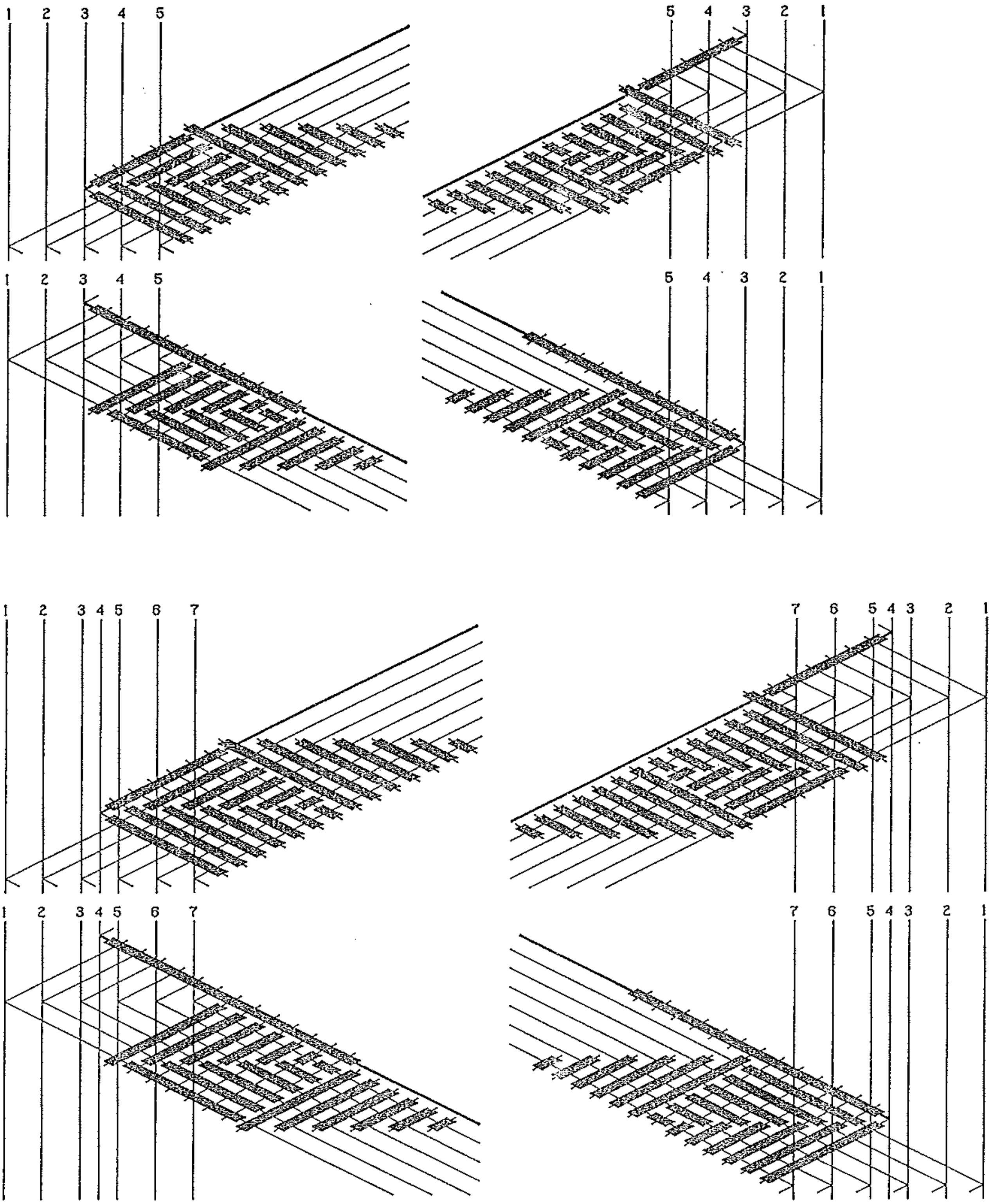

Fig. 740 Cont. — The initial and final half-cycle coding sets. (non semi row-coding; $y_p = A + 1$).

The first-return string-run contains $2A = 10$ half-cycles, hence:
half-cycles $1, 11, 21, 31, 41$ are identically coded, the first-return string-run shows that they start at $l_{i_j} = 1_1$ and end at $r_{i_j} = 1_1$;
half-cycles $3, 31, 23, 33, 43$ are identically coded, the first-return string-run shows that they start at $l_{i_j} = 3_5$ and end at $r_{i_j} = 2_2$;
half-cycles $5, 15, 25, 35, 45$ are identically coded, the first-return string-run shows that they start at $l_{i_j} = 5_4$ and end at $r_{i_j} = 4_3$;
half-cycles $7, 17, 27, 37, 47$ are identically coded, the first-return string-run shows that they start at $l_{i_j} = 4_3$ and end at $r_{i_j} = 5_4$;
half-cycles $9, 19, 29, 39, 49$ are identically coded, the first-return string-run shows that they start at $l_{i_j} = 2_2$ and end at $r_{i_j} = 3_5$;
half-cycles $2, 12, 22, 32, 42$ are identically coded, the first-return string-run shows that they start at $r_{i_j} = 1_1$ and end at $l_{i_j} = 3_5$;
half-cycles $4, 14, 24, 34, 44$ are identically coded, the first-return string-run shows that they start at $r_{i_j} = 2_2$ and end at $l_{i_j} = 5_4$;
half-cycles $6, 16, 26, 36, 46$ are identically coded, the first-return string-run shows that they start at $r_{i_j} = 4_3$ and end at $l_{i_j} = 4_3$;
half-cycles $8, 18, 28, 38, 48$ are identically coded, the first-return string-run shows that they start at $r_{i_j} = 5_4$ and end at $l_{i_j} = 2_2$;
half-cycles $10, 20, 30, 40, 50$ are identically coded. the first-return string-run shows that they start at $r_{i_j} = 3_5$ and end at $l_{i_j} = 1_1$.

From the half-cycle tables we can again read the half-cycle braiding algorithms.

It should be noted that we do not have to draw up the grid-diagram of our Flores Knot, although in general we like to have the grid-diagram of a knot we braid. Hence we can delay drawing the grid-diagram till after we have compiled the half-cycle braiding algorithms from the half-cycle tables:

1. $1_1 \longrightarrow 1_1$: Free run.
2. $3_5 \longleftarrow 1_1$: o.
3. $3_5 \longrightarrow 2_2$: u.
4. $5_4 \longleftarrow 2_2$: $2u$.
5. $5_4 \longrightarrow 4_3$: u.
6. $4_3 \longleftarrow 4_3$: $2u$
7. $4_3 \longrightarrow 5_4$: u.
8. $2_2 \longleftarrow 5_4$: $2u$.
9. $2_2 \longrightarrow 3_5$: $4o$.
10. $1_1 \longleftarrow 3_5$: $o - u - 3o$.
11. $1_1 \longrightarrow 1_1$: $u - 3o - u$.
12. $3_5 \longleftarrow 1_1$: $5u - o$.
13. $3_5 \longrightarrow 2_2$: $4u - o - u$.
14. $5_4 \longleftarrow 2_2$: $2u - 3o - 2u$.
15. $5_4 \longrightarrow 4_3$: $3u - 2o - u$.
16. $4_3 \longleftarrow 4_3$: $3u - 2o - 2u$.
17. $4_3 \longrightarrow 5_4$: $2u - 3o - u$.
18. $2_2 \longleftarrow 5_4$: $4u - o - 2u$.
19. $2_2 \longrightarrow 3_5$: $u - 8o$.
20. $1_1 \longleftarrow 3_5$: $6o - u - 4o$.
21. $1_1 \longrightarrow 1_1$: $u - 4o - u - 3o - 2u$.
22. $3_5 \longleftarrow 1_1$: $7u - o - u - 3o$.

23. $3_5 \longrightarrow 2_2$: $o - 4u - o - u - 2o - 3u$.
24. $5_4 \longleftarrow 2_2$: $2u - 4o - 2u - o - 3u$.
25. $5_4 \longrightarrow 4_3$: $3u - 2o - u - o - 4u$.
26. $4_3 \longleftarrow 4_3$: $3u - 3o - 2u - 2o - 2u$.
27. $4_3 \longrightarrow 5_4$: $2u - 3o - 6u$.
28. $2_2 \longleftarrow 5_4$: $4u - 2o - 2u - 3o - u$.
29. $2_2 \longrightarrow 3_5$: $u - 4o - u - 8o$.
30. $1_1 \longleftarrow 3_5$: $5o - u - 5o - u - 4o$.
31. $1_1 \longrightarrow 1_1$: $u - 5o - 4u - 4o - 2u$.
32. $3_5 \longleftarrow 1_1$: $u - o - u - 4o - 5u - o - u - 4o$.
33. $3_5 \longrightarrow 2_2$: $5o - 5u - o - u - 2o - 3u$.
34. $5_4 \longleftarrow 2_2$: $u - 3o - 2u - 4o - 2u - o - 4u$.
35. $5_4 \longrightarrow 4_3$: $8u - 2o - u - o - 4u$.
36. $4_3 \longleftarrow 4_3$: $2u - 2o - 3u - 3o - 2u - 2o - 3u$.
37. $4_3 \longrightarrow 5_4$: $3u - o - 3u - 3o - 6u$.
38. $2_2 \longleftarrow 5_4$: $3u - o - 4u - 2o - 2u - 3o - 2u$.
39. $2_2 \longrightarrow 3_5$: $2u - 2o - 2u - 4o - u - 9o$.
40. $1_1 \longleftarrow 3_5$: $4o - u - 4o - u - 5o - 2u - 4o - u$.
41. $1_1 \longrightarrow 1_1$: $2u - 5o - 4u - 5o - u - 3o - 2u$.
42. $3_5 \longleftarrow 1_1$: $u - o - u - 5o - 5u - 5o - u - 4o$.
43. $3_5 \longrightarrow 2_2$: $5o - 5u - 5o - 2u - 2o - 3u$.
44. $5_4 \longleftarrow 2_2$: $u - 3o - 3u - 5o - 5u - o - 4u$.
45. $5_4 \longrightarrow 4_3$: $8u - 5o - 3u - o - 4u$.
46. $4_3 \longleftarrow 4_3$: $2u - 2o - 4u - 5o - 4u - 2o - 3u$.
47. $4_3 \longrightarrow 5_4$: $3u - o - 3u - 5o - 9u$.
48. $2_2 \longleftarrow 5_4$: $3u - o - 5u - 5o - 3u - 3o - 2u$.
49. $2_2 \longrightarrow 3_5$: $2u - 2o - 2u - 5o - 5u - 9o$.
50. $1_1 \longleftarrow 3_5$: $4o - u - 5o - 5u - 5o - 2u - 4o - u$.

The grid-diagrams of the Flores Knot and the Semi-Perfect Herringbone Pineapple Knot from which it has been derived are depicted in Fig. 741.

Although for the Flores Knots derived from Perfect or Semi-Perfect Herringbone Pineapple Knots we can calculate the half-cycle bight-boundaries on their first-return string-run by means of the general method for Nested Cylindrical Braids (see *The Braider*, Issue No. 19, pg. 417) as we have done here on pg. 936, it is easier to derive them from the readily to be determined half-cycle bight-boundaries on the first-return string-run of their associated Herringbone Pineapple Knots. The following conversions should then be used:

A=EVEN ; $z=\frac{A}{2}$

LEFT BIGHT-BOUNDARY			RIGHT BIGHT-BOUNDARY		
PINE		FLORES	PINE		FLORES
2	►	1_1	2	►	1
1	►	z_A	3	►	2
A	►	$(A-1)_{(A-1)}$	4	►	3
(A-1)	►	$(A-2)_{(A-2)}$	•		•
•		•	•		•
•		•	•		•
•		•	(z-1)	►	(z-2)
(z+1)	►	z_z	z	►	(z-1)
z	►	$(z-1)_{(z-1)}$	(z+1)	►	z
(z-1)	►	$(z-2)_{(z-2)}$	(z+2)	►	(z+1)
•		•	•		•
•		•	•		•
•		•	•		•
4	►	3_3	A	►	(A-1)
3	►	2_2	1	►	z.

A=ODD ; $z=\frac{A+1}{2}$

LEFT BIGHT-BOUNDARY			RIGHT BIGHT-BOUNDARY		
PINE		FLORES	PINE		FLORES
2	►	1_1	2	►	1
1	►	z_A	3	►	2
A	►	$A_{(A-1)}$	4	►	3
(A-1)	►	$(A-1)_{(A-2)}$	•		•
•		•	•		•
•		•	•		•
•		•	(z-1)	►	(z-2)
(z+1)	►	$(z+1)_z$	z	►	(z-1)
z	►	$(z-1)_{(z-1)}$	(z+1)	►	(z+1)
(z-1)	►	$(z-2)_{(z-2)}$	(z+2)	►	(z+2)
•		•	•		•
•		•	•		•
•		•	•		•
4	►	3_3	A	►	A
3	►	2_2	1	►	z.

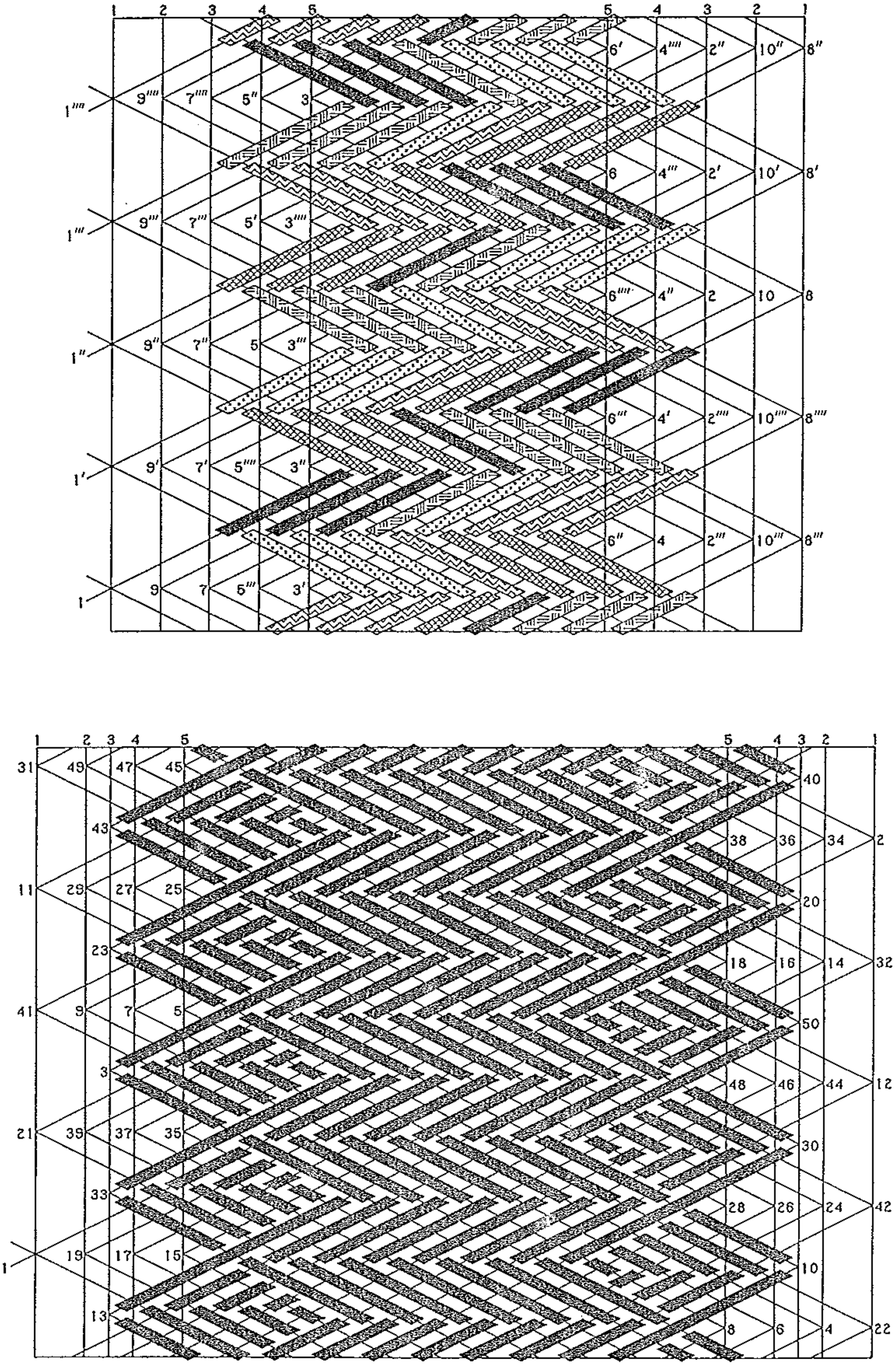

Fig. 741 — The Semi-Perfect Herringbone Pineapple Knot (upper grid-diagram) and Flores Knot derived from it (lower grid-diagram)

Example 2.:

Let $A = 6$ hence with $A_{l_2} = A_{r_2} = 1$ we obtain $A_{l_1} = A_{r_1} = 5$, and let the Flores Knot be derived from the Semi-Perfect Herringbone Pineapple Knot with $y_P = A + 1$. Let $x_P = 11$, hence $x_F = 11 + 2A = 23$. Let $B_{total} = 18$, hence $B^* = 3$.

Since $A = even$, hence $z = \frac{A}{2} = \frac{6}{2} = 3$, and $k = \left|\frac{x-A-3}{2}\right|_A = \left|\frac{23-6-3}{2}\right|_6 = 1$. Since $\left|\frac{x-A-3}{2}\right|_A = 1$, the first lower-left to upper-right half-cycle is $1_1 \longrightarrow A - 1 = 1_1 \longrightarrow 5$.[†]

The left bight-boundary position specification is 2222, hence $\mathcal{K}_l = 5$.
The left bight-boundary sequence specification is $1_1 3_6 5_5 4_4 3_3 2_2$.
The right bight-boundary position specification is 2222, hence $\mathcal{K}_r = 5$.
The right bight-boundary sequence specification is $5_1 3_2 1_3 2_4 3_5 4_6$.

Hence the string-run specification of this Flores Knot is:

$$(2222/23/2222)\{1_1 3_6 5_5 4_4 3_3 2_2 / 5_1 3_2 1_3 2_4 3_5 4_6\}18.$$

We can now readily calculate the Δ_{l_i} and the Δ_{r_i} values:

$\Delta_{l_i} = 8$ for $l_i = 1$. $\quad$ $\Delta_{r_i} = 8$ for $r_i = 1$.
$\Delta_{l_i} = 6$ for $l_i = 2$. $\quad$ $\Delta_{r_i} = 6$ for $r_i = 2$.
$\Delta_{l_i} = 4$ for $l_i = 3$. $\quad$ $\Delta_{r_i} = 4$ for $r_i = 3$.
$\Delta_{l_i} = 2$ for $l_i = 4$. $\quad$ $\Delta_{r_i} = 2$ for $r_i = 4$.
$\Delta_{l_i} = 0$ for $l_i = 5$. $\quad$ $\Delta_{r_i} = 0$ for $r_i = 5$.

The lower-left to upper-right half-cycle types of the Flores Knot are read from its string-run specification $(2222/23/2222)\{1_1 3_6 5_5 4_4 3_3 2_2 / 5_1 3_2 1_3 2_4 3_5 4_6\}18$:

$$1_1 \longrightarrow 5_1 \qquad 3_6 \longrightarrow 3_2 \qquad 5_5 \longrightarrow 1_3 \qquad 4_4 \longrightarrow 2_4 \qquad 3_3 \longrightarrow 3_5 \qquad 2_2 \longrightarrow 4_6$$

The first-return string-run of the associated Semi-Perfect Herringbone Pineapple Knot (first half-cycle is $1 \longrightarrow 1$ and $\Delta = |A + 1|_A = |6 + 1|_6 = 1$) is as follows:

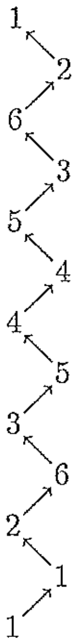

[†] See pg. 933.

By using the conversion table on pg. 948 we obtain for the first-return string-run of the Flores Knot:

$$\begin{tikzcd}
6/1_1 & \\
& 3_2/9 \arrow[ul] \\
9/3_6 \arrow[ur] & \\
& 1_3/12 \arrow[ul] \\
12/5_5 \arrow[ur] & \\
& 2_4/0 \arrow[ul] \\
0/4_4 \arrow[ur] & \\
& 3_5/6 \arrow[ul] \\
6/3_3 \arrow[ur] & \\
& 4_6/12 \arrow[ul] \\
12/2_2 \arrow[ur] & \\
& 5_1/0 \arrow[ul] \\
0/1_1 \arrow[ur] &
\end{tikzcd}$$

The nest-index numbers are again calculated with the following formulae:

$$I_{L_1} = 0 \quad ; \qquad I_{L_{n+1}} = \left| I_{L_n} + x_F + \Delta r_i + \tfrac{\Delta l_i + \Delta l_{i+1}}{2} \right|_B .$$

$$I_{R_1} = 0 \quad ; \qquad I_{R_{n+1}} = \left| I_{R_n} + x_F + \Delta l_i + \tfrac{\Delta r_i + \Delta r_{i+1}}{2} \right|_B .$$

$P_c = P_F = 2A + x_F - 4 = 12 + 23 - 4 = 31$.

g.c.d. (P_F , B^*) = g.c.d. $(31 , 3) = 1$, hence the component has no sub-components, consequently this Flores Knot requires one essential string (it is a single string knot).

This single string Flores Knot was derived from the Semi-Perfect Herringbone Pineapple Knot with $A = 6$; $x_P = 11$; $y = A + 1$; $B^* = 3$; $P_P = 21$, having g.c.d. (P_P , B^*) = g.c.d. $(21 , 3) = 3$, consequently this Semi-Perfect Herringbone Pineapple Knot requires three essential strings (it is a three string knot). However, the physical appearance of these two knots is the same.

In the half-cycle pattern arrangement we again indicate the number of crossings associated with a half-cycle under its half-cycle number.[†] On pp. 934-935 we discussed the calculation procedure of the number of crossings, and from the general schemes shown we obtain for our Example:

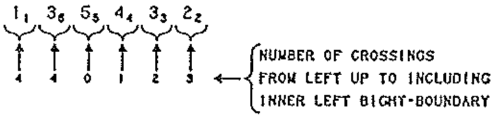
1₁ 3₆ 5₅ 4₄ 3₃ 2₂
4 4 0 1 2 3
NUMBER OF CROSSINGS FROM LEFT UP TO INCLUDING INNER LEFT BIGHT-BOUNDARY

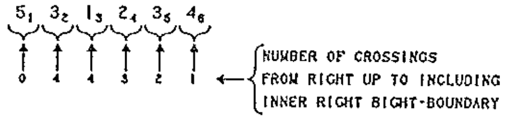
5₁ 3₂ 1₃ 2₄ 3₅ 4₆
0 4 4 3 2 1
NUMBER OF CROSSINGS FROM RIGHT UP TO INCLUDING INNER RIGHT BIGHT-BOUNDARY

Hence the half-cycle pattern arrangement of our Flores Knot will be as shown in Fig. 742.

[†] See *The Braider*, Issue No. 34, pg. 800.

1	2	3	4	5				5	4	3	2	1
		$\frac{23}{30}$			—	15	—			$\frac{24}{30}$		
$\frac{25}{26}$	$\frac{3}{26}$	$\frac{17}{26}$	$\frac{31}{26}$	$\frac{9}{26}$	—	12	—	$\frac{26}{25}$	$\frac{4}{25}$	$\frac{18}{25}$	$\frac{32}{25}$	$\frac{10}{30}$
		$\frac{11}{30}$			—	9	—			$\frac{12}{30}$		
$\frac{13}{26}$	$\frac{27}{26}$	$\frac{5}{26}$	$\frac{19}{26}$	$\frac{33}{26}$	—	6	—	$\frac{14}{25}$	$\frac{28}{25}$	$\frac{6}{25}$	$\frac{20}{25}$	$\frac{34}{30}$
		$\frac{35}{30}$			—	3	—			$\frac{36}{30}$		
$\frac{1}{26}$	$\frac{15}{26}$	$\frac{29}{26}$	$\frac{7}{26}$	$\frac{21}{26}$	—	0	—	$\frac{2}{25}$	$\frac{16}{25}$	$\frac{30}{25}$	$\frac{8}{25}$	$\frac{22}{30}$

Fig. 742 — The half-cycle pattern of the Flores Knot in Example 2.

Say that we use the non semi row-coding arrangement. Then with the aid of Fig. 740 Cont. (case $A = 6$) and the number of crossings on the half-cycles we can in the half-cycle tables for the lower-left to upper-right half-cycles and the lower-right to upper-left half-cycles enter the coding sequences (see Figs. 743 and 744).

23	☒	15	29	7	21	35	13	27	5	19	33	11	25	3	17	31	9	23	☒	15	29	7	21	35	13	27	5	19	33						
25	3	17	31	9	23	☒	15	29	7	21	35	13	27	5	19	33	11	25	3	17	31	9	23	☒	15	29	7	21	35						
11	25	3	17	31	9	23	☒	15	29	7	21	35	13	27	5	19	33	11	25	3	17	31	9	23	☒	15	29	7	21						
13	27	5	19	33	11	25	3	17	31	9	23	☒	15	29	7	21	35	13	27	5	19	33	11	25	3	17	31	9	23						
35	13	27	5	19	33	11	25	3	17	31	9	23	☒	15	29	7	21	35	13	27	5	19	33	11	25	3	17	31	9						
☒	15	29	7	21	35	13	27	5	19	33	11	25	3	17	31	9	23	☒	15	29	7	21	35	13	27	5	19	33	11						
o	o	o	o	o	u	o	o	o	o	o	o	u	u	u	u	u	u	o	o	o	o	o	o	u	o	o	o	o	o	23		35		11	
u	u	o	o	o	o	u	u	o	o	o	o	o	o	u	u	u	u	u	u	u	u	u	u	u	u	☒	☒	☒	☒		1		13		25
u	u	u	o	o	o	u	u	u	o	o	o	o	o	o	u	u	u	u	u	u	o	u	u	u	u	☒	☒	☒	☒		15		27		3
u	u	u	u	o	o	u	u	u	u	o	o	o	o	o	o	u	u	u	u	u	o	o	u	u	u	☒	☒	☒	☒		29		5		17
u	u	u	u	u	o	u	u	u	u	u	o	o	o	o	o	o	u	u	u	u	o	o	o	u	u	☒	☒	☒	☒		7		19		31
u	u	u	u	u	u	u	u	u	u	u	u	o	o	o	o	o	o	u	u	o	o	o	o	u	u	☒	☒	☒	☒		21		33		9

Fig. 743 — The half-cycle table for the lower-left to upper-right half-cycles.

24	22	8	30	16	2	36	34	20	6	28	14	12	10	32	18	4	26	24	22	8	30	16	2	36	34	20	6	28	14						
10	32	18	4	26	24	22	8	30	16	2	36	34	20	6	28	14	12	10	32	18	4	26	24	22	8	30	16	2	36						
12	10	32	18	4	26	24	22	8	30	16	2	36	34	20	6	28	14	12	10	32	18	4	26	24	22	8	30	16	2						
34	20	6	28	14	12	10	32	18	4	26	24	22	8	30	16	2	36	34	20	6	28	14	12	10	32	18	4	26	24						
36	34	20	6	28	14	12	10	32	18	4	26	24	22	8	30	16	2	36	34	20	6	28	14	12	10	32	18	4	26						
22	8	30	16	2	36	34	20	6	28	14	12	10	32	18	4	26	24	22	8	30	16	2	36	34	20	6	28	14	12						
o	o	o	o	o	o	o	o	o	o	o	u	u	u	u	u	u	o	o	o	o	o	o	u	o	o	o	o	o	u	24		36		12	
u	o	o	o	o	o	u	o	o	o	o	o	o	u	u	u	u	u	u	o	o	o	o	o	o	o	o	o	o	o		22		34		10
u	u	o	o	o	o	u	u	o	o	o	o	o	o	u	u	u	u	u	o	u	u	u	u	u	☒	☒	☒	☒	☒		8		20		32
u	u	u	o	o	o	u	u	u	o	o	o	o	o	o	u	u	u	u	o	o	u	u	u	u	☒	☒	☒	☒	☒		30		6		18
u	u	u	u	o	o	u	u	u	u	o	o	o	o	o	o	u	u	u	o	o	o	u	u	u	☒	☒	☒	☒	☒		16		28		4
u	u	u	u	u	o	u	u	u	u	u	o	o	o	o	o	o	u	u	o	o	o	o	u	u	☒	☒	☒	☒	☒		2		14		26

Fig. 744 — The half-cycle table for the lower-right to upper-left half-cycles.

The grid-diagrams of the Flores Knot and the Semi-Perfect Herringbone Pineapple Knot from which it has been derived are depicted in Fig. 745.

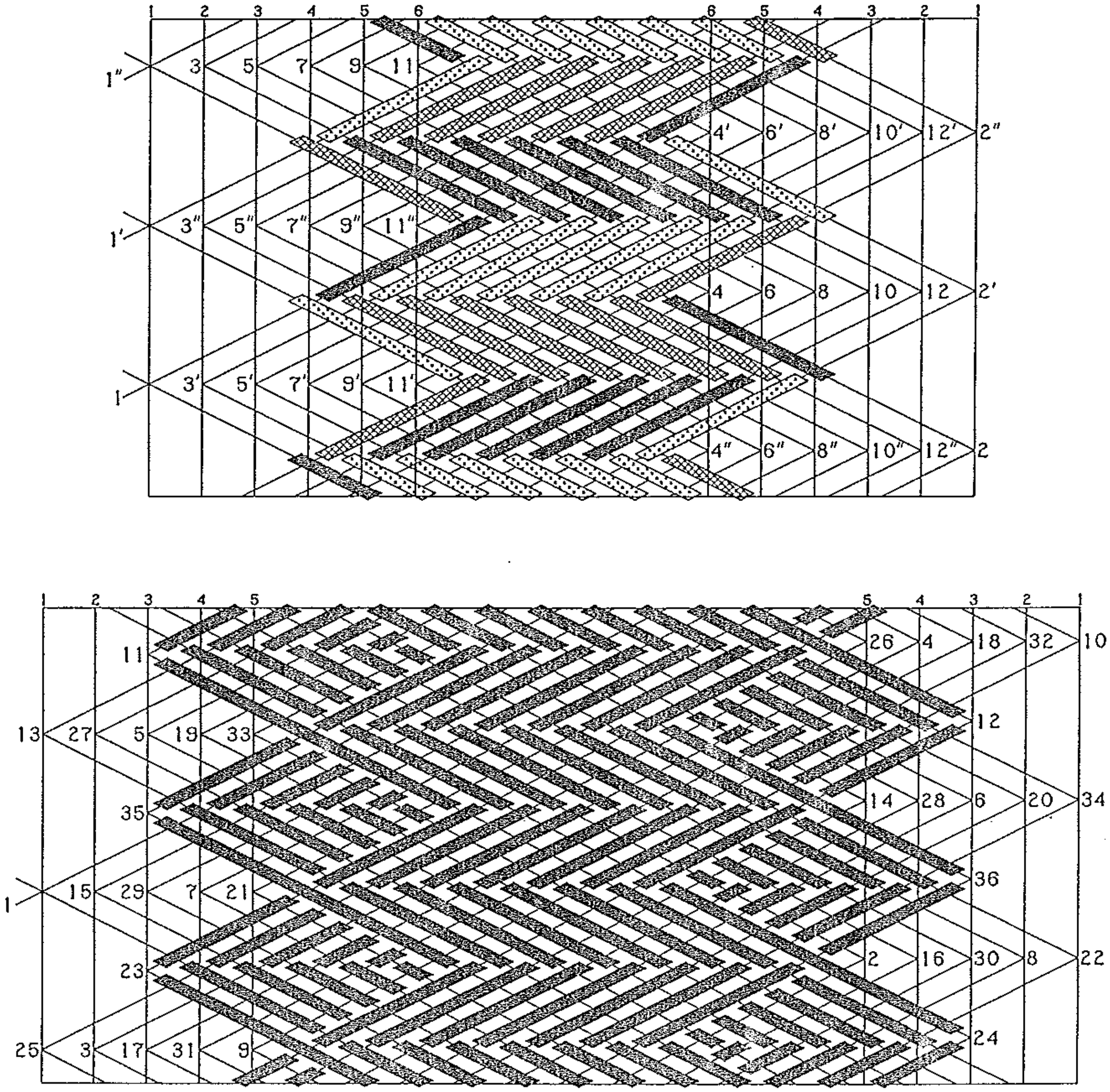

Fig. 745 — The Semi-Perfect Herringbone Pineapple Knot (upper grid-diagram) and Flores Knot derived from it (lower grid-diagram)

From the half-cycle tables (Figs. 743 and 744) we read the following half-cycle braiding algorithms:

1. $1_1 \longrightarrow 5_1$: Free run.
2. $2_2 \longleftarrow 5_1$: u.
3. $2_2 \longrightarrow 4_6$: o.
4. $3_3 \longleftarrow 4_6$: $o - 2u$.
5. $3_3 \longrightarrow 3_5$: $u - 2o$.
6. $4_4 \longleftarrow 3_5$: $2o - 2u$
7. $4_4 \longrightarrow 2_4$: $2u - 2o$.

8. $5_5 \longleftarrow 2_4$: $2o - 3u$.
9. $5_5 \longrightarrow 1_3$: $2u - 3o$.
10. $3_6 \longleftarrow 1_3$: $3o - 2u - 3o$.
11. $3_6 \longrightarrow 3_2$: $3o - 2u - 3o$.
12. $1_1 \longleftarrow 3_2$: $4o - u - 5o$.
13. $1_1 \longrightarrow 5_1$: $u - 4o - 4u$.
14. $2_2 \longleftarrow 5_1$: $4u - 2o - 2u - 2o$.
15. $2_2 \longrightarrow 4_6$: $u - o - 2u - 2o - 4u$.
16. $3_3 \longleftarrow 4_6$: $u - o - 2u - 2o - 2u - o - 2u$.
17. $3_3 \longrightarrow 3_5$: $u - o - 2u - 3o - u - o - 2u$.
18. $4_4 \longleftarrow 3_5$: $u - 6o - 2u - o - 2u$.
19. $4_4 \longrightarrow 2_4$: $3u - o - 2u - 3o - u - 2o - u$.
20. $5_5 \longleftarrow 2_4$: $2u - 5o - 4u - o - 2u$.
21. $5_5 \longrightarrow 1_3$: $7u - 3o - u - 2o - u$.
22. $3_6 \longleftarrow 1_3$: $3o - u - 3o - 4u - 7o$.
23. $3_6 \longrightarrow 3_2$: $7o - 4u - 3o - u - 3o$.
24. $1_1 \longleftarrow 3_2$: $7o - 4u - 8o - u$.
25. $1_1 \longrightarrow 5_1$: $u - 3o - u - 4o - 8u$.
26. $2_2 \longleftarrow 5_1$: $4u - o - 2u - 5o - 2u - 3o - u$.
27. $2_2 \longrightarrow 4_6$: $3u - 2o - 2u - 4o - 4u - o - 3u$.
28. $3_3 \longleftarrow 4_6$: $3u - 2o - 3u - 4o - 3u - 2o - 3u$.
29. $3_3 \longrightarrow 3_5$: $3u - o - 4u - 4o - 3u - 2o - 3u$.
30. $4_4 \longleftarrow 3_5$: $u - 3o - 2u - 6o - 3u - o - 4u$.
31. $4_4 \longrightarrow 2_4$: $4u - o - 4u - 5o - 2u - 3o - 2u$.
32. $5_5 \longleftarrow 2_4$: $2u - 10o - 5u - o - 4u$.
33. $5_5 \longrightarrow 1_3$: $11u - 5o - 2u - 4o - u$.
34. $3_6 \longleftarrow 1_3$: $u - 5o - u - 5o - 6u - 11o$.
35. $3_6 \longrightarrow 3_2$: $5o - u - 6o - 5u - 6o - u - 5o$.
36. $1_1 \longleftarrow 3_2$: $11o - 6u - 6o - u - 5o - u$.

⋆⋆ *In practice we would not braid the Flores Knots in Examples 1 and 2 in accordance with the half-cycle braiding algorithms shown since the long string-length required would make the braiding process quite cumbersome. With a long string-length we would, of course, braid a Flores Knot by starting at the centre of the required string-length. How would you handle this and how would you then assemble the necessary half-cycle braiding algorithms? Give for the Examples 1 and 2 the half-cycle braiding algorithms for such a construction method.*

Since a Flores Knot is in appearance identical to a Herringbone Pineapple Knot, only for $A = 2$ does it offer an advantage over the Herringbone Pineapple Knot with respect to the overall calculation procedures which are involved with the derivation of the half-cycle braiding algorithms. For $A > 2$, however, these overall calculation procedures are simpler for the Herringbone Pineapple Knots, hence we would only use a Flores Knot with $A > 2$ when its number of essential strings gives us a desired lay out which is not achievable with a Herringbone Pineapple Knot. For example, if for $A = 5$ with $x = 12$ a single string knot showing a Herringbone Pineapple pattern is desired, then these requirements would be fulfilled for $B^* = 5$ by a Flores knot, while for $B^* = 7$ by a Perfect Herringbone Pineapple Knot.

THE BRAIDER

No.41 FEBRUARY 2005.

CONTENTS

pg.

Solutions to the Questions in Issue No.40 955

Transition from two Round Braids to one Round Braid, and vice versa 964

The Braider's Notebook 973

A quarterly publication
for
the braiding artisan

Resale of this publication or copies thereof is strictly prohibited

Copyright ©2005 by:

A.G. Schaake; 21 Sundown Cresc.; Hamilton; New Zealand.
D. Van Tassel; Box 335; Craig, Co 81626-0335; U.S.A.
F.J.M. Masurel; Ganzenzijde 4; 2317XG Leiden; Nederland.

All rights reserved. No part of this publication may be reproduced, stored in a retrieval system, or transmitted, in any form or by any means, electronic, mechanical, photo-copying, recording, or otherwise, without prior written permission.

This publication is available to braiding artisans only.

Copies may be obtained from:

A.G. Schaake,
21 Sundown Cresc.,
Hamilton,
New Zealand.

Solutions to the Questions in Issue No. 40

Question on pg. 931.

For both Flores Knots in Fig. 731 $p/b = 13/12$, and hence both have the same path in the RKT.

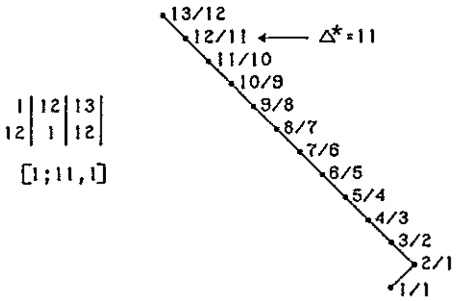

For the Flores Knot depicted by the left-hand grid-diagram in Fig. 731 the algorithm diagram is as follows:

i	→	11	10	9	8	7	6	5	4	3	2	1	0		
$h{=}4n{+}3$	→	u	o	u	o	o	u	u	o	o	u	o	u		
$h{=}4n{+}1\,;\,h{\neq}1$	→	o	o	o	u	u	o	o	u	u	o	o	o		
	⊢	.	.	.	.	.	.	.	.	.	.	.	.	⊣	
		u	u	u	u	o	o	u	u	o	o	u	o	←	$h{=}4n{+}2$
		o	u	o	o	u	u	o	o	u	u	u	u	←	$h{=}4n{+}4$
		0	1	2	3	4	5	6	7	8	9	10	11	←	i

In the above algorithm diagram $0 \leq n \leq 5$. Note that the first half-cycle is always a free run.

From this algorithm diagram we read the following half-cycle braiding algorithms:

half-cycle 1		:	$L \longrightarrow R$	Free Run.
half-cycle 2	$i = 0$	:	$L \longleftarrow R$	u.
half-cycle 3	$i = 0$	:	$L \longrightarrow R$	u.
half-cycle 4	$i \leq 1$	:	$L \longleftarrow R$	$u - o$.
half-cycle 5	$i \leq 1$	:	$L \longrightarrow R$	$2o$.
half-cycle 6	$i \leq 2$	:	$L \longleftarrow R$	$3u$.
half-cycle 7	$i \leq 2$	:	$L \longrightarrow R$	$u - o - u$.
half-cycle 8	$i \leq 3$	:	$L \longleftarrow R$	$2o - u - o$.
half-cycle 9	$i \leq 3$	:	$L \longrightarrow R$	$u - 3o$.
half-cycle 10	$i \leq 4$	:	$L \longleftarrow R$	$o - 4u$.
half-cycle 11	$i \leq 4$	:	$L \longrightarrow R$	$2o - u - o - u$.
half-cycle 12	$i \leq 5$	:	$L \longleftarrow R$	$2u - 2o - u - o$.
half-cycle 13	$i \leq 5$	:	$L \longrightarrow R$	$o - 2u - 3o$.
half-cycle 14	$i \leq 6$	:	$L \longleftarrow R$	$u - 2o - 4u$.
half-cycle 15	$i \leq 6$	:	$L \longrightarrow R$	$2u - 2o - u - o - u$.
half-cycle 16	$i \leq 7$	:	$L \longleftarrow R$	$2o - 2u - 2o - u - o$.
half-cycle 17	$i \leq 7$	:	$L \longrightarrow R$	$u - 2o - 2u - 3o$.
half-cycle 18	$i \leq 8$	:	$L \longleftarrow R$	$o - 2u - 2o - 4u$.
half-cycle 19	$i \leq 8$	:	$L \longrightarrow R$	$2o - 2u - 2o - u - o - u$.
half-cycle 20	$i \leq 9$	:	$L \longleftarrow R$	$2u - 2o - 2u - 2o - u - o$.
half-cycle 21	$i \leq 9$	:	$L \longrightarrow R$	$o - 2u - 2o - 2u - 3o$.

half-cycle 22 $i \leq 10$: $L \longleftarrow R$ $u - 2o - 2u - 2o - 4u$.
half-cycle 23 $i \leq 10$: $L \longrightarrow R$ $o - u - 2o - 2u - 2o - u - o - u$.
half-cycle 24 $i \leq 11$: $L \longleftarrow R$ $4u - 2o - 2u - 2o - u - o$.

For the Flores Knot depicted by the right-hand grid-diagram in Fig. 731 the algorithm diagram is as follows:

$$\begin{array}{cccccccccccccccc}
i & \rightarrow & 11 & 10 & 9 & 8 & 7 & 6 & 5 & 4 & 3 & 2 & 1 & 0 & & \\
h{=}4n{+}3 & \rightarrow & u & u & u & o & o & u & u & o & o & u & u & u & & \\
h{=}4n{+}1\,;\,h{\neq}1 & \rightarrow & o & o & o & u & u & o & o & u & u & o & o & o & & \\
 & \vdash & \cdot & \cdot & \cdot & \cdot & \cdot & \cdot & \cdot & \cdot & \cdot & \cdot & \cdot & \cdot & \dashv & \\
 & & u & o & u & u & o & o & u & u & o & o & u & o & \leftarrow & h{=}4n{+}2 \\
 & & o & u & o & o & u & u & o & o & u & u & o & u & \leftarrow & h{=}4n{+}4 \\
 & & 0 & 1 & 2 & 3 & 4 & 5 & 6 & 7 & 8 & 9 & 10 & 11 & \leftarrow & i
\end{array}$$

In the above algorithm diagram $0 \leq n \leq 5$. Note that the first half-cycle is always a free run.

From this algorithm diagram we read the following half-cycle braiding algorithms:

half-cycle 1 : $L \longrightarrow R$ Free Run.
half-cycle 2 $i = 0$: $L \longleftarrow R$ u .
half-cycle 3 $i = 0$: $L \longrightarrow R$ u .
half-cycle 4 $i \leq 1$: $L \longleftarrow R$ $u - o$.
half-cycle 5 $i \leq 1$: $L \longrightarrow R$ $2o$.
half-cycle 6 $i \leq 2$: $L \longleftarrow R$ $u - o - u$.
half-cycle 7 $i \leq 2$: $L \longrightarrow R$ $3u$.
half-cycle 8 $i \leq 3$: $L \longleftarrow R$ $2o - u - o$.
half-cycle 9 $i \leq 3$: $L \longrightarrow R$ $u - 3o$.
half-cycle 10 $i \leq 4$: $L \longleftarrow R$ $o - 2u - o - u$.
half-cycle 11 $i \leq 4$: $L \longrightarrow R$ $2o - 3u$.
half-cycle 12 $i \leq 5$: $L \longleftarrow R$ $2u - 2o - u - o$.
half-cycle 13 $i \leq 5$: $L \longrightarrow R$ $o - 2u - 3o$.
half-cycle 14 $i \leq 6$: $L \longleftarrow R$ $u - 2o - 2u - o - u$.
half-cycle 15 $i \leq 6$: $L \longrightarrow R$ $2u - 2o - 3u$.
half-cycle 16 $i \leq 7$: $L \longleftarrow R$ $2o - 2u - 2o - u - o$.
half-cycle 17 $i \leq 7$: $L \longrightarrow R$ $u - 2o - 2u - 3o$.
half-cycle 18 $i \leq 8$: $L \longleftarrow R$ $o - 2u - 2o - 2u - o - u$.
half-cycle 19 $i \leq 8$: $L \longrightarrow R$ $2o - 2u - 2o - 3u$.
half-cycle 20 $i \leq 9$: $L \longleftarrow R$ $2u - 2o - 2u - 2o - u - o$.
half-cycle 21 $i \leq 9$: $L \longrightarrow R$ $o - 2u - 2o - 2u - 3o$.
half-cycle 22 $i \leq 10$: $L \longleftarrow R$ $u - 2o - 2u - 2o - 2u - o - u$.
half-cycle 23 $i \leq 10$: $L \longrightarrow R$ $2u - 2o - 2u - 2o - 3u$.
half-cycle 24 $i \leq 11$: $L \longleftarrow R$ $4u - 2o - 2u - 2o - u - o$.

First question on pg. 933.

For both Flores Knots in Fig. 733 $p/b = 13/12$, and hence both have the same path in the RKT as the two Flores Knots in Fig. 731.

For the Flores Knot depicted by the left-hand grid-diagram in Fig. 733 the algorithm diagram is as follows:

$$\begin{array}{cccccccccccccccc}
i & \rightarrow & 11 & 10 & 9 & 8 & 7 & 6 & 5 & 4 & 3 & 2 & 1 & 0 & & \\
h{=}4n{+}3 & \rightarrow & u & u & u & u & o & o & u & u & o & o & u & o & & \\
h{=}4n{+}1\,;\, h{\neq}1 & \rightarrow & o & u & o & o & u & u & o & o & u & u & u & u & & \\
 & \vdash & \cdot & \cdot & \cdot & \cdot & \cdot & \cdot & \cdot & \cdot & \cdot & \cdot & \cdot & \cdot & \dashv & \\
 & & u & o & u & o & o & u & u & o & o & u & o & u & \leftarrow & h{=}4n{+}2 \\
 & & o & o & o & u & u & o & o & u & u & o & o & o & \leftarrow & h{=}4n{+}4 \\
 & & 0 & 1 & 2 & 3 & 4 & 5 & 6 & 7 & 8 & 9 & 10 & 11 & \leftarrow & i
\end{array}$$

In the above algorithm diagram $0 \leq n \leq 5$. Note that the first half-cycle is always a free run.

From this algorithm diagram we read the following half-cycle braiding algorithms:

half-cycle 1		:	$L \longrightarrow R$	Free Run.
half-cycle 2	$i = 0$	:	$L \longleftarrow R$	u.
half-cycle 3	$i = 0$	:	$L \longrightarrow R$	o.
half-cycle 4	$i \leq 1$	:	$L \longleftarrow R$	$2o$.
half-cycle 5	$i \leq 1$	:	$L \longrightarrow R$	$2u$.
half-cycle 6	$i \leq 2$	:	$L \longleftarrow R$	$u - o - u$.
half-cycle 7	$i \leq 2$	:	$L \longrightarrow R$	$o - u - o$.
half-cycle 8	$i \leq 3$	:	$L \longleftarrow R$	$u - 3o$.
half-cycle 9	$i \leq 3$	:	$L \longrightarrow R$	$4u$.
half-cycle 10	$i \leq 4$	:	$L \longleftarrow R$	$2o - u - o - u$.
half-cycle 11	$i \leq 4$	:	$L \longrightarrow R$	$u - 2o - u - o$.
half-cycle 12	$i \leq 5$	:	$L \longleftarrow R$	$o - 2u - 3o$.
half-cycle 13	$i \leq 5$	:	$L \longrightarrow R$	$2o - 4u$.
half-cycle 14	$i \leq 6$	:	$L \longleftarrow R$	$2u - 2o - u - o - u$.
half-cycle 15	$i \leq 6$	:	$L \longrightarrow R$	$o - 2u - 2o - u - o$.
half-cycle 16	$i \leq 7$	:	$L \longleftarrow R$	$u - 2o - 2u - 3o$.
half-cycle 17	$i \leq 7$	:	$L \longrightarrow R$	$2u - 2o - 4u$.
half-cycle 18	$i \leq 8$	:	$L \longleftarrow R$	$2o - 2u - 2o - u - o - u$.
half-cycle 19	$i \leq 8$	:	$L \longrightarrow R$	$u - 2o - 2u - 2o - u - o$.
half-cycle 20	$i \leq 9$	:	$L \longleftarrow R$	$o - 2u - 2o - 2u - 3o$.
half-cycle 21	$i \leq 9$	:	$L \longrightarrow R$	$2o - 2u - 2o - 4u$.
half-cycle 22	$i \leq 10$	:	$L \longleftarrow R$	$o - u - 2o - 2u - 2o - u - o - u$.
half-cycle 23	$i \leq 10$	:	$L \longrightarrow R$	$3u - 2o - 2u - 2o - u - o$.
half-cycle 24	$i \leq 11$	:	$L \longleftarrow R$	$3o - 2u - 2o - 2u - 3o$.

For the Flores Knot depicted by the right-hand grid-diagram in Fig. 733 the algorithm diagram is as follows:

$$\begin{array}{cccccccccccccccc}
i & \rightarrow & 11 & 10 & 9 & 8 & 7 & 6 & 5 & 4 & 3 & 2 & 1 & 0 & & \\
h{=}4n{+}3 & \rightarrow & u & o & u & u & o & o & u & u & o & o & u & o & & \\
h{=}4n{+}1\,;\, h{\neq}1 & \rightarrow & o & u & o & o & u & u & o & o & u & u & o & u & & \\
 & \vdash & \cdot & \cdot & \cdot & \cdot & \cdot & \cdot & \cdot & \cdot & \cdot & \cdot & \cdot & \cdot & \dashv & \\
 & & u & u & u & o & o & u & u & o & o & u & u & u & \leftarrow & h{=}4n{+}2 \\
 & & o & o & o & u & u & o & o & u & u & o & o & o & \leftarrow & h{=}4n{+}4 \\
 & & 0 & 1 & 2 & 3 & 4 & 5 & 6 & 7 & 8 & 9 & 10 & 11 & \leftarrow & i
\end{array}$$

In the above algorithm diagram $0 \leq n \leq 5$. Note that the first half-cycle is always a free run.

From this algorithm diagram we read the following half-cycle braiding algorithms:

half-cycle 1		:	$L \longrightarrow R$	Free Run.
half-cycle 2	$i = 0$	:	$L \longleftarrow R$	u.
half-cycle 3	$i = 0$	:	$L \longrightarrow R$	o.
half-cycle 4	$i \leq 1$	:	$L \longleftarrow R$	$2o$.
half-cycle 5	$i \leq 1$	:	$L \longrightarrow R$	$o - u$.
half-cycle 6	$i \leq 2$	:	$L \longleftarrow R$	$3u$.
half-cycle 7	$i \leq 2$	:	$L \longrightarrow R$	$o - u - o$.
half-cycle 8	$i \leq 3$	:	$L \longleftarrow R$	$u - 3o$.
half-cycle 9	$i \leq 3$	:	$L \longrightarrow R$	$2u - o - u$.
half-cycle 10	$i \leq 4$	:	$L \longleftarrow R$	$2o - 3u$.
half-cycle 11	$i \leq 4$	:	$L \longrightarrow R$	$u - 2o - u - o$.
half-cycle 12	$i \leq 5$	:	$L \longleftarrow R$	$o - 2u - 3o$.
half-cycle 13	$i \leq 5$	:	$L \longrightarrow R$	$2o - 2u - o - u$.
half-cycle 14	$i \leq 6$	:	$L \longleftarrow R$	$2u - 2o - 3u$.
half-cycle 15	$i \leq 6$	:	$L \longrightarrow R$	$o - 2u - 2o - u - o$.
half-cycle 16	$i \leq 7$	:	$L \longleftarrow R$	$u - 2o - 2u - 3o$.
half-cycle 17	$i \leq 7$	:	$L \longrightarrow R$	$2u - 2o - 2u - o - u$.
half-cycle 18	$i \leq 8$	:	$L \longleftarrow R$	$2o - 2u - 2o - 3u$.
half-cycle 19	$i \leq 8$	:	$L \longrightarrow R$	$u - 2o - 2u - 2o - u - o$.
half-cycle 20	$i \leq 9$	:	$L \longleftarrow R$	$o - 2u - 2o - 2u - 3o$.
half-cycle 21	$i \leq 9$	:	$L \longrightarrow R$	$2o - 2u - 2o - 2u - o - u$.
half-cycle 22	$i \leq 10$	:	$L \longleftarrow R$	$2u - 2o - 2u - 2o - 3u$.
half-cycle 23	$i \leq 10$	:	$L \longrightarrow R$	$o - 2u - 2o - 2u - 2o - u - o$.
half-cycle 24	$i \leq 11$	:	$L \longleftarrow R$	$3o - 2u - 2o - 2u - 3o$.

Second question on pg. 933.

For the Perfect Herringbone Pineapple Knot in Fig. 730:

$A = 2$; $B^* = 6$; $x_P = 9$; $y_P = A - 1 = 2 - 1 = 1$; $k = \left|\frac{x_P - A - 1}{2}\right|_A = \left|\frac{9-2-1}{2}\right|_2 = 1$, hence $1 \longrightarrow 1$ is the first lower-left to upper-right half-cycle; $\Delta = |y|_A = |1|_2 = 1$; $P_P = 2A + x_P - 2 = 4 + 9 - 2 = 11$; g.c.d. $(P_P, B^*) =$ g.c.d. $(11, 6) = 1$.

Its first-return string-run is thus as follows:

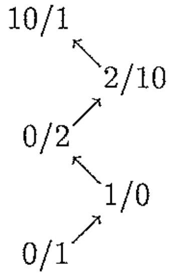

For calculating the nest-index numbers we use the formulae:[†]

$$I_{L_1} = 0 \quad ; \quad I_{L_{n+1}} = \left|I_{L_n} + 4A + x_P - (l_n + l_{n+1} + 2r_n)\right|_B .$$
$$I_{R_1} = 0 \quad ; \quad I_{R_{n+1}} = \left|I_{R_n} + 4A + x_P - (r_n + r_{n+1} + 2l_{n+1})\right|_B .$$

The half-cycle pattern arrangement of this Perfect Herringbone Pineapple Knot is then as depicted in Fig. 746.

[†] See *The Braider*, Issue No. 26, pg. 593.

1	2				2	1
$\frac{5}{10}$	$\frac{7}{8}$	—	10	—	$\frac{4}{9}$	$\frac{6}{9}$
$\frac{9}{10}$	$\frac{11}{8}$	—	8	—	$\frac{8}{9}$	$\frac{10}{9}$
$\frac{13}{10}$	$\frac{15}{8}$	—	6	—	$\frac{12}{9}$	$\frac{14}{9}$
$\frac{17}{10}$	$\frac{19}{8}$	—	4	—	$\frac{16}{9}$	$\frac{18}{9}$
$\frac{21}{10}$	$\frac{23}{8}$	—	2	—	$\frac{20}{9}$	$\frac{22}{9}$
$\frac{1}{10}$	$\frac{3}{8}$	—	0	—	$\frac{24}{9}$	$\frac{2}{9}$

Fig. 746 — The half-cycle pattern of the Perfect Herringbone Pineapple Knot.

From this half-cycle pattern in Fig. 746 we derive the half-cycle table for the lower-left to upper-right half-cycles (the left table in Fig. 747) and the half-cycle table for the lower-right to upper-left half-cycles (the right table in Fig. 747).

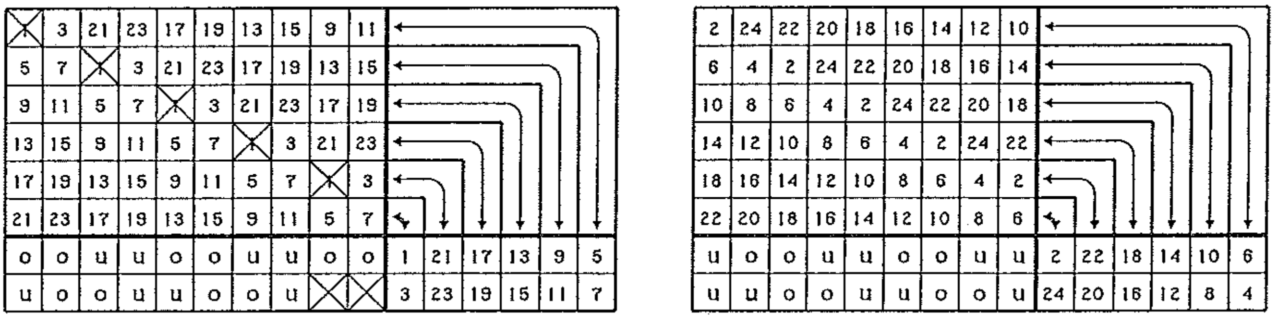

~~1~~	3	21	23	17	19	13	15	9	11						
5	7	~~1~~	3	21	23	17	19	13	15						
9	11	5	7	~~1~~	3	21	23	17	19						
13	15	9	11	5	7	~~1~~	3	21	23						
17	19	13	15	9	11	5	7	~~1~~	3						
21	23	17	19	13	15	9	11	5	7						
o	o	u	u	o	o	u	u	o	o	1	21	17	13	9	5
u	o	o	u	u	o	o	u	☒	☒	3	23	19	15	11	7

2	24	22	20	18	16	14	12	10						
6	4	2	24	22	20	18	16	14						
10	8	6	4	2	24	22	20	18						
14	12	10	8	6	4	2	24	22						
18	16	14	12	10	8	6	4	2						
22	20	18	16	14	12	10	8	6						
u	o	o	u	u	o	o	u	u	2	22	18	14	10	6
u	u	o	o	u	u	o	o	u	24	20	16	12	8	4

Fig. 747 — The half-cycle tables for the Perfect Herringbone Pineapple Knot.

From the half-cycle tables in Fig. 747 we read the half-cycle braiding algorithms for the Perfect Herringbone Pineapple Knot:

half-cycle 1 : 1 ⟶ 1 Free Run.
half-cycle 2 : 2 ⟵ 1 Free Run.
half-cycle 3 : 2 ⟶ 2 Free Run.
half-cycle 4 : 1 ⟵ 2 u.
half-cycle 5 : 1 ⟶ 1 o.
half-cycle 6 : 2 ⟵ 1 u.
half-cycle 7 : 2 ⟶ 2 o.
half-cycle 8 : 1 ⟵ 2 $2u - o$.
half-cycle 9 : 1 ⟶ 1 $2o - u$.
half-cycle 10 : 2 ⟵ 1 $u - 2o$.
half-cycle 11 : 2 ⟶ 2 $u - o - u$.
half-cycle 12 : 1 ⟵ 2 $2u - 2o - u$.
half-cycle 13 : 1 ⟶ 1 $2o - 2u - o$.
half-cycle 14 : 2 ⟵ 1 $u - 2o - 2u$.
half-cycle 15 : 2 ⟶ 2 $u - 2o - u - o$.
half-cycle 16 : 1 ⟵ 2 $2u - 2o - 2u - o$.
half-cycle 17 : 1 ⟶ 1 $2o - 2u - 2o - u$.
half-cycle 18 : 2 ⟵ 1 $u - 2o - 2u - 2o$.
half-cycle 19 : 2 ⟶ 2 $u - 2o - 2u - o - u$.
half-cycle 20 : 1 ⟵ 2 $2u - 2o - 2u - 2o - u$.

half-cycle 21 : $1 \longrightarrow 1$ $2o - 2u - 2o - 2u - o$.
half-cycle 22 : $2 \longleftarrow 1$ $u - 2o - 2u - 2o - 2u$.
half-cycle 23 : $2 \longrightarrow 2$ $u - 2o - 2u - 2o - u$.
half-cycle 24 : $1 \longleftarrow 2$ $2u - 2o - 2u - 2o - u$.

For the Perfect Herringbone Pineapple Knot in Fig. 732:

$A = 2$; $B^* = 6$; $x_P = 9$; $y_P = A + 1 = 2 + 1 = 3$; $k = \left|\frac{x_P - A - 3}{2}\right|_A = \left|\frac{9-2-3}{2}\right|_2 = 2$, hence $1 \longrightarrow 2$ is the first lower-left to upper-right half-cycle; $\Delta = |y|_A = |3|_2 = 1$; $P_P = 2A + x_P - 2 = 4 + 9 - 2 = 11$; g.c.d.$(P_P, B^*) =$ g.c.d.$(11, 6) = 1$.

Its first-return string-run is thus as follows:

$$\begin{tikzcd}
10/1 & \\
& 1/10 \arrow[ul] \\
10/2 \arrow[ur] & \\
& 2/0 \arrow[ul] \\
0/1 \arrow[ur] &
\end{tikzcd}$$

For calculating the nest-index numbers we use the formulae:

$$I_{L_1} = 0 \quad ; \quad I_{L_{n+1}} = \left|I_{L_n} + 4A + x_P - (l_n + l_{n+1} + 2r_n)\right|_B .$$
$$I_{R_1} = 0 \quad ; \quad I_{R_{n+1}} = \left|I_{R_n} + 4A + x_P - (r_n + r_{n+1} + 2l_{n+1})\right|_B .$$

The half-cycle pattern arrangement of this Perfect Herringbone Pineapple Knot is then as depicted in Fig. 748.

1	2				2	1
$\frac{5}{9}$	$\frac{3}{9}$	—	10	—	$\frac{6}{8}$	$\frac{4}{10}$
$\frac{9}{9}$	$\frac{7}{9}$	—	8	—	$\frac{10}{8}$	$\frac{8}{10}$
$\frac{13}{9}$	$\frac{11}{9}$	—	6	—	$\frac{14}{8}$	$\frac{12}{10}$
$\frac{17}{9}$	$\frac{15}{9}$	—	4	—	$\frac{18}{8}$	$\frac{16}{10}$
$\frac{21}{9}$	$\frac{19}{9}$	—	2	—	$\frac{22}{8}$	$\frac{20}{10}$
$\frac{1}{9}$	$\frac{23}{9}$	—	0	—	$\frac{2}{8}$	$\frac{24}{10}$

Fig. 748 — The half-cycle pattern of the Perfect Herringbone Pineapple Knot.

From this half-cycle pattern in Fig. 748 we derive the half-cycle table for the lower-left to upper-right half-cycles (the left table in Fig. 749) and the half-cycle table for the lower-right to upper-left half-cycles (the right table in Fig. 749).

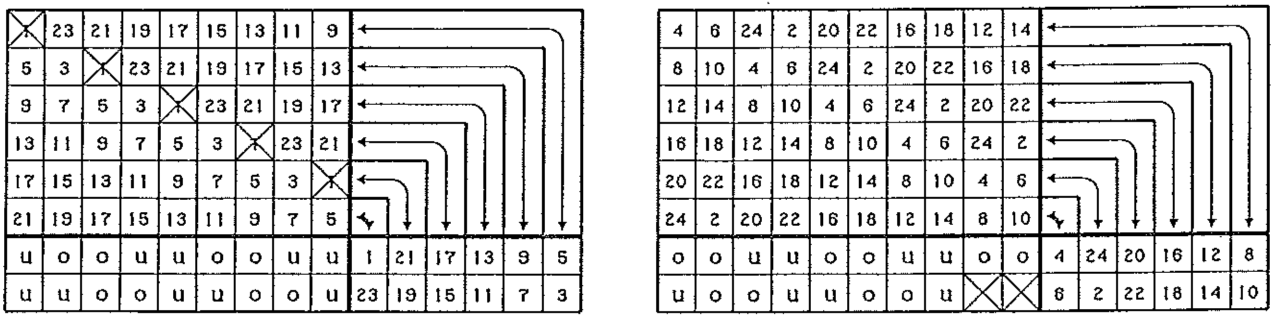

☒	23	21	19	17	15	13	11	9						
5	3	☒	23	21	19	17	15	13						
9	7	5	3	☒	23	21	19	17						
13	11	9	7	5	3	☒	23	21						
17	15	13	11	9	7	5	3	☒						
21	19	17	15	13	11	9	7	5						
u	o	o	u	u	o	o	u	u	1	21	17	13	9	5
u	u	o	o	u	u	o	o	u	23	19	15	11	7	3

4	6	24	2	20	22	16	18	12	14						
8	10	4	6	24	2	20	22	16	18						
12	14	8	10	4	6	24	2	20	22						
16	18	12	14	8	10	4	6	24	2						
20	22	16	18	12	14	8	10	4	6						
24	2	20	22	16	18	12	14	8	10						
o	o	u	u	o	o	u	u	o	o	4	24	20	16	12	8
u	o	o	u	u	o	o	u	☒	☒	6	2	22	18	14	10

Fig. 749 — The half-cycle tables for the Perfect Herringbone Pineapple Knot.

Note that these half-cycle tables can be obtained directly from the half-cycle tables in Fig. 747 (See *The Braider*, Issue No. 28, pg. 656).

From the half-cycle tables in Fig. 749 we read the half-cycle braiding algorithms for the Perfect Herringbone Pineapple Knot:

half-cycle 1 : $1 \longrightarrow 2$ Free Run.
half-cycle 2 : $2 \longleftarrow 2$ Free Run.
half-cycle 3 : $2 \longrightarrow 1$ Free Run.
half-cycle 4 : $1 \longleftarrow 1$ o.
half-cycle 5 : $1 \longrightarrow 2$ Free Run.
half-cycle 6 : $2 \longleftarrow 2$ o.
half-cycle 7 : $2 \longrightarrow 1$ $2u$.
half-cycle 8 : $1 \longleftarrow 1$ $2o - u$.
half-cycle 9 : $1 \longrightarrow 2$ $u - o$.
half-cycle 10 : $2 \longleftarrow 2$ $u - o - u$.
half-cycle 11 : $2 \longrightarrow 1$ $2u - 2o$.
half-cycle 12 : $1 \longleftarrow 1$ $2o - 2u - o$.
half-cycle 13 : $1 \longrightarrow 2$ $u - 2o - u$.
half-cycle 14 : $2 \longleftarrow 2$ $u - 2o - u - o$.
half-cycle 15 : $2 \longrightarrow 1$ $2u - 2o - 2u$.
half-cycle 16 : $1 \longleftarrow 1$ $2o - 2u - 2o - u$.
half-cycle 17 : $1 \longrightarrow 2$ $u - 2o - 2u - o$.
half-cycle 18 : $2 \longleftarrow 2$ $u - 2o - 2u - o - u$.
half-cycle 19 : $2 \longrightarrow 1$ $2u - 2o - 2u - 2o$.
half-cycle 20 : $1 \longleftarrow 1$ $2o - 2u - 2o - 2u - o$.
half-cycle 21 : $1 \longrightarrow 2$ $u - 2o - 2u - 2o - u$.
half-cycle 22 : $2 \longleftarrow 2$ $u - 2o - 2u - 2o - u$.
half-cycle 23 : $2 \longrightarrow 1$ $2u - 2o - 2u - 2o - u$.
half-cycle 24 : $1 \longleftarrow 1$ $2o - 2u - 2o - 2u - 2o$.

Question on pg. 954.

Since we prefer to employ the usual procedures for calculating the half-cycle pattern and the half-cycle tables as previously discussed, the braiding procedure to be followed should be such that these half-cycle tables can also be used for the derivation of the half-cycle braiding algorithms associated with starting at the centre of the required string-length. We can then employ one of the following two construction procedures:

1. First braid the table half-cycles $1 \leq h_t \leq B$, starting with table half-cycle $h_t = B$, in the reverse direction. Read for h_t the intersection codings from right to left for $h_t < h \leq (B+1)$. Then braid the table half-cycles $(B+1) \leq h_t \leq 2B$, starting with table half-cycle $h_t = (B+1)$, in the normal direction. Read for h_t the intersection codings from left to right for $1 < h \leq h_t$.

2. First braid the table half-cycles $(B+1) \leq h_t \leq 2B$, starting with table half-cycle $h_t = (B+1)$, in the normal direction. Read for h_t the intersection codings from left to right for $(B+1) < h \leq h_t$. Then braid the table half-cycles $1 \leq h_t \leq B$, starting with table half-cycle $h_t = B$, in the reverse direction. Read for h_t the intersection codings from right to left for $h = 1$ and $h_t < h \leq 2B$.

Construction procedure **1.** is to be preferred when we already have for the normal braiding direction the half-cycle braiding algorithms for the half-cycles $1 \leq h_t \leq 2B$.

In order to show both construction procedures we shall follow for **Example 1.** construction procedure **1.**, and for **Example 2.** construction procedure **2.**.

For the Flores Knot in **Example 1.** we first braid the table half-cycles $1 \leq h_t \leq 25$, starting with $h_t = B = 25$, in the reverse direction. We read for h_t the intersection codings from right to left for $h_t < h \leq 26$. Then we braid the table half-cycles $26 \leq h_t \leq 50$, starting with table half-cycle $h_t = B + 1 = 26$, in the normal direction. We read for h_t the intersection codings from left to right for $1 < h \leq h_t$. This results in the following half-cycle braiding algorithms:

1. $(h_t = 25 \text{ rev.})$ $5_4 \longleftarrow 4_3$: Free run.
2. $(h_t = 24 \text{ rev.})$ $5_4 \longrightarrow 2_2$: Free Run.
3. $(h_t = 23 \text{ rev.})$ $3_5 \longleftarrow 2_2$: o.
4. $(h_t = 22 \text{ rev.})$ $3_5 \longrightarrow 1_1$: $2o$.
5. $(h_t = 21 \text{ rev.})$ $1_1 \longleftarrow 1_1$: $o - u$.
6. $(h_t = 20 \text{ rev.})$ $1_1 \longrightarrow 3_5$: $2u - o$.
7. $(h_t = 19 \text{ rev.})$ $2_2 \longleftarrow 3_5$: $u - o - u$.
8. $(h_t = 18 \text{ rev.})$ $2_2 \longrightarrow 5_4$: $2o - 2u$.
9. $(h_t = 17 \text{ rev.})$ $4_3 \longleftarrow 5_4$: $u - o - u$.
10. $(h_t = 16 \text{ rev.})$ $4_3 \longrightarrow 4_3$: $2o - 2u$.
11. $(h_t = 15 \text{ rev.})$ $5_4 \longleftarrow 4_3$: $u - o - u$.
12. $(h_t = 14 \text{ rev.})$ $5_4 \longrightarrow 2_2$: $u - o - 2u$.
13. $(h_t = 13 \text{ rev.})$ $3_5 \longleftarrow 2_2$: $6o$.
14. $(h_t = 12 \text{ rev.})$ $3_5 \longrightarrow 1_1$: $3o - u - 3o$.
15. $(h_t = 11 \text{ rev.})$ $1_1 \longleftarrow 1_1$: $2o - u - 3o - u$.
16. $(h_t = 10 \text{ rev.})$ $1_1 \longrightarrow 3_5$: $6u - 3o$.
17. $(h_t = 9 \text{ rev.})$ $2_2 \longleftarrow 3_5$: $o - 4u - 2o - 2u$.
18. $(h_t = 8 \text{ rev.})$ $2_2 \longrightarrow 5_4$: $2u - 3o - 4u$.
19. $(h_t = 7 \text{ rev.})$ $4_3 \longleftarrow 5_4$: $3u - 3o - 2u$.
20. $(h_t = 6 \text{ rev.})$ $4_3 \longrightarrow 4_3$: $3u - 2o - u - o - 2u$.
21. $(h_t = 5 \text{ rev.})$ $5_4 \longleftarrow 4_3$: $2u - 3o - 3u$.
22. $(h_t = 4 \text{ rev.})$ $5_4 \longrightarrow 2_2$: $4u - o - u - 2o - u$.
23. $(h_t = 3 \text{ rev.})$ $3_5 \longleftarrow 2_2$: $u - 10o$.
24. $(h_t = 2 \text{ rev.})$ $3_5 \longrightarrow 1_1$: $8o - u - 4o$.
25. $(h_t = 1 \text{ rev.})$ $1_1 \longleftarrow 1_1$: $u - 4o - 2u - 4o - 2u$.

---

26. $(h_t = 26)$ $4_3 \longleftarrow 4_3$: $3u - 3o - 2u - 2o - 2u$.
27. $(h_t = 27)$ $4_3 \longrightarrow 5_4$: $2u - 3o - 6u$.
28. $(h_t = 28)$ $2_2 \longleftarrow 5_4$: $4u - 2o - 2u - 3o - u$.
29. $(h_t = 29)$ $2_2 \longrightarrow 3_5$: $u - 4o - u - 8o$.
30. $(h_t = 30)$ $1_1 \longleftarrow 3_5$: $5o - u - 5o - u - 4o$.
31. $(h_t = 31)$ $1_1 \longrightarrow 1_1$: $u - 5o - 4u - 4o - 2u$.
32. $(h_t = 32)$ $3_5 \longleftarrow 1_1$: $u - o - u - 4o - 5u - o - u - 4o$.
33. $(h_t = 33)$ $3_5 \longrightarrow 2_2$: $5o - 5u - o - u - 2o - 3u$.
34. $(h_t = 34)$ $5_4 \longleftarrow 2_2$: $u - 3o - 2u - 4o - 2u - o - 4u$.
35. $(h_t = 35)$ $5_4 \longrightarrow 4_3$: $8u - 2o - u - o - 4u$.
36. $(h_t = 36)$ $4_3 \longleftarrow 4_3$: $2u - 2o - 3u - 3o - 2u - 2o - 3u$.
37. $(h_t = 37)$ $4_3 \longrightarrow 5_4$: $3u - o - 3u - 3o - 6u$.
38. $(h_t = 38)$ $2_2 \longleftarrow 5_4$: $3u - o - 4u - 2o - 2u - 3o - 2u$.
39. $(h_t = 39)$ $2_2 \longrightarrow 3_5$: $2u - 2o - 2u - 4o - u - 9o$.

40. ($h_t = 40$) $1_1 \longleftarrow 3_5$: $4o - u - 4o - u - 5o - 2u - 4o - u$.
41. ($h_t = 41$) $1_1 \longrightarrow 1_1$: $2u - 5o - 4u - 5o - u - 3o - 2u$.
42. ($h_t = 42$) $3_5 \longleftarrow 1_1$: $u - o - u - 5o - 5u - 5o - u - 4o$.
43. ($h_t = 43$) $3_5 \longrightarrow 2_2$: $5o - 5u - 5o - 2u - 2o - 3u$.
44. ($h_t = 44$) $5_4 \longleftarrow 2_2$: $u - 3o - 3u - 5o - 5u - o - 4u$.
45. ($h_t = 45$) $5_4 \longrightarrow 4_3$: $8u - 5o - 3u - o - 4u$.
46. ($h_t = 46$) $4_3 \longleftarrow 4_3$: $2u - 2o - 4u - 5o - 4u - 2o - 3u$.
47. ($h_t = 47$) $4_3 \longrightarrow 5_4$: $3u - o - 3u - 5o - 9u$.
48. ($h_t = 48$) $2_2 \longleftarrow 5_4$: $3u - o - 5u - 5o - 3u - 3o - 2u$.
49. ($h_t = 49$) $2_2 \longrightarrow 3_5$: $2u - 2o - 2u - 5o - 5u - 9o$.
50. ($h_t = 50$) $1_1 \longleftarrow 3_5$: $4o - u - 5o - 5u - 5o - 2u - 4o - u$.

For the Flores Knot in **Example 2.** we first braid the table half-cycles $19 \leq h_t \leq 36$, starting with $h_t = B+1 = 19$, in the normal direction. We read for h_t the intersection codings from left to right for $19 < h \leq h_t$. Then we braid the table half-cycles $1 \leq h_t \leq 18$, starting with table half-cycle $h_t = B = 18$, in the reverse direction. We read for h_t the intersection codings from right to left for $h = 1$ and $h_t < h \leq 2B$. This results in the following half-cycle braiding algorithms:

1. ($h_t = 19$) $4_4 \longrightarrow 2_4$: Free run.
2. ($h_t = 20$) $5_5 \longleftarrow 2_4$: u.
3. ($h_t = 21$) $5_5 \longrightarrow 1_3$: o.
4. ($h_t = 22$) $3_6 \longleftarrow 1_3$: $o - u - o$.
5. ($h_t = 23$) $3_6 \longrightarrow 3_2$: $o - u - o$.
6. ($h_t = 24$) $1_1 \longleftarrow 3_2$: $5o$.
7. ($h_t = 25$) $1_1 \longrightarrow 5_1$: $u - 2o - 2u$.
8. ($h_t = 26$) $2_2 \longleftarrow 5_1$: $5u - o$.
9. ($h_t = 27$) $2_2 \longrightarrow 4_6$: $2u - 2o - 2u$.
10. ($h_t = 28$) $3_3 \longleftarrow 4_6$: $o - 2u - o - 3u$.
11. ($h_t = 29$) $3_3 \longrightarrow 3_5$: $2u - 2o - u - o - u$.
12. ($h_t = 30$) $4_4 \longleftarrow 3_5$: $u - 4o - u - o - u$.
13. ($h_t = 31$) $4_4 \longrightarrow 2_4$: $2u - o - u - 2o - u - o - u$.
14. ($h_t = 32$) $5_5 \longleftarrow 2_4$: $2u - 3o - 3u - o - u$.
15. ($h_t = 33$) $5_5 \longrightarrow 1_3$: $5u - 2o - u - o - u$.
16. ($h_t = 34$) $3_6 \longleftarrow 1_3$: $2o - u - 2o - 3u - 5o$.
17. ($h_t = 35$) $3_6 \longrightarrow 3_2$: $5o - 3u - 2o - u - 2o$.
18. ($h_t = 36$) $1_1 \longleftarrow 3_2$: $5o - 3u - 6o - u$.

---

19. ($h_t = 18$ rev.) $4_4 \longrightarrow 3_5$: $2u - o - 2u - 2o - 3u - o - 2u$.
20. ($h_t = 17$ rev.) $3_3 \longleftarrow 3_5$: $2u - o - 3u - 3o - 2u - o - 3u$.
21. ($h_t = 16$ rev.) $3_3 \longrightarrow 4_6$: $u - 2o - u - 4o - 2u - o - 3u$.
22. ($h_t = 15$ rev.) $2_2 \longleftarrow 4_6$: $3u - o - 3u - 4o - u - 2o - 2u$.
23. ($h_t = 14$ rev.) $2_2 \longrightarrow 5_1$: $2u - 6o - 4u - o - 2u$.
24. ($h_t = 13$ rev.) $1_1 \longleftarrow 5_1$: $8u - 4o - 2u - 2o - u$.
25. ($h_t = 12$ rev.) $1_1 \longrightarrow 3_2$: $u - 3o - u - 3o - 5u - 7o$.
26. ($h_t = 11$ rev.) $3_6 \longleftarrow 3_2$: $4o - u - 4o - 4u - 5o - u - 3o$.
27. ($h_t = 10$ rev.) $3_6 \longrightarrow 1_3$: $8o - 4u - 5o - u - 3o - u$.
28. ($h_t = 9$ rev.) $5_5 \longleftarrow 1_3$: $2u - 3o - 2u - 4o - 10u$.
29. ($h_t = 8$ rev.) $5_5 \longrightarrow 2_4$: $4u - o - 3u - 5o - 2u - 3o - 2u$.
30. ($h_t = 7$ rev.) $4_4 \longleftarrow 2_4$: $3u - 2o - 3u - 5o - 4u - o - 4u$.

31. $(h_t = 6 \text{ rev.})$ $4_4 \longrightarrow 3_5$: $3u - 2o - 3u - 5o - 3u - 2o - 3u$.
32. $(h_t = 5 \text{ rev.})$ $3_3 \longleftarrow 3_5$: $4u - o - 4u - 5o - 4u - 2o - 3u$.
33. $(h_t = 4 \text{ rev.})$ $3_3 \longrightarrow 4_6$: $2u - 3o - 2u - 6o - 4u - o - 4u$.
34. $(h_t = 3 \text{ rev.})$ $2_2 \longleftarrow 4_6$: $5u - o - 5u - 5o - 3u - 3o - 3u$.
35. $(h_t = 2 \text{ rev.})$ $2_2 \longrightarrow 5_1$: $2u - 4o - u - 6o - 5u - o - 5u$.
36. $(h_t = 1 \text{ rev.})$ $1_1 \longleftarrow 5_1$: $12u - 6o - 2u - 4o - 2u$.

Transition from two Round Braids to one Round Braid, and vice versa

A transition between two 8-string round braids, each with a 4-string round braid core, and one 12-string round braid with an 8-string round braid outer core over a 4-string round braid inner core.

BRAIDING TYPE																																			
12 STRING MANTLE												8 STRING OUTER CORE								4 STRING INNER CORE				8 STRING MANTLE								4 STRING CORE			
→						←						→				←				→		←		→				←				→		←	
U	O	U	O	U	O	O	U	O	U	O	U	U	O	U	O	O	U	O	U	U	O	O	U	U	O	U	O	O	U	O	U	U	O	O	U
1	1	1	1	1	1	1	1	1	1	1	1	1	1	1	1	1	1	1	1	1	1	1	1	1	1	1	1	1	1	1	1	1	1	1	1

Figs. 750, 751, 752, 753 and 754:

The 8-string round braid mantle has the strings A, B, C, D, E, F, G, H at one end and the strings 1, 2, 3, 4, 5, 6, 7, 8 at the other end. This 8-string round braid mantle goes over a 4-string round braid core, which has at one end the strings A^*, B^*, C^*, D^* and at the other end the strings 1^*, 2^*, 3^*, 4^*. Of the 8-string round braid mantle, the strings A, B, 1, 2 go over into a 4-string round braid inner core. Of the 4-string round braid core, the strings A^*, B^*, C^*, D^* and 1^*, 2^*, 3^*, 4^* go over into an 8-string round braid outer core. Of the 8-string round braid mantle, the strings C, D, E, F, G, H, 3, 4, 5, 6, 7, 8 go over into a 12-string round braid mantle which goes over the 8-string round braid outer core. See Figs. 750 & 751.

The strings A, B, 1, 2 go over into the 4-string round braid inner core, the preparation of which is depicted in the upper part of Fig. 750; bring A around the back of the left-hand 8-string round braid mantle from left to right, and bring 2 around the back of the right-hand 8-string round braid mantle from right to left. Note that in the 4-string round braid core the flesh-side of the strings is outermost. The braiding of this core continues as follows:

Bring 2 from the left around the back to the right, then along the front from right to left under 1, over A.

Bring 1 from the right around the back to the left, then along the front from left to right under B, over 2.

Bring B from the left around the back to the right, then along the front from right to left under A, over 1.

Bring A from the right around the back to the left, then along the front from left to right under 2, over B.

And so on.

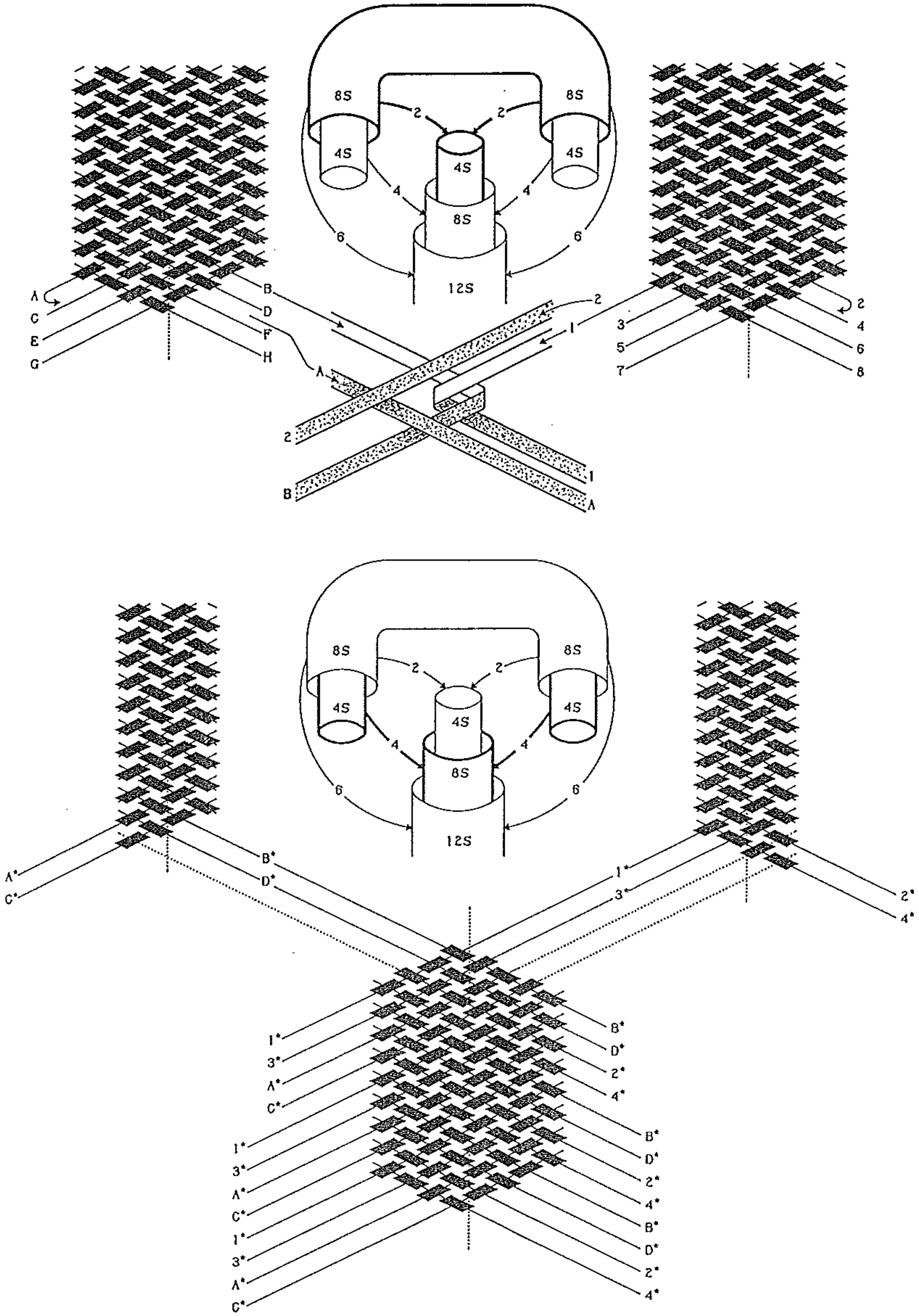

Fig. 750 — Transition from two 8-string over 4-string round braids to a 12-string over 8-string over 4-string round braid.

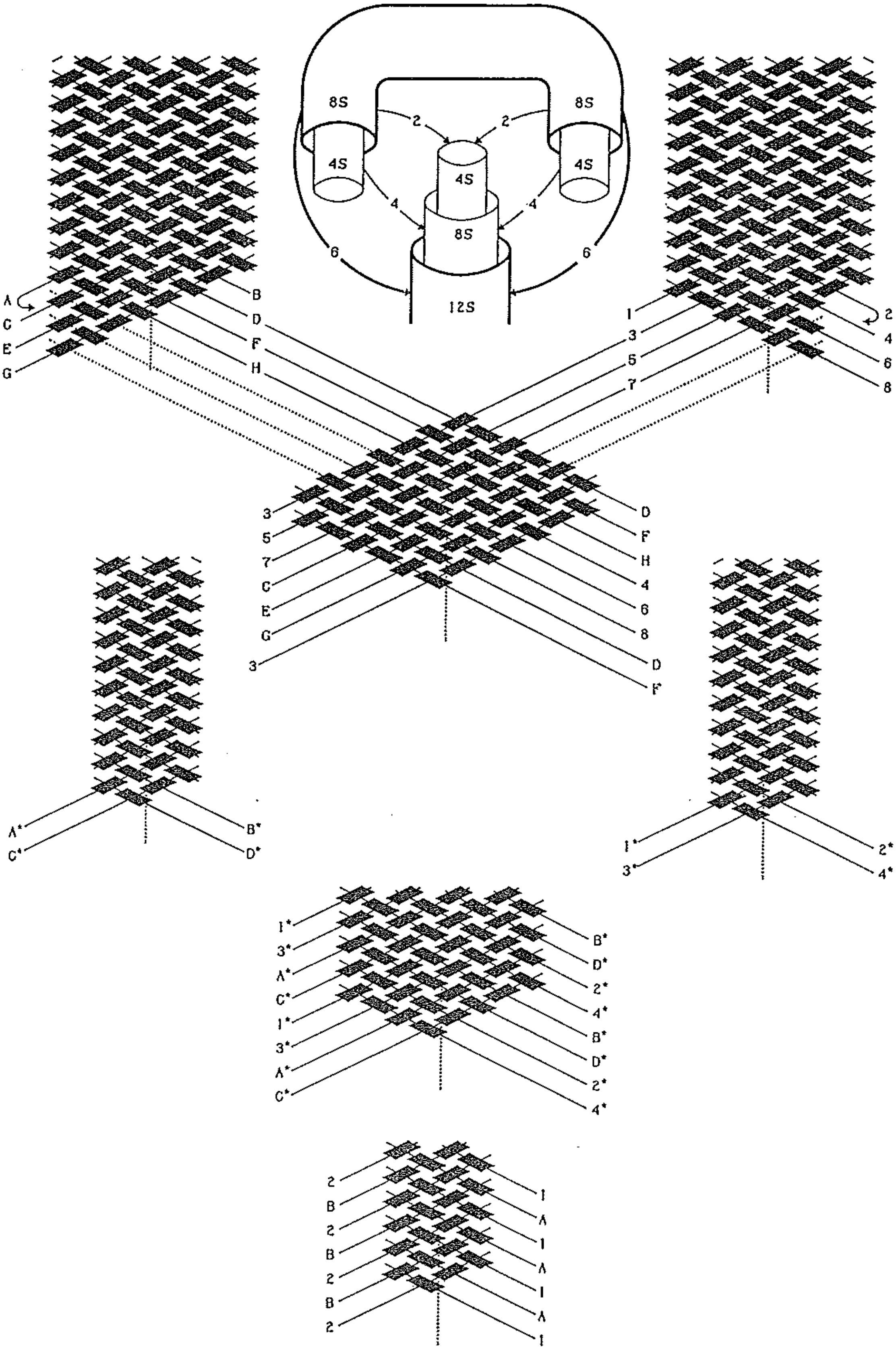

Fig. 751 — Transition from two 8-string over 4-string round braids to a 12-string over 8-string over 4-string round braid.

The strings A^*, B^*, C^*, D^* and 1^*, 2^*, 3^*, 4^* go over into an 8-string round braid outer core.

Form the crossings between the strings B^*, D^*, 1^*, 3^* as depicted in the lower part of Fig. 750.

Next bring A^* from the left around the back to the right, then along the front from right to left under 2^*, over 4^*, under B^*, over D^*.

Bring 2^* from the right around the back to the left, then along the front from left to right under C^*, over 1^*, under 3^*, over A^*.

Bring C^* from the left around the back to the right, then along the front from right to left under 4^*, over B^*, under D^*, over 2^*.

Bring 4^* from the right around the back to the left, then along the front from left to right under 1^*, over 3^*, under A^*, over C^*.

Bring 1^* from the left around the back to the right, then along the front from right to left under B^*, over D^*, under 2^*, over 4^*.

Bring B^* from the right around the back to the left, then along the front from left to right under 3^*, over A^*, under C^*, over 1^*.

Bring 3^* from the left around the back to the right, then along the front from right to left under D^*, over 2^*, under 4^*, over B^*.

Bring D^* from the right around the back to the left, then along the front from left to right under A^*, over C^*, under 1^*, over 3^*.

Bring A^* from the left around the back to the right, then along the front from right to left under 2^*, over 4^*, under B^*, over D^*.

Bring 2^* from the right around the back to the left, then along the front from left to right under C^*, over 1^*, under 3^*, over A^*.

Bring C^* from the left around the back to the right, then along the front from right to left under 4^*, over B^*, under D^*, over 2^*.

Bring 4^* from the right around the back to the left, then along the front from left to right under 1^*, over 3^*, under A^*, over C^*.

And so on.

The strings C, D, E, F, G, H, 3, 4, 5, 6, 7, 8 go over into the 12-string round braid mantle.

Form the crossings between the strings D, F, H, 3, 5, 7 as depicted in the upper part of Fig. 751.

Next bring 4 from the right around the back to the left, then along the front from left to right under C, over E, under G, over 3, under 5, over 7.

Bring C from the left around the back to the right, then along the front from right to left under 6, over 8, under D, over F, under H, over 4.

Bring 6 from the right around the back to the left, then along the front from left to right under E, over G, under 3, over 5, under 7, over C.

Bring E from the left around the back to the right, then along the front from right to left under 8, over D, under F, over H, under 4, over 6.

Bring 8 from the right around the back to the left, then along the front from left to right under G, over 3, under 5, over 7, under C, over E.

Bring G from the left around the back to the right, then along the front from right to left under D, over F, under H, over 4, under 6, over 8.

Bring D from the right around the back to the left, then along the front from left to right under 3, over 5, under 7, over C, under E, over G.

Bring 3 from the left around the back to the right, then along the front from right to left under F, over H, under 4, over 6, under 8, over D.

Bring F from the right around the back to the left, then along the front from left to right under 5, over 7, under C, over E, under G, over 3.

Bring 5 from the left around the back to the right, then along the front from right to left under H, over 4, under 6, over 8, under D, over F.

Bring H from the right around the back to the left, then along the front from left to right under 7, over C, under E, over G, under 3, over 5.

Bring 7 from the left around the back to the right, then along the front from right to left under 4, over 6, under 8, over D, under F, over H.

Bring 4 from the right around the back to the left, then along the front from left to right under C, over E, under G, over 3, under 5, over 7.

Bring C from the left around the back to the right, then along the front from right to left under 6, over 8, under D, over F, under H, over 4.

Bring 6 from the right around the back to the left, then along the front from left to right under E, over G, under 3, over 5, under 7, over C.

Bring E from the left around the back to the right, then along the front from right to left under 8, over D, under F, over H, under 4, over 6.

Bring 8 from the right around the back to the left, then along the front from left to right under G, over 3, under 5, over 7, under C, over E.

Bring G from the left around the back to the right, then along the front from right to left under D, over F, under H, over 4, under 6, over 8.

And so on.

The 12-string round braid mantle has the strings 1^*, 2^*, 3^*, 4^*, 5^*, 6^*, 7^*, 8^*, 9^*, 10^*, 11^*, 12^*. The preparation of the strings is shown in Fig. 753.

The 8-string round braid outer core has the strings A, B, C, D, E, F, G, H. The preparation of the strings is shown in the lower part of Fig. 752.

The 4-string round braid inner core, which has the flesh-side of its strings outermost, has the strings 1, 2, 3, 4. The preparation of the strings is shown in the upper part of Fig. 752:

Bring 1 around the back from right to left with the hair-side up on left. Place 1 between 2 and 4.

Bring 2 around the back from left to right with the hair-side up on right. Place 2 below 3.

Ensure that the crossings Y and Z are at the same level, and that the crossings X and V are at the same level.

Braid from the 8-string round braid outer core, hence with the strings A, B, C, D, E, F, G, H, the two 4-string cores as shown in the lower part of Fig. 754. For the preparation stage, bring A from the left around the back to the right, then along the front from right to left under B, over D, under F, over H.

Bring B from the right around the back to the left, then along the front from left to right under C, over E, under G.

Bring C from the left around the back to the right, then along the front from right to left under D, over F, under H.

Bring D from the right around the back to the left, then along the front from left to right under E, over G.

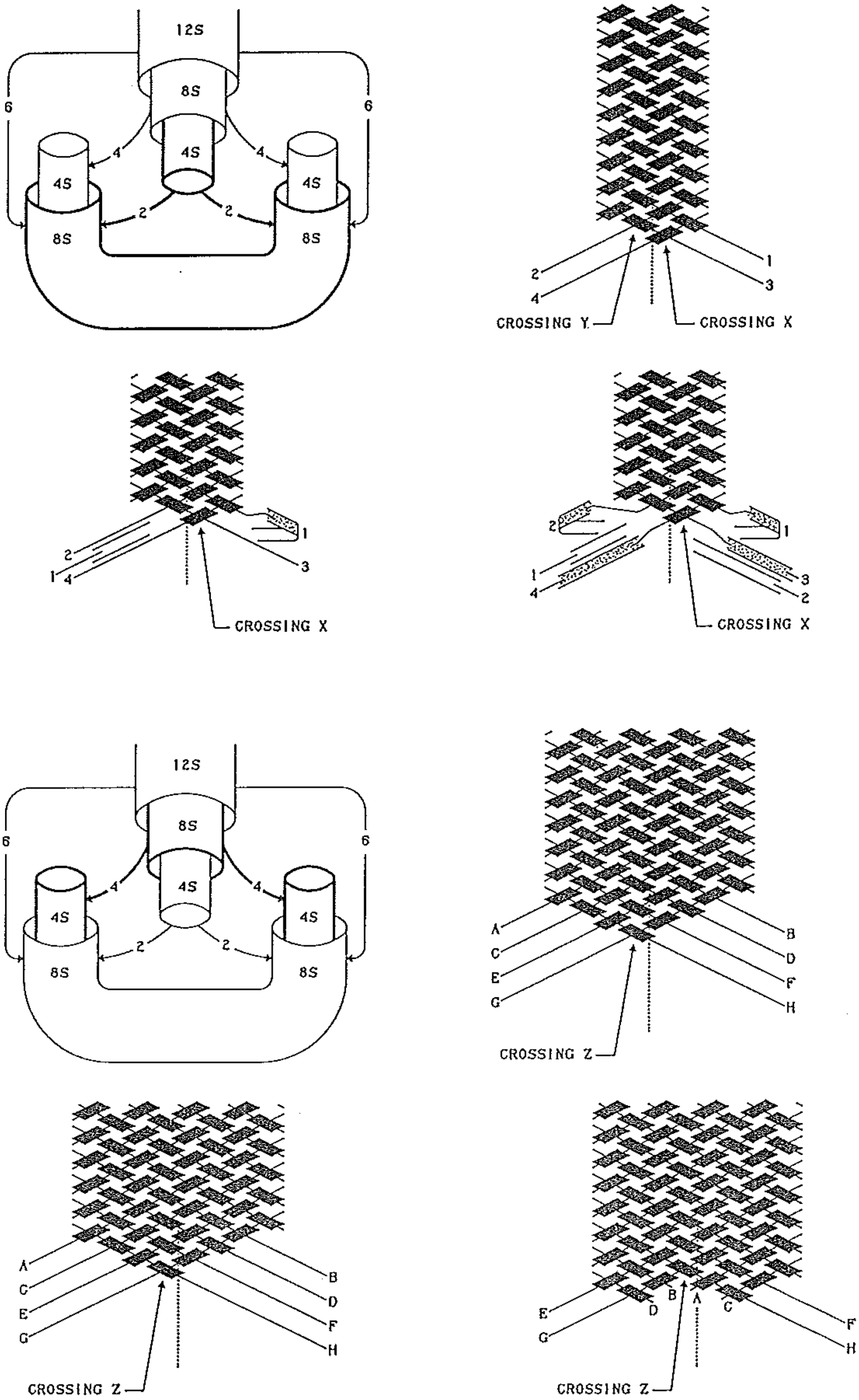

Fig. 752 — Preparation of the 4-string round braid inner core and of the 8-string round braid outer core.

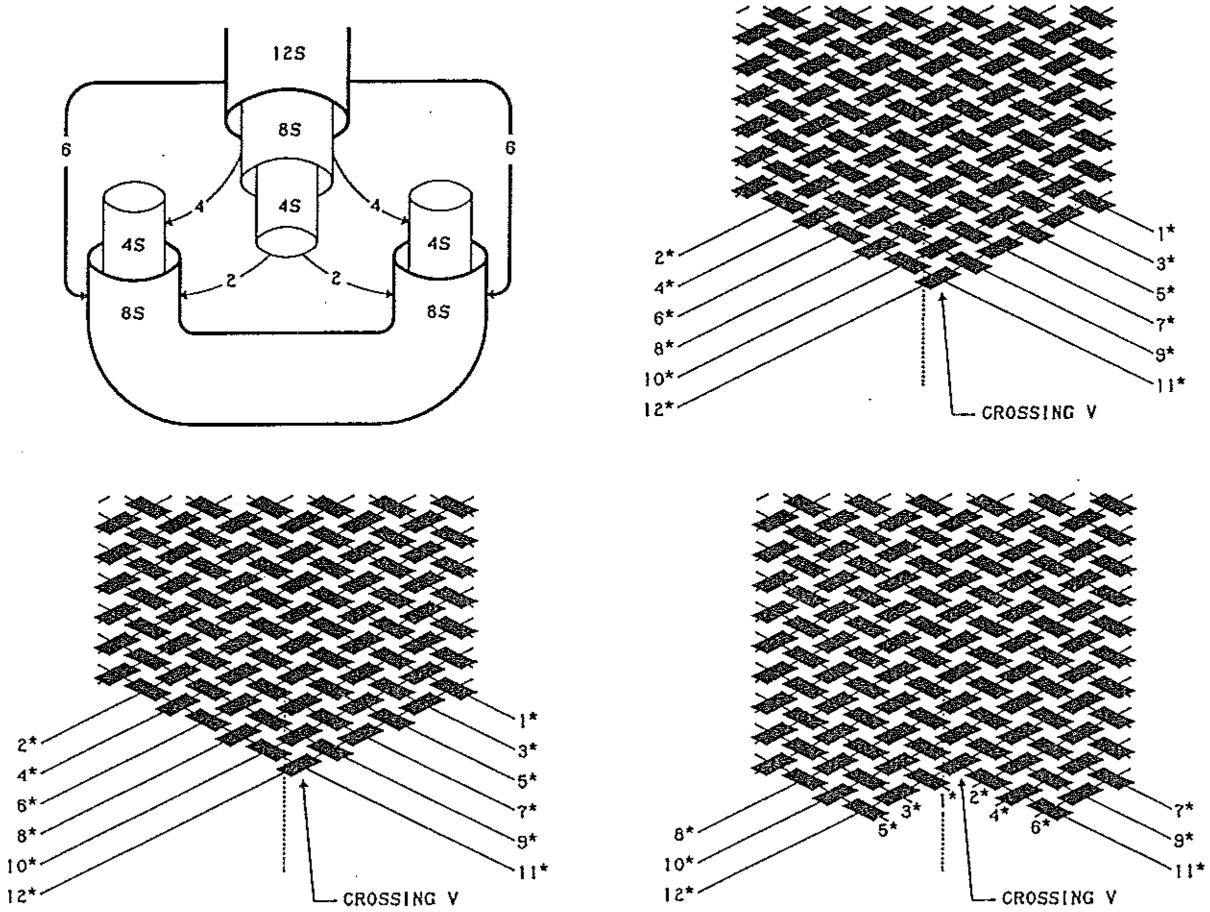

Fig. 753 — Preparation of the 12-string round braid mantle.

The left 4-string core:

Bring *E* from the left around the back to the right, then along the front from right to left under *B*, over *D*.

Bring *B* from the right around the back to the left, then along the front from left to right under *G*, over *E*.

Bring *G* from the left around the back to the right, then along the front from right to left under *D*, over *B*.

Bring *D* from the right around the back to the left, then along the front from left to right under *E*, over *G*.

And so on.

The right 4-string core:

Bring *A* from the left around the back to the right, then along the front from right to left under *F*, over *H*.

Bring *F* from the right around the back to the left, then along the front from left to right under *C*, over *A*.

Bring *C* from the left around the back to the right, then along the front from right to left under *H*, over *F*.

Bring *H* from the right around the back to the left, then along the front from left to right under *A*, over *C*.

And so on.

Braid from the strings of the 12-string round braid mantle and the strings 1, 2, 3, 4 of the inner core, the two 8-string mantles as shown in the upper part of Fig. 754.

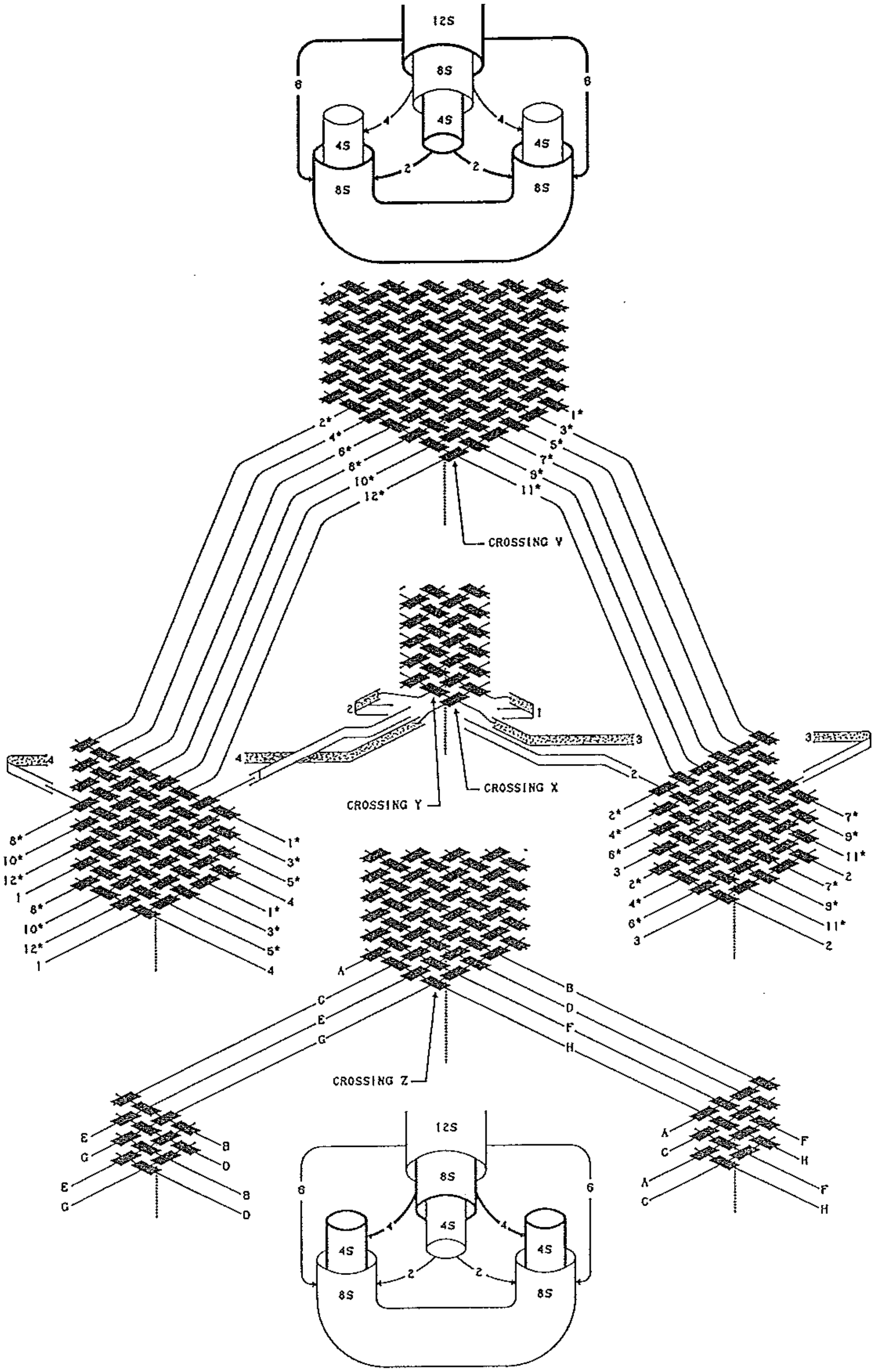

Fig. 754 — Transition from a 12-string over 8-string over 4-string round braid to two 8-string over 4-string round braids.

For the preparation stage, bring 1* from the right around the back to the left, then along the front from left to right under 2*, over 4*, under 6*, over 8*, under 10*, over 12*.

Bring 2* from the left around the back to the right, then along the front from right to left under 3*, over 5*, under 7*, over 9*, under 11*.

Bring 3* from the right around the back to the left, then along the front from left to right under 4*, over 6*, under 8*, over 10*, under 12*.

Bring 4* from the left around the back to the right, then along the front from right to left under 5*, over 7*, under 9*, over 11*.

Bring 5* from the right around the back to the left, then along the front from left to right under 6*, over 8*, under 10*, over 12*.

Bring 6* from the left around the back to the right, then along the front from right to left under 7*, over 9*, under 11*.

Bring 1 along the front to the left: over 4, over 1*, under 3*, over 5*.

Bring 4 around the back to the left, then along the front from left to right under 8*, over 10*, under 12*, over 1.

Bring 3 around the back to the right, then along the front from right to left over 7*, under 9*, under 11*.

Bring 2 along the front to the right under 2*, over 4*, under 6*, over 3.

The left 8-string mantle:

Bring 8* from the left around the back to the right, then along the front from right to left under 1*, over 3*, under 5*, over 4.

Bring 1* from the right around the back to the left, then along the front from left to right under 10*, over 12*, under 1, over 8*.

Bring 10* from the left around the back to the right, then along the front from right to left under 3*, over 5*, under 4, over 1*.

Bring 3* from the right around the back to the left, then along the front from left to right under 12*, over 1, under 8*, over 10*.

Bring 12* from the left around the back to the right, then along the front from right to left under 5*, over 4, under 1*, over 3*.

Bring 5* from the right around the back to the left, then along the front from left to right under 1, over 8*, under 10*, over 12*.

Bring 1 from the left around the back to the right, then along the front from right to left under 4, over 1*, under 3*, over 5*.

Bring 4 from the right around the back to the left, then along the front from left to right under 8*, over 10*, under 12*, over 1.

And so on.

The right 8-string mantle:

Bring 2* from the left around the back to the right, then along the front from right to left under 7*, over 9*, under 11*, over 2.

Bring 7* from the right around the back to the left, then along the front from left to right under 4*, over 6*, under 3, over 2*.

Bring 4* from the left around the back to the right, then along the front from right to left under 9*, over 11*, under 2, over 7*.

Bring 9* from the right around the back to the left, then along the front from left to right under 6*, over 3, under 2*, over 4*.

Bring 6* from the left around the back to the right, then along the front from right to left under 11*, over 2, under 7*, over 9*.

Bring 11* from the right around the back to the left, then along the front from left to right under 3, over 2*, under 4*, over 6*.

Bring 3 from the left around the back to the right, then along the front from right to left under 2, over 7*, under 9*, over 11*.

Bring 2 from the right around the back to the left, then along the front from left to right under 2*, over 4*, under 6*, over 3.

And so on.

THE BRAIDER'S NOTEBOOK

Most braidwork contains auxiliary knots. Their purpose, for example, may be to add weight to a section of the braidwork, to embellish the braidwork or to conceal local irregularities in the braidwork. It is important to ensure that such knots stay firmly in place at all times. A simple way to achieve this is for a knot-string to pass diametrically through the object the knot covers, and hence we ensure that the total number of bights of the knot is **even**.

When the knot is a Regular Knot, hence a Regular Cylindrical Braid requiring one essential string, then its number of parts p is **odd**, with g.c.d.$(p, b) = 1$. A string-run example of such a knot is shown in Fig. 755, where in the upper diagram the string-run has been split into two equal parts. One part forms the string-run half-cycles $1-2-3-4-5-6-7-8-9-10-11-12-13-14$ and the other part forms the string-run half-cycles $1'-2'-3'-4'-5'-6'-7'-8'-9'-10'-11'-12'-13'-14'$. We can braid these string-run half-cycles of the knot in two different ways: **1.** by parallel braiding or **2.** by series braiding.

By parallel braiding we braid first half-cycle 1, then half-cycle 1', then half-cycle 2, then half-cycle 2', then half-cycle 3, then half-cycle 3', and so on.

By series braiding we braid first the half-cycles $1-2-3-\cdots-14$, then the half-cycles $1'-2'-3'-\cdots-14'$.

Parallel braiding:

For the string-run half-cycles $1-2-3-\cdots-14$ or the string-run half-cycles $1'-2'-3'-\cdots-14'$, the algorithm diagram with $\Delta^* = 3$ is constructed in the usual way, resulting in the two inner rows of i-values. The outer two rows of i-values belong respectively to the string-run half-cycles $1'-2'-3'-\cdots-14'$ or to the string-run half-cycles $1-2-3-\cdots-14$ and are derived from the inner rows of i-values by adding or subtracting in modular fashion $\frac{b}{2}$. Thus for the half-cycles $1-2-3-\cdots-14$, the inner row of i-values are associated with their intersections with the half-cycles $1-2-3-\cdots-14$, and the outer row of i-values are associated with their intersections with the half-cycles $1'-2'-3'-\cdots-14'$. For the half-cycles $1'-2'-3'-\cdots-14'$, the inner row of i-values are associated with their intersections with the half-cycles $1'-2'-3'-\cdots-14'$, and the outer row of i-values are associated with their intersections with the half-cycles $1-2-3-\cdots-14$. From the inner row $i = 3$ we thus obtain the outer row $i = |3+7|_{14} = 10$ (or $i = |3-7|_{14} = 10$), from the inner row $i = 6$ we thus obtain the outer row $i = |6+7|_{14} = 13$ (or $i = |6-7|_{14} = 13$), from the inner row $i = 9$ we thus obtain the outer row $i = |9+7|_{14} = 2$ (or $i = |9-7|_{14} = 2$), etc. Hence for half-cycle 7 we obtain its half-cycle braiding algorithm by reading the sequential codings associated with $i = 2, 1, 0$. For half-cycle 8 we obtain its half-cycle braiding algorithm by reading the sequential codings associated with $i = 3, 2, 1, 0, 3$. For half-cycle 10′ we obtain its half-cycle braiding algorithm by reading the sequential codings associated with $i = 3, 2, 1, 4, 0, 3$. For half-cycle 13′ we obtain its half-cycle braiding algorithm by reading the sequential codings associated with $i = 3, 2, 5, 1, 4, 0, 3$.

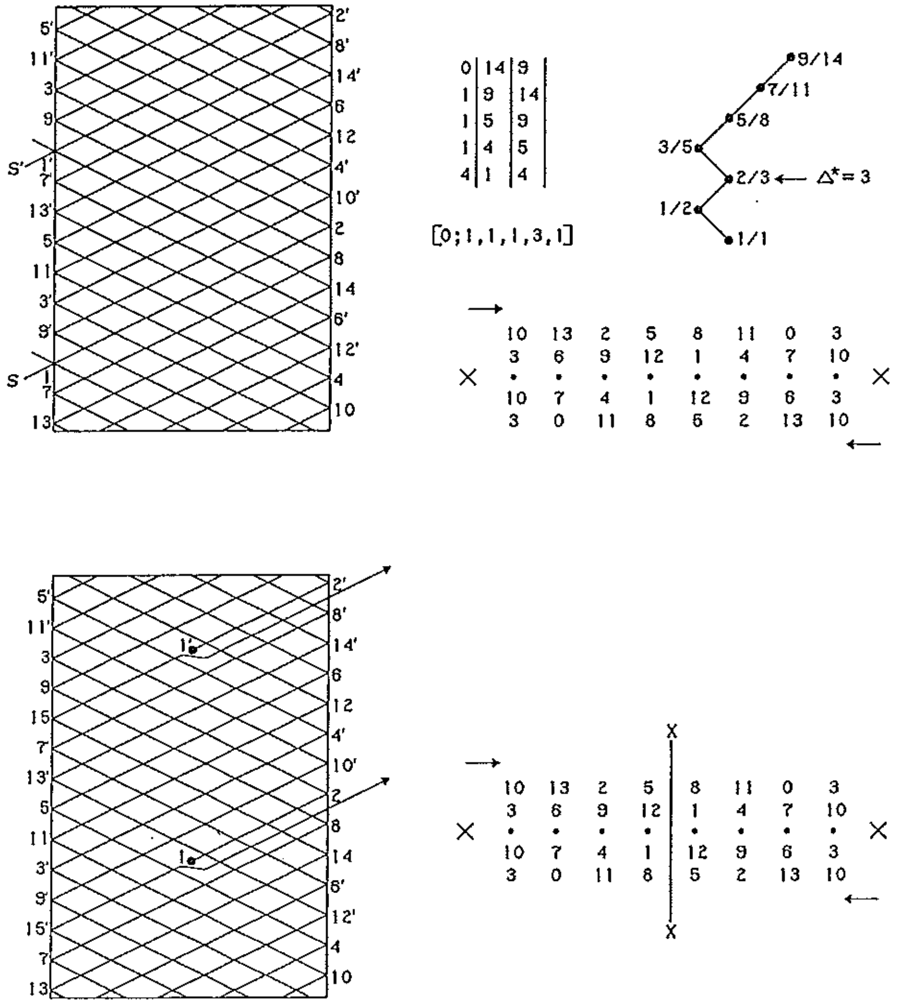

Fig. 755 — A Regular Knot with $p/b = 9/14$.

In the lower diagram of Fig. 755 the Standing Ends of the two strings have diametrically been joined. Hence the half-cycles 1 and 1′ run from the X—X line to the right, while the half-cycles 15 and 15′ are the last ones to be laid down; their half-cycle braiding algorithms are the sequential codings associated with $i = 3, 6, 2, 5$ followed by four unders. For half-cycle 7 we thus obtain its half-cycle braiding algorithm by reading the sequential codings associated with $i = 2, 1, 0$. For half-cycle 8 we obtain its half-cycle braiding algorithm by reading the sequential codings associated with $i = 3, 2, 1, 0$ (note that $i = 3$ in the outer lower row represents the intersection of half-cycle 8 with half-cycle 15 (the extended Standing End half-cycle 1′ left of the X—X line) and hence has to be neglected). For half-cycle 10′ we obtain its half-cycle braiding algorithm by reading the sequential codings associated with $i = 3, 2, 1, 0, 3$ (note that $i = 4$ in the inner lower row represents the intersection of half-cycle 10′ with half-cycle 15 (the extended Standing End half-cycle 1′ left of the X—X line) and hence has to be neglected). For half-cycle 13′ we obtain its half-cycle braiding algorithm by reading the sequential codings associated with $i = 3, 2, 5, 1, 4, 0, 3$.

Let the superimposed coding on this string-run be as shown in Fig. 756.

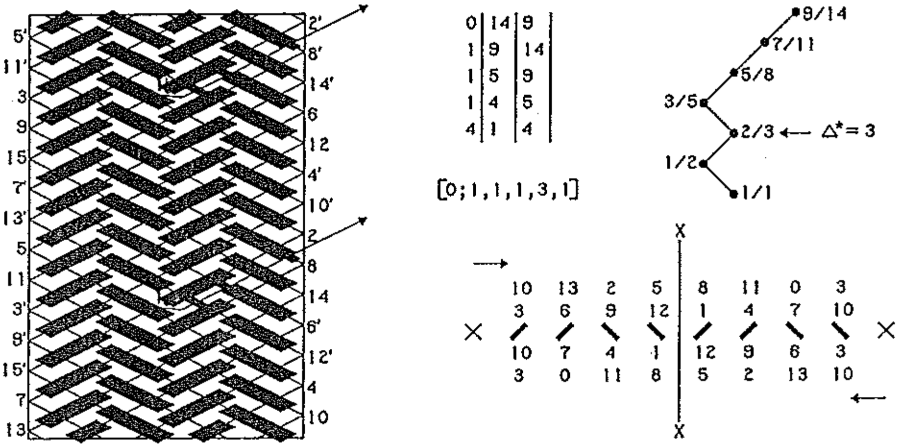

Fig. 756 — The superimposed coding on the string-run of Fig. 755.

The half-cycle braiding algorithms are then as follows:

half-cycles 1 & 1′ :		:	$L \longrightarrow R$:	Free run.
half-cycles 2 & 2′ :	$i = 0$;	$i \neq 0$ left of X–X :	$L \longleftarrow R$:	Free run.
half-cycles 3 & 3′ :	$i = 0$;	:	$L \longrightarrow R$:	u .
half-cycles 4 & 4′ :	$i \leq 1$;	$i \neq 1$ left of X–X :	$L \longleftarrow R$:	u .
half-cycles 5 & 5′ :	$i \leq 1$;	:	$L \longrightarrow R$:	$o - u$.
half-cycles 6 & 6′ :	$i \leq 2$;	$i \neq 2$ left of X–X :	$L \longleftarrow R$:	$u - o - u$.
half-cycles 7 & 7′ :	$i \leq 2$;	:	$L \longrightarrow R$:	$u - o - u$.
half-cycles 8 & 8′ :	$i \leq 3$;	$i \neq 3$ left of X–X :	$L \longleftarrow R$:	$o - u - o - u$.
half-cycles 9 & 9′ :	$i \leq 3$;	:	$L \longrightarrow R$:	$o - u - o - 2u$.
half-cycles 10 & 10′ :	$i \leq 4$;	$i \neq 4$ left of X–X :	$L \longleftarrow R$:	$o - u - o - 2u$.
half-cycles 11 & 11′ :	$i \leq 4$;	:	$L \longrightarrow R$:	$o - u - 2o - 2u$.
half-cycles 12 & 12′ :	$i \leq 5$;	$i \neq 5$ left of X–X :	$L \longleftarrow R$:	$o - 2u - 2o - 2u$.
half-cycles 13 & 13′ :	$i \leq 5$;	:	$L \longrightarrow R$:	$o - 2u - 2o - 2u$.
half-cycles 14 & 14′ :	$i \leq 6$;	$i \neq 6$ left of X–X :	$L \longleftarrow R$:	$2o - 2u - 2o - 2u$.
half-cycles 15 & 15′ :	$i \leq 6$;	unders right of X–X :	$L \longrightarrow R$:	$2o - 6u$.

Series braiding:

By series braiding we braid first the half-cycles $1 - 2 - 3 - \cdots - 14 - 15$, then the half-cycles $1' - 2' - 3' - \cdots - 14' - 15'$. By series braiding it is more convenient to number these two sets of half-cycles sequentially as in Fig. 757; thus we braid first half-cycles $1 - 2 - 3 - \cdots - 14 - 15$, then the half-cycles $15^* - 16 - 17 - \cdots - 28 - 29$. The i-value $\frac{h_e - 2}{2}$ to the left of the line X—X (hence in the bottom row of the algorithm diagram), associated with the string-run $1 - 2 - 3 - \cdots - 14 - 15$; $15^* - 16 - 17 - \cdots - 28 - 29$, must be neglected for the even numbered half-cycle h_e (intersection of half-cycle h_e with half-cycle 1 (the extended Standing End half-cycle 1 left of the X—X line). The i-values $\frac{h_o - 3}{2}$ to the right of the line X—X (hence in the top row of the algorithm diagram), associated with half-cycle 15, correspond to unders. The i-values $\frac{h_o - 3}{2}$ to the left of the line X—X (hence in the top row of the algorithm diagram), associated with half-cycle 15^*, must be neglected. The i-value $\left|\frac{h_e - 2}{2} - \frac{b}{2}\right|_b$ to the right of the line X—X (hence in the bottom row of the algorithm diagram), associated with the even numbered half-cycle h_e of the string-run $15^* - 16 - 17 - \cdots - 28 - 29$, corresponds to an $o - \star$, where the $\star$ stands for the coding that is associated with $i = \left|\frac{h_e - 2}{2} - \frac{b}{2}\right|_b$. Note that $\left|\frac{h_e-2}{2}-\frac{b}{2}\right|_b$ is identical to $\left|\frac{h_e-2}{2}+\frac{b}{2}\right|_b$. The i-values $\frac{h_o-3}{2}$ to the right of the line X—X (hence in the top row of the algorithm diagram), associated with half-cycle 29, correspond to unders.

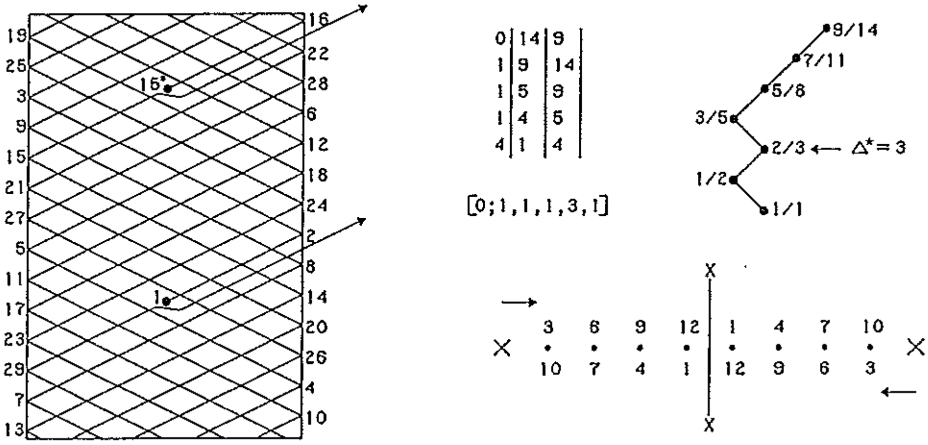

Fig. 757 — Half-cycle numbering for series braiding.

Thus for half-cycle 10 we obtain its half-cycle braiding algorithm by reading the sequential codings associated with $i = 3, 1$ (bottom row, right to left). Note that $i = 4$ in the bottom row represents the intersection of half-cycle 10 with half-cycle 1 (the extended Standing End half-cycle 1 left of the X—X line) and hence has to be neglected. For half-cycle 15 we obtain its half-cycle braiding algorithm by reading the sequential codings associated with $i = 3, 6$ (top row, left to right) followed by two unders. For half-cycle 15* we obtain its half-cycle braiding algorithm by reading the sequential codings associated with $i = 1, 4$ (top row, left to right). Note that $i = 3, 6$ in the top row are to the left of the X—X line and hence have to be neglected. For half-cycle 18 we obtain its half-cycle braiding algorithms by reading the sequential codings associated with $i = 3, 6, 1, 4, 7$ (bottom row, right to left). For half-cycle 22 we obtain its half-cycle braiding algorithms by reading the sequential codings o and those associated with $i = 3, 6, 9, 1, 4, 7$ (bottom row, right to left). Note that $i = \left|\frac{22-2}{2}-\frac{14}{2}\right|_{14} = 3$ in the bottom row, situated at the right of the X—X line, gives us the $o - \star$ codings, where the $\star$-coding is associated with $i = 3$; furthermore that $i = \frac{22-2}{2} = 10$ in the bottom row represents the intersection of half-cycle 22 with half-cycle 1 (the extended Standing End half-cycle 1 left of the X—X line) and hence has to be neglected.

Let the superimposed coding on this string-run be as shown in Fig. 758.

The half-cycle braiding algorithms are then as follows:

half-cycle 1 :		:	$L \longrightarrow R$:	Free run.
half-cycle 2 :	$i = 0$;	$i \neq 0$ left of X–X :	$L \longleftarrow R$:	Free run.
half-cycle 3 :	$i = 0$;	:	$L \longrightarrow R$:	Free run.
half-cycle 4 :	$i \leq 1$;	$i \neq 1$ left of X–X :	$L \longleftarrow R$:	Free run.
half-cycle 5 :	$i \leq 1$;	:	$L \longrightarrow R$:	o.
half-cycle 6 :	$i \leq 2$;	$i \neq 2$ left of X–X :	$L \longleftarrow R$:	o.
half-cycle 7 :	$i \leq 2$;	:	$L \longrightarrow R$:	o.
half-cycle 8 :	$i \leq 3$;	$i \neq 3$ left of X–X :	$L \longleftarrow R$:	$2o$.
half-cycle 9 :	$i \leq 3$;	:	$L \longrightarrow R$:	$2o$.
half-cycle 10 :	$i \leq 4$;	$i \neq 4$ left of X–X :	$L \longleftarrow R$:	$2o$.
half-cycle 11 :	$i \leq 4$;	:	$L \longrightarrow R$:	$3o$.
half-cycle 12 :	$i \leq 5$;	$i \neq 5$ left of X–X :	$L \longleftarrow R$:	$3o$.

half-cycle 13 : $i \leq 5$; : $L \longrightarrow R$: $3o$.
half-cycle 14 : $i \leq 6$; $i \neq 6$ left of X–X : $L \longleftarrow R$: $4o$.
half-cycle 15 : $i \leq 6$; unders right of X–X : $L \longrightarrow R$: $2o - 2u$.
half-cycle 15* : $i \leq 6$; : $L \longrightarrow R$: $2o$.
half-cycle 16 : $i \leq 7$; $i \neq 7$ left of X–X ; coding $o - \star =$ none for
$i = |7 - 7|_{14} = 0$ right of X–X : $L \longleftarrow R$: $4o$.
half-cycle 17 : $i \leq 7$; : $L \longrightarrow R$: $4o - u$.
half-cycle 18 : $i \leq 8$; $i \neq 8$ left of X–X ; coding $o - \star =$ none for
$i = |8 - 7|_{14} = 1$ right of X–X : $L \longleftarrow R$: $4o - u$.
half-cycle 19 : $i \leq 8$; : $L \longrightarrow R$: $4o - u$.
half-cycle 20 : $i \leq 9$; $i \neq 9$ left of X–X ; coding $o - \star =$ none for
$i = |9 - 7|_{14} = 2$ right of X–X : $L \longleftarrow R$: $2o - u - 2o - u$.
half-cycle 21 : $i \leq 9$; : $L \longrightarrow R$: $2o - u - 2o - u$.
half-cycle 22 : $i \leq 10$; $i \neq 10$ left of X–X ; coding $o - \star = 2o$ for
$i = |10 - 7|_{14} = 3$ right of X–X : $L \longleftarrow R$: $3o - u - 2o - u$.
half-cycle 23 : $i \leq 10$; : $L \longrightarrow R$: $2o - u - 2o - 2u$.
half-cycle 24 : $i \leq 11$; $i \neq 11$ left of X–X ; coding $o - \star =$ none for
$i = |11 - 7|_{14} = 4$ right of X–X : $L \longleftarrow R$: $2o - u - 2o - 2u$.
half-cycle 25 : $i \leq 11$; : $L \longrightarrow R$: $2o - u - 2o - 2u$.
half-cycle 26 : $i \leq 12$; $i \neq 12$ left of X–X ; coding $o - \star =$ none for
$i = |12 - 7|_{14} = 5$ right of X–X : $L \longleftarrow R$: $2o - 2u - 2o - 2u$.
half-cycle 27 : $i \leq 12$; : $L \longrightarrow R$: $2o - 2u - 2o - 2u$.
half-cycle 28 : $i \leq 13$; $i \neq 13$ left of X–X ; coding $o - \star = 2o$ for
$i = |13 - 7|_{14} = 6$ right of X–X : $L \longleftarrow R$: $3o - 2u - 2o - 2u$.
half-cycle 29 : $i \leq 13$; unders right of X–X : $L \longrightarrow R$: $2o - 6u$.

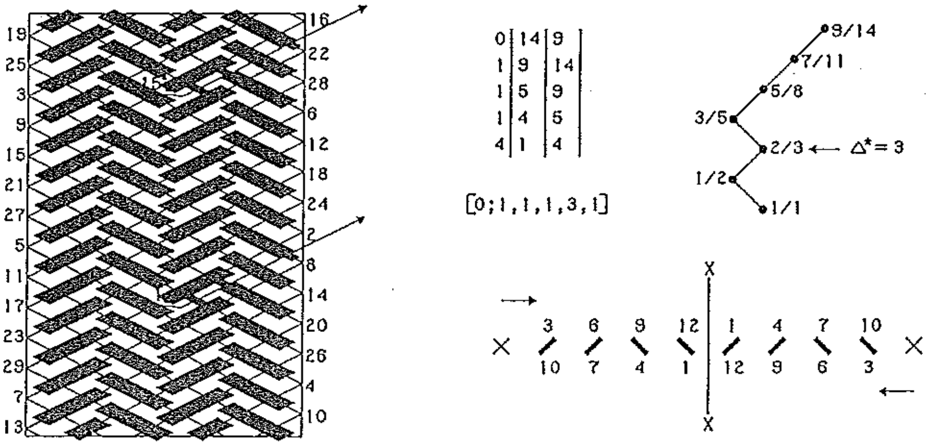

Fig. 758 — The superimposed coding on the string-run of Fig. 757.

When the knot is a Semi-Regular Knot, hence a Regular Cylindrical Braid with g.c.d. $(p, b) = \lambda$, where λ is the number of essential strings required, then we ensure that $\frac{b}{\lambda} = even$ and $\frac{p}{\lambda} = odd$. We furthermore ensure that the string-run of one of the interbraided Regular Knots passes diametrically through the object the Semi-Regular Knot covers. An example of such a Semi-Regular Knot is shown in Fig. 759 where the string-run of the component Regular Knot, which passes diametrically through the object the Semi-Regular Knot covers, is $1-2-3-4-5$; $1'-2'-3'-4'-5'$. One part of this component forms the string-run half-cycles $1-2-3-4-5$ and the other part forms the string-run half-cycles $1'-2'-3'-4'-5'$. We can again braid these string-run half-cycles in two different ways: **1.** by parallel braiding or **2.** by series braiding.

By parallel braiding we braid first half-cycle 1, then half-cycle 1′, then half-cycle 2, then half-cycle 2′, then half-cycle 3, then half-cycle 3′, and so on.

By series braiding we braid first the half-cycles $1-2-3-4-5$, then the half-cycles $1'-2'-3'-4'-5'$.

Parallel braiding:

For the string-run half-cycles $1-2-3-4-5$ or the string-run half-cycles $1'-2'-3'-4'-5'$, the algorithm diagram with $\Delta^* = 1$ is constructed in the usual way, resulting in the two inner rows of i-values. The outer two rows of i-values belong respectively to the string-run half-cycles $1'-2'-3'-4'-5'$ or to the string-run half-cycles $1-2-3-4-5$ and are derived from the inner rows of i-values by adding or subtracting in modular fashion $\frac{b}{2}$. Thus for the half-cycles $1-2-3-4-5$, the inner row of i-values are associated with their intersections with the half-cycles $1-2-3-4-5$, and the outer row of i-values are associated with their intersections with the half-cycles $1'-2'-3'-4'-5'$. For the half-cycles $1'-2'-3'-4'-5'$, the inner row of i-values are associated with their intersections with the half-cycles $1'-2'-3'-4'-5'$, and the outer row of i-values are associated with their intersections with the half-cycles $1-2-3-4-5$.

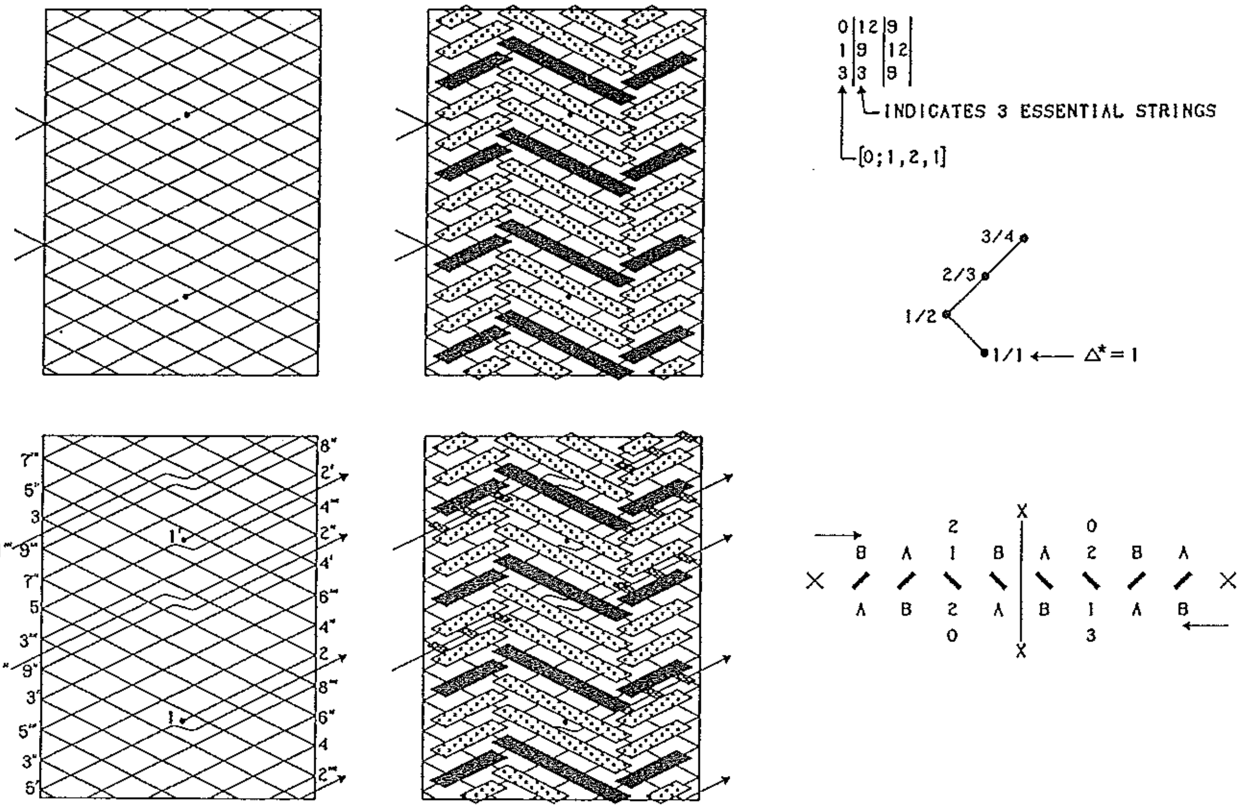

Fig. 759 — A Semi-Regular Knot with $p/b = 9/12$.

For the string-run $1-2-3-4-5$; $1'-2'-3'-4'-5'$ the half-cycle braiding algorithms are then as follows:

half-cycles 1 & 1′ : : $L \longrightarrow R$: Free run.
half-cycles 2 & 2′ : $i=0$; $i \neq 0$ left of X–X : $L \longleftarrow R$: Free run.
half-cycles 3 & 3′ : $i=0$; : $L \longrightarrow R$: u.
half-cycles 4 & 4′ : $i \leq 1$; $i \neq 1$ left of X–X : $L \longleftarrow R$: $2o$.
half-cycles 5 & 5′ : $i \leq 1$; : $L \longrightarrow R$: $2u$.

Next we interbraid the Regular Knot $1'' - 2'' - 3'' - \cdots - 8'' - 9''$, and finally we interbraid the Regular Knot $1''' - 2''' - 3''' - \cdots - 8''' - 9'''$. We position the starting-points of the half-cycles $5'$, $1''$ and $1'''$ regularly around the left-hand bight-boundary. Let half-cycle $5'$ start at bight-index number $I_0 = 0$, then half-cycle 5 starts at bight-index number $I_0' = \frac{b}{2} = 6$, half-cycle $1''$ starts at bight-index number $I_0'' = \frac{b}{3} = 4$, and half-cycle $1'''$ starts at bight-index number $I_0''' = 2 \times \frac{b}{3} = 8$. Thus from each of the positions 1 and $1'$ we have two parallel strings to the right-hand bight-boundary (hence to the right of the X—X line), ending at this bight-boundary respectively at bight-index number $I_0 = 0$ and bight-index number $I_0' = 6$. Furthermore, we have two parallel strings from each of the left bight-boundary bight-index numbers $I_0'' = 4$ and $I_0''' = 8$ to respectively the right bight-boundary bight-index numbers $I_0'' = 4$ and $I_0''' = 8$. An **even** numbered half-cycle to be laid down which will intersect such an already laid down parallel pair of strings will do so in the sequence $o - \star$ when the intersection is to the right of the X—X line and in the sequence $\star - o$ when the intersection is to the left of the X—X line. Hence for the **even** numbered half-cycles of the string-run sequence $1'' - 2'' - 3'' - \cdots - 8'' - 9''$, such intersections to the right of the X—X line are associated with the right bight-boundary bight-index numbers $I_0 = 0$ and $I_0' = 6$; there are no such intersections to the left of the X—X line. For the **even** numbered half-cycles of the string-run sequence $1''' - 2''' - 3''' - \cdots - 8''' - 9'''$, such intersections to the right of the X—X line are associated with the right bight-boundary bight-index numbers $I_0 = 0$, $I_0' = 6$, and $I_0'' = 4$, while such intersections to the left of the X—X line are associated with the right bight-boundary bight-index number $I_0'' = 4$. Thus for half-cycle $2''$, an $o - \star$ intersection occurs on the second intersection-column from the right ($|0 - 4|_b + nb = |0 - 4|_{12} + 12n = 8 + 12n$, and $|6 - 4|_b + nb = |6 - 4|_{12} + 12n = 2 + 12n = 2 + 12n$ (or $8 - 6 + nb = 2 + 12n$)). For half-cycle $4''$ there is no such an intersection ($|0 - (4 + p)|_b + nb = |0 - (4 + 9)|_{12} + 12n = 11 + 12n$, and $|6 - (4 + p)|_b + nb = |6 - (4 + 9)|_{12} + 12n = 5 + 12n$ (or $11 - 6 + nb = 5 + 12n$)). For half-cycle $6''$, an $o - \star$ intersection occurs on the second intersection-column from the right ($|0 - (4 + 2p)|_b + nb = |0 - (4 + 18)|_{12} + 12n = 2 + 12n$, and $|6 - (4 + 2p)|_b + nb = |6 - (4 + 18)|_{12} + 12n = 8 + 12n$ (or $2 + 6 + nb = 8 + 12n$)). For half-cycle $8''$ there is no such an intersection ($|0 - (4 + 3p)|_b + nb = |0 - (4 + 27)|_{12} + 12n = 5 + 12n$, and $|6 - (4 + 3p)|_b + nb = |6 - (4 + 27)|_{12} + 12n = 11 + 12n$ (or $5 + 6 + nb = 11 + 12n$)). For half-cycle $2'''$, an $o - \star$ intersection occurs on the fourth intersection-column from the right and a $\star - o$ intersection occurs on the eighth intersection-column from the right ($|0 - 8|_b + nb = |0 - 8|_{12} + 12n = 4 + 12n$, $|6 - 8|_b + nb = |6 - 8|_{12} + 12n = 10 + 12n$ (or $4 + 6 + nb = 10 + 12n$), and $|4 - 8|_b + nb = |4 - 8|_{12} + 12n = 8 + 12n$). For half-cycle $4'''$, an $o - \star$ intersection occurs on the first intersection-column from the right ($|0 - (8 + p)|_b + nb = |0 - (8 + 9)|_{12} + 12n = 7 + 12n$, $|6 - (8 + p)|_b + nb = |6 - (8 + 9)|_{12} + 12n = 1 + 12n$ (or $7 - 6 + nb = 1 + 12n$), and $|4 - (8 + p)|_b + nb = |4 - (8 + 9)|_{12} + 12n = 11 + 12n$). For half-cycle $6'''$, an $o - \star$ intersection occurs on the second and the fourth intersection-column from the right ($|0 - (8 + 2p)|_b + nb = |0 - (8 + 18)|_{12} + 12n = 10 + 12n$, $|6 - (8 + 2p)|_b + nb = |6 - (8 + 18)|_{12} + 12n = 4 + 12n$ (or $10 - 6 + nb = 4 + 12n$), and $|4 - (8 + 2p)|_b + nb = |4 - (8 + 18)|_{12} + 12n = 2 + 12n$). For half-cycle $8'''$, an $o - \star$ intersection occurs on the first intersection-column from the right and a $\star - o$ intersection occurs on the fifth intersection-column from the right ($|0 - (8 + 3p)|_b + nb = |0 - (8 + 27)|_{12} + 12n = 1 + 12n$, $|6 - (8 + 3p)|_b + nb = |6 - (8 + 27)|_{12} + 12n = 7 + 12n$ (or $1 + 6 + nb = 7 + 12n$), and $|4 - (8 + 3p)|_b + nb = |4 - (8 + 27)|_{12} + 12n = 5 + 12n$).

For the string-runs $1'' - 2'' - 3'' - \cdots - 8'' - 9''$ and $1''' - 2''' - 3''' - \cdots - 8''' - 9'''$ we thus use the following algorithm diagram:

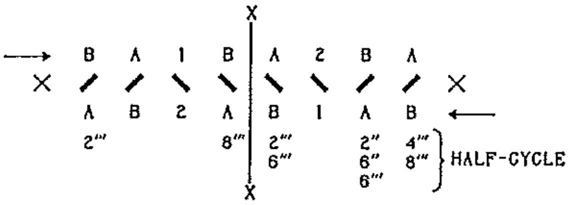

The intersections to the left of the X—X line on the first half-cycle of the string-runs $1'' - 2'' - 3'' - \cdots - 8'' - 9''$ and $1''' - 2''' - 3''' - \cdots - 8''' - 9'''$ are **unders.** The intersections to the right of the X—X line on the last half-cycle of the string-runs $1'' - 2'' - 3'' - \cdots - 8'' - 9''$ and $1''' - 2''' - 3''' - \cdots - 8''' - 9'''$ are **unders.**

For the string-run $1'' - 2'' - 3'' - \cdots - 8'' - 9''$ the half-cycle braiding algorithms are:

half-cycle $1''$: $i = A$: $L \longrightarrow R$: $2u - o$.
half-cycle $2''$: $i = A$ & $i = 0$: $L \longleftarrow R$: $o - u - o - u$.
half-cycle $3''$: $i = A$ & $i = 0$: $L \longrightarrow R$: $o - u - o$.
half-cycle $4''$: $i = A$ & $i \leq 1$: $L \longleftarrow R$: $u - 2o - u$.
half-cycle $5''$: $i = A$ & $i \leq 1$: $L \longrightarrow R$: $o - 2u - o$.
half-cycle $6''$: $i = A$ & $i \leq 2$: $L \longleftarrow R$: $o - u - 3o - u$.
half-cycle $7''$: $i = A$ & $i \leq 2$: $L \longrightarrow R$: $o - 3u - o$.
half-cycle $8''$: $i = A$ & $i \leq 3$: $L \longleftarrow R$: $u - 3o - u$.
half-cycle $9''$: $i = A$ & $i \leq 3$: $L \longrightarrow R$: $o - 4u$.

For the string-run $1''' - 2''' - 3''' - \cdots - 8''' - 9'''$ the half-cycle braiding algorithms are:

half-cycle $1'''$: $i = A, B$: $L \longrightarrow R$: $4u - 2o$.
half-cycle $2'''$: $i = A, B$ & $i = 0$: $L \longleftarrow R$: $2u - 3o - 2u - o$.
half-cycle $3'''$: $i = A, B$ & $i = 0$: $L \longrightarrow R$: $2o - 2u - 2o$.
half-cycle $4'''$: $i = A, B$ & $i \leq 1$: $L \longleftarrow R$: $o - 2u - 3o - 2u$.
half-cycle $5'''$: $i = A, B$ & $i \leq 1$: $L \longrightarrow R$: $2o - 3u - 2o$.
half-cycle $6'''$: $i = A, B$ & $i \leq 2$: $L \longleftarrow R$: $u - o - u - 5o - 2u$.
half-cycle $7'''$: $i = A, B$ & $i \leq 2$: $L \longrightarrow R$: $2o - 4u - 2o$.
half-cycle $8'''$: $i = A, B$ & $i \leq 3$: $L \longleftarrow R$: $o - 2u - 5o - 2u$.
half-cycle $9'''$: $i = A, B$ & $i \leq 3$: $L \longrightarrow R$: $2o - 6u$.

Series braiding:

Series braiding affects only the braiding of the sequence $1 - 2 - 3 - 4 - 5$; $1' - 2' - 3' - 4' - 5'$ which is then braided in the sequence $1 - 2 - 3 - 4 - 5$; $5^* - 6 - 7 - 8 - 9$.

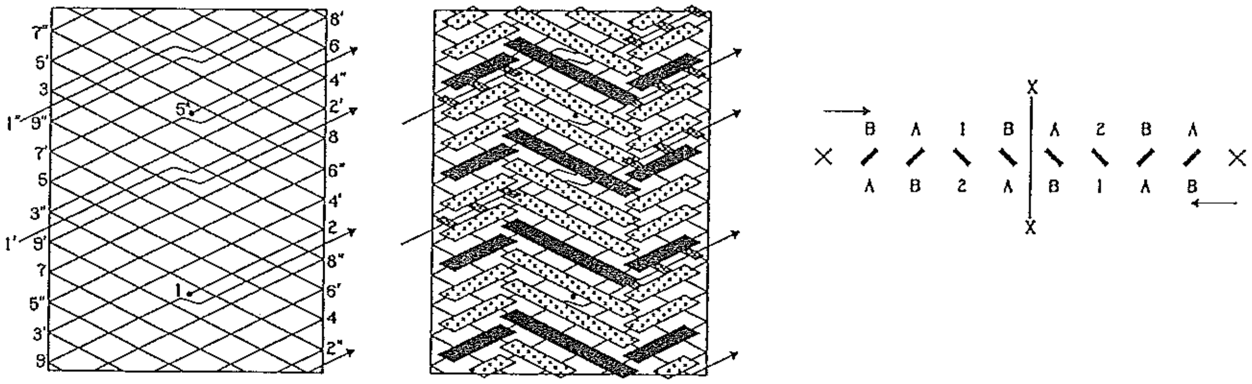

Fig. 760 — Half-cycle numbering for series braiding.

THE BRAIDER

No.42 **MAY 2005.**

CONTENTS

pg.
Braided Slit Braids 981
The Components of Semi-Perfect Herringbone Pineapple Knots 993

A quarterly publication
for
the braiding artisan

Resale of this publication or copies thereof
is strictly prohibited

Copyright ©2005 by:

A.G. Schaake; 21 Sundown Cresc.; Hamilton; New Zealand.
D. Van Tassel; Box 335; Craig, Co 81626-0335; U.S.A.
F.J.M. Masurel; Ganzenzijde 4; 2317XG Leiden; Nederland.

All rights reserved. No part of this publication may be reproduced, stored in a retrieval system, or transmitted, in any form or by any means, electronic, mechanical, photo-copying, recording, or otherwise, without prior written permission.

This publication is available to braiding artisans only.

Copies may be obtained from:

A.G. Schaake,
21 Sundown Cresc.,
Hamilton,
New Zealand.

Braided Slit Braids

Slit braids have been discussed in many different publications. In *The Braider*, Issue No. 1, pp. 13-15, can be found an article on basic slit braids which goes into much greater detail than is found in other publications.

In Bruce Grant's book *The Encyclopedia of Rawhide and Leather Braiding* these basic slit braids can be found on pp. 50, 51, 68, 69, 200 and 201. The written instructions for a somewhat different slit braid can be found in the 4th paragraph on pg. 200 with its associated drawings in figs. 4, 5, 6 and 7 on pg. 201. His text calls this a '-- *more fancy method of making this braid*--' and the desired result is depicted in fig. 6 where the view of the edges gives the appearance of a four-string braid. This is a simple form of a **braided slit braid** and one in which, although the idea is not difficult to understand, the braiding process itself can easily result in a final product with not the best of appearances.

A **braided slit braid** of much greater quality was noted as being a part of, and the attachment for, a quirt lash. The quirt was made by a Mexican sheepherder using mostly scraps of old leather recycled from worn out horse equipment. While the materials used were of generally only fair to poor quality, the braiding skills were quite good.

The braid has a square cross-section as shown in the centre of Fig. 761. If side 'a' has the appearance shown to the left of the cross-section view in Fig. 761, then side 'b' will be the mirror-image of side 'a'. If side 'c' has the appearance shown to the right of the cross-section view in Fig. 761, then side 'd' will be identical to side 'c'.

While there are, no doubt, many applications for these braided slit braids, we will limit our discussion to the general construction process needed to make similar quirt lashes. The lash as drawn in Fig. 761 is braided from three straps of leather. We will return to this braid shortly, but first we can look at a two strap braid. The preferred material used for these lashes is leather or rawhide.

In Fig. 762 is depicted a similar braided lash, but made from two straps rather than three. Again the braid will have a square cross-section as shown in the centre of Fig. 762. If side 'a' has the appearance shown to the left of the cross-section view in Fig. 762, then side 'b' will be the mirror-image of side 'a'. If side 'c' has the appearance shown to the right of the cross-section view in Fig. 762, then side 'd' will be identical to side 'c'.

This braid may be made as follows using two straps of material. In Fig. 763, top row left, the outermost strap is on the left labelled and identified as strand 1 while on the right it is labelled and identified as strand 2. The innermost strap is on the left labelled and identified as strand 3 while on the right it is labelled and identified as strand 4. This gives an initial left to right strand order of 1–3–4–2. Strand 1 is shown with its initial slit cut in for braiding to begin. The braiding proceeds as follows:

> **Fig. 763, top row right** — Pass strand 3 through the slit made in strand 1. This will result in the left to right strand order 3–1–4–2. Cut a slit in strand 2.
>
> **Fig. 763, bottom row left** — Pass strand 4 then strand 1 through the slit made in strand 2. This will result in the left to right strand order 3–2–1–4. Cut a slit in strand 3.
>
> **Fig. 763, bottom row centre** — Pass strand 2 through the slit made in strand 3. This will result in the left to right strand order 2–3–1–4. Cut a slit in strand 4.

Fig. 763, bottom row right — Pass strand 1 then strand 3 through the slit made in strand 4. This will result in the left to right strand order 2–4–3–1.

This completes half a periodic sequence of the braid. If the flesh-side of the leather or rawhide is outermost on the two straps at the beginning of the braid as depicted in Fig. 763, top row left, then at the completion of the stage depicted in Fig. 763, bottom row right, the braid will have the appearance of Fig. 762 where the braided portion has the flesh-side outermost while the remainder of the lash-strands will have the hair-side outermost.

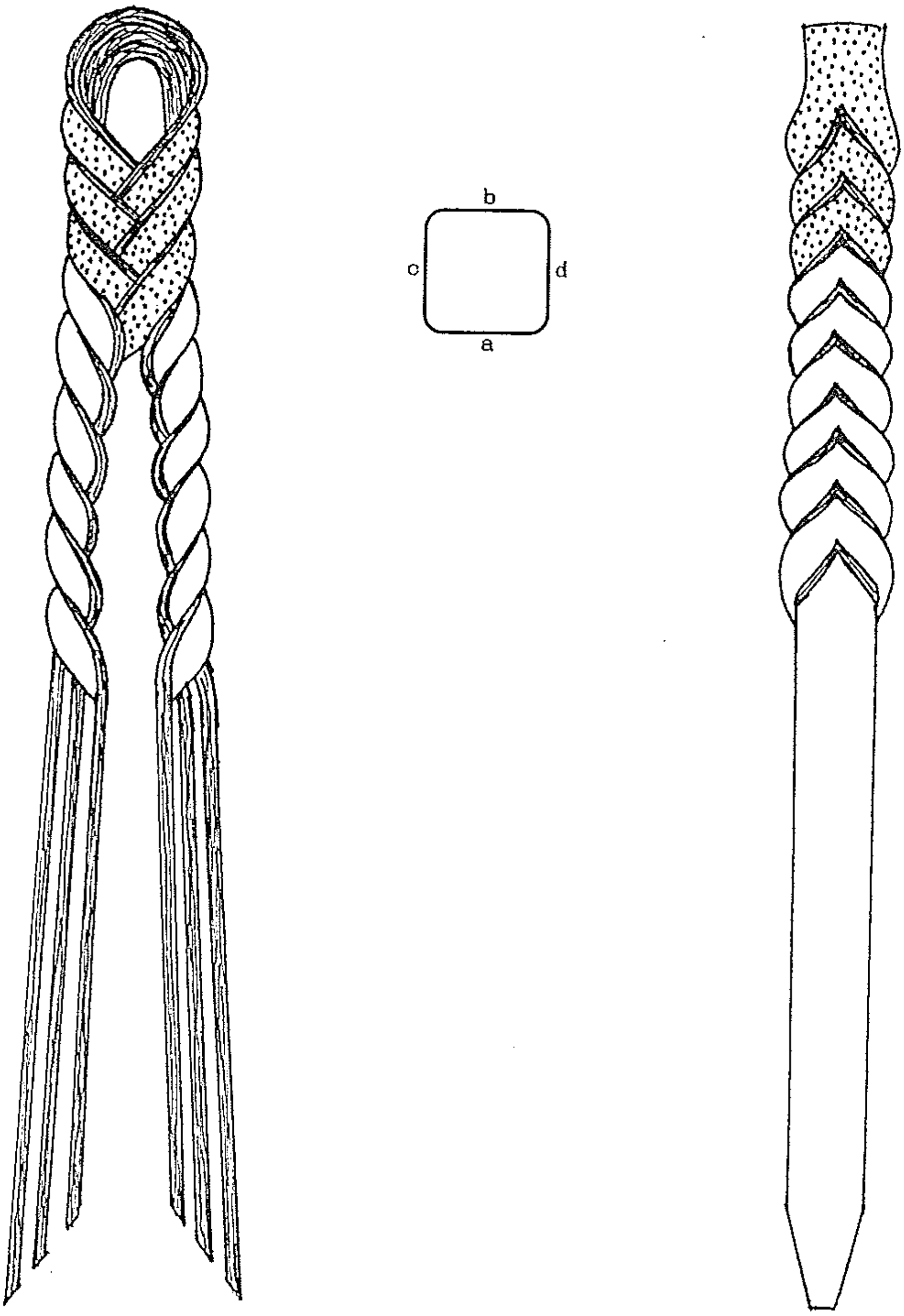

Fig. 761 — A braided slit braid made from three straps.

To continue the braid beyond the stage depicted in Fig. 763, bottom row right, we begin by cutting a slit in strand 2. Then:

1. — Pass strand 4 through the slit made in strand 2. This will result in the left to right strand order 4–2–3–1. Cut a slit in strand 1.

2. — Pass strand 3 then strand 2 through the slit made in strand 1. This will result in the left to right strand order 4–1–2–3. Cut a slit in strand 4.

3. — Pass strand 1 through the slit made in strand 4. This will result in the left to right strand order 1–4–2–3. Cut a slit in strand 3.

4. — Pass strand 2 then strand 4 through the slit made in strand 3. This will result in the left to right strand order 1–3–4–2.

This completes the consecutive half periodic sequence (the second half periodic sequence) of the braid, and hence a full periodic sequence of the braid has been completed. The final left to right strand order 1–3–4–2 is identical to that shown in Fig. 763, top row left. The second half periodic sequence will have doubled the length of the braided portion shown in Fig. 762, but the additional braided portion will have the hair-side outermost. The remainder of the lash-strands will now have the flesh-side outermost.

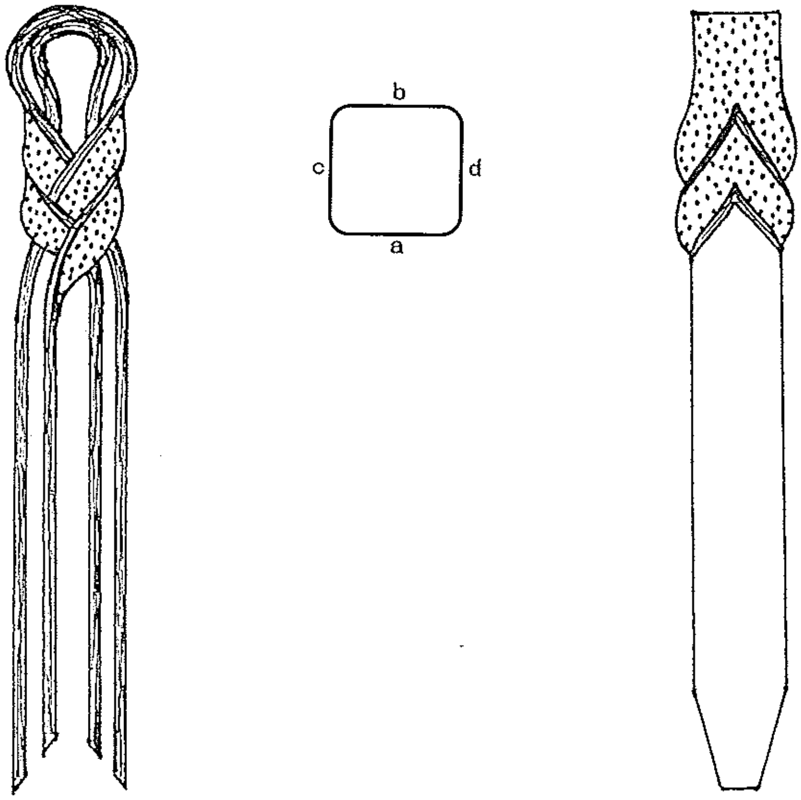

Fig. 762 — A braided slit braid made from two straps.

The braid may be continued for any length by repeating the steps beginning with the step shown in Fig. 763, top row left, and ending at the completion of any half periodic sequence.

The braided slit braid can easily be extended to a three or more strap braid. It will again have a square cross-section as shown in the centre of Fig. 764 for a three strap braided slit braid. If side 'a' has the appearance shown to the left of the cross-section view in Fig. 764, then side 'b' will be the mirror-image of side 'a'. If side 'c' has the appearance shown to the right of the cross-section view in Fig. 764, then side 'd' will be identical to side 'c'.

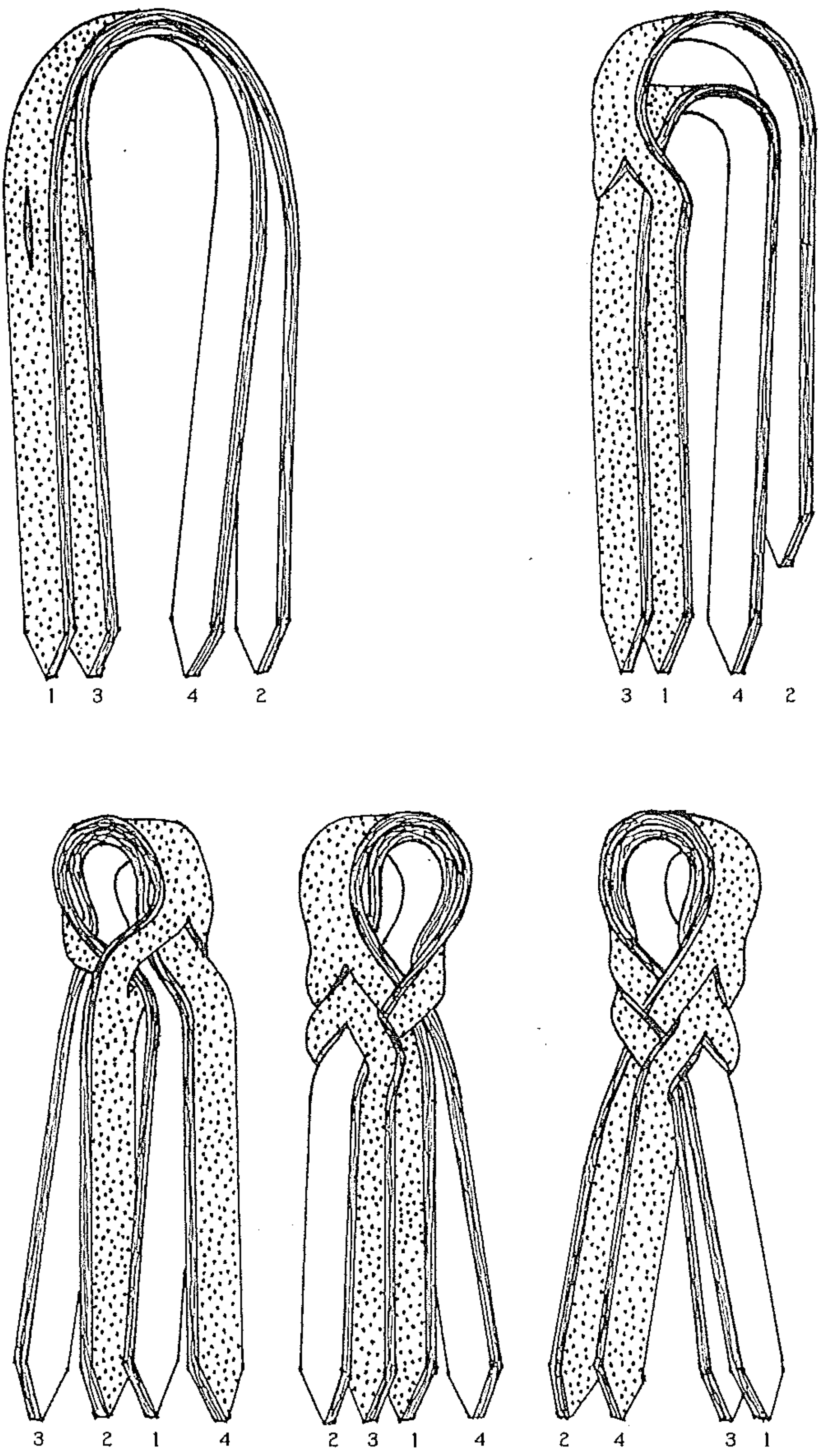

Fig. 763 — Braiding the first half periodic sequence of a two strap braided slit braid.

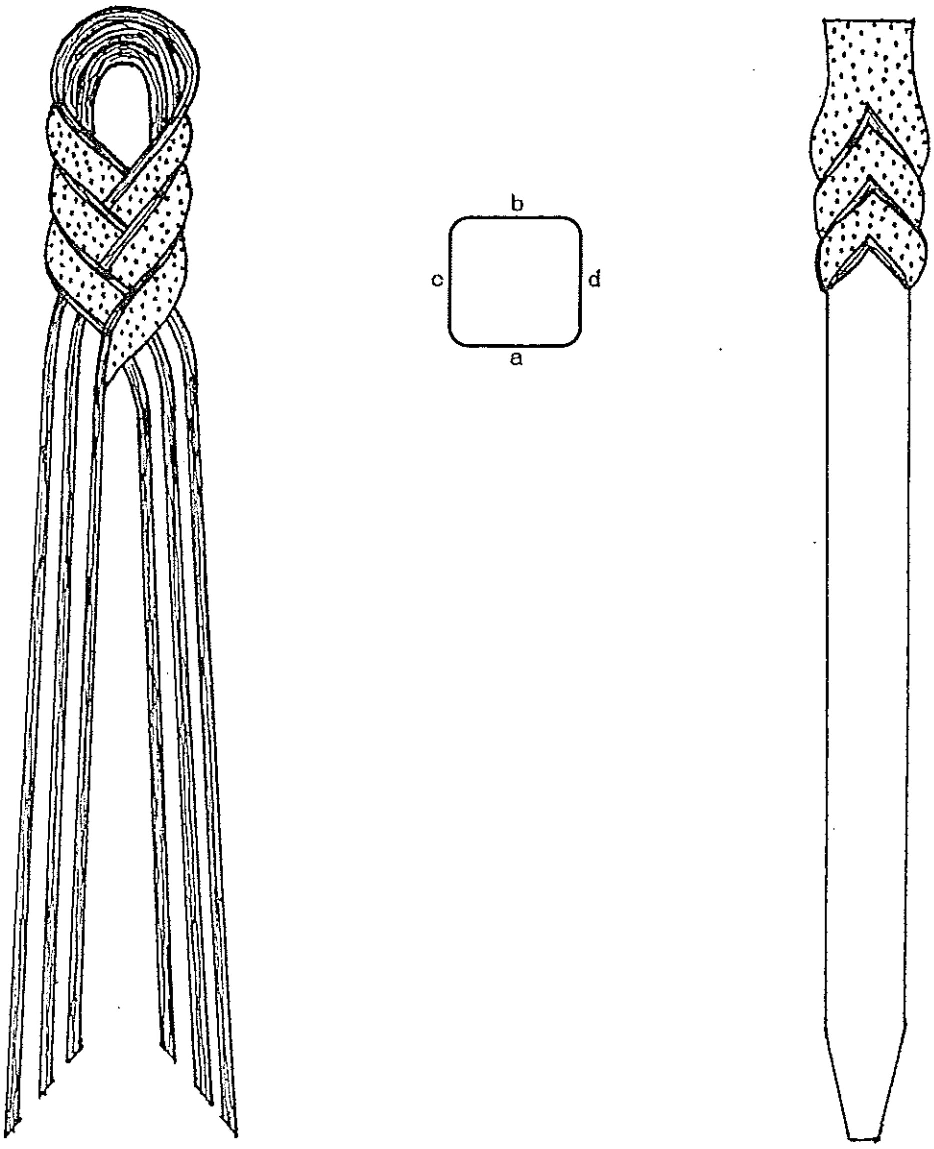

Fig. 764 — A braided slit braid made from three straps.

This three strap braided slit braid may be made as follows:

In the leftmost drawing of Fig. 765 the outermost strap is on the left labelled and identified as strand 1 while on the right it is labelled and identified as strand 2. The middle strap is on the left labelled and identified as strand 3 while on the right it is labelled and identified as strand 4. The innermost strap is on the left labelled and identified as strand 5 while on the right it is labelled and identified as strand 6. This gives an initial left to right strand order of 1–3–5–6–4–2. Strand 1 is shown with its initial slit cut in for braiding to begin. The braiding proceeds as follows:

Fig. 765, central drawing — Pass strand 3 and then strand 5 through the slit made in strand 1. This will result in the left to right strand order 3–5–1–6–4–2. Cut a slit in strand 2.

Fig. 765, rightmost drawing — Pass strand 4 then strand 6 then strand 1 through the slit made in strand 2. This will result in the left to right strand order 3–5–2–1–6–4. Cut a slit in strand 3.

— Pass strand 5 then strand 2 through the slit made in strand 3. This will

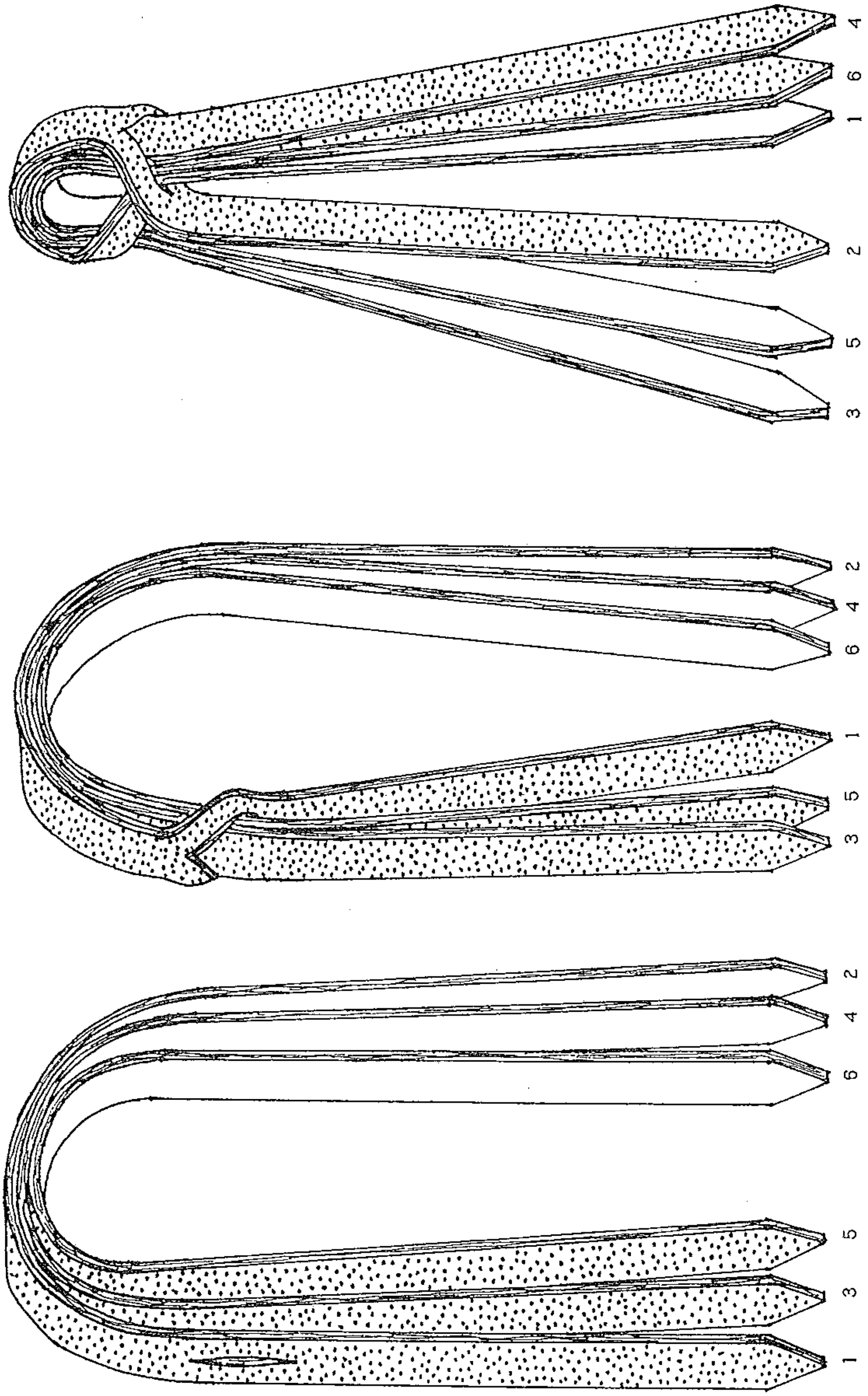

Fig. 765 — The initial steps in braiding the first half periodic sequence of a three strap braided slit braid.

result in the left to right strand order 5–2–3–1–6–4. Cut a slit in strand 4.
— Pass strand 6 then strand 1 then strand 3 through the slit made in strand 4. This will result in the left to right strand order 5–2–4–3–1–6. Cut a slit in strand 5.
— Pass strand 2 then strand 4 through the slit made in strand 5. This will result in the left to right strand order 2–4–5–3–1–6. Cut a slit in strand 6.
— Pass strand 1 then strand 3 then strand 5 through the slit made in strand 6. This will result in the left to right strand order 2–4–6–5–3–1.

This completes half a periodic sequence of the braid. If the flesh-side of the leather or rawhide is outermost on the three straps at the beginning of the braid as depicted in the leftmost drawing of Fig. 765 then at the completion of the first half periodic sequence of the braid, the braid will have the appearance of Fig. 764 where the braided portion has the flesh-side outermost while the remainder of the lash-strands will have the hair-side outermost.

To continue the braid through the next half periodic sequence we begin by cutting a slit in strand 2. Then:

1. — Pass strand 4 then strand 6 through the slit made in strand 2. This will result in the left to right strand order 4–6–2–5–3–1. Cut a slit in strand 1.
2. — Pass strand 3 then strand 5 then strand 2 through the slit made in strand 1. This will result in the left to right strand order 4–6–1–2–5–3. Cut a slit in strand 4.
3. — Pass strand 6 then strand 1 through the slit made in strand 4. This will result in the left to right strand order 6–1–4–2–5–3. Cut a slit in strand 3.
4. — Pass strand 5 then strand 2 then strand 4 through the slit made in strand 3. This will result in the left to right strand order 6–1–3–4–2–5. Cut a slit in strand 6.
5. — Pass strand 1 then strand 3 through the slit made in strand 6. This will result in the left to right strand order 1–3–6–4–2–5. Cut a slit in strand 5.
6. — Pass strand 2 then strand 4 then strand 6 through the slit made in strand 5. This will result in the left to right strand order 1–3–5–6–4–2.

This completes the consecutive (the second) half periodic sequence of the braid, and hence a full periodic sequence of the braid has been completed. The final left to right strand order 1–3–5–6–4–2 is identical to that shown in the leftmost drawing of Fig. 765. The second half periodic sequence will have doubled the length of the braided portion shown in Fig. 764, but the additional braided portion will have the hair-side outermost. The remainder of the lash-strands will now have the flesh-side outermost.

The braid may be continued for any length by repeating the steps beginning with the step shown in the leftmost drawing of Fig. 765, and ending at the completion of any half periodic sequence. Also at the end of any half periodic sequence we can begin the basic slit braid as shown on pg. 201, figs. 1 , 2 and 3 in Grant's *Encyclopedia of Rawhide and Leather Braiding* using three strands in each braid. Then the braid will appear as used on the Mexican quirt and shown in Fig. 761.

We can also make similar quirt lashes by making the braided slit braid reversed to what is normal procedure. Such a braid is every bit as good as the braids shown above.

As in all braided slit braids a careful placement of the slits is critical to the appearance of the finished product. Smooth face pliers are very useful in making these reversed braided slit braids lie properly.

For a two strap lash the braid will again have a square cross-section as shown in the centre of Fig. 766.

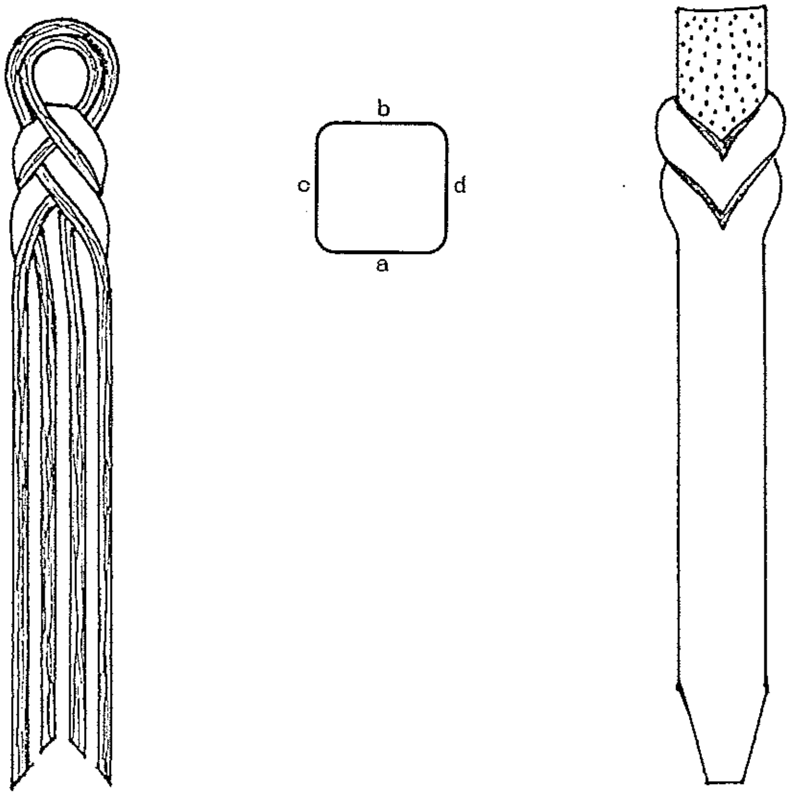

Fig. 766 — A reversed braided slit braid made from two straps.

If side 'a' has the appearance shown to the left of the cross-section view in Fig. 766, then side 'b' will be the mirror-image of side 'a'. If side 'c' has the appearance shown to the right of the cross-section view in Fig. 766, then side 'd' will be identical to side 'c'.

This braided slit braid may be made as follows using two straps of material. In Fig. 767, top row left, the innermost strap is on the left labelled and identified as strand 1 while on the right it is labelled and identified as strand 2. The outermost strap is on the left labelled and identified as strand 3 while on the right it is labelled and identified as strand 4. This gives an initial left to right strand order of 3–1–2–4. Strand 1 is shown with its initial slit cut in for braiding to begin. The braiding proceeds as follows:

Fig. 767, top row right — Pass strand 2 then strand 4 through the slit made in strand 1. This will result in the left to right strand order 3–2–4–1. Cut a slit in strand 2.

Fig. 767, bottom row left — Pass strand 3 through the slit made in strand 2. This will result in the left to right strand order 2–3–4–1. Cut a slit in strand 3.

Fig. 767, bottom row centre — Pass strand 4 then strand 1 through the slit made in strand 3. This will result in the left to right strand order 2–4–1–3. Cut a slit in strand 4.

Fig. 767, bottom row right — Pass strand 2 through the slit made in strand 4. This will result in the left to right strand order 4–2–1–3.

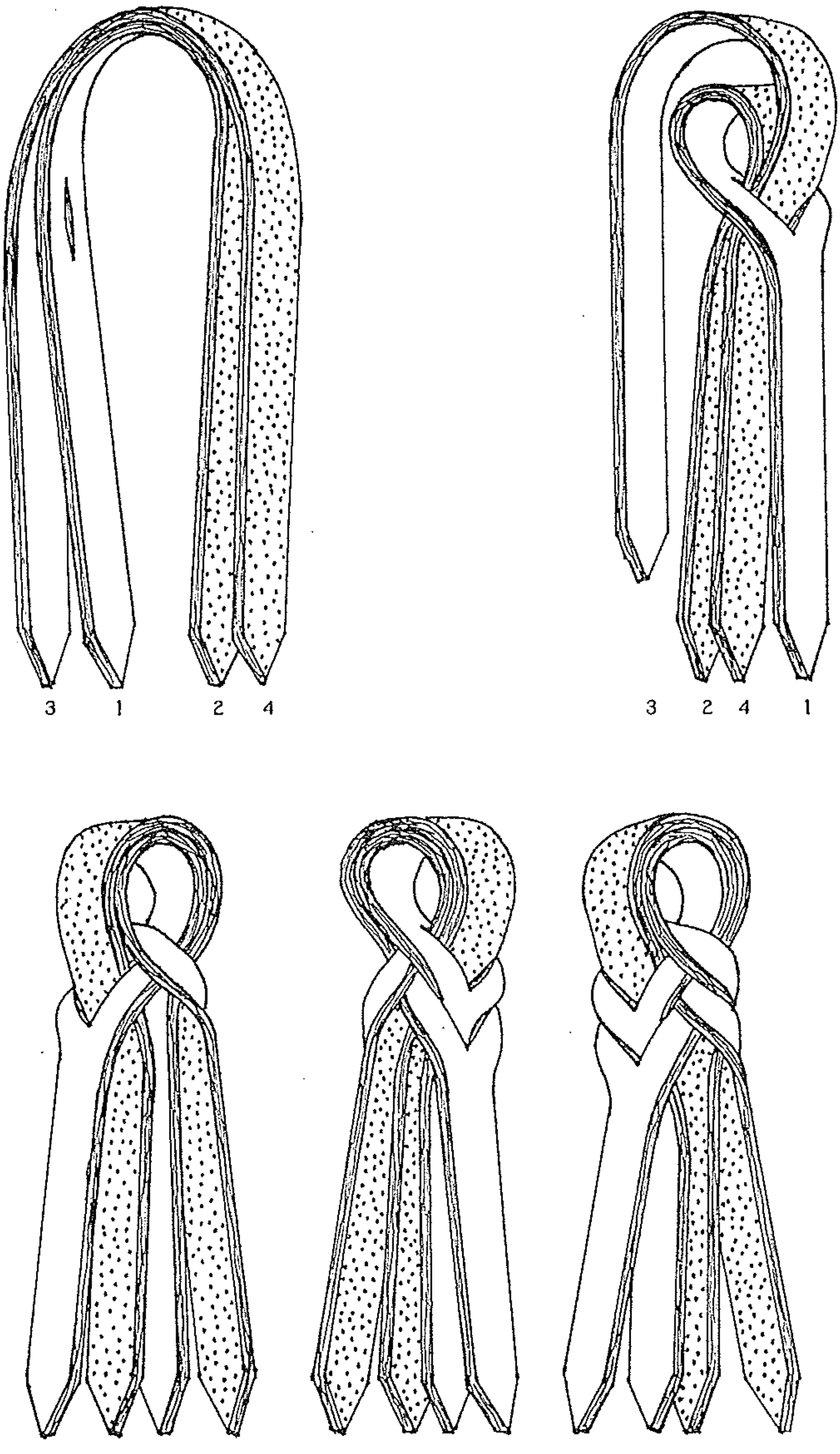

Fig. 767 — Braiding the first half periodic sequence of a two strap reversed braided slit braid.

This completes half a periodic sequence of the braid. If the flesh-side of the leather or rawhide is outermost on the two straps at the beginning of the braid as depicted in Fig. 767, top row left, then at the completion of the stage depicted in Fig. 767, bottom row right, the braid will have the appearance of Fig. 765 where the braided portion and the remainder of the lash strands have the hair-side outermost.

To continue the braid beyond the stage depicted in Fig. 767, bottom row right, we begin by cutting a slit in strand 2. Then:

1. — Pass strand 1 then strand 3 through the slit made in strand 2. This will result in the left to right strand order 4–1–3–2. Cut a slit in strand 1.
2. — Pass strand 4 through the slit made in strand 1. This will result in the left to right strand order 1–4–3–2. Cut a slit in strand 4.
3. — Pass strand 3 then strand 2 through the slit made in strand 4. This will result in the left to right strand order 1–3–2–4. Cut a slit in strand 3.
4. — Pass strand 1 through the slit made in strand 3. This will result in the left to right strand order 3–1–2–4.

This completes the consecutive half periodic sequence of the braid, and hence a full periodic sequence of the braid has been completed. The final left to right strand order 3–1–2–4 is identical to that shown in Fig. 767, top row left. The second half periodic sequence will have doubled the length of the braided portion shown in Fig. 766, but the additional braided portion as well as the remainder of the lash strands will have the flesh-side outermost.

The braid may be continued for any length by repeating the steps beginning with the step shown in Fig. 767, top row left, and ending at the completion of any half periodic sequence.

The reversed braided slit braid can easily be extended to a three or more strap braid. It will again have a square cross-section as shown in the centre of Fig. 768 for a three strap reversed braided slit braid. If side 'a' has the appearance shown to the left of the cross-section view in Fig. 768, then side 'b' will be the mirror-image of side 'a'. If side 'c' has the appearance shown to the right of the cross-section view in Fig. 764, then side 'd' will be identical to side 'c'.

This three strap braided slit braid may be made as follows:

In the leftmost drawing of Fig. 769 the innermost strap is on the left labelled and identified as strand 1 while on the right it is labelled and identified as strand 2. The middle strap is on the left labelled and identified as strand 3 while on the right it is labelled and identified as strand 4. The outermost strap is on the left labelled and identified as strand 5 while on the right it is labelled and identified as strand 6. This gives an initial left to right strand order of 5–3–1–2–4–6. Strand 1 is shown with its initial slit cut in for braiding to begin. The braiding proceeds as follows:

Fig. 769, central drawing — Pass strand 2 then strand 4 then strand 6 through the slit made in strand 1. This will result in the left to right strand order 5–3–2–4–6–1. Cut a slit in strand 2.

Fig. 765, rightmost drawing — Pass strand 3 then strand 5 through the slit made in strand 2. This will result in the left to right strand order 2–5–3–4–6–1. Cut a slit in strand 3.

— Pass strand 4 then strand 6 then strand 1 through the slit made in strand 3. This will result in the left to right strand order 2–5–4–6–1–3. Cut a slit in strand 4.

— Pass strand 5 then strand 2 through the slit made in strand 4. This will result in the left to right strand order 4–2–5–6–1–3. Cut a slit in strand 5.

— Pass strand 6 then strand 1 then strand 3 through the slit made in strand 5. This will result in the left to right strand order 4–2–6–1–3–5. Cut a slit in strand 6.
— Pass strand 2 then strand 4 through the slit made in strand 6. This will result in the left to right strand order 6–4–2–1–3–5.

This completes half a periodic sequence of the braid. If the flesh-side of the leather or rawhide is outermost on the three straps at the beginning of the braid as depicted in the leftmost drawing of Fig. 769 then at the completion of the first half periodic sequence of the braid, the braid will have the appearance of Fig. 768 where the braided portion and the remainder of the lash strands will have the hair-side outermost.

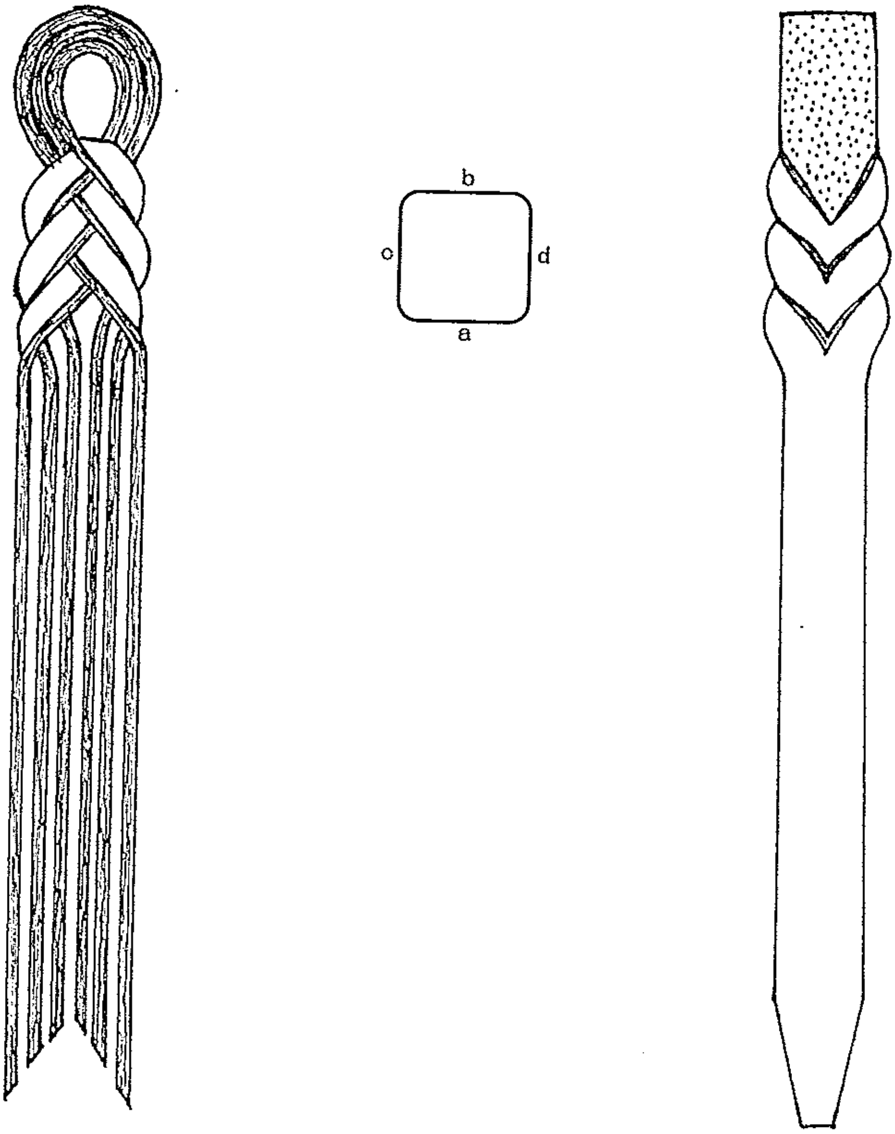

Fig. 768 — A reversed braided slit braid made from three straps.

To continue the braid through the next half periodic sequence we begin by cutting a slit in strand 2. Then:

1. — Pass strand 1 then strand 3 then strand 5 through the slit made in strand 2. This will result in the left to right strand order 6–4–1–3–5–2. Cut a slit in strand 1.
2. — Pass strand 4 then strand 6 through the slit made in strand 1. This

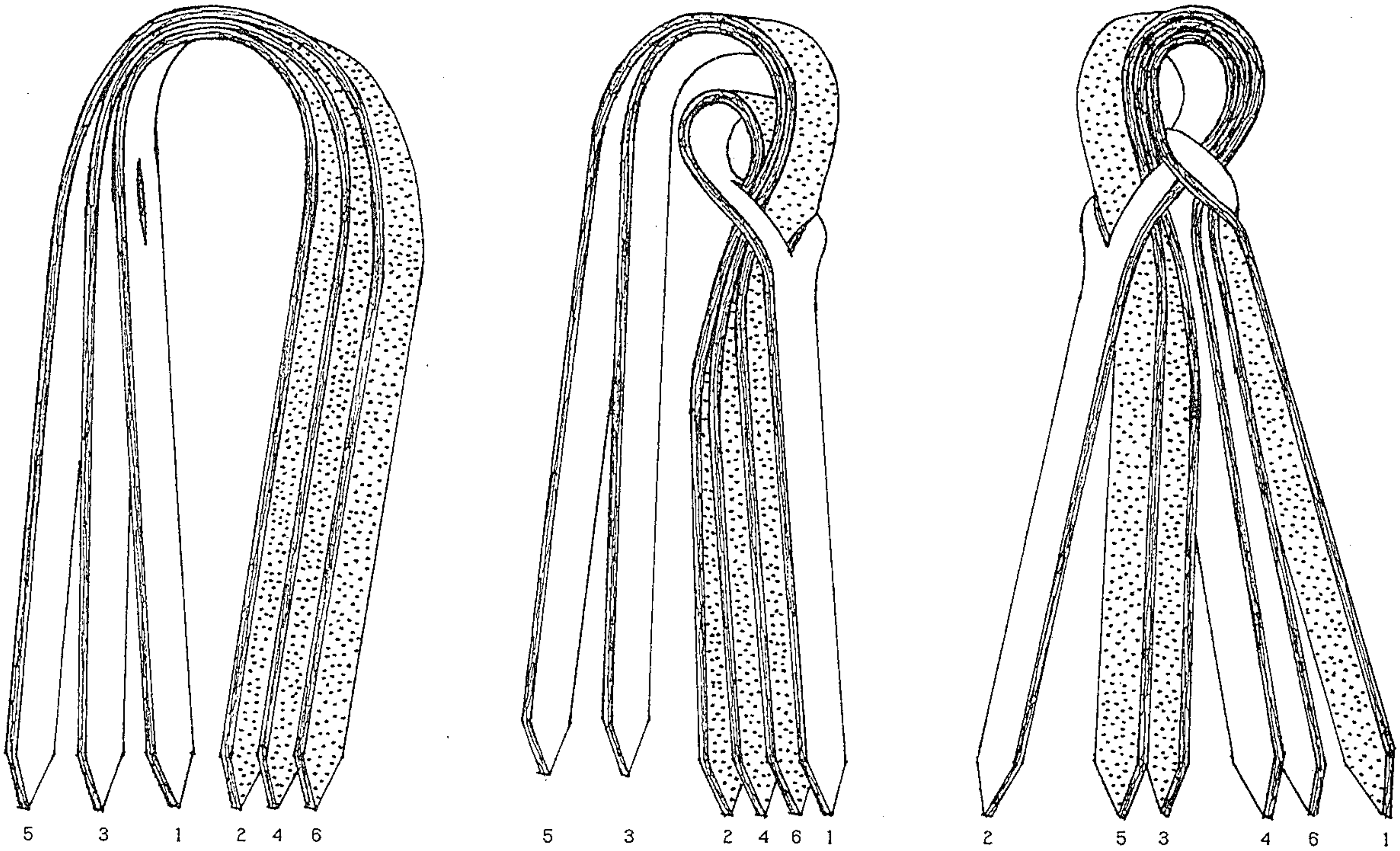

Fig. 769 — The initial steps in braiding the first half periodic sequence of a three strap reversed braided slit braid.

will result in the left to right strand order 1–6–4–3–5–2. Cut a slit in strand 4.

3. — Pass strand 3 then strand 5 then strand 2 through the slit made in strand 4. This will result in the left to right strand order 1–6–3–5–2–4. Cut a slit in strand 3.

4. — Pass strand 6 then strand 1 through the slit made in strand 3. This will result in the left to right strand order 3–1–6–5–2–4. Cut a slit in strand 6.

5. — Pass strand 5 then strand 2 then strand 4 through the slit made in strand 6. This will result in the left to right strand order 3–1–5–2–4–6. Cut a slit in strand 5.

6. — Pass strand 1 then strand 3 through the slit made in strand 5. This will result in the left to right strand order 5–3–1–2–4–6.

This completes the second consecutive half periodic sequence of the braid, and hence a full periodic sequence of the braid has been completed. The final left to right strand order 5–3–1–2–4–6 is identical to that shown in the leftmost drawing of Fig. 769. The second half periodic sequence will have doubled the length of the braided portion shown in Fig. 768, but the additional braided portion will have the flesh-side outermost. Also the remainder of the lash-strands will now have the flesh-side outermost.

The braid may be continued for any length by repeating the steps beginning with the step shown in the leftmost drawing of Fig. 769, and ending at the completion of any half periodic sequence.

All of these lash braids are most easily formed with the loop above the braid, fitting snug around an object. Arrangements of straps of different colours can be used for colour-patterns in the braided portions of the braids.

The Components of Semi-Perfect Herringbone Pineapple Knots

The overall string-run of all the components combined is characterised by either $y = A - 1$ or by $y = A + 1$.[†] Since $\Delta = A - 1$ for $y = A - 1$, and $\Delta = 1$ for $y = A + 1$ for these knots, the first-return string-run of a component visits each bight-boundary once (since $\text{g.c.d.}(A, \Delta) = 1 = \gamma$; hence since $\gamma = 1$, it follows that $\alpha = A$).[‡] Since $\alpha = A$, the number of components $\lambda = \text{g.c.d.}(B^*, P_{total})$ in a Semi-Perfect Herringbone Pineapple Knot are identical, and hence the Standing-End of each component can be placed at left bight-boundary 1. Consequently, the consecutive λ components have their Standing-Ends in consecutive nests at left bight-boundary 1. Note that the string-run of a component consists of one or more first-return string-runs ($\frac{B^*}{\lambda}$ first-return string-runs per component).

Let the λ components be divided into z sets, such that the string-run of a set is regularly distributed in the overall string-run of the knot. Hence when the components of a set have a colour that differs from the colour of the components of another set or from the colour of the components of some other sets, we obtain a regularly distributed colour-pattern. Note that each of the z sets of components consists of $\frac{\lambda}{z}$ components, and that when $z = 1$ there is no regular distributed colour-pattern since all components have then the same colour.

[†] See *The Braider*, Issue No. 28, pp. 644–645.

[‡] See *The Braider*, Issue No. 25, pg. 570.

If the Standing-End of the first component of a set is at left bight-boundary 1 of nest m, where $1 \leq m \leq B^*$, then the string-run of this set visits left bight-boundary 1 of nests $|m + nz|_{B^*}$, where n is a natural number. Hence the regular distribution of the string-run of a set must take place in z consecutive nests, thus in z consecutive nests the string-run of a set must visit each bight-boundary once.

Fig. 770 schematically shows two consecutive nests. Observe that $A = (r+1)z + t$, where $r = 0, 1, 2, 3, \cdots$ for $A \geq 3$. Note that either $2t - z = 0$, hence $z = 2t$, or that $2t - z = z$, hence $z = t$. When $z = t$, the two consecutive nests are identical and hence z must be 1; consequently there cannot be a regular distributed colour-pattern. When $z = 2t$, there are only two different consecutive nests, hence z must be 2 and $t = 1$, consequently A must be odd and λ must be even (hence B^* must be even).

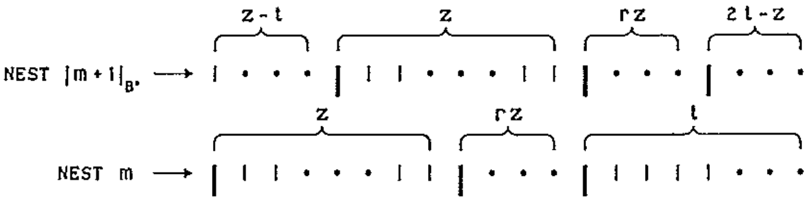

Fig. 770 — Two consecutive nests.

From the coding of an A-pass Semi-Perfect Herringbone Pineapple Knot, which requires $y = A - 1$ or $y = A + 1$ for its string-run, it follows that only two regular distributed colour-patterns are possible. Their appearance is that of spiralling zigzags with a left helix for $y = A + 1$, or with a right helix for $y = A - 1$ (see for example Fig. 771; for the two components the string-run and coding are shown on the right).

The string-run of each of the two component sets is that of a Periodic Regular Nested Cylindrical Braid (see *The Braider*, Issue No. 34) with $A_{l_1} = A_{r_1} = \frac{A+1}{2}$ and $A_{l_2} = A_{r_2} = \frac{A-1}{2}$. Since for the Semi-Perfect Herringbone Pineapple Knot $k = \left|\frac{x-A-1}{2}\right|_A$ when $y = A - 1$, or $k = \left|\frac{x-A-3}{2}\right|_A$ when $y = A + 1$, it follows that for each of the two component sets $k_{cs} = k$ and $x_{cs} = \frac{x}{2}$, furthermore that $y_{cs} = \left|\frac{x}{2} - (k+1)\right|_{2A}$ when $k = odd$ or that $y_{cs} = \left|\frac{x}{2} + A - (k+1)\right|_{2A}$ when $k = even$. The string-run specification for each of the two Periodic Regular Nested Cylindrical Braids is thus as follows:

$$\begin{aligned}&(111\cdots1/\tfrac{x}{2}/111\cdots1)\{(1)_1\,(A-1)_A\,(A-3)_{(A-1)}\,(A-5)_{(A-2)}\cdots(4)_{(A_{l_1}+2)}\\&(2)_{(A_{l_1}+1)}\,(A)_{(A_{l_1})}\,(A-2)_{(A_{l_1}-1)}\cdots(5)_{(3)}\,(3)_{(2)}\,/\\&(k)_{(1)}\,(k+2)_{(2)}\,(k+4)_{(3)}\cdots(2A_{r_2}-1)_{(A_{r_2}-\frac{k-1}{2})}\,(2A_{r_2}+1)_{(A_{r_2}+1-\frac{k-1}{2})}\\&(2)_{(A_{r_2}+2-\frac{k-1}{2})}\,(4)_{(A_{r_2}+3-\frac{k-1}{2})}\cdots(2A_{r_2}-2)_{(2A_{r_2}-\frac{k-1}{2})}\,(2A_{r_2})_{(2A_{r_2}+1-\frac{k-1}{2})}\\&(1)_{(2A_{r_2}+2-\frac{k-1}{2})}\,(3)_{(2A_{r_2}+3-\frac{k-1}{2})}\cdots(k-4)_{(2A_{r_2})}\,(k-2)_{(2A_{r_2}+1)}\}B \text{ for } k = odd\text{, or}\end{aligned}$$

$$\begin{aligned}&(111\cdots1/\tfrac{x}{2}/111\cdots1)\{(1)_1\,(A-1)_A\,(A-3)_{(A-1)}\,(A-5)_{(A-2)}\cdots(4)_{(A_{l_1}+2)}\\&(2)_{(A_{l_1}+1)}\,(A)_{(A_{l_1})}\,(A-2)_{(A_{l_1}-1)}\cdots(5)_{(3)}\,(3)_{(2)}\,/\\&(k)_{(1)}\,(k+2)_{(2)}\,(k+4)_{(3)}\cdots(2A_{r_2}-2)_{(A_{r_2}-\frac{k}{2})}\,(2A_{r_2})_{(A_{r_2}+1-\frac{k}{2})}\\&(1)_{(A_{r_2}+2-\frac{k}{2})}\,(3)_{(A_{r_2}+3-\frac{k}{2})}\cdots(2A_{r_2}-1)_{(2A_{r_2}+1-\frac{k}{2})}\,(2A_{r_2}+1)_{(2A_{r_2}+2-\frac{k}{2})}\\&(2)_{(2A_{r_2}+3-\frac{k}{2})}\,(4)_{(2A_{r_2}+4-\frac{k}{2})}\cdots(k-4)_{(2A_{r_2})}\,(k-2)_{(2A_{r_2}+1)}\}B \text{ for } k = even.\end{aligned}$$

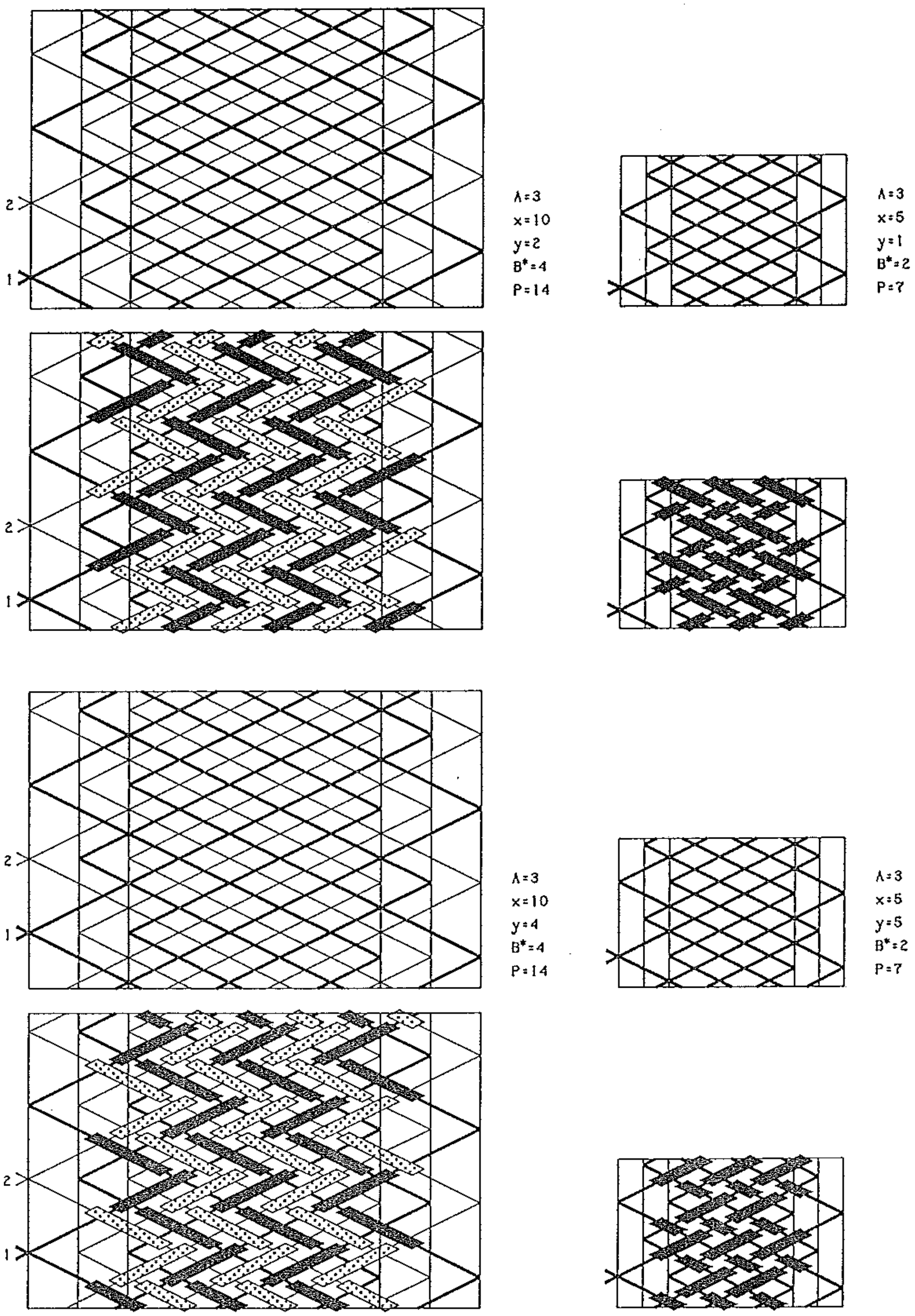

Fig. 771 — Two Semi-Perfect Herringbone Pineapple Knots.
Upper diagrams for $y = A - 1$; lower diagrams for $y = A + 1$.

The lowermost string-run diagram in Fig. 772 shows the string-run of a two component Regular Nested Cylindrical Braid on which a Herringbone Pineapple coding can be superimposed ($y = A - 1$). The third diagram from the top shows the string-run of each Periodic Regular Nested component. This string-run can be thought to be derived (via the second diagram from the top) from the string-run of the Regular Nested Cylindrical Braid shown in the uppermost diagram. This Regular Nested Cylindrical Braid consists of three Periodic Regular Nested components.

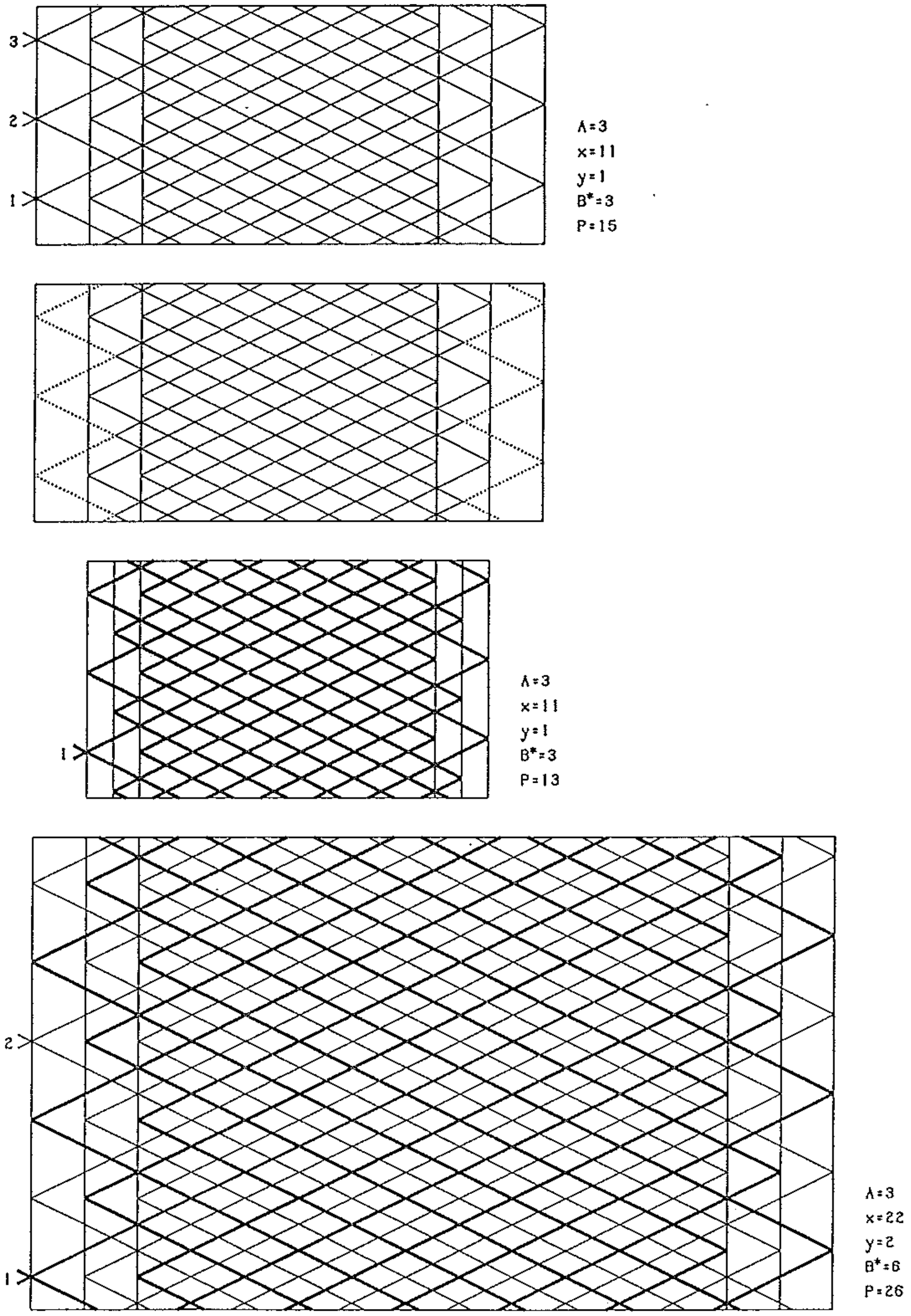

Fig. 772 — A two component Regular Nested Cylindrical Braid.

The lowermost grid-digram in Fig. 773 shows a Semi-Perfect Herringbone Pineapple Knot consisting of six interbraided Regular Knots. If we divide these six interbraided Regular Knots into two sets of three each (1, 2, 3 and 4, 5, 6), then with the components of a set having all the same colour, but different to the colour of the components of the other set, we obtain a spiralling zigzag colour-pattern with a right helix. Each set of three components can be thought to be derived from the Perfect Regular Nested Knot shown in the uppermost grid-diagram (see the string-run diagrams in Fig. 774).

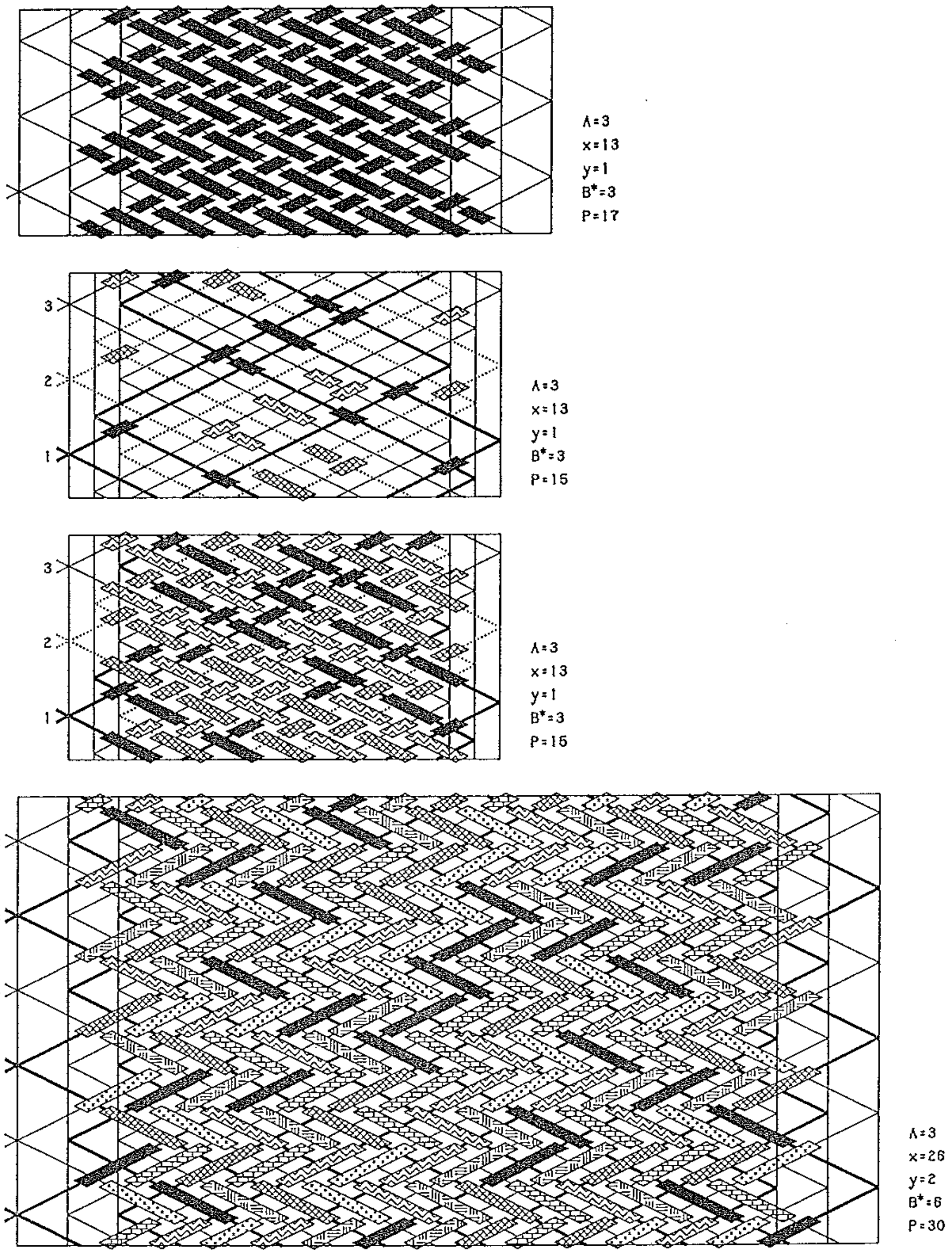

Fig. 773 — A six component Semi-Perfect Herringbone Pineapple Knot.

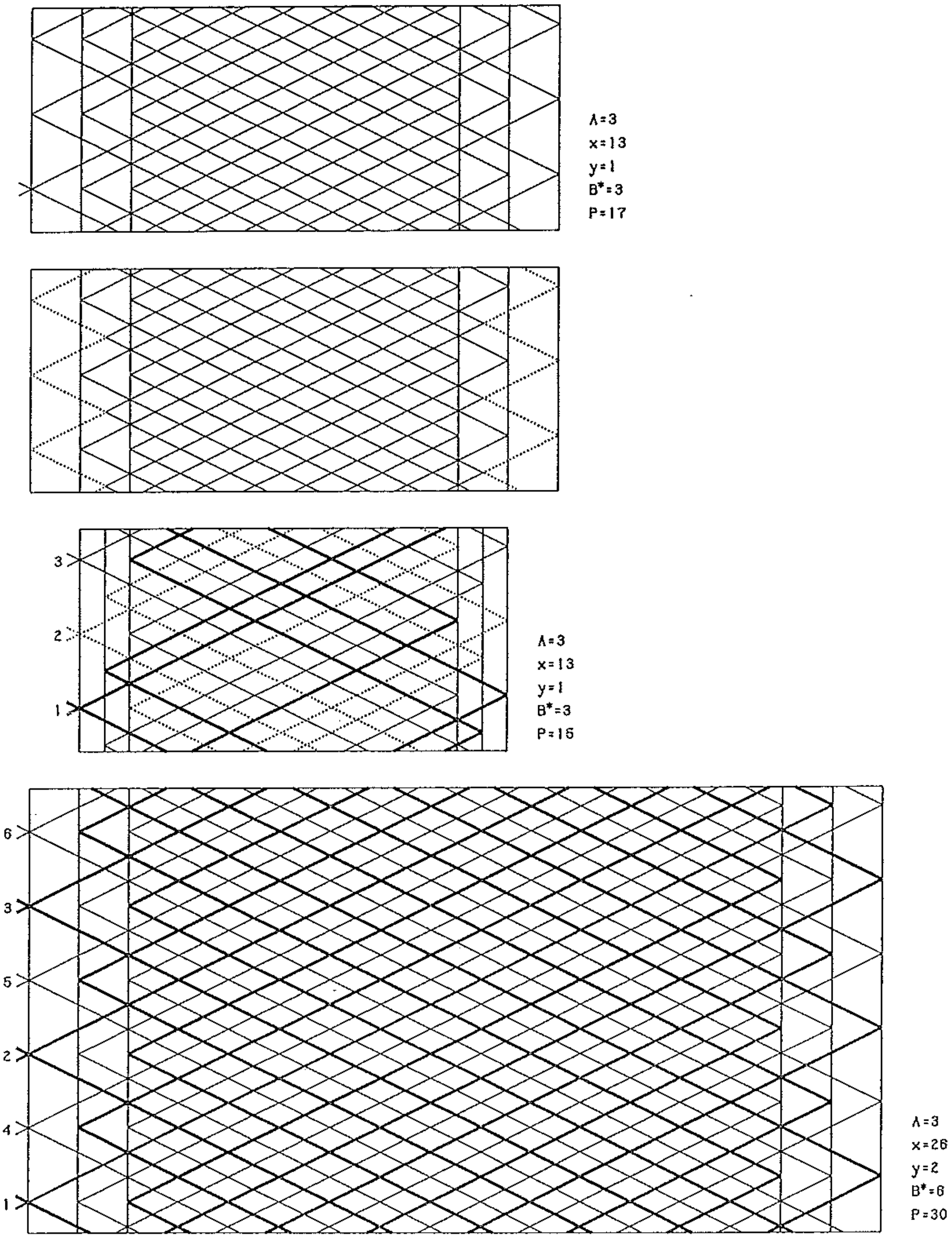

Fig. 774 — The string-run diagrams associated with the grid-diagrams in Fig. 773.

The lowermost string-run diagram in Fig. 775 shows the string-run of a two component Regular Nested Cylindrical Braid on which a Herringbone Pineapple coding can be superimposed ($y = A - 1$). The third diagram from the top shows the string-run of each Periodic Regular Nested component. This string-run can be thought to be derived from the string-run of the Perfect Regular Nested Knot shown in the uppermost diagram.

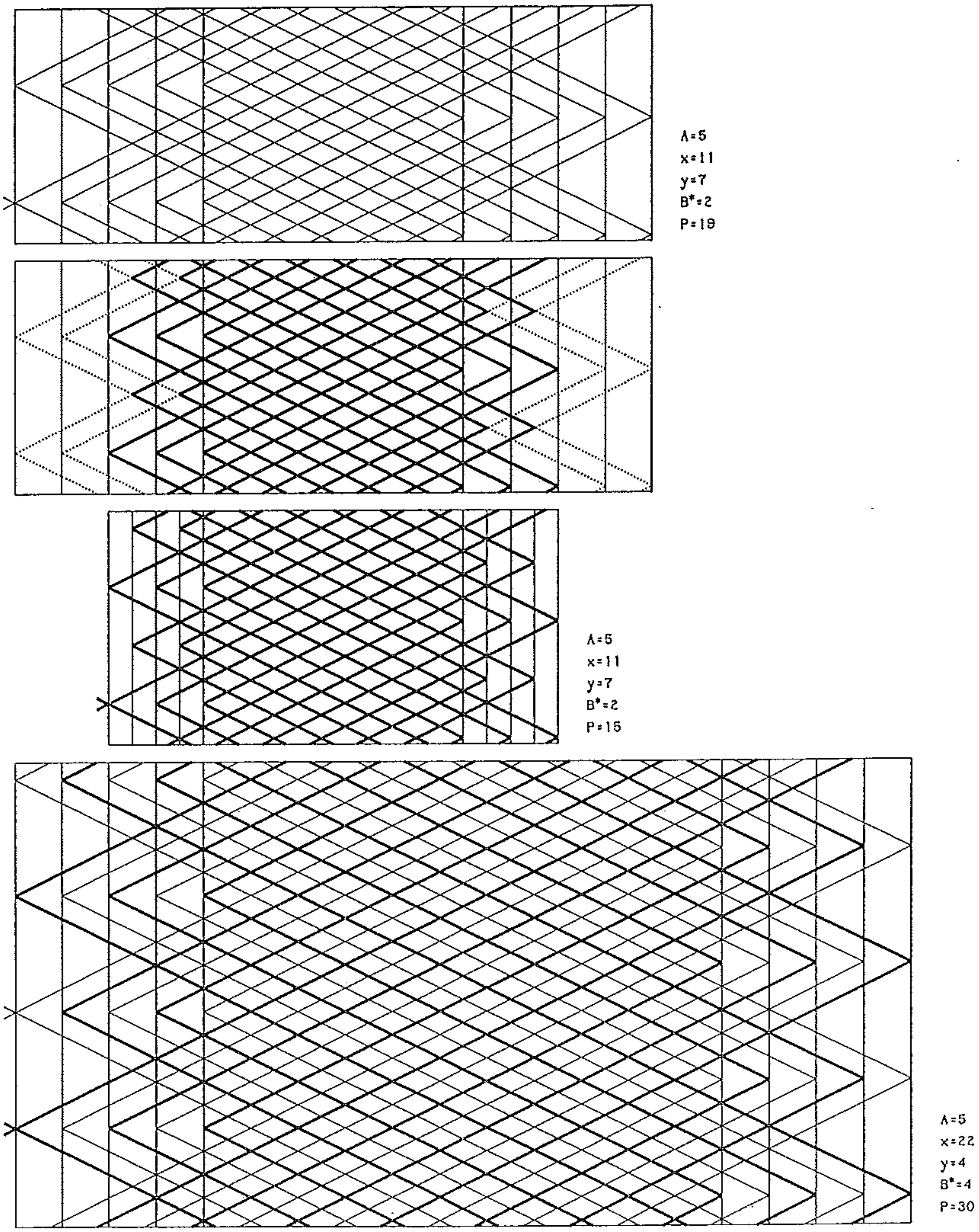

Fig. 775 — A two component Regular Nested Cylindrical Braid.

In Fig. 776 the string-runs associated with another two component Regular Nested Cylindrical Braid are shown on which a Herringbone Pineapple coding can be superimposed ($y = A - 1$). Each component is again a Perfect Periodic Regular Nested Knot and can be thought to be derived from the string-run of the Perfect Regular Nested Knot shown in the uppermost diagram.

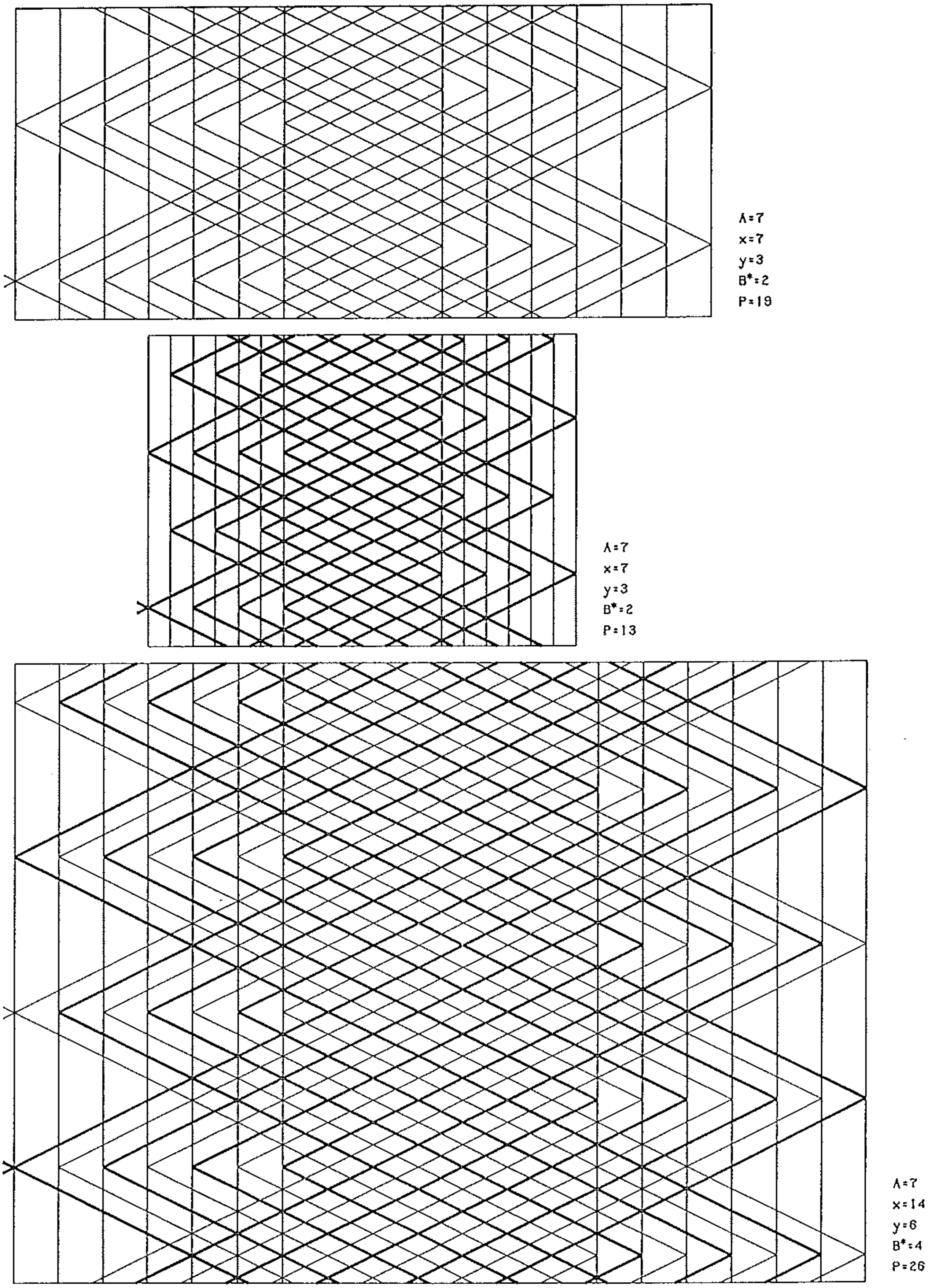

Fig. 776 — A two component Regular Nested Cylindrical Braid.

Fig. 777 shows a Semi-Perfect Herringbone Pineapple Knot consisting of six interbraided Perfect Nested Knots. If we divide these six interbraided Perfect Nested Knots into two sets of three each (1, 2, 3 and 4, 5, 6), then with the components of a set having all the same colour, but different to the colour of the components of the other set, we obtain a spiralling zigzag colour-pattern with a right helix. Each interbraided set of three components is a Periodic Regular Nested Cylindrical Braid.

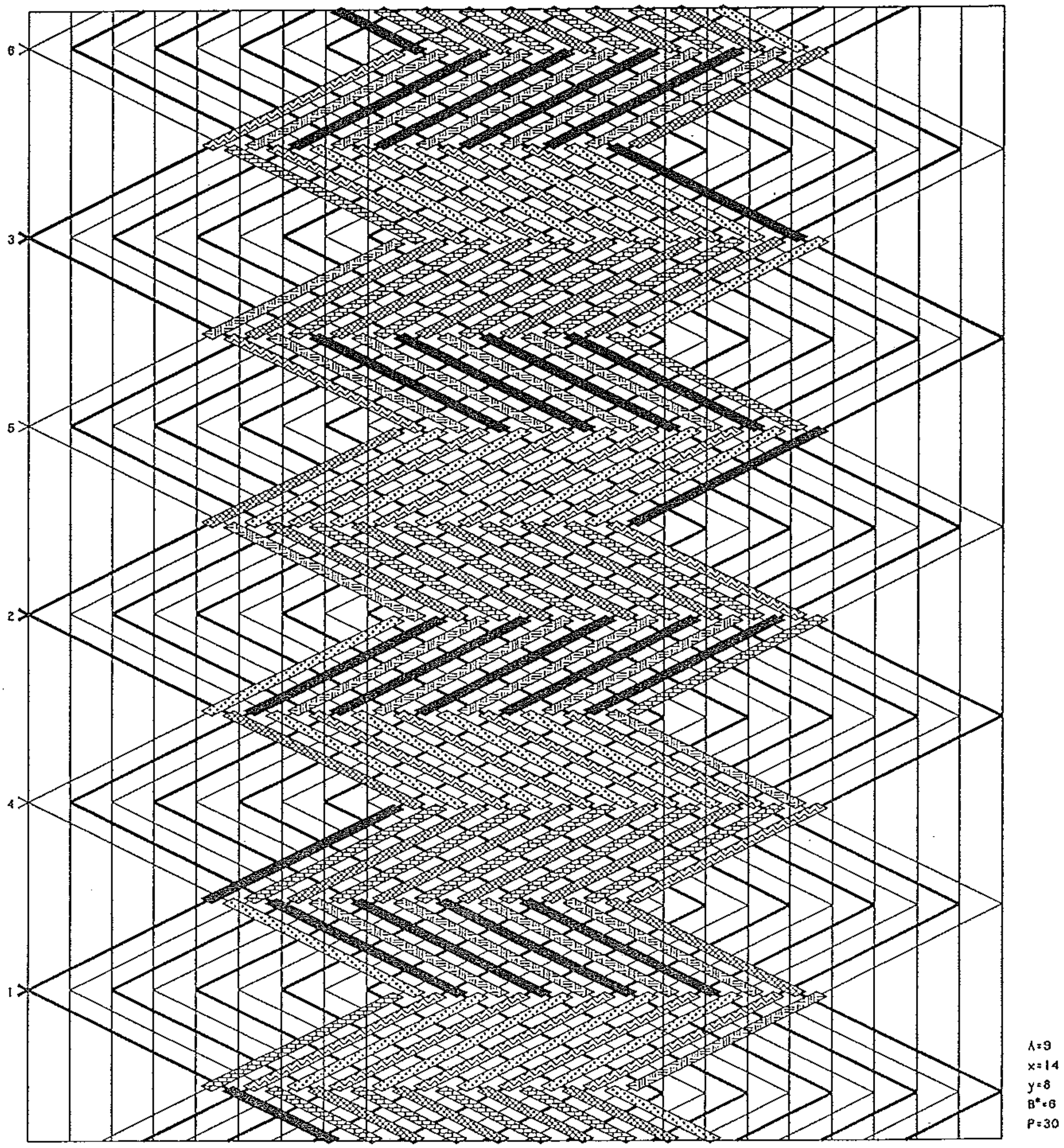

Fig. 777 — A six component Semi-Perfect Herringbone Pineapple Knot.

The lowermost diagram in Fig. 778 shows the string-run of a component set of three Perfect Nested components, while the uppermost diagrams in Fig. 778 show the string-run diagram and the grid-diagram of a Perfect Nested component.

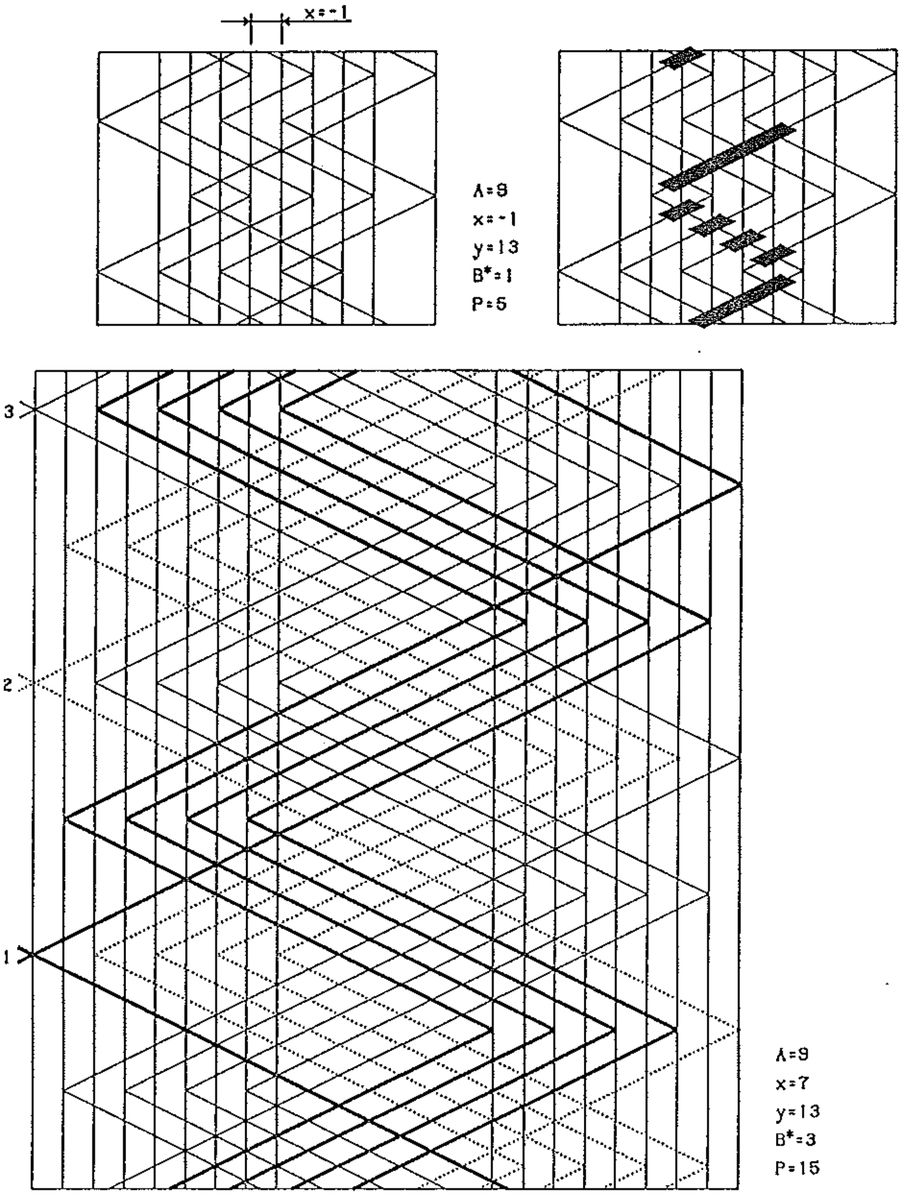

Fig. 778 — The string-run diagrams associated with the grid-diagram in Fig. 777.

The leftmost string-run diagram in Fig. 779 shows the string-run of a three component Regular Nested Cylindrical Braid on which a Herringbone Pineapple coding can be superimposed ($y = A - 1$). The lowermost right-hand diagram shows the string-run of each Periodic Regular Nested component. This string-run can be thought to be derived from the string-run of the three component Regular Nested Knot shown in the central right-hand diagram. Each component in this string-run diagram is the string-run of a Perfect Periodic Regular Nested Knot.

It is not possible to obtain for the string-run of the leftmost diagram in Fig. 779 a superimposed Herringbone Pineapple coding with a regular distributed colour-pattern since we cannot form two sets of interbraided components, each having an identical number of interbraided components ($\lambda = 3$, and since the natural number z must divide into 3, z can only be equal to 1, but when $z = 1$ a regular distributed colour pattern is not possible).

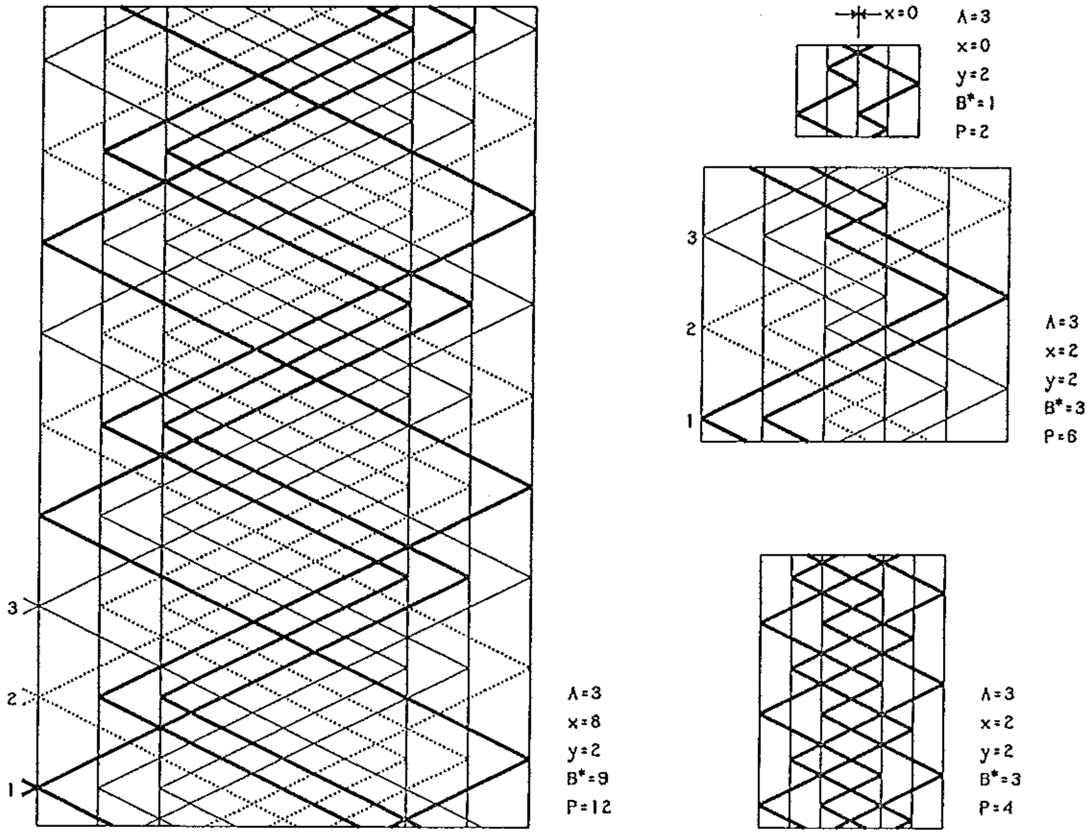

Fig. 779 — The string-run of a three component Semi-Perfect Herringbone Pineapple Knot with $A = 3$; $x = 8$; $k = 2$; $B^* = 9$.

With $z = 2$ and hence $t = 1$ the layout of the two consecutive nests m and $|m + 1|_{B^*}$ in Fig. 770, pg. 994, becomes as shown in Fig. 780.

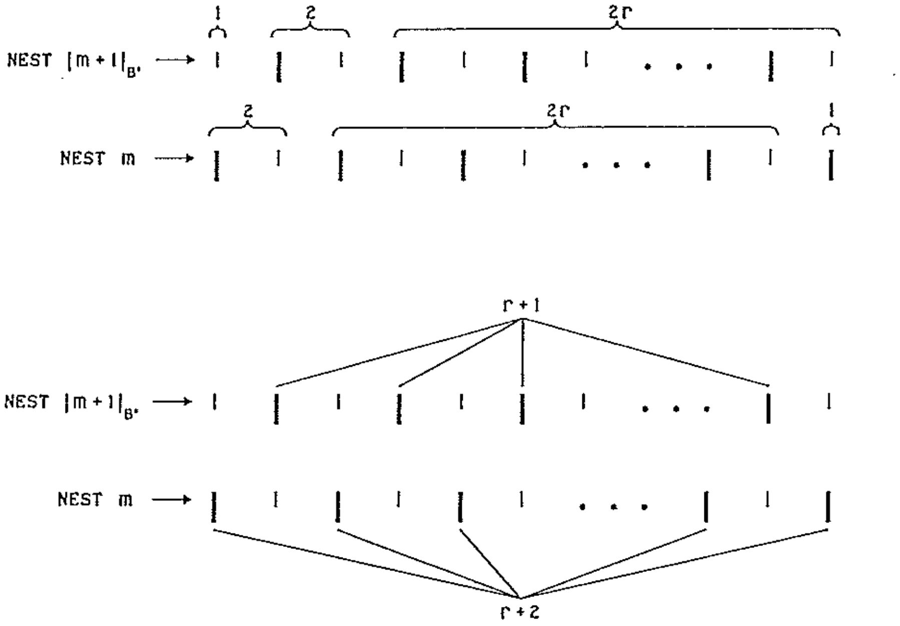

Fig. 780 — The layout of two consecutive nests with $z = 2$.

From this layout it will readily be seen that $A \geq 3$ and hence $r \geq 0$, consequently $A = odd$. From the lowermost layout in Fig. 780 it follows that each of the two component sets is a Periodic Regular Nested Cylindrical Braid with $A_{l_1} = A_{r_1} = \frac{A+1}{2}$ and $A_{l_2} = A_{r_2} = \frac{A-1}{2}$.

As we have seen, a regular distributed colour pattern in Semi-Perfect Herringbone Pineapple Knots consist of alternately coloured zigzag left (when $y = A+1$) or right (when $y = A-1$) helixes, where all the helixes of the same colour belong to a set (≥ 1) of components whose string-run is that of a Periodic Regular Nested Cylindrical Braid with $A_{l_1} = A_{r_1} = \frac{A+1}{2}$ and $A_{l_2} = A_{r_2} = \frac{A-1}{2}$. Note that this Periodic Regular Nested Cylindrical Braid is a special one since $A_{l_1} - A_{l_2} = A_{r_1} - A_{r_2} = 1$.

Once again we like to stress that various coding arrangements can be superimposed on a particular string-run, hence a particular string-run cannot tell us which coding form should be superimposed on it. However, a particular coding form may require a particular string-run. Here, for example, the string-run of each of the two component sets (the string-run of a Periodic Regular Nested Cylindrical Braid with $A_{l_1} - A_{l_2} = A_{r_1} - A_{r_2} = 1$) does **not** determine its superimposed coding and hence does **not** determine the colour-pattern of the overall braid, but the overall coding-pattern of the braid with its overall string-run particulars does determine the colour-pattern of the overall braid and the string-run of its components. Hence the alternately coloured zigzag left (when $y = A+1$) or right (when $y = A-1$) helix pattern of the overall braid determines its overall string-run particulars, its overall coding, the string-run particulars of the component sets and their coding, but the string-run particulars of the component sets do **not** determine their coding, hence do **not** determine the overall coding and colour-pattern.

It is therefore surprising that we still encounter in that Dutch braiding publication *Het Knoopeknauwertje* the question whether those alternately coloured zigzag helix patterns in certain Semi-Perfect Herringbone Pineapple Knots are due to Periodic Regular Nested Cylindrical Braids (*Het Knoopeknauwertje*, Issue No. 21, pg. 5), although its editor is well aware of the fact that a string-run does **not** determine the coding we can superimpose on it. More seriously, the question was raised on account of the results obtained from:

(*i*). Modifying the string-run of the Regular Nested Knot with the specification $(22/3/22)\{132/312\}6$, hence with $A = 3$; $x = 3$; $k = 3$; $B^* = 2$, into the string-run of the Periodic Regular Nested Knot with the specification $(11/3/11)\{1_1 2_3 3_2/1_1 3_2 2_3\}6$. Both these knots require one essential string.

(*ii*). Interbraiding the two string-runs of two Periodic Regular Nested Knots, each with the specification $(11/3/11)\{1_1 2_3 3_2/1_1 3_2 2_3\}6$, in order to obtain the string-run of the Regular Nested Knot with the specification $(22/6/22)\{132/312\}12$, hence with $A = 3$; $x = 6$; $k = 3$; $B^* = 4$.

Since $y = |x - 2(k+1)|_{2A} = 4 = A+1$ for the Regular Nested Knot with the specification $(22/6/22)\{132/312\}12$, we can superimpose on its string-run a Herringbone Pineapple coding.

The Semi-Perfect Herringbone Pineapple Knot $(22/6/22)\{132/312\}12$ is a 3-pass knot only, hence its two components, the Periodic Regular Nested Knots with specification $(11/3/11)\{1_1 2_3 3_2/1_1 3_2 2_3\}6$, have a string-run from which we cannot draw general conclusions about the type of Periodic Regular Nested Cylindrical Braids involved.

THE BRAIDER

No.43 **AUGUST 2005.**

CONTENTS

pg.
The Braider's Notebook 1005
Braid Design 1023

A quarterly publication
for
the braiding artisan

Resale of this publication or copies thereof
is strictly prohibited

Copyright ©2005 by:

A.G. Schaake; 21 Sundown Cresc.; Hamilton; New Zealand.
D. Van Tassel; Box 335; Craig, Co 81626-0335; U.S.A.
F.J.M. Masurel; Ganzenzijde 4; 2317XG Leiden; Nederland.

All rights reserved. No part of this publication may be reproduced, stored in a retrieval system, or transmitted, in any form or by any means, electronic, mechanical, photo-copying, recording, or otherwise, without prior written permission.

This publication is available to braiding artisans only.

Copies may be obtained from:

A.G. Schaake,
21 Sundown Cresc.,
Hamilton,
New Zealand.

THE BRAIDER'S NOTEBOOK

In *The Braider*, Issue No. 41, we discussed the Regular Cylindrical Braids with an even number of bights of which a string passes diametrically through its supporting object. In this issue we will look at the Regular Nested Cylindrical Braids with an even number of bights of which a string passes diametrically through its supporting object.

The Standard and Semi-Standard Herringbone Pineapple Knots:

We like to stress that it is essential to draw the grid-diagrams of the knots involved. This will then enable us to determine of which component knot the string-run should pass diametrically through the object to be covered by the Standard Herringbone Pineapple Knot.

Example 1.

Let $A = 2$, $x = 10$, $B^* = 6$. Hence $k = \left|\frac{x+A}{2} - 1\right|_A = \left|\frac{10+2}{2} - 1\right|_2 = |5|_2 = 1$.[†]

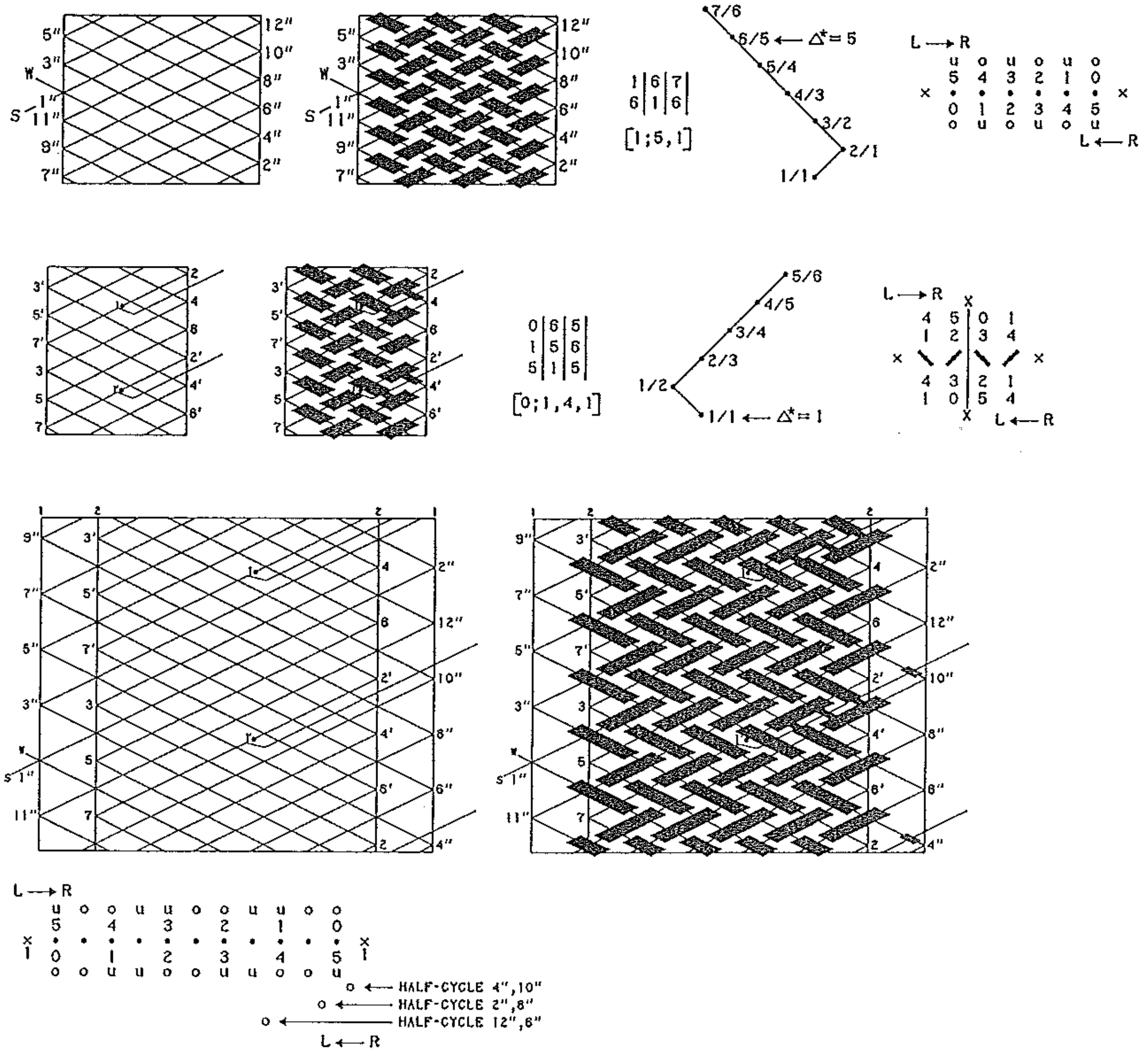

Fig. 781 — Example 1. -- the knots involved.

[†] See *The Braider*, Issue No. 23, pg. 521.

The coding of the lowermost right-hand grid-diagram shows that the component between left bight-boundary 2 and right bight-boundary 2 is the preferred one for having its string diametrically through the object over which the 2-pass Standard Herringbone Pineapple Knot is meant to sit. This component (an over-under coded Regular Knot) has 5-parts and 6-bights. Say we braid this component in the parallel braiding way. Then its half-cycle braiding algorithms are as follows:

half-cycle parts 1 & 1′ : : $L \longrightarrow R$: Free run.
half-cycles 2 & 2′ : $i = 0$; $i \neq 0$ left of X–X : $L \longleftarrow R$: Free run.
half-cycles 3 & 3′ : $i = 0$; : $L \longrightarrow R$: u .
half-cycles 4 & 4′ : $i \leq 1$; $i \neq 1$ left of X–X : $L \longleftarrow R$: $2u$.
half-cycles 5 & 5′ : $i \leq 1$; : $L \longrightarrow R$: $2u - o$.
half-cycles 6 & 6′ : $i \leq 2$; $i \neq 2$ left of X–X : $L \longleftarrow R$: $u - o - u - o$.
half-cycles 7 & 7′ : $i \leq 2$; : $L \longrightarrow R$: $u - o - 2u$.

Next we interbraid the component between left bight-boundary 1 and right bight-boundary 1. This component (an over-under coded Regular Knot) has 7-parts and 6-bights. Its algorithm diagram as the interbraid is shown below the lowermost string-run diagram and grid-diagram from which we read its half-cycle braiding algorithms:

half-cycle 1″ : ; $L \longrightarrow R$: $o - u - o - u - o$.
half-cycle 2″ : $i = 0$; $L \longleftarrow R$: $2o - u - o - u - 2o$.
half-cycle 3″ : $i = 0$; $L \longrightarrow R$: $o - u - o - u - 2o$.
half-cycle 4″ : $i \leq 1$; $L \longleftarrow R$: $2o - u - o - 2u - 2o$.
half-cycle 5″ : $i \leq 1$; $L \longrightarrow R$: $o - u - o - 2u - 2o$.
half-cycle 6″ : $i \leq 2$; $L \longleftarrow R$: $2o - u - 2o - 2u - 2o$.
half-cycle 7″ : $i \leq 2$; $L \longrightarrow R$: $o - u - 2o - 2u - 2o$.
half-cycle 8″ : $i \leq 3$; $L \longleftarrow R$: $2o - 2u - 2o - 2u - 2o$.
half-cycle 9″ : $i \leq 3$; $L \longrightarrow R$: $o - 2u - 2o - 2u - 2o$.
half-cycle 10″ : $i \leq 4$; $L \longleftarrow R$: $3o - 2u - 2o - 2u - 2o$.
half-cycle 11″ : $i \leq 4$; $L \longrightarrow R$: $2o - 2u - 2o - 2u - 2o$.
half-cycle 12″ : $i \leq 5$; $L \longleftarrow R$: $u - 3o - 2u - 2o - 2u - 2o$.

Although the above procedure, using the lowermost algorithm diagram form in Fig. 781 for obtaining the half-cycle braiding algorithms for interbraiding the second component, is suitable for 2-pass Standard Herringbone Pineapple Knots, it is in general not suitable for Standard or Semi-Standard Herringbone Pineapple Knots for which $A > 2$. After obtaining the half-cycle braiding algorithms for the foundation knot (the knot of which the string passes diametrically through the object over which it sits) we obtain the half-cycle braiding algorithms for the further interbraided components by the appropriate modifications of their half-cycle braiding algorithms associated with a normal braided foundation knot. In our Example above, the half-cycle braiding algorithms for the interbraided component between left bight-boundary 1 and right bight-boundary 1, associated with a normal braided foundation knot, are obtained from the following algorithm diagram[†]:

$$\begin{array}{cccccccc}
\longrightarrow & l_i - 1 & A - 1 & A - 1 & A - 1 & A - 1 & A - 1 & r_i - 1 \\
0 & \star & \star & \star & \star & \star & \star & \\
/ & \backslash & / & \backslash & / & \backslash & / & \backslash \\
 & \star & \star & \star & \star & \star & \star & 0 \\
l_i - 1 & A - 1 & A - 1 & A - 1 & A - 1 & A - 1 & r_i - 1 & \longleftarrow
\end{array}$$

[†] See *The Braider*, Issue No. 27, pg. 634.

where the positions of the stars are being occupied by the i-values of the complementary bight-number scheme associated with the component to be interbraided, and where the reference value above an upper star, or below a lower star, increases by 1 when its associated i-value is applicable to the half-cycle concerned, excepting the **last** entry $(r_i - 1)u$ which remains the same for each of the lower-left to upper-right half-cycles, and the **last** entry $(l_i - 1)u$ which remains the same for each of the lower-right to upper-left half-cycles. Hence, since $r_i = 1$, $l_i = 1$ and $\Delta^* = 5$ for $p/b = 7/6$, from the algorithm diagram:

$$\begin{array}{cccccccc}
\longrightarrow & 0 & 1 & 1 & 1 & 1 & 1 & 0 \\
\vdash & 5 & 4 & 3 & 2 & 1 & 0 & \\
/ & \backslash & / & \backslash & / & \backslash & / & \backslash \\
 & 0 & 1 & 2 & 3 & 4 & 5 & \dashv \\
0 & 1 & 1 & 1 & 1 & 1 & 0 & \longleftarrow
\end{array}$$

This algorithm diagram gives us the following half-cycle braiding algorithms:

half-cycle $1''$: ; $L \longrightarrow R$: $o - u - o - u - o$.
half-cycle $2''$: $i = 0$; $L \longleftarrow R$: $o - u - o - u - 2o$.
half-cycle $3''$: $i = 0$; $L \longrightarrow R$: $o - u - o - u - 2o$.
half-cycle $4''$: $i \leq 1$; $L \longleftarrow R$: $o - u - o - 2u - 2o$.
half-cycle $5''$: $i \leq 1$; $L \longrightarrow R$: $o - u - o - 2u - 2o$.
half-cycle $6''$: $i \leq 2$; $L \longleftarrow R$: $o - u - 2o - 2u - 2o$.
half-cycle $7''$: $i \leq 2$; $L \longrightarrow R$: $o - u - 2o - 2u - 2o$.
half-cycle $8''$: $i \leq 3$; $L \longleftarrow R$: $o - 2u - 2o - 2u - 2o$.
half-cycle $9''$: $i \leq 3$; $L \longrightarrow R$: $o - 2u - 2o - 2u - 2o$.
half-cycle $10''$: $i \leq 4$; $L \longleftarrow R$: $2o - 2u - 2o - 2u - 2o$.
half-cycle $11''$: $i \leq 4$; $L \longrightarrow R$: $2o - 2u - 2o - 2u - 2o$.
half-cycle $12''$: $i \leq 5$; $L \longleftarrow R$: $u - 2o - 2u - 2o - 2u - 2o$.

From the grid-diagram in Fig. 781 we see that for these half-cycles:

half-cycle $2''$ has one additional o before the first o.
half-cycle $4''$ has one additional o before the first o.
half-cycle $6''$ has one additional o after the first o.
half-cycle $8''$ has one additional o before the first o.
half-cycle $10''$ has one additional o before the first $2o$.
half-cycle $12''$ has one additional o after the first $2o$.

After making these adjustments we obtain the half-cycle braiding algorithms on pg. 1006.

Instead of using the algorithm diagrams in Fig. 781, it is simpler to make use of algorithm diagrams which show all the columns between left bight-boundary 1 and right bight-boundary 1. The bigger dots in such an algorithm diagram indicate the actual intersection columns associated with the component under consideration. The uppermost algorithm diagram in Fig. 782 is associated with the first component, the foundation knot, between left bight-boundary 2 and right bight-boundary 2. The lowermost algorithm diagram in Fig. 782 is associated with the second component between left bight-boundary 1 and right bight-boundary 1. The intersection between a lower-right to upper-left half-cycle of the second component with the outgoing half-cycle parts 7 & $7'$ of the foundation knot (which are **over**-crossings) are indicated by the i-value of the lower-right to upper-left half-cycle concerned (very small + sign with its associated small numeral for the i-value concerned indicates the position of this intersection (readily obtainable from the lowermost string-run diagram in Fig. 781)).

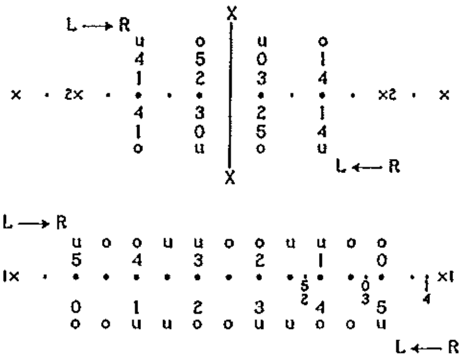

Fig. 782 — The algorithm diagrams showing all the columns between bight-boundaries $l_i = 1$ and $r_i = 1$.

Example 2.

Let $A = 5$, $x = 13$, $B^* = 6$. Hence $k = \left|\frac{x+A}{2} - 1\right|_A = \left|\frac{13+5}{2} - 1\right|_5 = |8|_5 = 3$. We have three components with n-parts and two components with $(n-2)$-parts, and since the total number of parts is $2A + x - 2 = 21$, it follows that $5n = 25$, hence $n = 5$. Thus we have three components with 5-parts and two components with 3-parts. Since g.c.d. $(3, B^*) =$ g.c.d. $(3, 6) = 3$, each of the two components with 3-parts require three essential strings, hence each consists of 3 sub-components with each sub-component having 1-part. We are thus dealing with a Semi-Standard Herringbone Pineapple Knot.

In fact we have met this Semi-Standard Herringbone Pineapple Knot in *The Braider*, Issue No. 27, pp. 629-633, where it was braided in the normal way. There the foundation knot was the component between left bight-boundary 1 and right bight-boundary 3, the second component between left bight-boundary 2 and right bight-boundary 2, the third component between left bight-boundary 3 and right bight-boundary 1, the sub-components of the fourth component between left bight-boundary 5 and right bight-boundary 4, and the sub-components of the fifth component between left bight-boundary 4 and right bight-boundary 5.

Let's now braid this Semi-Standard Herringbone Pineapple Knot with the foundation knot between left bight-boundary 2 and right bight-boundary 2, the string-run of which passes diametrically through the object over which this Semi-Standard Herringbone Pineapple Knot sits. Then the second component we braid between left bight-boundary 1 and right bight-boundary 3, the third component between bight-boundary 3 and right bight-boundary 1, the sub-components of the fourth component between left bight-boundary 5 and right bight-boundary 4, and the sub-components of the fifth component between left bight-boundary 4 and right bight-boundary 5. See Fig. 783.

Hence the half-cycle braiding algorithms for the foundation knot (the first component) are those of the foundation knot in Example 1 with the replacement of o by u and vice versa except for half-cycles 7 & 7′ where right of line X–X we have unders:

half-cycle parts 1 & 1′ :		:	$L \longrightarrow R$:	Free run.
half-cycles 2 & 2′ :	$i = 0$;	$i \neq 0$ left of X–X :	$L \longleftarrow R$:	Free run.
half-cycles 3 & 3′ :	$i = 0$;	:	$L \longrightarrow R$:	o .
half-cycles 4 & 4′ :	$i \leq 1$;	$i \neq 1$ left of X–X :	$L \longleftarrow R$:	$2o$.
half-cycles 5 & 5′ :	$i \leq 1$;	:	$L \longrightarrow R$:	$2o - u$.
half-cycles 6 & 6′ :	$i \leq 2$;	$i \neq 2$ left of X–X :	$L \longleftarrow R$:	$o - u - o - u$.
half-cycles 7 & 7′ :	$i \leq 2$;	:	$L \longrightarrow R$:	$o - 3u$.

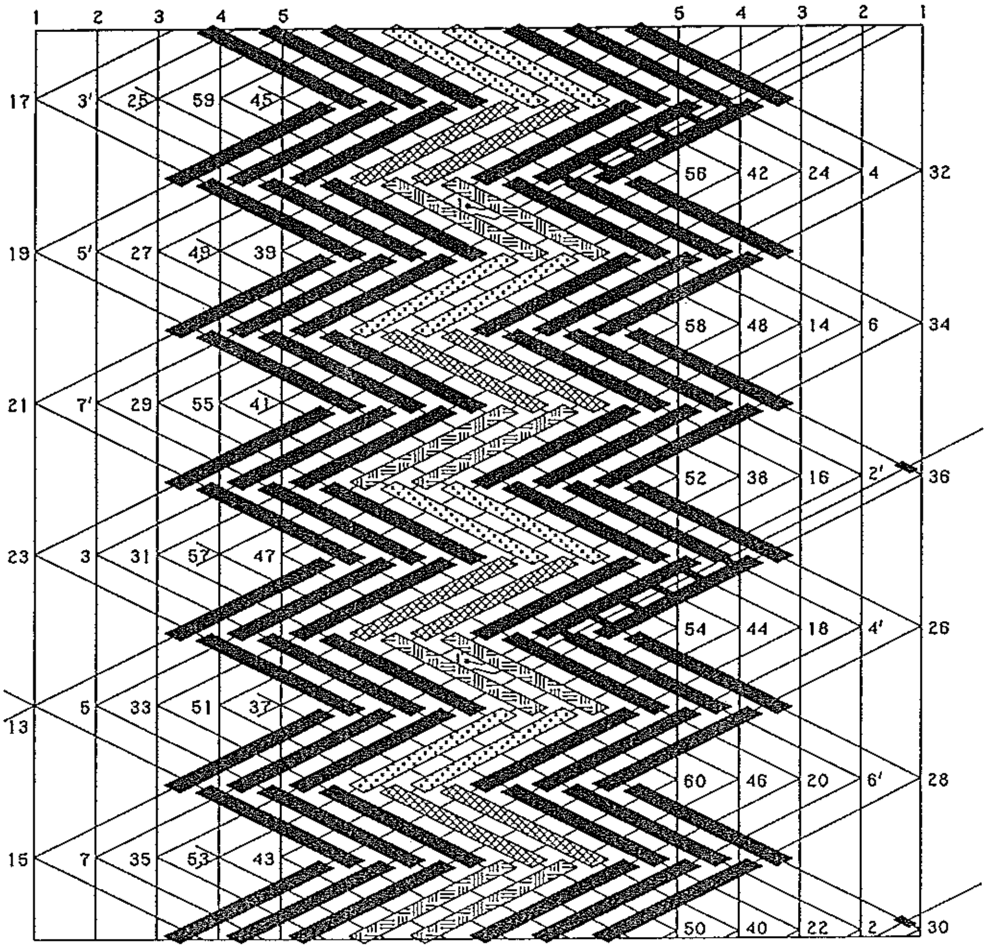

Fig. 783 — The Semi-Standard Herringbone Pineapple Knot of Example 2.

The second component between left bight-boundary 1 and right bight-boundary 3 would have the following half-cycle braiding algorithms when the foundation knot between left bight-boundary 2 and right bight-boundary 2 would have been braided in the normal way without its string going diametrically through the object over which it sits (hence for the second component $A = 2$, $l_i = 1$, $r_i = 2$):

half-cycle 13 : $L \longrightarrow R$ $o - u - o - u$.
half-cycle 14 $i = 0$: $L \longleftarrow R$ $u - o - u - o$.
half-cycle 15 $i = 0$: $L \longrightarrow R$ $o - u - o - u$.
half-cycle 16 $i \leq 1$: $L \longleftarrow R$ $u - 2o - u - o$.
half-cycle 17 $i \leq 1$: $L \longrightarrow R$ $2o - u - o - u$.
half-cycle 18 $i \leq 2$: $L \longleftarrow R$ $u - 2o - 2u - o$.
half-cycle 19 $i \leq 2$: $L \longrightarrow R$ $2o - 2u - o - u$.
half-cycle 20 $i \leq 3$: $L \longleftarrow R$ $u - 2o - 2u - 2o$.
half-cycle 21 $i \leq 3$: $L \longrightarrow R$ $2o - 2u - 2o - u$.
half-cycle 22 $i \leq 4$: $L \longleftarrow R$ $u - 2o - 2u - 2o - u$.
half-cycle 23 $i \leq 4$: $L \longrightarrow R$ $2o - 2u - 2o - 2u$.
half-cycle 24 $i \leq 5$: $L \longleftarrow R$ $u - 2o - 2u - 2o - u$.

These half-cycle braiding algorithms and the half-cycle braiding algorithms for the half-cycles 25 to 60 on pp. 632-633 (see *The Braider*, Issue No. 27) have now to be modified as follows:

half-cycle 14 has one additional o before the first o.
half-cycle 18 has one additional o before the first u.
half-cycle 20 has one additional o after the first o.
half-cycle 24 has one additional o before the first u.
half-cycle 26 has one additional o before the first o.
half-cycle 28 has one additional o before the first u.
half-cycle 30 has one additional o before the first o.
half-cycle 32 has one additional o after the first o.
half-cycle 34 has one additional o after the first u.
half-cycle 36 has one additional o before the first o.
half-cycle 42 has one additional o after the first u.
half-cycle 44 has one additional o after the first u.
half-cycle 46 has one additional o after the second o.
half-cycle 48 has one additional o after the second o.
half-cycle 54 has one additional o after the first u.
half-cycle 56 has one additional o after the first u.

Hence the actual half-cycle braiding algorithms for the half-cycles 13 to 60 are as follows:

half-cycle 13 : $L \longrightarrow R$ $o - u - o - u$.
half-cycle 14 $i = 0$: $L \longleftarrow R$ $u - 2o - u - o$.
half-cycle 15 $i = 0$: $L \longrightarrow R$ $o - u - o - u$.
half-cycle 16 $i \leq 1$: $L \longleftarrow R$ $u - 2o - u - o$.
half-cycle 17 $i \leq 1$: $L \longrightarrow R$ $2o - u - o - u$.
half-cycle 18 $i \leq 2$: $L \longleftarrow R$ $o - u - 2o - 2u - o$.
half-cycle 19 $i \leq 2$: $L \longrightarrow R$ $2o - 2u - o - u$.
half-cycle 20 $i \leq 3$: $L \longleftarrow R$ $u - 3o - 2u - 2o$.
half-cycle 21 $i \leq 3$: $L \longrightarrow R$ $2o - 2u - 2o - u$.
half-cycle 22 $i \leq 4$: $L \longleftarrow R$ $u - 2o - 2u - 2o - u$.
half-cycle 23 $i \leq 4$: $L \longrightarrow R$ $2o - 2u - 2o - 2u$.
half-cycle 24 $i \leq 5$: $L \longleftarrow R$ $o - u - 2o - 2u - 2o - u$.

half-cycle 25 : $L \longrightarrow R$ $2u - 2o - 2u - 2o$.
half-cycle 26 $i = 0$: $L \longleftarrow R$ $3o - 2u - 2o - 2u$.
half-cycle 27 $i = 0$: $L \longrightarrow R$ $2u - 2o - 2u - 2o$.
half-cycle 28 $i \leq 1$: $L \longleftarrow R$ $4o - 2u - 2o - 2u$.
half-cycle 29 $i \leq 1$: $L \longrightarrow R$ $2u - 3o - 2u - 2o$.
half-cycle 30 $i \leq 2$: $L \longleftarrow R$ $4o - 3u - 2o - 2u$.
half-cycle 31 $i \leq 2$: $L \longrightarrow R$ $2u - 3o - 3u - 2o$.
half-cycle 32 $i \leq 3$: $L \longleftarrow R$ $4o - 3u - 3o - 2u$.
half-cycle 33 $i \leq 3$: $L \longrightarrow R$ $2u - 3o - 3u - 3o$.
half-cycle 34 $i \leq 4$: $L \longleftarrow R$ $3o - u - o - 2u - 3o - 3u$.
half-cycle 35 $i \leq 4$: $L \longrightarrow R$ $2u - 3o - 3u - 3o - u$.
half-cycle 36 $i \leq 5$: $L \longleftarrow R$ $4o - 3u - 3o - 3u$.

half-cycle 37 : $L \longrightarrow R$ $3u - 3o - 3u$.
half-cycle 38 $i = 0$: $L \longleftarrow R$ $3u - 3o - 3u$.
half-cycle 39 $i = 0$: $L \longrightarrow R$ $3u - 3o - 3u$.
half-cycle 40 $i \leq 1$: $L \longleftarrow R$ $3u - 3o - 3u$.
half-cycle 41 $i = X$: $L \longrightarrow R$ $3u - 4o - 3u$.

half-cycle 42	$i = 0\,;\, i = X$:	$L \longleftarrow R$	$u - o - 2u - 4o - 3u$.
half-cycle 43	$i = 0\,;\, i = X$:	$L \longrightarrow R$	$3u - 4o - 3u$.
half-cycle 44	$i \leq 1\,;\, i = X$:	$L \longleftarrow R$	$u - o - 2u - 4o - 3u$.
half-cycle 45	$i = X, Y$:	$L \longrightarrow R$	$3u - 4o - 4u$.
half-cycle 46	$i = 0\,;\, i = X, Y$:	$L \longleftarrow R$	$3u - 5o - 4u$.
half-cycle 47	$i = 0\,;\, i = X, Y$:	$L \longrightarrow R$	$3u - 4o - 4u$.
half-cycle 48	$i \leq 1\,;\, i = X, Y$:	$L \longleftarrow R$	$3u - 5o - 4u$.

half-cycle 49	:	$L \longrightarrow R$	$3u - 4o - 4u$.
half-cycle 50	$i = 0$:	$L \longleftarrow R$	$4u - 4o - 3u$.
half-cycle 51	$i = 0$:	$L \longrightarrow R$	$3u - 4o - 4u$.
half-cycle 52	$i \leq 1$:	$L \longleftarrow R$	$4u - 4o - 3u$.
half-cycle 53	$i = X$:	$L \longrightarrow R$	$3u - 5o - 4u$.
half-cycle 54	$i = 0\,;\, i = X$:	$L \longleftarrow R$	$u - o - 3u - 5o - 3u$.
half-cycle 55	$i = 0\,;\, i = X$:	$L \longrightarrow R$	$3u - 5o - 4u$.
half-cycle 56	$i \leq 1\,;\, i = X$:	$L \longleftarrow R$	$u - o - 3u - 5o - 3u$.
half-cycle 57	$i = X, Y$:	$L \longrightarrow R$	$3u - 5o - 5u$.
half-cycle 58	$i = 0\,;\, i = X, Y$:	$L \longleftarrow R$	$4u - 5o - 4u$.
half-cycle 59	$i = 0\,;\, i = X, Y$:	$L \longrightarrow R$	$3u - 5o - 5u$.
half-cycle 60	$i \leq 1\,;\, i = X, Y$:	$L \longleftarrow R$	$4u - 5o - 4u$.

Instead of using the above procedure, it is simpler to make use of algorithm diagrams which show all the columns between left bight-boundary 1 and right bight-boundary 1.

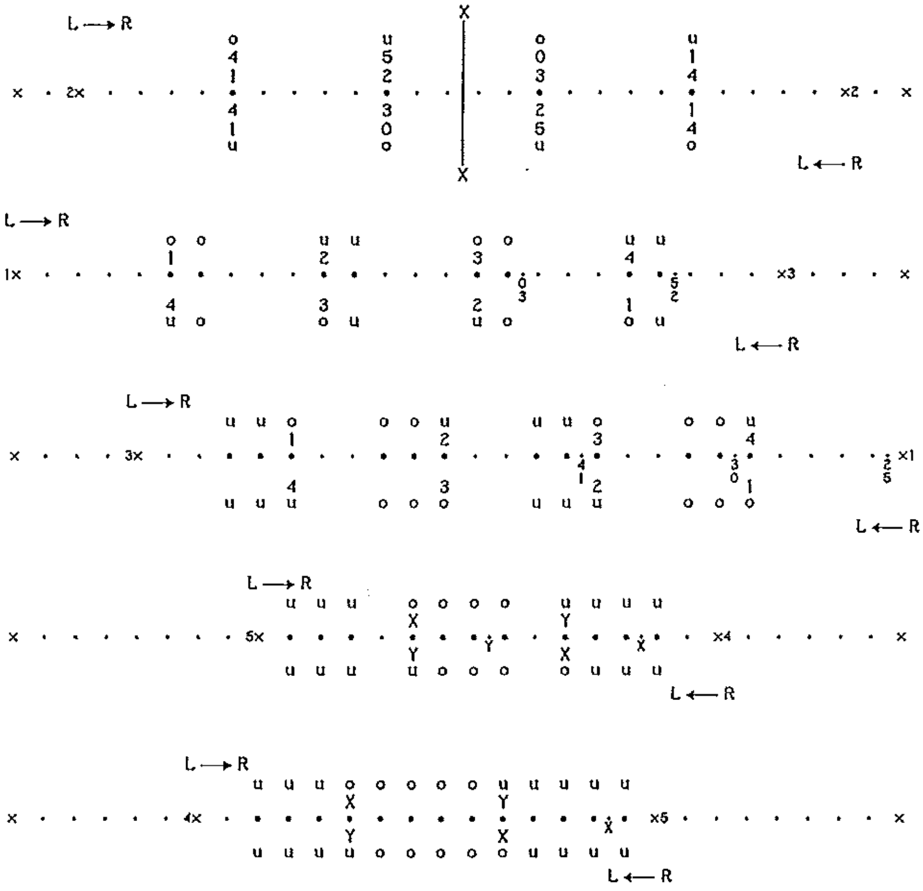

Fig. 784 — The algorithm diagrams showing all the columns between bight-boundaries $l_i = 1$ and $r_i = 1$.

The bigger dots in these algorithm diagrams indicate the actual intersection-columns associated with the component under consideration. In Fig. 784 we have the following sequence of algorithm diagrams:

The uppermost diagram is associated with the first component, the foundation knot, between left bight-boundary 2 and right bight-boundary 2. The next is associated with the second component between left bight-boundary 1 and right bight-boundary 3. The next is associated with the third component between left bight-boundary 3 and right bight-boundary 1. The next is associated with the fourth component between left bight-boundary 5 and right bight-boundary 4. And the lowermost is associated with the fifth component between left bight-boundary 4 and right bight-boundary 5.

The over-crossings between a lower-right to upper-left half-cycle of a component with the outgoing half-cycle parts 7 & 7′ of the foundation knot are indicated by a very small + sign and its associated small numeral for the i-value of the half-cycle concerned (readily obtainable from the string-run diagram or the grid-diagram in Fig. 783)).

Note that for the first to be braided sub-component of the components 4 and 5 the X and Y positions are neglected; for the second sub-component the bigger X and smaller X positions are to be taken into account; and for the third sub-component the positions with bigger X and Y and smaller Y when present are to be taken into account.

The Perfect and Semi-Perfect Herringbone Pineapple Knots:

First we calculate the first-return string-run with its associated nest-index numbers for braiding the knot in the normal way with its first half-cycle starting on its associated left bight-boundary (hence with its string-run not passing diametrically through the object over which it sits). For these nest-index numbers we use the formulae:[†]

$$I_{R_1} = I_{L_1} = 0$$
$$I_{L_{n+1}} = |I_{L_n} + 4A + x - (l_n + l_{n+1} + 2r_n)|_B$$
$$I_{R_{n+1}} = |I_{R_n} + 4A + x - (r_n + r_{n+1} + 2l_n)|_B$$

The number of crossings associated with a half-cycle are for this case calculated with the formula $2A + x - 1 - (l_n + r_n)$.[‡] Then we construct the half-cycle pattern for this case and then modify the half-cycle numbers so as to comply with the string passing diametrically through the object over which the knot sits (we shall again use parallel braiding).

For the **Perfect Herringbone Pineapple Knots** the string-run consists of two equal sections starting with the half-cycle parts 1 and 1′ respectively and ending with the outgoing half-cycles $(B+1)$ and $(B+1)'$ respectively. Half-cycle $(B+1)'$ and extended half-cycle part 1 occupy the same position on the left bight-boundary l_i at nest-index number $I_{L_1} = I_{L_{(B+1)'}} = 0$, while half-cycle $(B+1)$ and extended half-cycle part 1′ occupy the same position on the left bight-boundary $\left|l_i + \frac{AB^*}{2}\right|_A$ at nest-index number $I_{L_{1'}} = I_{L_{(B+1)}} = A\left\lceil \frac{B^*}{2} - \frac{l_i - 1}{A}\right\rceil$.[††]

Two sequential half-cycle numbers h_n and $(h_n + 2A)$, or $(h_n)'$ and $(h_n + 2A)'$, where $1 \leq h_n \leq (AB^* + 1 - 2A)$, on the same bight-boundary are associated respectively with nest-index number I and nest-index number $\left|I + 2A^2 + A(x-2)\right|_B$.

[†] See *The Braider*, Issue No. 26, pp. 592-593.

[‡] See *The braider*, Issue No. 28, pg. 647.

[††] $\lceil x \rceil$ denotes the smallest whole number equal to or greater than x.

For the **Semi-Perfect Herringbone Pineapple Knots** we have a number of string-run types for the foundation knot (the knot with its string diametrically through the object over which the Semi-Perfect Herringbone Pineapple sits):

Type I — Example:

Let $A = 4$; $x = 9$; $B^* = 25$; $y = A + 1 = 5$. Hence $k = \left|\frac{x-A-3}{2}\right|_A = \left|\frac{9-4-3}{2}\right|_4 = 1$, and $\Delta = |y|_A = |5|_4 = 1$. $P = 2A + x - 2 = 2 \times 4 + 9 - 2 = 15$, hence $\lambda = \text{g.c.d.}(P, B^*) =$ $\text{g.c.d.}(15, 25) = 5$; each sub-component has thus $\frac{AB^*}{\lambda} = \frac{100}{5} = 20$ bights.

Let the extended half-cycle part 1 be on the bight-boundary l_i at nest-index number $I_{L_{l_i}} = 0$, and let the extended half-cycle part $1'$ be on the bight-boundary $(l_i)' = \left|l_i + \frac{AB^*}{2}\right|_A$ at nest-index number $I_{L_{(l_i)'}} = \left|I_{L_{l_i}} + A\left\lceil \frac{B^*}{2} - \frac{l_i - 1}{A}\right\rceil\right|_B$.

The first-return string-run and its associated nest-index numbers are calculated in the usual manner, then for the to bight-boundary 1 extended lower-left to upper-right half-cycles the index numbers at bight-boundary 1 are calculated with the formula $I_{\text{at } l_1} = \left|I_{L_n} + 1 - l_n + mI_{L_{(A+1)}}\right|_B$, where $1 \leq n \leq A+1$ and $0 \leq m \leq \frac{B^*}{\lambda} - 1$, while $I_{L_n} = \left|I_{L_{n-1}} + 4A + x - (l_{n-1} + l_n + 2r_{n-1})\right|_B$ for $2 \leq n \leq A+1$ and with $I_{L_1} = 0$ (these index numbers are shown on the extreme left of the first-return string-run). Hence $\left|I_{L_{(l_i)'}} - I_{L_{l_i}} + l_i - (l_i)'\right|_B = \frac{AB^*}{2} = \frac{B}{2} = \frac{100}{2} = 50$.

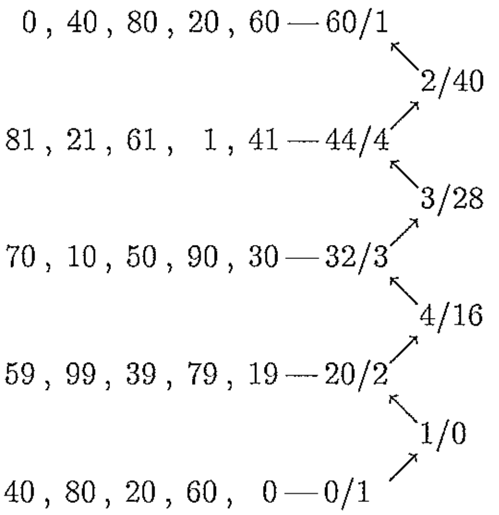

$$\begin{aligned}
I_{L_1} &= 0\,. \\
I_{L_2} &= |I_{L_1} + 4A + x - (l_1 + l_2 + 2r_1)|_B = \\
&\quad |0 + 4 \times 4 + 9 - (1 + 2 + 2 \times 1)|_{100} = 20\,. \\
I_{L_3} &= |I_{L_2} + 4A + x - (l_2 + l_3 + 2r_2)|_B = \\
&\quad |20 + 4 \times 4 + 9 - (2 + 3 + 2 \times 4)|_{100} = 32\,. \\
I_{L_4} &= |I_{L_3} + 4A + x - (l_3 + l_4 + 2r_3)|_B = \\
&\quad |32 + 4 \times 4 + 9 - (3 + 4 + 2 \times 3)|_{100} = 44\,. \\
I_{L_5} &= |I_{L_4} + 4A + x - (l_4 + l_5 + 2r_4)|_B = \\
&\quad |44 + 4 \times 4 + 9 - (4 + 1 + 2 \times 2)|_{100} = 60\,. \\
I_{R_1} &= 0\,. \\
I_{R_2} &= |I_{R_1} + 4A + x - (r_1 + r_2 + 2l_2)|_B = \\
&\quad |0 + 4 \times 4 + 9 - (1 + 4 + 2 \times 2)|_{100} = 16\,. \\
I_{R_3} &= |I_{R_2} + 4A + x - (r_2 + r_3 + 2l_3)|_B = \\
&\quad |16 + 4 \times 4 + 9 - (4 + 3 + 2 \times 3)|_{100} = 28\,. \\
I_{R_4} &= |I_{R_3} + 4A + x - (r_3 + r_4 + 2l_4)|_B = \\
&\quad |28 + 4 \times 4 + 9 - (3 + 2 + 2 \times 4)|_{100} = 40\,.
\end{aligned}$$

From the index numbers at the extreme left of the first-return string-run we see that $\left|I_{L_{(l_i)'}} - I_{L_{l_i}} + l_i - (l_i)'\right|_B = 50$ for $l_i = 1$ at nest-index number $I_{L_1} = 0$ and $(l_i)' = 3$ at nest-index number $I_{L_3} = 52$. Thus half-cycle part 1 can be associated with the lower-left to upper-right half-cycle starting on left bight-boundary 1 at nest-index number 0, and half-cycle part $1'$ can be associated with the lower-left to upper-right half-cycle starting on left bight-boundary 3 at nest-index number 52. Since this involves the string-run of one sub-component with 20 bights, the outgoing lower-left to upper-right half-cycles are 21 'coinciding' with half-cycle part $1'$, and $21'$ 'coinciding' with half-cycle part 1. In Fig. 785 a part of the string-run of the foundation knot is shown. Note the lengthways offset position for the diametrical string passage of the foundation knot due to the small x-value.

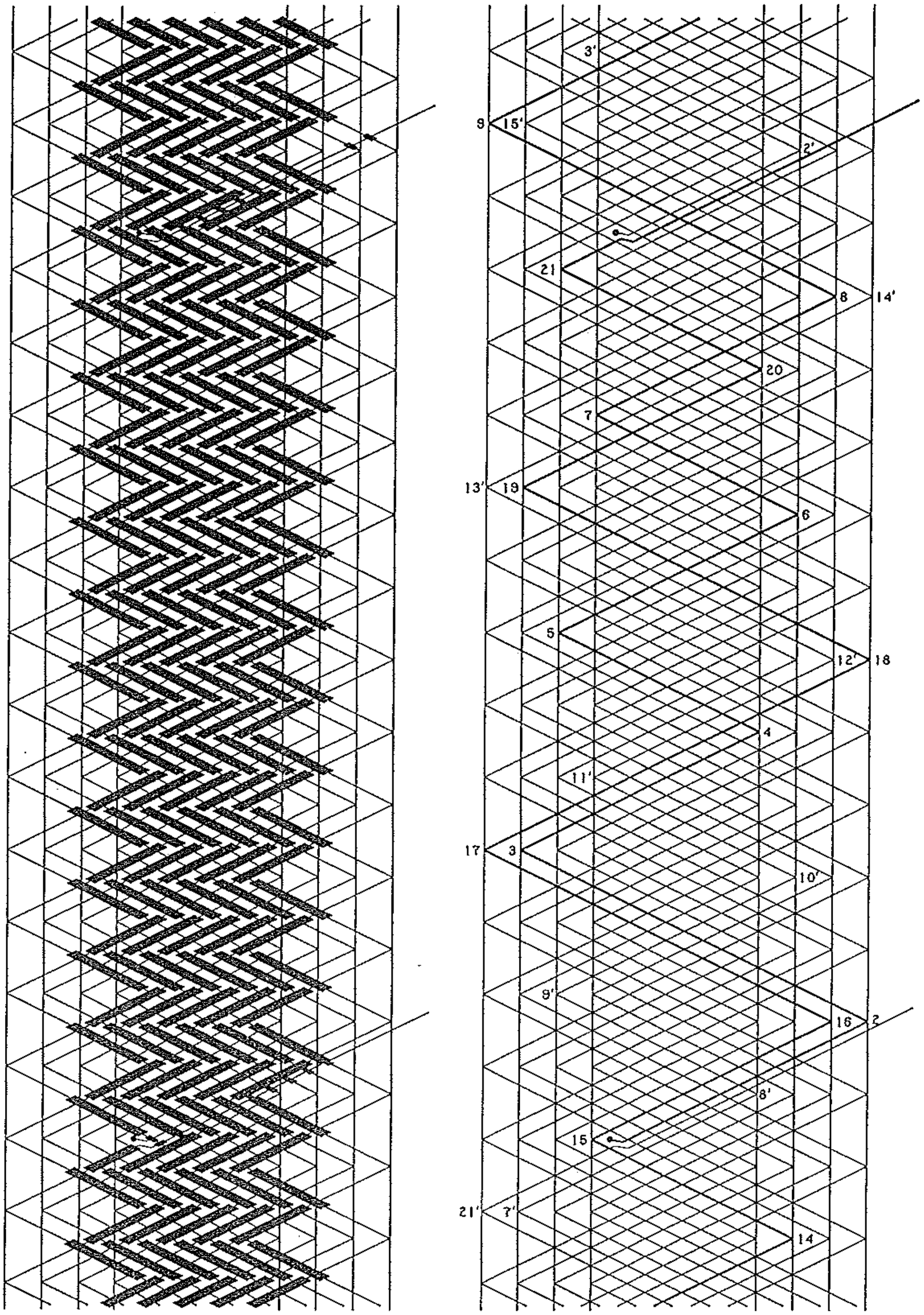

Fig. 785 — Part of grid-diagram and string-run diagram.

For greater x-values a more balanced position for the diametrical string passage of the foundation knot can be achieved (see for example Fig.thinspace786 where $x = 29$ and $B^* = 15$).

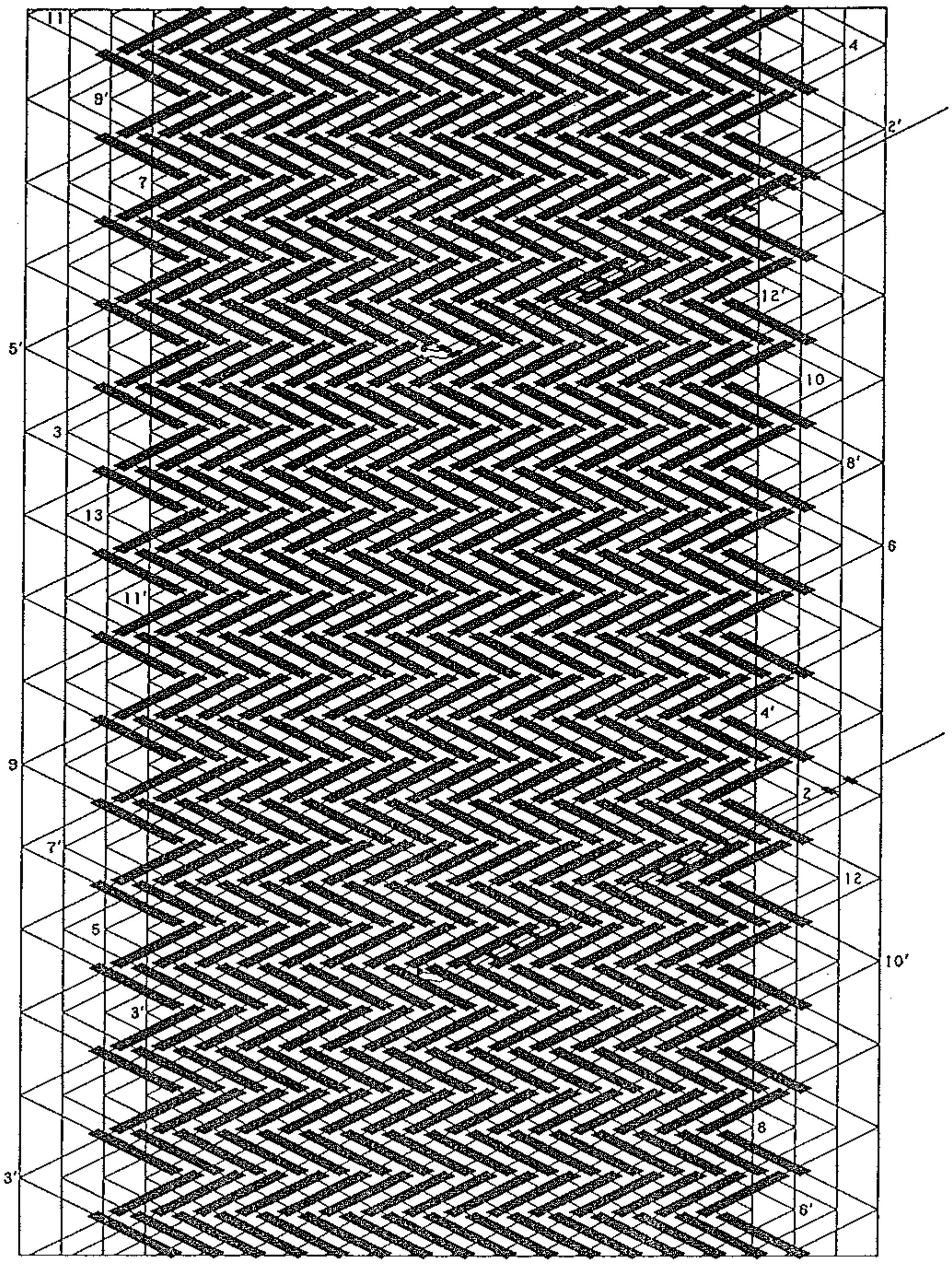

Fig. 786 — $A = 4$; $x = 29$; $y = A + 1 = 5$; $B^* = 15$. Hence $k = 3$ and $\Delta = 1$.

Type II — Example:

Let $A = 4$; $x = 19$; $B^* = 15$; $y = A + 1 = 5$. Hence $k = \left|\frac{x-A-3}{2}\right|_A = \left|\frac{19-4-3}{2}\right|_4 = 2$, and $\Delta = |y|_A = |5|_4 = 1$. $P = 2A + x - 2 = 2 \times 4 + 19 - 2 = 25$, hence $\lambda = \text{g.c.d.}\,(P, B^*) = \text{g.c.d.}\,(25, 15) = 5$; each sub-component has thus $\frac{AB^*}{\lambda} = \frac{60}{5} = 12$ bights.

Let the extended half-cycle part 1 be on the bight-boundary l_i at nest-index number $I_{L_{l_i}} = 0$, and let the extended half-cycle part $1'$ be on the bight-boundary $(l_i)' = \left|l_i + \frac{AB^*}{2}\right|_A$ at nest-index number $I_{L_{(l_i)'}} = \left|I_{L_{l_i}} + A\left[\frac{B^*}{2} - \frac{l_i - 1}{A}\right]\right|_B$.

The first-return string-run and its associated nest-index numbers are calculated in the usual manner, then for the to bight-boundary 1 extended lower-left to upper-right half-cycles the index numbers at bight-boundary 1 are calculated with the formula $I_{\text{at } l_1} = \left|I_{L_n} + 1 - l_n + mI_{L_{(A+1)}}\right|_B$, where $1 \le n \le A+1$ and $0 \le m \le \frac{B^*}{\lambda} - 1$, while $I_{L_n} = \left|I_{L_{n-1}} + 4A + x - (l_{n-1} + l_n + 2r_{n-1})\right|_B$ for $2 \le n \le A+1$ and with $I_{L_1} = 0$ (these index numbers are shown on the extreme left of the first-return string-run). Hence $\left|I_{L_{(l_i)'}} - I_{L_{l_i}} + l_i - (l_i)'\right|_B = \frac{AB^*}{2} = \frac{B}{2} = \frac{60}{2} = 30$.

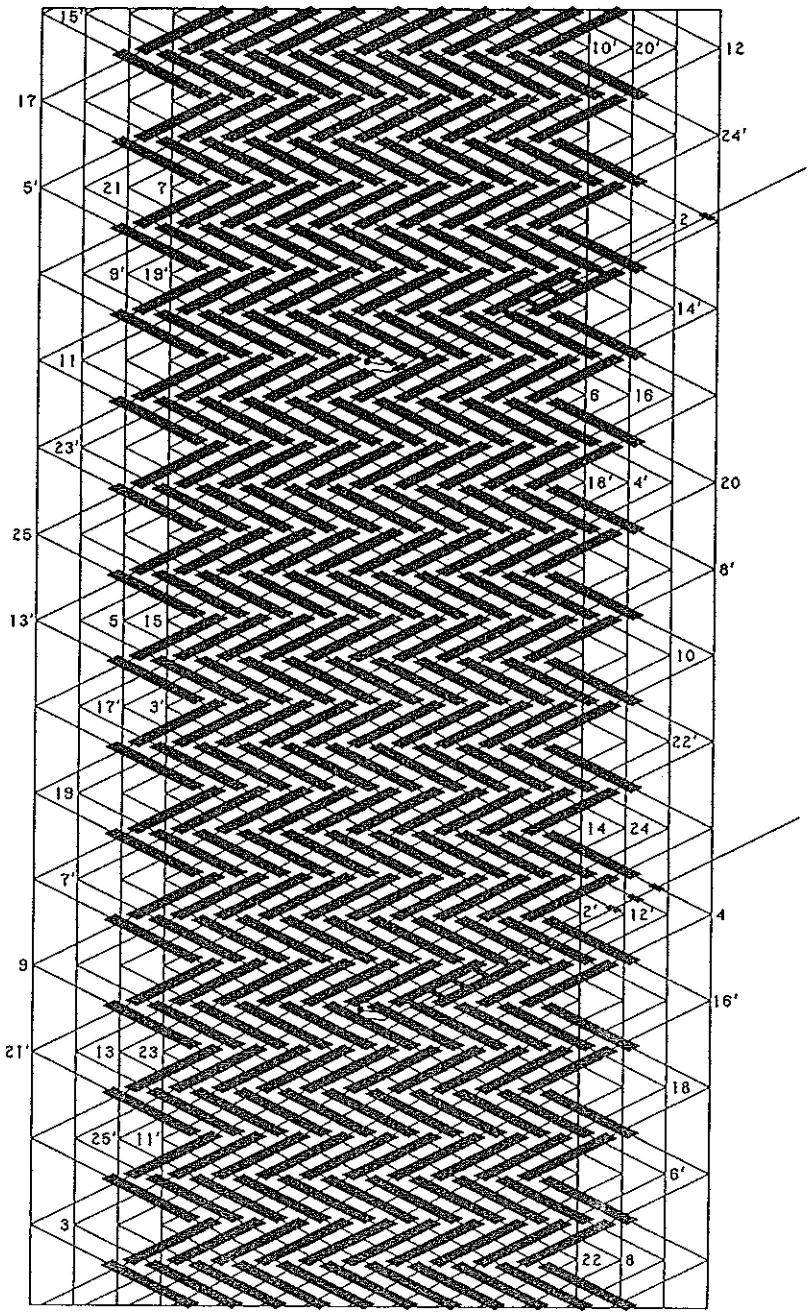

Fig. 787 — $A = 4$; $x = 19$; $y = A + 1 = 5$; $B^* = 15$. Hence $k = 2$ and $\Delta = 1$.

The index numbers at the extreme left of the first-return string-run clearly show that there isn't an l_i and $(l_i)'$, belonging to the same sub-component, for which $\left|I_{L_{(l_i)'}} - I_{L_{l_i}} + l_i - (l_i)'\right|_B = 30$. The grid-diagram (see Fig. 787) shows that we can place the string, which runs diametrically through the object over which the Semi-Perfect Herringbone Pineapple sits, between the lower-left to upper-right half-cycles which start on left bight-boundary $l_i = 1$ at $I_{L_{l_i}} = 0$ and on left bight-boundary $(l_i)' = 3$ at $I_{L_{(l_i)'}} = 32$. Note that the diametrically through string joins two sub-components, and hence the outgoing half-cycles are $\frac{2AB^*}{\lambda} + 1 = 25$ and $(\frac{2AB^*}{\lambda} + 1)' = 25'$ which respectively 'coincide' with half-cycle parts 1 and $1'$.

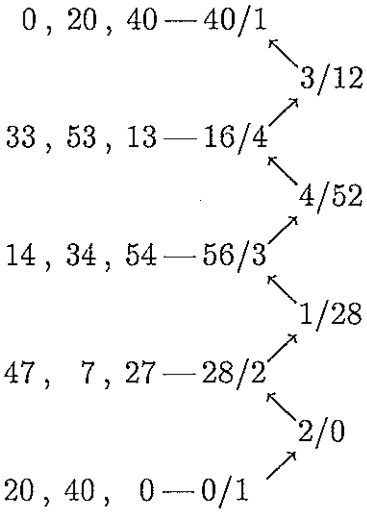

$$
\begin{aligned}
I_{L_1} &= 0\,.\\
I_{L_2} &= |I_{L_1} + 4A + x - (l_1 + l_2 + 2r_1)|_B = \\
&\quad |0 + 4 \times 4 + 19 - (1 + 2 + 2 \times 2)|_{60} = 28\,.\\
I_{L_3} &= |I_{L_2} + 4A + x - (l_2 + l_3 + 2r_2)|_B = \\
&\quad |28 + 4 \times 4 + 19 - (2 + 3 + 2 \times 1)|_{60} = 56\,.\\
I_{L_4} &= |I_{L_3} + 4A + x - (l_3 + l_4 + 2r_3)|_B = \\
&\quad |56 + 4 \times 4 + 19 - (3 + 4 + 2 \times 4)|_{60} = 16\,.\\
I_{L_5} &= |I_{L_4} + 4A + x - (l_4 + l_5 + 2r_4)|_B = \\
&\quad |16 + 4 \times 4 + 19 - (4 + 1 + 2 \times 3)|_{60} = 40\,.\\
I_{R_1} &= 0\,.\\
I_{R_2} &= |I_{R_1} + 4A + x - (r_1 + r_2 + 2l_2)|_B = \\
&\quad |0 + 4 \times 4 + 19 - (2 + 1 + 2 \times 2)|_{60} = 28\,.\\
I_{R_3} &= |I_{R_2} + 4A + x - (r_2 + r_3 + 2l_3)|_B = \\
&\quad |28 + 4 \times 4 + 19 - (1 + 4 + 2 \times 3)|_{60} = 52\,.\\
I_{R_4} &= |I_{R_3} + 4A + x - (r_3 + r_4 + 2l_4)|_B = \\
&\quad |52 + 4 \times 4 + 19 - (4 + 3 + 2 \times 4)|_{60} = 12\,.
\end{aligned}
$$

Type III — Example:

Let $A = 4$; $x = 19$; $B^* = 10$; $y = A + 1 = 5$. Hence $k = \left|\frac{x-A-3}{2}\right|_A = \left|\frac{19-4-3}{2}\right|_4 = 2$, and $\Delta = |y|_A = |5|_4 = 1$. $P = 2A + x - 2 = 2 \times 4 + 19 - 2 = 25$, hence $\lambda = \text{g.c.d.}(P, B^*) = \text{g.c.d.}(25, 10) = 5$; each sub-component has thus $\frac{AB^*}{\lambda} = \frac{40}{5} = 8$ bights.

Let the extended half-cycle part 1 be on the bight-boundary l_i at nest-index number $I_{L_{l_i}} = 0$, and let the extended half-cycle part $1'$ be on the bight-boundary $(l_i)' = \left|l_i + \frac{AB^*}{2}\right|_A$ at nest-index number $I_{L_{(l_i)'}} = \left|I_{L_{l_i}} + A\left[\frac{B^*}{2} - \frac{l_i-1}{A}\right]\right|_B$.

The first-return string-run and its associated nest-index numbers are calculated in the usual manner, then for the to bight-boundary 1 extended lower-left to upper-right half-cycles the index numbers at bight-boundary 1 are calculated with the formula $I_{\text{at } l_1} = \left|I_{L_n} + 1 - l_n + mI_{L_{(A+1)}}\right|_B$, where $1 \le n \le A+1$ and $0 \le m \le \frac{B^*}{\lambda} - 1$, while $I_{L_n} = \left|I_{L_{n-1}} + 4A + x - (l_{n-1} + l_n + 2r_{n-1})\right|_B$ for $2 \le n \le A+1$ and with $I_{L_1} = 0$ (these index numbers are shown on the extreme left of the first-return string-run). Hence $\left|I_{L_{(l_i)'}} - I_{L_{l_i}} + l_i - (l_i)'\right|_B = \frac{AB^*}{2} = \frac{B}{2} = \frac{40}{2} = 20$.

From the index numbers at the extreme left of the first-return string-run we see that $\left|I_{L_{(l_i)'}} - I_{L_{l_i}} + l_i - (l_i)'\right|_B = \frac{AB^*}{2} = \frac{B}{2} = \frac{40}{2} = 20$. For $(l_i)' = l_i$ with l_i at $I_{L_{l_i}} = 0$ and $(l_i)'$ at $I_{L'_{(l_i)}} = 20$

Thus half-cycle part 1 can be associated with the lower-left to upper-right half-cycle starting on left bight-boundary 3 at nest-index number 0, and half-cycle part $1'$ can be associated with the lower-left to upper-right half-cycle starting on left bight-boundary 3 at nest-index number 20. Since this involves the string-run of one sub-component with

$\frac{B}{\lambda} = \frac{40}{5} = 8$ bights, the outgoing lower-left to upper-right half-cycles are $9'$ 'coinciding' with half-cycle part 1, and 9 'coinciding' with half-cycle part $1'$.

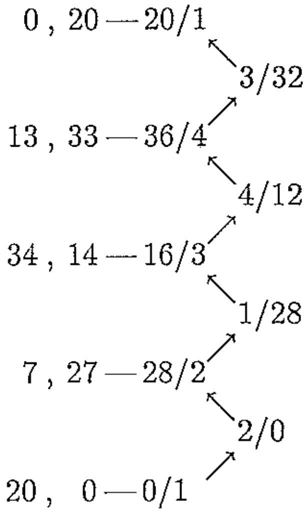

$$
\begin{aligned}
I_{L_1} &= 0\,.\\
I_{L_2} &= |I_{L_1} + 4A + x - (l_1 + l_2 + 2r_1)|_B = \\
&\quad |0 + 4 \times 4 + 19 - (1 + 2 + 2 \times 2)|_{40} = 28\,.\\
I_{L_3} &= |I_{L_2} + 4A + x - (l_2 + l_3 + 2r_2)|_B = \\
&\quad |28 + 4 \times 4 + 19 - (2 + 3 + 2 \times 1)|_{40} = 16\,.\\
I_{L_4} &= |I_{L_3} + 4A + x - (l_3 + l_4 + 2r_3)|_B = \\
&\quad |16 + 4 \times 4 + 19 - (3 + 4 + 2 \times 4)|_{40} = 36\,.\\
I_{L_5} &= |I_{L_4} + 4A + x - (l_4 + l_5 + 2r_4)|_B = \\
&\quad |36 + 4 \times 4 + 19 - (4 + 1 + 2 \times 3)|_{40} = 20\,.\\
I_{R_1} &= 0\,.\\
I_{R_2} &= |I_{R_1} + 4A + x - (r_1 + r_2 + 2l_2)|_B = \\
&\quad |0 + 4 \times 4 + 19 - (2 + 1 + 2 \times 2)|_{40} = 28\,.\\
I_{R_3} &= |I_{R_2} + 4A + x - (r_2 + r_3 + 2l_3)|_B = \\
&\quad |28 + 4 \times 4 + 19 - (1 + 4 + 2 \times 3)|_{40} = 12\,.\\
I_{R_4} &= |I_{R_3} + 4A + x - (r_3 + r_4 + 2l_4)|_B = \\
&\quad |12 + 4 \times 4 + 19 - (4 + 3 + 2 \times 4)|_{40} = 32\,.
\end{aligned}
$$

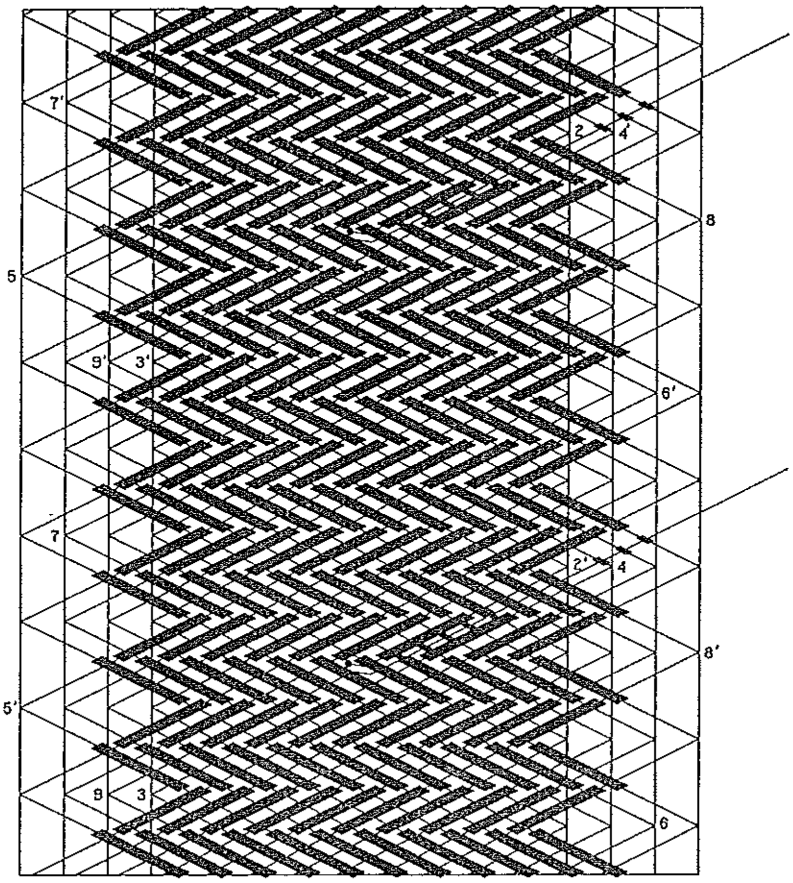

Fig. 788 — $A = 4$; $x = 19$; $y = A + 1 = 5$; $B^* = 10$. Hence $k = 2$ and $\Delta = 1$.

Besides these three string-run types I, II and III for the foundation knot, we have string-run types where the string-run from the diametrical passage position 1 describes a right helix while the string-run from the diametrical passage position $1'$ describes a left helix, or vice versa.

Example 3.

Fig. 785 shows the grid-diagram of a 2-pass Perfect Herringbone Pineapple Knot (hence $A = 2$), with its string passing diametrically through the object which it encircles. The further particulars of this knot are $x = 9$, $y = A - 1 = 1$, $B^* = 5$. Hence $k = \left|\frac{x-A-1}{2}\right|_A = \left|\frac{9-2-1}{2}\right|_2 = |3|_2 = 1$ and $\Delta = |y|_A = |1|_2 = 1$.

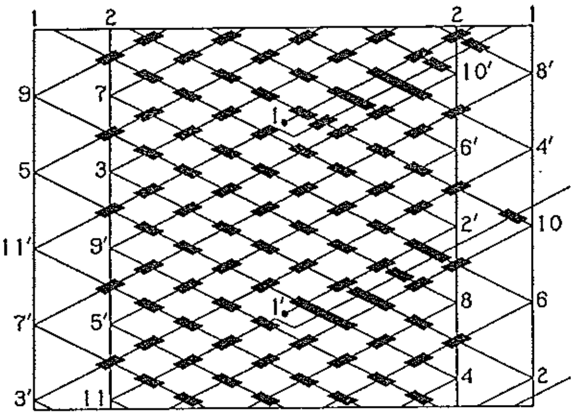

Fig. 789 — The Perfect Herringbone Pineapple Knot with $A = 2$, $x = 9$, $B^* = 5$, $y = A - 1$.

Hence in our Example with half-cycle $(B+1)' = 11'$ and extended half-cycle part 1 starting on left bight-boundary $l_i = 1$ at nest-index number $I_{L_1} = I_{L_{(B+1)'}} = I_{L_{11'}} = 0$, half-cycle $(B+1) = 11$ and extended half-cycle part $1'$ start on left bight-boundary $\left|l_i + \frac{AB^*}{2}\right|_A = \left|1 + \frac{10}{2}\right|_2 = 2$ at nest-index number $I_{L_{1'}} = I_{L_{(B+1)}} = I_{L_{11}} = A\left\lceil \frac{B^*}{2} - \frac{l_i - 1}{A} \right\rceil = 2\left\lceil \frac{5}{2} - \frac{1-1}{2} \right\rceil = 2 \times 3 = 6$.

Hence for our Example here we obtain the first-return string-run and half-cycle pattern shown in Fig. 790.

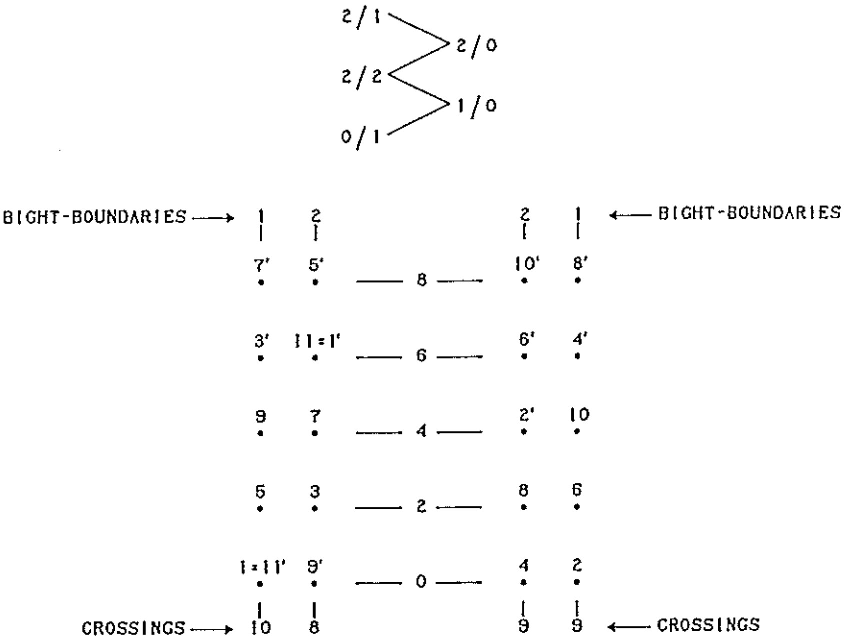

Fig. 790 — First-return string-run and half-cycle pattern for Example 3.

From the half-cycle pattern in Fig. 790 we assemble the half-cycle tables in Fig. 791.

In the odd-numbered half-cycle table the outgoing half-cycle $11'$ has two **unders** to the right of the heavy line in the penultimate bottom row. The outgoing half-cycle 11 has four **unders** to the right of the heavy line in the bottom row. In the even-numbered half-cycle tables neglect the crossed 2 and $2'$ and for half-cycle $2'$ neglect 2.

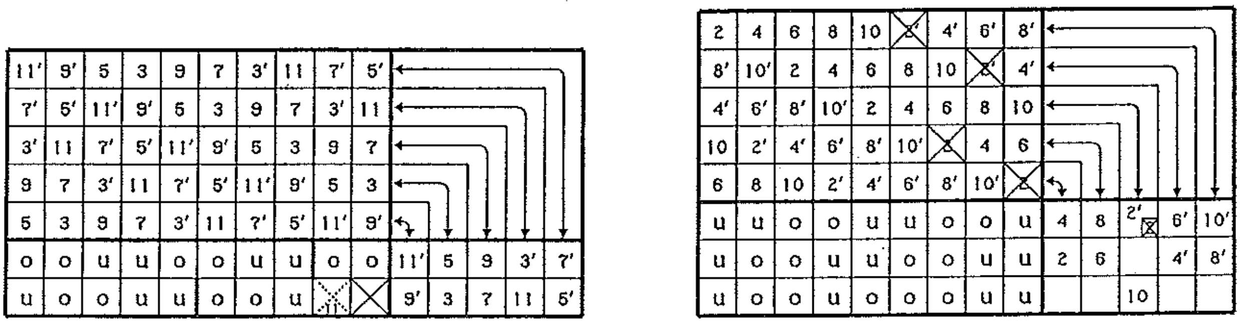

11′	9′	5	3	9	7	3′	11	7′	5′					
7′	5′	11′	9′	5	3	9	7	3′	11					
3′	11	7′	5′	11′	9′	5	3	9	7					
9	7	3′	11	7′	5′	11′	9′	5	3					
5	3	9	7	3′	11	7′	5′	11′	9′					
o	o	u	u	o	o	u	u	o	o	11′	5	9	3′	7′
u	o	o	u	u	o	o	u	$\cancel{11}$	☒	9′	3	7	11	5′

2	4	6	8	10	$\cancel{2'}$	4′	6′	8′					
8′	10′	2	4	6	8	10	$\cancel{2'}$	4′					
4′	6′	8′	10′	2	4	6	8	10					
10	2′	4′	6′	8′	10′	$\cancel{2}$	4	6					
6	8	10	2′	4′	6′	8′	10′	$\cancel{2}$					
u	u	o	o	u	u	o	o	u	4	8	2′ ☒	6′	10′
u	o	o	u	u	o	o	u	u	2	6		4′	8′
u	o	o	u	o	o	o	u	u			10		

Fig. 791 — The half-cycle tables for Example 3.

From the half-cycle tables in Fig. 791 we read the half-cycle braiding algorithms:

1. $\longrightarrow 1$: Free run.
$1'$. $\longrightarrow 2$: Free run.
2. $2 \longleftarrow 1$: u.
$2'$. $1 \longleftarrow 2$: Free run.
3. $2 \longrightarrow 2$: o.
$3'$. $1 \longrightarrow 1$: $2o$.
4. $1 \longleftarrow 2$: $o-u$.
$4'$. $2 \longleftarrow 1$: $o-2u$.
5. $1 \longrightarrow 1$: $u-3o$.
$5'$. $2 \longrightarrow 2$: $o-u-o$.
6. $2 \longleftarrow 1$: $2o-3u$.
$6'$. $1 \longleftarrow 2$: $2o-2u$.
7. $2 \longrightarrow 2$: $u-o-u-o-u$.
$7'$. $1 \longrightarrow 1$: $2u-o-u-2o$.
8. $1 \longleftarrow 2$: $u-2o-u-o-u$.
$8'$. $2 \longleftarrow 1$: $u-2o-u-o-2u$.
9. $1 \longrightarrow 1$: $o-2u-o-2u-2o$.
$9'$. $2 \longrightarrow 2$: $u-2o-2u-o-u$.
10. $2 \longleftarrow 1$: $u-2o-u-3o-2u$.
$10'$. $1 \longleftarrow 2$: $2u-2o-u-2o-u$.
11. $2 \longrightarrow$: $u-2o-6u$.
$11'$. $1 \longrightarrow$: $2o-2u-2o-4u$.

Example 4.

Fig. 792 shows the grid-diagram of a 5-pass Semi-Perfect Herringbone Pineapple Knot (hence $A = 5$), with its string passing diametrically through the object over which it sits. The further particulars of this knot are $x = 14$, $y = A+1 = 6$, $B^* = 4$. Hence $k = \left|\frac{x-A-3}{2}\right|_A = \left|\frac{14-5-3}{2}\right|_5 = |3|_5 = 3$; $P = 2A + x - 2 = 10 + 14 - 2 = 22$ and $\Delta = |y|_A = |6|_5 = 1$. The number of sub-components λ is equal to g.c.d.$(P, B^*) =$ g.c.d.$(22,4) = 2$, hence each sub-component has $\frac{B}{\lambda} = \frac{20}{2} = 10$ bights.†

---

† Compare this Example with Example 4 in *The Braider*, Issue No. 29.

Hence in our Example with half-cycle $(\frac{B}{\lambda}+1)' = 11'$ and extended half-cycle part 1 starting on left bight-boundary $l_i = 1$ at nest-index number $I_{L_1} = I_{L_{(\frac{B}{\lambda}+1)'}} = I_{L_{11'}} = 0$, half-cycle $(\frac{B}{\lambda}+1) = 11$ and extended half-cycle part $1'$ start on left bight-boundary $\left|l_i + \frac{AB^*}{2}\right|_A = \left|1 + \frac{20}{2}\right|_5 = 1$ at nest-index number $I_{L_{1'}} = I_{L_{(\frac{B}{\lambda}+1)}} = I_{L_{11}} = A\left\lceil \frac{B^*}{2} - \frac{l_i-1}{A}\right\rceil = 5\left\lceil \frac{4}{2} - \frac{1-1}{2}\right\rceil = 5 \times 2 = 10$.

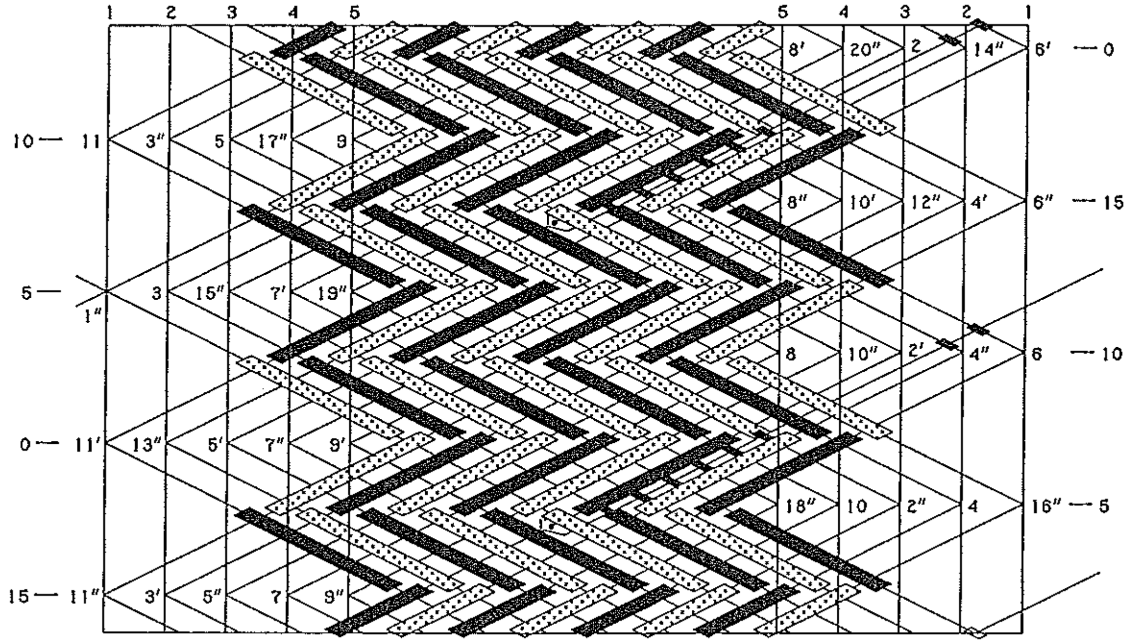

Fig. 792 — The 5-pass Semi-Perfect Herringbone Pineapple Knot of Example 4. Its first-return string-run and half-cycle pattern are depicted in Fig. 793.

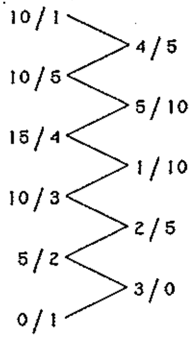

BIGHT-BOUNDARIES →	1	2	3	4	5		5	4	3	2	1	← BIGHT-BOUNDARIES
	11"	3'	5"	7	9"	— 15 —	8"	10'	12"	4'	6"	
	11=1'	3"	5	17"	9	— 10 —	8	10"	2'	4"	6	
	1"	3	15"	7'	19"	— 5 —	18"	10	2"	4	16"	
	1=11'	13"	5'	7"	9'	— 0 —	8'	20"	2	14"	6'	
CROSSINGS →	19	19	19	14	14		13	18	18	18	18	← CROSSINGS

Fig. 793 — First-return string-run and half-cycle pattern.

From the half-cycle pattern in Fig. 793 and the grid-diagram in Fig. 792 we assemble the half-cycle tables in Fig. 794. In the upper table (for the odd-numbered half-cycles from lower-left to upper-right) the codings to the right of the short heavy vertical line segment are **unders** for the half-cycles 11 and $11'$, while for the $''$ half-cycles the crossed-out $1''$ boxes are to be neglected. In the lower table (for the even-numbered half-cycles from lower-right to upper-left) the $2_\star$ and $2'_\star$ boxes are to be neglected for the half-cycles $2_\star$, $2'_\star$, $4_\star$, $4'_\star$, $6_\star$, $6'_\star$, $8_\star$, $8'_\star$, $10_\star$ and $10'_\star$, while the $_\star 2$ and $_\star 2'$ boxes are to be neglected for the half-cycles $_\star 8$ and $_\star 8'$. For the relevant even-numbered $''$ half-cycles the heavy lined boxes 2, $2'$, $_\star 2$ and $_\star 2'$ are associated with the indicated coding preceded by o.

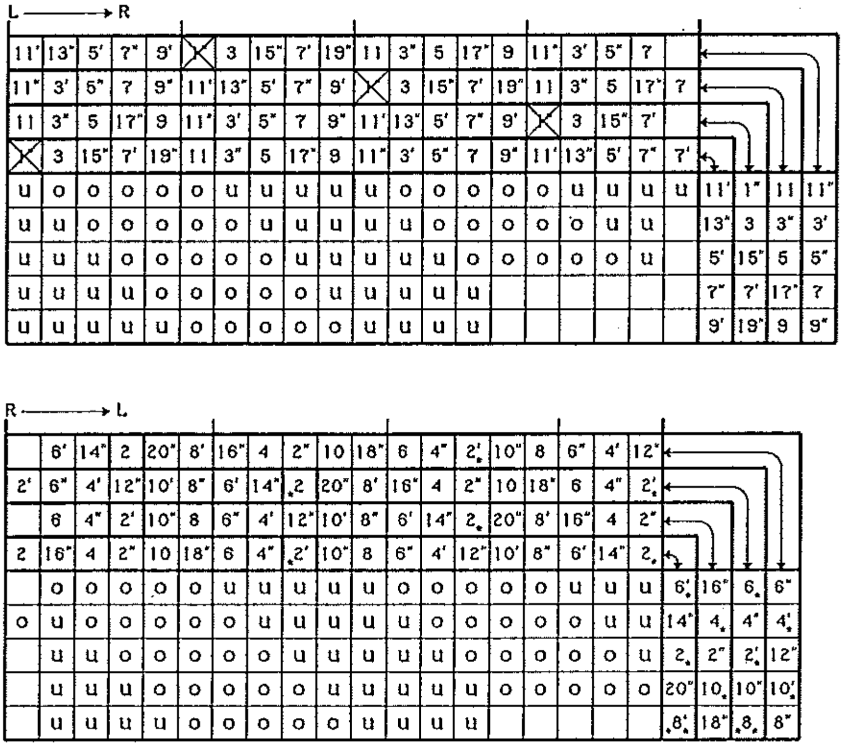

$11'$	$13''$	$5'$	$7''$	$9'$	☒	3	$15''$	$7'$	$19''$	11	$3''$	5	$17''$	9	$11''$	$3'$	$5''$	7					
$11''$	$3'$	$5''$	7	$9''$	$11'$	$13''$	$5'$	$7''$	$9'$	☒	3	$15''$	$7'$	$19''$	11	$3''$	5	$17''$	7				
11	$3''$	5	$17''$	9	$11''$	$3'$	$5''$	7	$9''$	$11'$	$13''$	$5'$	$7''$	$9'$	☒	3	$15''$	$7'$					
☒	3	$15''$	$7'$	$19''$	11	$3''$	5	$17''$	9	$11''$	$3'$	$5''$	7	$9''$	$11'$	$13''$	$5'$	$7''$	$7'$				
u	o	o	o	o	o	u	u	u	u	u	o	o	o	o	o	u	u	u	u	$11'$	$1''$	11	$11''$
u	u	o	o	o	o	o	u	u	u	u	u	o	o	o	o	o	u	u		$13''$	3	$3''$	$3'$
u	u	u	o	o	o	o	o	u	u	u	u	u	o	o	o	o	o	u		$5'$	$15''$	5	$5''$
u	u	u	u	o	o	o	o	o	u	u	u	u	u							$7''$	$7'$	$17''$	7
u	u	u	u	u	o	o	o	o	o	u	u	u	u							$9'$	$19''$	9	$9''$

	$6'$	$14''$	2	$20''$	$8'$	$16''$	4	$2''$	10	$18''$	6	$4''$	$2'_\star$	$10''$	8	$6''$	$4'$	$12''$				
$2'$	$6''$	$4'$	$12''$	$10'$	$8''$	$6'$	$14''$	$_\star 2$	$20''$	$8'$	$16''$	4	$2''$	10	$18''$	6	$4''$	$2'_\star$				
	6	$4''$	$2'$	$10''$	8	$6''$	$4'$	$12''$	$10'$	$8''$	$6'$	$14''$	$2_\star$	$20''$	$8'$	$16''$	4	$2''$				
2	$16''$	4	$2''$	10	$18''$	6	$4''$	$_\star 2'$	$10''$	8	$6''$	$4'$	$12''$	$10'$	$8''$	$6'$	$14''$	$2_\star$				
	o	o	o	o	o	u	u	u	u	u	o	o	o	o	o	u	u	u	$6'_\star$	$16''$	$6_\star$	$6''$
o	u	o	o	o	o	o	u	u	u	u	u	o	o	o	o	o	u	u	$14''$	$4_\star$	$4''$	$4'_\star$
	u	u	o	o	o	o	o	u	u	u	u	u	o	o	o	o	o	u	$2_\star$	$2''$	$2'_\star$	$12''$
	u	u	u	o	o	o	o	o	u	u	u	u	u	o	o	o	o	o	$20''$	$10_\star$	$10''$	$10'_\star$
	u	u	u	u	o	o	o	o	o	u	u	u	u						$_\star 8'_\star$	$18''$	$_\star 8_\star$	$8''$

Fig. 794 — The half-cycle tables for Example 4.

The half-cycle tables in Fig. 794 supply the following half-cycle braiding algorithms:

half-cycle part 1 $\longrightarrow 3 = r_i$: Free run.
half-cycle part $1'$ $\longrightarrow 3 = r_i$: Free run.
half-cycle 2 $l_i = 2 \longleftarrow 3 = r_i$: u.
half-cycle $2'$ $l_i = 2 \longleftarrow 3 = r_i$: u.
half-cycle 3 $l_i = 2 \longrightarrow 2 = r_i$: $2o$.
half-cycle $3'$ $l_i = 2 \longrightarrow 2 = r_i$: $2o$.
half-cycle 4 $l_i = 3 \longleftarrow 2 = r_i$: $o - 2u$.
half-cycle $4'$ $l_i = 3 \longleftarrow 2 = r_i$: $o - 2u$.
half-cycle 5 $l_i = 3 \longrightarrow 1 = r_i$: $u - o - u - o$.
half-cycle $5'$ $l_i = 3 \longrightarrow 1 = r_i$: $u - o - u - o$.
half-cycle 6 $l_i = 4 \longleftarrow 1 = r_i$: $o - 2u - o - u$.
half-cycle $6'$ $l_i = 4 \longleftarrow 1 = r_i$: $o - 2u - o - u$.
half-cycle 7 $l_i = 4 \longrightarrow 5 = r_i$: $u - 2o - u$.
half-cycle $7'$ $l_i = 4 \longrightarrow 5 = r_i$: $u - 2o - u$.
half-cycle 8 $l_i = 5 \longleftarrow 5 = r_i$: $u - o - 2u$.
half-cycle $8'$ $l_i = 5 \longleftarrow 5 = r_i$: $u - o - 2u$.

half-cycle 9 $l_i = 5 \longrightarrow 4 = r_i$: $2u - 2o - 2u$.
half-cycle $9'$ $l_i = 5 \longrightarrow 4 = r_i$: $2u - 2o - 2u$.
half-cycle 10 $l_i = 1 \longleftarrow 4 = r_i$: $2u - 2o - 2u - 2o$.
half-cycle $10'$ $l_i = 1 \longleftarrow 4 = r_i$: $2u - 2o - 2u - 2o$.
half-cycle 11 $l_i = 1 \longrightarrow$: $3o - 7u$.
half-cycle $11'$ $l_i = 1 \longrightarrow$: $3o - 7u$.

……

half-cycle $1''$ $l_i = 1 \longrightarrow 3 = r_i$: $u - 2o - 3u - 2o - 2u$.
half-cycle $2''$ $l_i = 2 \longleftarrow 3 = r_i$: $u - 4o - 2u - 3o - u$.
half-cycle $3''$ $l_i = 2 \longrightarrow 2 = r_i$: $u - 2o - 3u - 3o - u$.
half-cycle $4''$ $l_i = 3 \longleftarrow 2 = r_i$: $5o - 2u - 4o - u$.
half-cycle $5''$ $l_i = 3 \longrightarrow 1 = r_i$: $2u - 2o - 4u - 3o - u$.
half-cycle $6''$ $l_i = 4 \longleftarrow 1 = r_i$: $4o - 3u - 4o - 2u$.
half-cycle $7''$ $l_i = 4 \longrightarrow 5 = r_i$: $2u - 3o - 4u$.
half-cycle $8''$ $l_i = 5 \longleftarrow 5 = r_i$: $u - o - u - 4o - 3u$.
half-cycle $9''$ $l_i = 5 \longrightarrow 4 = r_i$: $4u - 2o - 3u$.
half-cycle $10''$ $l_i = 1 \longleftarrow 4 = r_i$: $2u - 5o - 3u - 4o$.
half-cycle $11''$ $l_i = 1 \longrightarrow 3 = r_i$: $u - 3o - 3u - 4o - 3u$.
half-cycle $12''$ $l_i = 2 \longleftarrow 3 = r_i$: $u - 4o - 4u - 5o - u$.
half-cycle $13''$ $l_i = 2 \longrightarrow 2 = r_i$: $u - 3o - 4u - 5o - 2u$.
half-cycle $14''$ $l_i = 3 \longleftarrow 2 = r_i$: $5o - u - o - 4u - 5o - 2u$.
half-cycle $15''$ $l_i = 3 \longrightarrow 1 = r_i$: $3u - 4o - 5u - 4o - u$.
half-cycle $16''$ $l_i = 4 \longleftarrow 1 = r_i$: $6o - 5u - 4o - 3u$.
half-cycle $17''$ $l_i = 4 \longrightarrow 5 = r_i$: $4u - 5o - 4u$.
half-cycle $18''$ $l_i = 5 \longleftarrow 5 = r_i$: $2u - o - 2u - 5o - 4u$.
half-cycle $19''$ $l_i = 5 \longrightarrow 4 = r_i$: $5u - 5o - 4u$.
half-cycle $20''$ $l_i = 1 \longleftarrow 4 = r_i$: $3u - 6o - 5u - 5o$.

Braid Design

We have met, in previous issues of *The Braider*, the 'conventional' grid-diagrams for depicting **round braids**. They had the advantage in clearly showing the actual braid-pattern of the round braid and hence are the normally employed grid-diagrams for these braids. However, a round braid can also be depicted by another type of grid-diagram — the **UT-OT grid-diagram** (UT = under turn, OT = over turn). Those readers who are in the possession of our Pamphlet No. 1 (published in January 1991) have already met this type of diagram which depicts **the braiding** of a **round braid** in the manner of a **flat braid**. Such a flat-braided round braid can be either kept and used in its flat-braided form or kept and used as a normal round braid. When it is kept and used in its flat-braided form we shall group it under the **flat tubular braids**, and call it a **primitive flat tubular braid**. Thus note that a **primitive flat tubular braid** is in essence a **round braid**, but that a **round braid** is **not** a **primitive flat tubular braid**.

These **primitive flat tubular braids** provide us with an opportunity to design a vast range of really beautiful 'new' braids. We shall start with a few very simple examples:

On the far right in Fig. 795 is depicted the conventional grid-diagram of an under-over coded 6-lead round braid and on the far left is depicted one of its two pictorial UT-OT diagram forms (depicted is the form where a 'half-cycle' of a front-facing string of a left helix (hence from upper-left to lower-right) starts at the left with an under; the other form starts at the left with an over). The UT-OT grid-diagram associated with this UT-OT pictorial diagram is shown by the central diagram. Note that every under-over coded round braid has two different UT-OT grid-diagrams.

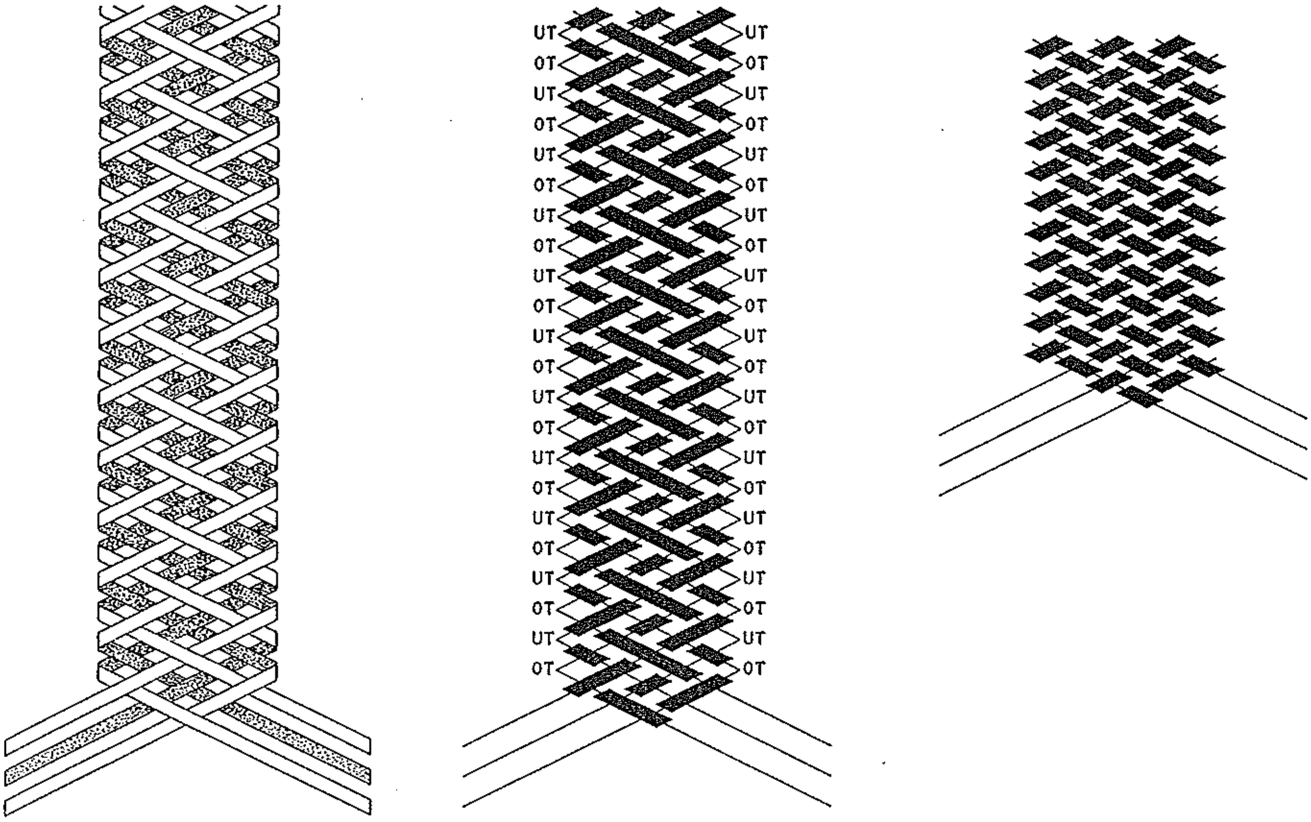

Fig. 795 — An UT-OT grid-diagram of a 6-lead under-over coded round braid.

In the upper-left pictorial diagram of Fig. 796 two of these in Fig. 795 pictorial UT-OT braids (shown again at the upper-right in Fig. 796) are placed side by side as indicated. All the right UT's and OT's of the left UT-OT braid and all the left UT's and OT's of the right UT-OT braid are cut and the cut-ends of their front-facing strings are joined and so are the cut-ends of their back-facing strings, while ensuring that at these joints the front-facing strings run behind the back-facing strings. The result of this is shown in the lower-left pictorial UT-OT diagram of Fig. 796, while on the lower-right is shown its associated UT-OT grid-diagram. This resulting braid is a kind of tubular flat braid that cannot take the shape of a round braid, in fact it appears as a beautiful flat braid.

If we had left at the joints the back-facing strings behind the front-facing strings we would have finished up with an UT-OT braid that can take the shape of a round braid. This UT-OT braid is shown by its UT-OT grid-diagram at the left in Fig. 797, while the conventional grid-diagram of this braid as a round braid is shown on the right in Fig. 797. Thus by braiding this round braid as an UT-OT braid while changing the string-run coding locally at the joint positions so as to comply with that shown in the lower-right diagram of Fig. 796, we obtain the tubular flat braid depicted there.

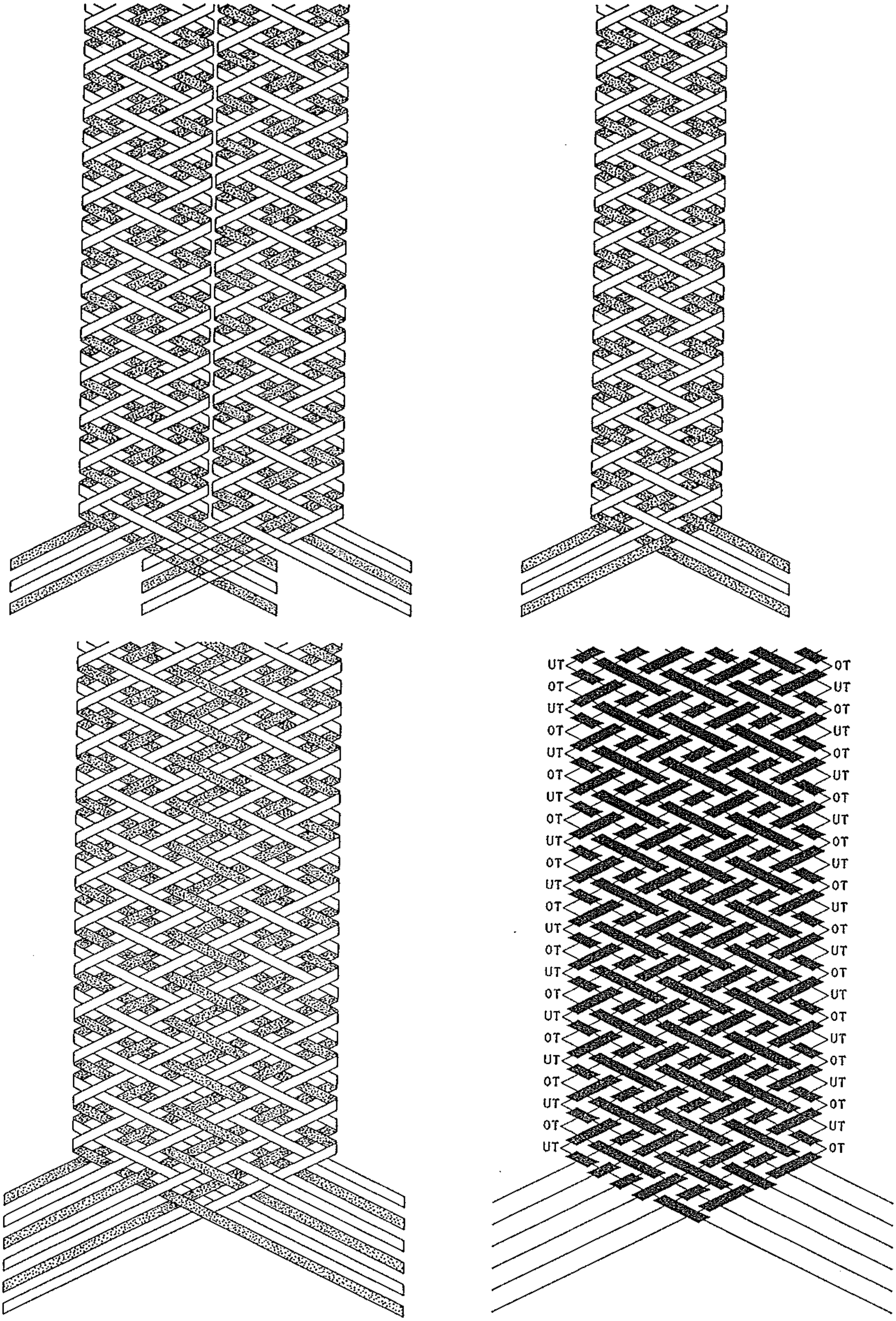

Fig. 796 —The development of a simple 12-lead tubular flat braid.

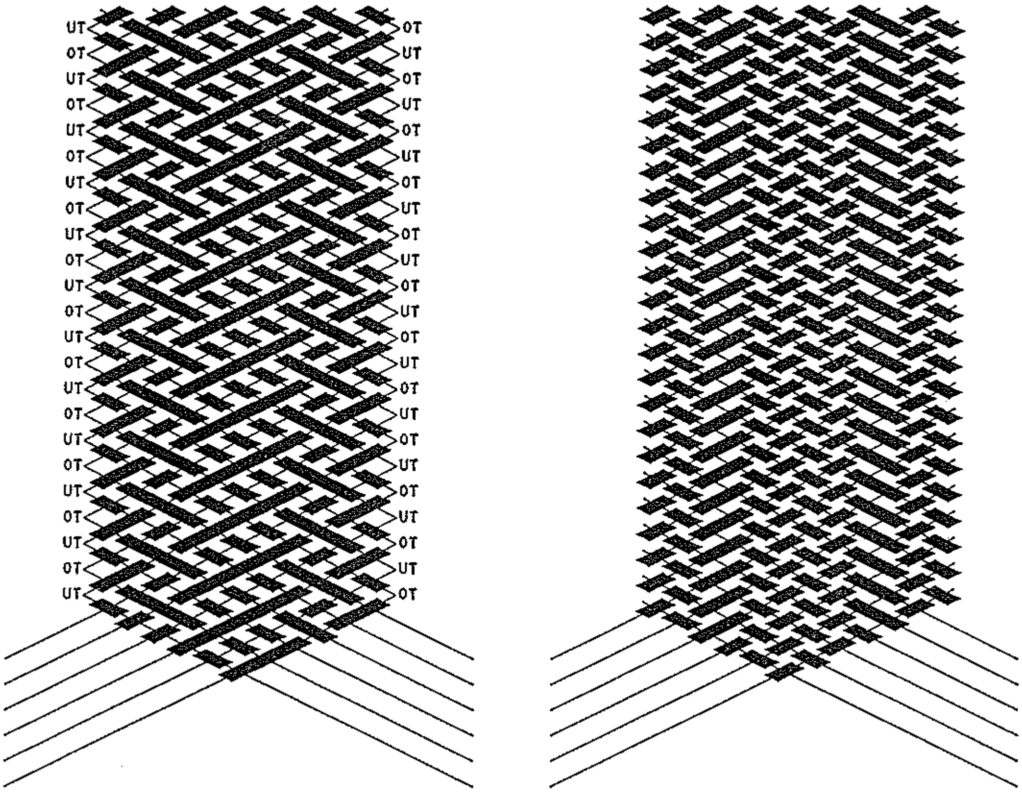

Fig. 797 — The associated 12-lead primitive flat tubular UT-OT braid and its conventional grid-diagram as a round braid.

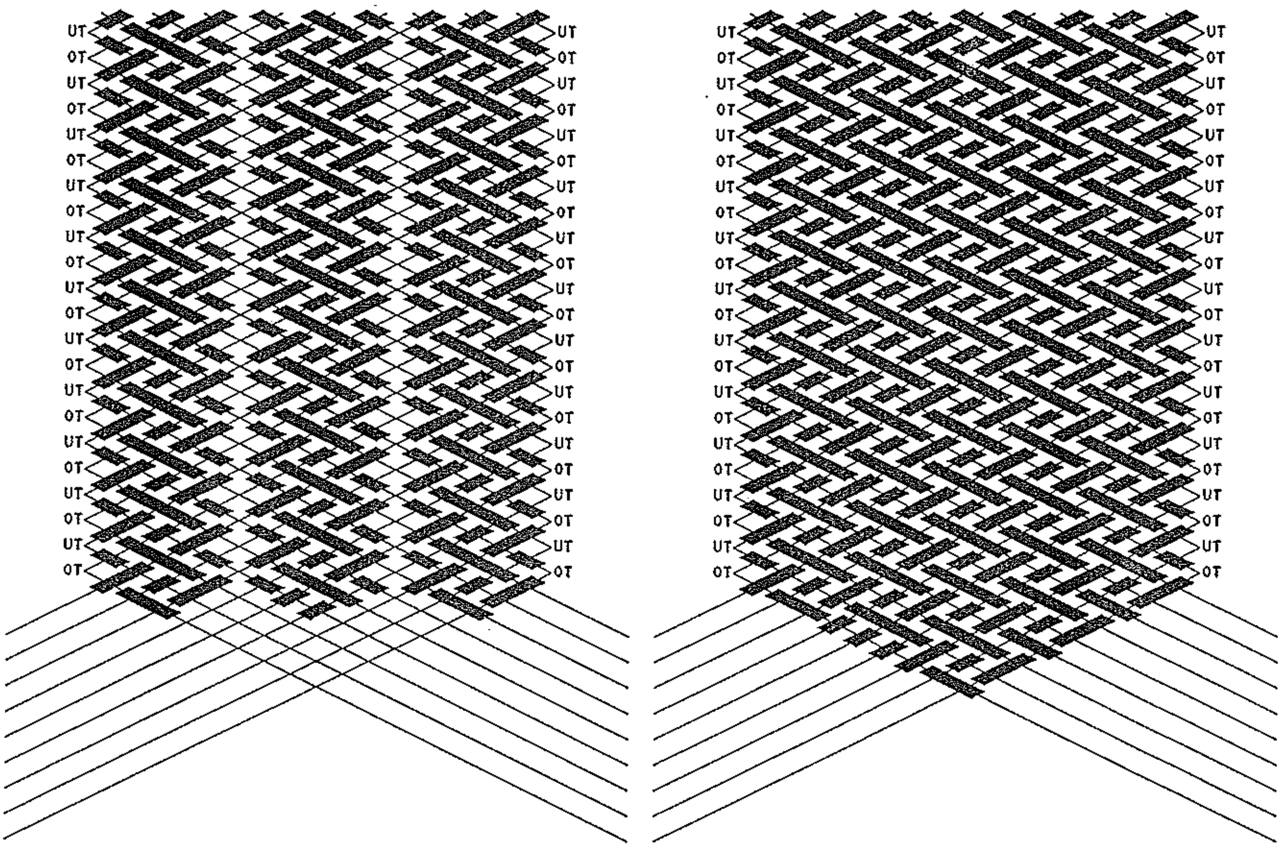

Fig. 798 — The development of a simple 18-lead tubular flat braid.

In Fig. 798 we have placed three of the UT-OT braids in Fig. 795 side by side and joined them together as in Fig. 796. The resulting braid is a beautiful tubular flat braid.

If we had again left at the joints the back-facing strings behind the front-facing strings we would have finished up with an UT-OT braid that can take the shape of a round braid. This UT-OT braid is shown by its UT-OT grid-diagram at the left in Fig. 799, while the conventional grid-diagram of this braid as a round braid is shown on the right in Fig. 799. Thus by braiding this round braid as an UT-OT braid while changing the string-run coding locally at the joint positions so as to comply with that shown in the right diagram of Fig. 798, we obtain the tubular flat braid depicted there.

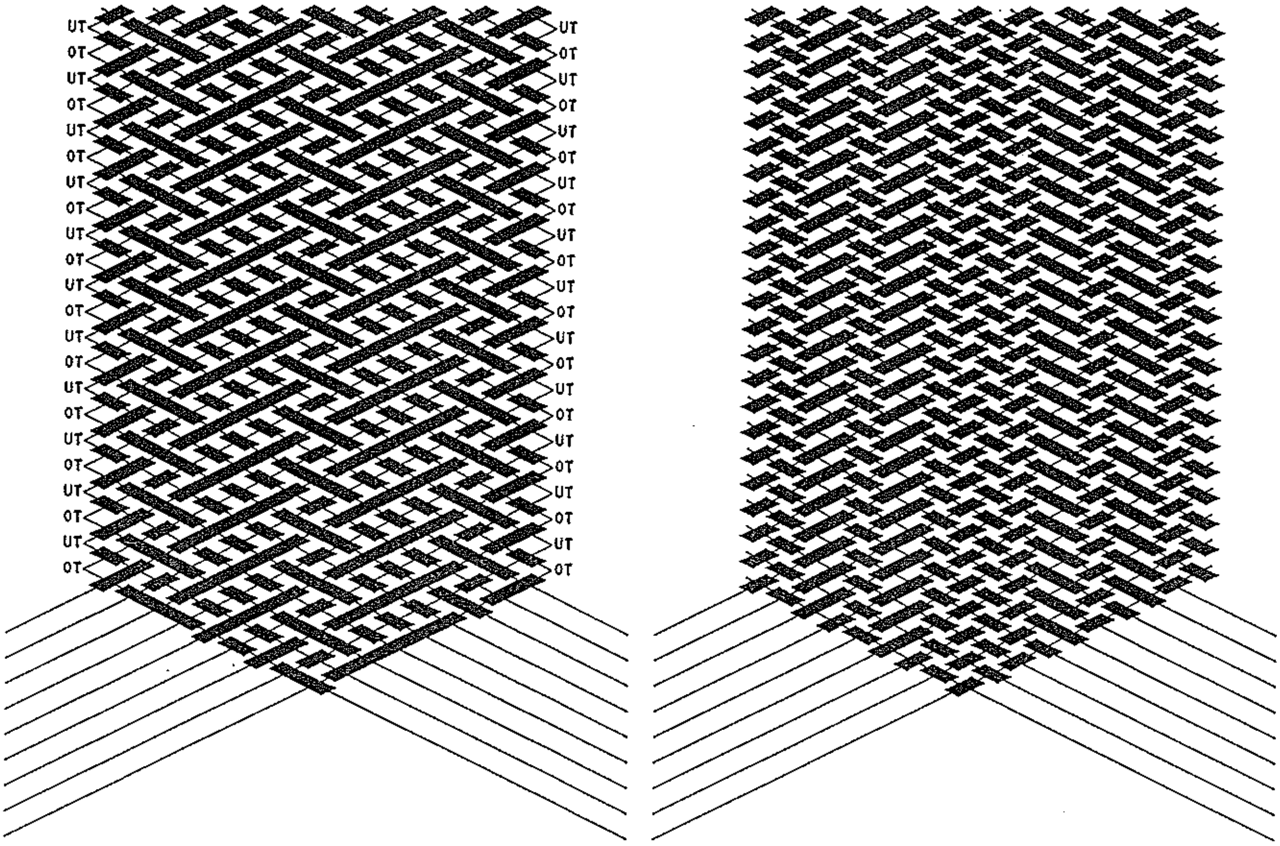

Fig. 799 — The associated 18-lead primitive flat tubular UT-OT braid and its conventional grid-diagram as a round braid.

The upper-right conventional round braid grid-diagram in Fig. 800 shows the under-over coded 4-lead round braid while its two UT-OT forms are shown to its left. When we place again two UT-OT grid-diagrams side by side, then for a balanced joint arrangement we need to use both these two UT-OT grid-diagram forms as shown on the lower-left in Fig. 800. After observing the same joining procedure as before, we obtain the lower-right UT-OT grid-diagram in Fig. 800. The resulting braid is again a beautiful tubular flat braid.

If we had left at the joints the back-facing strings behind the front-facing strings we would have finished up with an UT-OT braid that can take the shape of a round braid. This UT-OT braid is shown by its UT-OT grid-diagram at the left in Fig. 801, while the conventional grid-diagram of this braid as a round braid is shown on the right in Fig. 801. Thus by braiding this round braid as an UT-OT braid while changing the string-run coding locally at the joint positions so as to comply with that shown in the lower-right diagram of Fig. 800, we obtain the tubular flat braid depicted there.

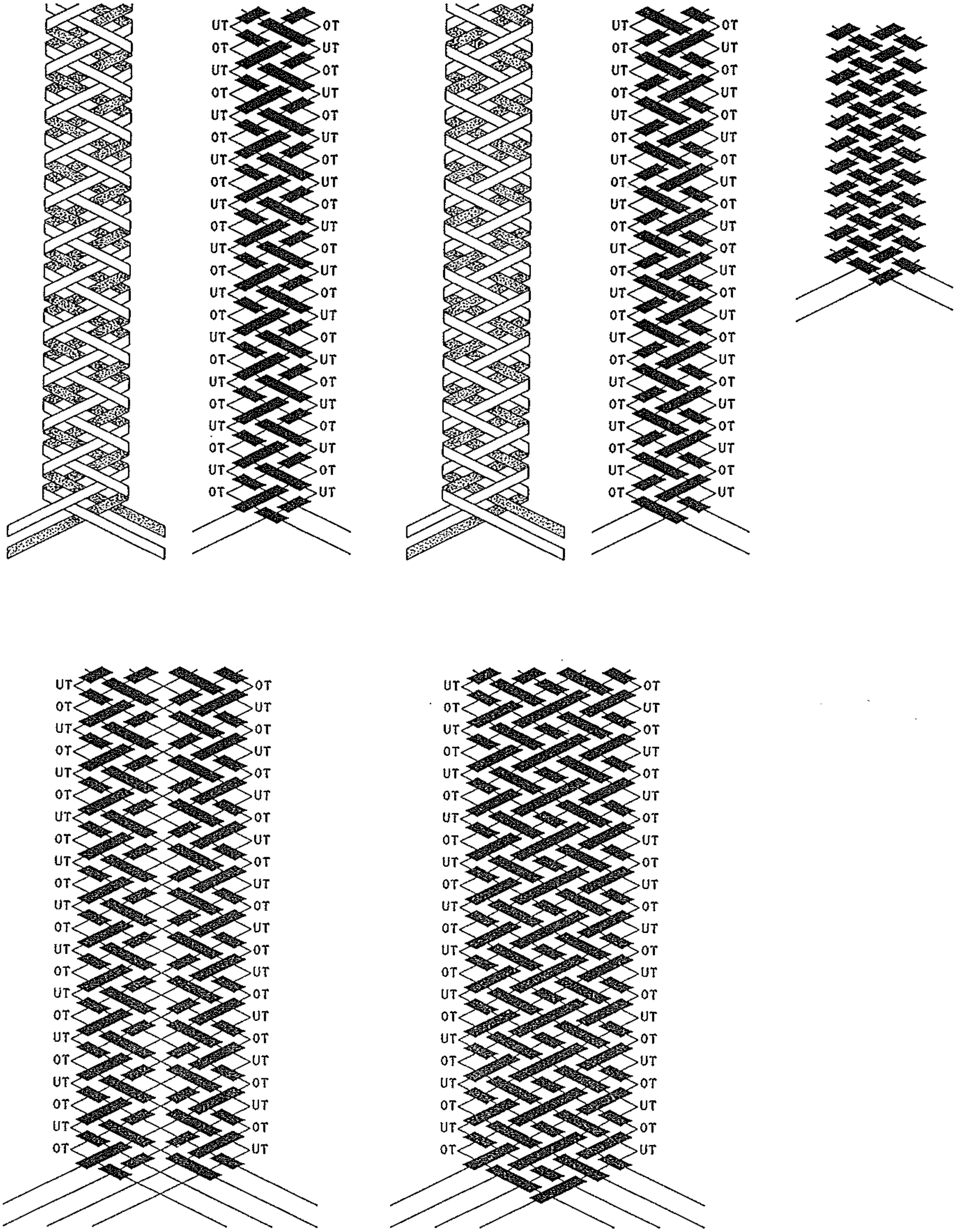

Fig. 800 — The development of a simple 8-lead tubular flat braid.

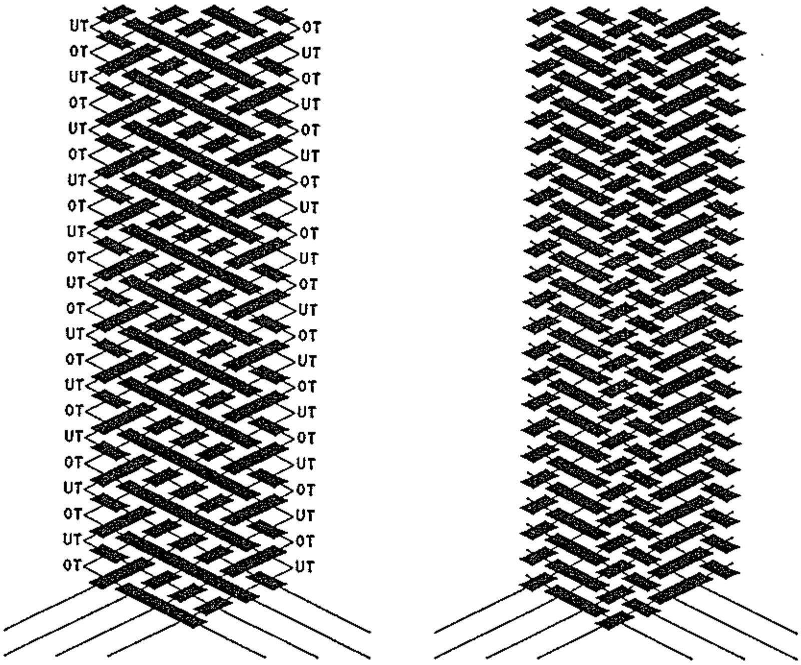

Fig. 801 — The associated 8-lead primitive flat tubular UT-OT braid and its conventional grid-diagram as a round braid.

In Fig. 802 we have added a further UT-OT braid to the right-hand side of the lower-left arrangement in Fig. 800. For a balanced joint arrangement this further UT-OT braid must be of the same form as the leftmost one. After observing the same joining procedure as before, we obtain the UT-OT grid-diagram on the right in Fig. 802. The resulting braid is again a beautiful tubular flat braid.

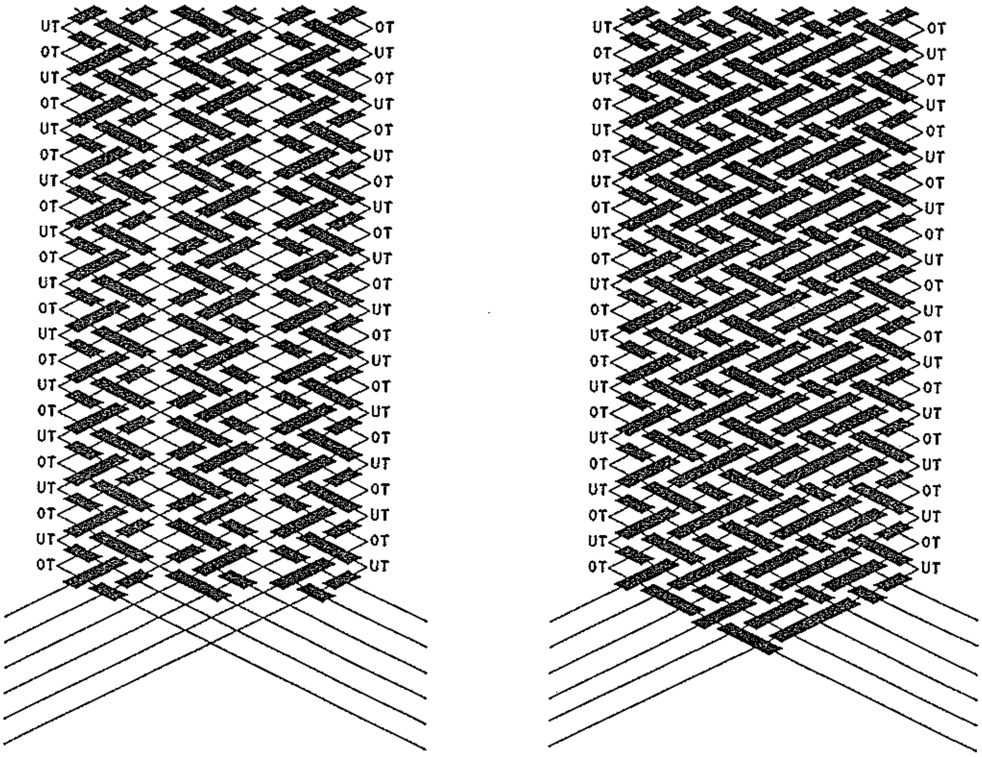

Fig. 802 — The development of a simple 12-lead tubular flat braid.

If we had left at the joints the back-facing strings behind the front-facing strings we would have finished up with an UT-OT braid that can take the shape of a round braid. This UT-OT braid is shown by its UT-OT grid-diagram at the left in Fig. 803, while the conventional grid-diagram of this braid as a round braid is shown on the right in Fig. 803. Thus by braiding this round braid as an UT-OT braid while changing the string-run coding locally at the joint positions so as to comply with that shown in the lower-right diagram of Fig. 802, we obtain the tubular flat braid depicted there.

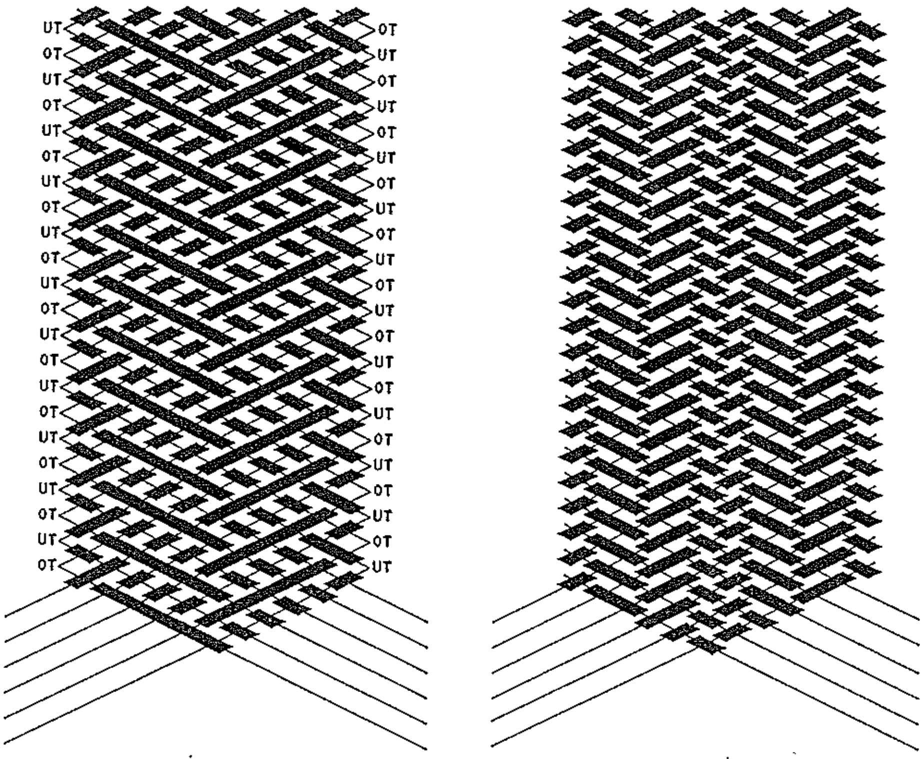

Fig. 803 — The associated 12-lead primitive flat tubular UT-OT braid and its conventional grid-diagram as a round braid.

As mentioned earlier, every under-over coded round braid has two different UT-OT grid-diagrams, hence two under-over coded primitive flat tubular UT-OT braid-forms. In the examples above of joining two or three under-over coded primitive flat tubular UT-OT braids, each with the same number of leads, we took the option for a front-facing string of a left helix in the leftmost of them to start at the left with an under.

Note that an under-over coded UT-OT braid does not show an under-over coding in its UT-OT grid-diagram. The codings shown are the codings of the actual string-crossings as well as of the virtual string-crossings.

⋆⋆ *Show that under an overall balanced and balanced joint construction procedure, a start at the left with an* **over** *for a front-facing string of a left helix in the leftmost under-over coded primitive flat tubular UT-OT braid creates the same UT-OT tubular flat braids as a start at the left with an* **under** *for a front-facing string of a left helix in the leftmost under-over coded primitive flat tubular UT-OT braid.*

Although we have kept here to the most simple tubular flat braids, tubular flat braids with a large variety of coding-patterns can be designed in a similar way. Furthermore, the tubular flat braids lead to 'new' forms of cylindrical braids — the **tubular flat torus braids.**

THE BRAIDER

No.44 **NOVEMBER 2005.**

CONTENTS

pg.
Solution to the Question in Issue No.43 1031
Braid Design 1031
Checkered Pineapple Knots 1040
Round Braids and their string sizes 1053

A quarterly publication
for
the braiding artisan

Resale of this publication or copies thereof
is strictly prohibited

Copyright ©2005 by:

A.G. Schaake; 21 Sundown Cresc.; Hamilton; New Zealand.
D. Van Tassel; Box 335; Craig, Co 81626-0335; U.S.A.
F.J.M. Masurel; Ganzenzijde 4; 2317XG Leiden; Nederland.

All rights reserved. No part of this publication may be reproduced, stored in a retrieval system, or transmitted, in any form or by any means, electronic, mechanical, photo-copying, recording, or otherwise, without prior written permission.

This publication is available to braiding artisans only.

Copies may be obtained from:

A.G. Schaake,
21 Sundown Cresc.,
Hamilton,
New Zealand.

Solution to the question in Issue No. 43

Question on pg. 1030.

Fig. 804 shows two rows of pictorial diagrams of under-over coded UT-OT braids with their UT-OT grid-diagrams immediately below them. In each of these two rows the first two diagrams from the left are associated with under-over coded UT-OT braids where $\frac{\text{leads}}{2} = \text{odd}$, and the last two diagrams from the left are associated with under-over coded UT-OT braids where $\frac{\text{leads}}{2} = \text{even}$. In the upper-row of pictorial UT-OT braids the first and third UT-OT braid from the left look towards the front of the braid while the second and fourth UT-OT braid from the left look towards the associated back of the braid. In the lower-row of pictorial UT-OT braids the first and third UT-OT braid from the left look towards the front of the braid while the second and fourth UT-OT braid from the left look towards the front of the associated braid turned through 180°.

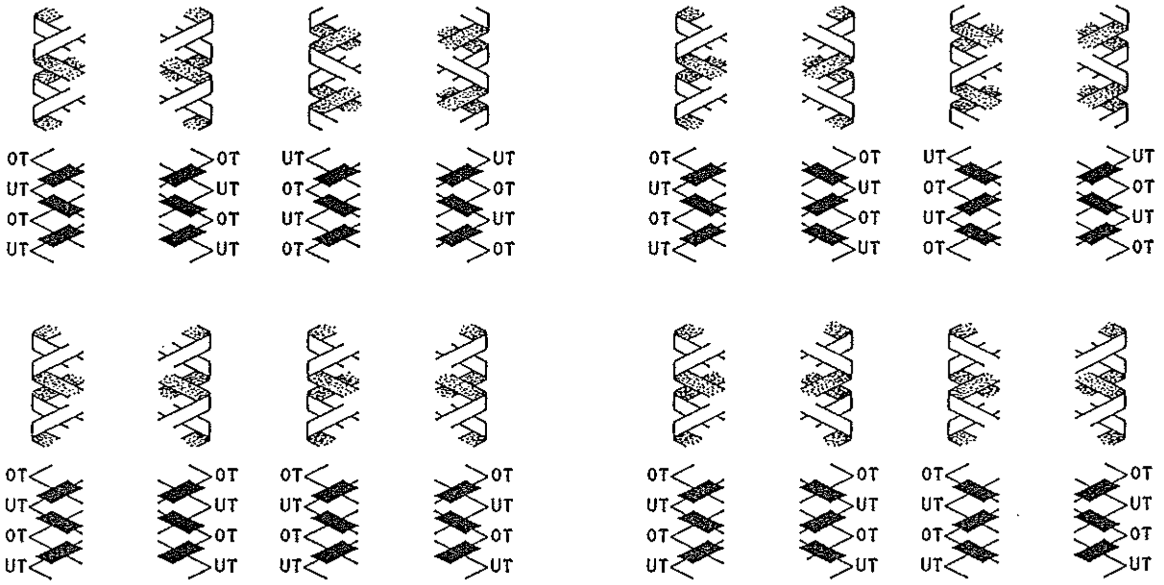

Fig. 804 — The under-over coded UT-OT braids.

Hence when in an under-over coded UT-OT braid the $\frac{\text{leads}}{2} = \text{odd}$ a front-facing left helix strand on the front of the braid starts at the left with an under, then when turning the back of this braid to the front, a front-facing left helix strand on the front of the braid starts at the left with an over (see upper left set of two diagrams); and when in an under-over coded UT-OT braid the $\frac{\text{leads}}{2} = \text{even}$ a front-facing left helix strand on the front of the braid starts at the left with an under, then when turning the front of this braid through 180°, a front-facing left helix strand on the front of the braid starts at the left with an over (see lower right set of two diagrams).

Braid Design

In issue No. 43 of *The Braider* we have seen on pp. 1023-1030 how we can design simple, but beautiful, 'new' braids with the aid of the diagrams of the **primitive flat tubular braids**. The reader will of course have realised that further 'new' braids can be designed by combining the diagrams of primitive flat tubular braids in other ways.

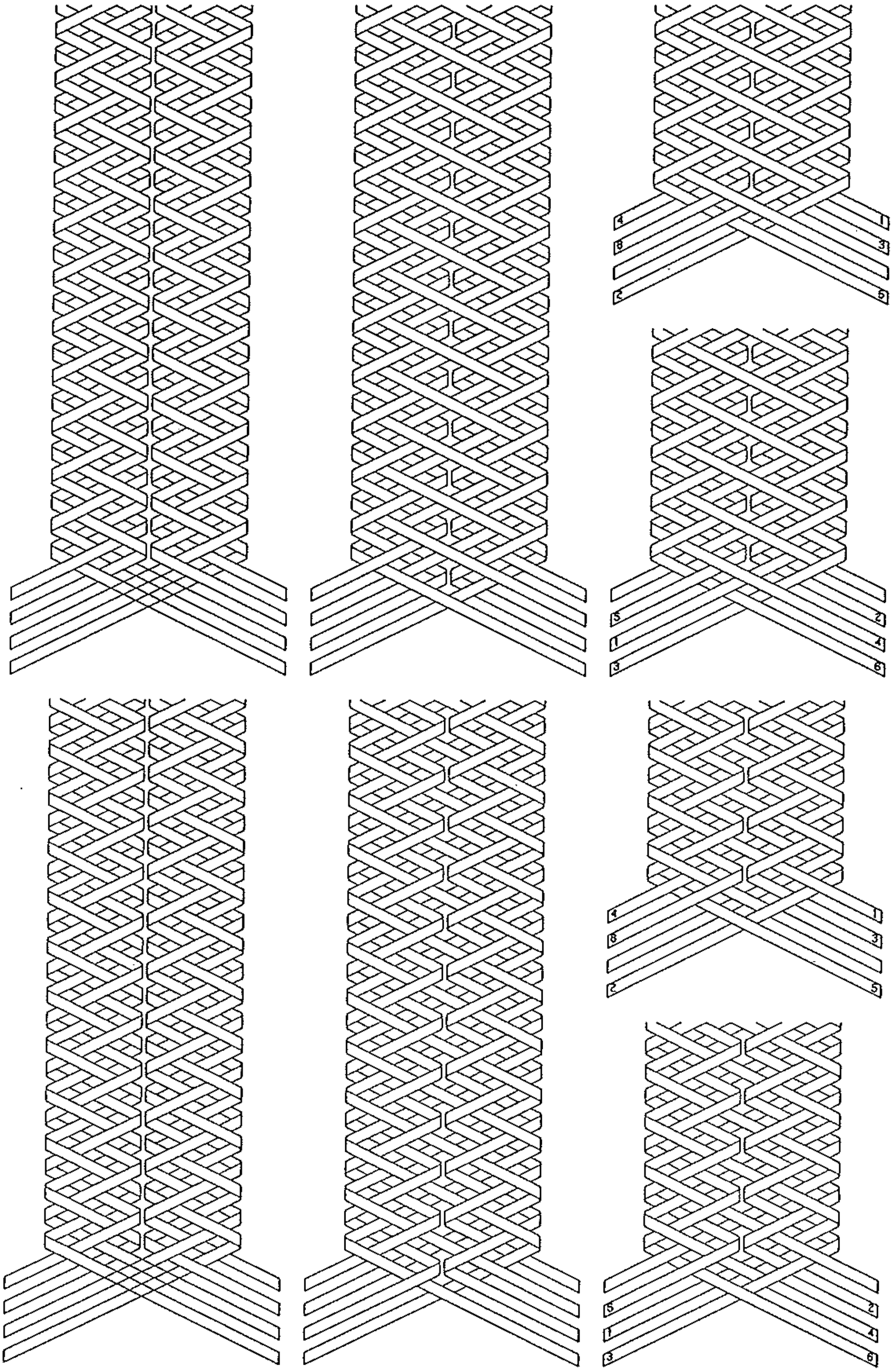

Fig. 805 — The designing of another 'new' braid.

We can, for example, design another 'new' braid by combining two under–over coded primitive flat tubular braid diagrams as depicted by the upper two left diagrams, or as depicted by the lower left two diagrams, in Fig. 805. Both methods give us the same 'new' braid (one is the other turned back to front). Again it is a beautiful 'new' braid, although a little harder to braid. Whether we use the upper or the lower braiding procedure depends on which surface of the final braid we want uppermost. Note that in this braid only the grainside of the strings is outermost.

We can design a large number of 'new' braids by combining more than two primitive flat tubular braids as well as by combining bigger ones, in fact the possibilities are limitless, however, the braiding of them becomes more and more difficult.

Let's now look at another way again to combine two four-string under–over coded primitive flat tubular braid diagrams.

The braid in Fig. 806 shows a flat front-side and two adjacent round braids on the back-side. An alternative braiding sequence for this braid is shown in Fig. 806A.

If we want to have the back-side of this braid on the front, hence the two adjacent round braids on the front, we braid it as depicted in Fig. 807; an alternative braiding sequence is shown in Fig. 807A. This beautiful braid is not difficult to produce, it should be braided nice and tight.

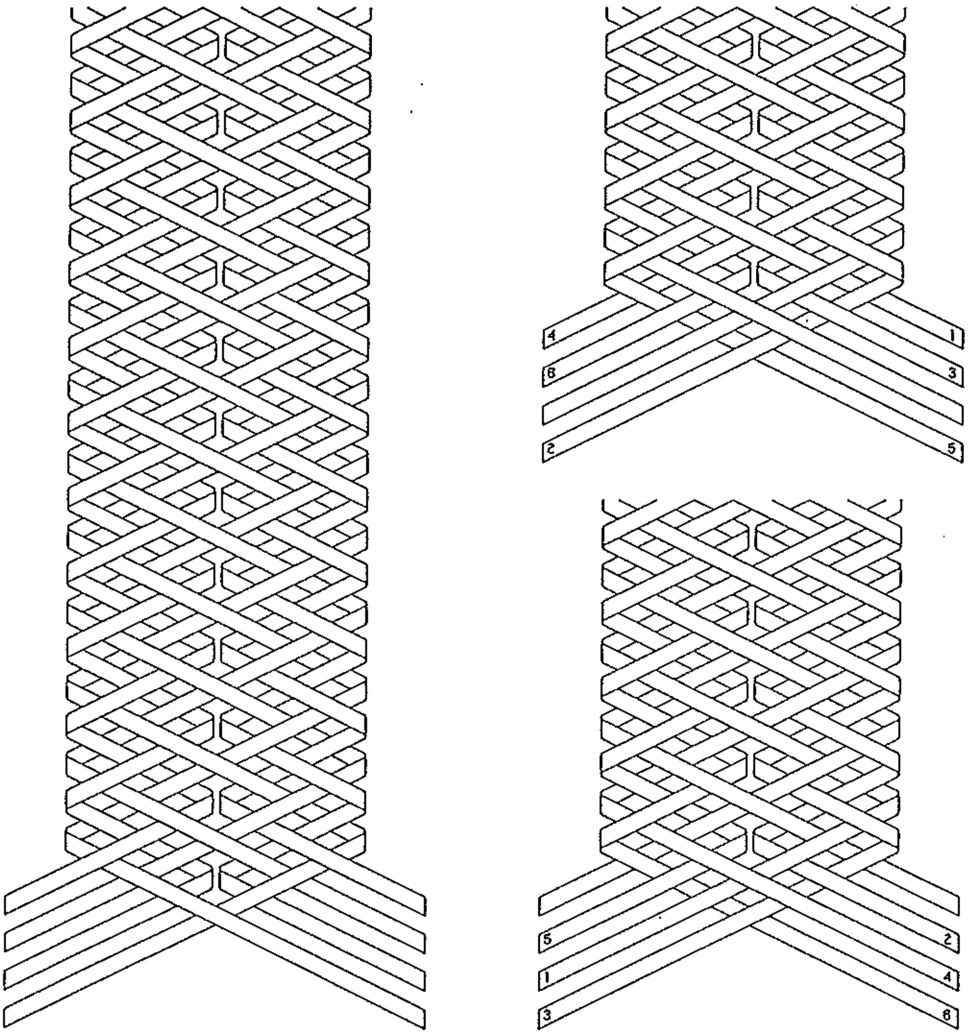

Fig. 806 — Designing a 'new' braid.

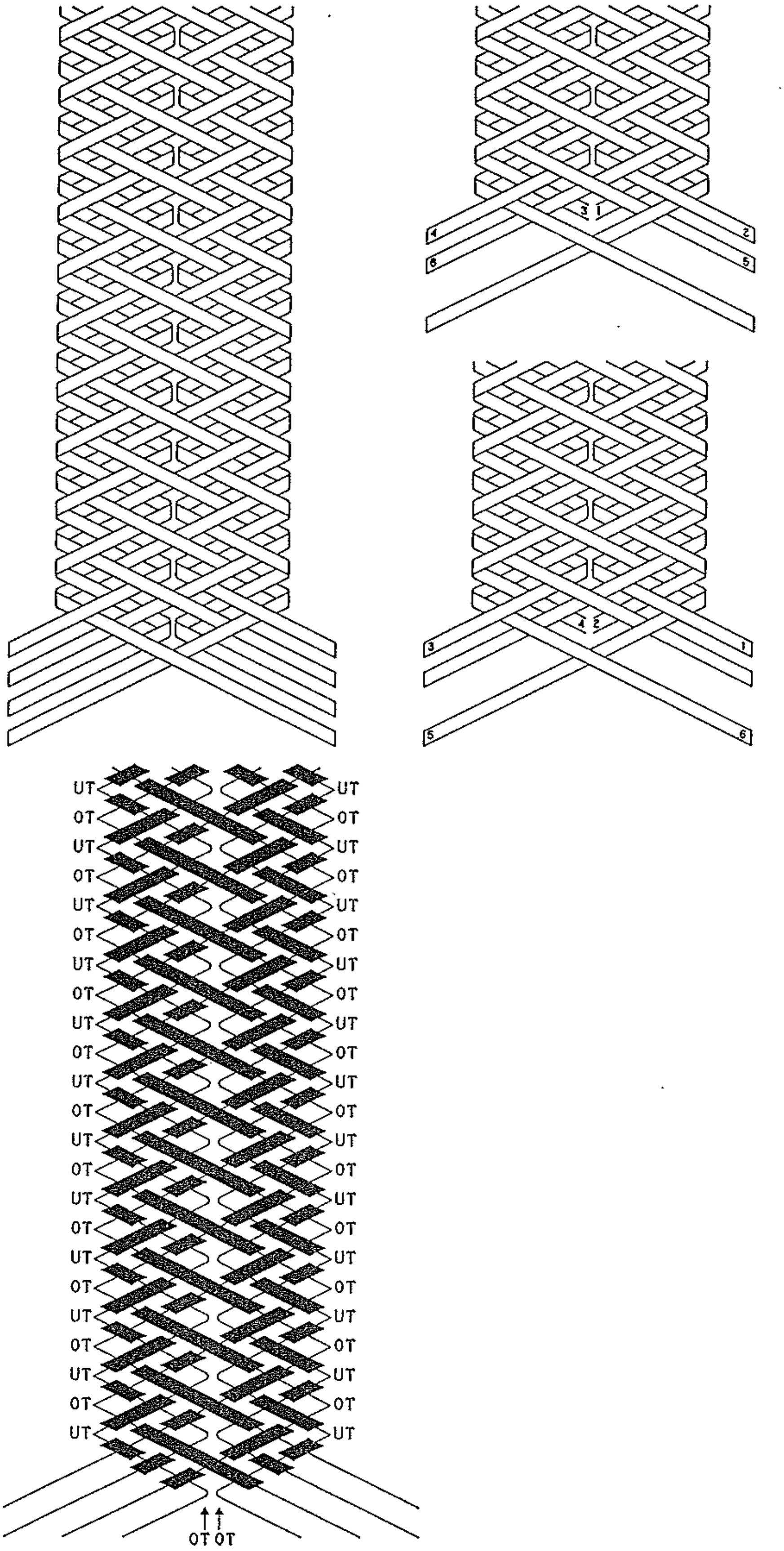

Fig. 806A — Designing a 'new' braid.

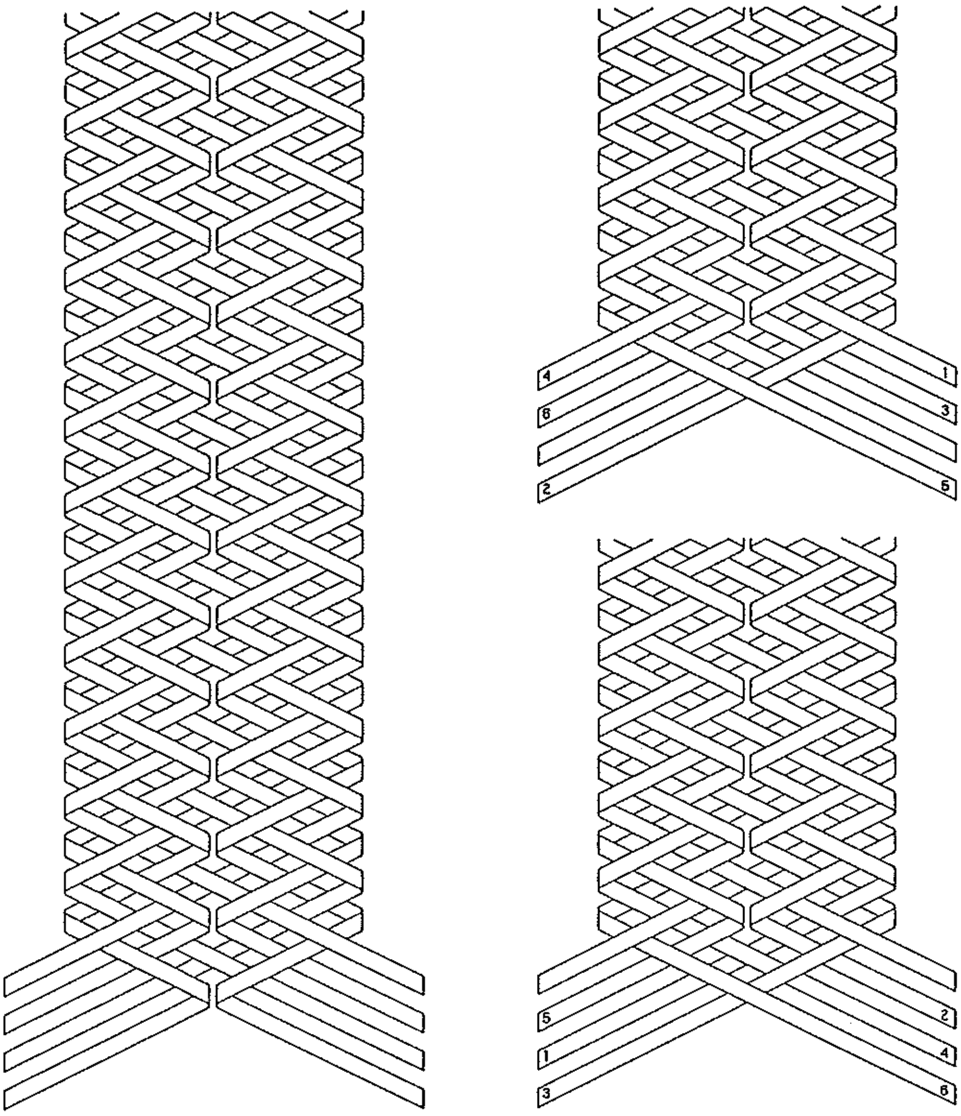

Fig. 807 — Designing a 'new' braid.

Note that not everywhere the grainside of the strings can be on the outside of the final braid, hence it is important to arrange the various strings in such a way that their grainsides and hence their fleshsides show a symmetric pattern. The same should be observed when, by combining more than two primitive flat tubular braids, it is not possible for the grainside of the strings to be everywhere on the outside of the final braid. Furthermore, by combining primitive flat tubular braids an overall balanced coding-pattern should be ensured.

The appearance of the braid in Fig. 806 (and hence the appearance of the braid associated with the alternative construction procedure in Fig. 806A) is similar to the appearance of the braid in Fig. 808 (and hence the appearance of the braid associated with the alternative construction procedure in Fig. 808A). Consequently the appearance of the braid in Fig. 807 (and hence the appearance of the braid associated with the alternative construction procedure in Fig. 807A) is similar to the appearance of the braid in Fig. 809 (and hence the appearance of the braid associated with the alternative construction procedure in Fig. 809A).

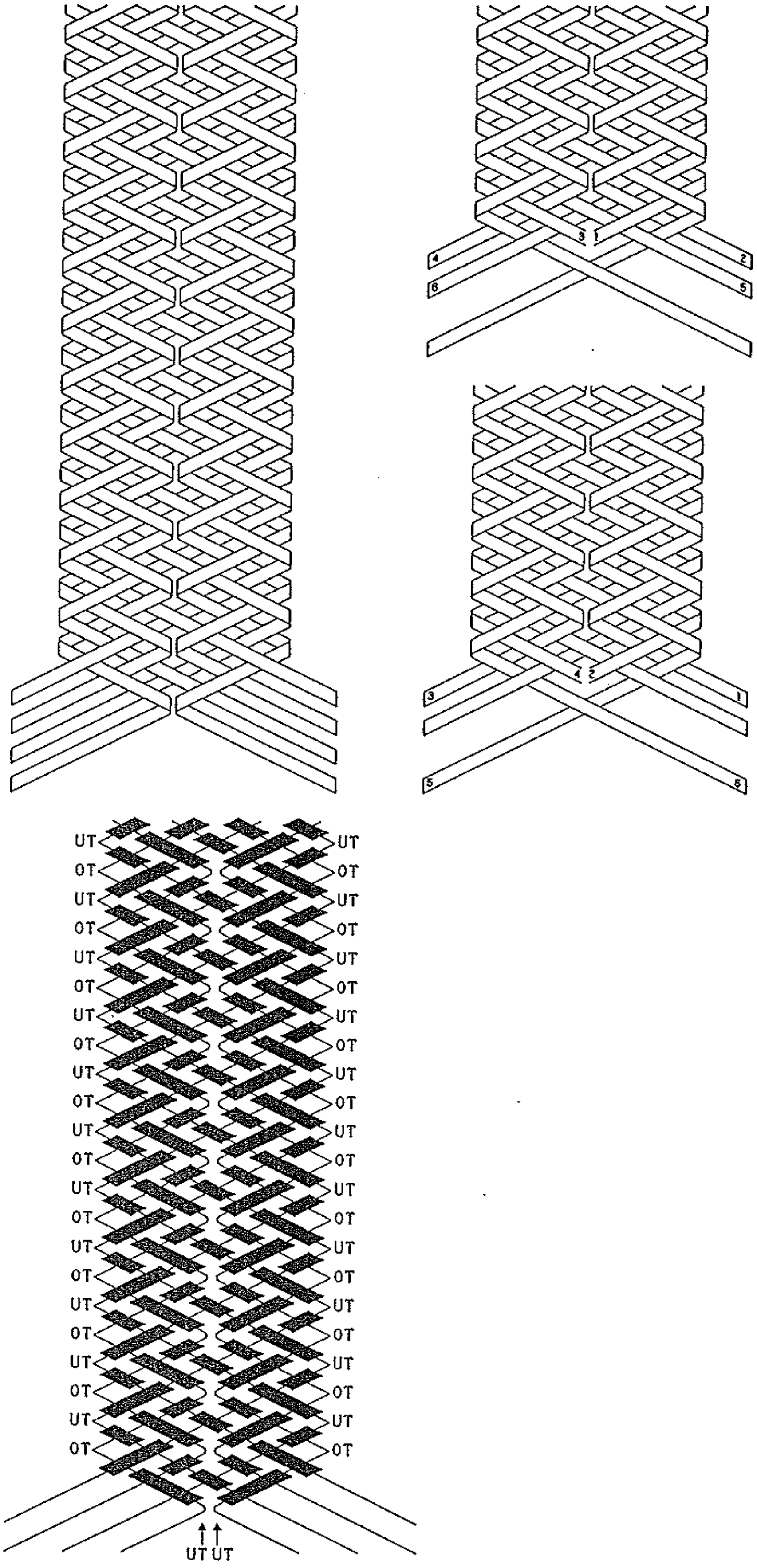

Fig. 807A — Designing a 'new' braid.

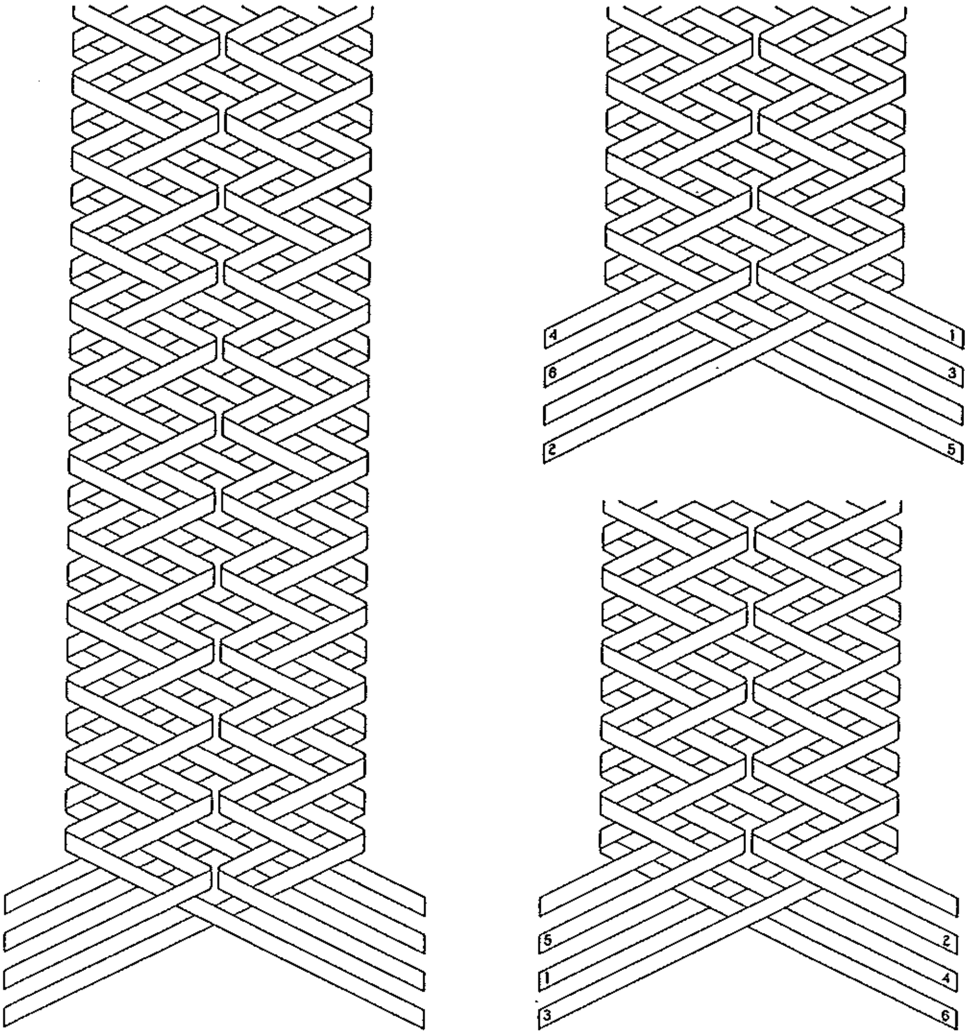

Fig. 808 — Designing a 'new' braid.

Since the appearance of the braid in Fig. 808 is similar to the appearance of the braid in Fig. 806 (and hence the appearance of the braid associated with its alternative construction procedure in Fig. 806A), the braid in Fig. 808 shows a flat front-side and two adjacent round braids on the back-side. An alternative braiding sequence for this braid is shown in Fig. 808A.

If we want to have the back-side of this braid on the front, hence the two adjacent round braids on the front, we braid it as depicted in Fig. 809; an alternative braiding sequence is shown in Fig. 809A.

The above discussed braids are small and hence their practical application is very limited. They are discussed here as an introduction to bigger similar braids of great practical value, formed by joining more and/or bigger primitive flat tubular braids of various coding arrangements. In addition, very attractive colour-patterns can be created. Although in our discussion here we have mainly used a pictorial representation of the UT-OT braids, in practice, however, we use of course UT-OT braid-diagrams. Any bigger round braid which forms an integral part of the created UT-OT braid should be provided with a braided core. The more complicated UT-OT braids so designed can be quite difficult to braid, but the serious braiding artisan will find here an eldorado of unlimited scope.

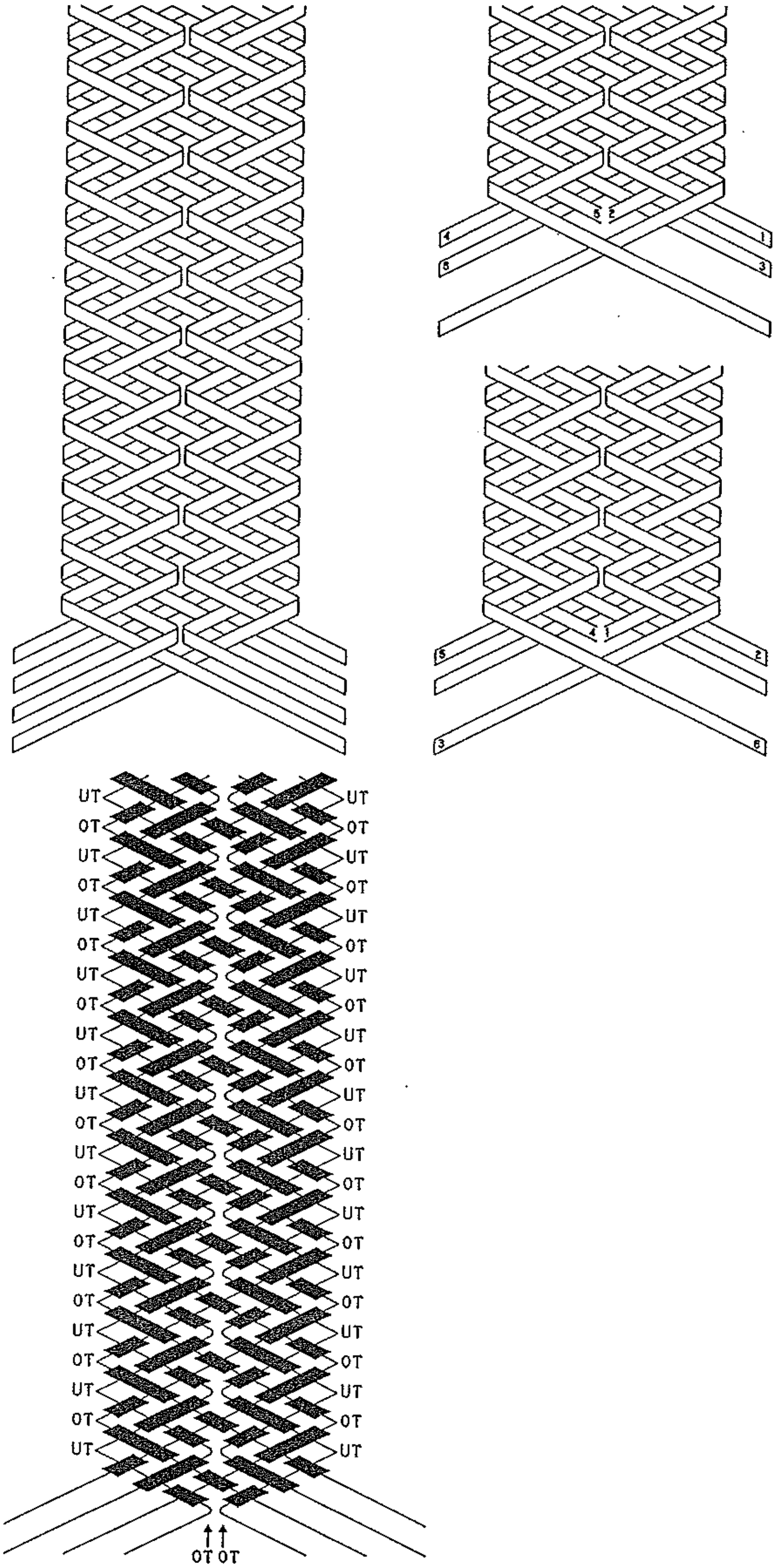

Fig. 808A — Designing a 'new' braid.

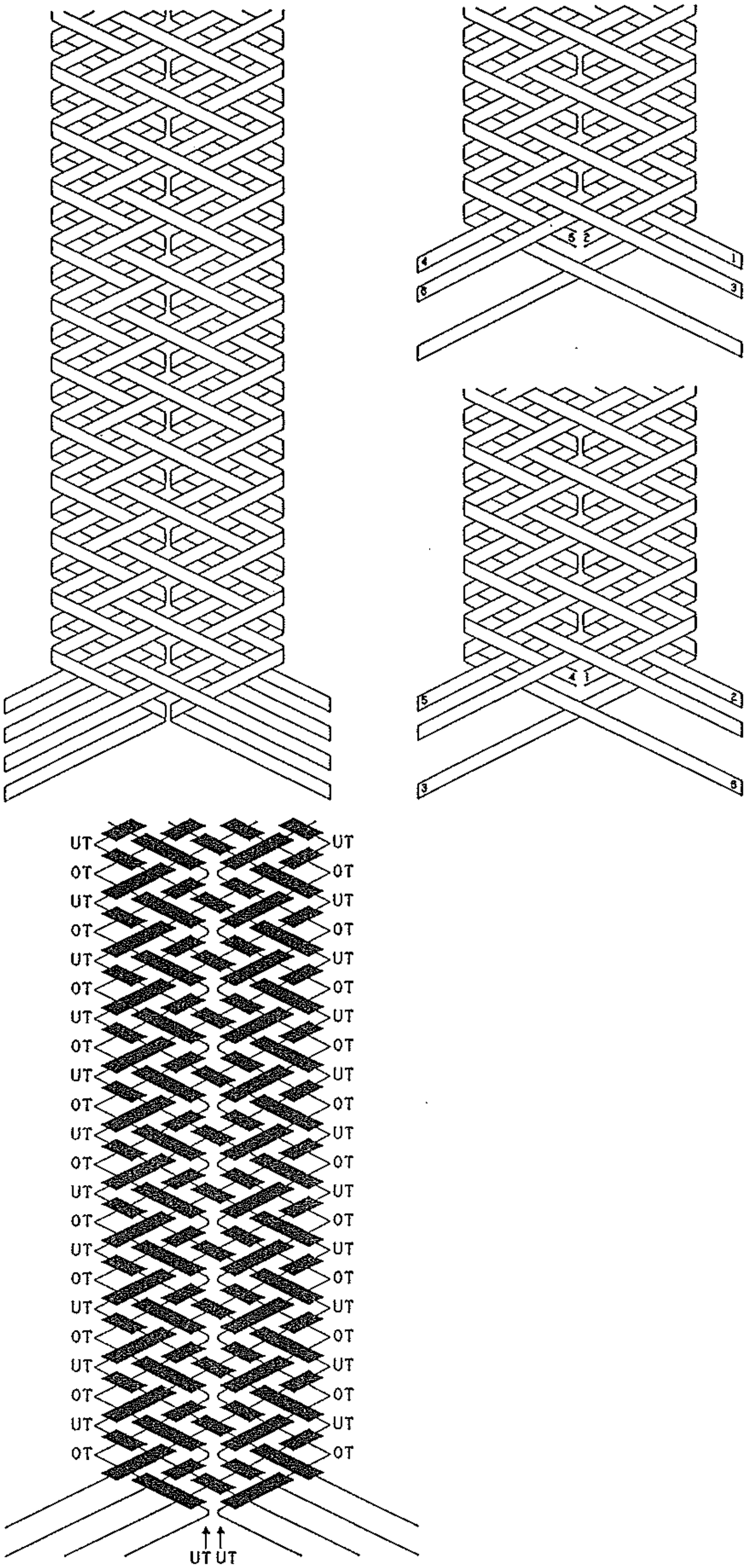

Fig. 809A — Designing a 'new' braid.

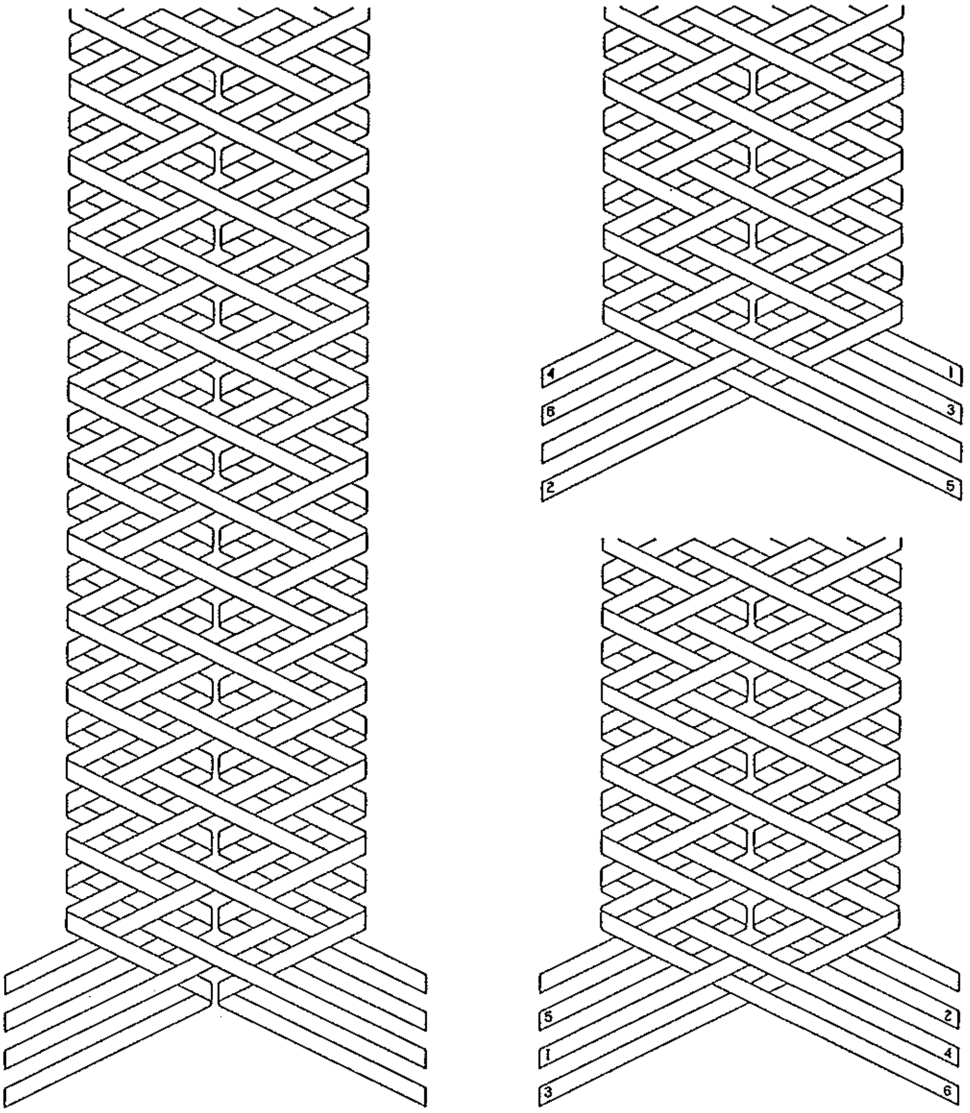

Fig. 809 — Designing a 'new' braid.

Checkered Pineapple Knots

The **essential** coding of Pineapple braids is shown in Fig. 810.[†] We shall again assume that the braiding-material is a flat string which has for each opposite face pair identical faces in size, shape, texture and colour.

The coding-patterns of Checkered Pineapple braids are depicted in Fig. 811. From these coding-patterns it follows that there are three types of Checkered Pineapple braids:

type 1. At the left bight-edge a coding-pattern as in the first row of diagrams in Fig. 811 and at the right bight-edge a coding-pattern as in the third row of diagrams in

---

[†] Don't confuse the essential coding of Pineapple braids with the essential coding of **Herringbone** Pineapple braids. See *The Braider*, Issue No. 23, pg. 523, Fig. 444.

Fig. 811. Note that this braid is its own mirror image, and that the same braid results with at the left bight-edge a coding-pattern as in the second row of diagrams in Fig. 811 and at the right bight-edge a coding-pattern as in the fourth row of diagrams in Fig. 811 (turn through 180°).

type 2. At the left bight-edge a coding-pattern as in the first row of diagrams in Fig. 811 and at the right bight-edge a coding-pattern as in the fourth row of diagrams in Fig. 811.

type 3. At the left bight-edge a coding-pattern as in the second row of diagrams in Fig. 811 and at the right bight-edge a coding-pattern as in the third row of diagrams in Fig. 811. Note that type 2 and type 3 are each others mirror image.

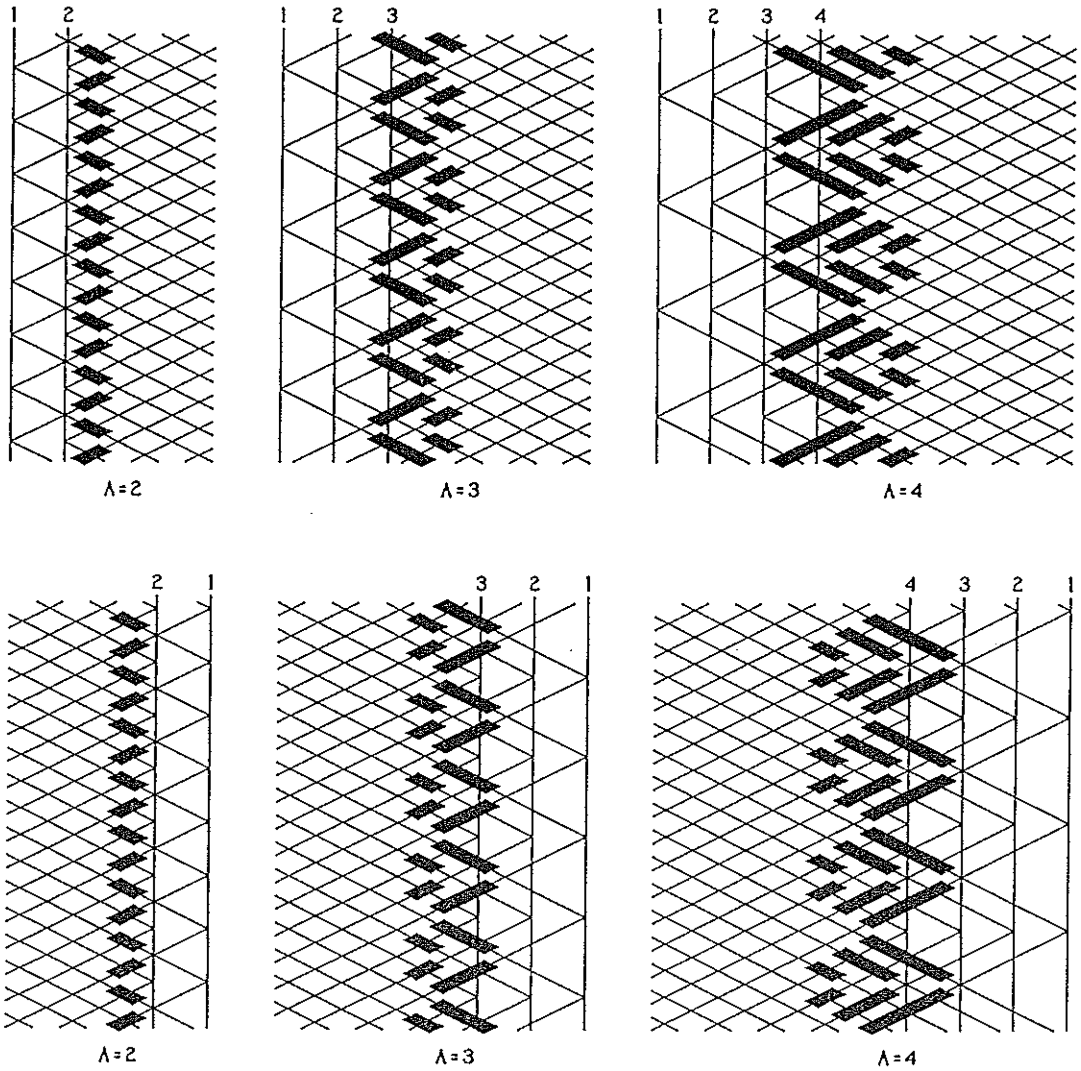

Fig. 810 — The essential Pineapple coding.

From the diagrams in Fig. 811 it immediately follows that the string-run of Checkered Pineapple Knots is the string-run of the Regular Nested Cylindrical Braids

$$(\underbrace{222\cdots2}_{(A-1)\text{ elements}}/3A+2+nA/\underbrace{222\cdots2}_{(A-1)\text{ elements}})\{1(A)(A-1)(A-2)\cdots2/(A)123\cdots(A-1)\}B\,,$$

where n is a whole number.†

Hence the Checkered Pineapple Knots are interbraids of A Regular Cylindrical

---

† See *The Braider*, Issue No. 22, pg. 502.

Braids, each with $P_c = 5 + n$ parts, and thus have a total of $P = A(5+n)$ parts.

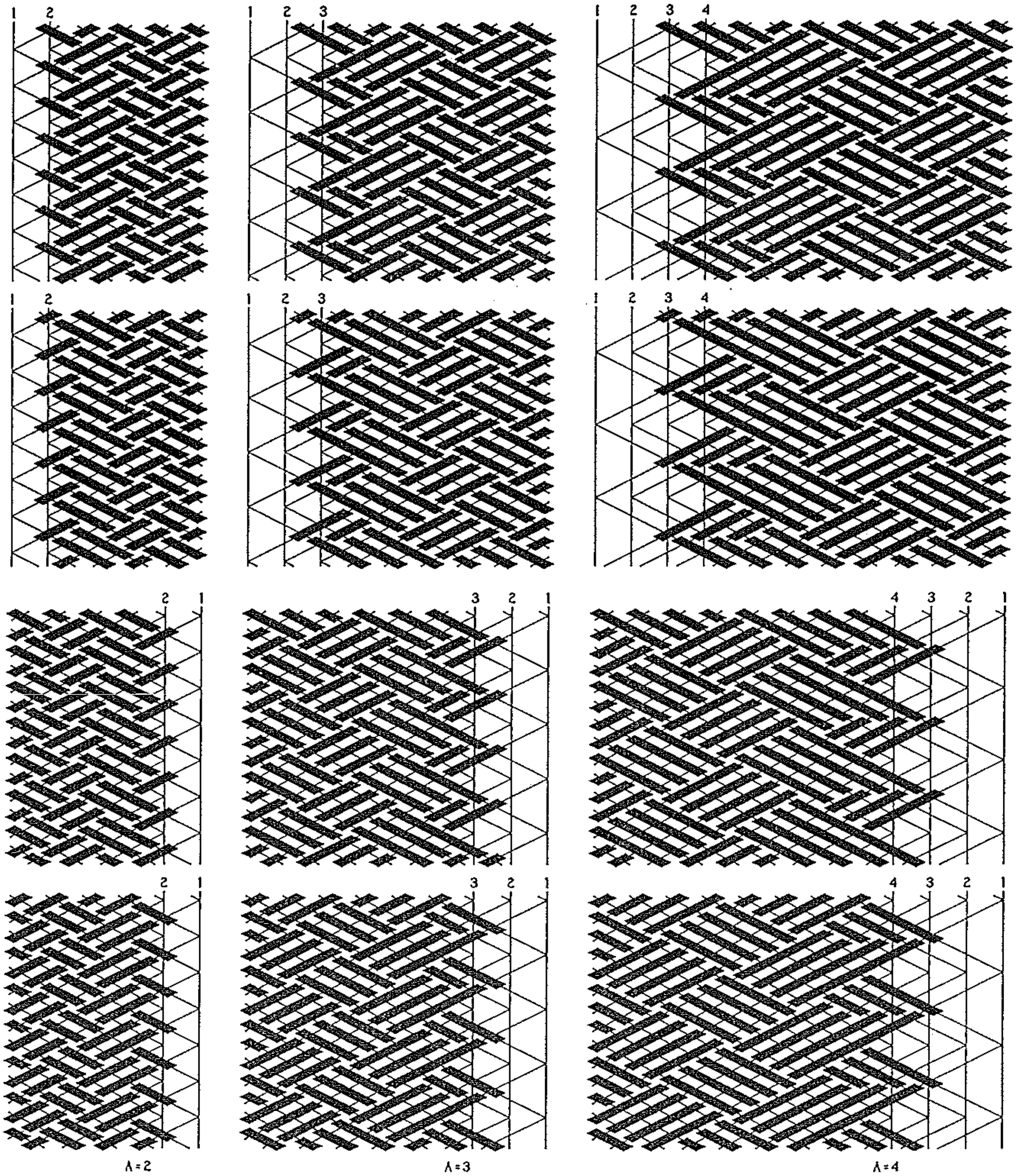

Fig. 811 — The coding-patterns of Checkered Pineapple braids.

$n =$ odd for types 2 & 3, thus $y = |2(A-1)+x|_{2A} = |x-2|_{2A} = |3A+nA|_{2A} = 0$.
$n =$ even for type 1, thus $y = |2(A-1)+x|_{2A} = |x-2|_{2A} = |3A+nA|_{2A} = A$.

From the diagrams in Fig. 811 it can readily be seen that the best way to braid an A-pass Checkered Pineapple Knot is to braid first a 2-pass Checkered Pineapple Knot and then progressively to enlarge it to a 3-pass, 4-pass, … , $(A-1)$-pass, A-pass Checkered Pineapple Knot by respectively interbraiding the Regular Cylindrical Braid component associated with the left to right bight-boundary pair $2 — 2$, a left to right bight-boundary pair which belongs to the set $2 — 3$ to $3 — 2$, ... , a left to right bight-boundary pair which belongs to the set $2 — (A-2)$ to $(A-2) — 2$, a left to right bight-boundary pair which belongs to the set $2 — (A-1)$ to $(A-1) — 2$.

Let P_c and B^* be coprime, hence g.c.d.$(P_c, B^*) = 1$, thus the interbraided Regular Cylindrical Braids are Regular Knots.

Type 1:

For a 2-pass type 1 Checkered Pineapple Knot the algorithm diagram for the foundation knot between left bight-boundary 1 and right bight-boundary 2 is:

$$\begin{array}{cc} \Delta^* & |2\Delta^*|_{B^*} \\ 0 & 0 \\ u & o \\ \cdot & \cdot \\ o & u \\ 0 & 0 \\ |(n+4)\Delta^*|_{B^*} & |(n+3)\Delta^*|_{B^*} \end{array} \underbrace{\left|\begin{array}{cc} |3\Delta^*|_{B^*} & |4\Delta^*|_{B^*} \\ 0 & 0 \\ u & o \\ \cdot & \cdot \\ o & u \\ 0 & 0 \\ |(n+2)\Delta^*|_{B^*} & |(n+1)\Delta^*|_{B^*} \end{array}\right|}_{n \text{ columns};\ n=P_c-5=\text{even} \geq 0} \begin{array}{cc} |(n+3)\Delta^*|_{B^*} & |(n+4)\Delta^*|_{B^*} \\ 0 & 0 \\ u & u \\ \cdot & \cdot \\ o & o \\ 0 & 0 \\ |2\Delta^*|_{B^*} & \Delta^* \end{array}$$

$$\begin{array}{cc} 0 & 0 \\ u & o \\ \cdot & \cdot \\ o & u \\ 0 & 0 \end{array} \quad \text{repeats.}$$

For the half-cycles from lower left to upper right the first line gives the i-values, the second line the reference quantities, the third line the coding and the fourth line the intersection columns. For the half-cycles from lower right to upper left the fourth line gives the intersection columns, the fifth line the coding, the sixth line the reference quantities and the seventh line the i-values. Each reference quantity is increased by 1 when its associated i-value is applicable for the half-cycle concerned.

For a 2-pass type 1 Checkered Pineapple Knot the algorithm diagram for the interbraided component between left bight-boundary 2 and right bight-boundary 1 is:

$$\begin{array}{ccc} & \Delta^* & |2\Delta^*|_{B^*} \\ 1 & 0 & 1 \\ u & o & o \\ \cdot & \cdot & \cdot \\ & u & u \\ & 1 & 1 \\ & |(n+4)\Delta^*|_{B^*} & |(n+3)\Delta^*|_{B^*} \end{array} \underbrace{\left|\begin{array}{cc} |3\Delta^*|_{B^*} & |4\Delta^*|_{B^*} \\ 1 & 1 \\ u & o \\ \cdot & \cdot \\ o & u \\ 1 & 1 \\ |(n+2)\Delta^*|_{B^*} & |(n+1)\Delta^*|_{B^*} \end{array}\right|}_{n \text{ columns};\ n=P_c-5=\text{even} \geq 0} \begin{array}{cc} |(n+3)\Delta^*|_{B^*} & |(n+4)\Delta^*|_{B^*} \\ 1 & 1 \\ u & o \\ \cdot & \cdot \\ o & u \\ 2 & 0 \\ |2\Delta^*|_{B^*} & \Delta^* \end{array}$$

$$\begin{array}{cc} 1 & 1 \\ u & o \\ \cdot & \cdot \\ o & u \\ 1 & 1 \end{array} \quad \text{repeats.}$$

For the lower left to upper right half-cycles, the first line gives the i-values where applicable, the second line the reference quantities, the third line the coding and the fourth line the intersection sets. For the lower right to upper left half-cycles, the fourth line gives the intersection sets, the fifth line the coding, the sixth line the reference quantities and the seventh line the i-values where applicable. Each reference quantity is increased by 1 when its associated i-value is applicable for the half-cycle concerned.

As mentioned earlier on pg. 1043 an A-pass type 1 Checkered Pineapple Knot with $A \geq 3$ is enlarged from a 2-pass type 1 Checkered Pineapple Knot by interbraiding the Regular Knot components between the left and right bight-boundary pairs $2 — (A-1)$ to and including $(A-1) — 2$. The algorithm diagram for these interbraids is:

$$\begin{array}{ccc|cc|ccc}
 & \Delta^* & |2\Delta^*|_{B*} & |3\Delta^*|_{B*} & |4\Delta^*|_{B*} & |(n{+}3)\Delta^*|_{B*} & |(n{+}4)\Delta^*|_{B*} & \\
 & l-1 & 2A-1-l & A-1 & A-1 & A-1 & l-1 & A-l \\
 & u & o & u & o & u & o & u \\
\cdot & \cdot & \cdot & \cdot & \cdot & \cdot & \cdot & \cdot \\
u & o & u & o & u & o & u & \\
A-r & r-1 & A-1 & A-1 & A-1 & 2A-1-r & r-1 & \\
 & |(n{+}4)\Delta^*|_{B*} & |(n{+}3)\Delta^*|_{B*} & |(n{+}2)\Delta^*|_{B*} & |(n{+}1)\Delta^*|_{B*} & |2\Delta^*|_{B*} & \Delta^* &
\end{array}$$

n columns; $n = P_c - 5 = \text{even} \geq 0$

$$\begin{array}{ccl}
A-1 & A-1 & \\
u & o & \\
\cdot & \cdot & \text{repeats.} \\
o & u & \\
A-1 & A-1 &
\end{array}$$

$$A \geq 3\,;\ 2 \leq l \leq A-1\,;\ 2 \leq r \leq A-1\,;\ r = A+1-l\,;\ l = A+1-r\,.$$

For the half-cycles from lower left to upper right the first line gives the i-values where applicable, the second line the reference quantities, the third line the coding and the fourth line the intersection sets. For the half-cycles from lower right to upper left the fourth line gives the intersection sets, the fifth line the coding, the sixth line the reference quantities and the seventh line the i-values where applicable. Each reference quantity is increased by 1 when its associated i-value is applicable for the half-cycle concerned.

Type 2:

For a 2-pass type 2 Checkered Pineapple Knot the algorithm diagram for the foundation knot between left bight-boundary 1 and right bight-boundary 2 is:

$$\begin{array}{ccc|cc|cc}
\Delta^* & |2\Delta^*|_{B*} & |3\Delta^*|_{B*} & |4\Delta^*|_{B*} & |5\Delta^*|_{B*} & |(n{+}3)\Delta^*|_{B*} & |(n{+}4)\Delta^*|_{B*} \\
0 & 0 & 0 & 0 & 0 & 0 & 0 \\
u & o & u & o & u & o & o \\
\cdot & \cdot & \cdot & \cdot & \cdot & \cdot & \cdot \\
o & u & o & u & o & u & u \\
0 & 0 & 0 & 0 & 0 & 0 & 0 \\
|(n{+}4)\Delta^*|_{B*} & |(n{+}3)\Delta^*|_{B*} & |(n{+}2)\Delta^*|_{B*} & |(n{+}1)\Delta^*|_{B*} & |n\Delta^*|_{B*} & |2\Delta^*|_{B*} & \Delta^*
\end{array}$$

$(n-1)$ columns; $n = P_c - 5 = \text{odd} \geq 1$

$$\begin{array}{ccl}
0 & 0 & \\
o & u & \\
\cdot & \cdot & \text{repeats.} \\
u & o & \\
0 & 0 &
\end{array}$$

For the half-cycles from lower left to upper right the first line gives the i-values, the second line the reference quantities, the third line the coding and the fourth line the intersection columns. For the half-cycles from lower right to upper left the fourth line gives the intersection columns, the fifth line the coding, the sixth line the reference quantities and the seventh line the i-values. Each reference quantity is increased by 1 when its associated i-value is applicable for the half-cycle concerned.

For a 2-pass type 2 Checkered Pineapple Knot the algorithm diagram for the interbraided component between left bight-boundary 2 and right bight-boundary 1 is:

$$\begin{array}{cccc|cc|cc}
 & \Delta^* & |2\Delta^*|_{B*} & |3\Delta^*|_{B*} & |4\Delta^*|_{B*} & |5\Delta^*|_{B*} & |(n+3)\Delta^*|_{B*} & |(n+4)\Delta^*|_{B*} \\
1 & 0 & 1 & 1 & 1 & 1 & 2 & 0 \\
u & o & o & u & o & u & o & u \\
\cdot & \cdot & \cdot & \cdot & \cdot & \cdot & \cdot & \cdot \\
 & u & u & o & u & o & u & o \\
 & 1 & 1 & 1 & 1 & 1 & 1 & 1 \\
 & |(n+4)\Delta^*|_{B*} & |(n+3)\Delta^*|_{B*} & |(n+2)\Delta^*|_{B*} & |(n+1)\Delta^*|_{B*} & |n\Delta^*|_{B*} & |2\Delta^*|_{B*} & \Delta^*
\end{array}$$

$(n-1)$ columns; $n=P_c-5=\text{odd}\geq 1$

$$\begin{array}{ccl}
1 & 1 & \\
o & u & \\
\cdot & \cdot & \text{repeats.} \\
u & o & \\
1 & 1 &
\end{array}$$

For the half-cycles from lower left to upper right the first line gives the i-values where applicable, the second line the reference quantities, the third line the coding and the fourth line the intersection sets. For the half-cycles from lower right to upper left the fourth line gives the intersection sets, the fifth line the coding, the sixth line the reference quantities and the seventh line the i-values where applicable. Each reference quantity is increased by 1 when its associated i-value is applicable for the half-cycle concerned.

An A-pass type 2 Checkered Pineapple Knot ($A \geq 3$) is enlarged from a 2-pass type 2 Checkered Pineapple Knot by interbraiding the Regular Knot components between the left and right bight-boundary pairs $2—(A-1)$ to and including $(A-1)—2$. The algorithm diagram for these interbraids is:

$$\begin{array}{cccc|cc|ccc}
 & \star & \star & \star & \star & \star & \star & \star & \\
 & l-1 & 2A-1-l & A-1 & A-1 & A-1 & A-2+l & A-l & \\
 & u & o & u & o & u & o & u & \\
\cdot & \cdot & \cdot & \cdot & \cdot & \cdot & \cdot & \cdot & \cdot \\
u & o & u & o & u & o & u & o & u \\
A-r & r-1 & A-1 & A-1 & A-1 & A-1 & A-1 & A-r & r-1 \\
 & \star & \star & \star & \star & \star & \star & \star &
\end{array}$$

$(n-1)$ columns; $n=P_c-5=\text{odd}\geq 1$

$$\begin{array}{ccl}
A-1 & A-1 & \\
o & u & \\
\cdot & \cdot & \text{repeats.} \\
u & o & \\
A-1 & A-1 &
\end{array}$$

$$A \geq 3\,;\ 2 \leq l \leq A-1\,;\ 2 \leq r \leq A-1\,;\ r = A+1-l\,;\ l = A+1-r\,.$$

For the half-cycles from lower left to upper right the stars in the first line give the i-values where applicable, the second line gives the reference quantities, the third line the coding and the fourth line the intersection sets. For the half-cycles from lower right to upper left the fourth line gives the intersection sets, the fifth line the coding, the sixth line the reference quantities and the stars in the seventh line give the i-values where applicable. Each reference quantity is increased by 1 when its associated i-value is applicable for the half-cycle concerned.

Type 3:

For a 2-pass type 3 Checkered Pineapple Knot the algorithm diagram for the foundation knot between left bight-boundary 1 and right bight-boundary 2 is:

$$\begin{array}{ccc|cc|cc}
\Delta^* & \lvert 2\Delta^*\rvert_{B*} & \lvert 3\Delta^*\rvert_{B*} & \lvert 4\Delta^*\rvert_{B*} & \lvert 5\Delta^*\rvert_{B*} & \lvert (n+3)\Delta^*\rvert_{B*} & \lvert (n+4)\Delta^*\rvert_{B*} \\
0 & 0 & 0 & 0 & 0 & 0 & 0 \\
u & u & o & u & o & u & o \\
\cdot & \cdot & \cdot & \cdot & \cdot & \cdot & \cdot \\
o & o & u & o & u & o & u \\
0 & 0 & 0 & 0 & 0 & 0 & 0 \\
\lvert (n+4)\Delta^*\rvert_{B*} & \lvert (n+3)\Delta^*\rvert_{B*} & \lvert (n+2)\Delta^*\rvert_{B*} & \lvert (n+1)\Delta^*\rvert_{B*} & \lvert n\Delta^*\rvert_{B*} & \lvert 2\Delta^*\rvert_{B*} & \Delta^*
\end{array}$$

$$\underbrace{\hspace{6em}}_{(n-1)\text{ columns};\ n=P_c-5=\text{odd}\geq 1}$$

$$\begin{array}{cc}
0 & 0 \\
u & o \\
\cdot & \cdot \\
o & u \\
0 & 0
\end{array}\ \text{repeats.}$$

For the half-cycles from lower left to upper right the first line gives the i-values, the second line gives the reference quantities of the coding associated with the intersection columns, the third line the coding of the intersection columns and the fourth line the intersection columns. For the half-cycles from lower right to upper left the fourth line gives the intersection columns, the fifth line the coding of the intersection columns, the sixth line the reference quantities of the coding associated with the intersection columns and the seventh line the i-values. Each reference quantity is increased by 1 when its associated i-value is applicable for the half-cycle concerned.

For a 2-pass type 3 Checkered Pineapple Knot the algorithm diagram for the interbraided component between left bight-boundary 2 and right bight-boundary 1 is:

$$\begin{array}{ccc|cc|ccc}
\Delta^* & \lvert 2\Delta^*\rvert_{B*} & \lvert 3\Delta^*\rvert_{B*} & \lvert 4\Delta^*\rvert_{B*} & \lvert 5\Delta^*\rvert_{B*} & \lvert (n+3)\Delta^*\rvert_{B*} & \lvert (n+4)\Delta^*\rvert_{B*} & \\
1 & 1 & 1 & 1 & 1 & 1 & 1 & \\
o & u & o & u & o & u & u & \\
\cdot & \cdot & \cdot & \cdot & \cdot & \cdot & \cdot & \cdot \\
u & o & u & o & u & o & o & u \\
0 & 2 & 1 & 1 & 1 & 1 & 0 & 1 \\
\lvert (n+4)\Delta^*\rvert_{B*} & \lvert (n+3)\Delta^*\rvert_{B*} & \lvert (n+2)\Delta^*\rvert_{B*} & \lvert (n+1)\Delta^*\rvert_{B*} & \lvert n\Delta^*\rvert_{B*} & \lvert 2\Delta^*\rvert_{B*} & \Delta^* &
\end{array}$$

$$\underbrace{\hspace{6em}}_{(n-1)\text{ columns};\ n=P_c-5=\text{odd}\geq 1}$$

$$\begin{array}{cc}
1 & 1 \\
u & o \\
\cdot & \cdot \\
o & u \\
1 & 1
\end{array}\ \text{repeats.}$$

For the half-cycles from lower left to upper right the first line gives the i-values where applicable, the second line gives the reference quantities of the coding associated with the intersection sets, the third line the coding associated with the intersection sets and the fourth line the intersection sets. For the half-cycles from lower right to upper left the fourth line gives the intersection sets, the fifth line the coding associated with the intersection sets, the sixth line the reference quantities of the coding associated with the intersection sets and the seventh line the i-values where applicable. Each reference quantity is increased by 1 when its associated i-value is applicable for the half-cycle concerned.

An A-pass type 3 Checkered Pineapple Knot ($A \geq 3$) is enlarged from a 2-pass type 3 Checkered Pineapple Knot by interbraiding the Regular Knot components between the left and right bight-boundary pairs $2—(A-1)$ to and including $(A-1)—2$. The algorithm diagram for these interbraids is:

$$\begin{array}{cccc|cc|ccc}
 & \star & \star & \star & \star & \star & \star & \star & \\
l-1 & A-l & A-1 & A-1 & A-1 & A-1 & A-1 & l-1 & A-l \\
u & o & u & o & u & o & u & o & u \\
\cdot & \cdot & \cdot & \cdot & \cdot & \cdot & \cdot & \cdot & \cdot \\
 & u & o & u & o & u & o & u & \\
 & A-r & A-2+r & A-1 & A-1 & A-1 & 2A-1-r & r-1 & \\
 & \star & \star & \star & \star & \star & \star & \star &
\end{array}$$

$(n-1)$ columns ; $n = P_c - 5 = \text{odd} \geq 1$

$$\begin{array}{cc}
A-1 & A-1 \\
u & o \\
\cdot & \cdot \\
o & u \\
A-1 & A-1
\end{array} \quad \text{repeats.}$$

$$A \geq 3\,;\ 2 \leq l \leq A-1\,;\ 2 \leq r \leq A-1\,;\ r = A+1-l\,;\ l = A+1-r\,.$$

For the half-cycles from lower left to upper right the stars in the first line give the i-values where applicable, the second line gives the reference quantities, the third line the coding and the fourth line the intersection sets. For the half-cycles from lower right to upper left the fourth line gives the intersection sets, the fifth line the coding, the sixth line the reference quantities and the stars in the seventh line give the i-values where applicable. Each reference quantity is increased by 1 when its associated i-value is applicable for the half-cycle concerned.

Example 1: type 1

Let $A = 2$; $B^* = 4$ and $n = 4$. Hence $P_c = n + 5 = 9$; $x = 3A + 2 + nA = 6 + 2 + 8 = 16$ and g.c.d. $(P_c, B^*) =$ g.c.d. $(9, 4) = 1$.

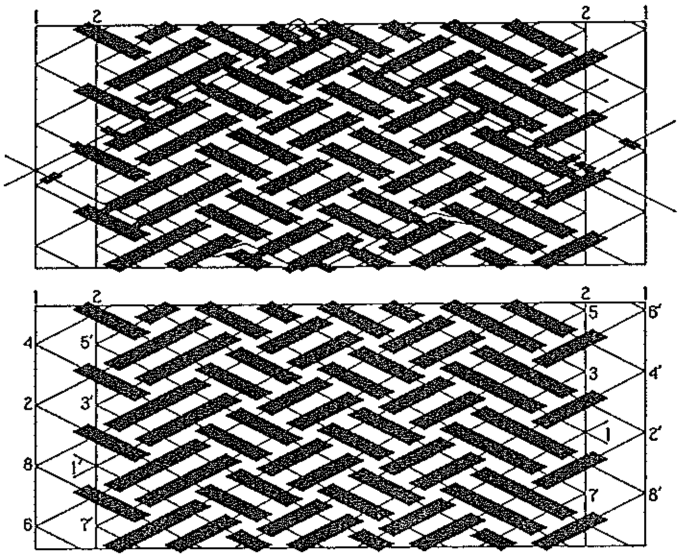

Fig. 812 — 2-pass Checkered Pineapple Knot of Example 1.

If we want to work away the string-ends as shown in the upper diagram of Fig. 812 then we braid the knot as shown in the lower diagram of Fig. 812. First we braid the foundation knot (a Regular Knot with $P_c/B^* = 9/4$) between left bight-boundary 1 and right bight-boundary 2, next we interbraid the component (a Regular Knot with $P_c/B^* = 9/4$) between left bight-boundary 2 and right bight-boundary 1. Before we can draw up the algorithm diagrams for these two components we need to know their

Δ^*-values (their Δ^*-values are the same since their P_c/B^*-values are the same), which we obtain from their path in the RKT:

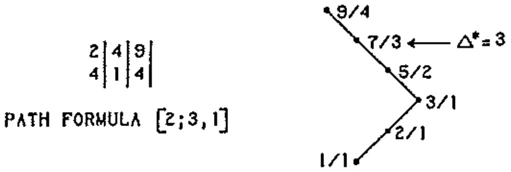

The algorithm diagram for the foundation knot is then:

$$\begin{array}{cccccccc}
3 & 2 & 1 & 0 & 3 & 2 & 1 & 0 \\
0 & 0 & 0 & 0 & 0 & 0 & 0 & 0 \\
u & o & u & o & u & o & u & u \\
. & . & . & . & . & . & . & . \\
o & u & o & u & o & u & o & o \\
0 & 0 & 0 & 0 & 0 & 0 & 0 & 0 \\
0 & 1 & 2 & 3 & 0 & 1 & 2 & 3
\end{array}$$

From this algorithm diagram we read its half-cycle braiding algorithms:

half-cycle 1	$L \longleftarrow R$		:	Free run.
half-cycle 2	$L \longrightarrow R$	$i = 0$	:	$o - u$.
half-cycle 3	$L \longleftarrow R$	$i = 0$	:	$2o$.
half-cycle 4	$L \longrightarrow R$	$i \leq 1$	:	$u - o - 2u$.
half-cycle 5	$L \longleftarrow R$	$i \leq 1$	:	$u - o - u - o$.
half-cycle 6	$L \longrightarrow R$	$i \leq 2$	:	$o - u - 2o - 2u$.
half-cycle 7	$L \longleftarrow R$	$i \leq 2$	:	$o - u - 2o - u - o$.
half-cycle 8	$L \longrightarrow R$	$i \leq 3$	:	$u - o - u - o - u - o - 2u$.

And the algorithm diagram for the interbraided knot is:

$$\begin{array}{ccccccccc}
 & 3 & 2 & 1 & 0 & 3 & 2 & 1 & 0 \\
1 & 0 & 1 & 1 & 1 & 1 & 1 & 1 & 1 \\
u & o & o & u & o & u & o & u & o \\
. & . & . & . & . & . & . & . & . \\
 & u & u & o & u & o & u & o & u \\
 & 1 & 1 & 1 & 1 & 1 & 1 & 2 & 0 \\
 & 0 & 1 & 2 & 3 & 0 & 1 & 2 & 3
\end{array}$$

From this algorithm diagram we read its half-cycle braiding algorithms:

half-cycle 1′	$L \longrightarrow R$		:	$u - o - u - o - u - o - u - o$.
half-cycle 2′	$L \longleftarrow R$	$i = 0$	:	$2o - u - 2o - u - o - 3u$.
half-cycle 3′	$L \longrightarrow R$	$i = 0$	:	$u - o - u - 2o - u - o - u - 2o$.
half-cycle 4′	$L \longleftarrow R$	$i \leq 1$	:	$2o - 2u - 2o - u - o - 4u$.
half-cycle 5′	$L \longrightarrow R$	$i \leq 1$	:	$u - o - 2u - 2o - u - o - 2u - 2o$.
half-cycle 6′	$L \longleftarrow R$	$i \leq 2$	:	$3o - 2u - 2o - u - 2o - 4u$.
half-cycle 7′	$L \longrightarrow R$	$i \leq 2$	:	$u - 2o - 2u - 2o - u - 2o - 2u - 2o$.
half-cycle 8′	$L \longleftarrow R$	$i \leq 3$	:	$u - 3o - 2u - 2o - 2u - 2o - 4u$.

Example 2: type 1

Let $A = 5$; $B^* = 4$ and $n = 2$. Hence $P_c = n + 5 = 7$; $x = 3A + 2 + nA = 15 + 2 + 10 = 27$ and $\text{g.c.d.}(P_c, B^*) = \text{g.c.d.}(7,4) = 1$.

First we braid the foundation knot (a Regular Knot with $P_c/B^* = 7/4$) between left bight-boundary 1 and right bight-boundary 5, next we interbraid the component (a Regular Knot with $P_c/B^* = 7/4$) between left bight-boundary 5 and right bight-boundary 1. Say we then interbraid the component (a Regular Knot with $P_c/B^* = 7/4$) between left bight-boundary 4 and right bight-boundary 2, next the component (a Regular Knot with $P_c/B^* = 7/4$) between left bight-boundary 2 and right bight-boundary 4 and then the component (a Regular Knot with $P_c/B^* = 7/4$) between left bight-boundary 3 and right bight-boundary 3.

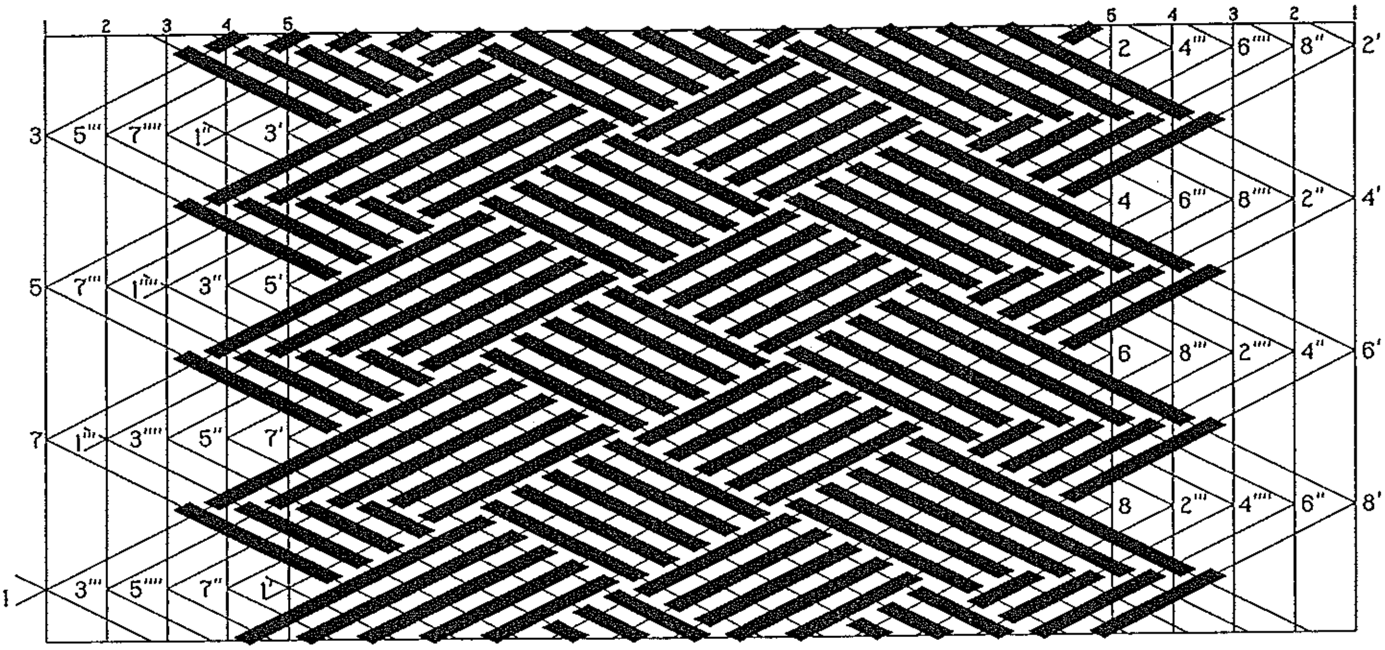

Fig. 813 — 5-pass Checkered Pineapple Knot of Example 2.

The Δ^*-values for the algorithm diagrams of these five components are obtained from their path in the RKT (Δ^*-values are the same since P_c/B^*-values are the same):

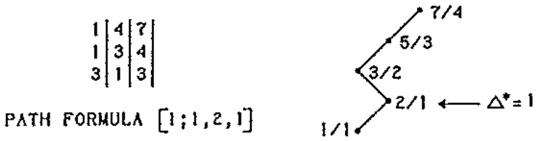

The algorithm diagram for the foundation knot is:

$$\begin{array}{cccccc}
1 & 2 & 3 & 0 & 1 & 2 \\
0 & 0 & 0 & 0 & 0 & 0 \\
u & o & u & o & u & u \\
\cdot & \cdot & \cdot & \cdot & \cdot & \cdot \\
o & u & o & u & o & o \\
0 & 0 & 0 & 0 & 0 & 0 \\
2 & 1 & 0 & 3 & 2 & 1
\end{array}$$

From this algorithm diagram we read its half-cycle braiding algorithms:

half-cycle 1 $L \longleftarrow R$: Free run.
half-cycle 2 $L \longrightarrow R$ $i = 0$: o.
half-cycle 3 $L \longleftarrow R$ $i = 0$: o.
half-cycle 4 $L \longrightarrow R$ $i \leq 1$: $2o - u$.
half-cycle 5 $L \longleftarrow R$ $i \leq 1$: $u - o - u$.
half-cycle 6 $L \longrightarrow R$ $i \leq 2$: $3o - u - o$.
half-cycle 7 $L \longleftarrow R$ $i \leq 2$: $u - 2o - 2u$.
half-cycle 8 $L \longrightarrow R$ $i \leq 3$: $2o - u - o - u - o$.

The algorithm diagram for the interbraided knot between left bight-boundary 5 and right bight-boundary 1 in the 5-pass Checkered Pineapple Knot (left bight-boundary 2 and right bight-boundary 1 in 2-pass Checkered Pineapple Knot) is:

$$\begin{array}{ccccccc}
 & 1 & 2 & 3 & 0 & 1 & 2 \\
1 & 0 & 1 & 1 & 1 & 1 & 1 \\
u & o & o & u & o & u & o \\
\cdot & \cdot & \cdot & \cdot & \cdot & \cdot & \cdot \\
 & & & & & & \\
 & u & u & o & u & o & u \\
 & 1 & 1 & 1 & 1 & 2 & 0 \\
 & 2 & 1 & 0 & 3 & 2 & 1
\end{array}$$

From this algorithm diagram we read its half-cycle braiding algorithms:

half-cycle $1'$ $L \longrightarrow R$: $u - o - u - o - u - o$.
half-cycle $2'$ $L \longleftarrow R$ $i = 0$: $2o - u - 2o - 2u$.
half-cycle $3'$ $L \longrightarrow R$ $i = 0$: $u - o - u - 2o - u - o$.
half-cycle $4'$ $L \longleftarrow R$ $i \leq 1$: $u - 2o - u - 2o - 3u$.
half-cycle $5'$ $L \longrightarrow R$ $i \leq 1$: $u - 2o - u - 2o - 2u - o$.
half-cycle $6'$ $L \longleftarrow R$ $i \leq 2$: $u - 3o - u - 2o - 4u$.
half-cycle $7'$ $L \longrightarrow R$ $i \leq 2$: $u - 3o - u - 2o - 2u - 2o$.
half-cycle $8'$ $L \longleftarrow R$ $i \leq 3$: $u - 3o - 2u - 2o - 4u$.

The algorithm diagram for the interbraided knot between left bight-boundary 4 and right bight-boundary 2 in the 5-pass Checkered Pineapple Knot (left bight-boundary 2 ($l = 2$) and right bight-boundary 2 ($r = 2$) in 3-pass Checkered Pineapple Knot) is:

$$\begin{array}{cccccccc}
 & 1 & 2 & 3 & 0 & 1 & 2 & \\
 & 1 & 3 & 2 & 2 & 2 & 1 & 1 \\
 & u & o & u & o & u & o & u \\
\cdot & \cdot & \cdot & \cdot & \cdot & \cdot & \cdot & \cdot \\
 & & & & & & & \\
u & o & u & o & u & o & u & \\
1 & 1 & 2 & 2 & 2 & 3 & 1 & \\
 & 2 & 1 & 0 & 3 & 2 & 1 &
\end{array}$$

From this algorithm diagram we read its half-cycle braiding algorithms:

half-cycle $1''$ $L \longrightarrow R$: $u - 3o - 2u - 2o - 2u - o - u$.
half-cycle $2''$ $L \longleftarrow R$ $i = 0$: $u - 3o - 2u - 3o - 2u - o - u$.
half-cycle $3''$ $L \longrightarrow R$ $i = 0$: $u - 3o - 2u - 3o - 2u - o - u$.
half-cycle $4''$ $L \longleftarrow R$ $i \leq 1$: $2u - 3o - 2u - 3o - 3u - o - u$.
half-cycle $5''$ $L \longrightarrow R$ $i \leq 1$: $2u - 3o - 2u - 3o - 3u - o - u$.
half-cycle $6''$ $L \longleftarrow R$ $i \leq 2$: $2u - 4o - 2u - 3o - 3u - 2o - u$.
half-cycle $7''$ $L \longrightarrow R$ $i \leq 2$: $2u - 4o - 2u - 3o - 3u - 2o - u$.
half-cycle $8''$ $L \longleftarrow R$ $i \leq 3$: $2u - 4o - 3u - 3o - 3u - 2o - u$.

The algorithm diagram for the interbraided knot between left bight-boundary 2 and right bight-boundary 4 in the 5-pass Checkered Pineapple Knot (left bight-boundary 2 ($l = 2$) and right bight-boundary 3 ($r = 3$) in 4-pass Checkered Pineapple Knot) is:

$$\begin{array}{cccccccc}
 & 1 & 2 & 3 & 0 & 1 & 2 & \\
 & 1 & 5 & 3 & 3 & 3 & 1 & 2 \\
 & u & o & u & o & u & o & u \\
\cdot & \cdot & \cdot & \cdot & \cdot & \cdot & \cdot & \cdot \\
 & & & & & & & \\
u & o & u & o & u & o & u & \\
1 & 2 & 3 & 3 & 3 & 4 & 2 & \\
 & 2 & 1 & 0 & 3 & 2 & 1 &
\end{array}$$

From this algorithm diagram we read its half-cycle braiding algorithms:

half-cycle $1'''$ $L \longrightarrow R$: $u - 5o - 3u - 3o - 3u - o - 2u$.
half-cycle $2'''$ $L \longleftarrow R$ $i = 0$: $2u - 4o - 3u - 4o - 3u - 2o - u$.
half-cycle $3'''$ $L \longrightarrow R$ $i = 0$: $u - 5o - 3u - 4o - 3u - o - 2u$.
half-cycle $4'''$ $L \longleftarrow R$ $i \leq 1$: $3u - 4o - 3u - 4o - 4u - 2o - u$.
half-cycle $5'''$ $L \longrightarrow R$ $i \leq 1$: $2u - 5o - 3u - 4o - 4u - o - 2u$.
half-cycle $6'''$ $L \longleftarrow R$ $i \leq 2$: $3u - 5o - 3u - 4o - 4u - 3o - u$.
half-cycle $7'''$ $L \longrightarrow R$ $i \leq 2$: $2u - 6o - 3u - 4o - 4u - 2o - 2u$.
half-cycle $8'''$ $L \longleftarrow R$ $i \leq 3$: $3u - 5o - 4u - 4o - 4u - 3o - u$.

The algorithm diagram for the interbraided knot between left bight-boundary 3 and right bight-boundary 3 in the 5-pass Checkered Pineapple Knot (hence $l = 3$ and $r = 3$ since this ends the interbraiding) is:

$$\begin{array}{cccccccc}
 & 1 & 2 & 3 & 0 & 1 & 2 & \\
 & 2 & 6 & 4 & 4 & 4 & 2 & 2 \\
 & u & o & u & o & u & o & u \\
\cdot & \cdot & \cdot & \cdot & \cdot & \cdot & \cdot & \cdot \\
u & o & u & o & u & o & u & \\
2 & 2 & 4 & 4 & 4 & 6 & 2 & \\
 & 2 & 1 & 0 & 3 & 2 & 1 &
\end{array}$$

From this algorithm diagram we read its half-cycle braiding algorithms:

half-cycle $1''''$ $L \longrightarrow R$: $2u - 6o - 4u - 4o - 4u - 2o - 2u$.
half-cycle $2''''$ $L \longleftarrow R$ $i = 0$: $2u - 6o - 4u - 5o - 4u - 2o - 2u$.
half-cycle $3''''$ $L \longrightarrow R$ $i = 0$: $2u - 6o - 4u - 5o - 4u - 2o - 2u$.
half-cycle $4''''$ $L \longleftarrow R$ $i \leq 1$: $3u - 6o - 4u - 5o - 5u - 2o - 2u$.
half-cycle $5''''$ $L \longrightarrow R$ $i \leq 1$: $3u - 6o - 4u - 5o - 5u - 2o - 2u$.
half-cycle $6''''$ $L \longleftarrow R$ $i \leq 2$: $3u - 7o - 4u - 5o - 5u - 3o - 2u$.
half-cycle $7''''$ $L \longrightarrow R$ $i \leq 2$: $3u - 7o - 4u - 5o - 5u - 3o - 2u$.
half-cycle $8''''$ $L \longleftarrow R$ $i \leq 3$: $3u - 7o - 5u - 5o - 5u - 3o - 2u$.

Example 3: type 2

Let $A = 3$; $B^* = 5$ and $n = 3$. Hence $P_c = n + 5 = 8$; $x = 3A + 2 + nA = 9 + 2 + 9 = 20$ and g.c.d.$(P_c, B^*) =$ g.c.d.$(8, 5) = 1$.

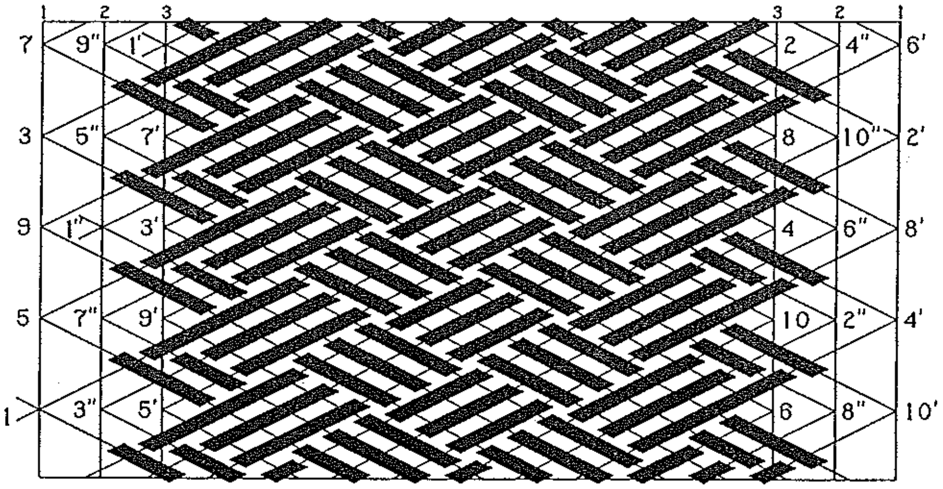

Fig. 814 — 3-pass Checkered Pineapple Knot of Example 3.

First we braid the foundation knot (a Regular Knot with $P_c/B^* = 8/5$) between left bight-boundary 1 and right bight-boundary 3, next we interbraid the component (a Regular Knot with $P_c/B^* = 8/5$) between left bight-boundary 3 and right bight-boundary 1. Next we interbraid the component (a Regular Knot with $P_c/B^* = 8/5$) between left bight-boundary 2 and right bight-boundary 2.

Again, before we can draw up the algorithm diagrams for these three components we need to know their Δ^*-values (their Δ^*-values are the same since their P_c/B^*-values are the same), which we obtain from their path in the RKT:

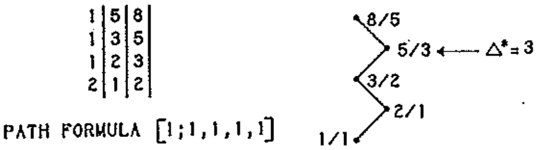

The algorithm diagram for the foundation knot is:

$$\begin{array}{ccccccc}
3 & 1 & 4 & 2 & 0 & 3 & 1 \\
0 & 0 & 0 & 0 & 0 & 0 & 0 \\
u & o & u & o & u & o & o \\
\cdot & \cdot & \cdot & \cdot & \cdot & \cdot & \cdot \\
o & u & o & u & o & u & u \\
0 & 0 & 0 & 0 & 0 & 0 & 0 \\
1 & 3 & 0 & 2 & 4 & 1 & 3
\end{array}$$

From this algorithm diagram we read its half-cycle braiding algorithms:

half-cycle 1 $L \longleftarrow R$: Free run.
half-cycle 2 $L \longrightarrow R$ $i = 0$: o.
half-cycle 3 $L \longleftarrow R$ $i = 0$: u.
half-cycle 4 $L \longrightarrow R$ $i \leq 1$: $u - 2o$.
half-cycle 5 $L \longleftarrow R$ $i \leq 1$: $o - u - o$.
half-cycle 6 $L \longrightarrow R$ $i \leq 2$: $2u - 2o$.
half-cycle 7 $L \longleftarrow R$ $i \leq 2$: $2o - u - o$.
half-cycle 8 $L \longrightarrow R$ $i \leq 3$: $3u - o - u - o$.
half-cycle 9 $L \longleftarrow R$ $i \leq 3$: $u - 2o - u - 2o$.
half-cycle 10 $L \longrightarrow R$ $i \leq 4$: $2u - o - u - o - u - o$.

The algorithm diagram for the interbraided knot between left bight-boundary 3 and right bight-boundary 1 in the 3-pass Checkered Pineapple Knot (left bight-boundary 2 and right bight-boundary 1 in 2-pass Checkered Pineapple Knot) is:

$$\begin{array}{cccccccc}
 & 3 & 1 & 4 & 2 & 0 & 3 & 1 \\
1 & 0 & 1 & 1 & 1 & 1 & 2 & 0 \\
u & o & o & u & o & u & o & u \\
\cdot & \cdot & \cdot & \cdot & \cdot & \cdot & \cdot & \cdot \\
 & u & u & o & u & o & u & o \\
 & 1 & 1 & 1 & 1 & 1 & 1 & 1 \\
 & 1 & 3 & 0 & 2 & 4 & 1 & 3
\end{array}$$

From this algorithm diagram we read its half-cycle braiding algorithms:

half-cycle 1′ $L \longrightarrow R$: $u - o - u - o - u - 2o$.
half-cycle 2′ $L \longleftarrow R$ $i = 0$: $o - u - o - u - 2o - 2u$.
half-cycle 3′ $L \longrightarrow R$ $i = 0$: $u - o - u - o - 2u - 2o$.
half-cycle 4′ $L \longleftarrow R$ $i \leq 1$: $o - 2u - o - u - 2o - 3u$.
half-cycle 5′ $L \longrightarrow R$ $i \leq 1$: $u - 2o - u - o - 2u - 2o - u$.

half-cycle 6′ $L \longleftarrow R$ $i \leq 2$: $o - 2u - o - 2u - 2o - 3u$.
half-cycle 7′ $L \longrightarrow R$ $i \leq 2$: $u - 2o - u - 2o - 2u - 2o - u$.
half-cycle 8′ $L \longleftarrow R$ $i \leq 3$: $2o - 2u - o - 2u - 2o - 4u$.
half-cycle 9′ $L \longrightarrow R$ $i \leq 3$: $u - 3o - u - 2o - 2u - 3o - u$.
half-cycle 10′ $L \longleftarrow R$ $i \leq 4$: $2o - 2u - 2o - 2u - 2o - 4u$.

The algorithm diagram for the interbraided knot between left bight-boundary 2 and right bight-boundary 2 in the 3-pass Checkered Pineapple Knot (hence $l = 2$ and $r = 2$ since this ends the interbraiding) is:

$$\begin{array}{ccccccccc}
 & 3 & 1 & 4 & 2 & 0 & 3 & 1 & \\
 & 1 & 3 & 2 & 2 & 2 & 3 & 1 & \\
 & u & o & u & o & u & o & u & \\
\cdot & \cdot & \cdot & \cdot & \cdot & \cdot & \cdot & \cdot & \cdot \\
u & o & u & o & u & o & u & o & u \\
1 & 1 & 2 & 2 & 2 & 2 & 2 & 1 & 1 \\
 & 1 & 3 & 0 & 2 & 4 & 1 & 3 &
\end{array}$$

From this algorithm diagram we read its half-cycle braiding algorithms:

half-cycle 1″ $L \longrightarrow R$: $u - 3o - 2u - 2o - 2u - 3o - u$.
half-cycle 2″ $L \longleftarrow R$ $i = 0$: $u - o - 2u - 2o - 2u - 3o - 2u - o - u$.
half-cycle 3″ $L \longrightarrow R$ $i = 0$: $u - 3o - 2u - 2o - 3u - 3o - u$.
half-cycle 4″ $L \longleftarrow R$ $i \leq 1$: $u - o - 3u - 2o - 2u - 3o - 2u - 2o - u$.
half-cycle 5″ $L \longrightarrow R$ $i \leq 1$: $u - 4o - 2u - 2o - 3u - 3o - 2u$.
half-cycle 6″ $L \longleftarrow R$ $i \leq 2$: $u - o - 3u - 2o - 3u - 3o - 2u - 2o - u$.
half-cycle 7″ $L \longrightarrow R$ $i \leq 2$: $u - 4o - 2u - 3o - 3u - 3o - 2u$.
half-cycle 8″ $L \longleftarrow R$ $i \leq 3$: $u - 2o - 3u - 2o - 3u - 3o - 3u - 2o - u$.
half-cycle 9″ $L \longrightarrow R$ $i \leq 3$: $2u - 4o - 2u - 3o - 3u - 4o - 2u$.
half-cycle 10″ $L \longleftarrow R$ $i \leq 4$: $u - 2o - 3u - 3o - 3u - 3o - 3u - 2o - u$.

Round Braids and their string sizes

The helix-angle of a helix on a cylinder is the angle between the helix and a line parallel to the centreline. In our calculations, however, we shall use its complement, indicated by α (see Fig. 815).

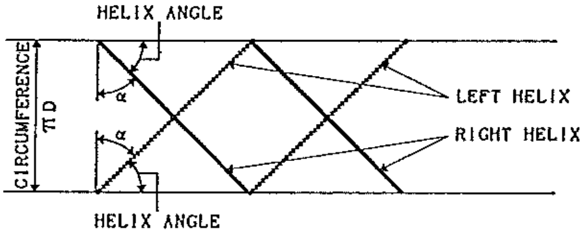

Fig. 815 — The helix angle and its complement α .

Say the core round braid has to be braided over a diameter D . Let for the core round braid the string-width be w , the string-thickness be t , the number of strings be $2b$ and the complement of the helix-angle be α . Then $bw = \pi(D + 2t) sin\alpha$, and with $\alpha = 45°$, hence $sin\alpha = \frac{1}{2}\sqrt{2} = 0.707$ we obtain $bw = 2.22(D + 2t)$. When we take $bw = 2(D + 2t)$, the angle between a right helix and a left helix is a little greater than

$90°$. Normally we choose a value for $2b$ and w, calculate the value for t and if that value is unsuitable we change $2b$ or w or both.

For two round braids over each other let for the core round braid the diameter over which it has to be braided be D. Let for the core round braid the string-width be w, the string-thickness be t and the number of strings be $2b_1$. For the mantle round braid let the string-width be w', the string-thickness be t' and the number of strings be $2b_2$. Let $w = rw'$ and $t = r^*t'$. Let the complement of the helix-angle for both braids be α. Then $b_2 - b_1 = \frac{\pi D(r-1) sin\alpha}{w} + \frac{2\pi t[2r+(\frac{r}{r^*}-1)] sin\alpha}{w}$. When the strings of both braids are identical in width and thickness, then $r = 1$ and $r^* = 1$, hence $b_2 - b_1 = \frac{4\pi t sin\alpha}{w} = n$. Thus the difference in the number of strings for the mantle and core round braids is equal to $2n$. These relationships are quite accurate in practice, provided the string preparation has been done properly. For thick string we have to take some off the width or the thickness to compensate for the discrepancy between theory and practice, and for thin string we add some to the width or the thickness. The string material is a more or less compressible medium which due to the tension during braiding decreases somewhat in width; furthermore it is not a homogeneous material and hence its properties are not constant along the entire string-length.

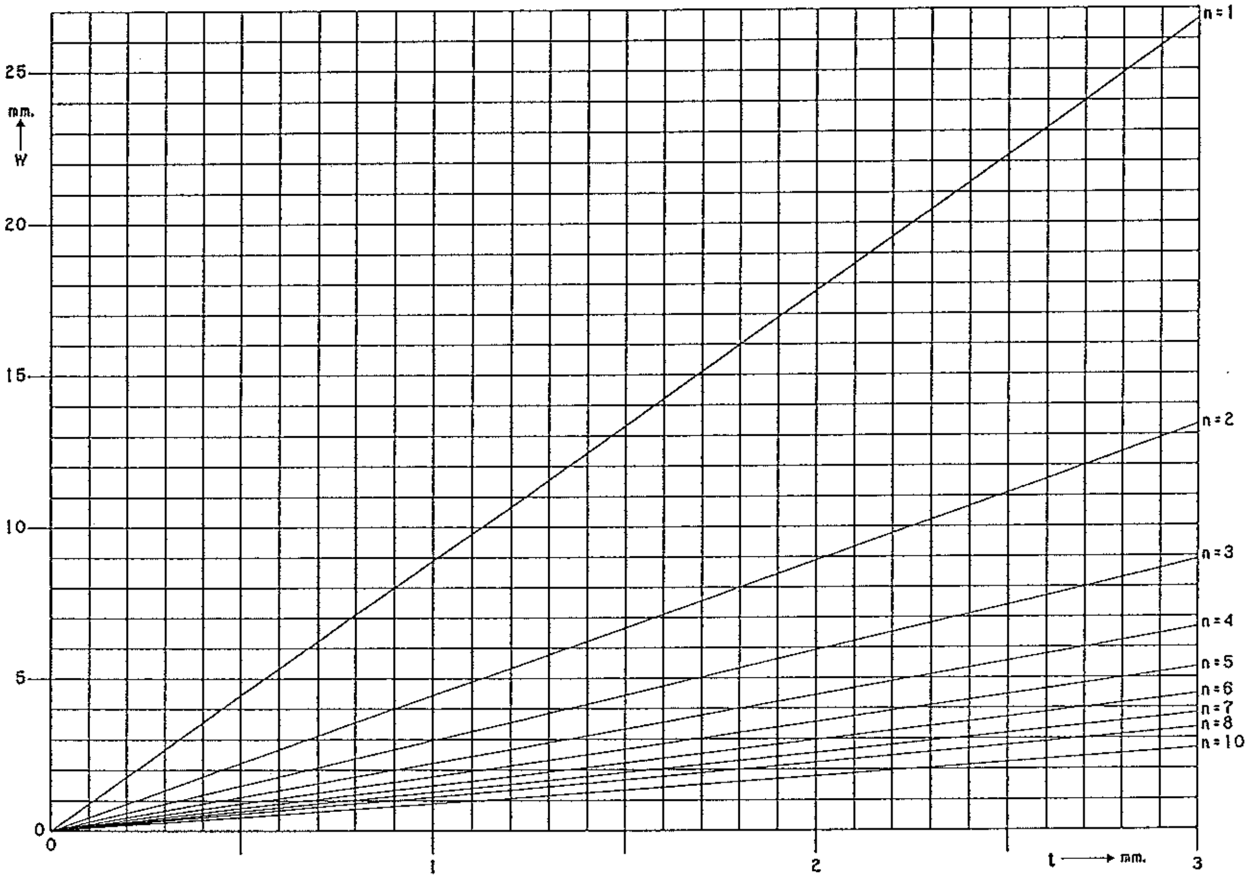

Fig. 816 — w, t, n graph for $\alpha = 45°$.

For a round braid over a core with varying diameters we first take the average diameter for the calculation of b_2, w', t', then we calculate the actual helix-pattern over the core and transfer that pattern to the core and lay the strings accordingly. Make sure that the string for building the various diameters of the core is relatively thin in order to prevent sudden steps.

THE BRAIDER

No.45 **FEBRUARY 2006.**

CONTENTS

pg.
The Glen Vandy Knots 1055
Braid Design 1059
Grant Knots 1066
The Single Bugler's Braid 1076

A quarterly publication for the braiding artisan

Resale of this publication or copies thereof is strictly prohibited

Copyright ©2006 by:

A.G. Schaake; 21 Sundown Cresc.; Hamilton; New Zealand.
D. Van Tassel; Box 335; Craig, Co 81626-0335; U.S.A.
F.J.M. Masurel; Ganzenzijde 4; 2317XG Leiden; Nederland.

All rights reserved. No part of this publication may be reproduced, stored in a retrieval system, or transmitted, in any form or by any means, electronic, mechanical, photo-copying, recording, or otherwise, without prior written permission.

This publication is available to braiding artisans only.

Copies may be obtained from:

A.G. Schaake,
21 Sundown Cresc.,
Hamilton,
New Zealand.

The Glen Vandy Knots

In *The Braider*, Issue No. 44 we discussed the Checkered Pineapple Knots and saw that for the types 2 and 3 the value of y is 0 (see pg. 1042). Although the value of n is an odd integer for these two types, hence the minimum n-value is equal to 1, we could relax this minimum n-value condition to $n = 0$ while retaining the y-value of 0. From the coding associated with the types 2 and 3 it will be observed that $2A+1 \le x \le 3A+2$ for $n = 0$. Since $y = |2(A-1)+x|_{2A}$ has to be zero, it follows that $x = 2A+2$. The knots of type 2 and type 3 with $n = 0$, $y = 0$ and $x = 2A+2$ are called **the Glen Vandy Knots.** An A-pass Glen Vandy Knot thus consists of A interbraided Regular Cylindrical Braids, each with $P_c = 4$ ($P_c = \frac{P_{total}}{A} = \frac{2A+x-2}{A}$), hence its string-run is the string-run of the Regular Nested Cylindrical Braid

$$(\underbrace{222\cdots2}_{(A-1)\text{ elements}}/2A+2/\underbrace{222\cdots2}_{(A-1)\text{ elements}})\{1(A)(A-1)(A-2)\cdots2/(A)123\cdots(A-1)\}B\,,$$

The upper row of diagrams in Fig. 817 show the coding-patterns of type 2 while the lower row of diagrams in Fig. 817 show the coding-patterns of type 3 Glen Vandy Knots.

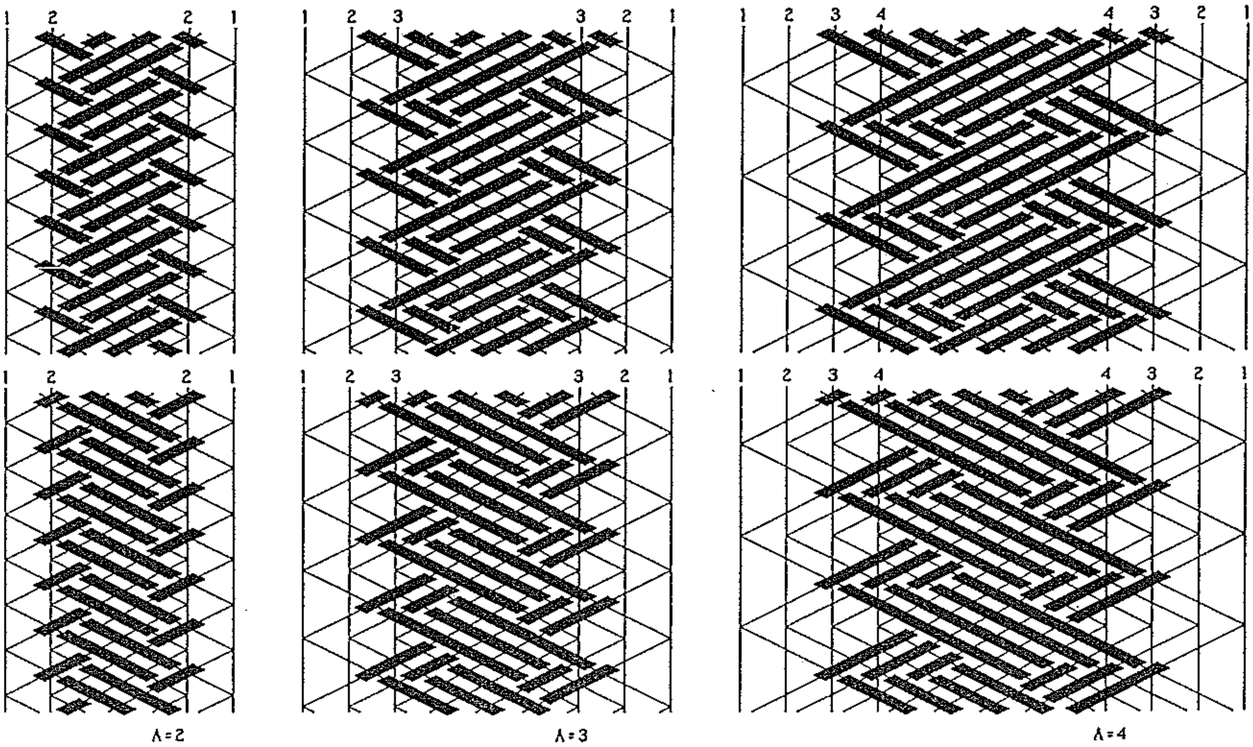

Fig. 817 — The coding-patterns of Glen Vandy Knots.

From the diagrams in Fig. 817 it can be seen that the best way to braid an A-pass Glen Vandy Knot is to braid first a 2-pass Glen Vandy Knot and then progressively to enlarge it to a 3-pass, 4-pass, … , $(A-1)$-pass, A-pass Glen Vandy Knot by respectively interbraiding the Regular Cylindrical Braid component associated with the left to right bight-boundary pair 2—2, a left to right bight-boundary pair which belongs to the set 2—3 to 3—2, … , a left to right bight-boundary pair which belongs to the set 2—$(A-2)$ to $(A-2)$—2, a left to right bight-boundary pair which belongs to the set 2—$(A-1)$ to $(A-1)$—2.

Let P_c and B^* be coprime, hence g.c.d.$(P_c, B^*) =$ g.c.d.$(4, B^*) = 1$ (consequently $B^* = odd$), thus the interbraided Regular Cylindrical Braids are Regular Knots.

Type 2:

For a 2-pass type 2 Glen Vandy Knot the algorithm diagram for the foundation knot between left bight-boundary 1 and right bight-boundary 2 is:

$$\begin{array}{ccc}
\Delta^* & |2\Delta^*|_{B*} & |3\Delta^*|_{B*} \\
0 & 0 & 0 \\
u & o & o \\
\cdot & \cdot & \cdot \\
o & u & u \\
0 & 0 & 0 \\
|3\Delta^*|_{B*} & |2\Delta^*|_{B*} & \Delta^*
\end{array}$$

For the half-cycles from lower left to upper right the first line gives the i-values, the second line the reference quantities, the third line the coding and the fourth line the intersection columns. For the half-cycles from lower right to upper left the fourth line gives the intersection columns, the fifth line the coding, the sixth line the reference quantities and the seventh line the i-values. Each reference quantity is increased by 1 when its associated i-value is applicable for the half-cycle concerned.

For a 2-pass type 2 Glen Vandy Knot the algorithm diagram for the interbraided component between left bight-boundary 2 and right bight-boundary 1 is:

$$\begin{array}{cccc}
 & \Delta^* & |2\Delta^*|_{B*} & |3\Delta^*|_{B*} \\
1 & 1 & 1 & 0 \\
u & o & o & u \\
\cdot & \cdot & \cdot & \cdot \\
 & u & u & o \\
 & 1 & 1 & 1 \\
 & |3\Delta^*|_{B*} & |2\Delta^*|_{B*} & \Delta^*
\end{array}$$

For the half-cycles from lower left to upper right the first line gives the i-values where applicable, the second line the reference quantities, the third line the coding and the fourth line the intersection sets. For the half-cycles from lower right to upper left the fourth line gives the intersection sets, the fifth line the coding, the sixth line the reference quantities and the seventh line the i-values where applicable. Each reference quantity is increased by 1 when its associated i-value is applicable for the half-cycle concerned.

An A-pass type 2 Glen Vandy Knot ($A \geq 3$) is enlarged from a 2-pass type 2 Glen Vandy Knot by interbraiding the Regular Knot components between the left and right bight-boundary pairs $2—(A-1)$ to and including $(A-1)—2$. The algorithm diagram for these interbraids is:

$$\begin{array}{ccccc}
 & \Delta^* & |2\Delta^*|_{B*} & |3\Delta^*|_{B*} & \\
 & l-1 & 2A-2 & A-l & \\
 & u & o & u & \\
\cdot & \cdot & \cdot & \cdot & \cdot \\
u & o & u & o & u \\
A-r & r-1 & A-1 & A-r & r-1 \\
 & |3\Delta^*|_{B*} & |2\Delta^*|_{B*} & \Delta^* &
\end{array}$$

$$A \geq 3\,;\; 2 \leq l \leq A-1\,;\; 2 \leq r \leq A-1\,;\; r = A+1-l\,;\; l = A+1-r\,.$$

For the half-cycles from lower left to upper right the first line gives the i-values where applicable, the second line gives the reference quantities, the third line the coding and the fourth line the intersection sets. For the half-cycles from lower right to upper left the fourth line gives the intersection sets, the fifth line the coding, the sixth line the reference quantities and the seventh line gives the i-values where applicable. Each reference quantity is increased by 1 when its associated i-value is applicable for the half-cycle concerned.

Type 3:

For a 2-pass type 3 Glen Vandy Knot the algorithm diagram for the foundation knot between left bight-boundary 1 and right bight-boundary 2 is:

$$\begin{array}{ccc}
\Delta^* & |2\Delta^*|_{B^*} & |3\Delta^*|_{B^*} \\
0 & 0 & 0 \\
o & u & u \\
\cdot & \cdot & \cdot \\
u & o & o \\
0 & 0 & 0 \\
|3\Delta^*|_{B^*} & |2\Delta^*|_{B^*} & \Delta^*
\end{array}$$

For the half-cycles from lower left to upper right the first line gives the i-values, the second line gives the reference quantities of the coding associated with the intersection columns, the third line the coding of the intersection columns and the fourth line the intersection columns. For the half-cycles from lower right to upper left the fourth line gives the intersection columns, the fifth line the coding of the intersection columns, the sixth line the reference quantities of the coding associated with the intersection columns and the seventh line the i-values. Each reference quantity is increased by 1 when its associated i-value is applicable for the half-cycle concerned.

For a 2-pass type 3 Glen Vandy Knot the algorithm diagram for the interbraided component between left bight-boundary 2 and right bight-boundary 1 is:

$$\begin{array}{cccc}
 & \Delta^* & |2\Delta^*|_{B^*} & |3\Delta^*|_{B^*} \\
 & 1 & 1 & 1 \\
 & u & u & o \\
\cdot & \cdot & \cdot & \cdot \\
u & o & o & u \\
1 & 1 & 1 & 0 \\
 & |3\Delta^*|_{B^*} & |2\Delta^*|_{B^*} & \Delta^*
\end{array}$$

For the half-cycles from lower left to upper right the first line gives the i-values where applicable, the second line gives the reference quantities of the coding associated with the intersection sets, the third line the coding associated with the intersection sets and the fourth line the intersection sets. For the half-cycles from lower right to upper left the fourth line gives the intersection sets, the fifth line the coding associated with the intersection sets, the sixth line the reference quantities of the coding associated with the intersection sets and the seventh line the i-values where applicable. Each reference quantity is increased by 1 when its associated i-value is applicable for the half-cycle concerned.

An A-pass type 3 Glen Vandy Knot ($A \geq 3$) is enlarged from a 2-pass type 3 Glen Vandy Knot by interbraiding the Regular Knot components between the left and right bight-boundary pairs $2—(A-1)$ to and including $(A-1)—2$. The algorithm diagram for these interbraids is:

$$\begin{array}{ccccc}
 & \scriptstyle\Delta^* & \scriptstyle|2\Delta^*|_{B^*} & \scriptstyle|3\Delta^*|_{B^*} & \\
l-1 & A-l & A-1 & l-1 & A-l \\
u & o & u & o & u \\
\cdot & \cdot & \cdot & \cdot & \cdot \\
 & u & o & u & \\
 & A-r & 2A-2 & r-1 & \\
 & \scriptstyle|3\Delta^*|_{B^*} & \scriptstyle|2\Delta^*|_{B^*} & \scriptstyle\Delta^* &
\end{array}$$

$$A \geq 3\,;\ 2 \leq l \leq A-1\,;\ 2 \leq r \leq A-1\,;\ r = A+1-l\,;\ l = A+1-r\,.$$

For the half-cycles from lower left to upper right the first line gives the i-values where applicable, the second line gives the reference quantities, the third line the coding and the fourth line the intersection sets. For the half-cycles from lower right to upper left the fourth line gives the intersection sets, the fifth line the coding, the sixth line the reference quantities and the seventh line gives the i-values where applicable. Each reference quantity is increased by 1 when its associated i-value is applicable for the half-cycle concerned.

In *The Braider*, Issue No. 16, pg. 367, an example of a 2-pass type 2 and of a 2-pass type 3 Glen Vandy Knot is shown.

For the upper knot the algorithm diagram of the foundation knot is:

$$\begin{array}{ccc}
\scriptstyle 1 & \scriptstyle 2 & \scriptstyle 3 \\
0 & 0 & 0 \\
u & o & o \\
\cdot & \cdot & \cdot \\
o & u & u \\
0 & 0 & 0 \\
\scriptstyle 3 & \scriptstyle 2 & \scriptstyle 1
\end{array}$$

while the algorithm diagram of the interwoven knot is:

$$\begin{array}{cccc}
 & \scriptstyle 1 & \scriptstyle 2 & \scriptstyle 3 \\
1 & 1 & 1 & 0 \\
u & o & o & u \\
\cdot & \cdot & \cdot & \cdot \\
 & u & u & o \\
 & 1 & 1 & 1 \\
 & \scriptstyle 3 & \scriptstyle 2 & \scriptstyle 1
\end{array}$$

For the lower knot the algorithm diagram of the foundation knot is:

$$\begin{array}{ccc}
\scriptstyle 1 & \scriptstyle 2 & \scriptstyle 3 \\
0 & 0 & 0 \\
o & u & u \\
\cdot & \cdot & \cdot \\
u & o & o \\
0 & 0 & 0 \\
\scriptstyle 3 & \scriptstyle 2 & \scriptstyle 1
\end{array}$$

while the algorithm diagram of the interwoven knot is:

$$\begin{array}{cccc} & {\scriptstyle 1} & {\scriptstyle 2} & {\scriptstyle 3}\\ & 1 & 1 & 1\\ & u & u & o\\ \cdot & \cdot & \cdot & \cdot\\ u & o & o & u\\ 1 & 1 & 1 & 0\\ & {\scriptstyle 3} & {\scriptstyle 2} & {\scriptstyle 1}\end{array}$$

Braid Design

Let's return to the 12-lead tubular flat braid in *The Braider*, Issue No. 43 (see the lower diagrams of Fig. 796), and form from this braid a cylindrical braid as depicted by the diagrams of Fig. 818. This cylindrical braid is then a **flat tubular torus braid**.

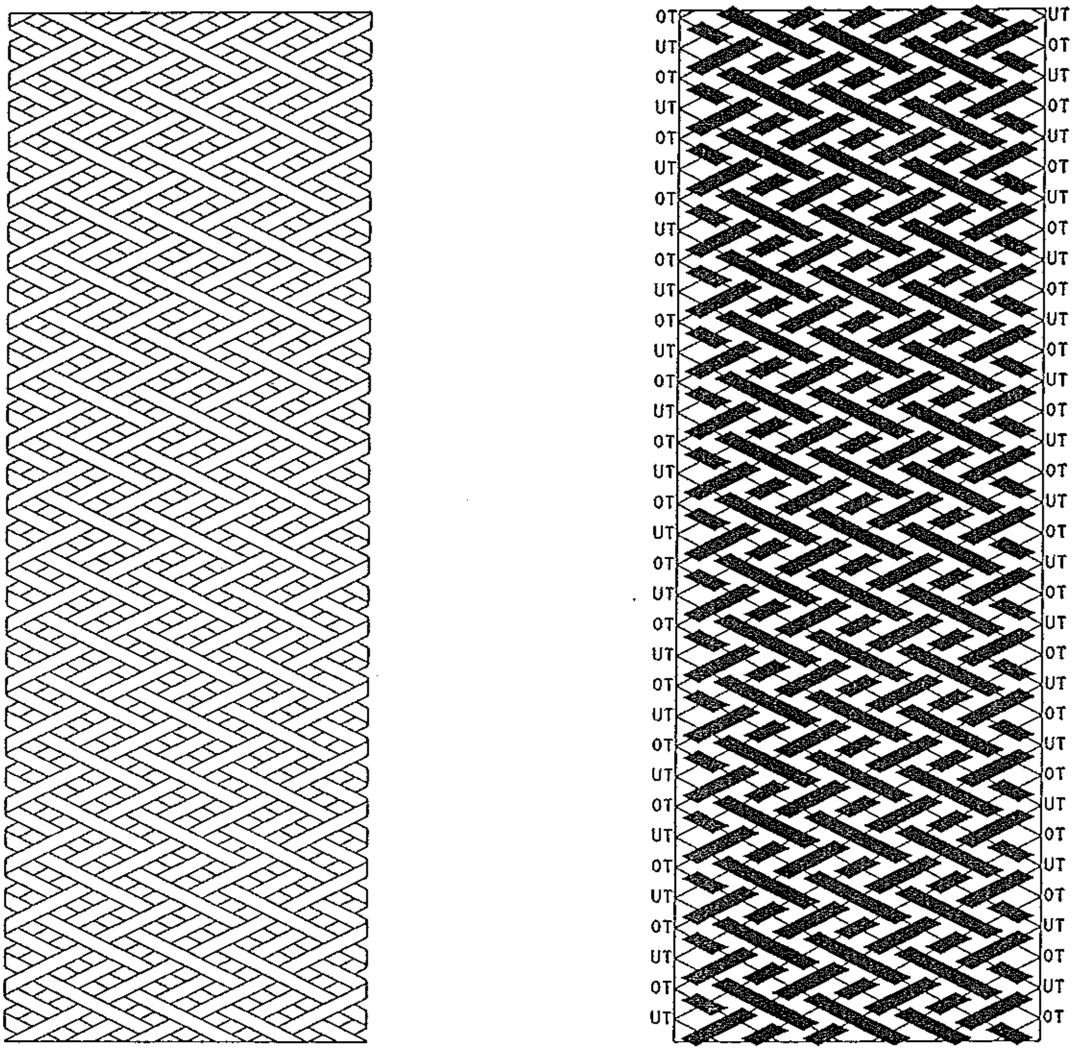

Fig. 818 — A $p/b = 12/34$ flat tubular torus braid.

The braid consists of two interbraided primitive flat torus braids: one having $p/b = 6/17$ with a right helix and one having $p/b = 6/17$ with a left helix. The one with a right helix has OT's on the left 'bight' boundary and UT's on the right 'bight' boundary, while the one with the left helix has UT's on the left 'bight' boundary and OT's on the right 'bight' boundary.[†] Say we first braid the primitive flat torus braid with the right helix as the foundation knot. The path-formula of a $p/b = 6/17$ Regular Knot is $[0; 2, 1, 4, 1]$ (obtained with the aid of Euclid's algorithm) and hence $\Delta^* = 14$.[‡] Hence the algorithm diagram for the foundation knot (the primitive flat torus braid with the right helix; odd numbered half-cycles from lower-left to upper-right start with OT, even numbered half-cycles from lower-right to upper-left start with UT) is:

$$\begin{array}{ccccc} 14 & 11 & 8 & 5 & 2 \\ o & o & u & o & o \\ \cdot & \cdot & \cdot & \cdot & \cdot \\ u & u & o & u & u \\ 2 & 5 & 8 & 11 & 14 \end{array}$$

From this algorithm diagram we read the following half-cycle braiding algorithms:

half-cycle 1: Free run.
half-cycle 2: $i = 0$: Free run.
half-cycle 3: $i = 0$: Free run.
half-cycle 4: $i \leq 1$: Free run.
half-cycle 5: $i \leq 1$: Free run.
half-cycle 6: $i \leq 2$: u.
half-cycle 7: $i \leq 2$: o.
half-cycle 8: $i \leq 3$: u.
half-cycle 9: $i \leq 3$: o.
half-cycle 10: $i \leq 4$: u.
half-cycle 11: $i \leq 4$: o.
half-cycle 12: $i \leq 5$: $2u$.
half-cycle 13: $i \leq 5$: $2o$.
half-cycle 14: $i \leq 6$: $2u$.
half-cycle 15: $i \leq 6$: $2o$.
half-cycle 16: $i \leq 7$: $2u$.
half-cycle 17: $i \leq 7$: $2o$.
half-cycle 18: $i \leq 8$: $o - 2u$.
half-cycle 19: $i \leq 8$: $u - 2o$.
half-cycle 20: $i \leq 9$: $o - 2u$
half-cycle 21: $i \leq 9$: $u - 2o$.
half-cycle 22: $i \leq 10$: $o - 2u$.
half-cycle 23: $i \leq 10$: $u - 2o$.
half-cycle 24: $i \leq 11$: $u - o - 2u$.
half-cycle 25: $i \leq 11$: $o - u - 2o$.
half-cycle 26: $i \leq 12$: $u - o - 2u$.
half-cycle 27: $i \leq 12$: $o - u - 2o$.
half-cycle 28: $i \leq 13$: $u - o - 2u$.
half-cycle 29: $i \leq 13$: $o - u - 2o$.
half-cycle 30: $i \leq 14$: $2u - o - 2u$.
half-cycle 31: $i \leq 14$: $2o - u - 2o$.
half-cycle 32: $i \leq 15$: $2u - o - 2u$.
half-cycle 33: $i \leq 15$: $2o - u - 2o$.
half-cycle 34: $i \leq 16$: $2u - o - 2u$.

The algorithm diagram for the interbraided knot (the primitive flat torus braid with the left helix; odd numbered half-cycles from lower-left to upper-right start with UT, even numbered half-cycles from lower-right to upper-left start with OT) is:

$$\begin{array}{ccccccccccc} & 14 & & 11 & & 8 & & 5 & & 2 & \\ u & u & o & u & u & o & u & u & o & u & u \\ \cdot & \cdot & \cdot & \cdot & \cdot & \cdot & \cdot & \cdot & \cdot & \cdot & \cdot \\ u & o & o & o & u & u & u & o & o & o & u \\ & 2 & & 5 & & 8 & & 11 & & 14 & \end{array}$$

From this algorithm diagram we read the following half-cycle braiding algorithms:

[†] Note that the OT's and UT's have changed place in the Figs. 818 & 796 since in Fig. 818 the braiding is from lower-left to upper-right and from lower-right to upper-left. Also note that the contact crossings in a primitive flat torus braid are not contact crossings in a primitive torus braid.

[‡] Note that each of the two interbraided primitive flat torus braids behaves as a Regular Knot.

half-cycle 1: $u - o - 2u - o - u$.
half-cycle 2: $i = 0$: $u - o - 2u - o - u$.
half-cycle 3: $i = 0$: $u - o - 2u - o - u$.
half-cycle 4: $i \leq 1$: $u - o - 2u - o - u$.
half-cycle 5: $i \leq 1$: $u - o - 2u - o - u$.
half-cycle 6: $i \leq 2$: $u - o - 2u - 2o - u$.
half-cycle 7: $i \leq 2$: $u - o - 2u - o - 2u$.
half-cycle 8: $i \leq 3$: $u - o - 2u - 2o - u$.
half-cycle 9: $i \leq 3$: $u - o - 2u - o - 2u$.
half-cycle 10: $i \leq 4$: $u - o - 2u - 2o - u$.
half-cycle 11: $i \leq 4$: $u - o - 2u - o - 2u$.
half-cycle 12: $i \leq 5$: $u - o - 2u - 3o - u$.
half-cycle 13: $i \leq 5$: $u - o - 3u - o - 2u$.
half-cycle 14: $i \leq 6$: $u - o - 2u - 3o - u$.
half-cycle 15: $i \leq 6$: $u - o - 3u - o - 2u$.
half-cycle 16: $i \leq 7$: $u - o - 2u - 3o - u$.
half-cycle 17: $i \leq 7$: $u - o - 3u - o - 2u$.
half-cycle 18: $i \leq 8$: $u - o - 3u - 3o - u$.
half-cycle 19: $i \leq 8$: $u - o - u - o - 2u - o - 2u$.
half-cycle 20: $i \leq 9$: $u - o - 3u - 3o - u$.
half-cycle 21: $i \leq 9$: $u - o - u - o - 2u - o - 2u$.
half-cycle 22: $i \leq 10$: $u - o - 3u - 3o - u$.
half-cycle 23: $i \leq 10$: $u - o - u - o - 2u - o - 2u$.
half-cycle 24: $i \leq 11$: $u - 2o - 3u - 3o - u$.
half-cycle 25: $i \leq 11$: $u - o - 2u - o - 2u - o - 2u$.
half-cycle 26: $i \leq 12$: $u - 2o - 3u - 3o - u$.
half-cycle 27: $i \leq 12$: $u - o - 2u - o - 2u - o - 2u$.
half-cycle 28: $i \leq 13$: $u - 2o - 3u - 3o - u$.
half-cycle 29: $i \leq 13$: $u - o - 2u - o - 2u - o - 2u$.
half-cycle 30: $i \leq 14$: $u - 3o - 3u - 3o - u$.
half-cycle 31: $i \leq 14$: $2u - o - 2u - o - 2u - o - 2u$.
half-cycle 32: $i \leq 15$: $u - 3o - 3u - 3o - u$.
half-cycle 33: $i \leq 15$: $2u - o - 2u - o - 2u - o - 2u$.
half-cycle 34: $i \leq 16$: $u - 3o - 3u - 3o - u$.

Similarly we can form a cylindrical braid as depicted in Fig. 819 from the 'tubular' braid in Fig. 807 (see *The Braider*, Issue No. 44, pg. 1035). This cylindrical braid consists of three components a primitive toroidal foundation knot with $p/b = 4/11$ and two primitive torus knots, each with $p/b = 2/11$ (one with a left-helix and one with a right-helix).

With the braiding direction for the odd-numbered half-cycles from lower-left to upper-right, the primitive toroidal foundation knot has OT bights, and with its Δ^*-value of 8, its algorithm diagram is:

$$\begin{array}{ccc} 8 & 5 & 2 \\ o & u & u \\ \cdot & \cdot & \cdot \\ u & o & o \\ 2 & 5 & 8 \end{array}$$

From this algorithm diagram we read the following half-cycle braiding algorithms for the foundation knot:

half-cycle 1: Free run.
half-cycle 2: $i = 0$: Free run.
half-cycle 3: $i = 0$: Free run.
half-cycle 4: $i \leq 1$: Free run.
half-cycle 5: $i \leq 1$: Free run.
half-cycle 6: $i \leq 2$: u.
half-cycle 7: $i \leq 2$: u.
half-cycle 8: $i \leq 3$: u.
half-cycle 9: $i \leq 3$: u.
half-cycle 10: $i \leq 4$: u.
half-cycle 11: $i \leq 4$: u.
half-cycle 12: $i \leq 5$: $o - u$.
half-cycle 13: $i \leq 5$: $2u$.
half-cycle 14: $i \leq 6$: $o - u$
half-cycle 15: $i \leq 6$: $2u$.
half-cycle 16: $i \leq 7$: $o - u$.
half-cycle 17: $i \leq 7$: $2u$.
half-cycle 18: $i \leq 8$: $2o - u$.
half-cycle 19: $i \leq 8$: $o - 2u$.
half-cycle 20: $i \leq 9$: $2o - u$.
half-cycle 21: $i \leq 9$: $o - 2u$.
half-cycle 22: $i \leq 10$: $2o - u$.

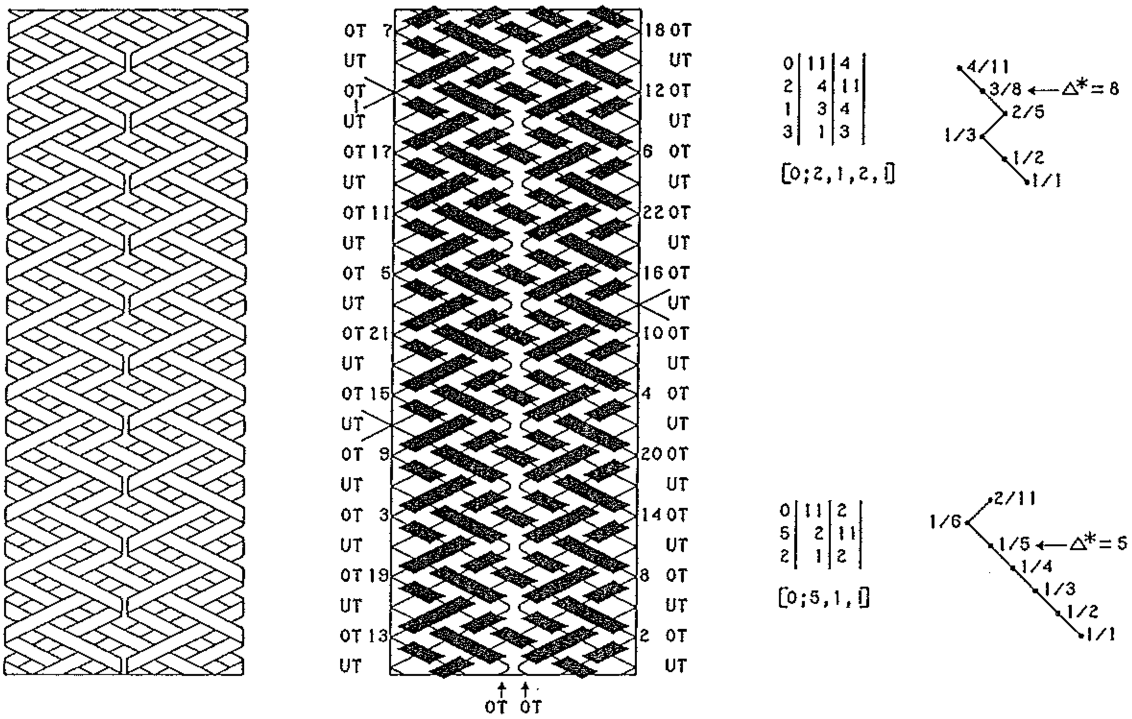

Fig. 819 — A toroidal braid.

For the interbraided left-hand primitive torus knot (left-helix) with $p/b = 2/11$ and hence $\Delta^* = 5$, the algorithm diagram is:

$$\begin{array}{ccc} & 5 & \\ u & u & o \\ \cdot & \cdot & \cdot \\ u & o & o \\ & 5 & \end{array}$$

From this algorithm diagram we read the following half-cycle braiding algorithms (odd numbered half-cycles from lower-left to upper-right and even numbered half-cycles from lower-right to upper-left):

half-cycle 1: : $u - o$.
half-cycle 2: $i = 0$: $o - u$.
half-cycle 3: $i = 0$: $u - o$.
half-cycle 4: $i \leq 1$: $o - u$.
half-cycle 5: $i \leq 1$: $u - o$.
half-cycle 12: $i \leq 5$: $2o - u$.
half-cycle 13: $i \leq 5$: $2u - o$.
half-cycle 14: $i \leq 6$: $2o - u$
half-cycle 15: $i \leq 6$: $2u - o$.
half-cycle 16: $i \leq 7$: $2o - u$.

half-cycle 6: $i \leq 2$: $o - u$.
half-cycle 7: $i \leq 2$: $u - o$.
half-cycle 8: $i \leq 3$: $o - u$.
half-cycle 9: $i \leq 3$: $u - o$.
half-cycle 10: $i \leq 4$: $o - u$.
half-cycle 11: $i \leq 4$: $u - o$.
half-cycle 17: $i \leq 7$: $2u - o$.
half-cycle 18: $i \leq 8$: $2o - u$.
half-cycle 19: $i \leq 8$: $2u - o$.
half-cycle 20: $i \leq 9$: $2o - u$.
half-cycle 21: $i \leq 9$: $2u - o$.
half-cycle 22: $i \leq 10$: $2o - u$.

For the interbraided right-hand primitive torus knot (right-helix) with $p/b = 2/11$ and hence $\Delta^* = 5$, the algorithm diagram is:

$$\begin{array}{ccc} & 5 & \\ o & o & u \\ \cdot & \cdot & \cdot \\ o & u & u \\ & 5 & \end{array}$$

From this algorithm diagram we read the following half-cycle braiding algorithms (odd numbered half-cycles from lower-right to upper-left and even numbered half-cycles from lower-left to upper-right):

half-cycle 1: : $u - o$.
half-cycle 2: $i = 0$: $o - u$.
half-cycle 3: $i = 0$: $u - o$.
half-cycle 4: $i \leq 1$: $o - u$.
half-cycle 5: $i \leq 1$: $u - o$.
half-cycle 6: $i \leq 2$: $o - u$.
half-cycle 7: $i \leq 2$: $u - o$.
half-cycle 8: $i \leq 3$: $o - u$.
half-cycle 9: $i \leq 3$: $u - o$.
half-cycle 10: $i \leq 4$: $o - u$.
half-cycle 11: $i \leq 4$: $u - o$.
half-cycle 12: $i \leq 5$: $2o - u$.
half-cycle 13: $i \leq 5$: $2u - o$.
half-cycle 14: $i \leq 6$: $2o - u$
half-cycle 15: $i \leq 6$: $2u - o$.
half-cycle 16: $i \leq 7$: $2o - u$.
half-cycle 17: $i \leq 7$: $2u - o$.
half-cycle 18: $i \leq 8$: $2o - u$.
half-cycle 19: $i \leq 8$: $2u - o$.
half-cycle 20: $i \leq 9$: $2o - u$.
half-cycle 21: $i \leq 9$: $2u - o$.
half-cycle 22: $i \leq 10$: $2o - u$.

Fig. 820 depicts a toroidal braid where four 4-lead under-over coded torus braids have been 'combined'. With the braiding direction for the odd-numbered half-cycles from lower-left to upper-right, the primitive toroidal foundation knot ($p/b = 8/11$) has OT bights, and with its Δ^*-value of 4, its algorithm diagram is:

$$\begin{array}{ccccccc} 4 & 8 & 1 & 5 & 9 & 2 & 6 \\ o & u & u & o & o & u & u \\ \cdot & \cdot & \cdot & \cdot & \cdot & \cdot & \cdot \\ u & o & o & u & u & o & o \\ 6 & 2 & 9 & 5 & 1 & 8 & 4 \end{array}$$

From this algorithm diagram we read the following half-cycle braiding algorithms for the foundation knot:

half-cycle 1: Free run.
half-cycle 2: $i = 0$: Free run.
half-cycle 3: $i = 0$: Free run.
half-cycle 4: $i \leq 1$: u.
half-cycle 5: $i \leq 1$: u.
half-cycle 6: $i \leq 2$: $u - o$.
half-cycle 7: $i \leq 2$: $2u$.
half-cycle 8: $i \leq 3$: $u - o$.
half-cycle 9: $i \leq 3$: $2u$.
half-cycle 12: $i \leq 5$: $o - 2u - o$.
half-cycle 13: $i \leq 5$: $o - u - o - u$.
half-cycle 14: $i \leq 6$: $o - 2u - o - u$
half-cycle 15: $i \leq 6$: $o - u - o - 2u$.
half-cycle 16: $i \leq 7$: $o - 2u - o - u$.
half-cycle 17: $i \leq 7$: $o - u - o - 2u$.
half-cycle 18: $i \leq 8$: $2o - 2u - o - u$.
half-cycle 19: $i \leq 8$: $o - 2u - o - 2u$.
half-cycle 20: $i \leq 9$: $2o - 2u - 2o - u$.

half-cycle 10: $i \le 4$: $o - u - o$.
half-cycle 11: $i \le 4$: $o - 2u$.

half-cycle 21: $i \le 9$: $o - 2u - 2o - 2u$.
half-cycle 22: $i \le 10$: $2o - 2u - 2o - u$.

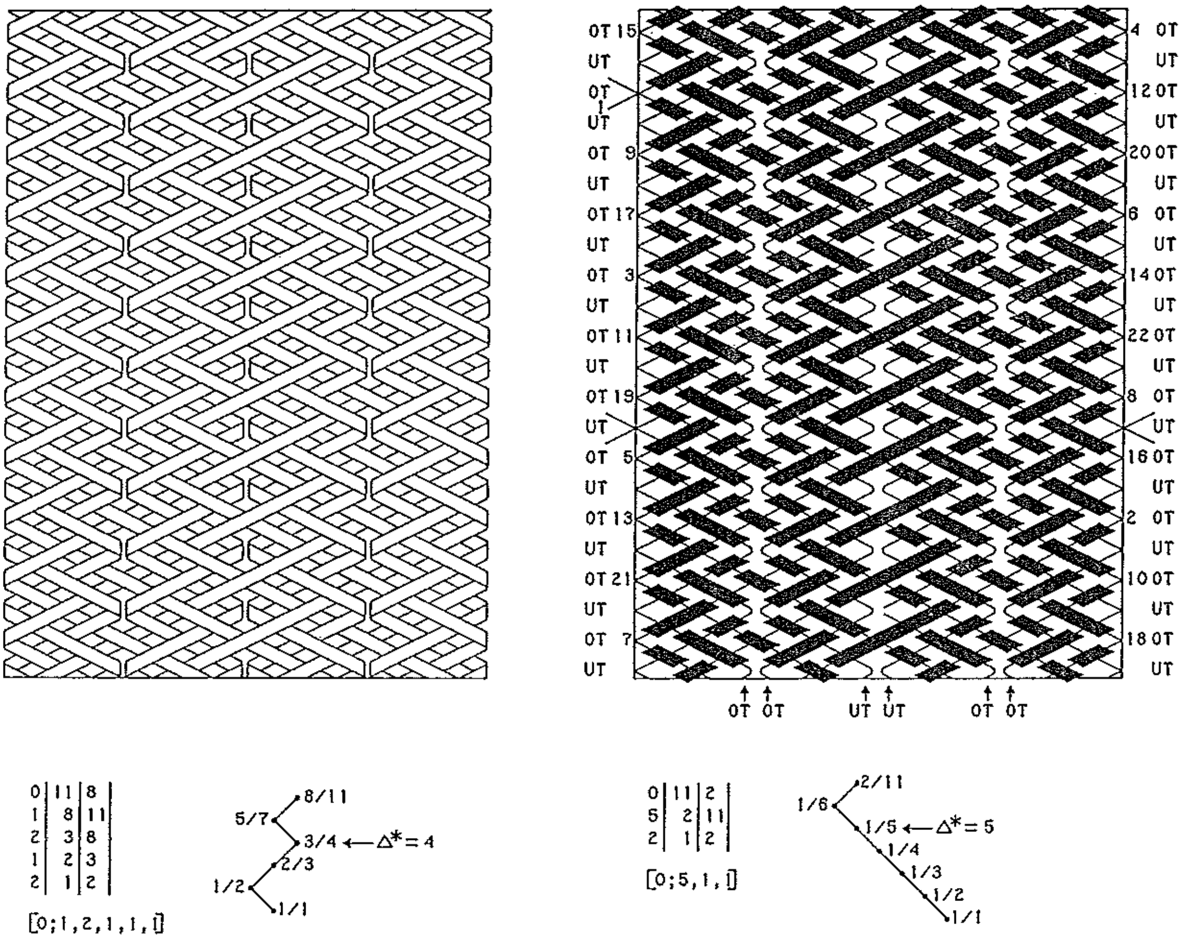

Fig. 820 — A toroidal braid formed from four 4-lead under-over coded torus braids.

The two interbraided left-helix primitive torus knots, each with $p/b = 2/11$ and hence $\Delta^* = 5$, are interbraided as the left-helix primitive torus knot in the toroidal foundation knot $p/b = 4/11$ we discussed earlier. Similarly, the two interbraided right-helix primitive torus knots, each with $p/b = 2/11$ and hence $\Delta^* = 5$, are interbraided as the right-helix primitive torus knot in the toroidal foundation knot $p/b = 4/11$ we discussed earlier.

A multitude of various toroidal braids can be designed by combining in similar ways various different torus braids. Furthermore, various toroidal braids can be designed by 'combining' torus braids and round braids; an example of such a braid is depicted in Fig. 821. With the braiding direction for the odd-numbered half-cycles from lower-left to upper-right, the toroidal foundation knot ($p/b = 15/11$) of that braid has OT bights. With its Δ^*-value of 8, its algorithm diagram is:

8	5	2	10	7	4	1	9	6	3	0	8	5	2
o	*u*	*u*	*o*	*o*	*u*	*u*	*o*	*o*	*u*	*u*	*o*	*o*	*u*
.	.	.	.	.	.	.	.	.	.	.	.	.	.
u	*o*	*o*	*u*	*u*	*o*	*o*	*u*	*u*	*o*	*o*	*u*	*u*	*o*
2	5	8	0	3	6	9	1	4	7	10	2	5	8

The interbraided left-helix primitive torus knot with $p/b = 2/11$ and the interbraided right-helix primitive torus knot with $p/b = 2/11$ are interbraided as in the earlier discussed toroidal foundation knot $p/b = 4/11$.

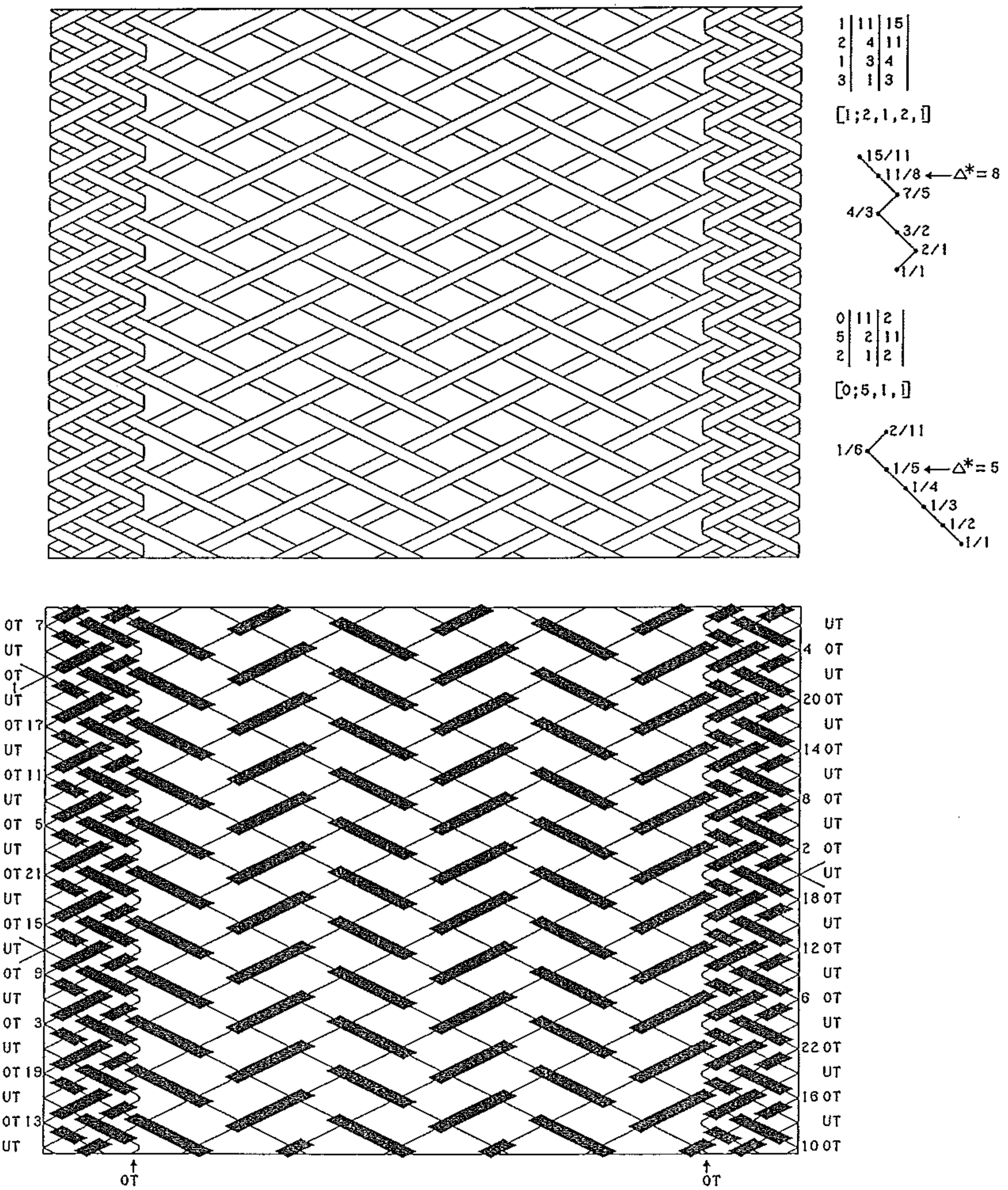

Fig. 821 — A toroidal braid.

From the algorithm diagram of the toroidal foundation knot ($p/b = 15/11$) we read the following half-cycle braiding algorithms for this foundation knot:

half-cycle 1: Free run.
half-cycle 2: $i = 0$: u.
half-cycle 3: $i = 0$: u.
half-cycle 4: $i \leq 1$: $2u$.
half-cycle 5: $i \leq 1$: $2u$.
half-cycle 6: $i \leq 2$: $4u$.

half-cycle 7: $i \leq 2$: $4u$.
half-cycle 8: $i \leq 3$: $5u$.
half-cycle 9: $i \leq 3$: $5u$.
half-cycle 10: $i \leq 4$: $6u$.
half-cycle 11: $i \leq 4$: $6u$.
half-cycle 12: $i \leq 5$: $6u - o - u$.
half-cycle 13: $i \leq 5$: $6u - o - u$.
half-cycle 14: $i \leq 6$: $4u - o - 2u - o - u$
half-cycle 15: $i \leq 6$: $4u - o - 2u - o - u$.
half-cycle 16: $i \leq 7$: $2u - o - 2u - o - 2u - o - u$.
half-cycle 17: $i \leq 7$: $2u - o - 2u - o - 2u - o - u$.
half-cycle 18: $i \leq 8$: $o - 2u - o - 2u - o - 2u - 2o - u$.
half-cycle 19: $i \leq 8$: $o - 2u - o - 2u - o - 2u - 2o - u$.
half-cycle 20: $i \leq 9$: $o - 2u - o - 2u - 2o - 2u - 2o - u$.
half-cycle 21: $i \leq 9$: $o - 2u - o - 2u - 2o - 2u - 2o - u$.
half-cycle 22: $i \leq 10$: $o - 2u - 2o - 2u - 2o - 2u - 2o - u$.

Grant Knots

If the string-run of a **Regular Nested Cylindrical Braid** with the essential coding of a **Pineapple Knot**[†] is modified in such a way that, at least at one set of two adjacent bight-boundaries with bight-boundary numbers greater than 1, the two consecutive bights $<<$ and/or $>>$ in each nest are respectively transformed to $\overset{<}{<}$ and $\overset{>}{>}$, the modified string-run with that essential Pineapple coding is then the string-run of a **Grant Knot**[‡] Similarly to the Herringbone Pineapple Knots with $y = A$, the Herringbone Grant Knots with $y = A$ we shall call the **Standard Herringbone Grant Knots.** Not only can the Standard Herringbone Grant Knots have the same colour-patterns as the Standard Herringbone Pineapple Knots and hence have identical appearances, the Standard Herringbone Grant Knots can have colour patterns which the Standard Herringbone Pineapple Knots cannot. Furthermore, the Standard Herringbone Grant Knots often require fewer essential strings. A few examples are shown in Fig. 822. When the Standard Herringbone Grant Knot has the same colour-pattern and requires the same number of essential strings as its associated Standard Herringbone Pineapple Knot, it will be more convenient to use the Standard Herringbone Pineapple Knot.

[†] See *The Braider*, Issue No. 44, pg. 1041, Fig. 810.

[‡] The best known books on braiding are no doubt the books by Bruce Grant (see *The Braider*, Issue No. 1, pp. 17-18). On pp. 418-419 of the *Encyclopedia of Rawhide and Leather Braiding* Bruce describes two knots he 'invented' (the **Bruce Knot** and the **Catharine Knot**) which he respectively named after himself and his wife, and thought to be small Herringbone-type knots. However, these knots are **Standard Herringbone Pineapple Knots**, hence do not deserve a special name (see the book *Braiding — Standard Herringbone Pineapple Knots — Vol 4/1*, by A.G. Schaake, J.C. Turner and D.A. Sedgwick, pg. 87). Consequently, in order to recognise his valuable contribution to braiding, the naming after him in the early nineteen eighties of a special family of knots, closely associated with Pineapple Knots, was felt to be justified.

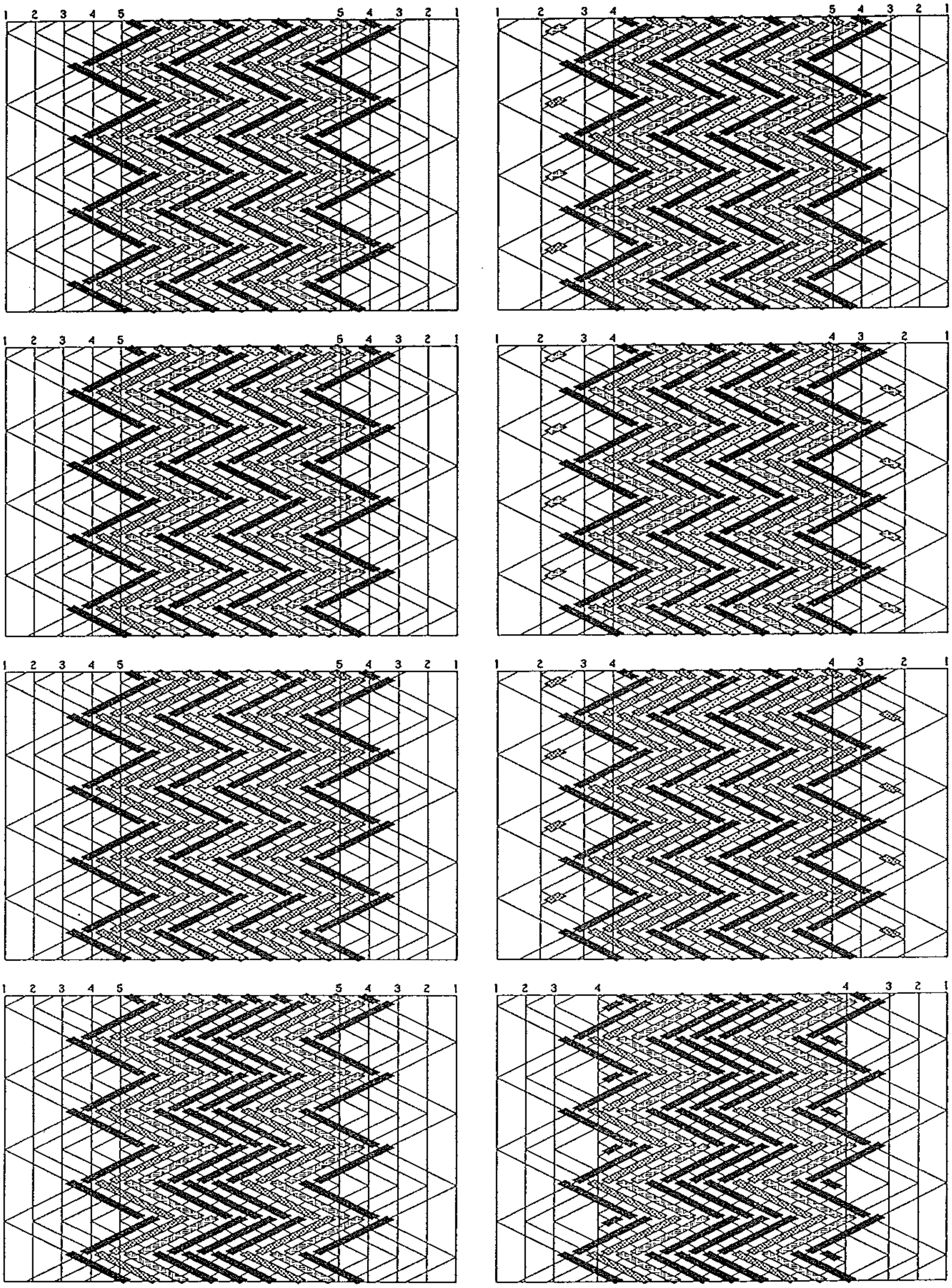

Fig. 822 — Some examples of 5-pass Standard Herringbone Pineapple Knots and their associated 5-pass Standard Herringbone Grant Knots.

In each row of two diagrams in Fig. 822, the Standard Herringbone Grant Knot is on the right and its associated Standard Herringbone Pineapple Knot is on the left. Each of the Standard Herringbone Pineapple Knots ($(2222/15/2222)\{15432/45123\}20$) requires five essential strings. The Standard Herringbone Grant Knots in the first three rows also require five essential strings, but those in the first two rows (respectively $(332/15/2222)\{1_1 4_5 3_4 2_2 2_3/4_1 5_2 1_3 2_4 3_5\}20$ & $(332/15/233)\{1_1 4_5 3_4 2_2 2_3/3_1 4_2 1_3 2_4 2_5\}20$) have a colour pattern which is different to that of their associated Standard Herringbone Pineapple Knots. The Standard Herringbone Grant Knot in the third row ($(332/15/233)\{1_1 4_5 3_4 2_2 2_3/3_1 4_2 1_3 2_4 2_5\}20$) has the same colour pattern as its associated Standard Herringbone Pineapple Knot and since both require the same number of essential strings, the latter should be used in an application. The Standard Herringbone Grant Knot in the fourth row ($(223/15/322)\{1_1 4_4 4_5 3_3 2_2/4_1 4_2 1_3 2_4 3_5\}20$) has the same colour pattern as its associated Standard Herringbone Pineapple Knot, but requires only three essential strings.

⋆⋆ *Say we want only two essential strings (of a different colour) in a 5-pass Standard Herringbone Grant Knot. How can we achieve that?*

After the Standard Herringbone Grant Knot has been designed (its grid-diagram), its algorithm diagrams can be drawn up and from them the half-cycle braiding algorithms can be read off.

For the Standard Herringbone Grant Knot depicted by the right-hand grid-diagram below, the string-colours (A, B, C, D) are indicated in the left-hand grid-diagram of its associated Standard Herringbone Pineapple Knot.

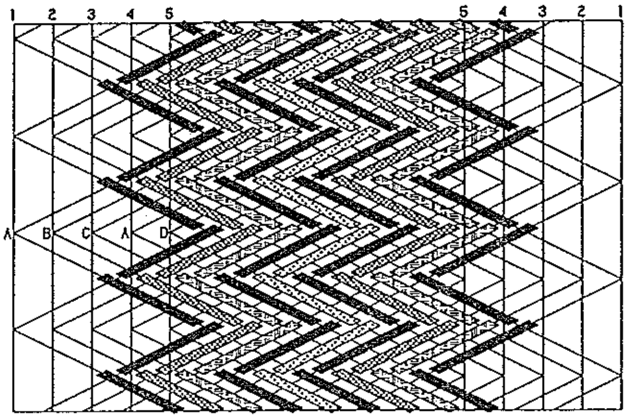

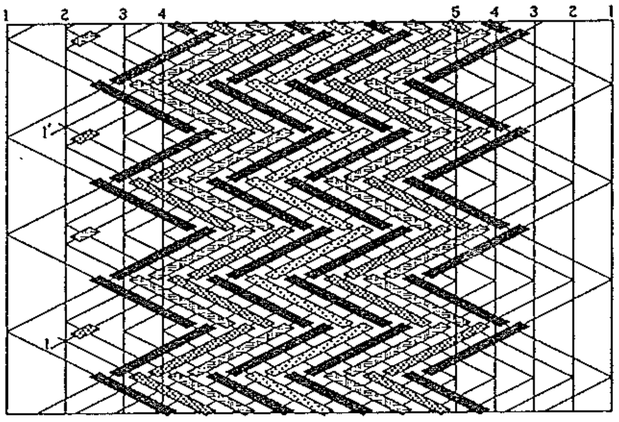

First we braid the component starting with half-cycle 1 and colour B, then we braid the component starting with half-cycle 1′ and colour C. Each of these two components has $p/b = 5/4$ and hence $\Delta^* = 3$. After these two components have been braided, the remaining components are braided as if the knot is a Standard Herringbone Pineapple Knot.

The algorithm diagram of the first to be braided component is:

$$\begin{array}{rccccl}
 & 3 & 2 & 1 & 0 & \\
\text{half-cycles 1, 5} \longrightarrow & u & o & u & o & \\
\text{half-cycles 3, 7} \longrightarrow & u & u & u & u & \\
 & \cdot & \cdot & \cdot & \cdot & \\
 & o & o & o & o & \longleftarrow \text{half-cycles 2, 6} \\
 & o & u & o & u & \longleftarrow \text{half-cycles 4, 8} \\
 & 0 & 1 & 2 & 3 &
\end{array}$$

From this algorithm diagram we read off the half-cycle braiding algorithms for the first to be braided component:

half-cycle 1: $L_1 \to R_1$: Free run.
half-cycle 2: $i = 0$: $R_1 \to L_1$: o.
half-cycle 3: $i = 0$: $L_1 \to R_2$: u.
half-cycle 4: $i \leq 1$: $R_2 \to L_1$: $u - o$.
half-cycle 5: $i \leq 1$: $L_1 \to R_1$: $u - o$.
half-cycle 6: $i \leq 2$: $R_1 \to L_1$: $3o$.
half-cycle 7: $i \leq 2$: $L_1 \to R_2$: $3u$.
half-cycle 8: $i \leq 3$: $R_2 \to L_1$: $u - o - u - o$.

The algorithm diagram of the next to be braided component is:

half-cycles 1′, 5′	→		3			2	1			0		
half-cycles 1′, 5′	→		u	o	o	u	u	o	o	u		
half-cycles 3′, 7′	→			3	2			1	0			
half-cycles 3′, 7′	→	o	u	u	o	o	u	u	o	o		
		.	.	.	.	.	.	.	.	.		
			o	o	u	u	o	o	u	u	←	half-cycles 2′, 6′
			0			1	2			3	←	half-cycles 2′, 6′
		u	u	o	o	u	u	o	o	u	←	half-cycles 4′, 8′
				0	1			2	3		←	half-cycles 4′, 8′

From this algorithm diagram we read off the half-cycle braiding algorithms for the second component:

half-cycle 1′: $L_1 \to R_2$: $4o$.
half-cycle 2′: $i = 0$: $R_2 \to L_1$: $u - o - u - 2o$.
half-cycle 3′: $i = 0$: $L_1 \to R_1$: $o - u - o - u - 2o$.
half-cycle 4′: $i \leq 1$: $R_1 \to L_1$: $3u - 2o - 2u$.
half-cycle 5′: $i \leq 1$: $L_1 \to R_2$: $2o - u - 2o - u$.
half-cycle 6′: $i \leq 2$: $R_2 \to L_1$: $u - 2o - 2u - 2o$.
half-cycle 7′: $i \leq 2$: $L_1 \to R_1$: $o - u - 2o - 2u - 2o$.
half-cycle 8′: $i \leq 3$: $R_1 \to L_1$: $u - 2o - 2u - 2o - 2u$.

As mentioned earlier, the remaining components of the Standard Herringbone Grant Knot are braided as if this Grant Knot is a Standard Herringbone Pineapple Knot, and hence for the remaining components we can use the algorithm diagrams of the equivalent components in its associated Standard Herringbone Pineapple Knot. Left bight-boundary 1 of the Grant Knot is equivalent to left bight-boundary 1 of the Pineapple Knot, left bight-boundary 3 of the Grant Knot is equivalent to left bight-boundary 4 of the Pineapple Knot, and left bight-boundary 4 of the Grant Knot is equivalent to left bight-boundary 5 of the Pineapple Knot.

The algorithm diagram for two components with $p/b = 5/4$, and hence $\Delta^* = 3$, is thus:[†]

$$\begin{array}{cccccc}
\longrightarrow & l_i - 1 & A - 1 & A - 1 & A - 1 & r_i - 1 \\
 & 3 & 2 & 1 & 0 & \\
/ & \backslash & / & \backslash & / & \backslash \\
 & 0 & 1 & 2 & 3 & \\
l_i - 1 & A - 1 & A - 1 & A - 1 & r_i - 1 & \longleftarrow
\end{array}$$

[†] Refer to *The Braider*, Issue No. 27, pg. 634.

The algorithm diagram for the component with $p/b = 3/4$, and hence $\Delta^* = 1$, is thus:[†]

$$\begin{array}{cccc} \longrightarrow & l_i - 1 & A - 1 & r_i - 1 \\ & 1 & 2 & \\ / & \backslash & / & \backslash \\ & 2 & 1 & \\ l_i - 1 & A - 1 & r_i - 1 & \longleftarrow \end{array}$$

The half-cycle braiding algorithms for the component with colour A between left bight-boundary 1 and right bight-boundary 4 in the final Standard Herringbone Grant Knot are:

half-cycle $1''$: $L_1 \rightarrow R_3$: $2o - 2u - 2o - 2u$.
half-cycle $2''$: $i = 0$: $R_3 \rightarrow L_1$: $2u - 2o - 2u - 3o$.
half-cycle $3''$: $i = 0$: $L_1 \rightarrow R_3$: $2o - 2u - 3o - 2u$.
half-cycle $4''$: $i \leq 1$: $R_3 \rightarrow L_1$: $2u - 2o - 3u - 3o$.
half-cycle $5''$: $i \leq 1$: $L_1 \rightarrow R_3$: $2o - 3u - 3o - 2u$.
half-cycle $6''$: $i \leq 2$: $R_3 \rightarrow L_1$: $2u - 3o - 3u - 3o$.
half-cycle $7''$: $i \leq 2$: $L_1 \rightarrow R_3$: $3o - 3u - 3o - 2u$.
half-cycle $8''$: $i \leq 3$: $R_3 \rightarrow L_1$: $3u - 3o - 3u - 3o$.

Note that for this component $l_i = 1$ and $r_i = 3$. Its string-run is between the bight-boundaries L_1 and R_3. When completed $A = 3$.

The half-cycle braiding algorithms for the component with colour A between left bight-boundary 3 and right bight-boundary 1 in the final Standard Herringbone Grant Knot are:

half-cycle $1'''$: $L_3 \rightarrow R_1$: $3u - 3o - 3u - 3o$.
half-cycle $2'''$: $i = 0$: $R_1 \rightarrow L_3$: $3o - 3u - 4o - 3u$.
half-cycle $3'''$: $i = 0$: $L_3 \rightarrow R_1$: $3u - 3o - 3u - 4o$.
half-cycle $4'''$: $i \leq 1$: $R_1 \rightarrow L_3$: $3o - 4u - 4o - 3u$.
half-cycle $5'''$: $i \leq 1$: $L_3 \rightarrow R_1$: $3u - 3o - 4u - 4o$.
half-cycle $6'''$: $i \leq 2$: $R_1 \rightarrow L_3$: $4o - 4u - 4o - 3u$.
half-cycle $7'''$: $i \leq 2$: $L_3 \rightarrow R_1$: $3u - 4o - 4u - 4o$.
half-cycle $8'''$: $i \leq 3$: $R_1 \rightarrow L_3$: $u - 4o - 4u - 4o - 3u$.

Note that for this component $l_i = 4$ and $r_i = 1$. Its string-run is between the bight-boundaries L_3 and R_1. When completed $A = 4$.

The half-cycle braiding algorithms for the component with colour D between left bight-boundary 4 and right bight-boundary 5 in the final Standard Herringbone Grant Knot are:

half-cycle $1''''$: $L_4 \rightarrow R_5$: $4u - 4o - 4u$.
half-cycle $2''''$: $i = 0$: $R_5 \rightarrow L_4$: $4u - 4o - 4u$.
half-cycle $3''''$: $i = 0$: $L_4 \rightarrow R_5$: $4u - 4o - 4u$.
half-cycle $4''''$: $i \leq 1$: $R_5 \rightarrow L_4$: $5u - 4o - 4u$.
half-cycle $5''''$: $i \leq 1$: $L_4 \rightarrow R_5$: $5u - 4o - 4u$.
half-cycle $6''''$: $i \leq 2$: $R_5 \rightarrow L_4$: $5u - 5o - 4u$.
half-cycle $7''''$: $i \leq 2$: $L_4 \rightarrow R_5$: $5u - 5o - 4u$.
half-cycle $8''''$: $i \leq 3$: $R_5 \rightarrow L_4$: $5u - 5o - 5u$.

Note that for this component $l_i = 5$ and $r_i = 5$. Its string-run is between the bight-boundaries L_4 and R_5. When completed $A = 5$.

[†] Refer to *The Braider*, Issue No. 27, pg. 634.

For the Standard Herringbone Grant Knot $(332/15/2222)\{1_1 4_5 3_4 2_2 2_3/45123\}20$ depicted by the right-hand grid-diagram below, the string-colours $(\mathrm{A},\mathrm{B},\mathrm{C},\mathrm{D})$ are indicated in the left-hand grid-diagram of its associated Standard Herringbone Pineapple Knot.

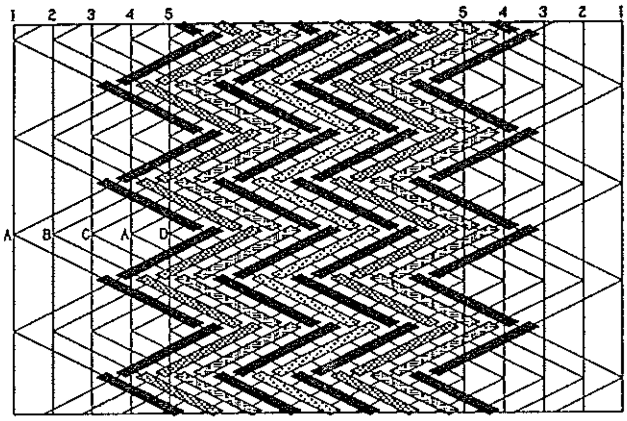

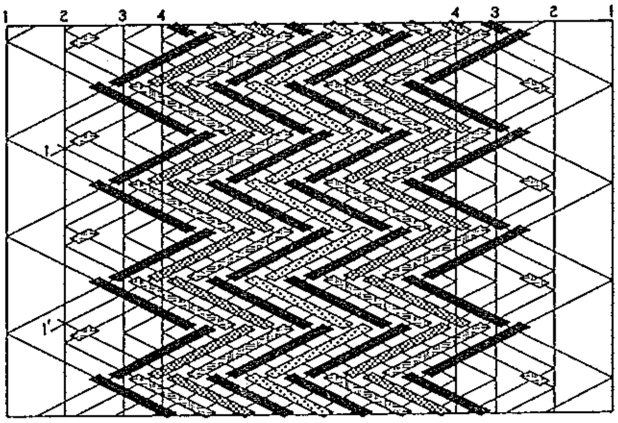

First we braid the component starting with half-cycle 1 and colour C, then we braid the component starting with half-cycle 1′ and colour B. Each of these two components is a Regular Knot with $p/b = 5/4$ and hence $\Delta^* = 3$. After these two components have been braided, the remaining components are braided as if the knot is a Standard Herringbone Pineapple Knot.

The algorithm diagram of the first to be braided component is:

$$\begin{array}{rccccl} & 3 & 2 & 1 & 0 & \\ \text{half-cycles 1, 3, 5, 7} \;\longrightarrow & u & o & u & o & \\ & \cdot & \cdot & \cdot & \cdot & \\ & o & u & o & u & \longleftarrow\; \text{half-cycles 2, 4, 6, 8} \\ & 0 & 1 & 2 & 3 & \end{array}$$

From this algorithm diagram we read off the half-cycle braiding algorithms for the first to be braided component:

half-cycle 1: $L_1 \to R_1$: Free run.
half-cycle 2: $i = 0$: $R_1 \to L_1$: o.
half-cycle 3: $i = 0$: $L_1 \to R_1$: o.
half-cycle 4: $i \leq 1$: $R_1 \to L_1$: $u - o$.
half-cycle 5: $i \leq 1$: $L_1 \to R_1$: $u - o$.
half-cycle 6: $i \leq 2$: $R_1 \to L_1$: $o - u - o$.
half-cycle 7: $i \leq 2$: $L_1 \to R_1$: $o - u - o$.
half-cycle 8: $i \leq 3$: $R_1 \to L_1$: $u - o - u - o$.

The algorithm diagram of the next to be braided component is:

$$\begin{array}{rcccccccccl} & & 3 & & 2 & & 1 & & 0 & & \\ \text{half-cycles } 1', 3', 5', 7' \;\longrightarrow & u & o & o & u & u & o & o & u & u & \\ & \cdot & \cdot & \cdot & \cdot & \cdot & \cdot & \cdot & \cdot & \cdot & \\ & u & u & o & o & u & u & o & o & u & \longleftarrow\; \text{half-cycles } 2', 4', 6', 8' \\ & & 0 & & 1 & & 2 & & 3 & & \end{array}$$

From this algorithm diagram we read off the half-cycle braiding algorithms for the second component:

half-cycle 1′: $L_1 \to R_1$: $u - o - u - o - u$.
half-cycle 2′: $i = 0$: $R_1 \to L_1$: $u - o - u - o - 2u$.

half-cycle 3′ : $i = 0$: $L_1 \to R_1$: $u - o - u - o - 2u$.
half-cycle 4′ : $i \leq 1$: $R_1 \to L_1$: $u - o - u - 2o - 2u$.
half-cycle 5′ : $i \leq 1$: $L_1 \to R_1$: $u - o - u - 2o - 2u$.
half-cycle 6′ : $i \leq 2$: $R_1 \to L_1$: $u - o - 2u - 2o - 2u$.
half-cycle 7′ : $i \leq 2$: $L_1 \to R_1$: $u - o - 2u - 2o - 2u$.
half-cycle 8′ : $i \leq 3$: $R_1 \to L_1$: $u - 2o - 2u - 2o - 2u$.

As mentioned earlier, the remaining components of the Standard Herringbone Grant Knot are braided as if this Grant Knot is a Standard Herringbone Pineapple Knot, and hence for the remaining components we can use the algorithm diagrams of the equivalent components in its associated Standard Herringbone Pineapple Knot. Left bight-boundary 1 of the Grant Knot is equivalent to left bight-boundary 1 of the Pineapple Knot, left bight-boundary 3 of the Grant Knot is equivalent to left bight-boundary 4 of the Pineapple Knot, and left bight-boundary 4 of the Grant Knot is equivalent to left bight-boundary 5 of the Pineapple Knot. Right bight-boundary 1 of the Grant Knot is equivalent to right bight-boundary 1 of the Pineapple Knot, right bight-boundary 3 of the Grant Knot is equivalent to right bight-boundary 4 of the Pineapple Knot, and right bight-boundary 4 of the Grant Knot is equivalent to right bight-boundary 5 of the Pineapple Knot.

The algorithm diagram for two components with $p/b = 5/4$, and hence $\Delta^* = 3$, is thus:

$$\begin{array}{cccccc}
\longrightarrow & l_i - 1 & A - 1 & A - 1 & A - 1 & r_i - 1 \\
 & 3 & 2 & 1 & 0 & \\
/ & \backslash & / & \backslash & / & \backslash \\
 & 0 & 1 & 2 & 3 & \\
l_i - 1 & A - 1 & A - 1 & A - 1 & r_i - 1 & \longleftarrow
\end{array}$$

The algorithm diagram for the component with $p/b = 3/4$, and hence $\Delta^* = 1$, is thus:

$$\begin{array}{cccc}
\longrightarrow & l_i - 1 & A - 1 & r_i - 1 \\
 & 1 & 2 & \\
/ & \backslash & / & \backslash \\
 & 2 & 1 & \\
l_i - 1 & A - 1 & r_i - 1 & \longleftarrow
\end{array}$$

The half-cycle braiding algorithms for the component with colour A between left bight-boundary 1 and right bight-boundary 3 in the final Standard Herringbone Grant Knot are:

half-cycle 1″ : $L_1 \to R_2$: $2o - 2u - 2o - 2u$.
half-cycle 2″ : $i = 0$: $R_2 \to L_1$: $2u - 2o - 2u - 3o$.
half-cycle 3″ : $i = 0$: $L_1 \to R_2$: $2o - 2u - 3o - 2u$.
half-cycle 4″ : $i \leq 1$: $R_2 \to L_1$: $2u - 2o - 3u - 3o$.
half-cycle 5″ : $i \leq 1$: $L_1 \to R_2$: $2o - 3u - 3o - 2u$.
half-cycle 6″ : $i \leq 2$: $R_2 \to L_1$: $2u - 3o - 3u - 3o$.
half-cycle 7″ : $i \leq 2$: $L_1 \to R_2$: $3o - 3u - 3o - 2u$.
half-cycle 8″ : $i \leq 3$: $R_2 \to L_1$: $3u - 3o - 3u - 3o$.

Note that for this component $l_i = 1$ and $r_i = 3$. Its string-run is between the bight-boundaries L_1 and R_2. When completed $A = 3$.

The half-cycle braiding algorithms for the component with colour A between left bight-boundary 3 and right bight-boundary 1 in the final Standard Herringbone Grant Knot are:

half-cycle $1'''$: $L_3 \rightarrow R_1$: $3u - 3o - 3u - 3o$.
half-cycle $2'''$: $i = 0$: $R_1 \rightarrow L_3$: $3o - 3u - 4o - 3u$.
half-cycle $3'''$: $i = 0$: $L_3 \rightarrow R_1$: $3u - 3o - 3u - 4o$.
half-cycle $4'''$: $i \leq 1$: $R_1 \rightarrow L_3$: $3o - 4u - 4o - 3u$.
half-cycle $5'''$: $i \leq 1$: $L_3 \rightarrow R_1$: $3u - 3o - 4u - 4o$.
half-cycle $6'''$: $i \leq 2$: $R_1 \rightarrow L_3$: $4o - 4u - 4o - 3u$.
half-cycle $7'''$: $i \leq 2$: $L_3 \rightarrow R_1$: $3u - 4o - 4u - 4o$.
half-cycle $8'''$: $i \leq 3$: $R_1 \rightarrow L_3$: $u - 4o - 4u - 4o - 3u$.

Note that for this component $l_i = 4$ and $r_i = 1$. Its string-run is between the bight-boundaries L_3 and R_1. When completed $A = 4$.

The half-cycle braiding algorithms for the component with colour D between left bight-boundary 4 and right bight-boundary 4 in the final Standard Herringbone Grant Knot are:

half-cycle $1''''$: $L_4 \rightarrow R_4$: $4u - 4o - 4u$.
half-cycle $2''''$: $i = 0$: $R_4 \rightarrow L_4$: $4u - 4o - 4u$.
half-cycle $3''''$: $i = 0$: $L_4 \rightarrow R_4$: $4u - 4o - 4u$.
half-cycle $4''''$: $i \leq 1$: $R_4 \rightarrow L_4$: $5u - 4o - 4u$.
half-cycle $5''''$: $i \leq 1$: $L_4 \rightarrow R_4$: $5u - 4o - 4u$.
half-cycle $6''''$: $i \leq 2$: $R_4 \rightarrow L_4$: $5u - 5o - 4u$.
half-cycle $7''''$: $i \leq 2$: $L_4 \rightarrow R_4$: $5u - 5o - 4u$.
half-cycle $8''''$: $i \leq 3$: $R_4 \rightarrow L_4$: $5u - 5o - 5u$.

Note that for this component $l_i = 5$ and $r_i = 5$. Its string-run is between the bight-boundaries L_4 and R_4. When completed $A = 5$.

For the Standard Herringbone Grant Knot $(223/17/322)\{1_1 4_4 4_5 3_3 2_2/4_1 4_2 1_3 2_4 3_5\}20$ depicted by the right-hand grid-diagram below, the string-colours (A, B, C) are indicated in the left-hand grid-diagram of its associated Standard Herringbone Pineapple Knot.

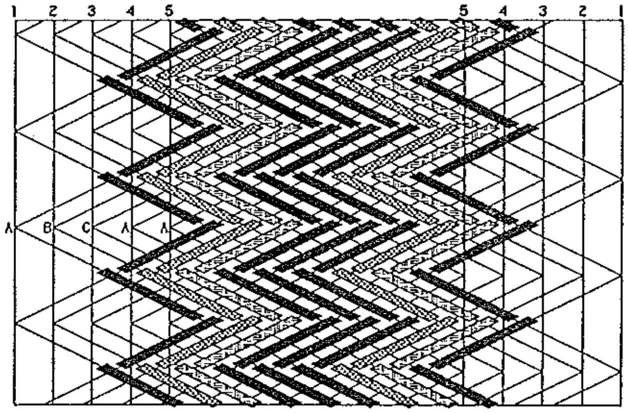

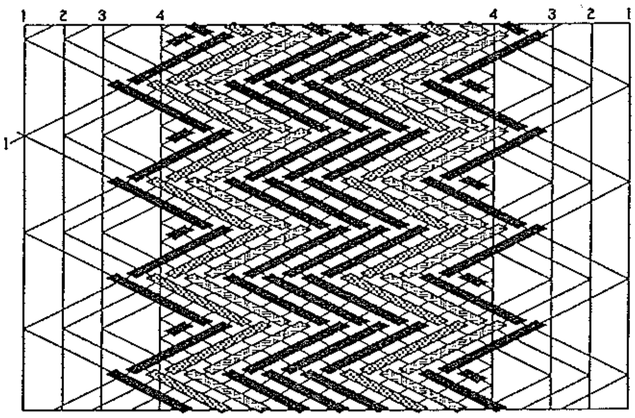

First we braid the component $(3/11/3)\{1_1 2_2 2_3/2_1 2_2 1_3\}12$, a 3-pass Standard Herringbone Grant Knot starting with half-cycle 1 and colour A, then we braid the two remaining components (Regular Knots) as if the knot is a Standard Herringbone Pineapple Knot. The first first-return string-run and the half-cycle pattern of the first to be braided component are shown in Fig. 823. From this half-cycle pattern we assemble the half-cycle table for the odd-numbered half-cycles (from lower left to upper right) and the half-cycle table for the even-numbered half-cycles (from lower right to upper left).[†] See Fig. 824.

[†] Refer to *The Braider*, Issue No. 28.

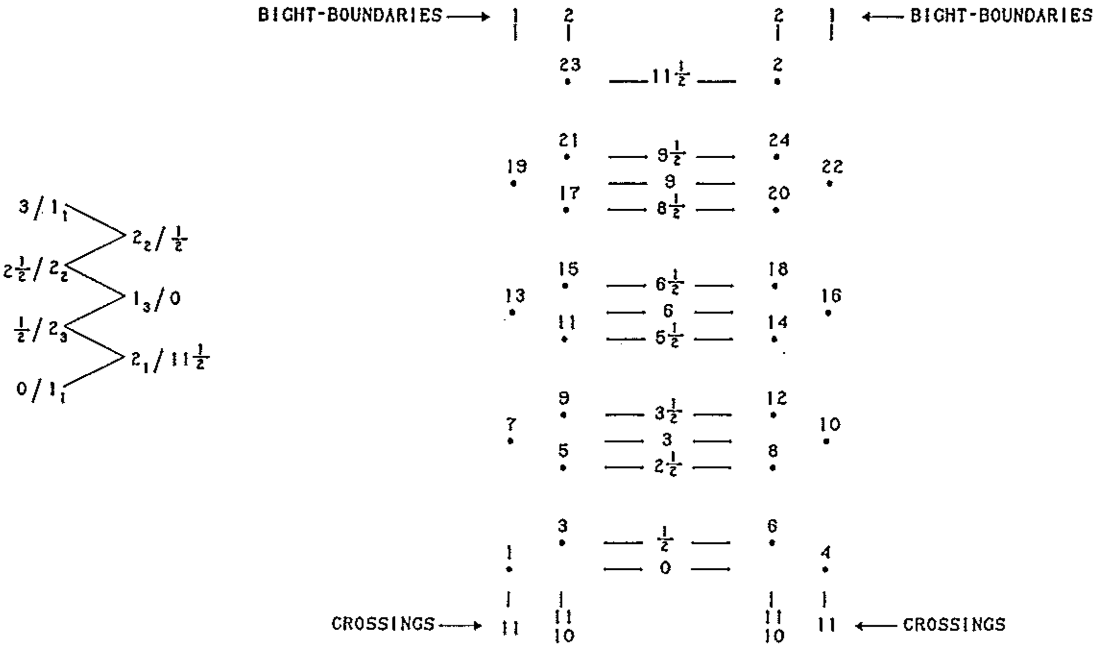

Fig. 823 — First-return string-run and half-cycle pattern.

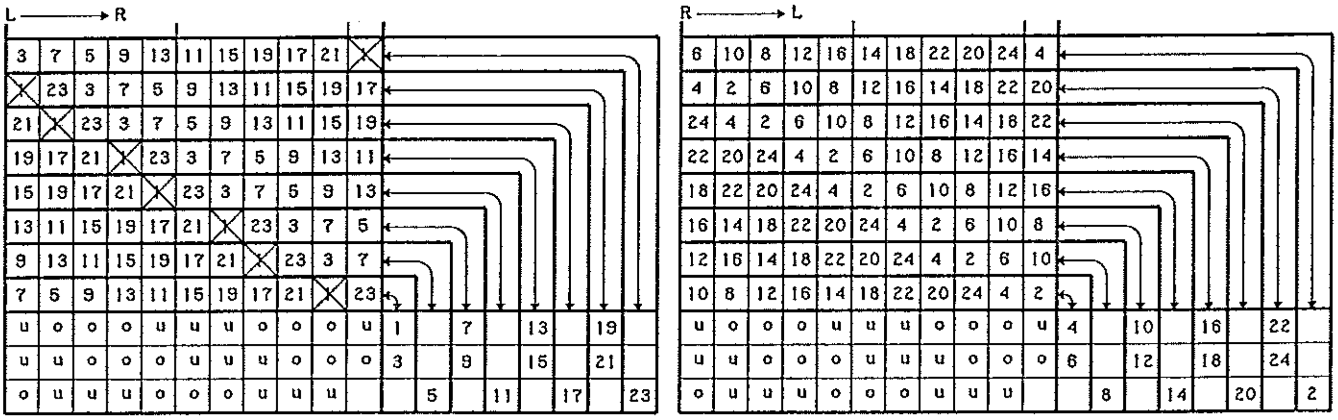

3	7	5	9	13	11	15	19	17	21	✕								
✕	23	3	7	5	9	13	11	15	19	17								
21	✕	23	3	7	5	9	13	11	15	19								
19	17	21	✕	23	3	7	5	9	13	11								
15	19	17	21	✕	23	3	7	5	9	13								
13	11	15	19	17	21	✕	23	3	7	5								
9	13	11	15	19	17	21	✕	23	3	7								
7	5	9	13	11	15	19	17	21	✕	23								
u	o	o	o	u	u	u	o	o	o	u	1		7		13		19	
u	u	o	o	o	u	u	u	o	o	o	3		9		15		21	
o	u	u	u	o	o	o	u	u	u			5		11		17		23

6	10	8	12	16	14	18	22	20	24	4								
4	2	6	10	8	12	16	14	18	22	20								
24	4	2	6	10	8	12	16	14	18	22								
22	20	24	4	2	6	10	8	12	16	14								
18	22	20	24	4	2	6	10	8	12	16								
16	14	18	22	20	24	4	2	6	10	8								
12	16	14	18	22	20	24	4	2	6	10								
10	8	12	16	14	18	22	20	24	4	2								
u	o	o	o	u	u	u	o	o	o	u	4		10		16		22	
u	u	o	o	o	u	u	u	o	o	o	6		12		18		24	
o	u	u	u	o	o	o	u	u	u			8		14		20		2

Fig. 824 — The half-cycle tables.

From these half-cycle tables we read the following half-cycle braiding algorithms:

half-cycle 1: $L_1 \to R_2$: Free run.
half-cycle 2: $R_2 \to L_2$: Free run.
half-cycle 3: $L_2 \to R_1$: Free run.
half-cycle 4: $R_1 \to L_2$: $o - u$.
half-cycle 5: $L_2 \to R_2$: u.
half-cycle 6: $R_2 \to L_1$: $2o$.
half-cycle 7: $L_1 \to R_2$: $2o - u$.
half-cycle 8: $R_2 \to L_2$: $2u$.
half-cycle 9: $L_2 \to R_1$: $3o$.
half-cycle 10: $R_1 \to L_2$: $u - 3o - u$.
half-cycle 11: $L_2 \to R_2$: $o - 3u$.
half-cycle 12: $R_2 \to L_1$: $2u - 3o$.
half-cycle 13: $L_1 \to R_2$: $2u - 3o - u$.
half-cycle 14: $R_2 \to L_2$: $3o - 3u$.

half-cycle 15: $L_2 \to R_1$: $3u - 3o$.
half-cycle 16: $R_1 \to L_2$: $o - 3u - 3o - u$.
half-cycle 17: $L_2 \to R_2$: $u - 3o - 3u$.
half-cycle 18: $R_2 \to L_1$: $2o - 3u - 3o$.
half-cycle 19: $L_1 \to R_2$: $2o - 3u - 3o - u$.
half-cycle 20: $R_2 \to L_2$: $3u - 3o - 3u$.
half-cycle 21: $L_2 \to R_1$: $3o - 3u - 3o$.
half-cycle 22: $R_1 \to L_2$: $u - 3o - 3u - 3o - u$.
half-cycle 23: $L_2 \to R_2$: $o - 3u - 3o - 3u$.
half-cycle 24: $R_2 \to L_1$: $2u - 3o - 3u - 3o$.

The remaining components of the Standard Herringbone Grant Knot are braided as if this Grant Knot is a Standard Herringbone Pineapple Knot, and hence for the remaining two components we can use the algorithm diagrams of the equivalent components in its associated Standard Herringbone Pineapple Knot. Left bight-boundary 2 of the Grant Knot is equivalent to left bight-boundary 2 of the Pineapple Knot, and left bight-boundary 3 of the Grant Knot is equivalent to left bight-boundary 3 of the Pineapple Knot. Right bight-boundary 2 of the Grant Knot is equivalent to right bight-boundary 2 of the Pineapple Knot, and right bight-boundary 3 of the Grant Knot is equivalent to right bight-boundary 3 of the Pineapple Knot.

The algorithm diagram for two components with $p/b = 5/4$, and hence $\Delta^* = 3$, is thus:

$$\begin{array}{cccccc}
\longrightarrow & l_i - 1 & A-1 & A-1 & A-1 & r_i - 1 \\
 & 3 & 2 & 1 & 0 & \\
/ & \backslash & / & \backslash & / & \backslash \\
 & 0 & 1 & 2 & 3 & \\
l_i - 1 & A-1 & A-1 & A-1 & r_i - 1 & \longleftarrow
\end{array}$$

The half-cycle braiding algorithms for the component with colour B between left bight-boundary 2 and right bight-boundary 3 in the final Standard Herringbone Grant Knot are:

half-cycle $1'$: $L_2 \to R_2$: $u - 3o - 3u - 3o - u$.
half-cycle $2'$: $i = 0$: $R_2 \to L_2$: $u - 3o - 3u - 4o - u$.
half-cycle $3'$: $i = 0$: $L_2 \to R_2$: $u - 3o - 3u - 4o - u$.
half-cycle $4'$: $i \leq 1$: $R_2 \to L_2$: $u - 3o - 4u - 4o - u$.
half-cycle $5'$: $i \leq 1$: $L_2 \to R_2$: $u - 3o - 4u - 4o - u$.
half-cycle $6'$: $i \leq 2$: $R_2 \to L_2$: $u - 4o - 4u - 4o - u$.
half-cycle $7'$: $i \leq 2$: $L_2 \to R_2$: $u - 4o - 4u - 4o - u$.
half-cycle $8'$: $i \leq 3$: $R_2 \to L_2$: $2u - 4o - 4u - 4o - u$.

Note that for this component $l_i = 2$ and $r_i = 2$. Its string-run is between the bight-boundaries L_2 and R_2. When completed $A = 4$.

The half-cycle braiding algorithms for the component with colour C between left bight-boundary 3 and right bight-boundary 2 in the final Standard Herringbone Grant Knot are:

half-cycle $1''$: $L_3 \to R_2$: $2u - 4o - 4u - 4o - u$.
half-cycle $2''$: $i = 0$: $R_2 \to L_3$: $u - 4o - 4u - 5o - 2u$.
half-cycle $3''$: $i = 0$: $L_3 \to R_2$: $2u - 4o - 4u - 5o - u$.
half-cycle $4''$: $i \leq 1$: $R_2 \to L_3$: $u - 4o - 5u - 5o - 2u$.
half-cycle $5''$: $i \leq 1$: $L_3 \to R_2$: $2u - 4o - 5u - 5o - u$.
half-cycle $6''$: $i \leq 2$: $R_2 \to L_3$: $u - 5o - 5u - 5o - 2u$.

half-cycle $7''$: $i \leq 2$: $L_3 \to R_2$: $2u - 5o - 5u - 5o - u$.
half-cycle $8''$: $i \leq 3$: $R_2 \to L_3$: $2u - 5o - 5u - 5o - 2u$.

Note that for this component $l_i = 3$ and $r_i = 2$. Its string-run is between the bight-boundaries L_3 and R_2. When completed $A = 5$.

The Single Bugler's Braid

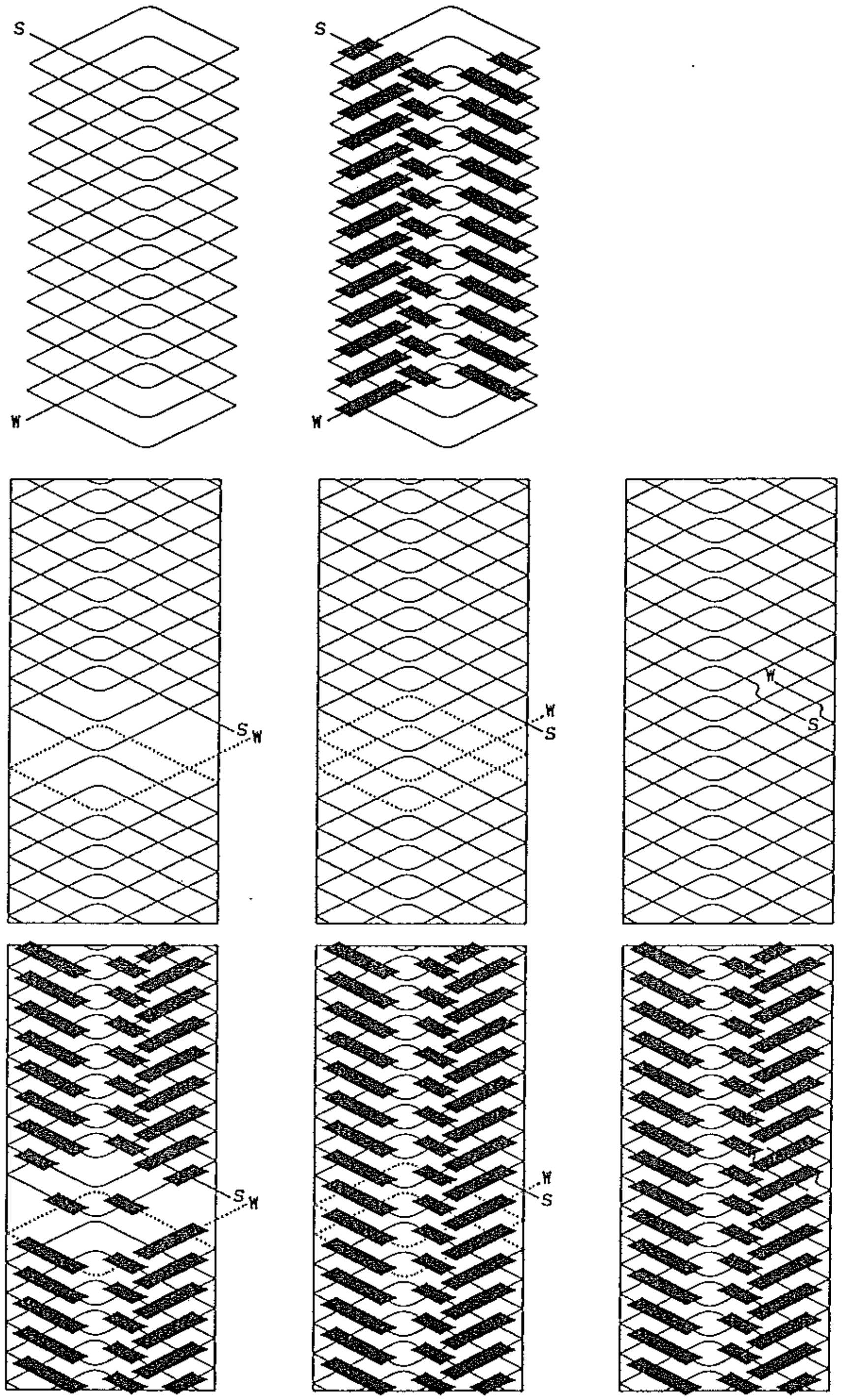

Fig. 825 — The Single Bugler's Braid.